FEDERAL EMERGENCY MANAGEMENT AGENCY

FEMA-288 / March 1997

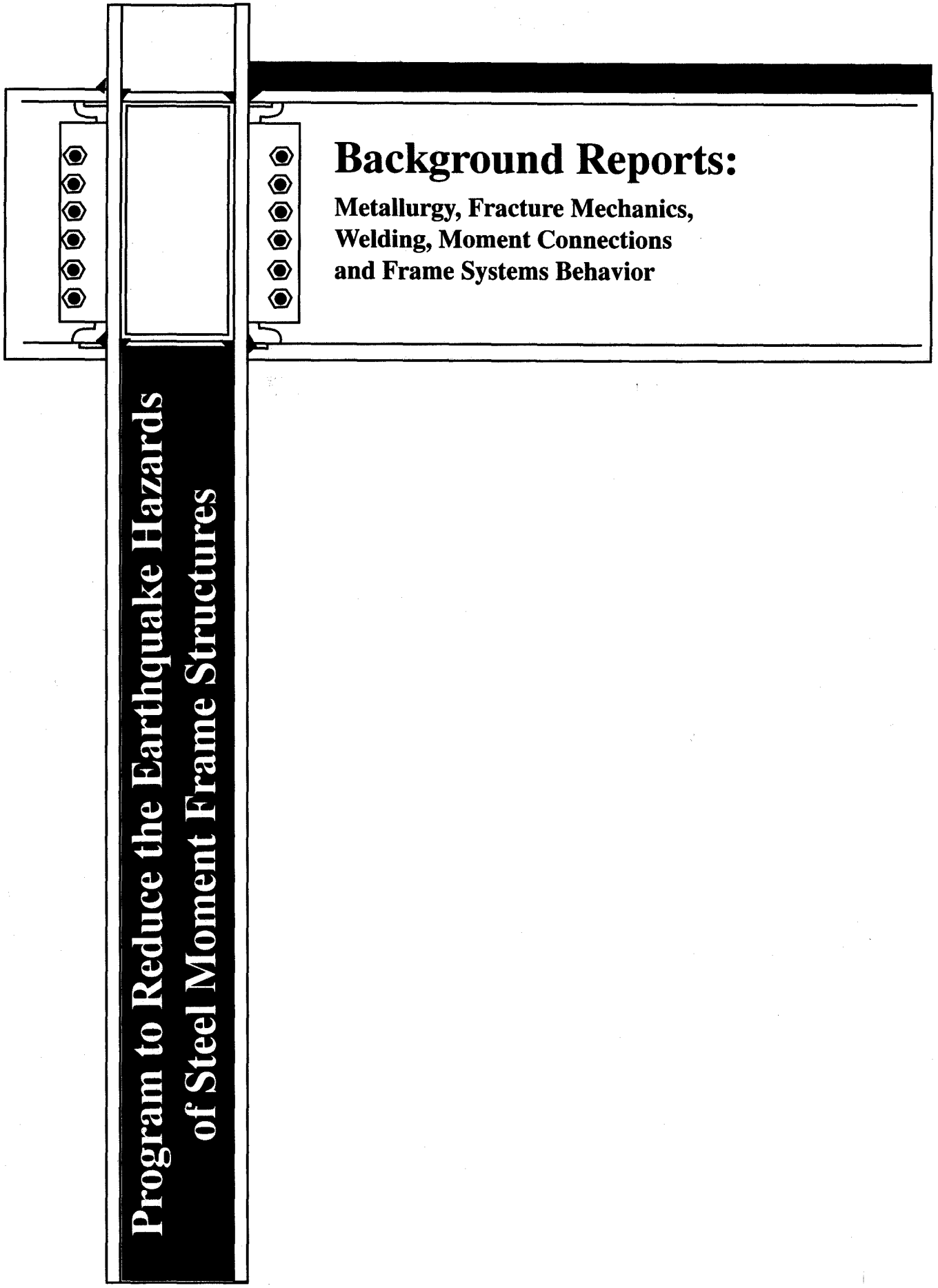

Background Reports:

Metallurgy, Fracture Mechanics, Welding, Moment Connections and Frame Systems Behavior

Program to Reduce the Earthquake Hazards of Steel Moment Frame Structures

BACKGROUND REPORTS: Metallurgy, Fracture Mechanics, Welding, Moment Connections and Frame Systems Behavior

Report No. SAC-95-09

SAC Joint Venture

a partnership of:
Structural Engineers Association of California (SEAOC)
Applied Technology Council (ATC)
California Universities for Research in Earthquake Engineering (CUREe)

Prepared for SAC Joint Venture Partnership by

Robert J. Dexter
John W. Fisher
Karl H. Frank
Eric J. Kaufmann
Helmut Krawinkler
Roberto T. Leon
Duane K. Miller
Egor P. Popov
K. C. Tsai

SAC Joint Venture Management Committee

SEAOC: William T. Holmes, Chairman, Arthur E. Ross
ATC: Edwin T. Huston, Christopher Rojahn
CUREe: Robin Shepherd, Geoffrey R. Martin.

SAC Technical Committee

Program Manager: Stephen A. Mahin
Project Director for Topical Investigations: James O. Malley
Project Director for Product Development: Ronald O. Hamburger

SAC Joint Venture
555 University Avenue, Suite 126
Sacramento, California 95825
916-427-3647

December, 1995

THE SAC JOINT VENTURE

SAC is a joint venture of the Structural Engineers Association of California (SEAOC), the Applied Technology Council (ATC), and California Universities for Research in Earthquake Engineering (CUREe), formed specifically to address both immediate and long-term needs related to solving the problems of the Welded Steel Moment Frame (WSMF) connection. SEAOC is a professional organization composed of more than 3,000 practicing structural engineers in California. The volunteer efforts of SEAOC's members on various technical committees have been instrumental in the development of the earthquake design provisions contained in the *Uniform Building Code* as well as the *National Earthquake Hazards Reduction Program (NEHRP) Recommended Provisions for Seismic Regulations for New Buildings.* The Applied Technology Council is a non-profit organization founded specifically to perform problem-focused research related to structural engineering and to bridge the gap between civil engineering research and engineering practice. It has developed a number of publications of national significance including ATC 3-06, which serves as the basis for the *NEHRP Recommended Provisions.* CUREe is a non-profit organization formed to promote and conduct research and educational activities related to earthquake hazard mitigation. CUREe's eight institutional members are: the California Institute of Technology, Stanford University, the University of California at Berkeley, the University of California at Davis, the University of California at Irvine, the University of California at Los Angeles, the University of California at San Diego, and the University of Southern California. This collection of university earthquake research laboratory, library, computer and faculty resources is among the most extensive in the United States. The SAC Joint Venture allows these three organizations to combine their extensive and unique resources, augmented by subcontractor universities and organizations from around the nation, into an integrated team of practitioners and researchers, uniquely qualified to solve problems related to the seismic performance of WSMF structures.

DISCLAIMER

This report is one of a series documenting a preliminary program of laboratory, field and analytical investigations and research conducted as part of Phase 1 of the Program to Reduce Earthquake Hazards of Steel Moment Frame Structures conducted by the SAC Joint Venture under funding from the Federal Emergency Management Agency. Information contained in this report was used in the development of the *Interim Guidelines: Evaluation, Repair, Modification and Design of Welded Steel Moment Frame Structures* (FEMA Report No. 267, August 1995). This report is being published to improve understanding of the basis for the *Interim Guidelines* and of the factors contributing to the seismic performance of steel moment frame structures. Opinions and recommendations contained in this report are those of the respective contributing author(s) and do not necessarily represent an official position of the SAC Joint Venture

The work contained in this report has been reviewed by a Technical Advisory Panel, comprising experts from a variety of fields, and the Project Technical Committee. Every attempt has been made to ensure its accuracy. However, it must be recognized that the report is of limited scope and has been completed within a short period of time. As a consequence, it may not account for work undertaken in other parts of the SAC Phase 1 Steel Project or by others; it may not address all of the facets of a problem in a consistent fashion; and it may contain information contrary to that incorporated into the *Interim Guidelines* or obtained in other SAC-directed investigations or in other investigations. The reader is cautioned that research is continuing at a rapid pace in this field, and that results of this continuing research may invalidate or suggest the need for modification of the results or recommendations contained herein.

No warranty is offered with regard to the results, findings and recommendations contained herein, either by the Federal Emergency Management Agency, the SAC Joint Venture, the individual joint venture partners, their directors, members or employees. These organizations and individuals do not assume any legal liability or responsibility for the accuracy, completeness, or usefulness of any of the information, products or processes included in this publication. The reader is cautioned to carefully review the material presented herein.

PREFACE

The Northridge Earthquake of January 17, 1994, dramatically demonstrated that the prequalified, welded beam-to-column moment connection commonly used in the construction of welded steel moment resisting frames (WSMFs) in the period 1970-1994 was much more susceptible to damage than previously thought. The stability of moment frame structures in earthquakes is dependent on the capacity of the beam-column connection to remain intact and to resist tendencies of the beams and columns to rotate with respect to each other under the influence of lateral swaying of the structure. The prequalified connections were believed to be ductile and capable of withstanding the repeated cycles of large inelastic deformation explicitly relied upon in the building code provisions for the design of these structures. Although many affected connections were not damaged, a wide spectrum of unexpected brittle connection fractures did occur, ranging from minor cracking observable only by detailed nondestructive testing (NDT) to complete severing of columns. At the time this damage was discovered, the structural steel industry and engineering profession had little understanding of the specific causes of this damage, the implications of this damage for building safety, or even if reliable methods existed to repair the damage which had been discovered. While no casualties or collapses occurred as a result of these connection failures, and some welded steel moment frame (WSMF) buildings were not damaged, the incidence of damage was sufficiently high in regions of strong ground motion to cause wide-spread concern by structural engineers and building officials with regard to the safety of these structures in seismically active regions.

In response to these concerns, the Federal Emergency Management Agency (FEMA) entered into a cooperative agreement with the SAC Joint Venture to perform a problem focused study of the seismic performance of welded steel moment connections and to develop interim recommendations for professional practice. Specifically, these recommendations were intended to address the inspection of earthquake affected buildings to determine if they had sustained significant damage; the repair of damaged buildings; the upgrade of existing buildings to improve their probable future performance; and the design of new structures to provide more reliable seismic performance. Within weeks of receipt of notification of FEMA's intent to enter into this agreement, the SAC Joint Venture published a series of two Design Advisories (SAC, 1994a; SAC, 1994b) These Design Advisories presented a series of papers, prepared by engineers and researchers engaged in the investigation of the damaged structures and presenting individual opinions as to the causes of the damage, potential methods of repair, and more reliable design of connections in the future. In February, 1995, Design Advisory No. 3 (SAC, 1995a) was published. This third advisory presented a synthesis of the data presented in the earlier publications, together with the preliminary recommendations developed in an industry workshop, attended by more than 50 practitioners, industry representatives and researchers, on methods of inspecting, repairing and designing WSMF structures. At the time this third advisory was published, significant disagreement remained within the industry and the profession as to the specific causes of the damage observed and appropriate methods for practice given that the damage had occurred. Consequently, the preliminary recommendations were presented as a series of issue statements, followed by the consensus opinions of the workshop attendees, where

consensus existed, and by majority and dissenting opinions where such consensus could not be formed.

During the first half of 1995, an intensive program of research was conducted to more definitively explore the pertinent issues. This research included literature surveys, data collection on affected structures, statistical evaluation of the collected data, analytical studies of damaged and undamaged buildings and laboratory testing of a series of full-scale beam-column assemblies representing typical pre-Northridge design and construction practice as well as various repair, upgrade and alternative design details. The findings of this research (SAC, 1995c; SAC, 1995d; SAC, 1995e; SAC, 1995f; SAC, 1995g; SAC, 1995h; SAC, in preparation) were used in the development of FEMA 267 *Interim Guidelines: Evaluation, Repair, Modification, and Design of Welded Steel Moment Frame Structures* (SAC, 1995b) in August, 1995. FEMA 267 provided the first definitive, albeit interim, recommendations for practice, following the discovery of connection damage in the Northridge earthquake.

As a result of these studies as well as independent research conducted by others, it is now known that a large number of factors contributed to the damage sustained by steel frame buildings in the Northridge earthquake. These included:

- design practice that favored the use of relatively few frame bays to resist lateral seismic demands, resulting in much larger member and connection geometries than had previously been tested
- standard detailing practice that resulted in the development of large inelastic demands at the beam to column connections
- detailing practice that often resulted in large stress concentrations in the beam-column connection
- the common use of welding procedures that resulted in deposition of low toughness weld metal in the critical beam flange to column flange joints
- relatively low levels of quality control and assurance in the construction process, resulting in welded joints that did not conform to the applicable quality standards
- detailing practice for welded joints that resulted in inherent stress risers and notches in zones of high stress
- excessively weak and flexible column panel zones that resulted in large secondary stresses in the beam flange to column flange joints
- large variations in material strengths relative to specified values
- the inherent inability of the material to yield under conditions of high tri-axial restraint such as exist at the center of the beam flange to column flange joints

In addition to these technical issues, review of the state-of-practice at the time of the Northridge earthquake indicated that many engineers engaged in the design of steel frames did not possess adequate knowledge or understanding of the basic materials and processes they were relying upon and specifying in their designs. The presence of a highly prescriptive set of building code provisions and industry standards resulted in a situation of near blind reliance on the efficacy of these standards and limited effort on the part of engineers to understand their basis, limits of applicability and critical issues pertinent to their application.

On the basis of preliminary research performed following the Northridge Earthquake, FEMA-267 was published in August, 1995. FEMA-267 presents an interim recommended design methodology to provide connections capable of more reliable seismic performance, as well as recommendations for the inspection, evaluation, repair and upgrade of existing buildings. Unlike previous engineering standards for these structures, the FEMA-267 recommendations require the engineer to exercise a high degree of judgment and understanding of the critical issues pertinent to steel moment-frame performance. The background papers contained in this publication are intended to provide a portion of the primary background information required to exercise such understanding and judgment. They provide a summary of the state of knowledge with regard to the production and properties of structural use steels, welding processes and procedures, fracture mechanics, the behavior of various types of welded and bolted connections and methods of predicting the demands on these connections using frame analysis, as it existed at the time of publication.

SAC is continuing, with FEMA funding, to perform additional research into the performance of moment resisting connections of various configurations. This work includes analytical evaluations of buildings and connections as well as additional large scale testing of connection assemblies. It is expected that in the course of these additional investigations, new information will be found that will either supplement or alter the validity of material presented in this publication. The SAC Joint Venture intends to prepare and FEMA to publish supplemental materials as appropriate.

It should be noted that individual authors of some papers have presented personal opinions and interpretations of the data presented, in some cases coupled with design recommendations. Engineers are cautioned to review the material presented carefully and to form their own opinions as to appropriate courses of action in applying this information. The opinions and recommendations contained herein do not necessarily reflect the recommendations of the Federal Emergency Management Agency, the SAC Joint Venture, or their individual employees, officers and directors.

The principal authors of the background reports included in this document are: K.H. Frank (University of Texas at Austin); D. K. Miller (The James F. Lincoln Arc Welding Foundation); J.W. Fisher, R.J. Dexter, and E.J. Kaufmann (Lehigh University); K.C. Tsai (National Taiwan University) and E.P. Popov (University of California at Berkeley); R.T. Leon (Georgia Institute of Technology); and H. Krawinkler (Stanford University).

SAC gratefully acknowledges the valuable input, support and cooperation provided by the FEMA Project Officer, Michael Mahoney and the FEMA Technical Advisor, Dr. Robert D.

Hanson. SAC also wishes to recognize the American Institute of Steel Construction, the American Iron and Steel Institute, the American Welding Society, the Lincoln Electric Company, the Structural Shape Producers Council, and the many engineers, fabricators, inspectors and researchers who contributed services, materials, data and invaluable advice and assistance in the completion of this project.

For additional information about the SAC Program to Reduce the Earthquake Hazards of Steel Moment Frame Structures see Appendix A.

Stephen A. Mahin
SAC Program Manager

Arthur E. Ross
Chair, SAC Phase 1 Joint Venture Management Committee

REFERENCES

SAC, 1994a, *Steel Moment Frame Advisory No. 1*, prepared by the SAC Joint Venture partnership of the Structural Engineers Association of California, the Applied Technology Council, and California Universities for Research in Earthquake Engineering, Sacramento, California.

SAC, 1994b, *Steel Moment Frame Advisory No. 2,* SAC Joint Venture, Sacramento, California.

SAC, 1995a, *Steel Moment Frame Connection Advisory No. 3,* SAC Joint Venture report 95-01, Sacramento, California.

SAC, 1995b, *Interim Guidelines: Evaluation, Repair, Modification, and Design of Welded Steel Moment Frame Structures,* prepared by the SAC Joint Venture, report 95-02, published by the Federal Emergency Management Agency, report FEMA-267, Washington, D.C.

SAC, 1995c, *Characterization of Ground Motions During the Northridge Earthquake of January 17, 1994,* SAC Joint Venture report 95-03, Sacramento, California.

SAC, 1995d, *Analytical and Field Investigations of Buildings Affected by the Northridge Earthquake of January 17, 1994,* SAC Joint Venture report 95-04, Volumes 1 and 2, Sacramento, California.

SAC, 1995e, *Parametric Analytical Investigations of Ground Motion and Structural Response, Northridge Earthquake of January 17, 1994,* SAC 95-05, Sacramento, California.

SAC, 1995f, *Surveys and Assessment of Damage to Buildings Affected by the Northridge Earthquake of January 17, 1994*, SAC Joint Venture report 95-06, Sacramento, California.

SAC, 1995g, *Case Studies of Steel Moment Frame Building Performance in the Northridge Earthquake of January 17, 1994*, SAC Joint Venture report 95-07, Sacramento, California.

SAC, 1995h, *Experimental Investigations of Materials, Weldments and Nondestructive Examination Techniques*, SAC Joint Venture report 95-08, Sacramento, California.

SAC, 1996, *Experimental Investigations of Beam-Column Subassemblages*, SAC Joint Venture report 96-01, Sacramento, California.

TABLE OF CONTENTS

PREFACE iii

1. STRUCTURAL STEELS, THEIR PHYSICAL AND METALLURGICAL PROPERTIES
   Karl H. Frank 1-1

2. WELDING OF SEISMICALLY RESISTANT STEEL STRUCTURES
   Duane K. Miller 2-1

3. FRACTURE MECHANICS OF WELDED STRUCTURAL STEEL CONNECTIONS
   John W. Fisher, Robert J. Dexter, Eric J. Kaufmann, ... 3-1

4. SEISMIC STEEL BEAM-COLUMN MOMENT CONNECTIONS
   K. C. Tsai, Egor P. Popov 4-1

5. SEISMIC PERFORMANCE OF BOLTED AND RIVETED CONNECTIONS
   Roberto T. Leon 5-1
   APPENDIX A: T-STUB CONNECTION DESIGN EXAMPLE 5-75

6. SYSTEMS GEHAVIOR OF STRUCTURAL STEEL FRAMES SUBJECTED TO EARTHQUAKE GROUND MOTIONS
   Helmut Krawinkler 6-1

APPENDIX A: SAC PROGRAM TO REDUCE THE EARTHQUAKE HAZARDS OF STEEL MOMENT FRAME STRUCTURES, AN OVERVIEW A-1

THE PHYSICAL AND METALLURGICAL PROPERTIES OF STRUCTURAL STEELS

Karl H. Frank
THE UNIVERSITY OF TEXAS AT AUSTIN

Abstract

This paper discusses the basics of steel making and the changes which have occurred in the steel making for structural steel shapes. The influence of alloys and heat treatment upon the finished steel's properties is presented. The specifications for the steels is reviewed and changes currently underway are discussed. The methods of determining the steels yield strength are discussed and the relationship of the values reported on the mill test to the actual strength are discussed. The influence of steel making practice upon the through thickness properties of the steel is discussed and the mechanism of lamellar tearing is presented.

Introduction

The design of moment frames for seismic loading relies upon the steel beams to form plastic hinges which dissipates the earthquake energy. The ductility and strength of the steel beam and the connection of the beam to the column govern the ability of the framing system to absorb the earthquake's energy. The paper discusses the roll of the steel making practice upon the ductility and strength of the beam and the changes that are occurring in the production of hot rolled steel sections.

Steel Production Process and Rolling Practice

The structural steel employed in most steel frames is either hot rolled carbon or high-strength low-alloy (HSLA) steel. The majority of the steel is made in either a basic-oxygen furnace (BOF) from iron or iron plus a charge of recycled scrap steel or in an electric-furnace from recycled scrap steel. The majority of structural shapes made in the U.S. is from electric furnace steel. The steel manufacturers using iron in a basic-oxygen furnace are called integrated producers since they first produce the iron by refining iron ore. Electric-furnace production of steel, was initially used by small specialty steel producers, which have been referred to as mini-mills. These smaller mills have grown and have become the larger producers of structural shapes in the U.S. Many steel mills in the U.S. and overseas are switching to electric furnace steel production to lower their costs.

The basic oxygen furnace removes the carbon from the steel by using oxygen blowing. The oxygen combines with the carbon to form carbon monoxide. Alloy additions are made in the ladle at the ladle treatment stage after the furnace is tapped and the molten metal is poured into the ladle. Normally these steels are produced as a semikilled steel. The term semikilled refers to the degree of oxygen removal. After the steel is produced, it is saturated with oxygen in the form of iron oxide. The degree to which the excess oxygen is removed or tied up by adding elements whose affinity for oxygen is greater than that of iron determines the degree of killing. Aluminum or ferrosilicon is added to the molten metal which ties up some of the dissolved oxygen in the steel. This prevents the formation of a rim of iron on the ingot mold but does not completely remove or tie up the oxygen as in a killed steel. Oxygen is still evolved during the solidification of the steel. Vacuum degassing of the steel to remove hydrogen,

oxygen and other gases is used when high purity is required. Calcium and other elements are used to reduce the level of sulfur and to remove or spheroidize sulfide inclusions.

Electric furnace production is done in a two step operation. First, a scrap charge is melted in the furnace. Second, the steel is poured into a ladle and moved to the ladle treatment station. The chemistry is checked at this stage and any alloy additions are made.

The molten steel is either poured into ingot molds or continuously strand cast into blooms or near net shape sections. A "heat of steel" is all the steel made from the same furnace batch. The chemical analysis of the molten steel is made and the results reported for all the shapes subsequently rolled from that heat of steel.

The ingots, blooms, or near net shape sections are then reheated to the rolling temperature and moved onto the rolling line. The steel is hot rolled to reduce the forces required to roll the shape and to provide the desired mechanical properties. The rolling process consists of passing the steel through a series of roller stands which progressively shape the steel into the desired shape. The use of strand cast blooms or near net shape sections reduces the amount of heating and rolling required and results in a more efficient rolling process. Many producers use these reduced size shapes to start the rolling process. The shape may make multiple passes in each stand with the position of the rollers changed either manually or by computer control to sequentially change the size of the steel. Some manufacturers use single pass rolling where the section is not reversed through the stand but passes directly from one roller stand to the next. The throughput of the rolling operation is increased using single pass rolling. However the number of roller stands and length of the rolling line must be increased which increases the construction cost of the rolling line.

Generally, more than one size shape can be rolled without the rolls being changed. The different size shapes can be accommodated by adjusting the thickness of the flange and web. The grouping of the shapes in the dimension tables found in Part 1 of AISC Manual of Steel Construction (ASD or LRFD) are shapes which can be made without changing the rolls. For example, a W24x68 and a W24x103 can be rolled with out changing the roll sizes. Consequently, both of these shapes can be made from the same heat of steel during the same rolling. The same heat of steel could also be used for other sections but would require changing the rolls in the mill.

After the section has been rolled to its final shape, it is cut to length at the hot saw and moved to the cooling bed. The test section for the mill tensile tests is normally taken from a short length of the section cut at the hot saw.

Residual stresses are formed in the sections due to the differential cooling of the section. The web to flange junction cools the slowest while the flange tips and the mid-height of the web cool faster. The shrinkage which occurs as flange tips and web mid-height region cool is not significantly restrained by the hotter softer parts of the section. However, the shrinkage of the areas with the slower cooling rates is restrained by the areas at a lower temperature. The result of this differential cooling and shrinkage is that the areas which cool the slowest are in tension. The faster cooling areas which resisted the shrinkage of the slower cooling areas are in compression. The resulting stresses are called residual stresses. In rolled W sections, the maximum residual tension is of the order of 0.3 to 0.5 F_y at the web to flange junction.

The section is next straightened in either a roller straightener or a gag press. Roller straightening or rotarizing the section consists of pulling the section through a series of offset rollers. The section is alternately bent about its weak axis. The alternating plastic deformation straightens the section. The cyclic deformation all but eliminates residual stress in the flanges of the section. Larger sections are

straightened by gagging. Gagging consists of bending the section using hydraulic rams against fixed supports. Gagging produces localized plastic deformation and does not remove the residual stress in the flange.

Introduction to Ferrous Metallurgy

Steel is an iron based material with less than 2% carbon and is a polycrystalline material made up of individual crystals. The individual crystals each have a different orientation of their crystal axis with respect to a reference axis. The areas with the same orientation are referred to as grains. Structural steels used in building construction are typically composed of two solid phases, ferrite and cementite, at room temperature. Each of these phases has a different atomic arrangement and contain different amounts of carbon and other alloys. The amount of each phase present at a given temperature is a function of the alloy content of the steel. An equilibrium phase diagram for an iron-carbon system (no other alloy) is shown below. Only a portion of the phase diagram is shown for simplicity. The upper portion of the phase diagram is a region of only one phase called austenite which is designated by the symbol γ. Steels with a carbon content below 0.80% enter a two phase region of ferrite, α, and γ as they cool and then enter a region of ferrite and cementite. The phase changes that a steel undergoes upon cooling or heating allow the steel to be heat treated and influence the weldability of the steel.

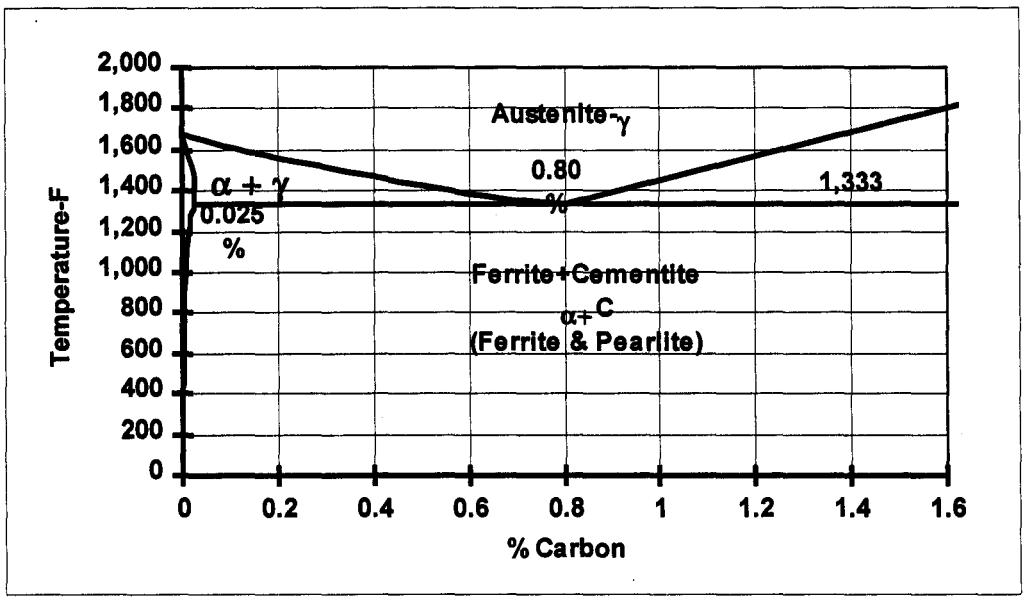

Figure 1- Iron-Carbon Phase Diagram

The phases shown in the figure are:

Austenite(γ): Face Centered Cubic atomic structure that can dissolve up to 2.06% carbon.

Ferrite(α): Body Centered Cubic atomic structure with a maximum solubility of carbon of 0.025%.

Cementite(C): Fe_3C, iron carbide or simply carbide.

Below 1333 ^{o}F two phases are present, carbide and ferrite. These phases are present in two distinct microstructures. One microstructure is called pearlite which is a two phase structure of ferrite and

carbide which results from a reaction called the eutectoid reaction. This reaction occurs if the steel is cooled slow enough to allow this reaction to occur. The eutectoid reaction can be written as:

$$\gamma \Leftrightarrow \alpha + \mathrm{C}.$$

This is a reversible reaction, that is upon reheating , austenite is formed. The reaction occurs at the eutectoid temperature of 1333 °F. The pearlite microstructure formed from the austenite is a lamellar structure consisting of alternating layers of ferrite and carbon rich cementite.

The second microstructure present below 1333 °F is ferrite when the carbon content is less than 0.80%. This is the ferrite formed above 1333 °F. If the carbon content exceeds 0.80%, the second microstructure present is carbide formed above 1333 °F.

The amount of each phase present and the composition of the phase is dependent upon the amount of carbon in the steel and the temperature. A steel with a carbon content of 0.20% will have the following phases and phase compositions at the temperatures listed below:

1,600°F: 100% Austenite with 0.20% Carbon

1,400°F: 33% Austenite with 0.55% Carbon , 67% Ferrite with 0.025% Carbon

1,334°F: 23% Austenite with 0.80% Carbon, 77% Ferrite with 0.025% Carbon

1,332°F: 23% Pearlite (ferrite and carbide in a lamellar structure) with 0.80% Carbon, 77% Ferrite with 0.025% Carbon

The ferrite in the material below the eutectoid temperature of 1,333 °F consists of ferrite grains formed above the eutectoid and the ferrite contained in the pearlite structure. The carbon content of the austenite above the eutectoid temperature increases as the temperature is lowered. This carbon comes from the material which transforms to ferrite as the temperature is lowered. The austenite which undergoes the eutectoid reaction will always have a composition of 0.80% carbon. The amount of austenite above the eutectoid temperature is a function of the carbon content. The higher the carbon content the more austenite. If the carbon content is equal to 0.80%, the material will be 100% austenite at a temperature just above the eutectoid temperature and at room temperature the microstructure will be 100% pearlite. The eutectoid reaction consists of the diffusion of carbon to form carbide from the adjacent austenite. The austenite with depleted carbon forms a ferrite layer adjacent to the carbide. The diffusion of the carbon takes time and the length of the reaction time is dependent upon the amount of austenite. Consequently, the reaction time is slower for higher carbon steels. Another microstructure, also consisting of ferrite and carbide, is formed if the transformation of austenite occurs at a lower temperature. It is suggested that at lower temperatures the ferrite forms first followed by the carbide. The resulting microstructure is called bainite. Bainite has a complex structure composed of ferrite with small particles of carbide precipitated at various crystal planes.

Steel is hot rolled when it is in the austenite range of the phase diagram. Upon cooling the steel goes through the phase changes to form a microstructure consisting of ferrite (formed above the eutectoid temperature) and pearlite formed from the eutectoid reaction. The properties of the steel are dependent upon the grain size of the steel for a given alloy. Smaller grain size steel has higher strength and ductility than a steel with a larger grain size.

Heat Treatment of Steel

The time required for the eutectoid reaction and the diffusion of carbon from the austenite to form ferrite above the eutectoid temperature allows the steel producer to heat treat the steel to produce another phase. Quenching the steel to a temperature below 230° C will produce martensite. This phase does not exist on the equilibrium phase diagram shown above since it is a metastable structure which has the same composition as the austenite from which it forms. The atomic structure is a body-centered tetragonal crystal structure. No diffusion is required to form martensite consequently it can form rapidly. Martensite is a very hard and brittle material. Normally martensite is tempered to lower its strength and improve its ductility and toughness. Tempering consists of reheating the steel to a temperature below the eutectoid temperature. The higher the tempering temperature the lower the strength and the higher the ductility of the tempered martensite. High strength A325 and A490 bolts are produced by quenching to form martensite followed by tempering. This can also be applied to structural plate. A514 and its pressure vessel equivalent A517 are structural plates produced by quenching and tempering.

The ability of a steel to form martensite upon quenching is dependent upon the time its takes to start the eutectoid reaction. The reaction time is dependent upon the temperature. The behavior is typically shown by a continuous cooling transformation diagram depicted in Figure 2. The start and end of the eutectoid reaction are shown by the curved solid lines on the diagram. The start and end of the formation of martensite are shown by the solid lines at the bottom of the figure. A quench which follows the lower dashed line will produce martensite. The line misses the nose of the curve defining the start of the reaction. Any cooling curve to the left of the nose will result in the formation of martensite. The upper dashed straight line which represents a slower cooling curve will result in the complete transformation of the austenite to pearlite. The lower horizontal curve which branches from the line which formed martensite will result in a bainite structure. In order to form bainite, the steel is cooled rapidly to miss the nose of the starting reaction curve and then allowed to cool at a slower rate above the M_S temperature.

Pearlite and bainite are much harder than the ferrite phase. Bainite is stronger and more ductile than pearlite. The lamellar structure of alternating layers of ferrite and carbide in pearlite and bainite provide the strength with reasonable ductility. If the carbide formed in a coarse grain structure without the surrounding layers of ferrite the steel would be hard and brittle. The finer the layers of ferrite and carbide the greater the ductility of the steel. Coarse pearlite is formed at slower cooling rates. The web-flange junction of a wide-flange shape has the slowest cooling rate and consequently the coarsest grain structure. In addition this zone is also the least hot worked. The toughness of this region may be increased by cooling the web-flange junction more quickly by spraying water on this region after rolling.

Bainitic steel is available from one manufacturer in rolled shapes. The steel is cooled by spraying water on the shape in the rolling line. The surface is cooled above the martensite formation temperature and below the nose of the start of the transformation curve. The outer surface transforms to bainite with the central portion of the thicker elements forming ferrite and pearlite. The pearlite formed is fine grained due to its rapid cooling relative to a section which is not quenched. The steel must be a low carbon and lean chemistry steel to insure that martensite is not formed during the quenching. Steels meeting ASTM A913 are bainitic steels which are marketed as QST (Quenching and Self-Tempering) steels. These steels have good weldability and toughness due to their low carbon content and fine grain structure. Their strength comes from the alloy additions and bainite structure. These steels should not be heated above 1100 ^{o}F during forming or post weld heat treatment. Their strength will be reduced upon cooling after heating to above this temperature. The heat affected zone (HAZ) in the base metal adjacent to the fusion line of a weld may also show a loss of strength due to the heating from the welding arc. The heat input as well as the interpass temperature should be reduced to maintain strength in the HAZ.

Steels with good hardenability have the starting reaction curve further to right in the cooling diagram. The further to the right that this starting curves lies, the slower the cooling rate required to form martensite. Since the outside of a steel cools faster then the interior, a steel with good hardenability can be hardened completely through its section with a slow cooling rate. The curve for the start of the eutectoid reaction moves further to the right as the carbon or alloy content increases. Other alloys also influence the shape of the curves and also modify the phase diagram.

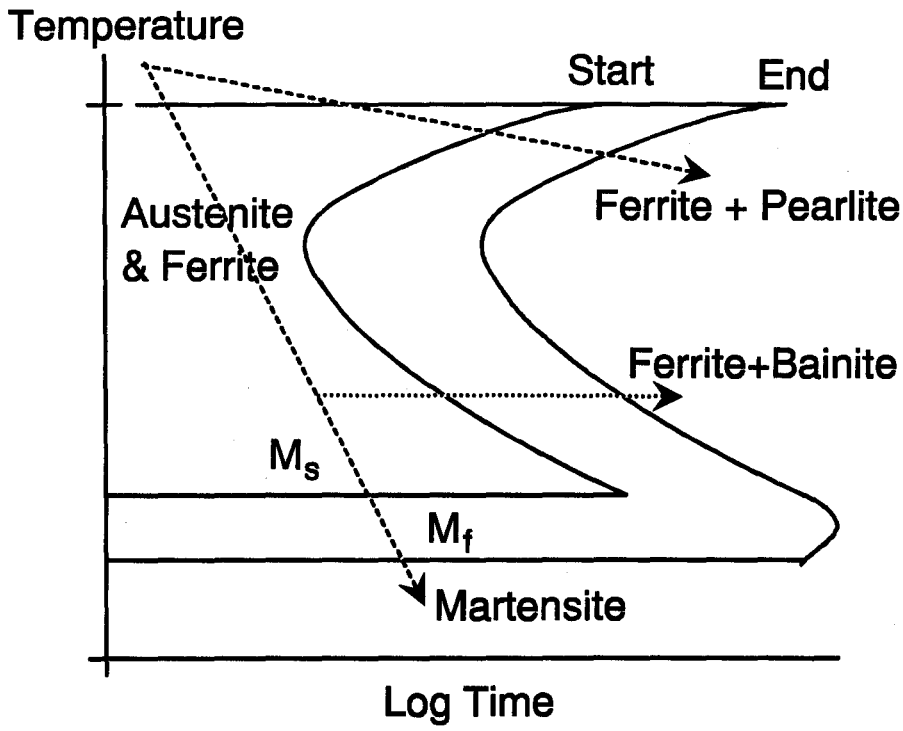

Figure 2 - Continuous Cooling Curve

Weldability of Steels

In general, steels with good hardenability are difficult to weld. Weld cracking will occur if martensite is formed during the cooling of the weldment. The critical region of a weldment is the heat affected zone of the base metal just adjacent to the fusion line. The steel in this region has been heated to the austenizing temperature and then cooled as the heat is conducted into the plate. Steels with high carbon content must be preheated to reduce the cooling rate to prevent the formation of martensite. Preheating the plate reduces the cooling rate since the cooling of the weldment is mainly by conduction of heat into the parent material and not by convection. Thicker material provides a greater heat sink which can increase the cooling rate. Consequently, the welding preheat temperature is increased when thicker material is welded. Care must be exercised when welding heat treated steels since high heat inputs and preheat temperatures may cause a strength reduction in the HAZ.

The term weldable steels is often used to classify steels which do not easily form martensite in the HAZ. Weldable steels are not easy to harden. Very rapid cooling rates are required to form martensite in a weldable steel. The carbon equivalent is used to characterize the weldability of the steel. The carbon equivalent relates the various elements in the steel to the equivalent amount of carbon which would produce similar welding behavior. Many carbon equivalent equations are available in the literature. They are all empirical equations which are based upon experimental studies of steels with

various amounts of alloys. The equations must be considered as indicators of expected behavior not as absolutes. The most commonly used formula for carbon equivalent (CE) is the IIW formula listed below.

$$CE = C + Mn/6 + (Cr + Mo + V)/5 + (Ni + Cu)/15$$

The percentage of each element is entered into the equation and the resulting CE is used as an index of weldability. Typically steels with carbon equivalents above 0.50% are considered to be difficult to weld. Care must be taken to slow the cooling rate of the weld when welding steels with high carbon equivalents. The preheat must be increased and the welding heat input increased. ASTM A6 contains supplemental requirement S74 which can be used to specify a maximum carbon equivalent for structural steel. Appendix X3 of ASTM A6 contains a commentary on the weldability of steel.

ASTM Specifications

The specification for the properties of structural steel, the dimensions of the rolled shapes, and the methods of testing are covered by the specifications of the American Society for Testing and Materials (ASTM). A summary of the applicable specifications is given in the following sections. The first section covers the material specifications and the second section covers the testing and dimensional specifications.

ASTM Specification A6 covers the general requirements for structural steel and A370 gives the test methods which must be followed. These specifications define the type of specimens to be used, the testing methods, and the sampling requirements. Other ASTM specifications which start with the letter E define the accuracy and type of equipment which must be used to measure the values specified in the product specifications. These detailed equipment and procedure specifications will not be discussed in this paper

ASTM Material Specification

Hot rolled shapes are available in the following material specifications and section size groups. The section size groups are contained in ASTM A6 Table A and in Table 1 Part 1 of the AISC Manual.

Low Carbon Steels:

ASTM A36-Shape Groups 1-5

ASTM A529 Grade 42-Shape Group 1

ASTM A529 Grade 50-Shape Groups 1-2

High-Strength Low-Alloy Steels:

ASTM A572 Grades 42 & 50-Shape Groups 1-5

ASTM A572 Grade 60-Shape Groups 1-2

ASTM A572 Grade 65-Shape Group 1

Corrosion Resistant High-Strength Low -Alloy Steels:

ASTM A242 Shape Groups 1-5

ASTM A588 -Shape Groups 1-5

The most common grades for steel buildings are A36 and A572 Gr. 50. These grades are available in all of the shape sizes. A529 Gr. 50 which is produced by the electric furnace mills has a yield strength comparable with A572 Gr. 50 without the alloying requirements and is available only in shape Group 1 and 2. A242 is an older specifications and is generally not available, although still listed in the AISC Manual. The yield strength of these older steels was less than 50 ksi in the larger section sizes.

ASTM Chemistry Requirements

The chemistry requirements for A36, A529, A572 Gr. 50, and A913 Gr. 50 are given below.

Table 1 - Chemistry Requirements for Structural Steels

Specification	C Max.	Mn	P Max.	S Max.	Si	Cu-min. if Specified
A36	.26	-	0.04	0.05	0.40 max.	0.20
A36 >426lb/ft	.26	0.85-1.35	0.04	0.05	0.15-0.40	0.20
A529 Gr. 50	0.27	1.35 max.	0.04	0.05		0.20
A572 Gr. 50**	0.23	0.50-1.35*	0.04	0.05		0.20
A572 Gr. 50 >426 lb/ft	0.23	0.50-1.35*	0.04	0.05	0.15-0.40	0.20
A913 Gr. 50	0.12	1.40 max.	0.03	0.03	0.40 max.	0.35 max.

* A maximum of manganese of 1.50% is permissible, with an associated reduction of the carbon maximum of 0.03%.

**Type 1-Columbium: 0.005-0.05, Type 2-Vanadium: 0.01-0.15, Type 3-Columbium(0.05 max,%)+Vanadium: 0.02-0.15, Type 4-Nitrogen: 0.015 max.

All of the above specifications limit the amount of carbon, phosphorus, and sulfur in the steel to provide good toughness and weldability. Carbon is the cheapest and easiest method of increasing the strength of a steel, however, carbon reduces the weldability of the steel since it increases the ability to harden the steel. High carbon steels require high preheats and large heat inputs to reduce the cooling rate in the heat affected zone (HAZ) to prevent the formation of hard martensite. The higher strength of A572 steel is attained with a lower carbon content by microalloying the steel with either vanadium or columbium. Phosphorus is an impurity in the steel and tends to segregate in steels causing weak areas. Sulfur is another impurity in the steel. One of the main functions of manganese is to combine with the sulfur to form MnS. MnS appears in steel as globular inclusions which upon hot rolling form elongated lamellar shaped discontinuities in the steel. The tearing of the low strength MnS inclusions in the presence of through-thickness strain is the primary cause of lamellar tearing. The steel producer must reduce the sulfur content of the steel to reduce the amount of these inclusions if lamellar tearing is a concern. Sulfide shape control can also be employed by the producer to reduce the aspect ratio of the

inclusion and thereby reduce the susceptibility of the steels to lamellar tearing. This is discussed further in the section on lamellar tearing.

The A529 specification is unusual since no alloying is specified. Steels made to this specification are from electric furnace mills. The strength of this steel comes from hot working and subsequent cooling of the steel in the rolling of the small shape sizes and from the residual elements from the scrap charge. Shape Groups 1 and 2 include all the M, S, C, MC, and L shapes with a thickness equal to or less than 3/4 in. as well as W shapes. The W shapes include W36 shapes up to 210 lb./ft and W14 shapes up to 132 lb./ft. These shapes would be typical of the shapes used in buildings of mid-height in seismic areas. A529 Gr. 50 is unusual in that it includes an upper limit on the tensile strength of 100 ksi with provisions for a supplemental limit of 90 ksi. No upper limit is contained in the A572 Gr. 50 specification. This specification will likely be superseded by a new grade 50 steel specification under development.

The overlap in the chemistry specification for these steels; A36, A529, and A572, allows producers to make steel that meets the chemistry specification of all three. A producer would have to add either Vanadium or Columbium to his steel to meet the alloy requirements of A572. ASTM Specification A6 section 7.1.2 requires that the producer, regardless of steel making practice, report the elements specified in the specification and also the analyses for copper, columbium, chromium, nickel, molybdenum, silicon and vanadium. The requirements for chemistry listed in the table above are heat analysis requirements. A check of the actual product analysis chemistry can be made subject to the product tolerance allowed in Table B of the A6 specification.

In addition to the elements listed for reporting, some concern has been expressed towards limiting the amount of the residual elements contained in electric furnace steel. The elements, which are required to be reported, as well as heavier elements such as tin and lead can sometimes be contained in the scrap charge used to make the steel. The producer buys different grades of scrap to control the chemistry of the steel. The influence of these elements and their interaction upon the weldability of the steel needs to be determined so that practical limits can be set. These limits need to balance the increase in cost of steel production (due to higher scrap steel costs) with the influence of the elements upon weldability. The steel maker does not know the precise chemistry content until after the steel has been melted. Imposing unrealistic requirements could force the maker to scrap whole heats of steel unnecessarily.

A new grade 50 steel specification for rolled shapes is under development. Limits on residual elements, maximum carbon equivalent, and limits on the yield to tensile ratio as well as a maximum yield strength are being considered in the specification development. This will be a specification for rolled shapes only. The future of the A36, A572 Gr. 50, and A529 specifications when this specification is adopted is uncertain. It is very unlikely that steels which have actual yield strengths below 50 ksi will be available in the future. Beams in seismic moment frames have typically been specified as A36 steel. The section size of the beams is normally controlled by elastic drift requirements. A36 steel is used to limit the moment demand on the columns to insure a strong column weak beam design. New designs should incorporate grade 50 beams. This will require either larger columns or columns using higher strength steel such as A913 Gr. 65. A913 is quenched self tempered steel available in Grades 50,60,65, and 70 ksi. The steel is quenched during the rolling process and allowed to cool slowly producing a bainite microstructure. The steel has a low carbon content and good toughness. The specification contains a Charpy V-Notch toughness of 40 ft-lb. at 70 ^{o}F. No other U.S. steel specification for rolled sections contains a mandatory toughness requirement. The steel is only available at this time from one

foreign supplier. The largest domestic supplier has a license to produce this material and provisions in his rolling line to perform the required quenching. It is likely that rolled shapes produced to this specification will be available domestically within the next ten years.

Typical Chemistry of Rolled Shapes

Table 2 lists chemistries from rolled shapes and plates from various producers. The chemistries are either from the mill test report or from a product analysis from a beam supplied as part of laboratory test programs. The second column indicates the production method of the steel producer, Elect. indicates a scrap based electric furnace steel and Intg. stands for an integrated steel producer. The electric furnace steels have significantly lower carbon and magnesium content than the steel produced by the integrated mills. The copper, nickel, and chromium content of the electric furnace steels are significantly higher. These alloying elements are not part of the A36 and A572 specifications and were not reported by the producers until the ASTM specifications were changed to require the reporting. These alloys come from the scrap used in the steel making. The strength of the electric furnace steels comes from these additional alloys as well as from the carbon and manganese content of the steel. A controversy exists about the significance of these additional alloying elements as well as other elements not listed in the table. The carbon equivalent calculated using the IIW formula given previously may not give an accurate indication of the weldability of these steels. The significance of large amounts of copper, copper contents as high as 0.65% have been reported, upon the performance of the steels is being debated. In addition, heavy elements such as tin which is currently not reported can reduce ductility and cause cracking.

The amount of these residual elements in the steel is dependent upon the quality of the scrap used in the steel production. One of the largest producers of high quality steel plate in the U.S. is a scrap based electric furnace producer. This producer has made steels meeting the stringent requirements for nuclear pressure vessels, offshore structures, and nuclear submarines. The scrap used by this producer is carefully analyzed and segregated. Scrap is a commercial commodity. The scarcer high quality scrap is considerably more expensive then scrap from automotive bodies.

In the last year, all of the producers of structural shapes in the U.S. have switched to electric furnace scrap based production. In addition, a large foreign producer of structural shapes has also changed to this economical method of steel production. The influence of these new steels upon the inelastic structural performance, weldability, and fracture toughness of rolled shapes needs to be evaluated. The second stage of the SAC research effort is directed at developing this knowledge.

Currently, under the leadership of the American Institute for Steel Construction, a new grade 50 steel specification is being developed. Included in this specification is the control of the alloying elements by a carbon equivalent formula and a maximum tensile strength or yield to tensile strength ratio. This specification is similar to the A529 specification which has similar requirements available as supplements. Maximum limits on some elements, such as copper, are also being discussed. This new specification will allow the producers to produce all the structural sizes without meeting the microalloying requirements of A572. The adoption of this new specification by ASTM is at least a year away. Steels meeting this specification may be available in late 1996.

Table 2 - Typical Steel Chemistries

Spec.	Prod.	Shape	C	Mn	P	S	Si	Cu	Ni	Cr	Mo	V	Nb
A36	Elect.	W36x150	.08	.65	.005	.03	.18	.33	.12	.10	.03	-	-
	Elect.	W21x57	.06	.61	.02	.02	.13	.35	.14	.11	.04	.01	.003
	Intg.	W36x150	.15	.85	.01	.02	.04	.15	.03	.04	.01	-	-
	Intg.	W24x62	.22	0.72	.01	.04	.07	.04	.01	.04	.01	-	-
A572 Gr. 50	Elect.	W30x148	.07	.89	.023	.02	.16	.41	.10	.11	.02	.03	.003
	Elect.	W14x257	.08	1.17	.025	.03	.21	.36	.10	.06	.02	.04	.004
	Intg.	W12x136	.19	1.26	.013	.02	.04	.11	.03	.05	.01	.06	-
	Intg.	W30x108	.18	1.18	.012	.02	.05	.02	.02	.04	.01	.04	.001

ASTM Mechanical Property Requirements

The producer is required to perform a tension test to determine the mechanical properties of the finished rolled product. The test sample is normally taken from a sample cut at the hot saw after all rolling has been completed. Two coupons from each heat of steel must be tested with the coupons from different as-produced pieces. The present ASTM requirements (ASTM A6 11.3.2) require the sample be taken from the web of rolled sections with the specimen oriented longitudinally. The web location has been the standard in the U.S. Some foreign specifications require that the tension specimen be taken from the flange of the section. The web was chosen in the U.S. since the S and C shapes, which historically were the first rolled shapes produced, have tapered flanges while the webs are flat. Since W shapes have essentially uniform thickness flanges, the tension specimen could also be taken from the flange. The ASTM Specification has just been changed to require that the tensile test specimen be taken from the flange. This change in the test specimen location will occur in steel shapes produced in 1997. The web of the section typically has a higher yield strength than the flange. The flange yield strength is often assumed to be approximately 95% of the web. The difference in strength is due to the greater amount of hot working of the steel in the thinner web and is also due to the faster cooling rate of the web which results in a cooler finishing temperature. The difference in strength between the web and flange is incorporated into the strength reduction factor ,Φ, used in determining the tension and bending capacity of steel shapes in the LRFD specifications.

Recent laboratory tests of rolled sections used in the SAC phase I research effort and other research programs has indicated that the yield strength of the flange is often much lower then the yield

point shown in the mill test report. The flange yield strength has been found to be as much as 25% less than the yield point of the web given in the mill test report. This difference is much greater then previous studies have indicated. The change of the test location in the ASTM Specification to the flange will eliminate the effect of test location upon this difference in reported and measured strengths. The flange location will provide a more realistic assessment of the bending capacity of the shape. The difference between measured tensile properties and the values reported on the mill test reports will be studied in the SAC phase II research program. This research will include the influence of testing methods upon the test results.

A summary of the mechanical property requirements of the A36, A529, and A572 Gr. 50 specifications are given below.

Table 3 Summary of Mechanical Properties

Specification	Min. Yield Point ksi	Min. Tensile Strength ksi	Max. Tensile Strength ksi	Percent Elongation-8 in. gage length	Percent Elongation-2 in. gage length
A36	36	58	80	20	21
A36 >426 lb./ft	36	58	-	20	19
A529 Gr. 50	50	70	100	18	21
A572 Gr. 50	50	65	-	18	21
A572 Gr. 50 >426 lb/ft	50	65	-	18	19

Both A36 and A529 Gr. 50 have an upper limit on the tensile strength which is intended to insure that the steel provided has the expected inelastic behavior. The upper limit prevents steels with high tensile strengths and, indirectly, high yield strengths from being supplied under these specifications, however the upper limit on tensile strength is not applicable to heavier A36 shapes. Also for these heavy shapes, the percent elongation of the 2 in. gage length specimen is reduced for both A36 and A572. Due to the large thickness of the web in these heavier sections, the smaller ½ in. round 2 in. gage length tensile specimen is normally used to measure the mechanical properties. The reduction in the elongation values and the lack of a cap on the tensile strength is eliminated for these heavier shapes due to the difficulty of the producers in meeting the requirements with these large shapes. Normally the amount of carbon and other alloying elements are increased in the heavier shapes in order to meet the yield strength requirements. The additional alloying is required since the heavier shapes receive less hot working during the rolling process, their cooling rate is slower, and their finishing temperature is higher. The higher alloy content used in these shapes increases the tensile strength and reduces the elongation. None of the specifications have an upper limit on the yield strength. It is possible for a producer to meet the tensile requirement of all three of the specifications. A steel which has a yield strength greater than 50 ksi and a tensile strength greater than 70 ksi but less than 80 ksi will meet the strength requirements of all three specifications. Some producers are currently certifying their product to multiple specifications. Dual grade steels meeting both the A36 and A572 Gr. 50 requirements are currently available in the market place.

The elongation values given for the two gage lengths are different to compensate for the size and geometry effect upon elongation between the 8 in. gage length x 1-1/2 in wide plate-type

specimen(A370 fig. 3) and the ½ in round 2 in. gage length specimen (A370 fig. 4). The two specimens yield different elongation values due to the difference in gage length and the constraint due to the axial symmetry of the round specimen. Most of the elongation is concentrated in the necked region of the specimen. This region of necking is a greater percentage of the overall gage length in the 2 in. gage length which results in a larger percent elongation relative to the 8 in. gage length. The symmetry of the round specimen constrains the plastic flow somewhat and tends to reduce the elongation. The elongation relationship between these two specimens can be estimated using the equation shown below from A370 A6:

$$\varepsilon = \varepsilon_0[4.47(\sqrt{A.}) / L]^a$$

where:

ε= Percent elongation on a standard test specimen having a gage length L and a cross-sectional area A,

a=0.4 for carbon-manganese steels with a tensile range of 40 to 85 ksi.

The standard practice within the industry is to use the plate-type specimen for thinner webs and use the round type specimen only for sections with thicker webs. The minimum web thickness that a 0.5 in round specimen can be obtained from is ¾ in. Normally the producers have used the plate-type specimen up to the capacity of their test machines. The area of the plate-type specimen is proportional to the web thickness. The maximum web thickness that can be tested in a plate-type specimen is less for higher strength steels due to the increase in area and corresponding increase in required load for the higher strength steels. The attached graph shows the relationship between elongation in the 0.5 in. round specimen and the plate type specimens for various plate thicknesses. Also shown are the ratio of the minimum elongation values for the 2 and 8 in. gage length specimens specified for the three steels. The upper curve is for the plate type 1-1/2 in. wide specimen with an 8 in. gage length. The ratio of the 2 to 8 in. gage length specimens specified in the A36 specification intersects this line at a thickness of approximately 1-3/4 in. This indicates that the specified minimum elongation for the two specimens are equivalent at this thickness. Since the curve decreases for greater thickness, the use of the 2 in. gage length specimen for thicker plates is more severe than using the plate type specimen with respect to elongation. The line for the grade 50 steels cross at about 1 inch. The lower thickness at the point of the intersection is due to the necessity to switch to the round specimen at a lower thickness due to the higher strength of the grade 50 material. ASTM A6 Section 11.5.2.1 requires that flat type full thickness specimens be used for material ¾ in. and under in thickness. The round 0.5 in. diameter specimen can only be used for material thicker than ¾ in. and the specimen should be approximately at the quarter-thickness of the material as specified in section 11.5.2.3 of A6.

ASTM A6 Section 11.5.2.1 also allows the use of the sheet type specimen shown in Fig. 3 of A370 for material ¾ in. and under in thickness. This sheet specimen is a full thickness specimen ½ in. wide using a 2 in. gage length. One producer uses this specimen exclusively since all of the sections he produces have a web thickness less than ¾ in. The line giving the relationship of the elongation between this sheet specimen and the round specimen is shown by the lower curve in the figure. The elongation of this flat 2 in. gage length specimen is larger than the 2 in. gage length round specimen. The elongation values from the ½ in. wide specimen will be larger than the same material tested in an 1-1/2 in. wide specimen with a gage length of 8 in or a 0.5 in. round specimen. The specification does not account for this difference in elongation value in the ½ in wide sheet specimen relative to the standard specimens used by most producers. The elongation values from the ½ in. wide specimen are almost twice that from the standard specimens. The large elongation values reported by the producer using the sheet type

specimen are not indications of a more ductile steel, they are simply due to the difference in test specimen geometry.

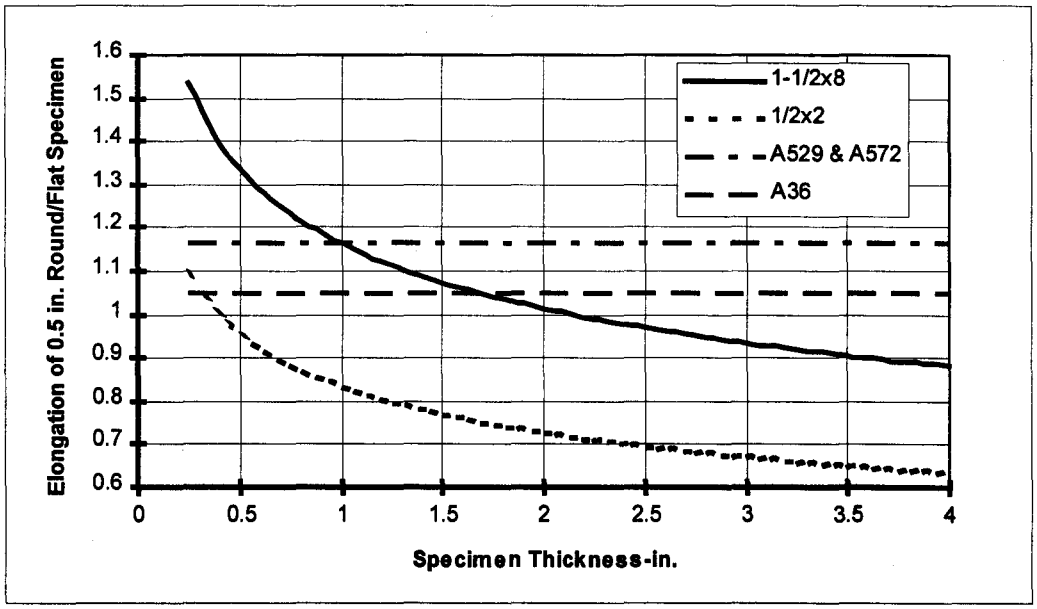

Figure 3 - Elongation Ratio Versus Flat Plate Specimen Thickness

The elongation values are allowed to be adjusted in accordance with ASTM A6 Section 11.6. This section allows the required percent elongation for thin specimens, thickness of specimen less than 0.312 in., using rectangular specimens to be adjusted. The base requirements can be adjusted downward by up to 7.5%. The elongation requirements for the 0.5 in. round specimens are also allowed to be adjusted when the material is over 3.5 in. thick. This adjustment cannot exceed 3%. This adjustment for thicker material is normally not encountered in rolled shapes since most webs are less than 3.5 in. thick.

Yield Strength of Rolled Shapes

The specifications for structural steels all specify a minimum yield point. Structural engineers normally use yield strength to describe the strength of a steel and use the yield strength to determine the moment and axial capacity of section. The difference between the yield strength and yield point of a steel is defined in ASTM A370 by the test methods used to obtain the value. A370 provides three methods of determining the yield point of a sample:

1. Drop of the Beam or Halt of the Pointer Method (A370 Section 13.1.1),
2. Autographic Diagram Method (A370 Section 13.1.2),
3. Total Extension Under Load Method (A370 Section 13.1.3).

The drop of beam method does not require that an extensometer be mounted on the specimen. Using electronically controlled test machines the drop of beam load can be determined by the change in slope of the loading versus displacement curve. The cross head displacement of the testing machine is used to determine the slope not the strain in the specimen which an extensometer measures. Methods 3 requires that an extensometer be placed on the specimen to measure the strain in the specimen. The total extension under load used to determine the yield point is 0.5% strain for steels with a specified yield point not over 80 ksi. The figure below shows the initial portion of a stress-strain curve for a steel. Many

steels exhibit an upper yield point, the peak shown in the graph. This point on the curve is the yield point determined by the autographic or drop of beam methods of determining the yield point. The yield strength of the material is the horizontal line after the upper yield point and is the material property which defines the inelastic strength of the steel. The value of the upper yield point is sensitive to the rate of loading as is the yield strength. However, the yield point shows a greater sensitivity to the rate of loading than the yield strength.

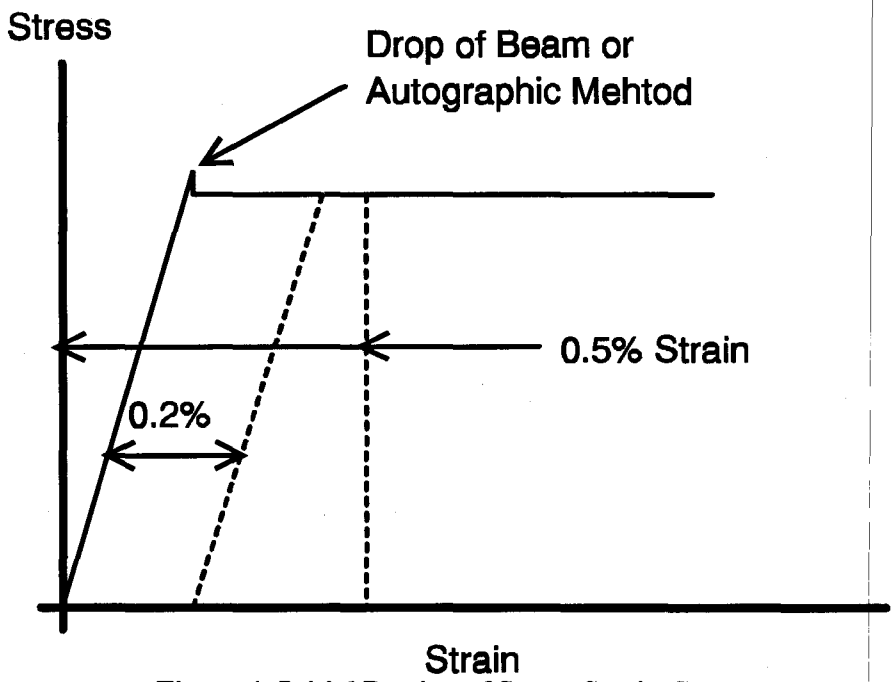

Figure 4 -Initial Portion of Stress-Strain Curve

The yield strength of a coupon is determined using the provisions of section 13.2 of A370. The yield strength can be determined using either the 0.2% offset method or the extension under load method. The offset and extension under load methods give essentially identical results and define the yield parameter (point or strength) as the level of the yield plateau. Some producers are using automated test machines which pick off the upper yield point peak of the curve automatically. The reporting of these peak values rather than the yield plateau value may explain the difference between the mill test values and the lower yield strength values found in the recent laboratory tests. This will be explored in the research contained in the SAC phase II research program.

The speed of testing has a marked affect upon the yield point and the yield strength of the test coupon. The producer who may be testing hundreds of specimens in a day may perform the tests as fast as allowed in the specification. The maximum cross head speed, the movement of the test machines grips relative to one another, that may be used for determining the yield point or strength is 1/16 in/min./in of reduced section of the coupon. If an 8 in. gage length specimen with a 10 in. long reduced section is tested, the maximum cross head speed is 5/8 in./min. The specification also gives this maximum testing speed in terms of stress. The maximum rate of stressing cannot exceed 100 ksi/min. The test machine may be sped up to ½ in./min./in of reduced section after the yield is measured. The loading or strain rates used in the mill tests are much higher than the material will be subjected to under gravity loads. The material's yield strength under static loading can be as much as 10% below the dynamic yield strength and even further below the yield point measured by the mill. This reduction in yield strength is important

when considering the capacity of structures under slowly applied gravity loads. A reduction in strength of 5% was used in determining the strength reduction factors, Φ, in the LRFD specification. On the other hand, the rapid loading which occurs in a steel frame during an earthquake will cause the yield strength of the steel to be at or above the value determined in the rapid mill test.

Survey of Shape Producers Results

The results of a survey performed for the Structural Steel Shape Producers Council is presented in this section. The database analyzed consisted of the tensile properties of rolled W shapes produced by six producers for 12 consecutive months, which were approximately coincident with the calendar year 1992. The survey consisted of 57,930 certified mill test reports on W shapes sold as ASTM A36, ASTM A572 Gr. 50, and Dual Grade (steel certified in accordance with both A36 and A572 Gr. 50). The data was analyzed by breaking it down by the six shape groups as defined in ASTM A6 and by steel specification. The distribution of data is given in the table below. The majority of data, 63.5%, came from shapes within Group 1. 63.1% of the steel included in the survey was certified as A36. Dual Grade steel had the least amount of data. Almost all of the data, 96.2%, for Dual Grade was from Shape Group 1 and 2. However much of the data from the A36 and A572 Gr. 50 databases also met the strength requirements for a Dual Grade steel. A steel with a yield point greater than 50 ksi, a tensile strength greater than 65 ksi but no more than 80 ksi meets the strength requirements for both steels. 39.2% of the A36 steel and 77.3% of the A572 Gr. 50 steel meet these Dual Grade strength requirements.

Table 4 Distribution of Data By Shape Group and Steel Specification

Shape Group	A36	Dual Grade	A572 Gr. 50	All Steels
1	23,675 64.7%	6,767 86.5%	6,340 46.8%	36,782 63.5%
2	11,030 30.2%	760 9.7%	5,065 37.4%	16,855 29.1%
3	1,271 3.5%	172 2.2%	1,152 8.5%	2,595 4.5%
4	567 1.6%	125 1.6%	923 6.8%	1,615 2.8%
5	27 0.07%	-	56 0.4%	83 0.1%
All Shapes	36,570 63.1%	7,824 13.5%	13,536 23.4%	57,930

Analysis of the data indicated that the distribution of yield point varied for each producer. An example of the variation by producer is shown in the figure below. The histogram of the data from two producers and for all the producers taken together is shown for A36 steel. All the shapes certified as A36 steel were included in the histogram. The producer labeled as 'I' had a much lower distribution of yield point than producer II. The variation exhibited by producer 'I' was similar to the distribution found in earlier surveys. The median yield strength for producer 'I' was approximately 45 ksi. Producer II on the other hand had a much higher distribution of yield point with a mean value of approximately 50 ksi. The mean yield point for all producers was 49 ksi.

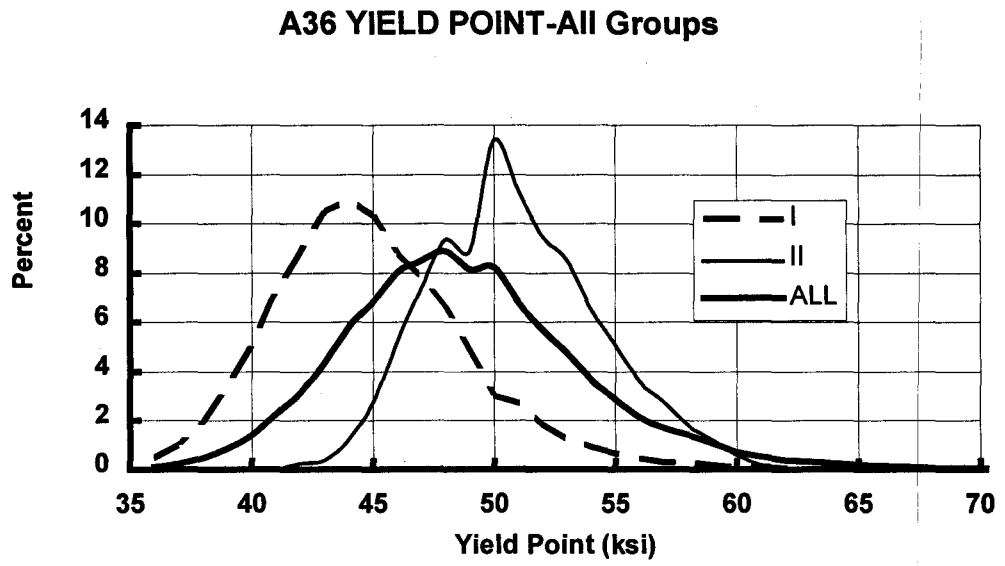

Figure 5 - Distribution of Data For Two Producers

Similar differences among the producers was found for other steels and statistics. The actual distribution of steel strengths for a particular building will be dependent upon the producer of the shapes.

The yield point data for Dual Grade and A572 Gr. 50 exhibited a truncated distribution. An example is shown in the figure below. The data shown is from Shape Group 2 and includes data from all the producers. The distribution for both of these steels shows a sharp drop off at 50 ksi. The A36 distribution is skewed but is much closer to a normal distribution than the higher strength steels.

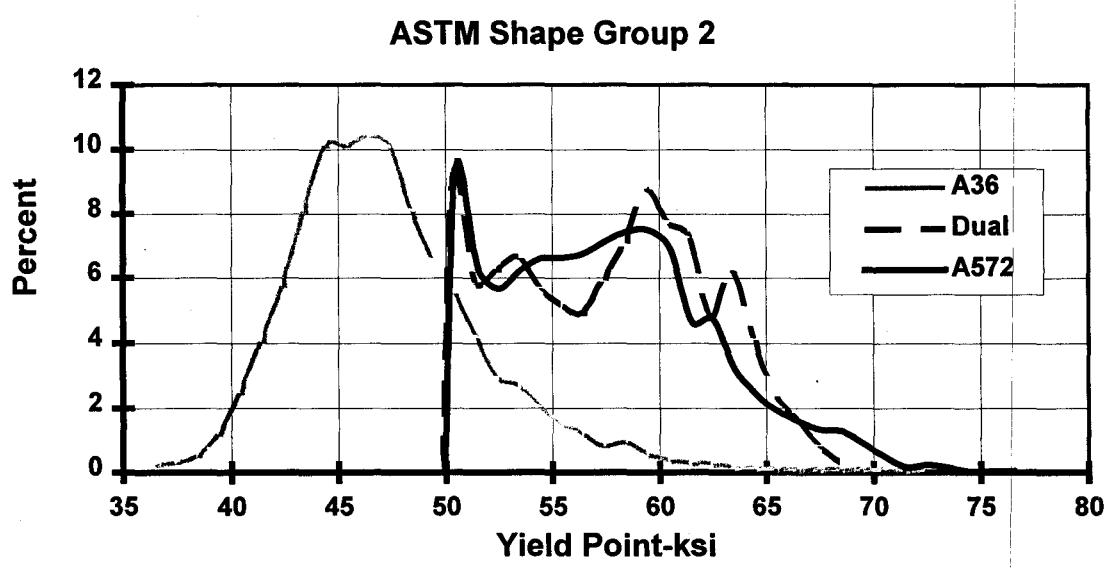

Figure 6 - Distribution of Data for Three Steel Specifications

The tensile specimens for a rolled shape is taken from the web of the section. Typically the flange has a lower yield point, approximately 95% of the web. The plot below is a cumulative frequency plot of the data shown above with the yield point taken as 95% of the mill test value. The data from the Dual Grade and A572 Gr. 50 steels was combined in the plot. Almost 25% of the data for the combined Dual and A572 Gr. 50 steels have an estimated flange yield point less than the minimum specified.

Since the mill tests are run at a rapid testing speed, the static yield strength of the flange of these beams may be as much as 5 ksi lower. The statistics for the static flange yield point can be estimated from the figure by subtracting 5 ksi from the abscissa. The data indicates that 50% of the Dual and A572 Gr. 50 shapes in Shape Group 2 may have a static flange yield point less than 50 ksi. This large population of shapes with low static flange yield strength indicates that yielding under slowly applied gravity loads may be of a concern. Note that the A36 data for the same shape group has less than 5% of its data below 36 ksi when the yield point is reduced by 5 ksi to estimate the static flange value.

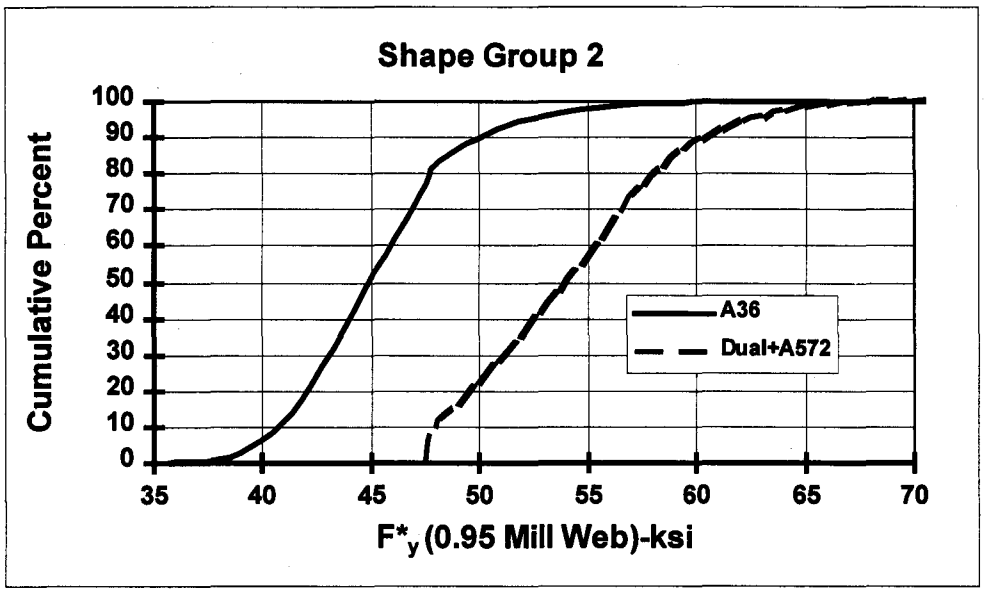

Figure 7 - Estimated Flange Yield Strength

The difference in the distribution of the yield point for A36 versus Dual and A572 Gr. 50 is also significant when designing moment frames, especially in seismic areas. Normally the size of the beams is controlled by elastic drift requirements. Large beams are used to stiffen the structure. A36 steel is often specified for the beams and A572 Gr. 50 for the columns to insure that the under seismic loading plastic hinges will form in the large beams not in the columns. However due to the skewed distribution of the 50 ksi yield point steels to the low side and the higher strength of the A36 steel, the hinge may form in the column. This is extremely likely if a Dual Grade beam is used. Consequently, a better and more reliable design approach would be to design for and specify A572 Gr. 50 for both the beam and column.

The survey also examined the variation in tensile strength and the yield to tensile ratio of the steels. The yield to tensile ratio of some of the steels was quite high. The maximum ratio was 0.986 for an A36 steel beam in shape Group 3. The mean value for A572 steel was 0.763 with 4.6% of the data above a value of 0.85. A total of 8% of the all the steel had yield to tensile values exceeding 0.85. The local buckling as well as connection behavior of sections is influenced by the yield to tensile ratio. Steels with high ratios have lower local buckling capacities and exhibit less ductility at connections.

Lamellar Tearing

During the rolling process the non-metallic magnesium sulfide (MnS) inclusions formed during the solidification of the steel are flattened. The largest dimensions of the inclusions after rolling are in a plane parallel to the rolling direction. These inclusions have little effect upon the steel's strength and ductility when the applied stresses are in the direction of rolling or transverse to the rolling direction in the plane of the material. However, the inclusion may have a dramatic influence upon the strength and ductility of the steel when the applied stresses are perpendicular to the surface of the steel. Stresses applied perpendicular to the surface, the so called Z direction, produce a stress normal to the plane of the flattened inclusions. This stress may cause the low strength inclusions to fracture. A lamellar tear results from the fractures in the inclusions linking up through further fracturing of the adjoining steel. The resulting fracture surface has a woody looking appearance. The figure below shows the orientation of the flattened inclusions and the mechanism of lamellar tearing. The inclusion size shown in the figures is not to scale, the actual size of the inclusion would be much smaller than shown in the figures.

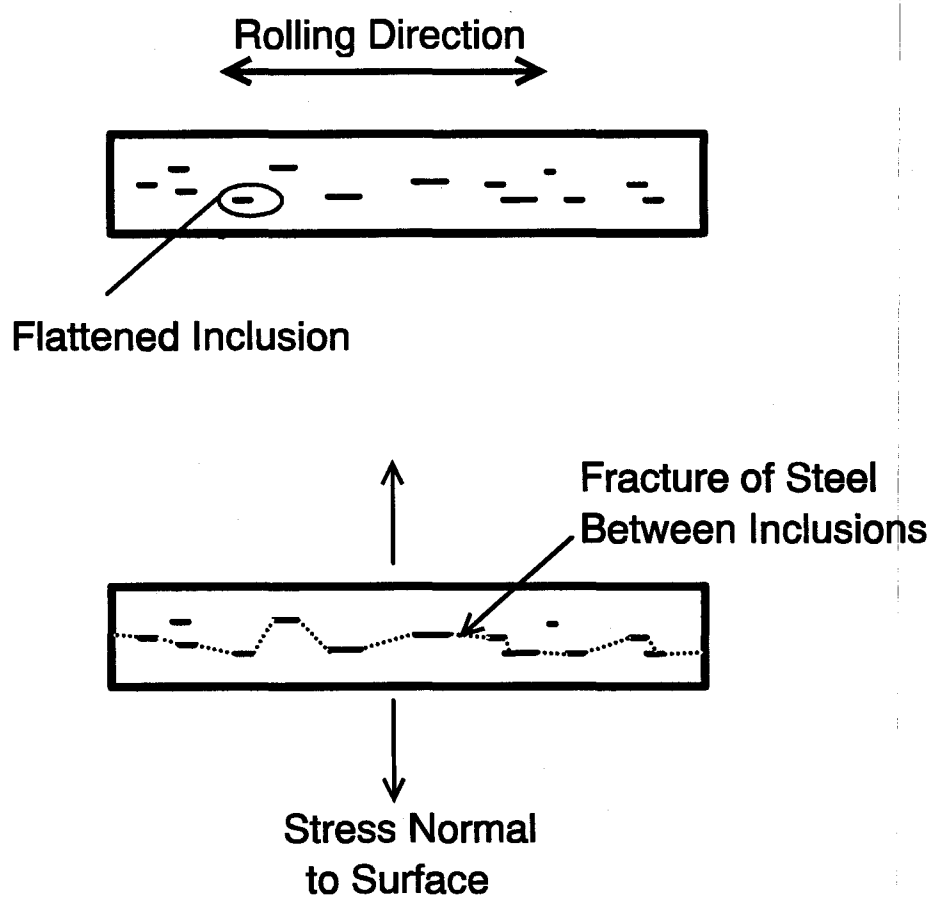

Figure 8 - Lamellar Tearing Mechanism

The strength of the material in the through thickness direction is a function of the size and distribution of the inclusions and the fracture toughness of the steel. Large inclusions increase the susceptibility of the material to lamellar tearing since the fracture of the large inclusions reduce the area of steel to support the applied stress. If the inclusions are all on the same plane, a plane of weakness results which drastically reduces the strength. A higher toughness steel increases the stress required to propagate the fracture in the steel between the inclusions.

The steel maker can increase the through thickness strength and ductility of the steel by reducing the sulfur content thereby reducing the number and size of the inclusions. The maximum sulfur content of structural steels has been reduced in the new ASTM specifications to a maximum of 0.035%. This small decrease from 0.040% will not significantly improve the steels through thickness strength. An additional approach used is called sulfide shape control. The producer adds materials, generally calcium, to change the shape of the inclusions. Steels plates are available with specified through thickness properties. These are commonly used in offshore platforms and other structures which use welded connections that produce significant through thickness stresses. These steels are normally made using vacuum degassed steel and other special processing. The performance of the steel in the through thickness direction is specified by a through thickness tensile test of the material. The governing criteria in this test is the reduction of area. Structural shapes are not generally available with guaranteed through thickness properties.

Lamellar tearing normally occurs during cooling following the welding of members or attachments to the surface of the steel. The residual stresses generated by the shrinkage of the weld initiate the tearing. The tear can start after the deposition of the first weld pass and then continue tearing as the subsequent welds are made. The tearing can also be localized which does not surface but is buried in the base material in the heat affected zone or even deeper within the plate. Lamellar tearing is easily found by ultrasonic inspection because the flat fracture surface at the inclusion provides a good reflector to the interrogating ultrasonic beam. Inspection prior to welding using a straight beam ultrasonic transducer will not eliminate lamellar tearing. The small inclusions, which can initiate a lamellar tear, are not found using the standard loss of back reflection techniques. This method of inspection will easily find complete separations or laminations. Tearing of the flat inclusions can also occur from service stresses. A crack which may initiate at the root of the weld will propagate along the path of least resistance in the steel. The low strength inclusion provides the easiest path of fracture propagation. The fracture toughness of the material for a crack propagating in the direction of rolling is much lower due to the inclusions and the orientation of the grains within the steel. The graphs shown in Figures 9 and 10 show the relationship between the Charpy V notch (CVN) toughness for the flange material for two directions of crack propagation for two column shapes. The core toughness is measured with the long axis of the Charpy specimen oriented in the direction of rolling taken from the web to flange junction core area. The transverse toughness was measured using a Charpy specimen with the longitudinal axis of the specimen perpendicular to the surface of the flange and the direction of crack extension in the rolling direction. The high toughness column has a CVN toughness of over 250 ft-lb. at room temperature. The short transverse specimens have more scatter and at room temperature had a CVN toughness from about 80 to 210 ft-lb. The scatter is due to the probability of the crack propagation path traversing through an inclusion. The low toughness values would be for specimens in which the crack propagation path traversed an inclusion. The lower toughness column had a room temperature toughness of about 30 ft-lb. The short transverse direction had a lower toughness, less than 10 ft-lb. The variability of the short transverse toughness is much less in this lower toughness material. The low toughness of this steel is not significantly affected by inclusions in the fracture path.

Summary and Conclusions

The production and specifications for rolled steel structural shapes is undergoing dramatic change. Steel for structural shapes is now almost exclusively produced in electric furnaces using scrap steel. The resulting steel has a lower carbon content with a higher alloy content from the scrap. The influence of the alloying elements from the scrap upon weldability is not well established. A new specification is under development which will have limits on some of these elements. The low carbon

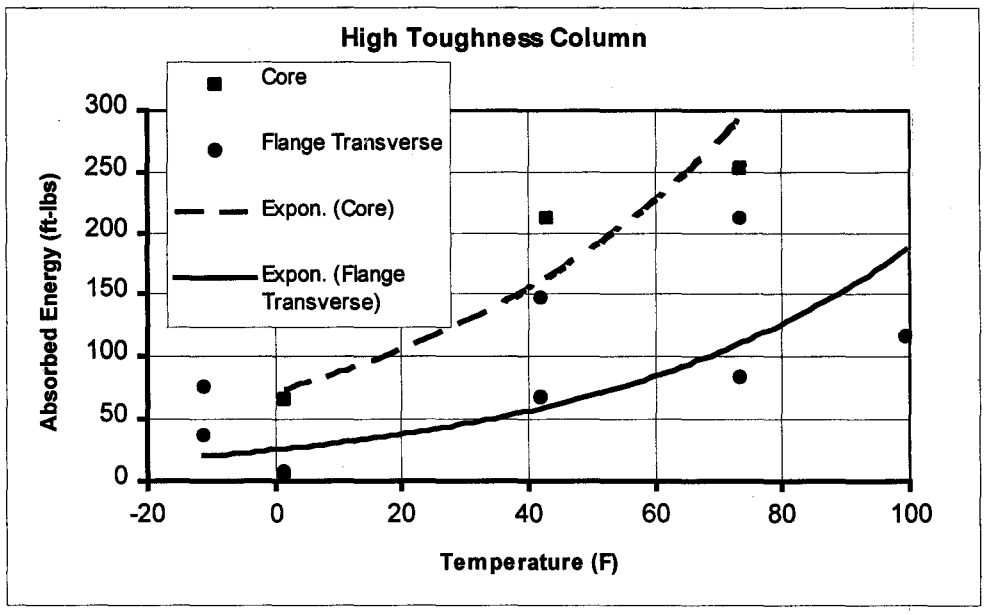

Figure 9 - Distribution of Toughness in High Toughness Column

content of steels increases the toughness of the steels relative to the higher carbon steels produced by the integrated mills.

The industry appears to be moving to a single strength level of grade 50 for rolled shapes. The rolled shapes produced to have a yield strength less than 50 ksi will generally not be available in the future. The practice of using lower strength steels for beams to insure that the plastic moment occurs in the beam rather than the column will not be possible in the future. The designer must design using grade 50 beams and either increase his column size, weaken his beam with a "dog-bone" flange, or use a higher strength column steel.

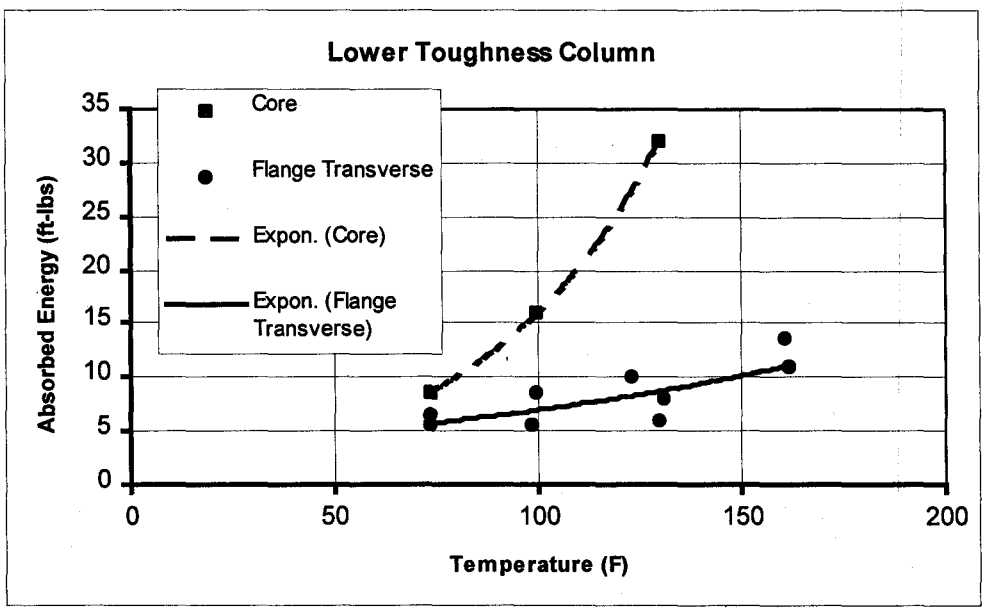

Figure 10 - Distribution of Toughness in Low Toughness Column

The skewed distribution of the strength of the grade 50 steels found in the shape producer's survey and the low test values found in the laboratory tests indicate that the actual yield strength of the steel is lower then expected. The moment produced by these beams will be less than the values based upon estimates based upon statistical data from integrated mill production. The change in the test location to the flange will upset the statistics of the recent shape producers survey. The producer must increase the strength of the steel by alloying in order to meet the strength requirements in the flange.

The SAC phase II research effort will provide information on the relationship between the mill test reports and the actual strength of the sections, the Charpy V-Notch toughness of the steels, the through thickness strength of the steels, and the variability of the properties. The results will clarify many of the issues about the new steels.

WELDING OF SEISMICALLY RESISTANT STEEL STRUCTURES

By Duane K. Miller, P.E.
The James F. Lincoln Arc Welding Foundation

1 Introduction

Arc welding has become a popular, widely used method for making steel structures more economical. Although not a new process, welding is still often misunderstood. Perhaps some of the confusion results from the complexity of the technology. To effectively and economically design a building that is to be welded, the engineer should have a knowledge of metallurgy, fatigue, fracture control, weld design, welding processes, welding procedure variables, nondestructive testing, and welding economics. Fortunately, excellent references are readily available, and industry codes specify the minimum standards that are required to be met. Finally, the industry is relatively mature. Although new developments are made every year, the fundamentals of welding are well understood, and many experienced engineers may be consulted for assistance.

The goal of this paper is to provide the engineer with a one-source reference to structural welding for seismic applications. Every effort has been made to at least touch on the major issues. Additional references are cited; the reader is urged to consult them when a more comprehensive treatment of a particular topic is needed.

Welding is the only joining method that creates a truly one-piece member. All the components of a welded steel structure act in unison, efficiently and effectively transferring loads from one piece to another. Only a minimum amount of material is required when welding is used for joining. Alternate joining methods, such as bolting, are generally more expensive and require the use of lapped plates and angles, increasing the number of pieces required for construction. With welded construction, various materials with different tensile strengths may be mixed, and otherwise unattainable shapes can be achieved. Along with these advantages, however, comes one significant drawback: any problems experienced in one element of a member may be transferred to another. For example, a crack that exists in the flange of a beam may propagate through welds into a column flange. This means that, particularly in a dynamically loaded structure that is to be joined by welding, all details must be carefully controlled. Interrupted, non-continuous backing bars, tack welds, and even seemingly minor arc strikes have resulted in cracks propagating through primary members. Attention to design details and weld quality is essential in seismic applications.

In order to best utilize the unique capabilities of welding, it is imperative to consider the entire design-fabrication-erection sequence. A properly designed welded connection not only transfers stresses safely, but also is economical to fabricate. Successful integration of design, welding processes, metallurgical considerations, inspection criteria, and in-service inspection depends upon mutual trust and free communication between the engineer and the fabricator.

This state-of-the-art report on welding and joining was prepared directly as a result of the problems that were revealed during the Northridge earthquake that occurred in California on January 17, 1994. References throughout to "Northridge" refer to this event. "Pre-Northridge" and "post-Northridge" are utilized to reference events with respect to January 1994. On January 17, 1995, by eerie coincidence,

the city of Kobe, Japan would be dramatically hit by the earthquake that is known by multiple names, including the "1995 Hyogoken-Nanbu Earthquake" and the "Hanshin Great Earthquake." Throughout this paper, it will be referred to as the "Kobe" earthquake. Arising from both of those events were many issues for which there are not definitive answers at this point in time. Areas that are less certain and in the need of research are identified throughout this paper. The reader is cautioned that as with any written document, new information may supersede what is contained herein. It is expected that the SAC Joint Venture will continue to be the primary source to obtain the latest up-to-date information that will be emerging from the post-Northridge and post-Kobe investigations that are underway even at the time of writing of this document.

2 Design of Welded Connections

A welded connection consists of two or more pieces of base metal joined together by weld metal. Engineers determine joint type and generally specify weld type and the required throat dimension. Fabricators select the joint details to be used.

2.1 Joint Types

When pieces of steel are brought together to form a joint, they will assume one of the five configurations presented in Fig. 2-1. Of the five, butt, tee, corner, and lap joints are common in construction. Coverplates on rolled beams, and angles to gusset plates would be examples of lap joints. Edge joints are more common for sheet metal applications. Joint types are merely descriptions of the relative positioning of the materials; the joint type does not imply a specific type of weld.

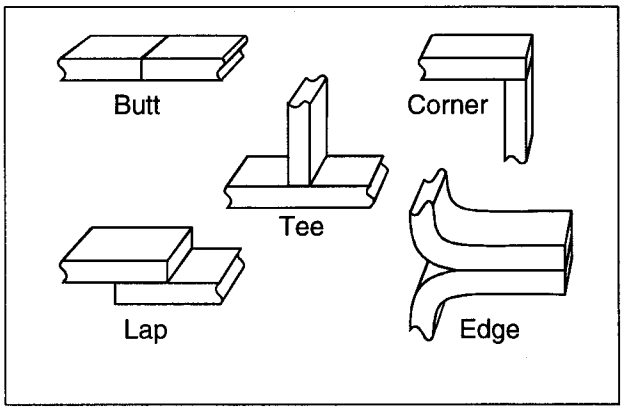

Figure 2-1 *Joint types*

2.2 Weld Types

Welds may be placed into three major categories: groove welds, fillet welds, and plug/slot welds (see Fig. 2-2). For groove welds, there are two subcategories: Complete Joint Penetration (CJP) groove welds and Partial Joint Penetration (PJP) groove welds (see Fig. 2-3). Plug welds are commonly used to weld decking to structural supports. Groove and fillet welds are of prime interest for major structural connections.

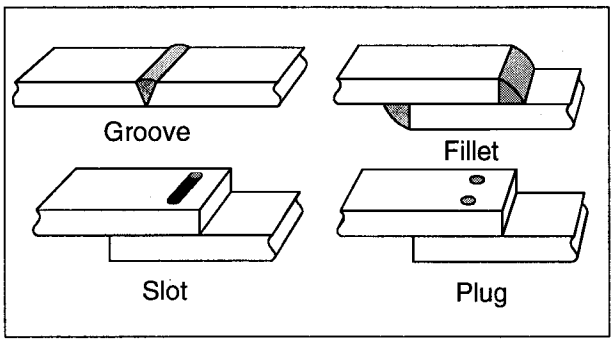

Figure 2-2 Major weld types

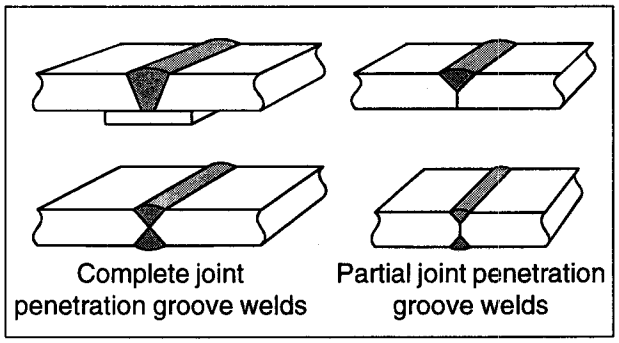

Figure 2-3 Types of groove welds

In Fig. 2-4, terminology associated with groove welds and fillet welds is described. Of great interest to the designer is the dimension noted as the "throat." The throat is the theoretical weakest plane in the weld which controls the design of many welds.

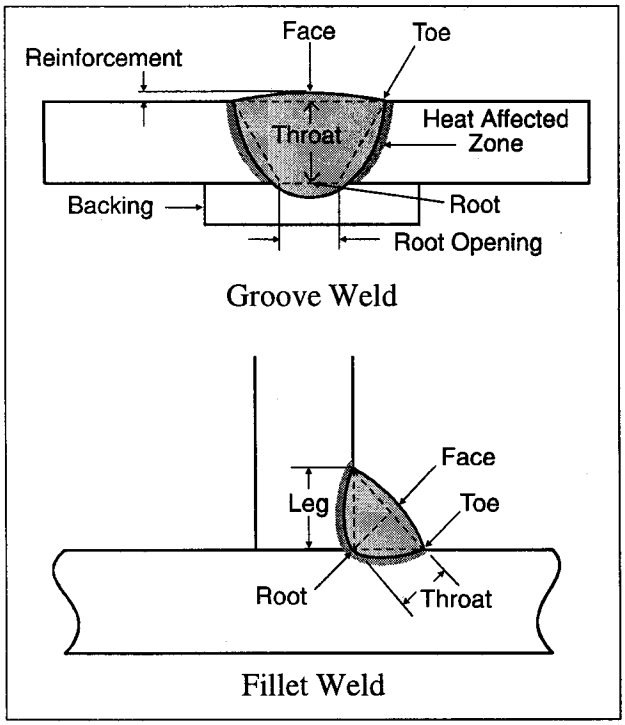

Figure 2-4 Weld terminology

2.2.1 Fillet Welds

Fillet welds have a triangular cross section and are applied to the surface of the materials they join. Fillet welds by themselves do not fully fuse the cross-sectional areas of parts they join, although it is still possible to develop full strength connections with fillet welds.

The size of a fillet weld is usually determined by measuring the leg size, even though the weld is designed by determining the required throat size. For equal legged, flat faced fillet welds applied to plates that are oriented 90° apart, the throat dimension is found by multiplying the leg size by 0.707 (i.e., sine 45°).

2.2.2 Complete Joint Penetration Groove Welds (CJP)

By definition, CJP groove welds have a throat dimension equal to the thickness of the plate they join (see Fig. 2-4). For prequalified welding procedure specifications, the American Welding Society D1.1-96 Structural Welding Code requires backing (see **2.9**) if a CJP weld is made from one side, and back gouging (see **3.12**) if a CJP weld is made from both sides. This ensures complete fusion throughout the thickness of the material being joined. Otherwise, procedure qualification testing is required to prove that the full throat is developed. A special exception to this is applied to tubular connections whose CJP groove welds may be made from one side without backing.

2.2.3 Partial Joint Penetration Groove Welds (PJP)

A PJP groove weld is one that, by definition, has a throat dimension less than the thickness of the materials it joins (see Fig. 2-3). An "effective throat" is associated with a partial joint penetration groove weld (see Fig. 2-5). This term is used to delineate the difference between the depth of groove preparation and the probable depth of fusion that will be achieved. When submerged arc welding (which has inherently deep penetration) is used, and the weld groove included angle is 60°, the D1.1-96 Code allows the

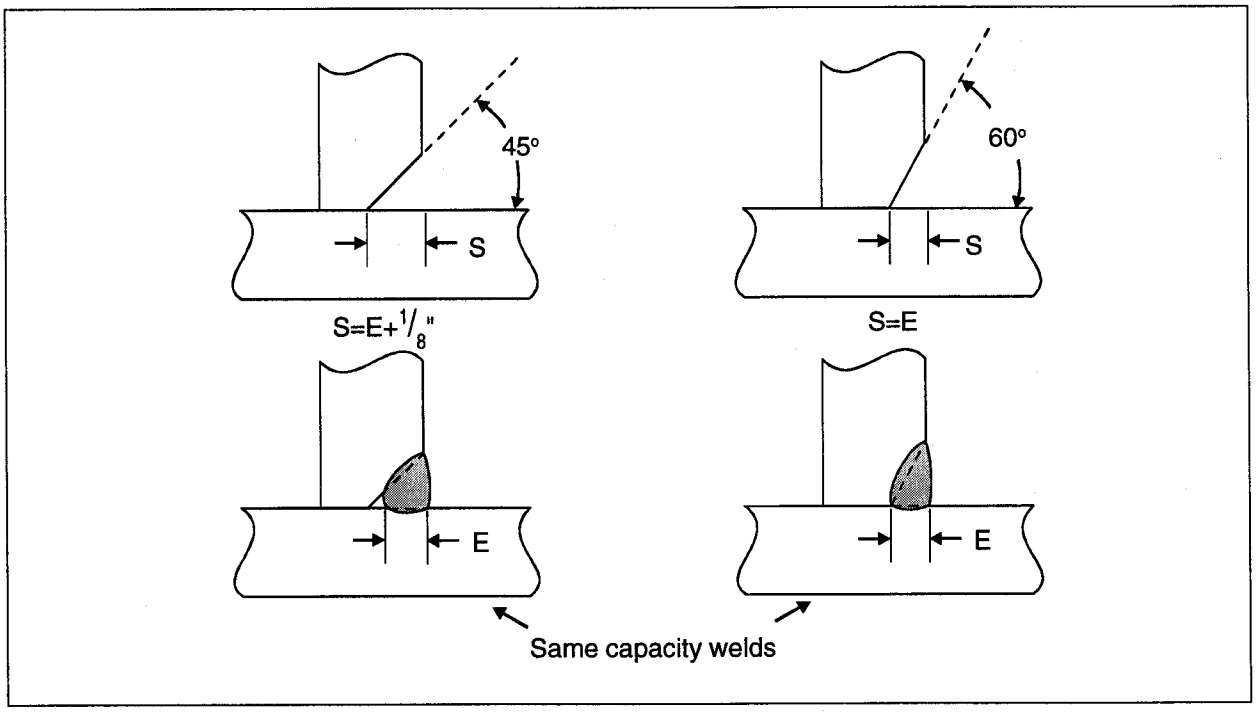

Figure 2-5 *PJP groove welds: "E" versus "S"*

designer to rely on the full depth of joint preparation to be used for delivering the required throat dimension. When other processes with less penetration are used, such as shielded metal arc welding, and when the groove angle is restricted to 45°, it is doubtful that fusion to the root of the joint will be obtained. Because of this, the D1.1-96 Code assumes that 1/8 in. of the PJP joint may not be fused. Therefore, the effective throat is assumed to be 1/8 in. less than the depth of preparation. This means that for a given included angle, the depth of joint preparation must be increased to offset the loss of penetration.

The effective throat on a PJP groove weld is abbreviated utilizing a capital "E." The required depth of groove preparation is designated by a capital "S." Since the engineer does not normally know which welding process a fabricator will select, it is only necessary for the engineer to specify the dimension for E. The fabricator then selects the welding process, determines the position of welding, and thus specifies the appropriate S dimension, which will be shown on the shop drawings. In most cases, both the S and E dimension will be contained on the welding symbols of shop drawings, the effective throat dimension showing up in parentheses.

2.2.4 Double-Sided Welds

Welds may be single or double. Double welds are made from both sides of the member (see Fig. 2-6). Double-sided welds may require less weld metal to complete the joint. This, of course, has advantages with respect to cost and is of particular importance when joining thick members. However, double-sided joints necessitate access to both sides. If the double joint necessitates overhead welding, the economies of less weld metal may be lost because overhead welding deposition rates are inherently slower. For joints that can be re-positioned, this is of little consequence. There are also distortion considerations where the double-sided joints have some advantages in balancing weld shrinkage strains.

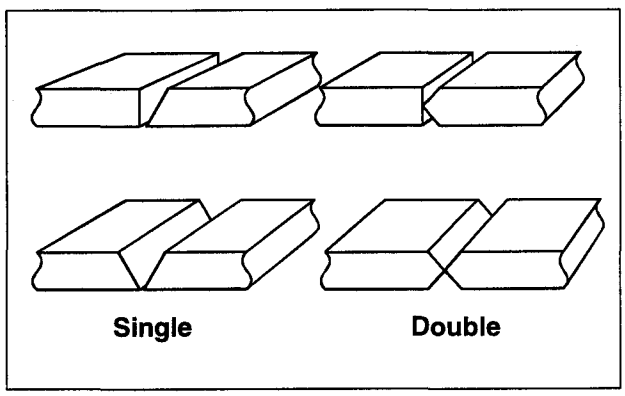

Figure 2-6 *Single versus double-sided joints*

2.2.5 Groove Weld Preparations

Within the groove weld category, there are several types of preparations (see Fig. 2-7). If the joint contains no preparation, it is known as a square groove. Except for thin sections, the square groove is rarely used. The bevel groove is characterized by one plate cut at a 90° angle, and a second plate with a bevel cut. A vee groove is similar to a bevel, except both plates are bevel cut. A "J" groove resembles a bevel, except the root has a radius, as opposed to a straight cut. A "U" groove is similar to two J grooves put together. For butt joints, vee and U groove details are typically used when welding in the flat position since it is easier to achieve uniform fusion when welds are placed upon the inclined surfaces of these details, versus the vertical edges of the bevel or J groove counterparts.

Properly made, any CJP groove preparation will yield a connection equal in strength to the connected material. The factors that separate the advantages of each type of preparation are largely fabrication related. Preparation costs of the various grooves differ. The flat surfaces of vee and bevel groove weld preparations are generally more economical to produce than the U and J counterparts, although less weld metal is usually required in the later examples. For a given plate thickness, the volume of weld metal required for the different types of grooves will vary, directly affecting fabrication costs. As the volume of weld metal cools, it generates residual stresses in the connection that have a direct effect on the extent of distortion and the probability of cracking or lamellar tearing. Reducing weld volume is generally advantageous in limiting these problems. The decision as to which groove type will be used is usually left to the fabricator who, based on knowledge, experience, and available equipment, selects the type of groove that will generate the required quality at a reasonable cost. In fact, design engineers should not specify the type of groove detail to be used, but rather determine whether a weld should be a CJP or a PJP.

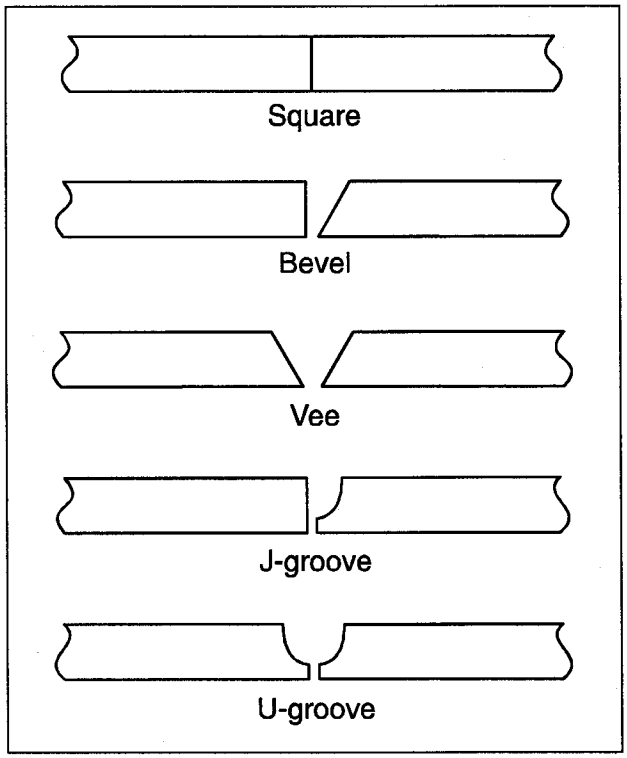

Figure 2-7 *Groove weld preparation*

2.2.6 Interaction of Joint Type and Weld Type

Every weld type cannot be applied to every type of joint. For example, butt joints can only be joined with groove welds. A fillet weld cannot be applied to a butt joint. Tee joints may be joined with fillet welds or groove welds. Similarly, corner joints may be joined with either groove welds or fillet welds. Lap joints would typically be joined with fillet welds or plug/slot welds. Table I illustrates possible combinations.

	Fillet	Groove	Plug/Slot
Butt	N.A.		N.A.
Tee	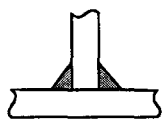	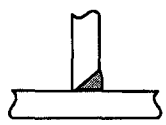	N.A.
Corner	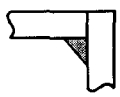	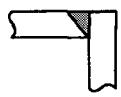	N.A.
Lap	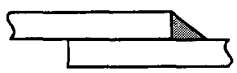	N.A.	

Table I *Weld type/joint type interaction*

2.3 Determining Weld Size

2.3.1 Strength of Welded Connections

A welded connection can be designed and fabricated to have a strength that matches or exceeds that of the steel it joins. This is known as a full strength connection and can be considered 100% efficient, that is, it is as strong as the base metal it joins. Welded connections can be designed so that if loaded to destruction, failure would occur in the base material. Poor weld quality, however, may adversely affect weld strength.

A connection that duplicates the base metal capacity is not always necessary and when unwarranted, its specification unnecessarily increases fabrication costs. In the absence of design information, it is possible to specify welds that have strengths equivalent to the base metal capacity. Assuming the base metal thicknesses has been properly selected, a weld that duplicates the strength of the base metal will be adequate as well. This, however, is a very costly approach. Economical connections cannot be designed on this basis. Unfortunately, the overuse of the complete joint penetration (CJP) detail and the requirement of "matching filler metal" (see **2.4**) serves as evidence that this is often the case.

2.3.2 Variables Affecting Welded Connection Strength

The strength of a welded connection is dependent on the weld metal strength and the area of weld that resists the load. Weld metal strength is a measure of the capacity of the deposited weld metal itself, measured in units such as ksi (kips per square inch). The connection strength reflects the combination of weld metal strength and cross sectional area, and would be expressed as a unit of force, such as kips. If the product of area times the weld metal strength exceeds the loads applied, the weld should not fail in static service. For cyclic dynamic service, fatigue must be considered as well.

For seismic applications, the design forces may be only a fraction of the actual forces experienced. It is generally desirable in these applications to detail connections so that load limiting behavior (i.e. yielding) occurs in the members and not in the connections. For welded construction, this requires yielding in the base metal before yielding in the weld metal.

The area of weld metal that resists fracture is the product of the theoretical throat multiplied by the length. The theoretical weld throat is defined as the minimum distance from the root of the weld to its theoretical face. For a CJP groove weld, the theoretical throat is assumed to be equal to the thickness of the plate it joins. Theoretical throat dimensions of several types of welds are shown in Fig. 2-8.

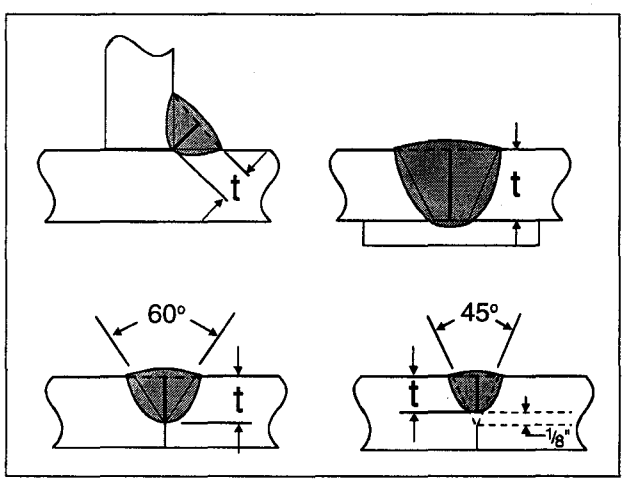

Figure 2-8 Theoretical throats

For fillet welds or partial joint penetration groove welds, using filler metal with strength levels equal to or less than the base metal, the theoretical failure plane is through the weld throat. When the same weld is made using filler metal with a strength level greater than that of the base metal, the failure plane may shift into the fusion boundary or heat affected zone. This is covered in detail in **2.4**. Most designers will calculate the load capacity of the base metal, as well as the capacity of the weld throat. The fusion zone and its capacity is not generally checked, as this is unnecessary when matching or undermatching weld metal is used. When overmatching weld is specifically selected, and the required weld size is deliberately reduced to take advantage of the overmatched weld metal, the designer must check the capacity of the fusion zone (controlled by the base metal) to ensure adequate capacity in the connection.

Complete joint penetration groove welds that utilize weld metal with strength levels exactly equal to the base metal will theoretically fail in either the weld or the base metal. Even with matching weld metal, the weld metal is generally slightly higher in strength than the base metal, the theoretical failure plane for transversely loaded connections is assumed to be in the base metal.

2.3.3 Determining Throat Size for Tension or Shear Loads

Connection strength is governed by three variables: weld metal strength, weld length, and weld throat. The weld length is often fixed, due to the geometry of the parts being joined, leaving one variable to be determined, namely, the throat dimension.

For tension or shear loads, the required capacity the weld must deliver is simply the force divided by the length of the weld. The result, in units of force per length (such as kips per inch) can be divided by the weld metal strength, in units of force per area (such as kips per square inch). The final result would be the required throat, in inches. Weld metal allowables which incorporate factors of safety can be used instead of the actual weld metal capacity. This directly generates the required throat size.

To determine the weld size, it is necessary to consider what type of weld is to be used. Assume the preceding calculation determined the need for a one inch throat size. If a single fillet weld is to be used, a throat of 1 in. would necessitate a leg size of 1.4 in., shown in Fig. 2-9. For double-sided fillets, two 0.7 in. leg size fillets could be used. If a single PJP groove weld is used, the effective throat would have to be 1 in. The actual depth of preparation of the production joint would be 1 in. or greater, depending on the welding procedure and included angle used. A double PJP groove weld would require two effective throats of 0.5 in. each. A final option would be a combination of partial joint penetration groove welds and external fillet welds. As shown in Fig. 2-9, a 60° included angle was utilized for the PJP groove weld and an unequal leg fillet weld applied externally. This acts to shift the effective throat from the normal 45° angle location to a 30° throat.

If the plates being joined are 1 in. thick, a CJP groove weld is the only type of groove weld that will effectively transfer the stress, since the throat on a CJP weld is equal to the plate thickness. PJP groove welds would be incapable of developing adequate throat dimensions for this application, although the use of a combination PJP-fillet weld would be a possibility.

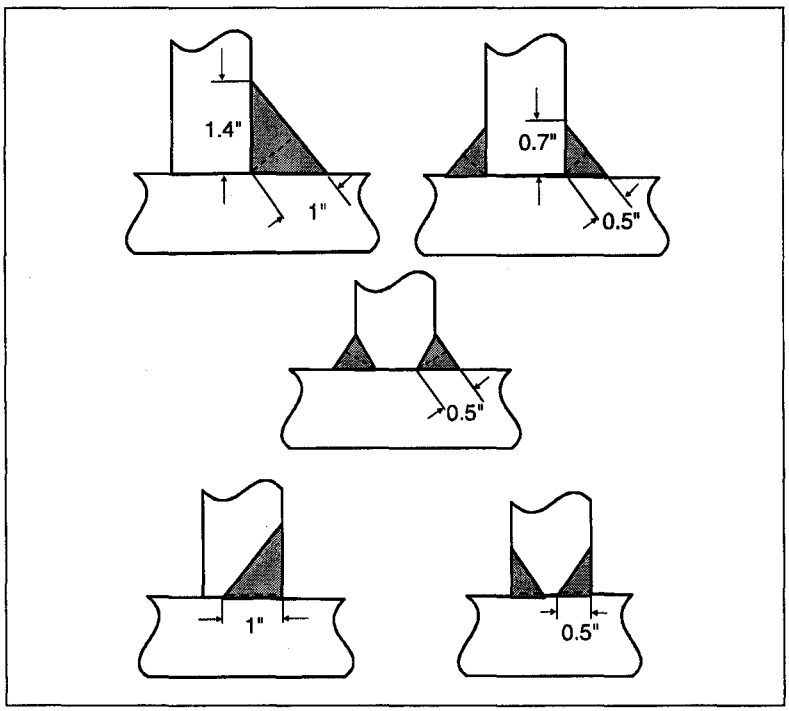

Figure 2-9 *Weld combinations with equal throat dimensions*

2.3.4 Determining Throat Size for Compressive Loads

When joints are only subject to compression, the unwelded portion of the joint may be milled-to-bear, reducing the required weld throat. Typical of these types of connections are column splices where partial joint penetration (PJP) groove welds frequently are used for static structures. There were few if any reports of column splice failures during the Northridge earthquake. Even so, there is concern about the suitability of these connection types in seismic applications because of the potential of fracture associated with net tensile loading on the splice. This is an area where more research is required.

2.3.5 Determining Throat Size for Bending or Torsional Loads

When a weld, or group of welds, is subject to bending or torsional loads, the weld(s) will not be uniformly loaded. In order to determine the stress on the weld(s), a weld size must be assumed and the resulting stress distribution calculated. An iterative approach may be used to optimize the weld size.

A simpler approach is to treat the weld as a line with no throat. Standard design formulas may be used to determine bending, vertical shear, torsion, etc. These formulas normally result in unit stresses. When applied to welds treated as a line, the formulas result in a force on the welds, measured in pounds per linear inch, from which the capacity of the weld metal, or applicable allowable values, may be used to determine the required throat size (Blodgett, 1966, ref. 26).

2.3.6 Weld Size for Longitudinal Welds

Longitudinal welds include the web-to-flange welds on I-shaped girders, and the welds on the corners of box girders. These welds primarily transmit horizontal shear forces resulting from the change in moment along the member. To determine the force between the members being joined, the following equation may be used:

$$f = \frac{Vay}{In}$$

where:

f	=	force on weld per unit length
V	=	total shear on section at a given position along the beam
a	=	area of flange connected by the weld
y	=	distance from the neutral axis of the whole section to the center of gravity of the flange
I	=	moment of inertia of the whole section
n	=	number of welds joining the flange to webs per joint

The resulting force per unit length is then divided by the allowable stress in the weld metal and the weld throat is attained.

This particular procedure is emphasized because the resultant value for the weld throat is nearly always less than the minimum allowable weld size (see **2.6**). The minimum size then becomes the controlling factor.

2.4 Filler Metal Strength Requirements

Filler metal strength may be classified as "matching," "undermatching," or "overmatching." Matching filler metal has the same or slightly higher minimum specified yield and tensile strength, compared to the minimum specified properties of the base material. Emphasis is placed on minimum specified properties, because actual properties are routinely higher. Matching filler metal for A572 Gr50 would be E70 classed electrodes, where the minimum specified filler metal/base metal properties for yield are 60/50 ksi and for tensile are 70/65 ksi. Even though the filler metal has slightly higher properties than the minimum specified strength of the base metal, this is considered to be a matching combination.

Too many engineers see the filler metal recommendations provided in codes that reference "matching" combinations for various grades of steel and assume that is the only option available. While this will never generate a non-conservative answer, it may eliminate better options. Matching filler metal tables are designed to give recommendations for the one unique situation where matching is required (e.g., CJPs in tension). Other alternatives should be considered, particularly when the residual stresses on the welded connection can be reduced in crack sensitive, or distortion prone configurations.

2.4.1 Matching Filler Metal

Matching filler metal is required for CJP groove welds loaded in tension. In order to achieve a full strength welded connection, the filler metal must have a strength that is at least equal to that of the material it joins.

2.4.2 Undermatching

Undermatching weld metal may be used for all weld types and loading types except one: complete joint penetration groove welds loaded in tension. For all other joints and other loading types, some degree of undermatching is permitted. For example, CJPs in compression may be made with weld metal that has strength of up to 10 ksi less than matching. CJPs in shear or loading parallel to the longitudinal axis may be made with undermatching filler material. All PJPs, fillet welds, and plug or slot welds may be made with undermatching weld metal. Design of the weld sizes, however, must incorporate the lower filler metal strength in order to ensure the welded connection has the proper capacity.

Undermatching may be used to reduce the concentration of stresses in the base material. Lower strength filler material generally will be more ductile than higher strength weld metal. In Fig. 2-10, the first weld was made with matching filler material. The second design utilizes undermatching weld metal. To obtain the same capacity in the second joint, a larger fillet weld has been specified. Since the residual stresses are assumed to be of the order of the yield point of the weaker material in the joint, the first example would have residual stresses in the weld metal and the base metal of approximately 100 ksi level. In the second example, the residual stresses in the base material would be approximately 60 ksi, since the filler metal has the lower yield point. These lower residual stresses will reduce cracking tendencies.

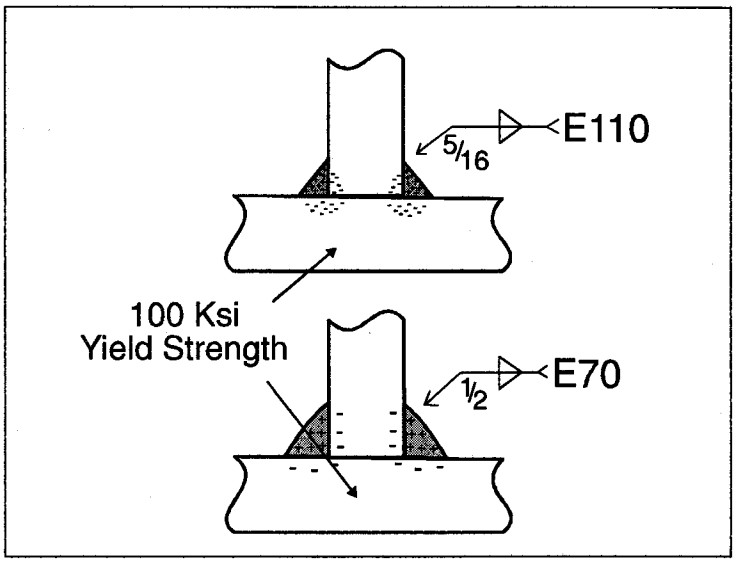

***Figure 2-10** Matching and undermatching filler metal*

In situations where the weld size is controlled by the minimum permitted size (see **2.6**), undermatching is a particularly desirable option. If a 1/4 in. fillet weld is required because of the minimum fillet weld size, it may be made of undermatching weld material without increasing the weld size due to the undermatching requirement.

2.4.3 Overmatching

Caution must be exercised when overmatching filler metal is deliberately used. The strength of fillet and PJP groove welds is controlled by the throat dimension, weld length, and capacity of the weld metal. In theory, overmatching filler metal would enable smaller weld sizes to be employed and yet create a weld of equal strength. However, the strength of a connection is dependent not only on the weld strength, but also on the strength of the fusion zone. As weld sizes are reduced, the fusion zone is similarly decreased in size. The capacity of the base metal is not affected by the selection of filler metal, so it remains unchanged. The reduction in weld size may result in an overstressing of the base metal.

Consider three tee joints containing PJP groove welds and illustrated in Fig. 2-11. A load is applied parallel to the weld; that is, the weld is subject to shear. The allowable stress on the groove weld is 0.30 X the nominal tensile strength of the weld metal, i.e. the "E" number (e.g., E60, E70, etc.). Allowable stress on the base metal shall not exceed 0.40 X the yield strength of the base metal. The first combination employs a very close match of weld metal to base metal, namely A572 Gr50 welded with E70 electrode. The second example examines the same steel welded with undermatching E60 electrode, and the final illustration shows an example of overmatching with E80 electrode.

The weld capacity in kips per inch has been determined by multiplying the weld throat by the weld metal allowable. In the undermatching case, notice that the weld controls. If the weld is properly designed, the base metal will not be overstressed. With matching weld metal, the loading on both the weld and the base metal is essentially the same. However, in the case of the overmatching combination, the weld has 20% more capacity than the base metal. If a designer overlooked loading on the base metal, the connection could easily be overloaded.

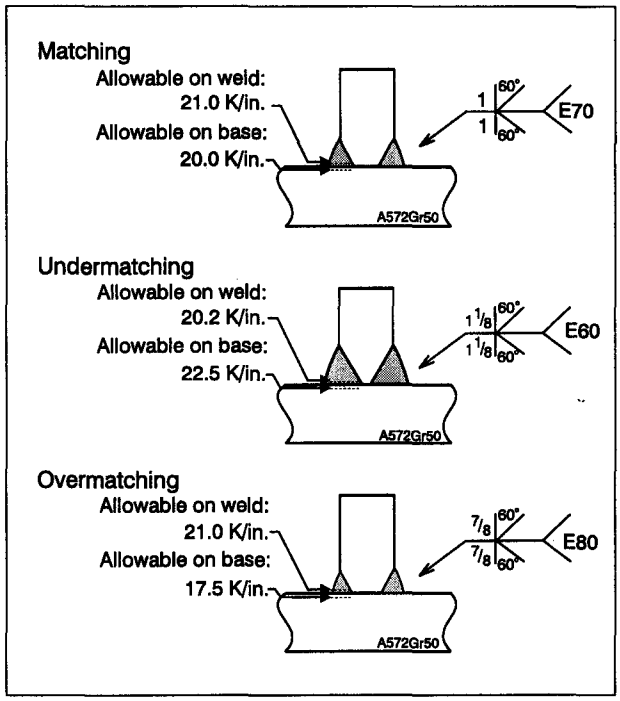

Figure 2-11 *Effect of filler metal strength level*

PJP groove welds should be carefully evaluated, particularly when loaded in shear and when overmatching weld metal is used. If they are loaded in tension, there is less concern since the base metal allowable is increased to 60% of the base metal yield strength, or a 50% increase over the shear value. Fillet welds applied to 90° oriented plates have a leg size that is 40% greater than the throat size. Finally, these concerns only exist when overmatching filler metal is used.

It should be noted, however, that all filler metal combinations will overmatch A36 steel. Particular caution should be taken when sizing PJP groove welds on this steel, to ensure that the base metal allowables are not exceeded.

For CJP groove weld applications, deliberate overmatching may be specified in order to ensure that the weld metal (which may contain a variety of weld discontinuities) stays elastic while the steel it joins becomes inelastic. This approach has been applied to pipelines and offshore structures, although research must be performed on this approach for structural applications, particularly when they are seismic loaded.

2.5 Selection of Weld Type

2.5.1 Options

As was presented in Table I, certain joints lend themselves to a variety of weld options, most notably the tee and corner joints. These may be joined by CJP or PJP groove welds, fillet welds or combination PJP and fillet welds. The selection of weld type for butt joints, whether CJP or PJP groove welds, is primarily dictated based on loading type and magnitude.

2.5.2 Considerations: Performance and Cost

Two factors must be considered when selecting weld types: performance and cost. The designer must be aware of the variations in performance that may be seen, using details to optimize performance. When multiple weld configuration options exist and the performance is expected to be the same, the economics of the different details should be considered.

2.5.3 Performance of Various Weld Types for Specific Joints

Butt Joints. Full strength tension butt joints must be made with CJP groove welds. When subject to compression or shear, PJP groove welds may be used, providing adequate throats can be developed. For static loaded conditions, PJP groove welds may be used in tensile applications, provided the resulting throat is sufficient to transfer the applied loads. Even in situations where fatigue loading is encountered, PJP groove welds may be used as long as the stress range does not exceed the allowable loading for the anticipated service life. Single-sided PJP groove welds must be restrained from rotation since tension at the root of the weld can result in a tearing action.

The suitability of PJP groove welds in applications that result in tensile loading due to seismically-induced forces is an area where little information is available. Since the PJP groove weld, by definition, does not have the capacity of the steel that it joins, loading that would be induced on these types of connections due to inelastic deformations of the steel would be extremely high. Until definitive information is available, PJP groove welds in butt joints connecting material that is loaded into the inelastic region should be avoided.

A common example of a butt joint in a structural application is the column splice. Traditionally, even in seismic applications, PJP groove welds have been used for these applications. The performance of these connections in earthquakes seems to have been adequate, although fracture would be inevitable if tensile loads were high enough. For these applications, the loading must be carefully assessed to ensure that the resultant weld throat is adequate to resist the applied tensile loads since code specified design loads may not adequately govern these demands.

Tee Joints. A common tee joint application in building framing is the beam-to-column moment connection. This is the type of joint that has received widespread attention as the result of the fractures experienced during the Northridge earthquake. In the Special Moment Resisting Frames (SMRF), both of the beam flanges will be subject to reversal of tensile loading due to lateral displacements. When the beam is subject to loads that result in inelastic deformations, the connections will be required to transmit these high forces. Under these loading conditions, tee joints are required to contain CJP groove welds in order to transmit the loads that result from lateral displacements.

Several aspects of this weld, joint and overall detail deserve special attention. The CJP details that may be applied to this connection include single bevel groove welds (the traditional detail), single J groove welds (which are difficult to use due to fit-up variations), and double bevel and double J groove details (which necessitate overhead welding). The traditional single bevel detail necessitates the use of steel backing, along with the corresponding implications discussed in **2.9**. All these details necessitate welding against the vertical column surface face, a more difficult situation than welding into vee grooves in butt joints.

For tee joints, the weld metal will apply shrinkage-induced strains that will act upon the through-thickness (Z-axis) properties of the steel, typically the weakest axis. Lamellar tearing (discussed in **6.3.4**) is always a concern for these type of connections, particularly when the weld metal volumes become larger, resulting in increased shrinkage strains and corresponding stresses.

When high service loads are transferred through the thickness of steel (as is done during seismic loading of SMRFs), the steel properties in the Z-axis must be considered. More research into specific steel requirements is needed, especially for the specific example of SMRFs.

The naturally occurring 90° interface between the un-reinforced groove weld and the column is not an optimum configuration since the interface constitutes a stress concentration. For "dynamic" applications, the D1.1-96 Code requires a reinforcing fillet weld be applied to reduce this stress concentration (D1.1-96, Fig. 3.4, Note J). Initial tests indicate advantages when groove welds are reinforced with fillet welds.

Tee joints also define the relative orientation of web-to-flange connections of fabricated plate girders. These members typically are subject to bending, and the loading transmitted across this joint consists of horizontal (or longitudinal) shear. For these situations, fillet welds or partial joint penetration groove welds are generally sufficient to transmit the relatively small forces involved.

The shear tab to column connection is also a tee joint. This connection traditionally has been made in the shop, and in the field, the beam web is bolted to the shear tab. The shear tab may be further connected with fillet welds to the beam flanges, depending on the Z_t/Z ratio. Post-Northridge investigations yielded data supporting the use of beam webs welded directly to column flanges, typically with CJP groove welds. The improved performance of the directly welded web appears to be related to the greater efficiency in load transfer through a welded connection vs. the bolted connection although more research needs to be done in this area (AWS, 1995, ref. 15). The use of a CJP groove weld (vs. fillet welds of equivalent strength) seems to be advantageous from a fracture viewpoint, since the naturally occurring lack of fusion plane between the two fillet welds is eliminated with the use of the CJP groove weld. There is insufficient data available regarding the suitability of various details in this area, so most engineers will default to the use of the more conservative CJP groove weld.

Tee joints also define the orientation of the continuity plate to both column flanges and the column web. Details regarding the most efficient types of welds for continuity plates, and the requirements for them, will be subject to future investigations. Continuity (or stiffener) plates are usually welded to the flanges with CJP groove welds, and to the web with fillet welds. The automatic specification of CJP groove welds throughout may cause additional fabrication problems, particularly when extremely heavy continuity plates are utilized. The accumulation of residual stresses can lead to a variety of fracture types in this region. Corners of continuity plates should be snipped, or angled at the corners, to prohibit the interaction of the longitudinal shrinkage forces from the web and flange welds. A minimum of 1-1/2 inches is recommended.

Corner Joints. When box columns are utilized, it is important that the size of the welds in the corner be sufficient to transfer the horizontal forces that would result from lateral displacements. This usually necessitates a yield-line analysis to ensure that the welding in the local area of the beam connection is sufficient to transfer those forces that are imposed (Blodgett, 1966, ref. 26). If the bending stresses in the column are sufficiently low, fillet welds or PJP groove welds are often utilized. If the loading in the area of the connection is significantly higher, the weld size can be increased in that area. It may be necessary for CJP groove welds to be used under some situations. It is not necessary, however, for the same weld detail to be used along the length of the joint.

Lap Joints. Lap joints would define the orientation of a shear tab to beam web connection. Depending on the specific Z_f/Z ratio, supplemental fillet welds may be applied around this lap joint. Lap joints are typically joined by fillet welds, sized for the loading transfer between the members. It is also possible to apply plug or slot welds to lapped connections, although these are rarely used for heavy material in structural applications.

2.5.4 Cost of Various Weld Types for Specific Joints

When performance is the same, cost differences become the most important issue in weld type selection. The difference can be dramatic.

Butt Joints. When PJP groove welds are acceptable, their costs (as compared to those of CJP groove welds) vary according to the square of the difference in throat size. For example, consider a weld on one inch thick steel. A PJP groove weld with a 1/2 in. throat may be acceptable while the CJP groove weld automatically has a throat of one inch. The cost of the PJP weld would be $(1/2)^2$ or 1/4 compared to the CJP at $(1)^2$ or 1. The PJP groove weld would cost only 25% as much as the CJP groove weld, resulting in a savings of 75%. However, in the case of butt joints, performance conditions may preclude this option.

Tee Joints. As seen in Fig. 2-12, several weld types can be used to create tee joints.

When the required throat dimension is 0.50 in. or less, external fillet welds are generally the lowest cost option. It is important to remember that a 0.50 in. throat requires a 3/4 in. leg sized fillet. The joints which incorporate PJP groove welds necessitate additional plate preparation time. The cost of this beveling operation can be offset by savings due to reduced weld metal volume. As larger throats are required, the combination PJP groove weld with external fillets becomes the most cost effective option.

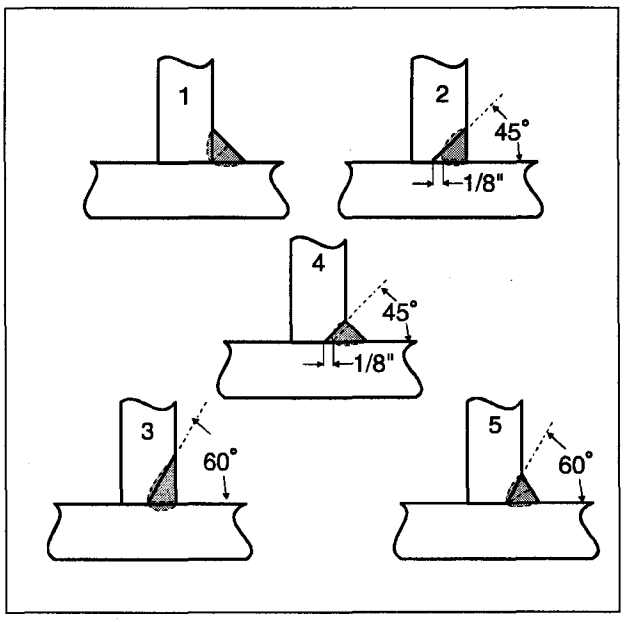

***Figure 2-12** Tee joint weld options*

Corner Joints. Internal access to the box section has a major influence on weld selection for corner joints. For large box sections, external PJP groove welds with internal fillets are economical choices. Small box sections are most economically welded with PJP groove welds until the required throat demands a CJP groove weld. This is rarely the case, however.

Lap Joints. Lap joints may be welded utilizing plug, slot, or fillet welds. Except in cases of very low levels of transferred load, fillet generally are utilized.

2.6 Minimum Weld Size

Many codes specify minimum weld sizes that are a function of plate thickness. These are not design related requirements, but rather reflect the inherent interaction of heat input and weld size.

2.6.1 Heat Input and Weld Size

Heat input and weld bead size (or cross sectional area) are directly related. Heat input is typically calculated with the following equation:

$$H = \frac{60\,EI}{1000\,S_w}$$

where

E = arc volts
I = amperage
S_w = travel speed (in./minute)
H = heat input (kilojoules/in.)

In order to create a larger weld in one pass, two approaches may be used: higher amperages (I), or slower travel speeds (S_w) must be employed. Notice that either procedure modification results in a higher heat input. Welding codes have specified minimum acceptable weld sizes with the primary purpose of dictating minimum heat input levels. For example, almost independent of the welding process used, a 1/4 in. fillet weld will require a heat input of approximately 20-30 kilojoules per inch. By prescribing a minimum fillet weld size, these specifications have, in essence, specified a minimum heat input.

Understanding that the minimum fillet weld size is related to heat input, it is also important to note that there is an inherent interaction of preheat and heat input. The prescribed minimum fillet weld sizes assume the required preheats are also applied. If a situation arises where it is impossible to construct the minimum fillet weld size, it may be appropriate to increase the required preheat to compensate for the reduced energy of welding (see **6.4.4**).

The minimum fillet weld size need never exceed the thickness of the thinner part. It is important to recognize the implications of this requirement. In some extreme circumstances, it may be possible that the connection involves a very thin plate being joined to an extremely thick plate. The code requirements would dictate that the weld need not exceed the size of the thinner part. However, under these circumstances, additional preheat based upon the thicker material may be justified.

2.6.2 Required Weld vs. Minimum Weld Sizes

When welds are properly sized based upon the forces they are required to transfer, the appropriate weld size frequently is found to be surprisingly small. Even on bridge plate girders that may be 18 to 20 feet deep, with flange thicknesses exceeding two inches, the required fillet weld size to transmit the horizontal shear forces may be in the range of a 3/32 in. continuous fillet. Intuition indicates that some-

thing would be wrong when trying to apply this small weld to join a flange that may be two inches thick to a web that is 3/4" thick. This is not to indicate a fault with the method used to determine weld size, but rather reveals the small shear forces involved. However, when attempts are made to fabricate this plate girder with these small weld sizes, extremely high travel speeds or very low currents would be required. This naturally would result in an extremely low heat input value. The cooling rates that would be experienced by the weld metal and the base material, specifically the heat affected zone, would be extremely high. A brittle microstructure could be formed. To avoid this condition, the minimum weld size would dictate that a larger weld is required. This is frequently the case for longitudinal welds that resist shear. Any further increase in specified weld size is unnecessary and directly increases fabrication costs.

2.6.3 Single Pass Minimum Sized Welds

Controlling the heat input by specifying the minimum fillet weld size necessitates that this minimum fillet weld be made in a single pass. If multiple passes are used to construct the minimum sized fillet weld, the intent of the requirement is circumvented. In the past, some recommendations included minimum fillet weld sizes of 3/8 in. and larger. A single pass 3/8 in. fillet weld can only be made in the flat or vertical position. In the horizontal position, multiple passes are required, and the spirit of the requirement is invalidated. For this reason, the largest minimum fillet weld in the D1.1-96, Table 5.8 code is 5/16 in. However, even this weld may necessitate multiple passes, depending on the particular welding process used. For example, a quality 5/16 in. fillet weld cannot be made in a single pass with the shielded metal arc welding process utilizing l/8 in. diameter electrodes, except perhaps in the vertical plane.

It may not be possible to make the required minimum sized fillet weld in a single weld pass under all conditions. For example, it is impossible to make a 5/16 in. fillet weld in a single pass in the overhead position. Under these conditions, it is important to remember the principals that underlie the code requirements. For the preceding example, the overhead fillet weld would necessitate three weld passes. Each weld pass would be made with approximately one-third of the heat input normally associated with the 5/16 in. fillet weld. These subjects are addressed in detail in Section **6.4**. In order to ensure satisfactory results, it would be desirable to utilize additional preheat to offset the naturally resulting lower heat input that would result from each of these weld passes.

2.6.4 Minimum Sized Groove Welds

When complete joint penetration groove welds are made, there is no need to specify the minimum weld size, because the weld size will be the thickness of the base material being joined. This is not the case, however, for partial joint penetration groove welds, so the various codes typically specify minimum PJP groove weld sizes as well. When making CJP groove welds, it is a good practice to make certain that the individual passes applied to the groove meet or exceed the minimum weld size for PJP groove welds.

2.7 Weld Symbols

The American Welding Society has standardized a system of designating welds by symbols that communicate the desired weld location, size, and type. AWS publication "A2.4 Standard Symbols for Welding, Brazing and Nondestructive Examination" defines the symbols in detail (AWS, 1991, ref. 11). The symbol consists, as a minimum, of a reference line and an arrow. The arrow points to the joint location (see Fig. 2-13). Symbols, or miniature pictures, of the desired weld are drawn above or below the reference line.

Weld symbols are designed to be communication tools. If they fail to completely communicate the intention of the detailer to the shop, it makes little difference whether the symbol is technically "correct". Confusing details warrant sketches that accurately tell the shop what is required. Notes in the tail are very helpful. Designers have made mistakes in symbols and communicated incorrect information to the shop. Confusing symbols, even though technically correct, have been misinterpreted by welders, resulting in delays and rework. Remember: communicate with weld symbols — don't confuse with weld symbols.

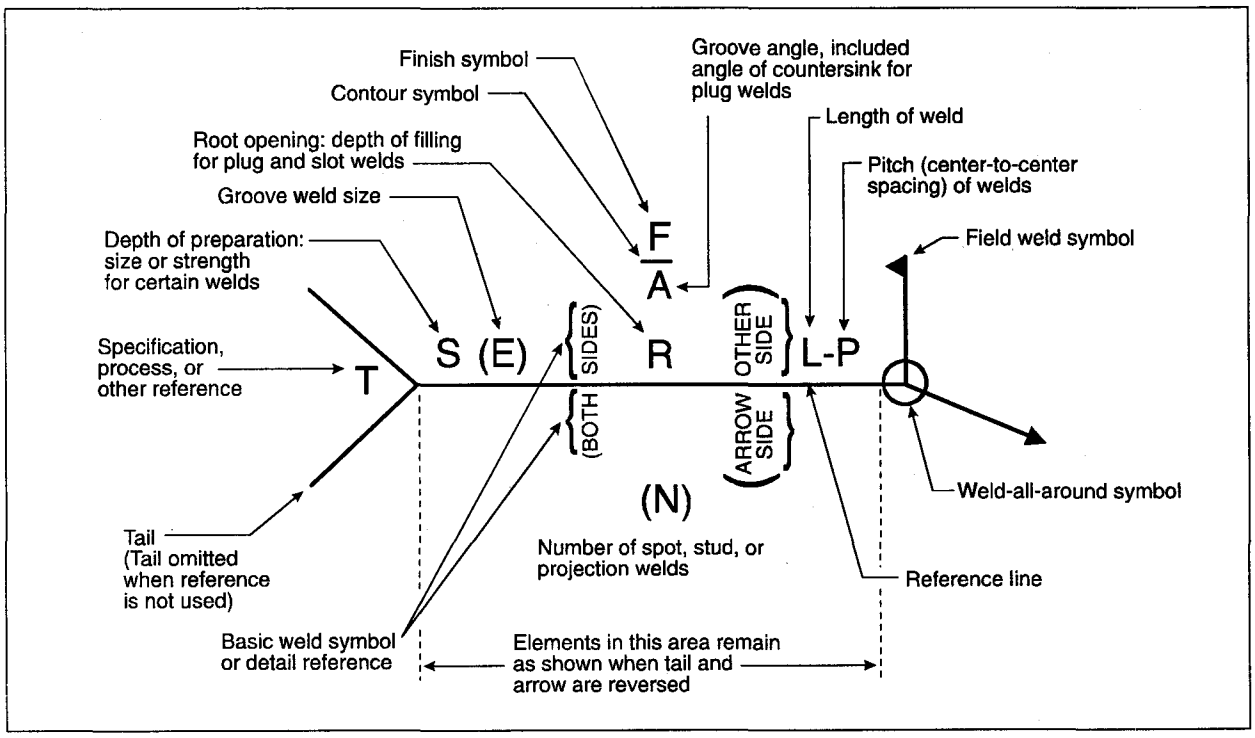

Figure 2-13 Weld symbols

2.8 Weld Joints

Weld joints fit into one of two broad categories: prequalified, and qualified by testing. Prequalified joints are those details which have a proven history of acceptable performance. They are an essential part of a prequalified welding procedure specification (WPS, **see 4.4.2**). The D1.1-96 code allows the fabricator to use these prequalified joints without again proving their adequacy. The combination of root opening, included angle, the applicable thickness, etc., is arranged to ensure fusion to the root of the joint, electrode access, and, in some cases, to reflect economies associated with that particular

detail. For example, some joints are inefficient in their use of weld metal for heavy plates, although very economical for thinner plates. A prequalified joint may be restricted to the thinner plate in order to encourage the fabricator to choose a more cost effective detail.

Tolerances applied to prequalified joints fall into one of two categories: as-detailed and as-fit. The as-detailed tolerances allow the detailer to select slightly modified variations of the prequalified joints without requiring qualification. The as-fit tolerances apply to shop or field assembly of the steel as compared to the dimensions required by the print. The tolerances are cumulative with respect to the final as-fit dimensions. As long as the actual joint detail fits into these tolerances, it is considered prequalified. When the dimensions deviate from prequalified requirements, they require qualification by test.

A joint qualified by test is as good as a prequalified joint. It should be noted, however, that the size of the plates associated with procedure qualification testing seldom duplicates the restraint or cooling rates that will be seen in production. The success achieved using smaller qualification plates may generate a false sense of security. When radical departures from established conditions are to be evaluated, more extensive testing may be justified. These changes would include new processes, new base metals, greater material thicknesses than commonly used, and significant procedure changes (for instance, deletion of all preheat). Such changes may justify more evaluation than routine procedure qualification testing.

2.9 Weld Backing

When there is a gap between two members to be joined, it is difficult to bridge the space with weld metal. On the other hand, when two members are tightly abutted to each other, it is difficult to obtain complete fusion. To overcome these problems, an auxiliary material is added behind the members to act as a support for the weld metal. This is known as weld backing (Fig. 2-14). Weld backing fits into one of two categories: fusible-permanent steel backing, or removable backing.

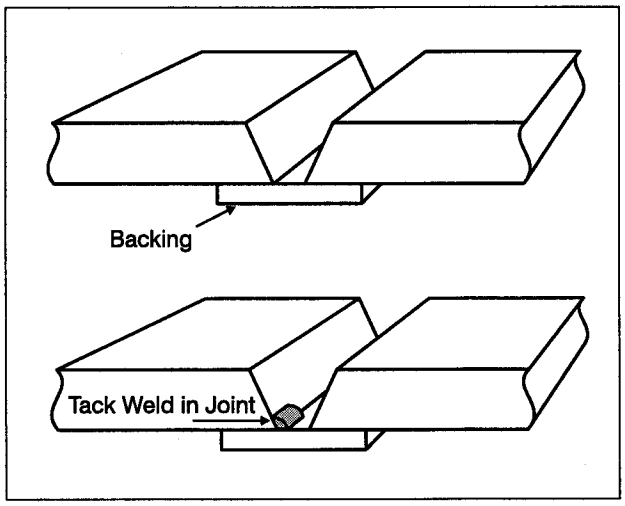

Figure 2-14 *Weld backing*

2.9.1 Fusible Backing

Fusible steel backing, commonly known as backing bars, becomes part of the final structure when left in place, so the quality of steel used for backing, the method of joining the backing, and the continuity of backing, are all critical. Steel that would meet quality requirements for primary members should be used for backing. In general, however, notch toughness properties are not specified for backing. The backing must be continuous for the length of the joint. If multiple pieces of steel backing are to be used in a single joint, they must be joined with complete joint penetration groove welds before being applied to the joint they are to back. Welds joining segments of backing bars should be inspected with radiographic or ultrasonic inspection to ensure soundness. Interrupted backing bars have been the source of fracture, as well as fatigue crack initiation, and are unacceptable even in static structures.

For building construction, steel backing is frequently used in order to compensate for dimensional variations that inevitably occur under field conditions. In order to maintain plumb columns, there will be slight variations in the dimensions between the columns in a bay. Since the beams are cut to length without knowing the exact dimensions that will occur, an oversized gap will often result between the beam and the column. Steel backing is inserted underneath this gap, and weld metal is used to bridge this space. It is important to remember, however, that the steel backing becomes part of the final structure if it is left in place. A proper welded connection is illustrated in Fig. 2 - 15. In this tee joint, even with the proper fusion to the root, the backing creates a notch-like condition that, when subject to tensile loading, could result in fracture initiation. This is discussed in a companion paper by J. Fisher. Indeed, this was the common point of fracture initiation in Northridge-damaged connections. Because of this condition, as well as to facilitate inspection at the weld root, a common post-Northridge specification requirement is to remove steel backing from bottom beam flange connections (AWS, 1995, ref. 15). And, when a reinforcing fillet weld is applied, the geometric severity of this transition region is significantly reduced.

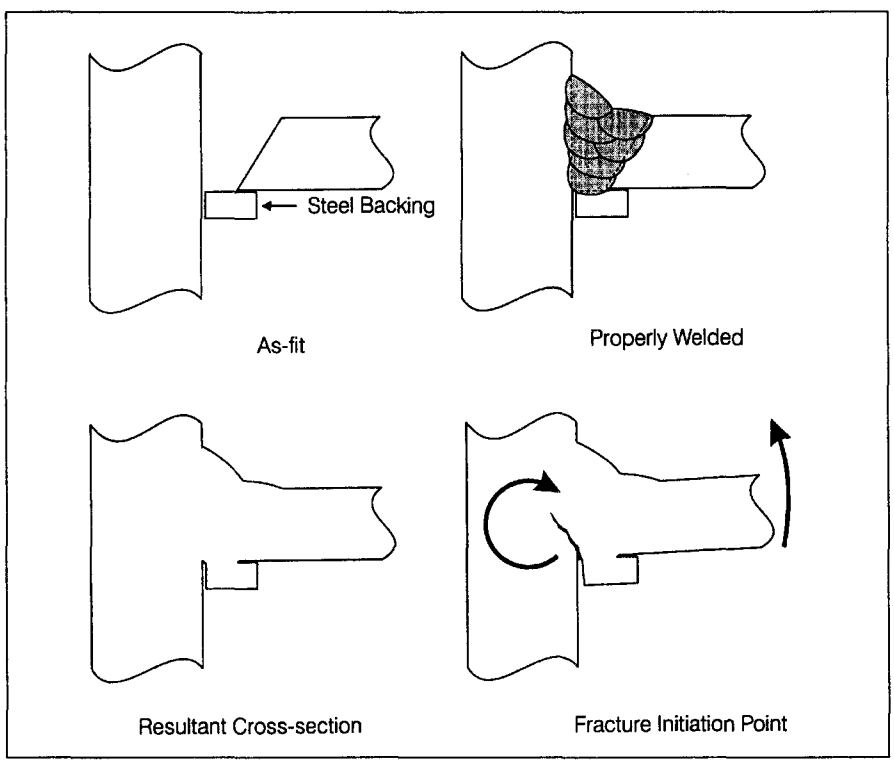

Figure 2-15 *Weld backing and fracture initiation*

Not all backing is required to be removed. For welds subject to horizontal shear (such as corner joints in box columns), backing can be left in place. In butt joints, the degree of stress amplification that occurs due to backing left in place is much less severe than what occurs in T-joints. It must be recognized that backing removal is an expensive operation, and particularly when done in the overhead position, requires considerable welder skill. Some recommendations have not required removal of top beam flange-to-column connection backing because the removal operation (gouge, clean, inspect and re-weld) must be performed through the weld access hole. This difficult operation may do more harm than good. Still, additional work needs to be done in this area before prescriptive requirements can be established.

2.9.2 Removable Backing

Removable backing includes fiberglass tapes, ceramic tiles, and fluxes attached to flexible tape. Removable backing generally is applied when the joint is to be welded with an open arc process such as flux core or shielded metal arc welding. Such backing is applied to the joint with some type of adhesive before the joint is welded. Upon completion of the welding operation, the temporary backing is removed. Ideally, the resulting back bead is acceptable and no further work is required. If the back bead is not acceptable, cosmetic grinding or back gouging and subsequent rewelding may be required.

Removable backing may be less costly for the fabricator than using the alternatives of double-sided joints or fusible backing. A major obstacle in the use of many of these types of backing is the adhesive that holds the material in place. This is particularly a concern when preheat is required. In some situations, mechanical means have been used to assist in holding the backing in place. When supports are attached by tack welds, care should be exercised to ensure that appropriate techniques are employed.

Because of concerns that arose after Northridge about steel backing in tee joints that is left in place, there is increased interest in ceramic backing. Welding procedures that employ ceramic backing must be qualified by test for work done in accordance to the D1.1- 96, para. 5.10. Welders must be trained in the proper use of these materials. Ceramic is nonconductive, requiring that the welder establish a "bridge" between the two steel members to be welded in order to maintain the electrical arc between the two members. While this can be accomplished fairly readily with small root opening dimensions (such as 1/4 in.) it becomes increasingly difficult with larger root openings (such as 1/2 in.). Wide, thin root passes on ceramic-backed joints may crack due to high shrinkage stresses imposed on small weld throats.

One benefit of the activity of fusible backing removal is that it permits the weld joint to be back gouged to sound material. The root of the weld joint is always the most problem-prone region. The center of the length of the bottom beam flange to column weld is difficult to make, since the welder must work through the weld access hole. This is also one of the most difficult areas to inspect with confidence. In a typical beam-to-column connection, the bottom beam flange to column weld must be interrupted mid-length due to interference with the web. This area is particularly sensitive to workmanship problems, and is also a difficult region to inspect with ultrasonic testing. The back gouging operations provide the opportunity for visual verification that sound weld metal has been obtained, particularly in the center of the joint length. This is similar to the D1.1 code requirement for back gouging of double-sided joints. When ceramic backing is used, it still would be advisable to grind or back gouge the joint to sound metal in order to ensure weld quality, and to apply a reinforcing fillet weld to provide a more gradual transition in the area.

2.9.3 Copper Backing

Another type of removable backing would be a copper chill bar placed under the joint. Because of the high thermal conductivity of copper, the large difference in melting points of copper versus steel, and physical and chemical differences between the metals, molten weld metal can be supported by copper and the two materials rarely fuse together. This makes copper an attractive material to use for weld backing. However, this practice is discouraged or prohibited by many codes, because of the possibility of the arc impinging itself on the copper, and drawing some of the melted copper into the weld metal. Copper promotes centerline cracking (see **6.3.1**). This would, of course, be unacceptable. As a practical matter, fabricators avoid this practice simply because the copper backing is extremely expensive, and is rapidly ruined when the arc melts a portion of the copper. Copper backing can be used successfully under controlled conditions which generally involve mechanized welding, and joints that do not utilize root openings.

In some situations, the fabricator will mill a groove in a copper chill bar, and fill the groove with clean, dry submerged arc flux. The flux then acts as the backing, and ensures the arc does not melt any of the copper. This is an efficient method and does not have the same ramifications as welding directly against copper. To ensure tight fit of the copper to the back of the joint, pneumatic, mechanical, or hydraulic pressure may be applied to achieve close alignment. Any temporary welds made to attach the backing system to the structural member must employ appropriate welding techniques.

2.10 Weld Tabs

Weld tabs, commonly known as starting and run off tabs, are added to the ends of joints in order to facilitate quality welding for the full length of the joint. The start and finish ends of weld beads are known to be more defect-prone than the continuous weld between these points. Under starting conditions, the weld pool must be established, adequate shielding developed, and thermal equilibrium established. At the termination of a weld, the crater experiences rapid cooling with the extinguishing arc. Shielding is reduced. Cracks and porosity are more likely to occur in craters than at other points of the weld. Starts and stops can be placed on these extension tabs and subsequently removed upon the completion of the weld (see Fig. 2-16).

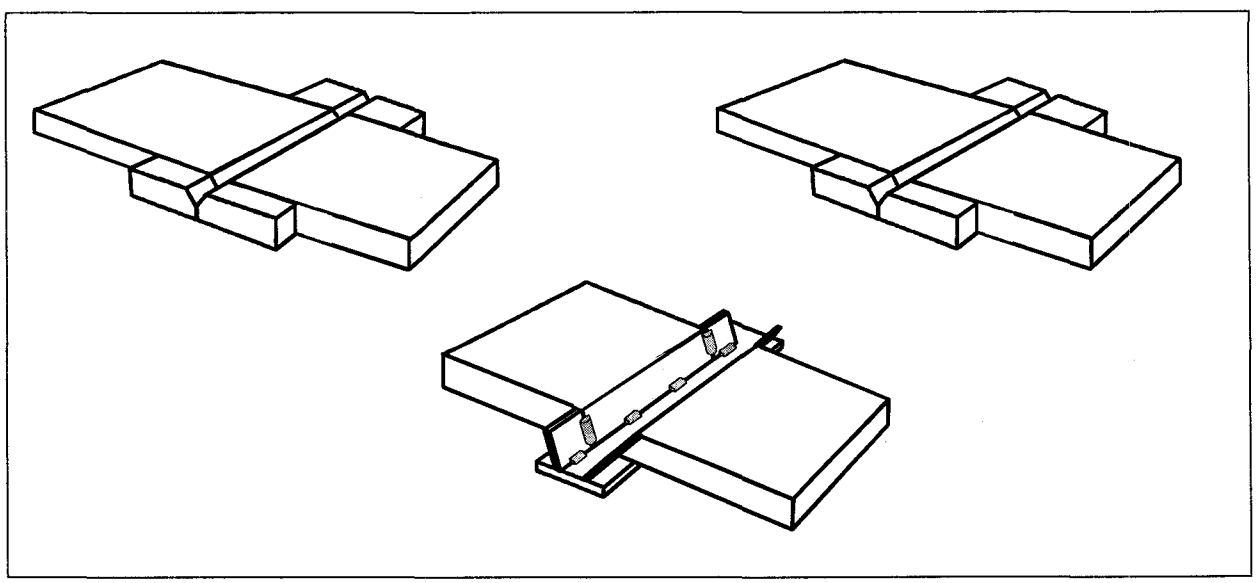

Figure 2-16 *Examples of weld tabs*

It is preferable to attach the weld tabs by tack welding within the joint (in Fig. 2-16, notice the tack welds in the third example). Preheat requirements must be met when attaching weld tabs, unless the production weld is made with the submerged arc welding process that will remelt these zones. It is important for weld tabs to have the same geometry as the weld joint to ensure the full throat or plate thickness dimension is maintained at the ends of the weld joint.

Post-Northridge investigations revealed a variety of abuses regarding the use of weld tabs. Predominant was the use of "end dams," small pieces of steel that were placed perpendicular to the longitudinal axis of the weld. These devices do not constitute weld tabs as required by the D1.1 code (AWS, 1995, ref. 15).

Post-Northridge specifications often have called for the removal of weld tabs since it is likely that these regions will contain weld metal of lesser quality (AWS, 1995, ref. 15). When weld tabs are removed, it is possible to verify that uniform fusion has been achieved at the ends of the weld joint. Where lack of fusion is observed, these areas can be removed by grinding, providing the depth of lack of fusion is minimal. For greater depths, more extensive weld repair may be required.

The resultant contour between the beam flange and column flange should be made with a slight radius, although the largest radius possible will be equivalent to the root opening of the original weld joint, typically 1/4 - 1/2 inch in size. Perhaps too much has been made of the weld termination issue for beam-to-column connections where the columns are I-shaped sections, because the center of the length of this weld is most severely loaded, not the ends. Just the opposite condition exists, however, when box columns are utilized. While most of the Northridge fractures initiated in the center of the length of the beam-to-column weld, just the opposite was observed in some Kobe fractures, since the most severely loaded portion of the weld is at the ends of the weld length. When weld metal of questionable quality in the weld tab is left in place, a fracture can initiate in these regions, and propagate along the length of the weld (AWS, 1995, ref. 15). Weld tabs are removed for bridge fabrications, and since 1989, weld tab removal has been required by AISC specifications when "jumbo" sections or heavy built-up sections are joined in tension applications by CJP groove welds (AISC, 1994, ref. 4).

2.11 Welds in Combination with Bolts

In connections where loads are transferred through both welds and mechanical fasteners (bolts, rivets), it has been traditional to assume that the welds are required to be designed to transfer the full load. After the development of high-strength bolts, slip critical connections began to be used that relied on both welds and bolts to transfer loads. This led to the typical pre-Northridge joint detail that utilized welded flanges and bolted web connections. Research indicates that better performance can be achieved by directly welding the beam web to the column flange vs. the bolted connection. This is probably the result of the greater rigidity achieved with the welded connections, particularly when the beam is subject to inelastic loading levels. Several successful post-Northridge connection details have utilized welded webs (AWS, 1995, ref. 15). Alternate detailing may permit the use of bolted web connections in the future, but additional research must be conducted in this area.

2.12 Weld Access Holes

Weld access holes are provided in the web of beam sections to be joined to columns. The access hole in the upper flange connection permits the application of weld backing. The lower weld access hole permits access for the welder to make the bottom flange groove weld. AISC and AWS prescribe minimum weld access hole sizes for these connections (AWS D1.1-96, para. 5.17, Fig 5.2). It must be

emphasized that these minimum dimensions can be increased for specific requirements necessitated by the weld process, overall geometry, etc. The designer must be certain that the resultant section loss is acceptable.

In order to provide ample access for electrode placement, visibility of the joint, and effective cleaning of the weld bead, it is imperative to provide adequate access.

In addition to offering access for welding operations, properly sized weld access holes provide an important secondary function: they prevent the interaction of the residual stress fields generated by the vertical weld associated with the web connection, and the horizontal weld between the beam flange and column face. The weld access hole acts as a physical barrier to preclude the interaction of these residual stress fields that can result in cracking.

It is best for the weld access hole to terminate in an area of residual compressive stress (Blodgett, 1995, ref. 27). More ductile behavior can be obtained under these conditions.

Weld access holes must be properly made. Nicks, gouges, and other geometric discontinuities can act as stress risers increasing local stress levels and acting as points of fracture initiation. This type of fracture was seen on occasion in Northridge, but was common in the Kobe event. AISC requires that weld access holes be ground to a bright finish on applications where tension splices are applied to heavy sections (AISC, 1994, ref. 4). Although not mandated by the codes, these requirements for tension members may be needed for successful fabrication of compression members when connection details typically associated with tension members are applied to compression members, e.g., CJP groove welds (Blodgett, 1993, ref. 28). It is unknown whether these types of measures will be required for connections in seismic applications. At a minimum, however, good workmanship with smooth contours appears to be necessary in order to obtain acceptable behavior.

2.13 Fatigue

The following information applies to structures subject to low stress range, high cycle fatigue, such as bridges. The relative applicability of these principles to the high stress range, low cycle loading associated with seismic events is unknown at this time. More research is required in this area.

Similarities that *appear* to be common between traditional fatigue and seismic loading include: careful attention to load paths and uniform loading on welds, required minimum weld metal notch toughness; removal of weld backing and weld tabs in some situations; the need for high quality (sound) weld metal; and the importance of attention to geometric irregularities.

Fatigue behavior due to the stress range from variable loads is the most important single difference between bridges and buildings. Buildings subject to static loading are not required to resist cyclic, repetitive loading. For bridge construction, fatigue considerations are essential. The selection of design details and assurance of weld quality are both critical. The smallest neglected detail can result in the failure of a major bridge member, even when the structure has seen years of acceptable service.

Welding adds two additional elements to those items that must be considered when fatigue conditions are addressed. First, welded structures contain residual stresses that are always present and assumed to be near the yield point of the base material. Any superimposed, fluctuating load will generate

stresses that will add to the residual stresses, resulting in localized plastic deformation. Stated another way, a fluctuating load that may cause fatigue cracking in a welded structure can be so small that it would not induce plastic deformation in a non-welded structure.

The second element unique to welding is the inherent geometry associated with certain welds in various joints. For example, the reinforcement on a groove weld in a butt joint causes a geometric stress raiser located at the weld toe. Fillet welded tee joints have a more severe geometric stress concentration, particularly when loaded perpendicular to their length.

Weld discontinuities also act as geometric stress risers. The most severe stress riser is a crack. Rounded, volumetric discontinuities such as porosity and slag inclusions are less severe. The least detectable types of weld discontinuities are internal to the weld and must be observed with nondestructive testing methods. Surface discontinuities and inherent geometric stress concentrations such as undercut, excessive weld reinforcement, and even fillet weld toes are generally more severe than internal discontinuities, and are readily observable. The most severe type of weld discontinuity would be a crack that extends to the surface; fortunately, such defects are readily observable with the less sophisticated types of inspection.

2.14 Effect of Design on Welding Costs

Effective cost control begins with a good design. Selection of hard-to-fabricate details unnecessarily increases the cost of fabrication. Perhaps the greatest error committed by inexperienced designers is the imposition of CJP groove welds in applications where fillet welds or PJP groove welds would have provided a cost-saving alternative. While covered extensively in **2.2**, this bears repeating due to the frequency of its misuse.

Communication between all parties associated with structural design and fabrication must be encouraged. Good cost saving ideas presented by competent fabricators deserve a fair hearing by the engineers and acceptance when warranted. The American Institute of Steel Construction (AISC) through its fabrication membership can provide assistance in determining the most cost effective approaches. Savings achieved in design frequently outweigh all other possible savings achieved through efficient fabrication practices.

2.15 Access for Welding

It is imperative that the design allow for easy access for welding and subsequent inspection. Welds with inadequate access will frequently suffer from poor quality that may not be detected due to reduced access for inspection.

In general, access requires a minimum of at least 18 in. of clear space around the weld joint. The welder must be able to reach this free space, and have good visibility. Mechanized equipment may necessitate more space. For tighter configurations, an understanding of the specific process and equipment being used is helpful.

3 Welding and Cutting Processes

3.1 Welding Process Fundamentals

Arc welding is one of several fusion processes for joining metal. By the generation of intense heat, metal at the joint between two parts is melted and caused to mix — directly or, more commonly, with the addition of an intermediate molten filler metal. Upon cooling and solidification, a metallurgical bond results. The resulting metallurgical bond is due to the same physical atomic behavior that gives a single piece of steel its strength.

In arc welding, the intense heat needed to melt metal is produced by an electric arc. The arc is formed between the work to be welded and an electrode that is manually or mechanically moved along the joint (or the work may be moved under a stationary electrode). The electrode generally is a specially prepared rod or wire that not only conducts the current and sustains the arc, but also melts and supplies filler metal to the joint. The electrode may also be a carbon or tungsten rod, the sole purpose of which is to carry the current and sustain the electric arc between its tip and the workpiece. When a non-consumed electrode is used and the joint requires added metal for fill, that metal is supplied by a separately applied filler metal rod or wire. Most welding in the manufacture of structural steel products where filler metal is required, however, is accomplished with the first type of electrode — the type that supplies filler metal as well as providing the conductor for carrying electric current.

3.1.1 Heat and Filler Metal

The basic arc welding circuit is illustrated in Fig. 3-1. An AC or DC power source fitted with whatever controls may be needed is connected by a work cable to the workpiece and by a "hot" cable to an electrode holder of some type, which makes electrical contact with the welding electrode. When the circuit is energized and the electrode tip is touched to the workpiece, then withdrawn and held close to the spot of contact, an arc is created across the gap. The arc generates intense heat at the tip of the electrode--more than adequate for melting most metals. The heat produced melts the base metal in the vicinity of the arc and any filler metal supplied by the electrode or by a separately introduced rod or wire.

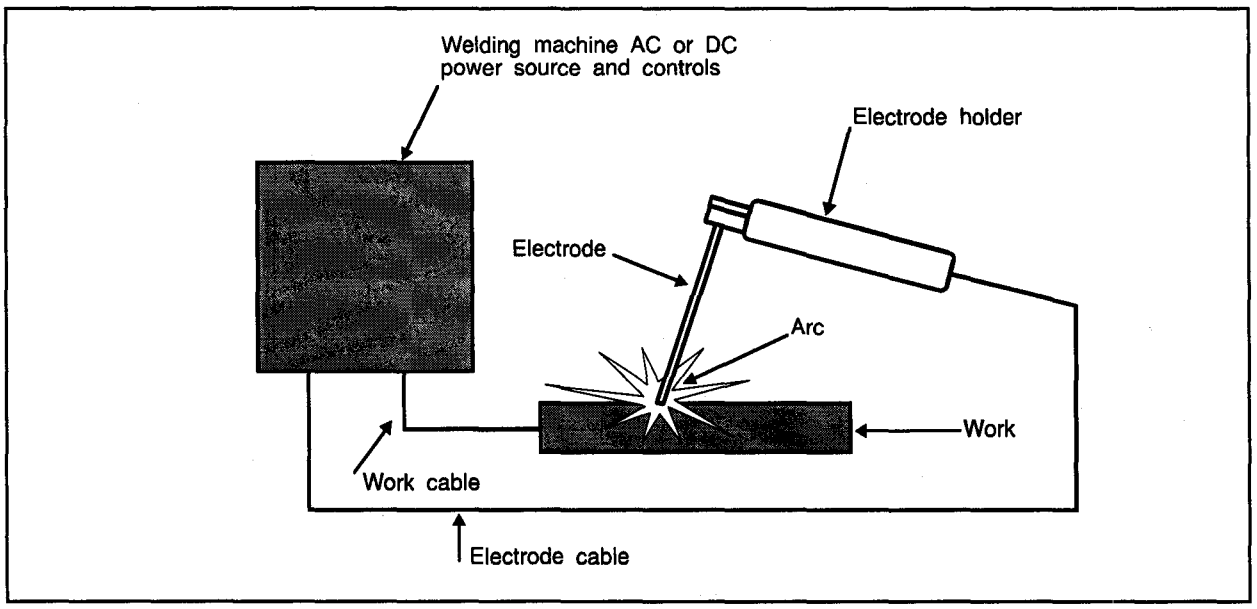

Figure 3-1 Typical welding circuit

A common puddle of molten metal is produced, called a weld pool or puddle. This pool solidifies behind the electrode that is moved along the joint being welded. The result is a fusion bond and the metallurgical unification of the workpieces.

While the main function of the arc is to supply heat, it has other functions that are important to the success of arc welding processes. It can be adjusted or controlled to transfer molten metal from the electrode to the work, to remove surface films, to bring about complex gas-slag metal reactions and various metallurgical changes, as well as to provide the necessary arc force to penetrate the base metal and hold liquid metal in place.

Filler metal is introduced into the arc with most of the arc welding processes. The term filler metal refers to the product that will be melted and added to the molten weld pool. When the filler metal conducts electrical current, it is known as the electrode. Rods are filler metals that do not carry current. Filler metal composition is generally designed to be different than the weld metal composition, in that the weld metal will be composed of both filler metal and base metal.

Filler metals are heated and melted by electrical energy. The current that is conducted through the electrode first heats the filler metal by electrical resistance. In the region of the arc, the extremely high electrical resistance of the arc then melts the filler and the base metal.

3.1.2 Shielding and Fluxing

Use of the heat of an electric arc to join metals, however, requires more than simply establishing the arc and moving the electrode with respect to the weld joint. Metals at high temperatures react with the main constituents of air — oxygen and nitrogen. While these gases can be dissolved in the liquid metal, their solubility is significantly lowered as the metal cools and solidifies. With this decrease in solubility, the gases will come out of solution. If these gases exit as the metal solidifies, a cylindrical cavity known as porosity may be left behind. While this is always undesirable, it is acceptable in limited amounts under specific conditions.

Much lower levels of these gases, particularly nitrogen, may be retained in the solidified steel, causing ordinarily excellent weld metal properties to deteriorate dramatically. Notch toughness is particularly affected by the inclusion of nitrogen. For these reasons, shielding must be provided to protect the molten metal from harmful atmospheric elements. Shielding of the molten puddle, as well as weld metal droplets transferring across the arc, is accomplished in one of two ways, or both: gas shielding or slag shielding.

Gas shielding consists of either an externally supplied gas, such as carbon dioxide, that physically displaces the atmosphere, or a gas that is generated as a result of heating of the electrode flux ingredients. Slag shielding results from the melting of flux ingredients. This slag creates a barrier that prohibits the molten metal from contacting the atmosphere. Some processes utilize both concepts of shielding.

While the primary purpose of the shielding gas is to protect the molten metal, it also significantly affects arc behavior. The shielding gas may be mixed with small levels of a second, third, or even a fourth gas component in order to improve arc stability, puddle fluidity, and other welding characteristics.

In addition to providing slag protection to the molten metal, flux ingredients may also provide a cleaning action. The fluxing action consists of breaking down oxides that are present on the steel surface and aids in "wetting" of the weld pool edges to the steel surface, thus improving bead contour. The flux also cleanses the weld pool of impurities and floats these to the surface slag.

Fig. 3-3 illustrates the shielding of the welding arc and molten pool with a SMAW covered "stick" electrode — the type used in most manual arc welding. The extruded covering on the electrode, under the heat of the arc, generates a gaseous shield that prevents air from coming in contact with the molten metal. It also supplies ingredients that react with deleterious substances on the metals, such as oxides, and ties these substances up chemically in a slag that rises to the top of the pool and crusts over the newly solidified metal. The slag can assist in supporting liquid metal and helps to "mold" the metal to a desirable profile. This slag, even after solidification, has a protective function; it minimizes contact of the very hot solidified metal with air until the temperature is lowered to a point where reaction of the metal with air is lessened, and retards the weld cooling rate.

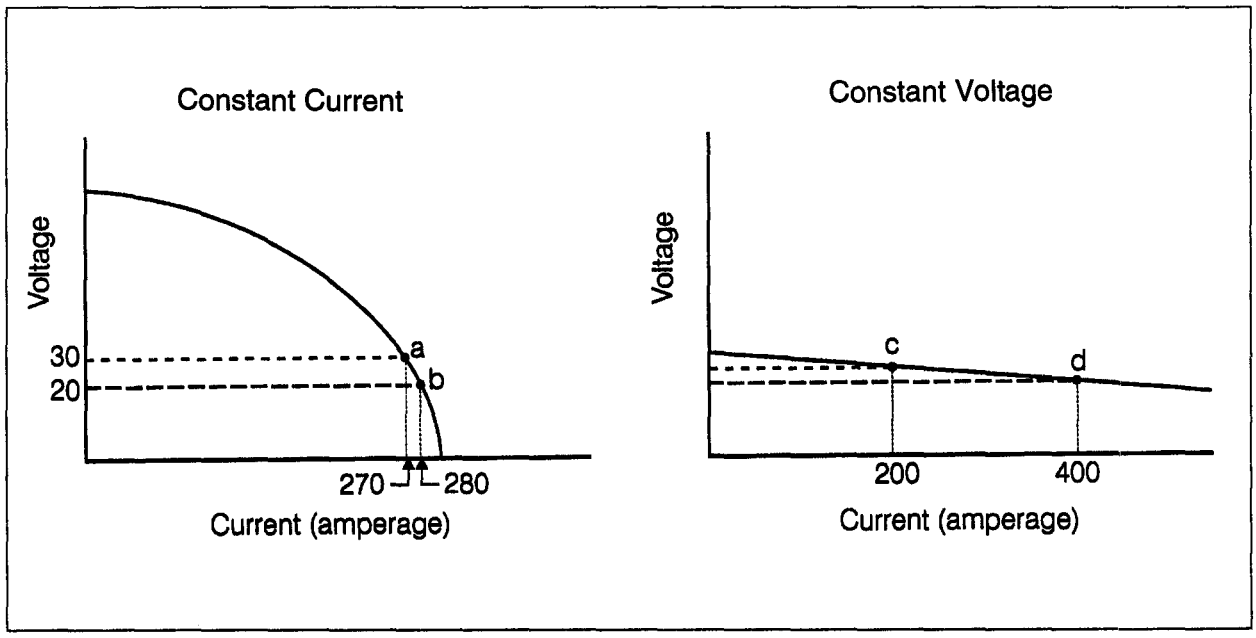

Figure 3-2 Electrical characteristics

3.2 Power Sources

A variety of types of power supplies can be used in arc welding to deliver the required electrical power to the welding circuit. Where electrical input power is available, electric power sources are used that convert the high voltage, 60 hertz power into the type of power required for welding. Where primary electrical input is not available, engine-driven equipment may be used to generate the required welding power. The welding power may be characterized as AC (Alternating Current) or DC (Direct Current). Most of the semiautomatic welding processes today employ DC output.

The output characteristics of the power supply may be identified as either Constant Current (CC) or Constant Voltage (CV). The output characteristics of these two types of machines are illustrated in Fig. 3-2. For the CC system, within the range of operation of the welding processes, the current (or amperage) is relatively constant. A significant change in voltage results in a negligible change in amperage. This can be visualized by observing a change from Point A (30 volts) to Point B (20 volts), a difference of 33%. For this rather large change in voltage, the amperage has only changed from 270 to 280 amps, or, approximately 4%. By contrast, in constant voltage welding, the change from Point C to Point D involves a 200% change in amperage (200 vs. 400 amps). The voltage remains relatively constant, changing from 25 to 20 volts, a decrease of 20%.

Constant current output is used for SMAW, GTAW, and some SAW welding. Constant voltage output is used for GMAW, FCAW, and some SAW processes. For a CC system, the current is determined by the welding power source setting, and the arc length determines the voltage. For constant voltage welding, the power source settings determine the voltage, and the current that is delivered is a function of the wire feed speed.

3.3 Filler Metal Specifications

The American Welding Society produces a series of "AWS Filler Metal Specifications" that give the requirements for classification of welding electrodes. The requirements include chemical composition and mechanical properties of weld metal, weld metal soundness tests, usability tests, and tests that relate to the control and measurement of diffusible hydrogen in weld metal. Requirements for standard sizes, lengths, marking, manufacturing, and packaging are included in these specifications. The AWS Committee is known as the "A5" committee, and the documents and committee activities are in conformance with ANSI standards. There are currently 31 different filler metal specifications, covering electrodes for carbon and low alloy steels, copper and copper alloys, stainless steel, aluminum, nickel, titanium, magnesium, zirconium, as well as brazing materials. Welding processes include SMAW, GMAW, SAW, FCAW, GTAW, EGW/ESW, and brazing. Of primary interest for structural steel applications are those filler metal specifications for carbon and low alloy steels, and for SMAW, GMAW, FCAW, SAW, and EGW/ESW. These are summarized below:

PROCESS	CARBON STEEL SPECIFICATION	LOW ALLOY STEEL SPECIFICATION
SMAW	A5.1	A5.5
FCAW	A5.20	A5.29
GMAW	A5.18	A5.28
SAW	A5.17	A5.23
ESW	<- A5.25 ->	
EGW	<- A5.26 ->	

In a general way, the AWS A5 documents are for welding electrodes, what ASTM specifications are for steel.

Manufacturers of electrodes will report on a Certificate of Conformance the test results that verify their particular products are in conformance with the applicable A5 specification. These reports show the typical properties that will be obtained when welding is performed under the conditions specified in the A5 documents, although some variation will naturally result due to production variations over the course of time. The characteristics of individual welds are a function of complex chemical and thermal reactions that are dependent on a variety of variables. It must be understood that the properties

of deposited weld metal may not be the same as those obtained in the manufacturer's Certificate of Conformance that conforms to the applicable A5 filler metal specification.

This behavior is reported in the A5 documents. For example, quoting from the A5.5 specification, A6.1 and A6.2 read as follows:

> "**A6.1** - Weld metal properties may vary widely, according to the size of the electrode and amperage used, size of the weld beads, base-metal thickness, joint geometry, preheat and interpass temperatures, surface condition, base-metal composition, dilution, etc.
>
> Because of the profound effect of these variables, a test procedure was chosen for this specification which would represent good welding practice and minimize variation of the most potent of these variables.
>
> **A6.2** - It should be recognized that welding practices may be different. The differences encountered may alter the properties of the weld metal. For example, interpass temperatures may range from sub-freezing to several hundred degrees. No single temperature or reasonable range of temperatures can be chosen for classification tests which would be representative of all the conditions encountered in production work. Properties of production welds may vary accordingly, depending on the particular welding conditions.
>
> Weld metal properties may not duplicate, or even closely approach, the values listed and prescribed for test welds."

For these reasons, it is important to understand the role of Welding Variables (discussed in **4.2**) and the role of Welding Procedure Specifications (discussed in **4.3**). The specific parameters that are required by the filler metal specification are not, in general, suitable for all the types of welding that will be encountered. Differences will naturally result because of the specific constraints associated with the actual weld joint. Perhaps the most significant deviation that is routinely encountered is the difference between single pass fillet weld applications, and the multiple pass groove welds that are used for product classification. Single pass welds generally will have a greater level of admixture, making the corresponding base metal composition more significant in terms of weld composition. The weld metal in multiple pass welds benefits from the refinement afforded by subsequent weld passes, while single pass welds will be essentially as-cast grain structures.

The yield and tensile strength of actual welds, as compared to the test welds conducted under the controls of the A5 documents, will not be significantly different unless extreme variations in welding parameters are encountered. The notch toughness of the weld deposits, in contrast, is fairly sensitive to welding conditions. The notch toughness obtained from actual weld deposits may vary significantly from that reported on the A5 classification test. In order to maintain acceptable properties, and notch toughness in particular, it is important that the welding procedures utilized in production be in conformance with good welding practice.

3.4 Shielded Metal Arc Welding (SMAW)

3.4.1 Process Description

The shielded metal arc welding (SMAW) process, commonly known as stick electrode welding or manual welding, is the most popular of the arc welding processes. It is characterized by versatility, simplicity and flexibility (see Fig. 3-1 and 3-3).

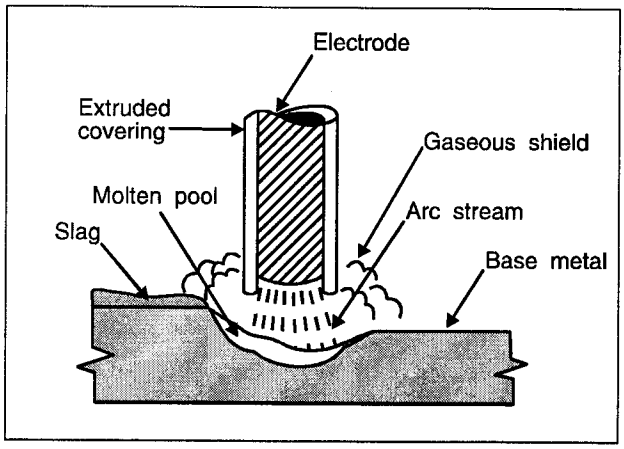

Figure 3-3 *SMAW process*

To persons only casually acquainted with welding, "arc welding" usually means shielded metal arc welding. The SMAW process commonly is used for tack welding, fabrication of miscellaneous components, and repair welding. SMAW also is used in the field for erection, maintenance and repairs. Because of its relative inefficiency, SMAW seldom is used for primary fabrication of structures. SMAW has earned a reputation for depositing high quality welds dependably. It is, however, inherently slower and more costly than other methods of welding.

Shielded metal arc welding may utilize either DC (direct current) or AC (alternating current). Generally speaking, DC is used for smaller diameter electrodes, typically those with a diameter of less than 3/16 in. Larger electrodes utilize AC to eliminate undesirable arc blow conditions.

Electrodes used on AC must be designed specifically to operate in this mode where the current changes direction 120 times per second on 60 Hertz power. All AC electrodes will operate acceptably on DC. The opposite is not necessarily true.

3.4.2 SMAW Filler Metals

The American Welding Society (AWS) publishes a variety of filler metal specifications that are developed by the A5 Committee (AWS, various dates, ref.8); A5.1 addresses the particular requirements for mild steel covered electrodes used with the shielded metal arc welding process. The specification A5.5 similarly covers the low alloy electrodes.

For welding on steels with minimum specified yield strengths exceeding 50 Ksi, all electrodes should be of the low hydrogen type with specific coatings that are designed to be extremely low in moisture. Water (H_2O) will break down into its components hydrogen and oxygen under the intensity of the arc. This hydrogen can then enter into the weld deposit and may lead to unacceptable weld heat

affected zone cracking under certain conditions. Low hydrogen electrodes have coatings that are comprised of materials that are very low in hydrogen.

Under the A5.1 nomenclature, the electrodes are classified based on a four or five digit number that follows the letter E (for electrode). The electrode classification is imprinted on the coating near the end of the electrode, as well as on the electrode package. An example of the numbering system is shown in Fig. 3-4.

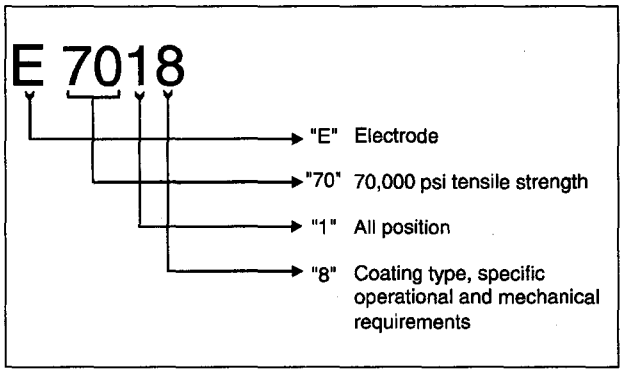

Figure 3-4 *SMAW electrode classification*

Low Hydrogen Electrode Classifications

The term "low hydrogen" was initially used to separate those SMAW electrodes capable of depositing weld metal with low levels of diffusible hydrogen from non-low hydrogen electrodes such as E6010 and E6012 that contain (by design) coating moisture levels of 2 - 4%. The low hydrogen classifications also were capable of depositing weld metal with minimum specified levels of notch toughness. This led to an unfortunate, and technically incorrect, misunderstanding where "low hydrogen" became somewhat synonymous with "notch tough" weld metal. Non-low hydrogen weld metal from E6010 electrodes, for example, is required to meet minimum notch toughness requirements. When applied to processes other than SMAW, specification of electrodes capable of depositing weld metal that is low in diffusible hydrogen does not ensure the weld metal will have minimum specified notch toughness properties.

The D1.1-96 Code does not currently define "low hydrogen" nor do the AWS A5 filler metal specifications. The preheat tables for prequalified welding procedure specifications list one set of preheat values for "non-low hydrogen electrodes", and another series of values for SMAW with low hydrogen electrodes and FCAW, SAW and GMAW, grouping all electrodes used with these other processes with low-hydrogen SMAW. This implies a similarity in expected maximum levels of diffusible hydrogen (D1.1-96, Table 3.2).

The low hydrogen electrodes that fit into the A5.1 classification include E7015, E7016, E7018, and E7028. The E7015 electrodes operate on DC only. E7016 electrodes operate on either AC or DC. The E7018 electrodes operate on AC or DC and include approximately 25% iron powder in their coatings; this increases the rate at which metal may be deposited. An E7028 electrode contains approximately 50% iron powder in the coating, enabling it to deposit metal at even higher rates. However, as the nomenclature shows, the "2" would indicate that this electrode is suitable for flat and horizontal welding only.

Under the low alloy specification, A5.5, a similar format is used to identify the various electrodes. The most significant difference, however, is the inclusion of a suffix letter and number indicating the alloy content. An example would be an "E8018-C3" electrode, with the suffix "-C3" indicating the electrode nominally contains 1% nickel. A "-C1" electrode nominally contains 2.5% nickel. Some electrodes carry the "-W" designation that indicates the presence of alloys capable of giving the electrode atmospheric corrosion resistance for weathering applications.

Hydrogen Designators

In 1991, the American Welding Society began to issue filler metal specifications which include optional supplemental designators indicating the maximum level of hydrogen that may be present in the deposit. These designators follow the standard AWS classification and consist of the letter H followed by a single or double digit, for example "E7018-H8." An "H8" indicates that the deposit contains a maximum diffusible hydrogen content of 8 milliliters per 100 grams. Most standard low hydrogen electrodes must deposit weld metal with a maximum of 16 ml/100 g of diffusible hydrogen under the specific test conditions. However, manufacturers may optionally show an H8 or an H4 if their particular electrodes are capable of delivering these extra low levels of diffusible hydrogen. While "low hydrogen" electrodes are required by the D1.1-96 code for welding on steels with minimum specified yield strength of 50 ksi or greater, the engineer should be careful to avoid over-specification of extra-low hydrogen levels in this regard. There is generally a consumable cost premium associated with the lower diffusible hydrogen products. Even more importantly, current filler metal technology is such that high notch toughness weld metal and consumables with good operating characteristics are not always available with the lowest hydrogen designations. In fact, some consumables delivering very low diffusible hydrogen content weld metal have poor notch toughness. Just because one electrode may be capable of depositing lower levels of hydrogen, it should not be arbitrarily specified unless it is required for a specific application.

In AWS A5.1, the electrodes listed include both low hydrogen and non-low hydrogen electrodes. In AWS D1.1-96, Table 3.1, Group I steels may be welded with non-low hydrogen electrodes. This would include A36 steel. From Group II steels and higher, low hydrogen electrodes are required. These steels would include A572 grade 50. For most structural steel fabrication today, low hydrogen electrodes are prescribed to offer additional assurance against hydrogen induced cracking. When low hydrogen electrodes are used, the required levels of preheat (as identified in Table 3.2 of D1.1-96) are actually lower, offering additional economic advantages to the contractor.

All the low hydrogen electrodes listed in AWS A5.1 have minimum specified notch toughnesses of at least 20 ft.- lbs. in 0°F. There are electrode classifications that have no reported notch toughnesses (such as E6012, E6013, E6014, E7024) but these are not low hydrogen electrodes. Although there is no direct correlation between the low hydrogen nature of various electrodes and notch toughness requirements, in the case of SMAW electrodes in A5.1, the low hydrogen electrodes all have reported minimum notch toughness requirements.

Care of Low Hydrogen SMAW Electrodes

In the U.S., low hydrogen electrodes typically are supplied in hermetically sealed cans. When electrodes are so supplied, they may be used without any preconditioning; that is, they need not be heated before use. Once electrodes are removed from the hermetically sealed container, they should be placed in a holding oven to avoid the pick up of moisture from the atmosphere. These holding ovens generally are electrically heated devices that can accommodate several hundred pounds of electrodes. They hold the electrodes at a temperature of approximately 250^0 F. Electrodes to be used in fabrication are taken from

these ovens. Fabricators should establish a practice of limiting the amount of electrodes discharged at any given time. Once the electrode is exposed to the atmosphere, it may begin to pick up moisture. The D1.1 code limits the total exposure time as a function of the electrode type. Electrodes used to join high strength steels (which are particularly susceptible to hydrogen cracking) must be carefully cared for, and their exposure to the atmosphere strictly limited (D1.1-96, para. 5.3.2.2, Table 5.1).

Some electrodes are supplied in cardboard containers, a common practice in Europe. This is not commonly done for structural fabrication in the U.S., although the practice is acceptable if specific guidelines are followed. The electrodes must be preconditioned before welding. Typically, this means baking them at temperatures in the 700 to 900°F range to remove any residual moisture. In all cases, the electrode manufacturer's guidelines should be followed to ensure a baking procedure that eliminates retained moisture. Electrodes removed from damaged hermetically sealed cans should be similarly baked at high temperature. The manufacturer's guidelines should be consulted and followed to ensure that the electrodes are properly conditioned.

3.5 Flux Cored Arc Welding (FCAW)

Flux cored arc welding (FCAW) is a process that uses an arc between a continuous filler metal electrode and the weld pool. The electrode always is tubular. Inside the metal sheath is a combination of materials that may include metallic powder and flux. FCAW may be applied automatically or semiautomatically.

The flux cored arc welding process has become the most popular semiautomatic process for structural steel fabrication and erection. Production welds that are short, change direction, are difficult to access, must be done out-of-position (e.g., vertical or overhead), or are part of a short production run, generally will be made with semiautomatic FCAW.

When the application lends itself to mechanized welding, most fabricators will select the submerged arc welding process (see **3.6**). Flux cored arc welding may be used in the mechanized mode, but the intensity of arc rays from a high current flux cored arc, as well as a significant volume of smoke, make alternatives such as submerged arc welding more desirable.

3.5.1 Advantages of FCAW

The flux cored arc welding process offers two distinct advantages over shielded metal arc welding. First, the electrode is continuous. This eliminates the built-in starts and stops that are inevitable with shielded metal arc welding. Not only does this have an economic advantage because the operating factor is raised, but the number of arc starts and stops, a potential source of weld discontinuities, is reduced.

Another major advantage is that increased amperages can be used with flux cored arc welding. With SMAW, there is a practical limit to the amount of current that may be used. The covered electrodes are 9 to 18 inches long, and if the current is raised too high, electrical resistance heating within the unused length of electrode will become so great that the coating ingredients may overheat and "break down." With the continuous flux cored electrodes, the tubular electrode is passed through a contact tip, where electrical energy is transferred to the electrode. The short distance from the contact tip to the end of the electrode, known as electrode extension or "stickout," prohibits the build up of heat due to electrical resistance. This electrode extension distance is typically 3/4 inch to 1 inch for flux cored electrodes, although it may be as high as two or three inches for some process variations.

Smaller diameter flux cored electrodes are suitable for all position welding. The larger electrodes, using higher electrical currents, typically are restricted to use in the flat and horizontal positions. Although the equipment required for flux cored welding is more expensive and more complicated than that for SMAW, most fabricators and erectors find the process much more economical than shielded metal arc welding.

3.5.2 FCAW Equipment and Procedures

As with all wire fed processes, flux cored arc welding requires a power source, wire feeder, and gun and cable assembly (see Fig. 3-5). The power supply is a direct current source, although either electrode positive or electrode negative polarity may be used. The four primary variables used to determine welding procedures are voltage, wire feed speed, electrode extension, and travel speed. For a given wire feed speed and electrode extension, a specific amperage will be delivered to maintain stable welding conditions.

As the wire feed speed is increased, the amperage will be increased. On some equipment, the wire feed speed control is called amperage control. Regardless of the name, it is a rheostat that regulates the speed of the DC motor that drives the electrode through the gun and cable. The most accurate way, however, to establish welding procedures, is to reference the wire feed speed (WFS), since electrode extension, polarity and electrode diameter will also affect amperage. For a fixed wire feed speed, a shorter electrical stickout will result in higher amperages. If procedures are set based on wire feed speed, the resulting amperage verifies that proper electrode extensions are being used. However, if amperage is used to set welding procedures, an inaccurate electrode extension may go undetected.

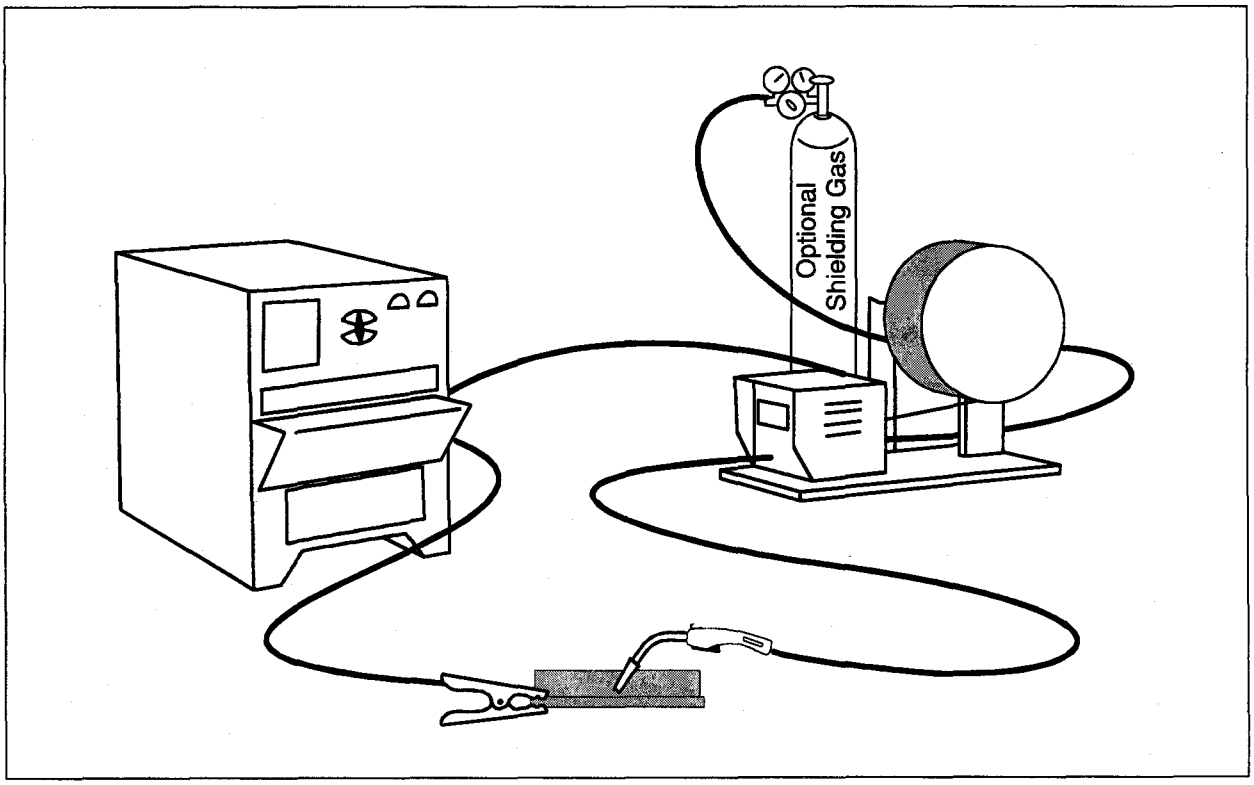

Figure 3-5 FCAW equipment

3.5.3 Self Shielded and Gas Shielded FCAW

Within the category of flux cored arc welding, there are two specific subsets: self shielded flux core (FCAW-ss) and gas shielded flux core (FCAW-g). Self shielded flux cored electrodes require no external shielding gas (see Fig. 3-6). The entire shielding system results from the flux ingredients contained within the core of the tubular electrode. This unique system is described in detail in **3.5.5**. The gas shielded (see Fig. 3-7) varieties of flux cored electrodes utilize, in addition to the flux core, an externally supplied shielding gas. In many cases, pure CO_2 is used, although mixtures of CO_2 and argon may be used.

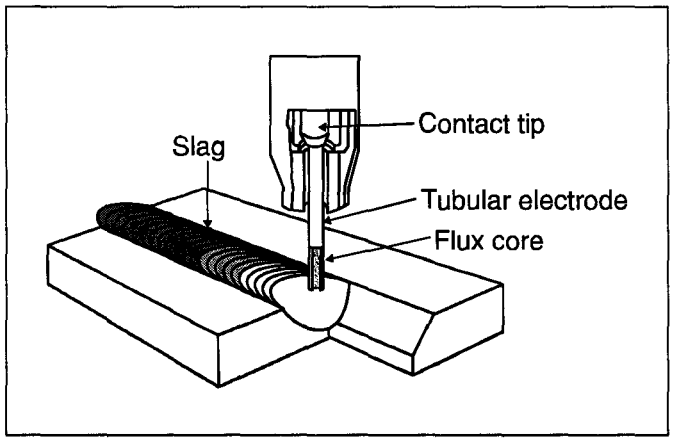

Figure 3-6 *Self shielded FCAW*

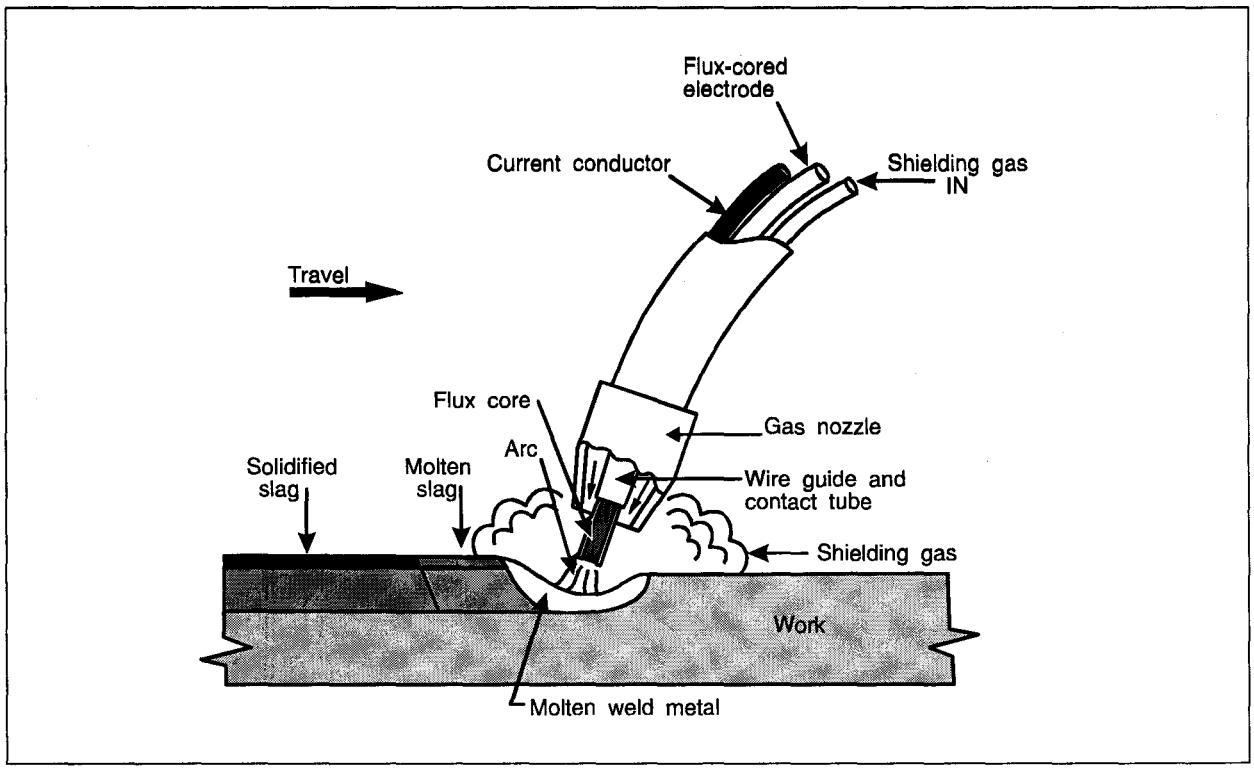

Figure 3-7 *Gas shielded FCAW*

Both types of flux cored arc welding are capable of delivering weld deposits featuring consistency, high quality, and excellent mechanical properties. In general, the fabricator will utilize the process that offers the greatest advantages for the particular environment. Self shielded flux cored electrodes are ideal for field welding situations. Since no externally supplied shielding gas is required, the process may be used in high winds without adversely affecting the quality of the deposit. With any of the gas shielded processes, wind shields must be erected to preclude interference with the gas shield in windy weather. Many fabricators with large shops have found self shielded flux core offers advantages when the shop door is left open or fans are used to improve ventilation. Finally, recent developments in the technology have made this process capable of delivering weld deposits with very high notch toughness and lower diffusible hydrogen levels.

Gas shielded flux cored electrodes tend to be more versatile than self shielded flux cored electrodes and, in general, provide better arc action. Operator appeal is usually higher. While the gas shield must be protected from winds and drafts, this is not difficult in most shop fabrication situations. Weld appearance is very good, and quality is outstanding. Higher strength gas shielded FCAW electrodes are available while current technology limits self shielded FCAW deposits to 90 ksi tensile strength or less.

Table **3.1** describes various FCAW electrodes listed in AWS A5.20 and A5.29. All of these electrodes are considered low hydrogen. Some of the electrodes have minimum specified notch toughness values although others do not. Some are gas shielded while others are self-shielded. Some are restricted to single pass applications, and others have restrictions on the thickness for their application. The electrical polarity used for the various electrodes is also shown. For critical applications in buildings that are subject to seismic loading, minimum notch toughness levels should be specified.

3.5.4 Advantages and Limitations of FCAW-ss

The welding process of choice for field erectors for the last 25 years has been FCAW-ss. This was the commonly used process for fabrication of steel structures throughout the United States, and specifically most, if not all, of the structures affected by the Northridge earthquake were fabricated by this process. Its advantages are reviewed in order to provide an understanding of why it was the preferred process. In addition, its limitations are outlined to highlight areas of potential concern.

The chief advantage of the FCAW-ss process is its ability to deposit quality weld metal under field conditions generally involving wind. In order to utilize gas shielded processes under these conditions, it is necessary to erect windshields to preclude movement of the shielding gas with respect to the molten weld puddle. While tents and other housings can be created to minimize this problem, such activities can be costly and are often a fire hazard. In addition, adequate ventilation must be provided for the welder. The most efficient windshields may preclude adequate ventilation. Under conditions of severe shielding loss, weld porosity will be exhibited. At much lower levels of shielding loss, the mechanical properties (toughness and ductility) may be negatively affected, although there will be no physical evidence that this is taking place.

The graph shown in Fig. 3-8 illustrates the effect of shielding gas loss on weld deposits, as well as the resistance to this problem with the FCAW-ss process (Boniszewski, 1992, ref. 29). The D1.1 code specifically limits wind velocity in the vicinity of a weld to a maximum of 5 miles per hour (D1.1-96, para. 5.12.1). This roughly corresponds with the point as shown in Fig. 3-8, where the properties of the gas shielded GMAW process become approximately equal to those of FCAW-ss.

A variety of other gas-related issues are also eliminated, including ensuring availability of gas, handling of high pressure cylinders (always a safety concern), theft of cylinders, protection of gas distribution hosing under field conditions, and the cost of shielding gas. Leaks in the delivery system obviously waste shielding gas, but the leak can also allow entry of air into the delivery system. Weld quality can be affected in the same way as shielding loss. Most field erectors have found it advantageous to utilize the gasless process and circumvent all such potential problems.

The FCAW-ss process also permits very high deposition rates. This has obvious productivity advantages, but must be carefully controlled to ensure that the required level of weld quality is consistently achieved. High deposition rates must be balanced with appropriate travel speeds to ensure that code mandated maximum bead sizes are maintained. Failure to do so will reduce notch toughness, reduce weld soundness (e.g., fusion), decrease heat affected zone toughness, and may decrease the weld metal yield and tensile strength.

Because the FCAW-ss welding gun assemblies are free from gas nozzles associated with gas shielded processes, the visibility of the arc is enhanced, and access into smaller areas is possible. This is particularly significant when welding in the constrained conditions of beam to column connections, and specifically when welding through weld access holes.

SMAW also may be used under field conditions. However, compared to FCAW, it results in much lower deposition rates and reduced penetration. Most importantly, the semiautomatic welding processes offer the advantage of fewer arc starts and stops, always an area of potential welding problems.

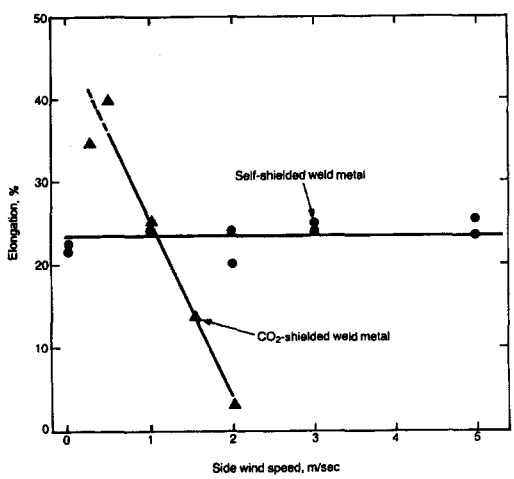

Comparison of the effect of side-wind speed on tensile elongation of: (a) CO_2-shielded and (b) self-shielded ferritic steel weld metals.
(a) Autio, Kettunen and Ström (1980); (b) Japanese work, IIW Doc. XII-317-66 (1966).

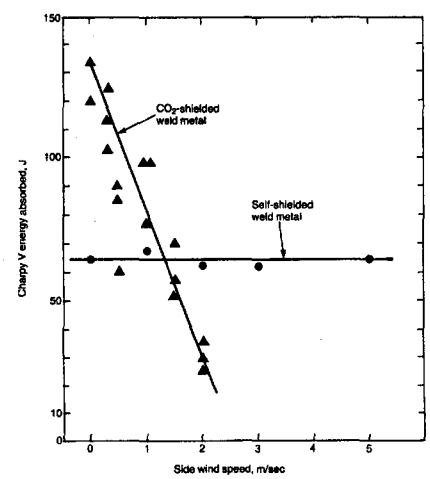

Comparison of the effect of side-wind speed on Charpy V-notch impact toughness of: (a) CO_2-shielded and (b) self-shielded ferritic steel weld metals. (a) Autio, Kettunen and Ström (1980), data generated at room temperature; (b) Japanese work, IIW Doc. XII-317-66 (1966), data generated at 0°C.

***Figure 3-8** Effect of wind on weld properties (Boniszewski, 1992, ref. 29)*

When an arc is initiated, a small amount of time is necessary for welding conditions to reach equilibrium. In the area of the start, the steel will be at a lower temperature than after the arc is initiated. It takes time for the shielding system to be established, so shielding is reduced under starting conditions. When the weld is terminated, the rapid withdrawal of the thermal energy delivered by the welding process causes an increase in the cooling rate. A reduction in shielding associated with the termination of the arc can also lead to inferior weld properties. For these reasons, weld tabs (see **2.10**) are employed in order to place weld starts and stops in the tab area outside the length of the weld joint. However, because of the finite length of SMAW electrodes, this process automatically requires that, except for very short weld joint lengths, weld starts and stops be contained within the joint itself. While it is possible to make high-quality welds under these conditions, it is easier to ensure quality when the continuous wire-fed semiautomatic processes are employed.

For shop fabrication, wind is less of a problem than under field conditions. Still, many fabrication shops would utilize FCAW-ss because of the advantages outlined above, including advantages of productivity. Wind can be a problem in fabrication shops that are not enclosed. Even in enclosed facilities, the breeze from opening a shop door can negatively effect weld properties. Fans used to cool the welder and to provide for ventilation can affect weld deposits. Finally, smoke exhaust equipment that regulates air quality may negatively effect the deposit characteristics of gas shielded methods, while the FCAW-ss remains immune.

FCAW-ss is more sensitive to variations in electrode extension and arc voltage than is FCAW-g. The range of suitable applications for a single size and classification of FCAW-ss electrode is more limited than for the gas-shielded counterpart. "Operator friendliness" for FCAW-g is generally superior to FCAW-ss.

3.5.5 Metallurgy of FCAW-ss

In section **3.1.2**, two forms of protection from the atmospheric gases that can contaminate weld metal were described: shielding and fluxing. FCAW-ss uniquely relies on a third mechanism as the primary method of protecting the weld metal from the atmosphere. Instead of excluding the atmosphere (as is done with gas shielding), or providing a slag as a physical barrier, FCAW-ss uses aluminum as a deoxidizer and denitrider. Aluminum is typically present at a level of 0.5 - 1.5%, significantly higher than the aluminum contents typically found in steels. Low levels of aluminum in both base metal and weld metal have been known to cause a reduction in toughness, so the higher levels of aluminum found in the weld deposits of FCAW-ss have generated justifiable curiosity. When present at levels of 1%, the behavior of aluminum is significantly different than that obtained at the 0.1% level, for example. Significant quantities of nitrogen may be contained in the weld metal of FCAW-ss, but this nitrogen is typically in the compound of Al-N. While the nitrogen content may be 500 ppm, the available 10,000 ppm level of aluminum ensures that there is always excess aluminum to ensure formation of Al-N (which requires an Al:N ratio of approximately 2:1). The remaining aluminum therefore acts as an alloying agent in the iron.

The iron-aluminum phase diagram shows that, at aluminum contents of approximately 1%, the gamma loop is closed, and the austenite to ferrite transformation is eliminated. This means that, at room temperature, the resulting weld metal is Delta-ferrite and has not undergone transformations as it solidifies and cools. These transformations aid in grain refinement. To restore the transformations necessary for grain refining, other alloying agents must be added, including carbon, manganese, and nickel. Electrodes such as E70T-4 and E70T-7 utilize carbon in levels of approximately 0.20% to restore the gamma loop and provide for some degree of grain refinement. However, these products do not have minimum

levels of notch toughness. Where notch toughness is required, alloy additions of manganese and/or nickel are often used. These alloys also expand the gamma loop, allowing for grain refining transformations to take place. The carbon content of these types of weld deposits is typically less than 0.08% (Boniszewski, 1992, ref. 29).

3.5.6 Intermixing of Weld Deposits

The unique characteristics of a properly made FCAW-ss weld deposit have been discussed in **3.5.5**. The balance between aluminum and nitrogen, as well as carbon and other alloying elements, must be properly maintained to ensure the specified mechanical properties are obtained from the weld deposit. When weld processes that use consumables that derive their properties from significantly different metallurgical mechanisms are mixed in a single joint, however, there is the potential for negative interaction. For example, if a root pass is made with FCAW-ss, and the subsequent fill passes are made with SAW, the properties of the SAW deposit may be negatively affected in terms of ductility and toughness.

This phenomenon appears to be the result of the liberation of nitrogen and aluminum that were previously chemically combined as Al-N in the FCAW-ss deposit. The SAW weld metal, typically a carbon-manganese-silicon metallurgical system, does not contain the amount of aluminum necessary in order to preclude the formation of free nitrogen which can embrittle the steel. In addition, the SAW weld metal does not necessarily contain the balance of other metallic ingredients needed to overcome harmful effects of small aluminum additions. Thus, the notch toughness of the carbon-manganese-silicon weld metal deposited by the SAW process may be significantly reduced by the introduction of free nitrogen and small levels of aluminum. The traditional assumption is that this concern exists only for non-FCAW-ss weld deposits on top of FCAW-ss. However, preliminary tests indicate that there may be some concern with other combinations of welding processes.

The use of multiple weld processes in a single weld joint may occur for several reasons. Tack welding might be performed with one process, and the completion of the joint made with another. The more demanding welding conditions of root pass welding, and particularly open root joints (i.e., no backing) may dictate a different weld process for the root pass. Multiple processes also may result when repair welding is being performed with a separate process than the original method used to fabricate the joint. When non-FCAW-ss weld processes are used on top of welds made by FCAW-ss, the potential for negative effects must be investigated.

The resulting mechanical properties of subsequent welds will be dependent on many variables, including: the original composition of the FCAW-ss deposit; the degree of admixture (related to penetration) that will occur in the subsequent welding; and the actual level of mechanical properties delivered by the subsequent weld process when they are unaffected by FCAW-ss interactions. For example, when deep penetrating submerged arc welding is used upon high aluminum content FCAW-ss welds, the moderate notch toughness of undiluted SAW weld metal (which maybe 40 ft-lbs. @ -20°F) may decrease to less than 15 ft.-lbs. at the same temperature. In contrast, a shallow penetrating undiluted SMAW weld deposit made with E7018 may find the excellent notch toughness of 150 ft.-lbs. may decrease to 80 ft.-lbs. at the same temperature, even though the resultant toughness may be more than adequate for the application.

Two approaches can be taken with respect to this issue. First, the same process can be used throughout, eliminating potential concerns. Secondly, the potential interaction of the two processes can be evaluated by testing. This approach is recommended by the SAC Interim Guidelines (SAC Joint Venture, 1995, ref. 39). More research in this area is currently being conducted and will be made available to the SAC organization as results are finalized.

3.5.7 Shielding Gases for FCAW-g

Most of the gas shielded flux cored electrodes utilize carbon dioxide for the shielding media. However, electrodes may also be shielded with an argon-CO_2 mixture. The carbon dioxide content is typically 10% to 25%, with the balance composed of argon. This is done to enhance welding characteristics. In order to utilize the argon based shielding gases, arc voltages are typically reduced by two volts from the level used with carbon dioxide shielding.

The selection of shielding gas may affect mechanical properties, including yield and tensile strength, elongation, and notch toughness. This is largely due to the difference in alloy recovery--that is, the amount of alloy transferred from the filler material to the weld deposit. Carbon dioxide is a reactive gas that may cause some of the alloys contained in the electrode to be oxidized, and less alloy is transferred to the deposit. When a portion of this active carbon dioxide is replaced with an inert gas such as argon, recovery typically increases, resulting in more alloy in the weld deposit. Generally, this will result in higher yield and tensile strengths, accompanied by a reduction in elongation. The notch toughness of the weld deposit may go up or down, depending on the particular alloy whose recovery is increased.

3.5.8 FCAW Filler Metals

Filler metals for flux cored arc welding are specified in AWS A5.20 and A5.29. A5.20 covers mild steel electrodes, while A5.29 addresses low alloy materials. The classification format is shown in Fig. 3-9. A "1" in the position before the "T" indicates an all position electrode, while a "0" would be applied to an electrode designed for flat and horizontal welding only. The suffix indicates the type of electrode, whether self shielded or gas shielded, the level of impact properties required (if any), whether the electrode is suitable for single pass only or for multiple pass operation, the polarity to be used, and the chemical composition of the deposited metal. Positive polarity is always used for FCAW-g, although the self shielded electrodes may be used on either polarity, depending on their classification. Under A5.29 for alloy electrodes, a suffix letter followed by a number appears at the end. Common designations include "Ni1" indicating a nominal nickel content in the deposited metal of 1%. The letter "M" could appear at the end of the electrode classification. If this is done, the electrode has been designed for operation with mixed shielding gas, that is an Argon-CO_2 blend that consists of 75 - 80% Argon. Other suffix designators may be used that indicate increased notch toughness capabilities, and/or extra low diffusible hydrogen contents.

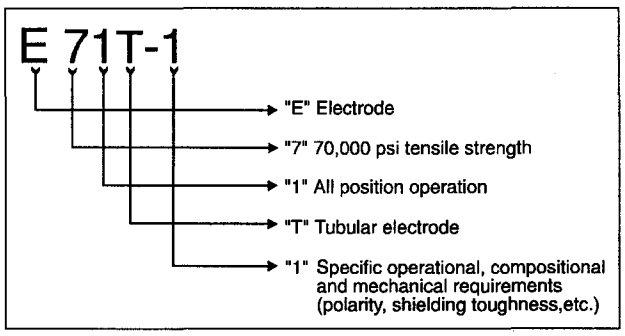

Figure 3-9 FCAW electrode classification

	FCAW ELECTRODE CLASSIFICATION			
AWS Classification [1]	Single / [2] Multiple Pass	CVN Requirements [3]	Polarity	Shielding Gas
AWS A5.20				
E7XT-1, -1M	M	20 @ 0	DC+	YES
E7XT-2 [(4)]	S	NONE	DC+	YES
E7XT-3 [(4)]	S	NONE	DC+	NO
E7XT-4	M	NONE	DC-	NO
E7XT-5, -5M	M	20 @ -20	DC+	YES
E7XT-6	M	20 @ -20	DC+	YES
E7XT-7	M	NONE	DC-	NO
E7XT-8	M	20 @ -20	DC-	NO
E7XT-9	M	20 @ -20	DC+	YES
E7XT-10 [(4)]	S	NONE	DC-	NO
E7XT-11	M	NONE	DC-	NO
E7XT-12, -12M	M	20 @ -20	DC+	YES
E7XT-13	S	NONE	DC-	NO
E7XT-14	S	NONE	DC-	NO
E7XT-G	M	NONE	Not Specified	Not Specified
E7XT-GS	S	NONE	Not Specified	Not Specified
AWS A5.29 [(5)]				
E6XT1 - Ni1	M	20 @ -20	DC+	YES
E6XT8 -K6	M	20 @ -20	DC-	NO
E7XT4 -K2	M	20 @ - 0	DC+	NO
E7XT5 -K6	M	20 @ -75	DC+	YES
E7XT7 -K2	M	20 @ -20	DC-	NO
E7XT8 -K2	M	20 @ -20	DC-	NO
E7XT8 -K6	M	20 @ -20	DC-	NO
E7XT8 - Ni1	M	20 @ -20	DC-	NO
E7XT8 - Ni2	M	20 @ -20	DC-	NO

Table 3.1

NOTES: 1) An "X" in the electrode classification will designate the welding positions possible. A "1" represents an all position electrode while a "O" indicates a flat and horizontal position only electrode.

2) "M" indicates single or multiple pass; "S" indicates single pass only.

3) The first number represents the energy level in foot-pounds, and the second number is the test temperature in degrees Fahrenheit.

4) These single pass electrodes are specifically exempted from prequalified usage in AWS D1.1, Table 3.1.

5) Not all A5.29 electrodes are listed as many are of a tensile strength level (>80 KSI) that is not required for most building construction, or are classified in the post weld heat treated (stress relieved) condition.

3.6 Submerged Arc Welding (SAW)

Submerged arc welding differs from other arc welding processes (see Fig. 3-10) in that a blanket of fusible granular material called flux is used for shielding the arc and the molten metal. The arc is struck between the workpiece and a bare wire electrode, the tip of which is submerged in the flux. Since the arc is completely covered by the flux, it is not visible and the weld is made without the flash, spatter, and sparks that characterize the open-arc processes. The nature of the flux is such that very little smoke or visible fumes are developed.

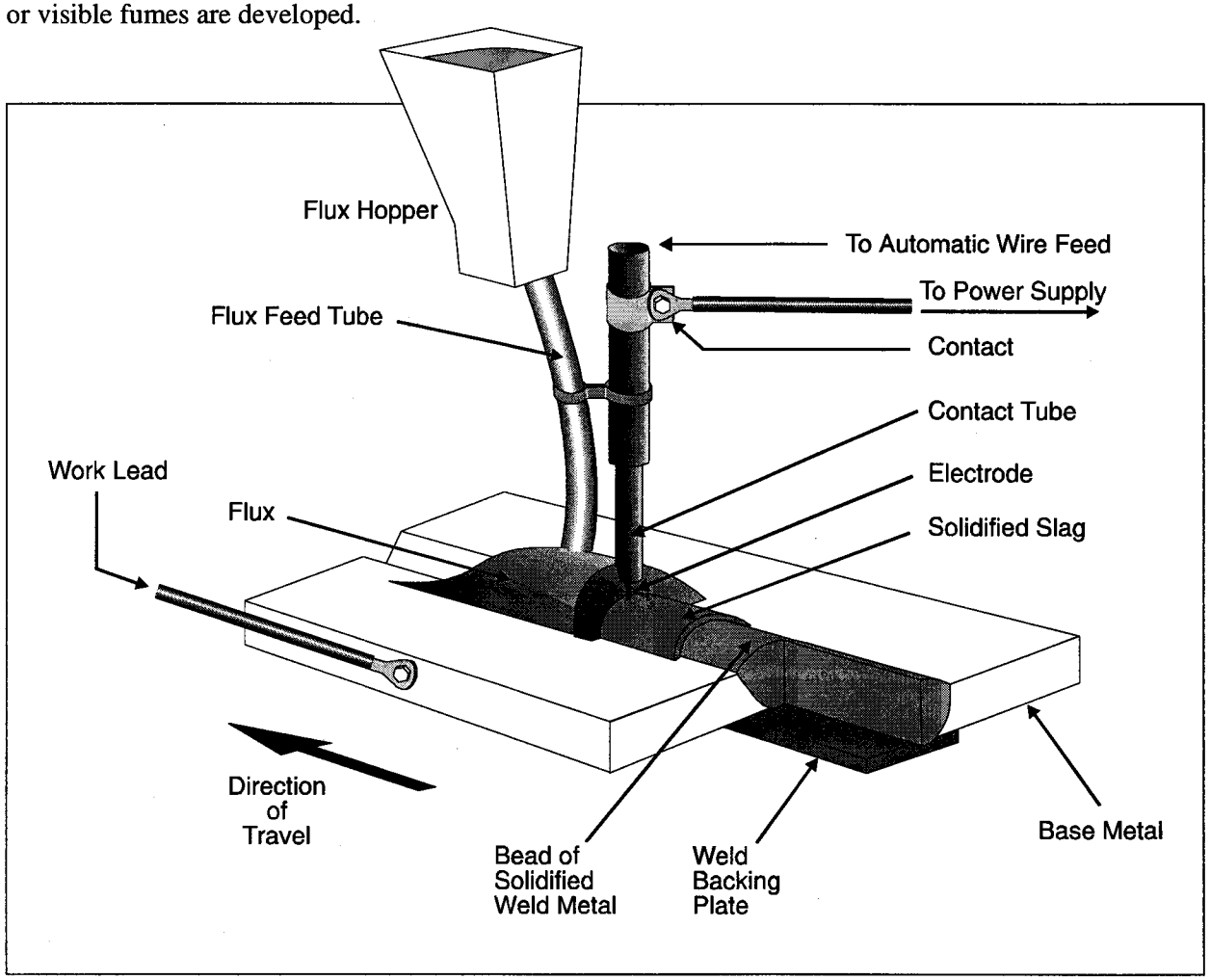

Figure 3-10 *SAW process*

The process is typically fully mechanized, although semiautomatic operation is often used. The electrode is fed mechanically to the welding gun, head, or heads. In semiautomatic welding, the welder moves the gun, usually equipped with a flux-feeding device, along the joint.

Flux feed may be by gravity flow through a nozzle concentric with the electrode from a small hopper atop the torch or it may be through a concentric nozzle tube connected to an air-pressurized flux tank. Flux may also be applied in advance of the welding operation or ahead of the arc from a hopper run along the joint. Many fully mechanized installations are equipped with vacuum systems to pick up the unfused flux left after welding for reuse.

During welding, the heat of the arc melts some of the flux along with the tip of the electrode, as illustrated in Fig. 3-11. The tip of the electrode and the welding zone are always shielded by molten flux, surrounded by a layer of unfused flux. The electrode is maintained a short distance above the workpiece. As the electrode progresses along the joint, the lighter molten flux rises above the molten metal in the form of a slag. The weld metal, having a higher melting (freezing) point, solidifies while the slag above it is still molten. The slag then freezes over the newly solidified weld metal, continuing to protect the metal from contamination while it is very hot and reactive with atmospheric oxygen and nitrogen. Upon cooling and removal of any unmelted flux for reuse, the slag is easily peeled from the weld.

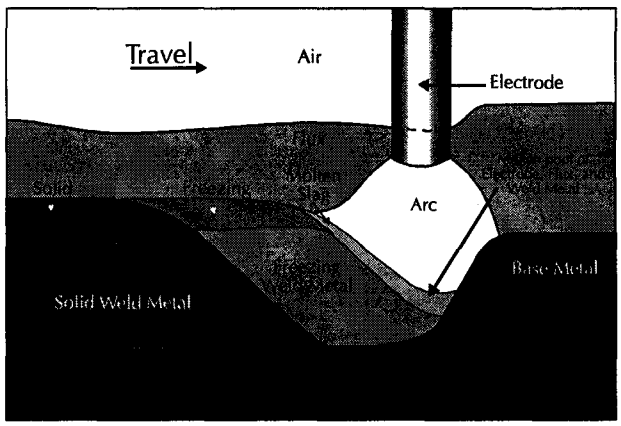

Figure 3-11 SAW cross section

3.6.1 Advantages of SAW

High currents can be used in submerged arc welding and extremely high heat input levels can be developed. Because the current is applied to the electrode a short distance above its arc, relatively high amperages can be used on small diameter electrodes. This results in extremely high current densities on relatively small cross sections of electrode. Currents as high as 600 A can be carried on electrodes as small as 5/64 in., giving a density on the order of 125,000 A/in.^{2} — 6 to 10 times that carried on stick electrodes. This results in high deposition rates and deep penetration.

The insulating blanket of flux above the arc prevents rapid escape of heat and concentrates it in the welding zone. Not only are the electrode and base metal melted rapidly, but the fusion is deep into the base metal. The deep penetration allows the use of small welding grooves, thus minimizing the amount of filler metal per foot of joint and permitting fast welding speeds. Fast welding, in turn, minimizes the total heat input into the assembly and thus tends to limit problems of heat distortion. Even relatively thick joints can be welded in one pass by the submerged arc welding process.

Welds made under the protective layer of flux have good ductility, toughness, and a uniform bead appearance. Since the process develops a minimum amount of smoke, the surrounding plate surfaces remain clear of smoke deposits. The high quality of submerged arc welds, the high deposition rates, the deep penetration characteristics, and the easy adaptability of the process to full mechanization make it ideal for the fabrication of structural members.

One of the greatest benefits of the process is the freedom from the open arc. This allows multiple arcs to be operated in a tight, confined area without the need for extensive shields to guard the operators

from arc flash. Extremely high amperages may be used that would be impractical for an open arc process. Yet this advantage also proves to be one of the chief drawbacks of the process; it does not allow the operator to observe the weld puddle. When SAW is applied semi-automatically, the operator must learn to carefully propel the torch in a fashion to ensure uniform bead contour. The experienced operator relies on the uniform formation of a slag blanket to indicate the nature of the deposit. For single pass welds, this is mastered fairly readily; however, for multiple pass welding, the skills required are significant. Therefore, most submerged arc welding applications are mechanized. The nature of the joint must then lend itself to automation if the process is to prove viable. Long, uninterrupted straight seams are ideal applications for submerged arc welding. Short, intermittent welds are better made with one of the open arc processes.

Multiple Electrode SAW refers to a variation of submerged arc welding which utilizes at least two separate power supplies, two separate wire drives, and feeds two electrodes independently. In most applications, the lead electrode operates on DC current, while the trail electrode is operated with AC. This is done to minimize the potentially negative interaction of magnetic fields between the two electrodes.

3.6.2 SAW Electrode Classification

Submerged arc filler materials are classified under AWS A5.17 for mild steel and AWS A5.23 for low alloy filler materials. Both fluxes and electrodes are covered under these specifications. Since submerged arc welding is a two-component process, that is, flux and electrode, the classification system is slightly different than for other filler materials.

Electrodes are classified based on the composition of the electrode. Under A5.17, the electrode will carry a classification that consists of two letters, one or two numerical digits and, in some cases, a final letter, as illustrated in Fig. 3-12. The first letter is an E, which stands for electrode. The second letter will be L, M, or H, referring to a low, medium, or high level of manganese in the electrode. The next one or two digits refer to the nominal carbon content in hundredths of a percent. A "12" in this location, for example, would indicate a nominal carbon content of 0.12%. It should be emphasized that this is the nominal value; it is possible to have higher and lower carbon contents in a specific electrode. In some cases, the electrode will be made of killed steel. When this is the case, silicon normally is added and the electrode will have a "K" at the end of the classification.

Electrodes classified under A5.23, the low alloy variety, have a more complex nomenclature, because of the variety of alloys that may be involved. The most important alloys for structural welding are the "Ni," or nickel alloys, and "W," or weathering alloys.

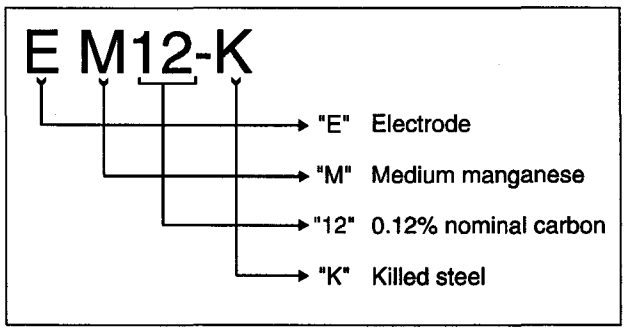

Figure 3-12 SAW electrode classification

3.6.3 SAW Flux Classification

Fluxes are always classified in conjunction with an electrode. The flux-electrode combination must meet specific mechanical property requirements. After a flux is selected and a classification test plate welded, a flux-electrode classification may be established. Specimens are extracted from the weld deposit to obtain the mechanical properties of the flux-electrode combination. As illustrated in Fig. 3-13, the classification will follow the format of an F followed by a single or two digit number, an A or P, a single digit and a hyphen which separates the electrode classification. Thus, a typical flux-electrode may be classified as an F7A2-EM12K. The "F" stands for flux, and the "7" indicates all of the following: a 70-95 ksi tensile strength deposit, a 58,000 psi minimum yield strength, and a minimum of 22% elongation. The "A" indicates the deposit is tested in the as-welded condition. The "2" after the "A" indicates that the particular flux-electrode combination is capable of delivering a minimum notch toughness of 20 ft.-lbs. at -20°F, where the "2" refers to the temperature (e.g. - 20°F). A zero at this location would refer to 20 ft.-lbs. at 0°F.

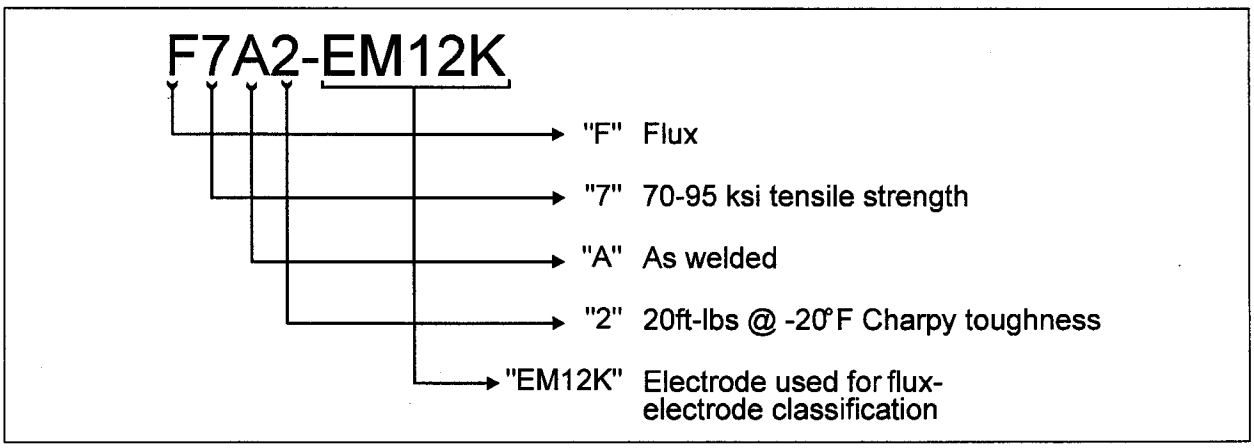

Figure 3-13 *SAW flux-electrode classification*

Because of the popularity of the submerged arc welding process for pressure vessel fabrication where assemblies are routinely stress relieved, submerged arc products may be classified in the post weld heat treated, or stress relieved, condition. When this is done, a "P" replaces the "A". For structural work, which is seldom stress relieved, the "A" classification is more common.

When a structural member will be stress relieved, it is important to examine the effect this will have on weld properties. The tensile strength may decrease. In many applications, there is a sufficient margin in the filler metal capacity to allow for some softening in the deposit under stress relief while still retaining a metal that is stronger than the base material. The engineer should be aware, however, that flux-electrode combinations classified in the post weld stress relieved condition may not exhibit notch toughness when used in the as-welded condition. Investigation into weld metal properties is warranted whenever the weld will be treated differently than the filler metal classification condition. In addition, the behavior of the base metal and the heat affected zone under stress relief conditions should be investigated.

For products classified under A5.23, a format similar to that of A5.17 is used, with this major exception: at the end of the flux-electrode classification, a weld deposit composition is specified. For example, an F7A2-ENi1-Ni1 would indicate that the electrode, an ENi1, delivers an F7A2 deposit when used with a specific flux. In addition, the deposit has a composition that meets the requirements of an

Ni1. In this case, a nickel bearing electrode deposits a weld that contains nickel. The example is straightforward. However, it is also possible to use alloy fluxes which, with mild steel electrodes, are capable of delivering alloy weld metal. In this case, a typical classification may be an F7A2-EL12-Nil. In this example, an EL12 electrode (a non-alloy electrode that contains a low level of manganese) is used with an alloy flux. The result is an alloyed deposit. This is commonly done when nickel bearing deposits are desired on weathering steel that will not be painted.

3.6.4 Reclaiming and Care of Flux

Only part of the flux deposited from a hopper or a gun is fused in welding. The unfused, granular flux may be recovered for future use and is known as reclaimed flux. The unmelted flux does not undergo chemical changes and is therefore capable of delivering quality welds when used the next time. However, this flux may be contaminated in the act of recovery. If it comes in contact with oil, moisture, dirt, scale or other contaminants, the weld deposit made with reclaimed flux may suffer. Care should be exercised to ensure that flux is not thus contaminated. The method of flux recovery varies from sweeping up the flux with broom and pans, to vacuum recovery systems.

Larger pieces of fused slag should be separated from the recovered flux in order to avoid flux feeding problems. The automated systems typically have screening to handle this. The fused slag may be chemically different than the unfused flux. For less critical applications, this slag may be crushed and thoroughly inter-mixed with new flux. This is sometimes called "recycled flux," but since recovered flux can be referred to by the same term, a better description for this product is "crushed slag." Performance and mechanical properties of recrushed slag may differ from those of virgin flux.

Flux must be stored so that it remains dry. The guidelines of the flux manufacture regarding storage and usage of the flux must be followed. In use, granules of flux that are reclaimed must not come in direct contact with water since weld cracking can result if this flux is reused. Fluxes can be contaminated with moisture from the atmosphere, so exposure should be limited. When not in use, flux hoppers should be covered or otherwise protected from the atmosphere.

3.7 Gas Metal Arc Welding (GMAW)

Gas metal arc welding utilizes the same equipment as is used in flux cored arc welding (see Fig. 3-14). Indeed, the two processes are very similar. The major differences are: gas metal arc uses a solid or metal cored electrode, and leaves no appreciable amount of residual slag (see Fig. 3-15).

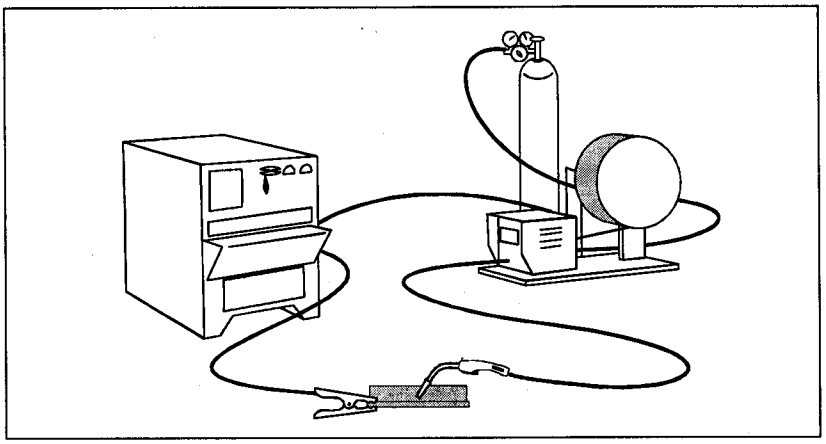

Figure 3-14 GMAW equipment

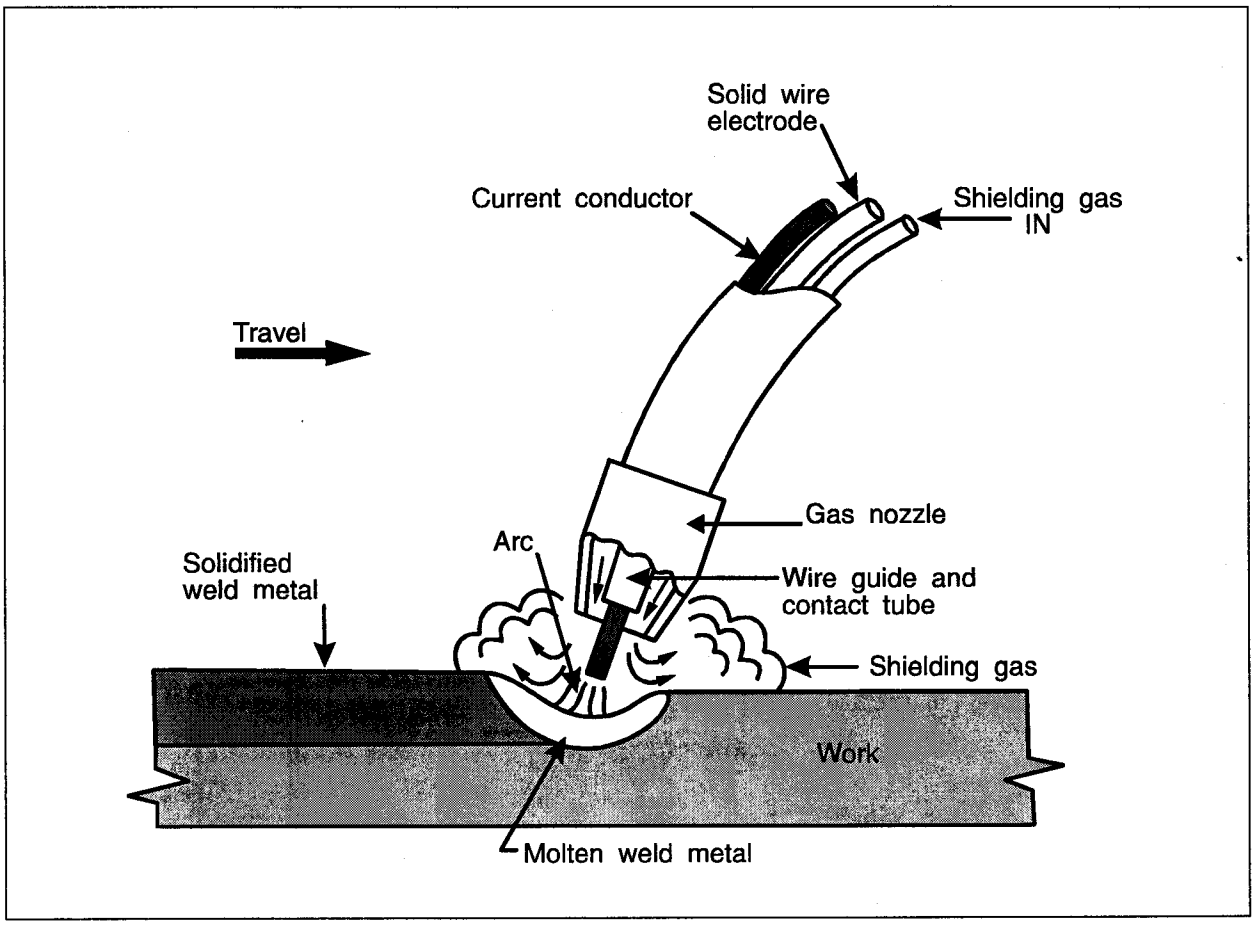

Figure 3-15 GMAW welding process

Gas metal arc has not been a particularly popular method of welding in the typical fabrication shop because of its sensitivity to mill scale, rust, limited puddle control, and sensitivity to shielding loss. Newer GMAW metal cored electrodes, however, are beginning to be used in the fabrication of structures with good success.

GMAW may be referred to as "MIG" (Metal Inert Gas), solid wire and gas, "mini-wire" or "microwire" welding. The shielding gas used may be carbon dioxide or blends of argon with either CO_2 or small levels of oxygen, or both. Gas metal arc is commonly applied in one of four ways: short arc transfer, globular transfer, spray arc transfer, and pulsed arc transfer.

GMAW typically employs solid electrodes, although metal cored electrodes could be used. In either case, the process is essentially free of fluxing ingredients that, after they have performed their function, form a slag over the weld deposit. Fluxing agents permit the welding of materials that contain surfaces that are less than optimum for ideal welding conditions. These situations include mill scale, rust, and other surface contaminants. Because GMAW does not contain fluxing ingredients, this process is restricted to welding on relatively clean materials. Common examples include sheet steel that is pickled and oiled. When the process is applied to hot rolled material, the mill scale may be removed by shot-blasting prior to welding in order to overcome the problems of these oxides.

3.7.1 Short Arc Transfer

Short arc transfer is ideal for welding on thin gauge materials. It is generally unsuitable for structural steel fabrication purposes. In this mode of transfer, the small diameter electrode, typically 0.035 in. or 0.045 in. is fed at a moderate wire feed speed at relatively low voltages. The electrode will touch the workpiece, resulting in a short in the electrical circuit. The arc will actually go out at this point, and very high currents will flow through the electrode, causing it to heat and melt. Just as excessive current flowing through a fuse causes it to blow, so the shorted electrode will separate from the work, initiating a momentary arc. A small amount of metal will be transferred to the work at this time.

The cycle will repeat itself again once the electrode shorts to the work. This occurs up to 200 times per second, creating a characteristic buzz to the arc. This mode of transfer is ideal for sheet metal, but results in significant fusion problems if applied to heavy materials. A phenomenon known as cold lap or cold casting may result where the metal does not fuse to the base material. This is unacceptable since the welded connections will have virtually no strength. Great caution must be exercised in the application of the short arc mode to heavy plates. The use of short arc on heavy plates is not totally prohibited, however, since it is the only mode of transfer that can be used out of position with gas metal arc welding, unless specialized equipment is used. Weld joint details must be carefully designed when short arc transfer is used. Welders must pass specific qualification tests before using this mode of transfer. The mode of transfer is often abbreviated as GMAW-s, and is not prequalified (D1.1-96, para. 3.2.1).

3.7.2 Spray Arc Transfer

Spray arc transfer is characterized by high wire feed speeds at relatively high voltages. A fine spray of molten drops, all smaller in diameter than the electrode diameter, is ejected from the electrode toward the work. Unlike short arc transfer, the arc in spray transfer is continuously maintained. High quality welds with particularly good appearance are the result. The shielding used for spray arc transfer is composed of at least 80% argon, with the balance made up of either carbon dioxide or oxygen. Typical mixtures would include 90-10 Argon-CO_2, and 95-5 Argon-Oxygen. Relatively high arc voltages are used with the spray mode of transfer. However, due to the intensity of the arc, spray arc is restricted to applications in the flat and horizontal position, because of the puddle fluidity, and lack of a slag to hold the molten metal in place.

3.7.3 Globular Transfer

Globular transfer is a mode of gas metal arc that results when high concentrations of carbon dioxide are used. Carbon dioxide is not an inert gas. Rather, it is active. Therefore, GMAW that uses CO_2 may be referred to as "MAG," for Metal Active Gas. With high concentrations of CO_2 in the shielding gas, the arc no longer behaves in a spray-like fashion, but larger globs of metal are ejected from the end of the electrode. This mode of transfer, while resulting in deep penetration, generates relatively high levels of spatter. Weld appearance can be poor. Like the spray mode, it is restricted to the flat and horizontal position. Globular transfer may be preferred over spray transfer because of the low cost of CO_2 shielding gas and the lower level of heat experienced by the operator.

3.7.4 Pulsed Arc Transfer

Another mode of transfer in gas metal arc welding is pulsed arc. In this mode, a background current is continuously applied to the electrode. A pulsing peak current is optimally applied at a rate that is proportional to the wire feed speed.

With this mode of transfer, the power supply delivers a pulse of current which, ideally, ejects a single droplet of metal from the electrode. The power supply returns to a lower background current which maintains the arc. This occurs between 100 and 400 times per second. One advantage of pulsed arc transfer is that it can be used out-of-position. For flat and horizontal work, it will not be as fast as spray transfer. However, used out-of-position, it is free of the problems associated with gas metal arc short circuiting mode. Weld appearance is good and quality can be excellent. The disadvantage of pulsed arc transfer is that the equipment is slightly more complex and more costly. The joints are still required to be relatively clean, and out-of-position welding is still more difficult than with processes that generate a slag that can support the molten puddle.

3.7.5 Metal Cored Electrodes

A relatively new development in gas metal arc welding is the use of metal cored electrodes. This is similar to flux cored arc welding in that the electrode is tubular, but the core material does not contain slag forming ingredients. Rather, a variety of metallic powders is contained in the core, resulting in exceptional alloy control. The resulting weld is essentially slag-free, just as with other forms of GMAW. The use of metal cored electrodes offers many fabrication advantages. Compared to spray transfer, metal cored electrodes require less amperage to obtain the same deposition rates. They have increased ability to handle mill scale and other surface contaminants. When used out-of-position, they offer greater resistance to the cold lapping phenomenon so common with short arc transfer. Finally, metal cored electrodes permit the use of high amperages that may not be practical with solid electrodes, resulting in higher deposition rates.

The properties obtained from metal cored deposits can be excellent. Appearance is very good. Because of the ability of the filler metal manufacturer to control the composition of the core ingredients, mechanical properties obtained from metal cored deposits may be more consistent than those obtained with solid electrodes.

3.7.6 Filler Metal Classification

Mild steel gas metal arc electrodes are classified according to AWS A5.17. AWS A5.28 covers classification of low alloy electrodes. Mechanical properties are determined from weld deposits. Chemical compositional requirements are based on electrode analysis for solid electrodes. Cored electrodes have compositional requirements based on deposit analysis. The format for classification to A5.18 is shown in Fig. 3-16. Classification is made under specific welding conditions that generally promote

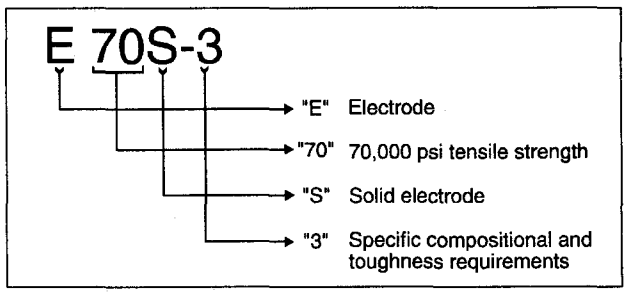

Figure 3-16 GMAW electrode classification

globular-type transfer. Carbon dioxide shielding gas is typically required. For classification of low alloy electrodes, a suffix is used to denote the electrode composition. These suffixes follow formats similar to those used for the submerged arc electrodes previously discussed.

3.8 Electroslag/Electrogas Welding (ESW/EGW)

Electroslag and electrogas welding are closely related processes that offer high deposition welding in the vertical plane. Properly applied, these processes offer tremendous savings over alternative, out-of-position, methodology and in many cases, savings over flat position welding. Although the two processes have similar applications and mechanical set up, there are fundamental differences in the arc characteristics.

Electroslag and electrogas are mechanically similar in that both utilize copper dams or shoes that are applied to either side of a square edged butt joint (see Fig. 3-17, 3-18). An electrode or multiple electrodes are fed into the joint. A starting sump is typically applied for the beginning of the weld. As the electrode is fed into the joint, a puddle is established that progresses vertically. The copper dams, which are commonly water cooled, chill the weld metal and prevent it from escaping from the joint. The weld is completed in one pass.

In building construction, applications for this process with traditional connection designs is somewhat limited. However, it can be highly efficient in the manufacture of tree columns. In the shop, the beam flange-to-column welds can be made with the column in the horizontal plane. With the proper equipment and tooling, all four flange welds can be made simultaneously. In addition, continuity plate welds can be made with this process. Future connection designs may utilize configurations that are more conducive to these processes.

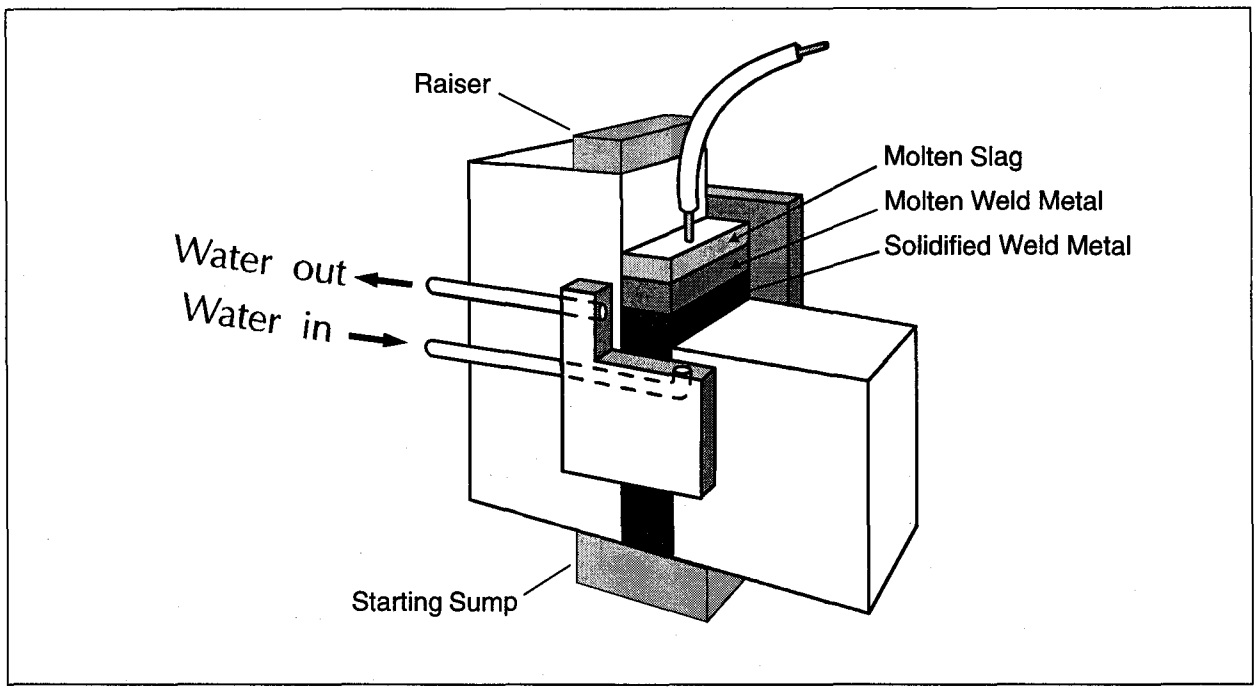

Figure 3-17 ESW process

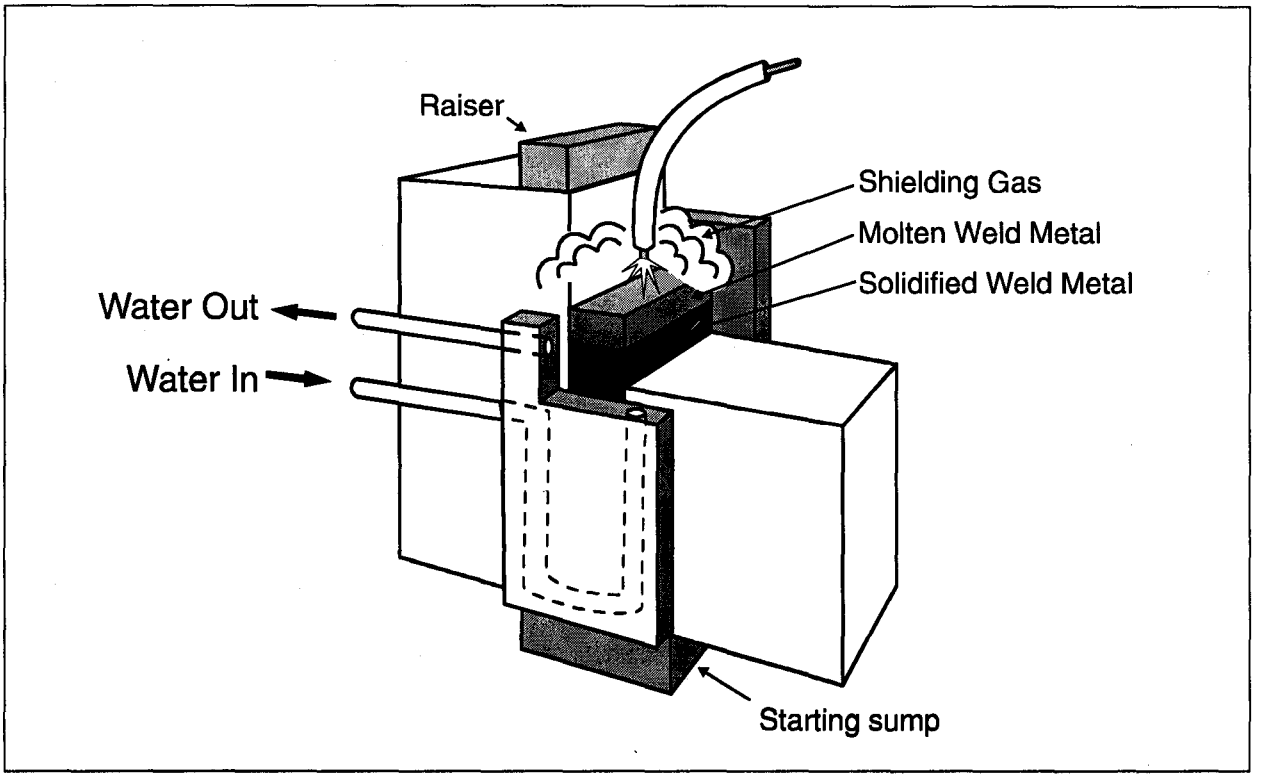

Figure 3-18 EGW process

Another common application is for the welding of continuity plates inside box columns. It is possible to weld three sides of the continuity plate to the interior of the box prior to closing the box with the fourth side. However, once this closure is made, access to the final side of the continuity plate is restricted. It is possible to use these processes to make this final closure weld by operating through a hole in the outside of the box column. This approach is very popular in the Far East where box columns have more widespread utilization.

3.8.1 Electroslag Welding

In electroslag welding, a granular flux is metered into the joint during the welding operation. At the beginning, an arc, similar to that of submerged arc welding, is established between the electrode and the sump.

After the initial flux is melted into a molten slag, the electrical characteristics change. The slag, which is carefully designed to be electrically conductive, will conduct the welding current from the electrode through the slag into the pieces of steel to be joined. As high currents are passed through the slag, it becomes very hot. The electrode is fed through the hot slag and melts. Technically, electroslag welding is not an arc welding process, but a resistance welding process. Once the arc is extinguished and the resistance melting process is stabilized, the weld continues vertically to completion. A small amount of slag is consumed as it chills against the water cooled copper shoes. In some cases, steel dams are used to retain the puddle. After completion of the weld, the steel dams stay in place, and become part of the final product. Slag must be replenished, and additional flux is continuously added to compensate for the loss.

One aspect of electroslag welding that must be considered is the very high heat input associated with the process. This causes a large heat affected zone (HAZ) that may have a lower notch toughness. The HAZ performance is dependent not only on the heat input, but also on the nature of the steel. While all processes develop a heat affected zone, the large size of the electroslag heat affected zone justifies additional scrutiny. Advances in steel technology have resulted in improved steels, featuring higher cleanliness and toughness, that better retain the HAZ properties in ESW/EGW welds.

3.8.2 Electrogas Welding

Electrogas welding is different from electroslag, inasmuch as no flux is used. Electrogas welding is a true arc welding process and is conceptually more like gas metal arc or flux cored arc welding. A solid or tubular electrode is fed into the joint that is flooded with an inert gas shield. The arc progresses vertically while the puddle is retained by the water cooled dams.

3.8.3 New Developments

A relatively new development in high deposition vertical welding utilizes a self-shielded flux cored electrode. Like electrogas welding, it is an arc welding process. However, a slag is formed on the surface as it progresses vertically. No gas is used. As the flux cored electrode is fed into the joint, the required flux additions are simultaneously supplied by the electrode. This helps overcome one of the problems with electroslag welding, which is that either too much or too little slag will result in welding problems (Lincoln Electric, 1995, ref. 30).

3.9 Gas Tungsten Arc Welding (GTAW)

The gas tungsten arc welding process (see Fig. 3-19), colloquially called TIG welding, is rarely used in the construction of structural steel members. However, it may be specified to meet some unique requirements, or for a repair welding procedure. GTAW uses a non-consumed electrode composed of

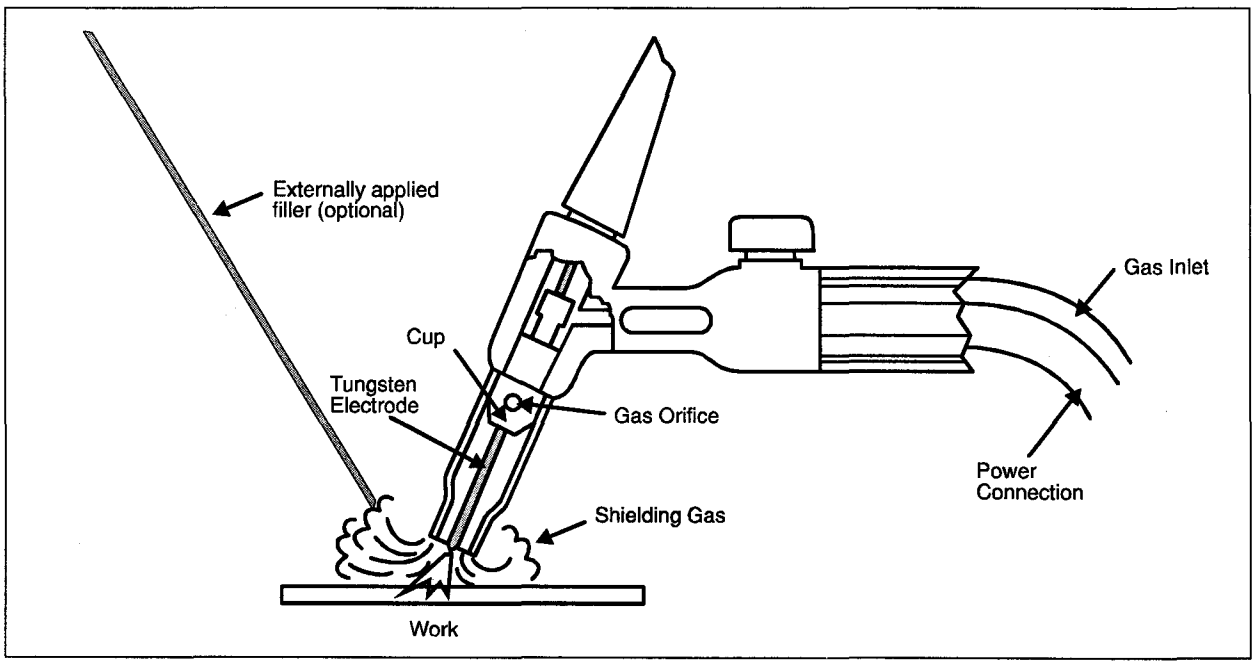

Figure 3-19 *Gas tungsten arc welding (GTAW)*

tungsten, a metal with a very high melting point. Between the tungsten and the work, an arc is established that results in heating of the base material. A filler rod may or may not be used. The area is shielded with an inert gas, typically argon, although helium or mixtures of argon and helium may be used. GTAW is ideally suited for welding on non-ferrous materials, such as stainless steel and aluminum.

3.10 Oxyfuel Cutting (OFC)

Oxyfuel cutting (OFC) is commonly used to sever steels and to prepare bevels (see Fig. 3-20). In this process, the metal is heated to its ignition temperature, or kindling point, by a series of preheat flames. After this temperature is attained, a high velocity stream of pure oxygen is introduced, which causes oxidation or "burning" to occur. The force of the oxygen stream blows the oxides out of the joint, resulting in a successful cut. The oxidation process also generates additional thermal energy, which is radially and axially conducted into the surrounding steel, increasing the temperature of the steel ahead of the cut. The next portion of the steel is raised to the kindling temperature and the cut proceeds.

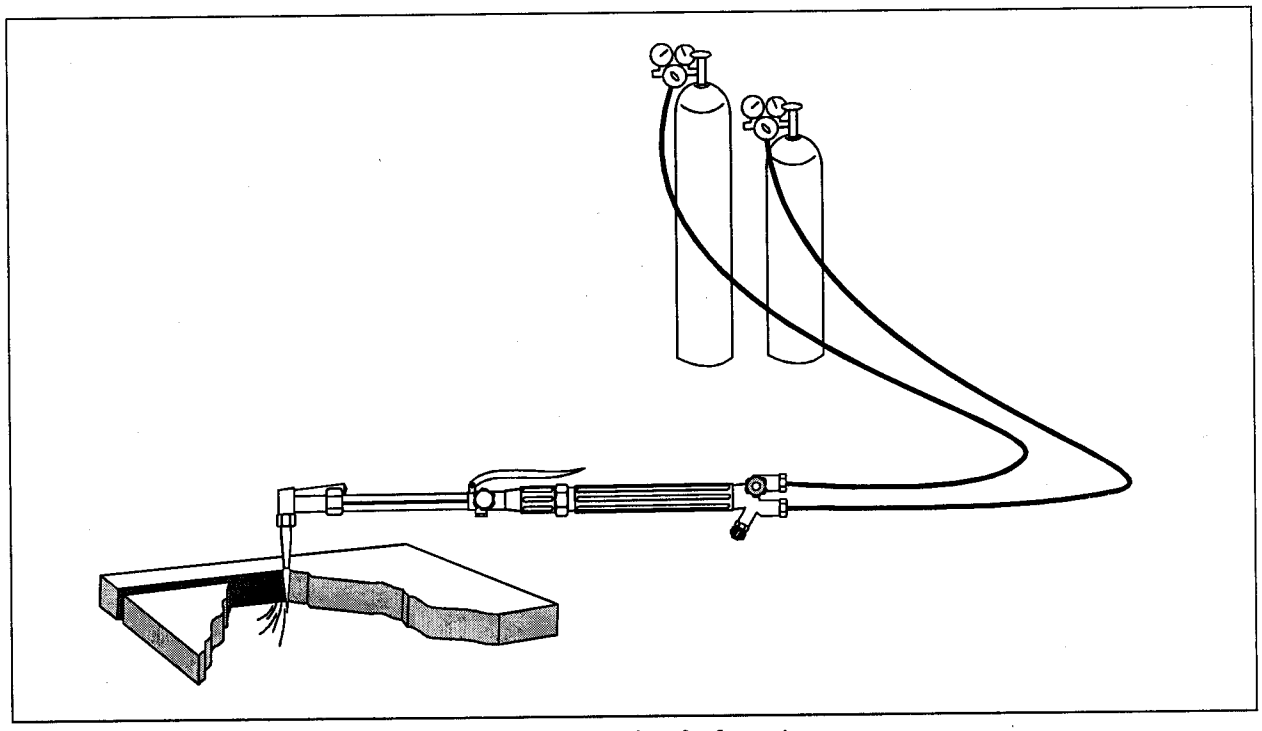

Figure 3-20 *Oxyfuel cutting*

Carbon and low alloy steels are easily cut with the oxyfuel process. Alloy steels are readily cut, but with greater difficulty than mild steel. The level of difficulty is a function of the alloy content. When the alloys are increased to the levels found in stainless steels, oxyfuel cutting cannot be used unless the process is modified by injecting flux or iron rich powders into the oxygen stream. Aluminum cannot be cut with the oxyfuel process. Oxyfuel cutting is commonly regarded as the most economical way to sever steel plates greater than 1/2" in thickness. It can be used to cut steels that are even thicker than those typically used in construction.

3.10.1 Gases Used in Oxyfuel Cutting

Any of a variety of fuel gases may be used for oxyfuel cutting, with the decision largely dependent on local economics. Popular gases include natural gas, propane, acetylene, and a variety of proprietary gases offering unique advantages. Because of its role in the primary cutting stream, oxygen is always used as the second gas. In addition to this function, a percentage of the oxygen is mixed with the fuel gas in ideal proportions to ensure proper combustion.

NOTE: Oxygen is incorrectly called "air" in some fabricating shops. Air from the atmosphere contains only 21% oxygen and is significantly different than the 100% pure oxygen used for cutting. The unintentional confusion of oxygen with air has resulted in fatal accidents. When compressed oxygen is inadvertently used to power air tools, for example, an explosion can result. While most people recognize that fuel gases are dangerous, it can be argued that oxygen requires even more careful handling.

3.10.2 Oxyfuel Equipment

The oxyfuel cutting process may be manual, where the torch is manipulated by an operator, or automated. Simple mechanization may involve an electrically powered carriage that holds the torch in the proper position and assures uniform travel speeds. Sophisticated automation may involve multiple torch cutting systems with automatic height sensors. These systems may be controlled by CAD/CAM programs. Mechanization offers two distinct advantages: quality and economy.

With the smooth travel offered by mechanical devices, the resulting cut will have a superior appearance. Higher cutting speeds may be used, resulting in greater economies. In the modern fabrication shop, oxyfuel cutting routinely is done with a torch propelled by some mechanical means.

3.10.3 Effect of Oxyfuel Cutting on Steel Properties

As a result of chemical and thermal effects experienced by steel during oxyfuel cutting, the surface of the cut edge changes. Along the cut edge, there is a thin boundary of steel which will contain a higher level of carbon than the average for the steel. Historically, many believed this increased carbon came from the oxyfuel flame. However, the correct explanation is that the carbon has migrated from the kerf of the cut. During the oxidation process, carbon will leave the kerf and attach itself to the adjoining steel. This region of increased carbon is very thin. However, because of the thermal effects that will be imposed upon the edge, it can play a significant role in the performance of that edge (Wilson, 1990, ref. 42).

Immediately adjacent to the cut, the steel will be heated to a temperature above the transformation point of the steel. The surrounding steel, acting as a heat sink, will cause the thermal cut edge to cool very rapidly. The edge may obtain a higher strength or hardness than the surrounding steel. Coupled with the enriched carbon previously described, very hard microstructures may develop along the edge of the steel that, in rare cases, can even contain microcracks.

In addition to the chemical and thermal effects described, the cut edge will contribute to distortion. As the cut edge experiences expansion due to the heat of the cutting process, and subsequent contraction upon cooling, it is possible to induce residual stresses that cause distortion. Even if distortion does not occur, residual stresses will be present in the cut member.

3.10.4 Visual Inspection of Cut Edges

Visual inspection of thermally cut edges is very important. During the cutting process, it is not uncommon to uncover inclusions, laminations, or other discontinuities in the steel. Careful inspection of the thermally cut edges at this point in time may eliminate the necessity of weld repairs in the future. Frequently, gouges in a mechanized cut are an indication of some discontinuity in the steel that interrupted the thermal cut. Smooth, uniform cut edges provide an assurance of uniformity in the steel.

Defects in thermally cut edges may be repaired by grinding or welding. Specific code provisions apply in these situations. The depth and nature of the discontinuity will dictate whether repair welding will be permitted. It is important to distinguish between edges which will be exposed, versus edges on which weld metal will be deposited. Exposed edges must be uniform and free of any notches or gouges which would adversely affect the performance of the member.

In many situations, simple grinding of the discontinuity to provide a smooth contour will be acceptable. This "fairing in" of the adjoining metal effectively eliminates the notch without introducing the potentially harmful residual stresses of welding.

3.10.5 Weld Joints vs. Exposed Edges

If the oxyfuel process is used to prepare a joint on which welding material will be placed, the concern about residual stress and localized hardened zones is reduced. The energy of the arc will melt part of the base material and effectively erase the thermal cycle experienced during cutting. In its place will be the thermal history created by the weld, which must always be considered in welding.

On thermally cut edges that will not receive weld metal deposits, the previously mentioned microcracks may be a concern. Heavy sections of low alloy steels (plates with a thickness of 4 in. or greater) may require a preheat of 150°F to be applied before cutting. Not only is the cooling rate reduced when this is done, but the effectiveness of cutting is increased, resulting in a higher quality cut surface. This is not typically done when the surfaces will have weld metal deposited upon them. Even if micro cracks are present on these surfaces, the penetration of welding will remelt these zones and eliminate these problems. It is important, however, that the surfaces on which weld metal will be placed be free of the scale that may be present after the cutting process. This thin layer of scale is typically removed with a chipping hammer or wire brushing.

3.11 Plasma Arc Cutting (PAC)

The plasma arc cutting process (see Fig. 3-21) was initially developed to cut the various materials

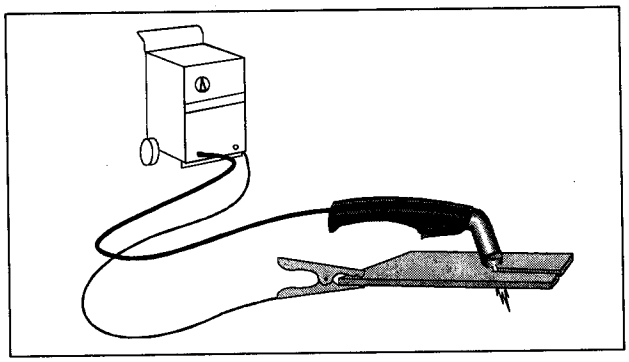

Figure 3-21 *Plasma arc cutting process*

that cannot be severed using the oxyfuel process: stainless steel and aluminum. It was found, however, that plasma arc cutting offered economic advantages when applied to thinner sections of mild steel, specifically, material less than one inch in thickness. Higher travel speeds were possible with plasma arc cutting and the area of heated base material was reduced, minimizing the effect of the metallurgical changes, as well as reducing distortion.

Plasma arc cutting is a thermal and mechanical process. The physics of plasma arc cutting consist of heating the material until molten and expelling it with a high velocity plasma stream. Unlike oxyfuel cutting, the process does not rely on oxidation. Because high energies can be introduced through the arc, the process is capable of extremely high travel speeds. The thermal energy generated during the oxidation process with oxyfuel cutting is not present in plasma, and hence, on thicker sections, plasma cutting is not economically justifiable. Thick section cutting with plasma arc is typically restricted to those materials that do not oxidize readily with oxyfuel.

3.11.1 Plasma Arc Cutting Equipment

Plasma arc cutting equipment is significantly different than that required for oxyfuel cutting. The source of energy is a power source that externally resembles that of an arc welder. Plasma arc cutting requires much higher voltages than are used with welding. This necessitates a significant difference in machine design.

3.11.2 Effects of PAC on Steel Properties

The effects of plasma arc cutting on steel are similar in many respects to the effects of oxyfuel cutting. However, there are distinct differences that should be understood. Like oxyfuel cutting, the plasma cutting system generates a small region that is heated and subsequently cooled by the surrounding materials. On thin plate, however, this zone is significantly smaller than with oxyfuel cutting, because of the higher speeds that are generated by the plasma arc process, and distortion may be reduced. Unlike oxyfuel cutting, plasma arc cutting does not result in an enrichment of carbon on the surface of the cut. However, depending on the gases that can be used in the cutting process, surface compounds may be deposited. These are largely compounds of nitrogen that come from the nitrogen or air used for the cutting gas. When the affected surfaces are welded, porosity may result. A series of complex interactions of cutting speed, gas type, and steel composition are involved. Under most conditions when this is encountered, the cut surfaces are ground before welding to remove any contamination.

With plasma arc cutting, the kerf typically will be composed of one side that has a 90° cut and the second side which will have a 3-5° bevel. When possible, the 90° cut is applied to the "good" side and the beveled side becomes the "scrap" side. Careful planning of the cutting sequence can minimize this problem.

3.12 Air Arc Gouging (AAG)

The air carbon arc gouging system utilizes an electric arc to melt the base material, and a high velocity jet of compressed air subsequently blows it away (see Fig. 3-22). The air carbon gouging torch looks much like a manual electrode holder, but in place of a metallic electrode, a carbon electrode with a copper sheath is used. As current is conducted through the base material, it is heated without depositing any metal. A valve in the torch handle permits compressed air to flow through three air ports. As the air hits the molten material, a combination of oxidation and expulsion of metal takes place, leaving a smooth cavity behind. The air carbon arc gouging system is capable of removing metal at a much higher rate than can be deposited by most welding processes. It is a powerful tool to remove metal at low cost.

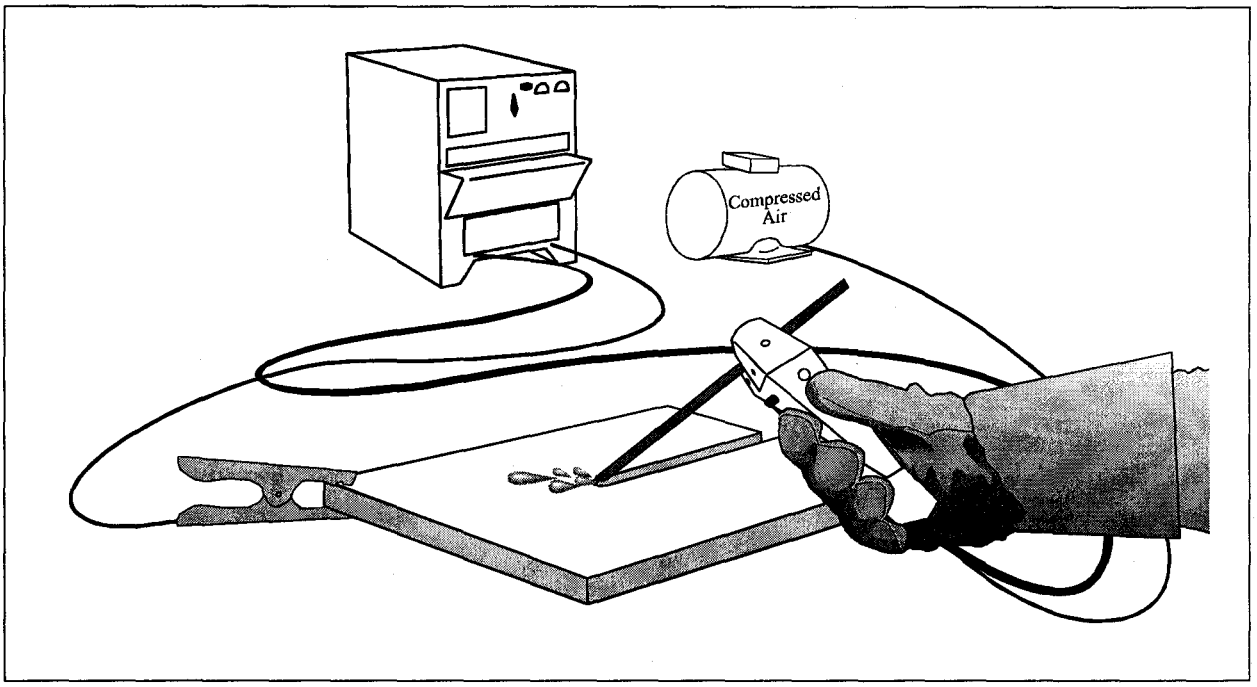

Figure 3-22 *Air arc gouging*

Air arc gouging may be used in the initial preparation of J or U grooves (see Fig. 3-23). On complete joint penetration groove welds made without backing, air arc gouging may be used to ensure that 100% fusion is obtained (see Fig. 3-24). Under this sequence, the first passes are applied from one side of the joint and the second side is gouged to solid metal. Air arc gouging may also be used to remove welds containing discontinuities.

Like the previously mentioned cutting processes, air arc gouging will leave behind a small region which may contain hardened microstructures or carbon deposits. However, most gouged surfaces will receive subsequent weld metal. The surfaces need only be clean, and the heat of welding will eliminate any potential problem with hardened zones caused by gouging.

Air arc electrodes are available in a variety of sizes. Larger electrodes require higher currents and remove metal more rapidly. It is important to realize that the electrode size will determine the joint geometry obtained after cutting. It is desirable for the root of the weld to have a generous radius and the sides of the joint to have an included angle of sufficient size to permit easy access. Improperly used, the air arc gouging system will generate small included groove angles, which make quality welding difficult. Any gouged joint should have a configuration that permits easy access to the root and is conducive to good fusion.

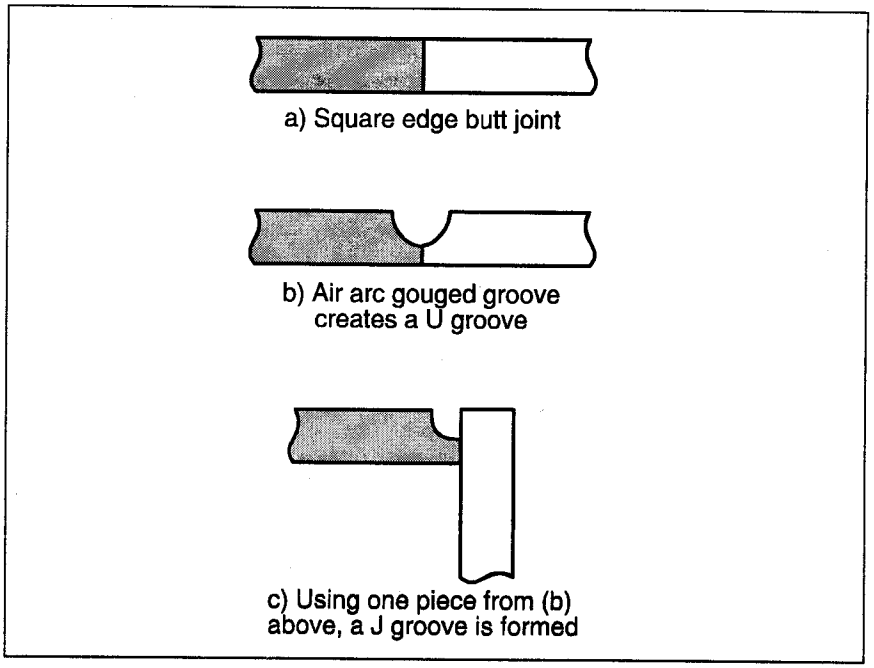

Figure 3-23 *Preparation of J and U grooves by AAG*

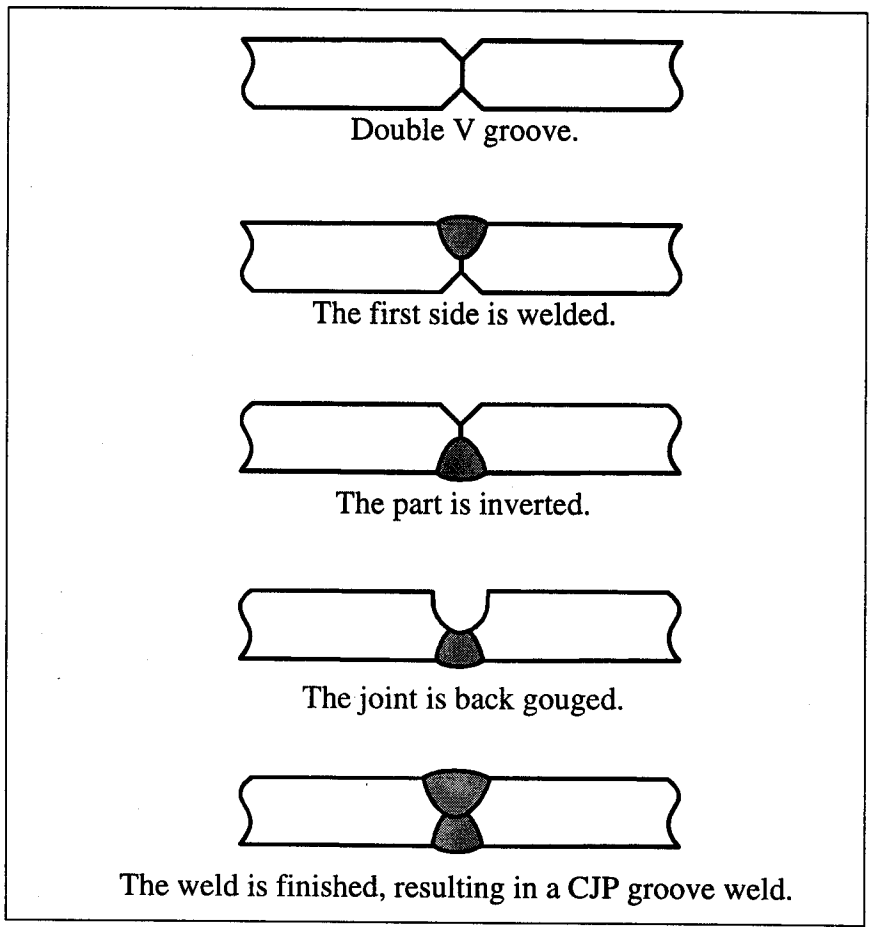

Figure 3-24 *Back gouging sequences to obtain CJP groove welds*

Air carbon arc gouging may be done either manually or mechanically. For preparation of the initial joint, the gouging system typically is automated. In this case, the electrode is automatically fed into the joint and the torch is propelled along the length of the joint. Quality and productivity are both enhanced by this system. For excavation of unacceptable weld metal, the manual mode of air arc gouging usually is applied. The power supply required for air arc gouging is similar to that used for production welding and in many situations, the same equipment will be used for welding and for gouging. Either AC or DC+ may be used, although DC+ is preferred. Special carbon electrodes must be used for AC, while all carbons may be used for DC operations.

3.13 Plasma Arc Gouging (PAG)

A relatively new development is the application of plasma arc equipment for gouging (see Fig. 3-25). The process is identical to plasma arc cutting, but the small diameter orifice is replaced with a larger one, resulting in a broader arc. More metal is heated, and a larger, broader stream of hot, high velocity plasma gas is directed toward the work. When the torch is inclined to the work surface, the metal can be removed in a fashion similar to air carbon arc gouging. The applications of the process are similar to those for air carbon arc gouging. The decision of whether to use air carbon gouging or plasma arc gouging depends on the availability of equipment and the relative economies as determined by the fabricator.

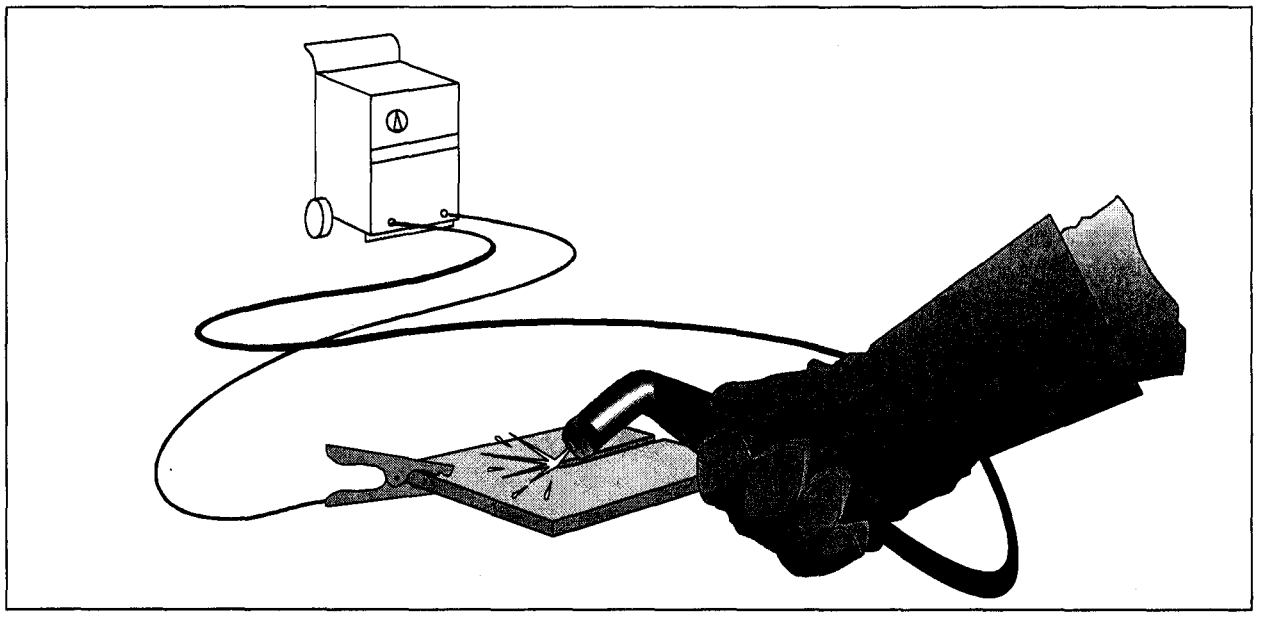

Figure 3-25 Plasma arc gouging

3.14 Flame Shrinking

Flame shrinking is a term used to describe the various operations that can be employed to shape or straighten steel members that require dimensional changes. Fabricators frequently utilize flame shrinking to adjust the camber and sweep, as well as to correct for unacceptably distorted members. The same process can be used to correct steel that has been bent or twisted due to overloads, unexpected collisions, and fire damage. It is a powerful tool that, in the hands of an experienced practitioner, can restore significantly distorted material to acceptable configurations.

The process relies on thermal expansion, constraint, localized upsetting, and subsequent cooling of steel. When steel is heated under conditions where complete restraint is offered in two orthogonal directions, all the volumetric expansion that takes place will occur in the third direction. If the amount of expansion exceeds the yield point strains for the particular material involved, thermal upsetting (i.e., plastic deformations) will occur in the region where the material is restrained. Upon cooling, the same volume of material that was previously heated must geometrically shrink. If it is not restrained in the same three orthogonal directions, it will be free to shrink in all three directions, resulting in a geometric change from the original configuration. The principles of expansion, constraint, and subsequent cooling that enable the heat shrinking process to work are the same principles that govern distortion that occurs during welding. By carefully controlling the expansion, constraint, and cooling of materials, flame shrinking can be utilized to move the material into a new configuration, or restore it to a previously acceptable configuration.

The techniques employed for flame shrinking will vary from simple approaches used to correct minor irregularities, to very complicated operations that require the experience and expertise of a specialist in the field. Multiple heating cycles with specific patterns are employed to correct complicated assemblies. A key aspect of the technique is to ensure a sufficient differential in temperature between the hot, expanded metal, and the cooler surrounding metal that provides the restraint. It necessitates that the torches used to heat the steel have the capacity to rapidly raise a portion of the material to the higher temperatures, whereupon localized expansion can occur before the thermal energy is conducted into the surrounding steel.

Under perfectly restrained conditions, a 50 Ksi yield strength steel will experience thermal upsetting with a net change in temperature of 256°F. Therefore, considering an ambient temperature of 70° F, thermal upsetting should occur if the steel is heated to 326° F. In practice, however, much higher temperatures are used because the region heated is rarely perfectly restrained and because of the greater efficiency that is gained. At higher temperatures, thermal conductivity decreases, thermal expansion increases, the yield strength decreases, and the modulus of elasticity decreases. All four of these activities increases the efficiency at which heat shrinking can occur. Excessively high temperatures, however, can damage the steel. For hot rolled materials, 1300°F is prescribed as the maximum temperature for these operations, while 1100°F is the temperature employed for most quench-and-tempered alloy steels, or 50°F below the final tempering temperature. The temperatures can be monitored by steel color change or the use of temperature indicating crayons.

For structures that have been damaged due to earthquakes, correction of bent or twisted members by heat shrinking may be much more desirable than removal of the bent members, and welding a replacement in place. Many issues must be considered before a project of this nature is begun; however, they are well beyond the scope of this paper (AISC, 1994, ref. 4; Roeder, 1985, ref. 38; Shanafelt and Horn, 1984, ref. 40).

4. Welding Procedures

4.1 Introduction

Within the welding industry, the term "welding procedure" is used to signify the combination of variables that are to be used to make a certain weld. These are recorded on a document known as a "Welding Procedure Specification" or "WPS". At a minimum, the WPS consists of the following:

WPS VARIABLES

Process	(SMAW, FCAW, etc.)
Electrode specification	(AWS A5.1, A5.20, etc.)
Electrode classification	(E7018, E71T-1, etc.)
Electrode diameter	(1/8 in., 5/32 in., etc.)
Electrical characteristics	(AC, DC+, DC-)
Base metal specification	(A36, A572 Gr50, etc.)
Minimum preheat and interpass temperature	
Welding current (amperage)	
Arc voltage	
Travel speed	
Position of welding	
Post weld heat treatment	
Shielding gas flow rate	
Joint design details	
Base material thickness	

The welding procedure is somewhat analogous to a cook's recipe. It outlines the steps required to make a quality weld under specific conditions.

4.2 Effects of Welding Variables

The effects of the variables are somewhat dependent on the welding process being employed, but general trends apply to all the processes. It is important to distinguish the difference between constant current (CC) and constant voltage (CV) electrical systems. Shielded metal arc welding is always done with a CC system. Flux cored welding and gas metal arc welding generally are performed with CV systems. Submerged arc welding may utilize either.

4.2.1 Amperage

Amperage is a measure of the amount of current flowing through the electrode and the work. It is a primary variable in determining heat input (see **4.2.7**). Generally, an increase in amperage means higher deposition rates, deeper penetration, and more admixture (see **6.1**). The amperage flowing through an electrical circuit is the same, regardless of where it is measured. It may be measured with a tong meter or with the use of an electrical shunt. The role of amperage is best understood in the context of heat input and current density considerations. For CV welding, an increase in wire feed speed will directly increase amperage. For SMAW on CC systems, the machine setting determines the basic amperage, although changes in the arc length (controlled by the welder) will further change amperage. Longer arc lengths reduce amperage.

4.2.2 Voltage

Arc voltage is directly related to arc length. As the voltage increases, the arc length increases, as does the demand for arc shielding. For CV welding, the voltage is determined primarily by the machine setting, so the arc length is relatively fixed in CV welding. For SMAW on CC systems, the arc voltage is determined by the arc length, which is manipulated by the welder. As arc lengths are increased with SMAW, the arc voltage will increase, and the amperage will decrease. Arc voltage also controls the width of the weld bead, with higher voltages generating wider beads. Arc voltage has a direct effect on the heat input computation.

The voltage in a welding circuit is not constant, but is composed of a series of voltage drops. Consider the following example: assume the power source delivers a total system voltage of 40 volts. Between the power source and the welding head or gun, there is a voltage drop of perhaps 3 volts associated with the input cable resistance. From the point of attachment of the work lead to the power source work terminal, there is an additional voltage drop of, say, 7 volts. Subtracting the 3 volts and the 7 volts from the original 40, this leaves 30 volts for the arc. This example illustrates how important it is to ensure that the voltages used for monitoring welding procedures properly recognize any losses in the welding circuit. The most accurate way to determine arc voltage is to measure the voltage drop between the contact tip and the work piece. This may not be practical for semiautomatic welding, so voltage is typically read from a point on the wire feeder (where the gun and cable connection is made), to the workpiece. For SMAW welding, voltage is not usually monitored, since it is constantly changing and cannot be controlled except by the welder. Skilled welders hold short arc lengths to deliver the best weld quality.

4.2.3 Travel Speed

Travel speed, measured in inches per minute, is the rate at which the electrode is moved relative to the joint. All other variables being equal, travel speed has an inverse effect on the size of the weld beads. As the travel speed increases, the weld size will decrease. Excessively low travel speeds may result in a reduction in penetration, as the arc impinges on a thick layer of molten metal and the weld puddle rolls ahead of the arc. Travel speed is a key variable used in computing heat input.

4.2.4 Electrode Extension

Electrode extension, also known as "stickout," is the distance from the contact tip to the end of the electrode. It applies only to the wire fed processes. As the electrode extension is increased in a constant voltage system, the electrical resistance of the electrode increases, causing the electrode to be heated. This is known as "I^2R heating." As the amount of heating increases, the arc energy required to melt the electrode decreases. Longer electrode extensions may be employed to gain higher deposition rates at a given amperage. When the electrode extension is increased without any change in wire feed speed, the amperage will decrease. This results in less penetration and less admixture. With the increase in electrical stickout, it is common to increase the machine voltage setting to compensate for the increased voltage drop across the electrode.

In constant voltage systems, it is possible to simultaneously increase the electrical stickout and wire feed speed in a balanced manner so that the current remains constant. When this is done, higher deposition rates are attained. Other welding variables such as voltage and travel speed must be adjusted to maintain a stable arc and to ensure quality welding.

4.2.5 Electrode Diameter

Larger electrodes can carry higher welding currents. For a fixed amperage, however, smaller electrodes result in higher deposition rates. This is because of the effect on current density discussed below.

4.2.6 Polarity

Polarity is a definition of the direction of current flow. Positive polarity (or reverse) is achieved when the electrode lead is connected to the positive terminal of the direct current (DC) power supply. The work lead would connect to the negative terminal. Negative polarity (or straight) occurs when the electrode is connected to the negative terminal. Alternating current (AC) is not a polarity, but a current type. With AC, the electrode is alternately positive and negative. Submerged arc welding is the only process that commonly uses both electrode positive and electrode negative polarity for the same filler metal. AC may also be used. For a fixed wire feed speed, a submerged arc electrode will require more amperage on positive polarity than on negative. For a fixed amperage, it is possible to utilize higher deposition rates with negative polarity than with positive. AC exhibits a mix of both positive and negative polarity characteristics.

The magnetic field that surrounds any DC conductor can cause a phenomenon known as arc blow, where the arc is physically deflected by the field. The strength of the magnetic field is proportional to the current squared, so this is a more significant potential problem with higher currents. AC is free of arc blow, and can be used to overcome this phenomenon.

4.2.7 Heat Input

Heat input is proportional to the welding amperage, times the arc voltage, divided by the travel speed. Higher heat inputs relate to larger weld cross sectional areas, and larger heat affected zones, which may negatively affect mechanical properties in that region. Higher heat input generally results in slightly decreased yield and tensile strength in the weld metal, and generally lower notch toughness because of the interaction of bead size and heat input. This is discussed in detail in **5.2.2.**

4.2.8 Current Density

Current density is determined by dividing the welding amperage by the cross sectional area of the electrode. For solid electrodes, the current density is therefore proportional to I/d^2. For tubular electrodes where current is conducted by the sheath, the current density is related to the area of the metallic cross section. As the current density increases, there will be an increase in deposition rates, as well as penetration. The latter will increase the amount of admixture for a given joint. Notice that this may be accomplished by either increasing the amperage or decreasing the electrode size. Because the electrode diameter is a squared function, a small decrease in diameter may have a significant effect on deposition rates and plate penetration.

4.2.9 Preheat and Interpass Temperature

Preheat and interpass temperature are used to control cracking tendencies, typically in the base materials. Regarding weld metal properties, for most carbon-manganese-silicon systems, a moderately high interpass temperature promotes good notch toughness. Excessively high preheat and interpass temperatures (greater than 550°F) will negatively affect notch toughness. When the base metal receives little or no preheat, the resultant rapid cooling may lead to a deterioration of notch toughness. (see Section **6.4**).

4.3 Purpose of Welding Procedure Specifications

The particular values for the variables identified in **4.1** and discussed in **4.2** have a significant effect on weld soundness, mechanical properties, and productivity. It is therefore critical that those procedural values used in the actual fabrication and erection be appropriate for the specific requirements of the applicable code and job specifications. Welds that will be architecturally exposed, for example, should be made with procedures that minimize spatter, encourage exceptional surface finish, and have limited or no undercut. Welds that will be covered with fireproofing, in contrast, would naturally have less restrictive cosmetic requirements.

Many issues must be considered when selecting welding procedure values. While all welds must have fusion to ensure their strength, the required level of penetration is a function of the joint design in the weld type. All welds are required to deliver a certain yield and/or tensile strength, although the exact level required is a function of the connection design. Not all welds are required to deliver minimum specified levels of notch toughness. Acceptable levels of undercut and porosity are a function of the type of loading applied to the weld. Determination of the most efficient means by which these conditions can be met cannot be left to the welders, but is determined by knowledgeable welding technicians and engineers who create written welding procedure specifications and communicate those requirements to welders by the means of these documents. The WPS is the primary tool that is used to communicate to the welder, supervisor, and the inspector how a specific weld is to be made. The welder is expected to be able to follow the WPS, although the welder may not know how or why each particular variable was selected. Welders are expected to ensure welding is performed in accordance with the WPS. Inspectors do not develop WPS's, but must ensure that they are available and are followed. The D1.1-96 Code is not prescriptive in its requirements regarding distribution of WPS's, although AWS recommends posting of these documents near the point of welding (AWS, 1995, ref. 15).

4.4 Development of WPS's

4.4.1 Selection of WPS Values

The suitability of a weld made by a skilled welder in conformance with the requirements of a WPS can only be as good as the WPS itself. The proper selection of procedural variable values must be achieved in order to have a WPS appropriate for the application. This is the job of the welding expert that generates or writes the WPS.

4.4.2 Prequalified WPS's

Under the D1.1 code (**3.1**), it is possible to utilize prequalified welding procedure specifications. In order for a WPS to be prequalified, it must meet all the requirements prescribed by the code. A prequalified WPS must specify a prequalified welding process, a prequalified joint, a prequalified steel, and must conform to all the procedural requirements contained in the code as they relate to welding variables. These items include electrode diameters, amperage levels, preheat temperatures, weld bead thicknesses, etc. Contained in the code is Annex - H, which lists the various requirements of a prequalified WPS. Failure to comply with one of these requirements necessitates that the welding procedure be qualified by test. If all the prequalified conditions are met, the WPS can be written and put into production without being subject to any qualification testing. Even though it is prequalified, the WPS must still be written. Welders must still be qualified. Although a WPS may meet all the prequalified requirements of the code, it is still preassumed that a knowledgeable welding expert is developing the WPS, and can judge its suitability for a given application based upon the expert's knowledge and experience.

4.4.3 Qualification of WPS's by Test

If a set of parameters proposed for use in production does not conform to all the requirements for a prequalified WPS, those particular parameters must be qualified by test. The D1.1 code prescribes the requirements which include nondestructive testing for soundness, and a variety of mechanical tests that determine the soundness and strength of the welded connection. The test results are recorded in a Procedure Qualification Record (PQR). The PQR will report the specific value for the welding variables that were tested, as well as the results of the nondestructive and mechanical tests that were performed on the test plate. PQR documents are typically not on the shop floor or the job site since they are of little value to production personnel. From the results of a successful procedure qualification test, a WPS will be developed from the parameters used for the test. The D1.1 code outlines the specific changes that can be made from the values that were used in the test. These are called "limitation of variables." It is possible, for example, to vary the amperage used on the WPS from the value used and recorded on the PQR. A variation of plus or minus 10% is permitted for amperage for FCAW. Thus, it is possible to write several WPS's from the results of a single PQR. Each WPS notes its supporting PQR. For production welding, whether the WPS is prequalified or qualified by test, the WPS is used in the same manner. Annex IV in the D1.1 code provides a synopsis of those variables that can be qualified by test.

New developments in welding are routinely subject to qualification testing since they do not have the history of satisfactory performance that is required before incorporation into the D1.1 code as a prequalified welding condition. For example, new steels, new filler metals, alternate joint details, as well as those welding processes that are particularly procedure sensitive (such as electroslag and electrogas welding) require qualification by test. After a satisfactory history of performance has been achieved, these advancements will be considered by D1 committee members for incorporation into prequalified WPS status.

4.5 Examples

To gain some insight into the thought process that may be utilized by a welding engineer in the development of a WPS, two examples will be given. In both cases, the weld is the same, namely, a 5/16 inch fillet weld. The specific application conditions, however, will necessitate that a separate WPS be developed for each situation. A sample WPS is included for each situation.

Situation One: The weld to be made is a 5/16 inch fillet weld that connects the shear tab to the column. This weld will be made in the fabrication shop with a column in the horizontal position. The fillet weld is applied to either side of a 1/2 inch shear tab. It is welded to a W 14 X 311 column with a flange thickness of 2-1/4 inches. The shear tab is made of A36 steel, while the column is of A572 Gr 50.

The welding engineer recognizes that for the grades of steel involved, and for the type of weld specified, a prequalified WPS could be written. The process of choice for this particular shop fabricator is gas shielded flux-cored arc welding, a prequalified welding process. From Table 3.1 of the D1.1 code, a list of prequalified filler metals is given. An E70T-1 is selected because, for semiautomatic welding, it is likely to be the most economical welding process considering deposition rate and cleanup time. The electrode operates on DC+ polarity. From experience, the engineer knows that 3/32 diameter is appropriate for the application, and specifies that the shielding gas should be CO_2 based upon the electrode manufacturer's recommendation and its low cost characteristics. From Table 3.2 of the D1.1 -96 code, the preheat is selected. It is controlled by the thicker steel, that is, the column flange, and required to be a minimum of 150°F since the column flange thickness is 2-1/4 inches. From recommendations supplied by the electrode manufacturer, the welding engineer selects a welding current of 460 amps, 31 volts, and specifies that the welding speed should be 15-17 inches per minute. The final variable is determined based upon experience. If any doubts existed, a simple fillet weld test could be made to verify the travel speed for the given amperage.

As a quick check, the engineer reviews Annex H to ensure that all the prequalified conditions have been achieved. Finally, these are tabulated on the WPS as illustrated in Fig. 4. 1 The particular form used was a copy from the D1.1 code, although any convenient format could have been used, provided all the required information was given.

Situation Two: The second weld to be made is also a 5/16 inch fillet weld, but in this case, the weld will be made in the field. The weld will be made between the shear tab described above, and the beam web. In this situation, the beam is a W36 X 150, specified to be of A36 steel. Under field conditions, the weld must be made in the vertical position.

The welding engineer again recognizes that the WPS for this application could be prequalified if all the applicable conditions are met. He selects self-shielded flux-cored arc welding in order to ensure high quality welds under windy conditions. This is a prequalified process. In D1.1-96, Table 3.1, he locates suitable filler metals and selects E71T-8, a self-shielded flux-cored electrode which operates on DC negative polarity. Because the welding will be made in the vertical position, a 0.068 inch diameter electrode is specified. From technical literature supplied by the filler metal manufacturer, a middle-of-the-range procedure suitable for vertical position welding is selected. The engineer specifies the current to be 250 amps, 19-21 volts, with a travel speed of 5.5-6.5 inches per minute. The controlling variable is the thickness of the beam web, which is 5/8 inch. In this situation, Table 3.2 of the D1.1 code does not require any minimum preheat. These parameters are recorded in the WPS shown in Fig. 4.2.

The two welds to be made are remarkably similar, and yet the WPS values specified are significantly different. In order to ensure that quality welds are delivered at economical rates, it is imperative that a knowledgeable individual establish WPS values. These values must be adhered to during fabrication and erection in order to ensure quality welds in the final structure.

WELDING PROCEDURE SPECIFICATION (WPS) Yes ☒
PREQUALIFIED X QUALIFIED BY TESTING ____
or PROCEDURE QUALIFICATION RECORDS (PQR) Yes ☐

Identification # 96-008
Revision 1 Date 4-96 By Y. LYE
Authorized by O. KAY Date ____
Type—Manual ☐ Semi-Automatic ☒
Machine ☐ Automatic ☐

Company Name ABC Fabricating
Welding Process(es) FCAW
Supporting PQR No.(s) N.A.

JOINT DESIGN USED
Type: T-joint, Fillet Weld 5/16"
Single ☐ Double Weld ☒
Backing: Yes ☐ No ☒
Backing Material:
Root Opening — Root Face Dimension —
Groove Angle: — Radius (J-U) —
Back Gouging: Yes ☐ No ☒ Method —

BASE METALS
Material Spec. ASTM A572 / A36
Type or Grade Gr 50 / —
Thickness: Groove — Fillet 1/2" → 2 1/4"
Diameter (Pipe) —

FILLER METALS
AWS Specification A5.20
AWS Classification E70T-1

SHIELDING
Flux — Gas X
Composition 100% CO_2
Electrode-Flux (Class) ____ Flow Rate 45 CFH
Gas Cup Size #4

PREHEAT
Preheat Temp., Min 150°F
Interpass Temp., Min 150°F Max —

POSITION
Position of Groove: — Fillet: HORIZ. (2F)
Vertical Progression: Up ☐ Down ☐ N.A.

ELECTRICAL CHARACTERISTICS
Transfer Mode (GMAW) Short-Circuiting ☐
Globular ☐ Spray ☐
Current: AC ☐ DCEP ☒ DCEN ☐ Pulsed ☐
Other —
Tungsten Electrode (GTAW)
Size: —
Type: —

TECHNIQUE
Stringer or Weave Bead:
Multi-pass or Single Pass (per side)
Number of Electrodes 1
Electrode Spacing Longitudinal —
Lateral —
Angle —
Contact Tube to Work Distance 1 1/8" ± 1/4"
Peening —
Interpass Cleaning: N.A.

POSTWELD HEAT TREATMENT
Temp. —
Time —

WELDING PROCEDURE

Pass or Weld Layer(s)	Process	Filler Metals		Current		Volts	Travel Speed	Joint Details
		Class	Diam.	Type & Polarity	Amps or Wire Feed Speed			
1	FCAW	E70T-1	3/32"	DC+	460A	31V	15-17 ipm	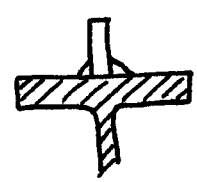

Form E-1 (Front)

Figure 4-1

WELDING PROCEDURE SPECIFICATION (WPS) Yes [X]
PREQUALIFIED X **QUALIFIED BY TESTING** ____
or PROCEDURE QUALIFICATION RECORDS (PQR) Yes [ ]

Identification # 12817
Revision 2 Date 3-89 By I. See
Authorized by J. Walk Date 4-89

Company Name XYZ Erectors
Welding Process(es) FCAW
Supporting PQR No.(s) N.A.

Type—Manual [ ] Semi-Automatic [X]
Machine [ ] Automatic [ ]

JOINT DESIGN USED
Type: Lap Joint - Fillet Weld 5/16"
Single [X] Double Weld [ ]
Backing: Yes [ ] No [X]
Backing Material:
Root Opening -- Root Face Dimension --
Groove Angle: -- Radius (J-U) --
Back Gouging: Yes [ ] No [X] Method --

POSITION
Position of Groove: ____ Fillet: Vertical (3F)
Vertical Progression: Up [X] Down [ ]

ELECTRICAL CHARACTERISTICS
Transfer Mode (GMAW) Short-Circuiting [ ] Globular [ ] Spray [ ]
Current: AC [ ] DCEP [ ] DCEN [X] Pulsed [ ]
Other ----
Tungsten Electrode (GTAW)
Size: ---
Type: ---

BASE METALS
Material Spec. ASTM A36/A36
Type or Grade ---
Thickness: Groove --- Fillet 1/2" - 5/8"
Diameter (Pipe) ---

TECHNIQUE
Stringer or Weave Bead: Weave
Multi-pass or Single Pass (per side) single
Number of Electrodes 1
Electrode Spacing Longitudinal ---
Lateral ---
Angle ---

FILLER METALS
AWS Specification S.20
AWS Classification E71T-8

SHIELDING
Flux --- Gas None
Composition --
Electrode-Flux (Class) -- Flow Rate --
Gas Cup Size --

Contact Tube to Work Distance 1/2" - 3/4"
Peening ---
Interpass Cleaning: N.A.

PREHEAT
Preheat Temp., Min None (70°F min.)
Interpass Temp., Min None Max ____

POSTWELD HEAT TREATMENT
Temp. ---
Time ---

WELDING PROCEDURE

Pass or Weld Layer(s)	Process	Filler Metals		Current		Volts	Travel Speed	Joint Details
		Class	Diam.	Type & Polarity	Amps or Wire Feed Speed			
1	FCAW	E71T-8	0.068"	DC-	250A (150 ipm)	19-21	5.5 - 6.5ipm	3F

Form E-1 (Front)

Figure 4-2

Welding of Seismically Resistant Steel Structures

4.6 Approval of WPS's

After a WPS is developed, it is typically submitted to the engineer for review. Many structural engineers have limited knowledge of welding, and thus delegate this task to the owner's inspector. However, not all capable welding inspectors are qualified to perform this function. When inspectors are empowered by the engineer to approve WPS's, the bounds of responsibilities can become confused. The inspector can easily assume other functions that should be the responsibility of the engineer, and are well outside the inspector's area of expertise and code authority. This can lead to "negotiating" between the inspector and the fabricator or erector, where the inspector "allows" deviation from some code requirements, providing other items are addressed to the inspector's satisfaction. This is an unacceptable practice. The inspector's primary role is to ensure conformance to the code and contract documents. The inspector is authorized to approve the fabrication, and is responsible to report non-conformances to the fabricator/erector and the engineer. It is inappropriate, for example, for the inspector to write WPS's, or to allow for deviation from written WPS requirements, even though such deviation may be appropriate for the specific situation. These types of abuses proliferate when the roles of inspector and engineer are not clearly understood and maintained.

4.7 Maintaining Weld Quality

After all the effort has been expended in developing a WPS, all too often it is filed away as the fulfillment of some "paperwork requirement", instead of being used for its primary purpose of communicating to welders, supervisors, and inspectors how welding is to be executed on actual projects. Not only can quality be compromised when WPS's are not available, but productivity can suffer as well. How this information is made available to the welder is generally left up to the particular contractor. Regardless of the method used, it must be available to the welder(s), supervisor(s) and inspector(s). The WPS is a communication tool. The welder's ability to follow a written welding procedure specification is part of welder qualification testing. To perform work under the D1.1 Code, the welder must be capable of following the written WPS requirements. There must be appropriate equipment available to ensure conformance to WPS requirements. These may be meters on the welding machine, or may be hand-held meters or other measuring devices.

5 Welding Process Selection and Cost Considerations

All of the common arc welding processes can be used to achieve the quality required for structural steel applications. While each may have a particular area of strength and/or weakness, the primary consideration as to which process will be used is largely cost driven. The availability of specialized equipment in one fabrication shop compared to the capabilities of a second shop may dictate significantly different approaches, both of which may prove to be cost effective. A history of successful usage offers a strong incentive for the fabricator to continue using a given process. The reasons for this go well beyond familiarity and comfort with a given approach. When welders and procedures are established with a given process, significant costs will be incurred with any change to a new, different approach.

5.1 Joint Requirements

The particular weld joint and its associated preparation dictate certain requirements in the welding process. Four characteristics must be considered: deposition rate, penetration ability, out-of-position capability, and high travel speed capacity. Each process exhibits different capabilities in these realms. Once the joint and its associated requirements are analyzed, they should be compared to the various process options and the ability of the process to achieve those requirements. A proper match of requirements and capabilities will lead to dependable and economical fabrication.

5.1.1 Deposition Rate Requirements

Some welds, such as large fillet welds and groove welds, require that high deposition rate welding be used (see Fig. 5-1). The cost of making these welds will be determined largely by the deposition rate of the process. The amount of weld material required may be measured in pounds per foot of joint. Once the deposition rate of a process in pounds per hour is known, it is possible to determine the number of feet of weld that can be made in a given hour. This, of course, translates directly to productivity rates. However, not all joints require high deposition rate welding. Small fillet welds are a notable example. If a weld joint requires only a small volume of material per length, a high deposition welding process must be operated at extremely high travel speeds in order to deliver the small weld size. Under these conditions, the travel speed capacity (which will be discussed later) rather than the deposition rate, becomes the controlling criterion.

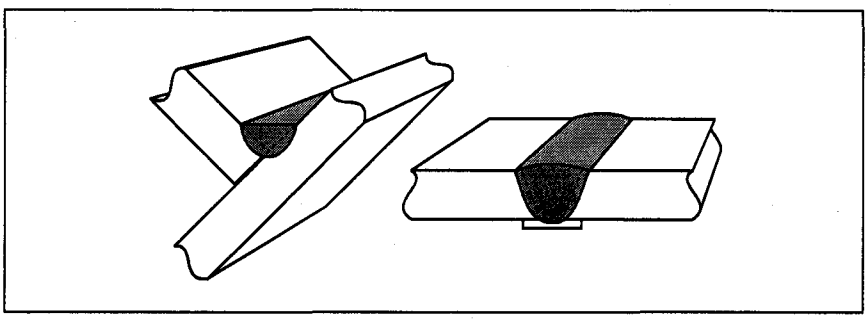

Figure 5-1 *Joints requiring substantial fill*

5.1.2 Penetration Requirements

The second criterion imposed by weld joints is the requirement for penetration. Examples are shown in Fig. 5-2 and would include any complete joint penetration groove weld that has a root face dimension. These joints will be made by welding from one side and back gouging from the second to ensure complete fusion.

With deeper penetration afforded by the welding process, a smaller amount of base metal will require removal by back gouging. Subsequent welding will then be proportionately reduced as well. It should be noted that while all welding requires fusion, not all joints require deep penetration. For example, simple fillet welds require fusion to the root of the joint, but do not require penetration beyond. This has a practical basis: verification of penetration beyond the root is impossible with visual inspection.

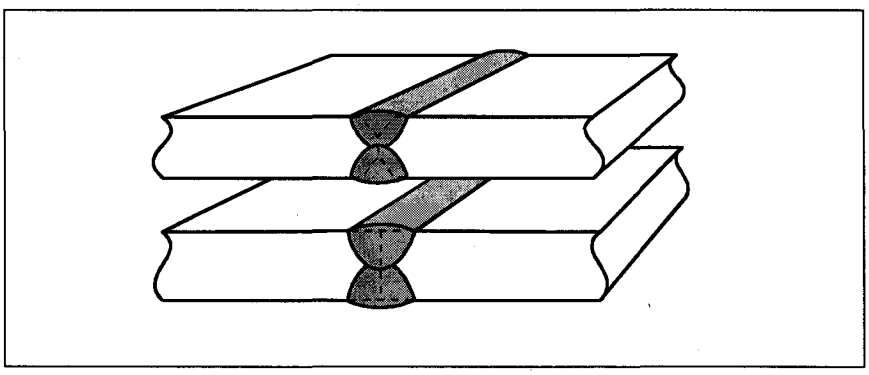

Figure 5-2 *Joints requiring substantial penetration*

Furthermore, the critical dimension in a fillet weld is the throat dimension. Fusion to the root, and not necessarily beyond, ensures that sufficient strength is generated, providing the weld is properly sized. While penetration can be verified with ultrasonic inspection, fillet welds routinely receive only visual or magnetic particle inspection. Thus, no penetration beyond the root is required, nor is design credit given to deeper penetration in fillet welds if it happens to be present. Fig. 5-3 illustrates this requirement.

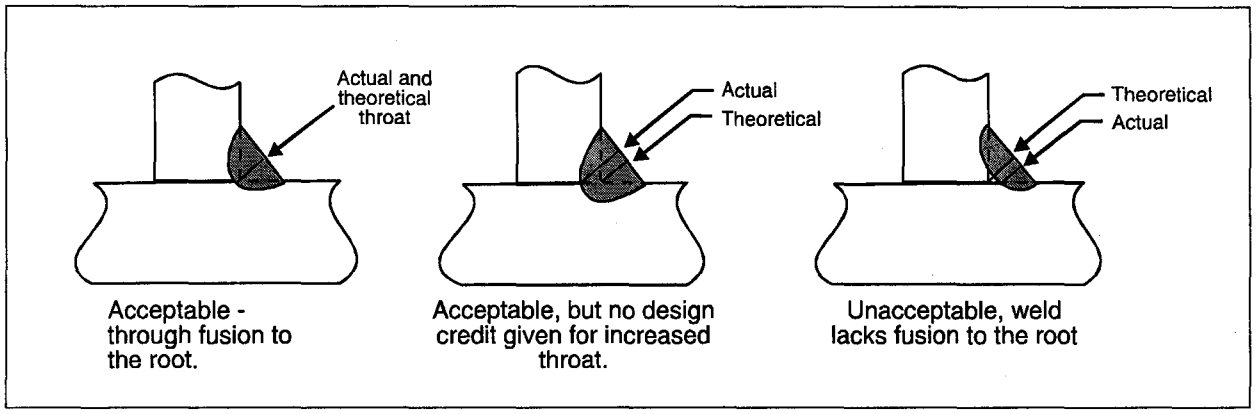

Figure 5-3 Fillet weld requirements

5.1.3 Out-of-Position Requirements

The out-of-position capability of a given welding process refers to the ability to deposit weld metal in the vertical or overhead positions. It is generally more economical to position the work in the flat and horizontal positions. However, this is usually impossible for field erection, and may be impractical under other conditions.

5.1.4 Travel Speed Requirements

It may not be possible for a high deposition welding process to be used at high travel speeds. The size of the droplet transferred, puddle fluidity, surface tension, and other factors combine to make some processes more capable of high travel speeds than others. High travel speeds are only required for making small welds.

5.2 Process Capabilities

After the joint is analyzed and specific requirements determined, these are compared to the capabilities of various processes. The process whose capabilities most closely match the requirements typically will be the best and most economical option.

5.2.1 Deposition Rate Capability

Submerged arc welding and electroslag/electrogas welding have the greatest ability to deliver high deposition rates. Multiple electrode applications of submerged arc welding extend this capability even further. For joints requiring high deposition rates, submerged arc welding and electroslag/electrogas welding are ideal processes to contribute to low cost welding. Where an open arc process is required, flux cored electrodes offer high deposition rates as well. The larger diameter electrodes, which run at higher electrical currents, are preferred.

5.2.2 Penetration Capability

Deep penetration is offered by the submerged arc welding process. While electroslag/electrogas also offers deep penetration, the joints on which electroslag are used typically do not require this capability. Where open arc processes must be used, the gas shielded flux cored electrodes are the ideal choice to provide deep penetration.

5.2.3 Out-of-Position Capability

Out-of-position capability is strongest for the flux cored and shielded metal arc welding processes. The slag coatings that are generated by these processes can be instrumental in retaining molten weld metal in the vertical and overhead positions.

5.2.4 High Travel Speed Capability

The requirement for high travel speed capability for welding structural steel members is fairly limited. This typically consists of the travel speed associated with making a 1/4 in. fillet weld. All of the popular processes, with the exception of electroslag/electrogas, are capable of making the 1/4 inch fillet welds under the proper conditions. Among the variables that need to be considered are electrode size and procedure variables. A common mistake of fabricators is to utilize a process and procedure capable of extremely high deposition rates, but limited travel speeds. Oversized welds can result from the inability to achieve high travel speeds. A more economical approach would be to optimize the procedure according to the desired travel speed. This may result in a lower deposition rate but a lower overall cost because overwelding has been eliminated.

5.3 Special Situations

5.3.1 Field Welding Outdoors

Self shielded flux cored welding is ideal for outdoor conditions. Quality deposits may be obtained without the erection of special wind shields and protection from drafts. Shielded metal arc welding is also suitable for these conditions, but is considerably slower.

5.3.2 Repair Welding

For small, isolated repairs, shielded metal arc welding is ideal. For larger repairs, the production criteria already considered should be reviewed.

5.3.3 Multiple Arc Automation Systems

Some projects permit multiple welding heads to be simultaneously operated in the same general vicinity. When this is done, submerged arc welding is an ideal choice. Because of the lack of glare and arc flash, an operator can control multiple arcs that are nearly impossible to control in a situation where the arc intensity from one torch would make it difficult to carefully control another. A typical example would be the use of welding systems that simultaneously make fillet welds on opposing sides of stiffeners.

5.3.4 Smoke and Fume Control

The easiest way to control smoke and fumes in the welding environment is to limit their initial generation. Here, submerged arc welding is ideal. Smoke exhaust guns are available for the flux cored arc welding processes. The most effective process for use with these smoke exhaust guns is FCAW-ss. Because the process is self shielded, there is no concern about the disruption of the gas shielding. See **10.** on arc welding safety.

5.4 Welding Cost Analysis

Welding is a labor intensive technology. Electricity, equipment depreciation, electrodes, gases, and fluxes constitute a very small portion of the total welding cost. Therefore, the prime focus of cost control will be reducing the amount of time required to make a weld.

The following example is given to illustrate the relative costs of material and labor, as well as to assess the effects of proper process selection. The example to be considered is the groove weld of beam flange to column connections. Since this is a multiple pass weld, the most appropriate analysis method is to consider the welding cost per weight of weld metal deposited, such as $/lb. Other analysis methods include cost per piece, ideal for manufacturers associated with the production of identical parts on a repetitive basis. Another method is cost per length, appropriate for single-pass welds with substantial length. The two welding processes to be considered are shielded metal arc welding and flux-cored arc welding. Either would generate high-quality welds when properly used.

To calculate the cost per weight of weld metal deposited, an equation taking the following format is used:

$$\text{Cost per weight} = \frac{\text{Electrode Cost}}{\text{Efficiency}} + \frac{\text{Electrode + Overhead Rate}}{\text{(Deposition Rate)(Operating Factor)}}$$

The cost of the electrode is simply the purchase cost of the welding consumable used. Not all of this filler metal is converted directly to deposited weld metal. There are losses associated with slag, spatter, and in the case of SMAW, the stub loss (the end portion of the electrode that is discarded). To account for these differences, an efficiency factor is applied. The following efficiency factors are typically used for the various welding processes:

SMAW:	65%
FCAW:	80%
GMAW:	90% (CO_2 shielding)
	98% (Mixed gas)
SAW:	100%

The cost to deposit the weld metal is determined by dividing the applicable labor and overhead rate by the deposition rate, that is, the amount of weld metal deposited in a theoretical, continuous one hour of production. This cannot be maintained under actual conditions since welding will be interrupted by many factors. These include necessary activities such as slag removal, replacement of electrode, re-positioning of the work or the welder with respect to the work, etc. For SMAW, replacement of electrodes takes place approximately every minute because of the finite length of the electrodes used. The following operating factors are typically used for the various processes and method of application:

Manual SMAW:	30%
Semiautomatic:	40%
Mechanized:	50%

The following examples are the actual procedures used by a field erector. The labor and overhead cost does not necessarily represent actual practice, but has been used to enable comparison of the relative cost of filler metals vs. the labor required to deposit the weld metal. Once the cost per deposited pound is known, it is a relatively simple activity to determine the quantity of weld metal required for a given project, and multiply it by the cost per weight to determine the cost of welding on the project.

PROCESS	SMAW	FCAW
Electrode Classification	E7018	E70TG-K2
Electrode Diameter	3/16"	7/64"
Amperage	225	430
Voltage	N.A.	27
Electrode Efficiency	60%	80%
Electrode Cost	$1.23/#	$2.27/#
Operating Factor	30%	40%
Deposition Rate	5.5#/hr.	14.5#/hr.
Labor and Overhead Rate	$50/hr.	$50/hr.

For SMAW: Cost per weight ($/#) $= \frac{1.23}{60\%} + \frac{50}{(5.5)(30\%)}$

$= 2.05 + 30.30 = \$32.35/\text{lb.}$

For FCAW: Cost per weight ($/#) $= \frac{2.27}{80\%} + \frac{50}{(14.5)(40\%)}$

$= 2.84 + 8.62 = \$11.46/\text{lb.}$

In the case of the SMAW example, the electrode cost is approximately 6% of the total cost. For the FCAW example, primarily due to a decrease in the labor content, the electrode cost is 25% of the total. By going to FCAW, the total cost of welding was decreased approximately 65%. While the FCAW electrode costs 85% more than the SMAW electrode, the higher electrode efficiency reduces the increase in electrode cost to only 39%.

The first priority that must be maintained when selecting weld processes and procedures is that the required weld quality can be achieved. For different welding methods which deliver the required quality, it is generally advantageous to utilize the method that results in higher deposition rates and higher operating factors. This will result in a reduction in welding time with a corresponding decrease in the total building erection cycle, which will generally translate to a direct savings for the final owner, not only reducing the cost of direct labor, but also reducing construction loan costs.

6 Metallurgical Considerations

Weld metal is composed of both filler material and base material. The base material has a significant effect on the weld metal properties. It is important to understand the influence that the base material may have upon weld metal, particularly since many welding problems are directly traceable to the base material.

6.1 Base Metal Considerations

Important information concerning base metal properties is contained in a companion paper by K. Frank. The mechanical properties and chemical compositions for various structural steels are contained therein. The base metal affects welded connections in three major ways. First, preheat and interpass temperature control will be largely determined by base metal chemistry and thickness. Secondly, all welds contain some base metal. The intermixing of filler metal and base metal is known as admixture. The contribution of the base metal composition may significantly affect strength, toughness, and the atmospheric corrosion resistance of the weld metal. Finally, base metal discontinuities may affect joint design and the probability of weld related problems.

Perhaps the most important characteristic of steel is its ability to be heat treated. The properties of the material can be dramatically altered, depending on the particular heating and cooling cycle to which the material is subjected. The heat that is inherently associated with the arc welding process can dramatically affect the properties in both the weld metal and base metal, necessitating a basic understanding of the effects of thermal changes on steel properties. These principles are well established, and many excellent sources exist to provide the reader with a greater understanding of these principles. A very basic explanation is offered so that the chemical and thermal behaviors that are subsequently addressed will be better understood.

Steel is composed of, at a minimum, carbon and iron. Pure iron is allotropic, assuming different crystalline structures depending on its temperature. For pure iron, under equilibrium conditions, it assumes a body-centered cubic (BCC) structure at temperatures of 1670° F and below. From 1670° - 2552° F, iron crystals are arranged in a face-centered cubic (FCC) configuration. Above 2552°F, and up to the melting point, iron reassumes the BCC arrangement. Each crystalline structure has its own unique density, properties, and a different ability to dissolve other elements (such as carbon). The addition of carbon into the steel changes these transformation points, and the transformations do not occur at discrete temperatures with the addition of the second element. If an iron-carbon material is heated from room temperature, some of the BCC will be converted to FCC at 1333°F (as opposed to the previous temperature of 1670°F). This is known as the lower transformation temperature. In order to make major changes to the properties of the steel, the BCC must be changed to FCC. Conversely, if temperatures are held below the lower transformation temperature, major changes in the steel will not occur.

All of the BCC is not converted to FCC until the steel is heated above the upper transformation temperature. Regardless of the amount of carbon present, this transformation is completed by the time 1670°F is reached. With additions of carbon, however, full transformation can be achieved at lower temperatures.

All of the aforementioned temperatures are obtained from an "equilibrium diagram". Iron with different carbon levels is raised to specific temperatures and held at that temperature until thermal equilibrium is established. After all crystalline transformations have had adequate time to occur, the crystalline structure is determined. In welding applications, the rate of change in thermal conditions is very rapid, and transformation temperatures may be different than the equilibrium values listed above. The room temperature BCC structure is often referred to as ferrite, and the higher temperature FCC material is known as austenite. The relationships become much more complicated when material is cooled rapidly. Time is required for the transformations to take place, and if austenite is cooled rapidly, it

can retain that structure down to temperatures of approximately 600°F. Rapid cooling rates are inherently part of the arc welding processes, so these transformations can be very complicated. The primary means by which acceptable HAZ properties are achieved in welded structures is to control the chemistry of the base metal, as well as the thermal cycle to which the region is subjected.

An important portion of the base metal that has a definite interaction with the welding operations is the heat affected zone (HAZ) that was created by the application of an arc weld, thermal cutting, or other heat sources. By definition, this part of the base metal has had its microstructure altered by the heat of welding or thermal cutting, which in turn may alter mechanical properties in this region. The region is very complex. Immediately adjacent to the weld is base metal that has approached the melting point of steel. Away from the weld is base metal that has been merely warmed. Between these two extremes, there are regions that have exceeded the lower transformation temperature as well as portions that have exceeded the upper transition temperature. The properties of these individual zones are a function of the base metal composition, the temperature to which the material was exposed, the time of exposure at elevated temperature, and the subsequent cooling rate. To further compound the complication, these zones may be subject to additional thermal activity that results from the subsequent passes associated with multiple pass welding. The mechanical properties of the base metal in the heat affected zone may be significantly altered from those of the unaffected material.

Most steels used in construction are hot rolled materials and the effects of the thermal cycles imposed by welding on the heat affected zone properties are fairly minimal. A fairly broad spectrum of preheat, interpass temperature, and heat input of welding can be used with these steels without serious changes to HAZ properties. The heat affected zones in some quenched-and-tempered steels are more sensitive to the same thermal cycles. In the case of 100 Ksi yield strength A514 steel, a relatively narrow range of preheat, interpass temperature, and heat input must be maintained in order to ensure adequate strength and toughness is maintained in this region, and to preclude cracking.

Very high welding heat inputs (exceeding 100 kj/in.) can result in heat affected zone softening and a deterioration in the toughness properties. Very low heat inputs (less than 20 kj/in.) can result in hardened heat affected zones that also have a reduction in toughness and an increased risk of cracking. Codes typically control these two extremes by specifying minimum weld sizes, as well as maximum weld bead dimensions. These are directly correlated to heat input. Control of minimum preheat and minimum interpass temperatures is also important since it controls the cooling rate that the weld and the heat affected zone will experience. Excessively high interpass temperatures (exceeding 600°F) can result in deterioration in both the weld metal and the heat affected zone toughness. The AWS D1.1-96 Code (para. 3.5, table 3.2) does not contain specific limits on maximum interpass temperatures, except when welding on some quenched-and-tempered steels. Interim specifications developed after the Northridge earthquake suggest that a 550°F maximum interpass temperature should be maintained where notch tough weld metal is required (AWS, 1995, ref. 15). This control on interpass temperature is probably adequate for heat affected zone properties in hot rolled steels, although more work must be done in this area.

6.2 Filler Metal Considerations

The selection of filler metal has many implications. Various electrodes operate in different ways, generating production advantages or limitations. One electrode may have greater resistance to porosity than another. The out-of-position performance of one may exceed that of another. These factors affect the fabricator and the welder; they also have significant economic implications. To the design engineer,

however, the most important elements are the mechanical properties obtained from the weld metal. The most significant mechanical properties are the tensile and yield strengths, and the notch toughness or Charpy values.

6.2.1 Filler Metal Yield and Tensile Strength

Most grades of structural steel are designated based on their minimum specified yield strength. There is a specific tensile strength associated with that yield strength. In filler materials, just the opposite is true, and the primary reference is to the tensile strength. The relationship of weld metal to base metal properties is covered in **2.4**.

6.2.2 Filler Metal Notch Toughness

Notch toughness may be defined as the ability of a material to absorb energy in the presence of a flaw. Stated another way, notch toughness may be considered the property of the material that resists the onset of a brittle fracture.

The American Welding Society filler metal specifications indicate the levels of notch toughness (as measured by the Charpy V-notch specimen) required for the various filler metal classifications. The energy level that has been selected by AWS is 20 ft.-lbs.; the testing temperature may vary. Commonly, -20 F is used, although testing may be performed at either higher or lower temperatures. It is not uncommon for a filler material, tested according to filler metal specifications, to deliver notch toughness in excess of 100 ft.-lbs. at -20 F.

The conditions under which the filler materials are to be classified are carefully regulated by the AWS filler metal specifications. In order to generate a repeatable test that only evaluates the filler metal performance, a test condition was selected that would minimize the effects of the multitude of interacting variables. For example, the base material type, joint preparation, thickness of material, preheat and interpass temperatures, number of weld passes and sequence, and other variables all are dictated by the filler metal specifications. These conditions do not necessarily duplicate production welding conditions, and frequently differ from them significantly (AWS, various dates, ref. 8).

Variables Affecting Notch Toughness

Deviation from filler metal classification test conditions may result in changes in mechanical properties, with notch toughness particularly likely to be affected. Many of the changes that are desirable or necessary for production welding will result in a decrease in the notch toughness of production welds compared to the filler metal classification test. Base metal composition, joint type, preheat interpass temperature, weld size and pass sequence significantly affect notch toughness. Therefore, poor procedures may result in a significant decrease in the notch toughness delivered by an otherwise exceptional filler material.

Grain Refinement and Toughness

Under ordinary circumstances, as-cast metallurgical products have relatively poor notch toughness. This would include items such as castings. Steels develop their good mechanical properties due to composition, controlled rolling, mechanical hot working of the steel, or through heat treatment. Weld

metal develops its excellent notch toughness by the composition, and refinement afforded by subsequent weld passes. When the previously deposited bead is "heat treated" by subsequent passes, the notch toughness of the steel in the region that has been refined will be improved.

This is illustrated in Fig. 6-1. The first bead that is deposited has an as-cast microstructure with relatively poor notch toughness. When the second pass is applied, a portion of the first bead is remelted. Important for notch toughness is the region in the first bead that was not melted, but was raised to a high temperature that resulted in a tempering or refinement of the previous as-cast microstructure. This small region, illustrated by the darker shaded area in the HAZ in the weld metal of bead number 1, will have improved notch toughness. Similarly, pass number 3 will remelt part of beads number 1 and 2, and refine a portion of beads 1 and 2, improving the localized notch toughness. Also note that there is a region in bead 1 that has been refined twice. This region may have even higher notch toughness.

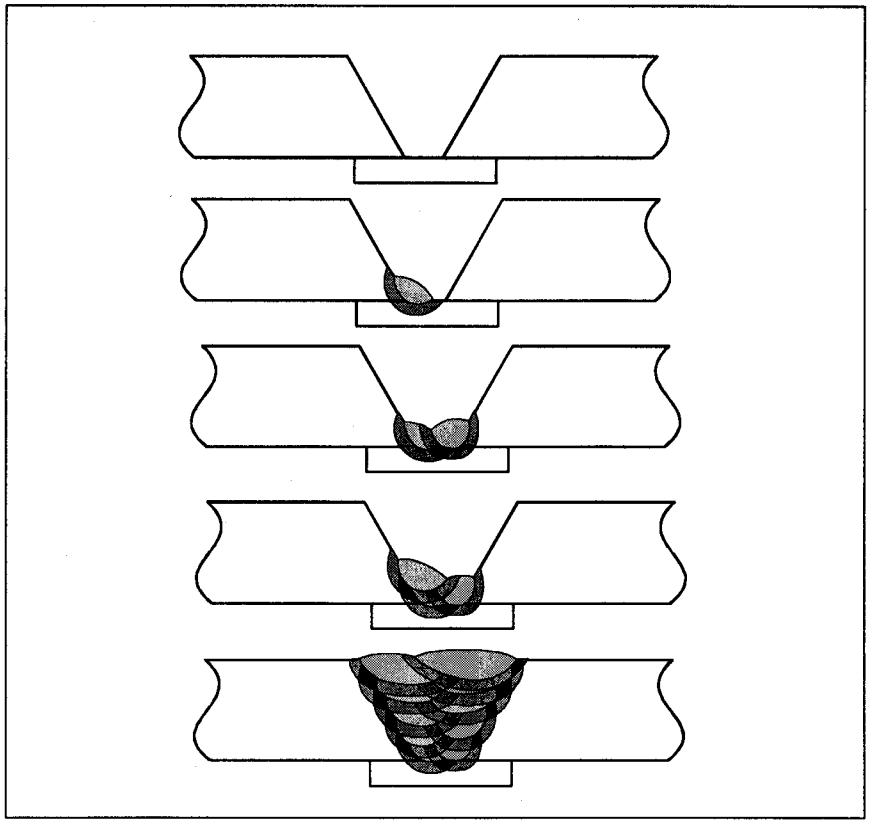

Figure 6-1 *Refinement due to multipass welding*

The final illustration in Fig. 6-1 shows a completed weld. Notice that the continual interaction of the beads has resulted in significant refinement of the previously deposited passes. Also, the last bead is totally unrefined. This is typical of all welded structures. This particular bead may exhibit the lowest localized notch toughness.

The resulting microstructure in the weld zone is very complex. Regions of as-cast weld metal, refined weld metal and twice refined weld metal exist. Each has a unique localized notch toughness. Of greater concern to the structural integrity is the composite notch toughness that results. Properly made, welds can have excellent notch toughness. Understanding the mechanics behind the development of this notch toughness is important.

It is imperative that the bead shape be proper to allow for generous refinement by subsequent weld passes. As is illustrated in Fig. 6-2, large welds will not be refined as completely by subsequent passes. Generally, this weld, made with a few passes, would exhibit poorer notch toughness. Fig. 6-1 shows smaller weld beads that have significant width and a relatively shallow depth. This is ideal for developing good notch toughness.

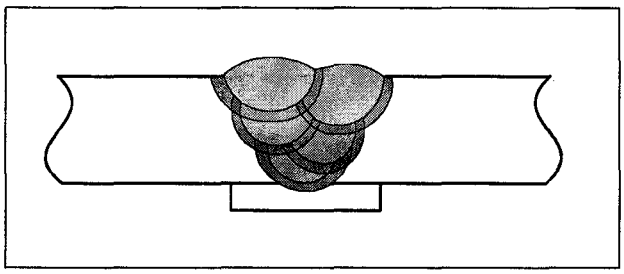

Figure 6-2 *Effect of large beads on refinement*

Heat Input and Toughness

Heat input was discussed in **2.5**. As the amperage is increased, resulting in a larger weld size, the heat input is increased. Similarly, as the travel speed is decreased, resulting in a larger weld size, the heat input is increased. Thus, it can be shown that the single pass weld cross sectional area is directly proportional to heat input.

As has been shown previously, large welds which do not receive significant refinement from subsequent passes, generally exhibit poor notch toughness. These welds are the result of higher heat input procedures. This has caused some people to believe that high heat input welding generates poor notch toughness. Whereas this trend is generally true, it misses the key variables involved. The most important variable is the bead size and shape, and the amount of subsequent refinement afforded by other weld passes. Interestingly, if the weld size and shape can be maintained at a constant level, research has shown that higher heat input will actually generate better notch toughness.

Specifying the heat input generally controls the weld size. However, for a given heat input, it is possible to generate a weld size and shape that will not generate good notch toughness properties. With a disproportionate emphasis on heat input, the importance of these other variables may be overlooked.

Toughness of Single vs. Multiple Pass Welds

Single pass welds do not have the benefit of grain refinement provided by subsequent weld passes. Greater emphasis is therefore placed on the composition of these welds, particularly with high admixture welds produced by SAW. To obtain good notch toughness, filler metals used to make single or limited pass welds usually employ higher levels of manganese.

Whereas single pass welds may exhibit less notch toughness than will be expected with multiple pass configurations, there is less need for high notch toughness in single pass welds. A common situation for a single pass weld would be for web-to-flange connections in a plate girder. The forces transferred by these welds are relatively small and the likelihood of brittle fracture is lessened under these conditions.

By contrast, the multiple pass welds of flange splices are critical welds subject to higher levels of stress and greater restraint. The thicker materials are more prone to brittle fracture. However, the welds applied in these joints are routinely multiple pass.

6.2.3 Filler Metal Composition and Weld Performance

The composition of weld metal usually is significantly different from that of the base materials it will join. In general, weld metals will contain lower levels of carbon and frequently higher levels of manganese and silicon than the base material. Weld metal solidifies and cools at a much higher rate than does steel when it is being made. The differences in thermal cycles necessitate the weld metal having a different chemical composition than the base metal in order to ensure that mechanical property requirements are met.

The behavior of the various alloys in base material has been well covered in other areas of this handbook. The role of these alloys in weld metal is sometimes slightly different than it is in base materials. The following summary explains the role of each element in the weld metal:

Carbon is the principal hardening agent in weld metal. It is typically held to levels of 0.06-0.15%.

Manganese is a primary element for strengthening weld metal. Typically it is present in the range of 1.0-1.8%. Manganese also overcomes the harmful effects of sulfur in the base material.

Silicon is usually present at levels of 0.4-0.8%. Silicon strengthens the weld metal and increases the fluidity of the weld puddle, assisting in obtaining uniform bead surface contours. It also acts as a deoxidizer.

Nickel in the amount of 1.0-4.0% is added as an alloy in the filler metals used to join weathering steels. Nickel is very effective at increasing toughness, but is a costly element to add.

Chromium & Molybdenum: Small percentages of these elements may be present in weld metal. When added to filler materials used on structural members, they usually are present as strengthening agents.

Phosphorus & Sulfur: These elements are not deliberately added, but are in the form of residual elements that are controlled to maximum permissible levels. Modern electrodes typically control sulphur and phosphorus contents to less than 0.010%.

Copper may be applied in small amounts to the surfaces of solid electrodes used in submerged arc welding and gas metal arc welding. This generally is held to a maximum of 0.50%. The copper on the surface of the electrode is present to aid in efficient electrical contact between the moving electrode and the fixed contact tip.

6.3 Weld Cracking During Fabrication

Several discontinuities may occur in welds or heat affected zones. Welds may contain porosity, slag inclusions or cracks. Of the three, cracks are by far the most detrimental. Whereas there are acceptable limits for slag inclusions and porosity in welds, cracks are never acceptable. Cracks in the vicinity of a weld indicate that one or more problems exist that must be addressed. A careful analysis of crack characteristics will make it possible to determine their cause and appropriate corrective measures.

For the purposes of this section, "cracking" will be distinguished from weld failure. Welds may fail due to overload, underdesign, or fatigue. The cracking discussed under this section has to do with solidification, cooling, and the stresses that develop due to weld shrinkage. Weld cracking occurs close to the time of fabrication. Hot cracks are those that occur at elevated temperatures and are usually solidification related. Cold cracks are those that occur after the weld metal has cooled to room temperature and may be hydrogen related. Neither is the result of service loads.

Most forms of cracking result from the shrinkage strains that occur as the weld metal cools. If the contraction is restricted, the strains will induce residual stresses that cause cracking. There are two opposing forces: the stresses induced by the shrinkage of the metal, and the surrounding rigidity of the base material. The shrinkage stresses increase as the volume of shrinking metal increases. Large weld sizes and deep penetrating welding procedures increase the shrinkage strains. The stresses induced by these strains will increase when higher strength filler metals and base materials are involved. When the stresses exceed the yield point, no further accumulation of stress is seen. The material simply yields. With a higher yield point, however, higher residual stresses will be present.

Opposing these residual stresses induced by shrinkage strains is the base metal rigidity. When thick, highly restrained plates are utilized, the strains imposed by the weld metal are largely self absorbed. That is, all shrinkage is restricted to the weld bead. When plates are relatively thin and flexible, however, the shrinking weld metal may pull the base material, redistributing the shrinkage strains. This causes distortion. Heavily restrained, normally ductile plates may be restricted from exhibiting their ductility, due to the very high triaxial (multidirectional) tensile strain that may develop in this region. The state of strain may cause the yield point to climb to a much higher value than the uniaxial yield point. This condition of strain causes the weld metal to experience even higher residual stresses which may exceed the uniaxial yield point.

Factors that increase the amount of strain on the metal will obviously increase cracking tendencies. However, particular attention must be paid to the restraint offered by the surrounding base material. Unfortunately, there is no simple way to describe restraint mathematically. However, experience has shown that when higher strength plate (greater than 50 ksi yield strength) in thicker sections (greater than 1-1/2 in.) intersect from all three geometrical directions, high restraint will be experienced at the intersection of these plates.

Under conditions of high restraint, extra precautions must be utilized to overcome the cracking tendencies which are described in the following sections. It is essential to pay careful attention to welding sequence, preheat and interpass temperature, post weld heat treatment, joint design, welding procedures, and filler material. The judicious use of peening as an in-process stress relief treatment may be necessary to fabricate highly restrained members.

Weld cracking may be characterized in one of the following ways: centerline cracking, heat affected zone cracking, and transverse cracking.

6.3.1 Centerline Cracking

Centerline cracking is characterized as a separation in the center of a given weld bead. If the weld bead happens to be in the center of the joint, as is always the case on a single pass weld, centerline cracks will be in the center of the joint. In the case of multiple pass welds, where several beads per layer may be applied, a centerline crack may not be in the geometric center of the joint, although it will always be in the center of the bead (see Fig. 6-3).

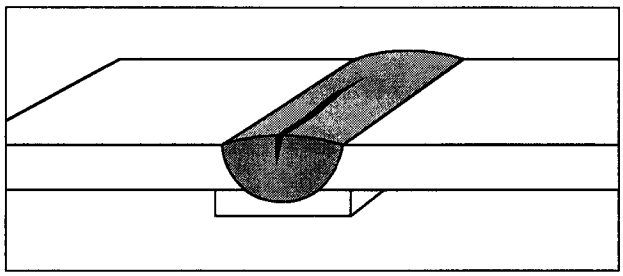

Figure 6-3 *Centerline cracking*

Centerline cracking is the result of one of the following three phenomena: segregation induced cracking, bead shape induced cracking, or surface profile induced cracking. Unfortunately, all three phenomena evidence themselves in the same type of crack, and it is often difficult to identify the cause. Moreover, experience has shown that often two or even all three of the phenomena will interact and contribute to the cracking problem. Understanding the fundamental mechanism of each of these types of centerline cracks will help in determining the corrective solutions.

Segregation Induced Cracking

Segregation induced cracking occurs when low melting point constituents in the admixture separate during the weld solidification process. As the weld metal solidifies, elements and compounds with low melting temperatures are forced into the liquid phases that are next to the solidifying metal. The enrichment of the remaining liquid material (typically concentrated in the center of the weld cross-section), with the low melting point materials, can lead to cracking.

When intermixed materials have a significantly different melting point than the basic iron-carbon weld metal, it is possible to have a liquid mixture in the center of the joint well after the majority of the weld has solidified. This is illustrated in Fig. 6-4. In Fig. 6-4a, the weld nugget is entirely molten. In Fig. 6-4b, solidification has begun. When materials solidify, segregation may occur. The result is a change in composition throughout the cross section of the solidified material. The grains of steel have begun to grow, perpendicular to the fusion interface. As this solidification proceeds, segregation occurs. In an iron-carbon system, the first materials to solidify are typically lower in carbon content because pure iron has a higher freezing point than iron-carbon mixtures.

The degree of segregation is a complex issue, and is a function of the solubility of the element or compound in liquid iron, as well as the rate of which solidification takes place. In general, however, the low carbon layer that begins to form forces higher levels of carbon into the center. Other low melting point constituents can also be forced into this liquid center. Part of the cross section is solidified, while a portion remains liquid. In Fig. 6-4c, solidification has progressed further. In Fig. 6-4d, solidification is nearly complete. Notice that the last portion of the bead to solidify is in the center of the cross section. This is the location that will contain any remaining components that have the lower freezing point.

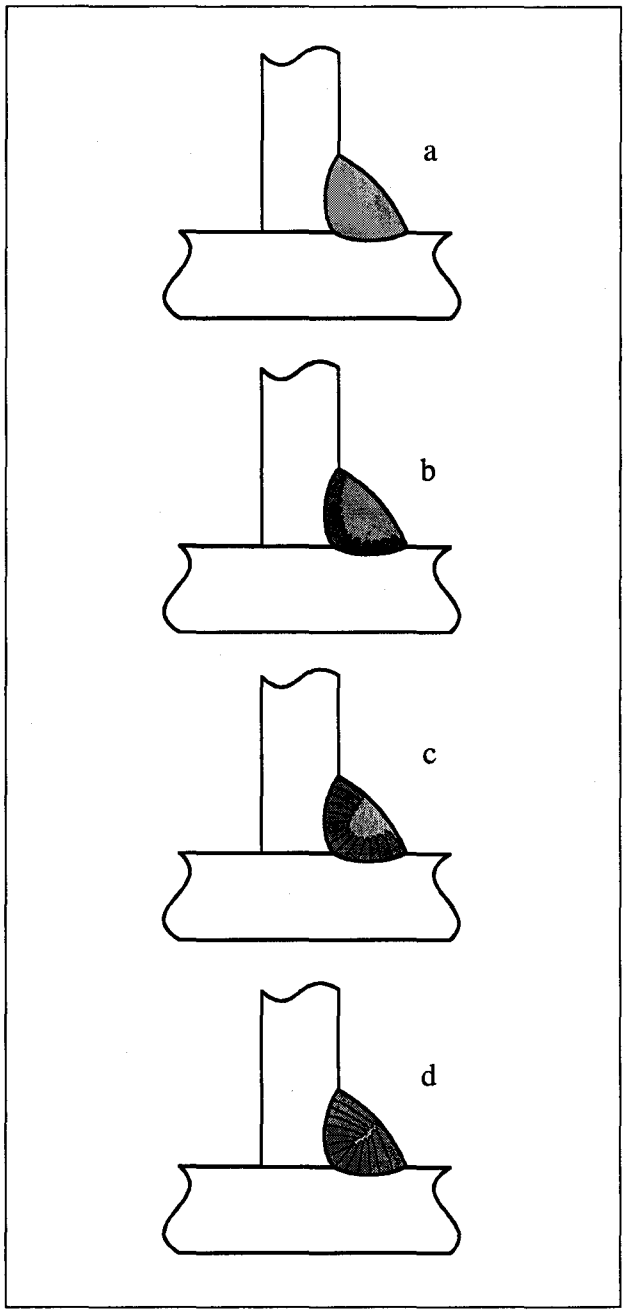

Figure 6-4 *Segregation induced cracking*

If the steels contain higher than desirable levels of sulfur, phosphorus, lead, or copper, these elements tend to segregate into the center of the solidifying weld bead. Perhaps the most frequently encountered contaminant from steel is sulfur. In the presence of iron, the sulfur will combine to form iron sulfide (FeS). Iron sulfide has a melting point of approximately 2,200°F. Steel, on the other hand, has a melting point of approximately 2,800°F. As the grains grow, iron sulfides are forced into the center of the joint. Well after all of this steel has solidified, the liquid iron sulfides with a melting point 600°F less than the steel will be contained in the center of the weld bead. As the steel cools, it contracts, pulling on the center of the weld bead which contains the weak liquid iron sulfide. As shown in Fig. 6-4d, the weld bead will crack.

Phosphorus, lead, and copper will act in a similar manner. The primary difference with these elements is that they do not form compounds, but are present in their basic form. The commercial welding processes are all capable of tolerating low levels of these contaminants. However, when higher levels are experienced, the segregation occurs and may result in centerline cracking. Whereas these elements may come from the filler material, they are more commonly the result of base material compositions; therefore, they must be controlled in the base materials.

When centerline cracking induced by segregation is experienced, several solutions may be implemented. Since the contaminant usually comes from the base material, the first consideration is to limit the amount of contaminant pick-up from the base material. This may be done by limiting the penetration of the welding process. In some cases, a joint redesign may be desirable. The extra penetration afforded by some of the processes is not necessary and can be reduced. This can be accomplished by using lower welding currents.

A buttering layer of weld material (see Fig. 6.5), deposited by a low energy process such as shielded metal arc welding, may effectively reduce the amount of pickup of contaminant into the weld admixture.

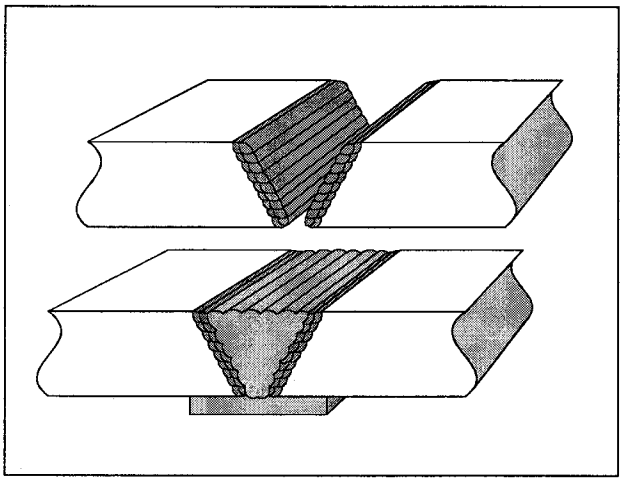

***Figure 6-5** Buttering*

In the case of sulfur, it is possible to overcome the harmful effects of iron sulfides by preferentially forming manganese sulfide. Manganese sulfide (MnS) forms when sufficient levels of manganese are present so that this compound is formed rather than iron sulfide. Manganese sulfide has a melting point of 2,900°F. In this situation, before the weld metal begins to solidify, manganese sulfides are formed which do not segregate. Steel producers utilize this concept when higher levels of sulfur are encountered in the iron ore. In welding, it is possible to use filler materials with higher levels of manganese to overcome the formation of low melting point iron sulfide. Unfortunately, this concept cannot be applied to contaminants other than sulfur.

Bead Shape Induced Cracking

The second type of centerline cracking is known as bead shape induced cracking. This is illustrated in Fig. 6-6 and is associated with deep penetrating processes such as SAW and CO_2 shielded FCAW. When a weld bead is of a shape where there is more depth than width to the weld cross section, the solidifying grains growing perpendicular to the steel surface intersect in the middle, but do not gain fusion across the joint. To correct for this condition, the individual weld beads must have at least as much width as depth. Recommendations vary from a 1:1 to a 1.4:1 width-to-depth ratio to remedy this condition. The total weld configuration, which may have many individual weld beads, can have an overall profile that constitutes more depth than width. If multiple passes are used in this situation, and each bead is wider than it is deep, a crack-free weld can be made.

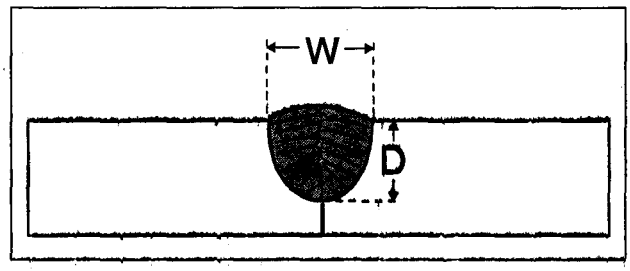

Figure 6-6 Bead shape induced cracking

Joint design affects the tendency toward centerline cracking induced by bead shape. The pre-qualified joints in welding specifications have taken this into consideration. Consider, for example, the three joints listed in Fig. 6-7. Known as a B-U2a, the combination of root opening and included angle is adjusted to ensure the bead shape of the root pass has an acceptable width-to-depth ratio. As the included angle is decreased, the tendency toward a narrow, deep bead increases. To compensate for this, a larger root opening is used. For PJP groove welds, the preferred configuration for a single bevel joint is

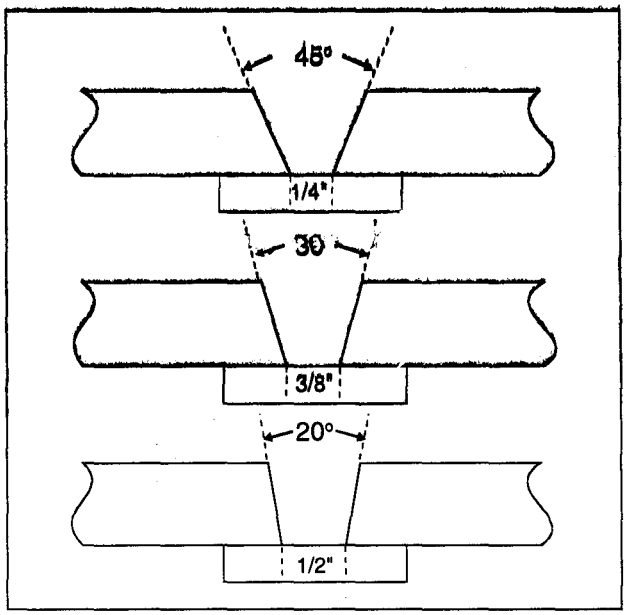

Figure 6-7 Acceptable root configurations

to have a minimum of a 60° included angle when the submerged welding process is used. With the deep penetration afforded by submerged arc welding, a 45° included angle could lead to unacceptable centerline cracking (see Fig. 6-8). Other processes may use smaller included angles, because they lack the penetration that would create this unacceptable relationship. However, these processes rarely obtain fusion down to the root under these tight joint configurations.

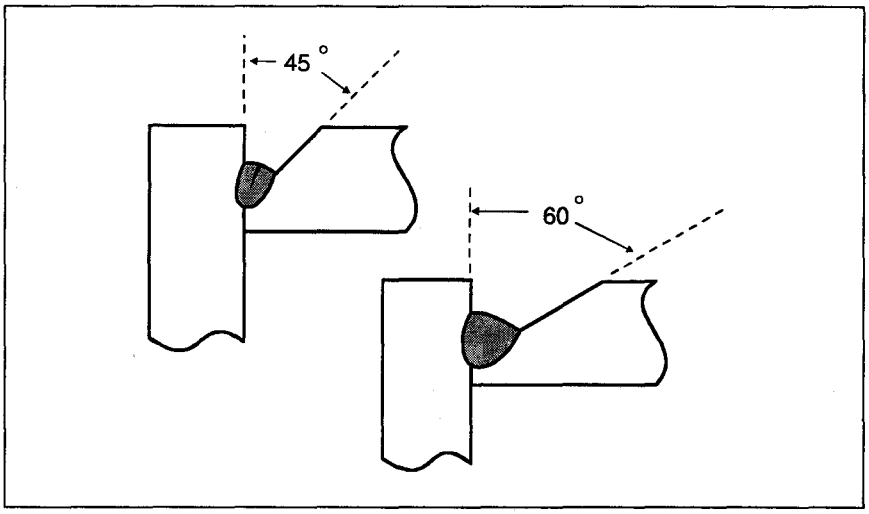

Figure 6-8 *Bead shape induced cracking and joint preparation*

Centerline cracking due to bead shape may occur in either groove welds or fillet welds. It is rarely experienced in fillet welds when applied to 90° tee joints. However, when skewed joints are specified, and the acute angle side is less than 70°, centerline cracking may occur. This is particularly true when the weld process has significant penetrating capability.

When centerline cracking due to bead shape is experienced, the obvious solution is to change the width-to-depth relationship. This may involve a change in joint design. Since the depth is a function of penetration, it is advisable to reduce the amount of penetration. This can be accomplished by utilizing lower welding amperages and larger diameter electrodes. All of these approaches will reduce the current density and limit the amount of penetration.

Surface Profile Induced Cracking

The final mechanism that generates centerline cracks is surface profile conditions. When concave weld surfaces are created, internal shrinkage stresses will place the weld metal on the surface into tension. Conversely, when convex weld surfaces are created, the internal shrinkage forces pull the surface into compression. These situations are illustrated in Fig. 6-9. Concave weld surfaces frequently are the result of high arc voltages. A slight decrease in arc voltage will cause the weld bead to return to a slightly convex profile and eliminate the cracking tendency. High travel speeds may also result in this configuration. A reduction in travel speed will increase the amount of fill and return the surface to a convex profile. Vertical down welding also has the tendency to generate these crack sensitive, concave surfaces. Vertical-up welding can remedy this situation by providing a more convex bead.

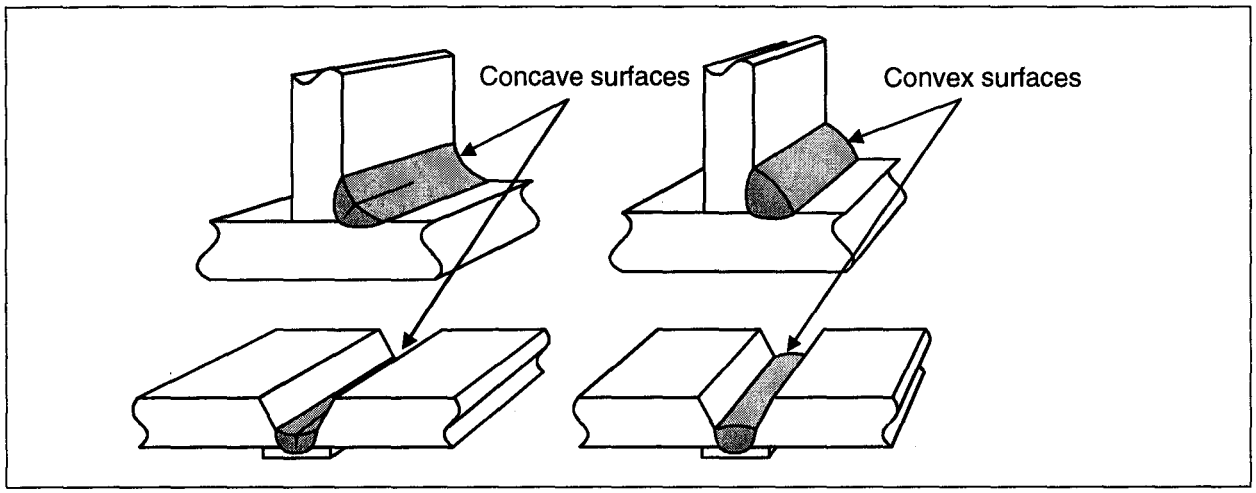

Figure 6-9 Surface profile induced cracking

6.3.2 Heat Affected Zone Cracking

Heat affected zone cracking (see Fig. 6-10) is characterized by separation that occurs immediately adjacent to the weld bead. The cracking occurs in the base material, and although it is certainly related to the welding process, the crack does not occur in the weld material. This type of cracking is also known as "underbead cracking," "toe cracking," or "delayed cracking." The small, potentially brittle region surrounding the weld bead, called the "heat affected zone" (HAZ), results from the thermal cycle experienced by this region during welding. Initially, the energy of the welding process raises this zone to a temperature above the transformation temperature, but lower than the melting point. After the steel has been raised to this temperature, its final properties will be dependent upon the cooling rate it experiences. The surrounding colder steel quickly cools the small region around the weld bead. It is possible for this zone to have hardnesses that approach the maximum possible for the steel. Along with this increase in hardness comes a decrease in ductility. This hardening is generally isolated to the base material (as opposed to the weld metal) due to the higher carbon and alloy content which increases the probability of cracking. Since the weld metal is not cracking, a change in filler material would generally not affect HAZ cracking.

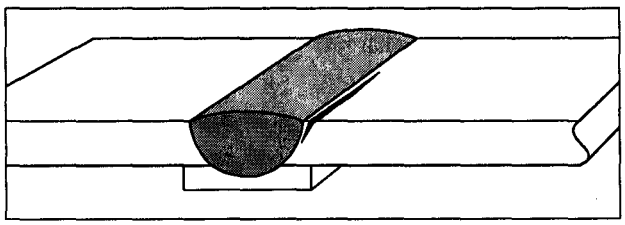

Figure 6-10 Heat affected zone cracking

Hydrogen is another factor that contributes to heat affected zone cracking. Moisture and organic compounds are the primary sources of hydrogen. They may be present on the steel, electrode, shielding materials, or even in the atmospheric humidity. Significant quantities of hydrogen can be dissolved in liquid weld material. As the weld metal begins to solidify, and particularly as it transforms from austenite to ferrite, the solubility for hydrogen decreases. Atomic hydrogen moves or diffuses within the weld metal at a rate exponentially proportional to the temperature. At ambient temperatures, the diffusion rates greatly decrease.

Atomic hydrogen, moving at random through the solidified weld metal, tends to accumulate around microscopic discontinuities in the heat affected zone that is significantly lower in temperature than the weld material. One theory suggests that as atomic hydrogen combines to form molecular hydrogen, a tremendous increase in internal pressure is experienced in this heat affected zone. A susceptible structure, the presence of hydrogen, and the residual stresses of welding will combine to cause cracking to occur. As is shown in Fig 6-11, three elements are required for hydrogen assisted cracking to occur. If any one of the three is decreased, hydrogen cracking can be minimized.

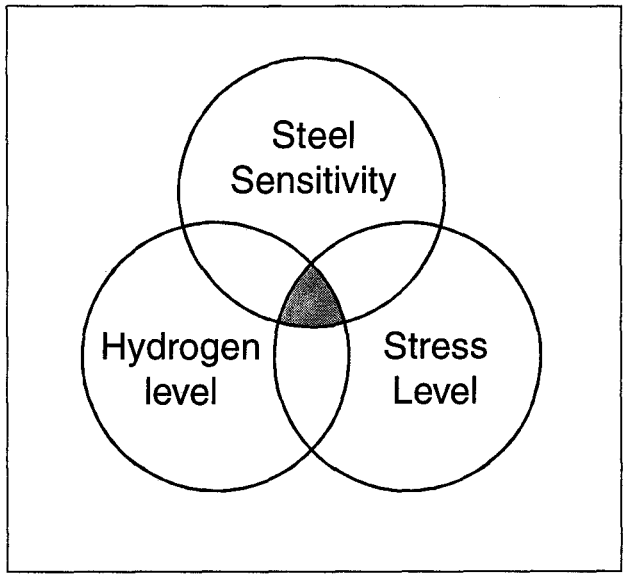

Figure 6-11 *Hydrogen cracking variables*

If steels that are not sensitive to hydrogen cracking are used, even fairly high levels of hydrogen can be experienced before the onset of any problems. These insensitive steels include low carbon and low alloy steels. Generally speaking, these are also low strength steels. Welding processes with even high levels of diffusible hydrogen have been successfully used without generating cracks, but they may be used only on steels which are lower in yield strength and less hardenable. Approved steels have greater resistance to hydrogen cracking than other options. A notable exception is the use of the A514 steels. These quenched and tempered materials are highly susceptible to hydrogen induced cracking. Notice that they have both higher alloy contents and higher strengths. For this reason, hydrogen must be more tightly controlled with these steels.

The diffusion of hydrogen through the weld metal requires time. Cracking may occur hours and even days after the time of fabrication. When steel is subject to this type of delayed cracking or welding, inspection periods are frequently delayed, typically by 48 hours, to ensure that any cracking will be found during final inspection.

The most effective way to reduce the hardness of the heat affected zone in a given steel is to preheat before welding and control the heat input and interpass temperature during welding. The preheat will slow the rate of cooling experienced by the heat affected zone, and the microstructures that develop will be softer and more ductile. The hydrogen diffusion rate is increased and the level of hydrogen is effectively lowered as well. In addition, there is a slight decrease in the residual stresses when preheat is applied. Thus, preheat addresses all three variables that contribute to this heat affected zone cracking problem.

In spite of all the attention hydrogen assisted heat affected zone cracking receives, it is infrequently experienced. This is largely due to the effectiveness of welding specifications. The use of good steels with lower hardenabilities, control of hydrogen in the welding processes, and generous preheat levels has greatly reduced this tendency. If heat affected zone cracking is experienced, it is important to review these variables. The practice of the fabricator with respect to storage of filler materials should be reviewed. Preheat should be carefully monitored. Mill test reports on these steels should be examined to ensure proper compliance for the chemical compositions. Lab analysis of the steel may be required to confirm the actual composition. If all variables appear to be proper and in compliance with the applicable welding specifications, it generally will be prudent to increase the level of preheat; the exception would be on the A514 grades of steel that are quenched and tempered. These boron alloyed steels may experience a version of heat affected zone cracking that occurs when this region is held at a high temperature too long. For this reason, these steels have specific maximum levels of preheat and interpass temperatures, as well as heat input. Under these conditions, lower levels of preheat may solve heat affected zone cracking tendencies.

It is possible to confuse underbead cracking with lamellar tearing (see **6.3.4**). The differences can usually be seen in the fracture surfaces. A lamellar tear generally reveals a grainy, coarse structure. It usually is highly oxidized and very coarse in appearance. On the other hand, heat affected zone cracking generally exhibits a smoother fracture resembling that of a brittle failure.

6.3.3 Transverse Cracking

Transverse cracking, also called cross cracking, is characterized as a crack within the weld metal perpendicular to the direction of travel (see Fig. 6-12). This is the least frequently encountered type of cracking, and is generally associated with weld metal that is very high in strength, significantly overmatching the base material.

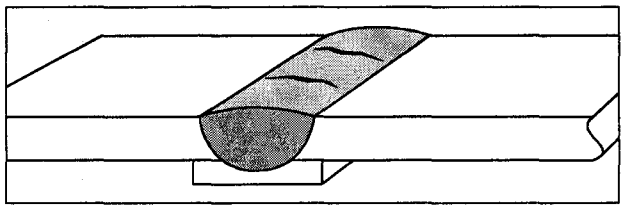

Figure 6-12 *Transverse cracking*

As the weld bead shrinks longitudinally, the surrounding base material resists this force by going into compression. The high strength of the surrounding steel in compression restricts the required shrinkage of the weld material. When the weld material is extremely high in strength, it has a reduced capacity to plastically deform. Due to the restraint of the surrounding base material, the weld metal may crack in the transverse direction.

Hydrogen is a key contributor to transverse cracking. Hydrogen cracking is normally associated with heat affected zone cracking. However, on lower carbon steels, HAZ cracking due to hydrogen may be replaced by hydrogen induced transverse cracking in the weld metal. Lower strength weld material, with a corresponding decrease in carbon and alloy levels, effectively solves the problem.

When transverse cracking is encountered, the strength of the weld metal should also be reviewed. Emphasis is placed upon the weld metal because the filler metal may deposit lower strength, highly ductile metal under normal conditions. However, with the influence of alloy pick-up, it is possible for the weld metal to exhibit extremely high strengths with reduced ductility. Using lower strength weld metal is an effective solution, but caution should be taken to ensure that the required joint strength is attained.

For fillet welds and PJP groove welds, undermatching is possible and is a frequently applied solution for situations where transverse cracking is expected. The common application of this concept is the web-to-flange weld of A514 steel. The 70 ksi filler metals are routinely used to make this connection. When higher strength filler material that would match the base material is used, the tendencies toward cracking, including transverse cracking, increase.

Preheat may have to be applied to alleviate transverse cracking. The preheat will assist in diffusing the excessive hydrogen. As preheat is applied, it will additionally expand the length of the weld joint, allowing the weld metal and the joint to contract simultaneously, and reducing the applied stress to the shrinking weld. This is particularly important when making circumferential welds. When the circumference of the materials being welded is expanded, the weld metal is free to contract along with the surrounding base material, reducing the transverse shrinkage stress. Finally, post weld hydrogen release treatments that involve holding the steel at 250 - 450°F for extended times will assist in diffusing any residual hydrogen.

6.3.4 Lamellar Tearing

Lamellar tearing is often a welding-related type of cracking that occurs in the base metal. It is caused by the shrinkage strains of welding acting perpendicular to planes of weakness in the steel. These planes are the result of inclusions in the base metal that have been flattened into very thin plates that are roughly parallel to the surface of the steel. When stressed perpendicular to the direction of rolling, the metallurgical bonds across these plates can separate. Since the various plates are not on the same plane, their fracture may jump between the plates, resulting in a "stair-stepped" pattern of fractures illustrated in Figure 6-13. This type of fracture generally occurs near the time of fabrication, and can be confused with under bead cracking, previously described in **6.3.2**. Some Northridge fractures had lamellar tearing-like fracture patterns. The significance of this type of fracture needs to be researched further.

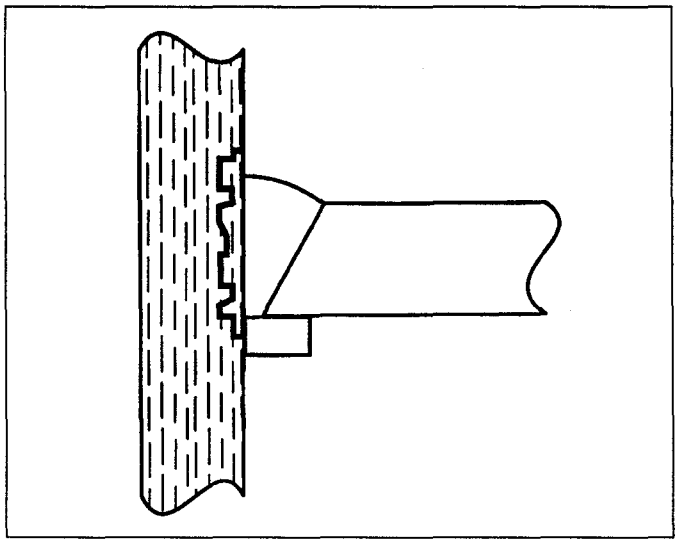

Figure 6-13 *Lamellar tearing*

Several approaches can be taken to overcome lamellar tearing. The first variable is the steel itself. Lower levels of inclusions within the steel will help mitigate this tendency. This generally means lower sulphur levels, although the characteristics of the sulphide inclusion are also important. Manganese sulphide is relatively soft, and when the steel is rolled at hot working temperatures of 1600-2000°F, the sulphide inclusions flatten significantly. If steel is first treated to reduce the sulfur, and then calcium treated, for example, the resultant sulphide is harder than the surrounding steel, and during the rolling process, is more likely to remain spherical. This type of material will have much less of a tendency toward lamellar tearing.

Current developments in steel-making practice have helped to minimize lamellar tearing tendencies. With continuously cast steel, the degree of rolling after casting is diminished. The reduction in the amount of rolling has directly affected the degree to which these laminations are flattened, and has correspondingly reduced lamellar tearing tendencies.

The second variable involves the weld joint design. For a specific joint detail, it may be possible to alternate the weld joint to minimize lamellar tearing tendencies. For example, on corner joints it is preferred to bevel the member in which lamellar tearing would be expected, that is, the plate that will be strained in the through-thickness direction. This is illustrated in Figure 6-14.

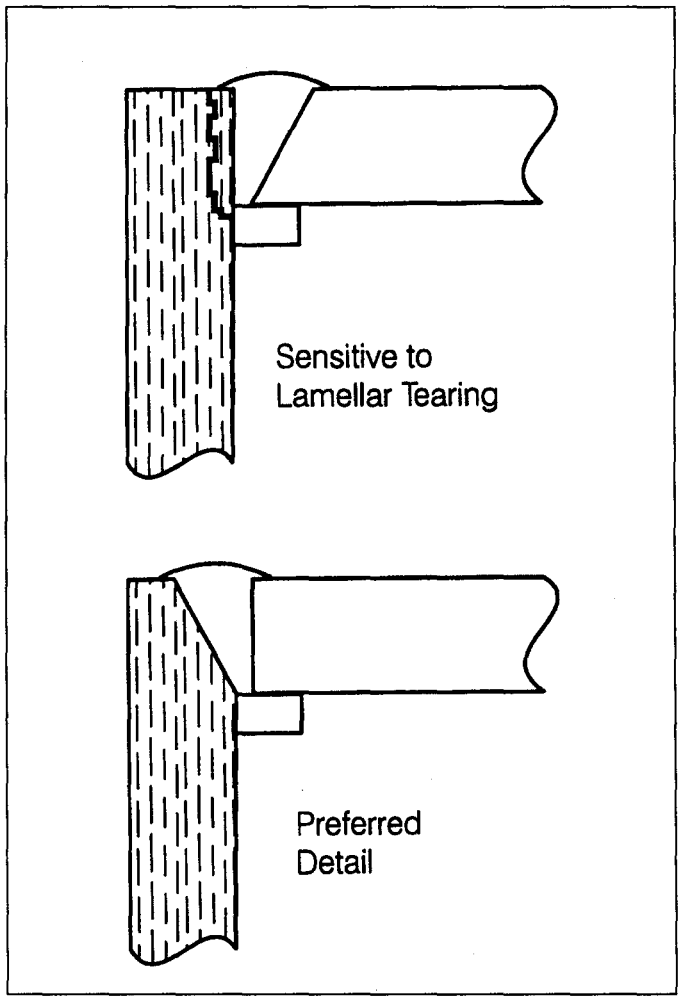

Figure 6-14 *Lamellar tearing*

A reduction in the volume of weld metal used will help to reduce the stress that is imposed in the through-thickness direction. For example, a single bevel groove weld with a 3/8" root opening and 30 degree included angle will require approximately 22% less weld metal for a 1-1/2" thick plate, compared to a 1/4" root opening and a 45° degree joint. The corresponding reduction in shrinkage stresses may be sufficient to eliminate lamellar tearing.

In extreme cases, it may be necessary to resort to special measures to minimize lamellar tearing, which may involve peening. This technique involves the mechanical deformation of the weld surface that results in compressive residual stresses that minimize the magnitude of the residual tensile stresses that naturally occur after welding. In order for peening to be effective, it is generally performed when the weld metal is warm (above 300°F), and must cause plastic deformation of the weld surface. The mechanical energy is generally imparted by a small, rounded, blunt instrument. The term "hammer peening" is descriptive of the forces involved.

Peening is restricted from being applied to root passes (because the partially completed weld joint could easily crack), as well as final weld layers, because the peening can inhibit appropriate visual weld inspection and embrittle the weld metal that will not be reheated (D1.1-96, para. 5.27).

Another specialized technique that can be used to overcome lamellar tearing tendencies is the "buttering layer" technique. With this approach, the surface of the steel where there might be a risk of lamellar tearing is milled to produce a slight cavity in which the butter layer can be applied. Individual weld beads are placed into this cavity. Since the weld beads are not constrained by being attached to a second surface, they solidify and cool, and thereby shrink, with a minimum level of applied stress to the material on which they are placed. After the butter layer is in place, it is possible to weld upon that surface with a much decreased level of concern about lamellar tearing. This concept is illustrated in Figure 6-15.

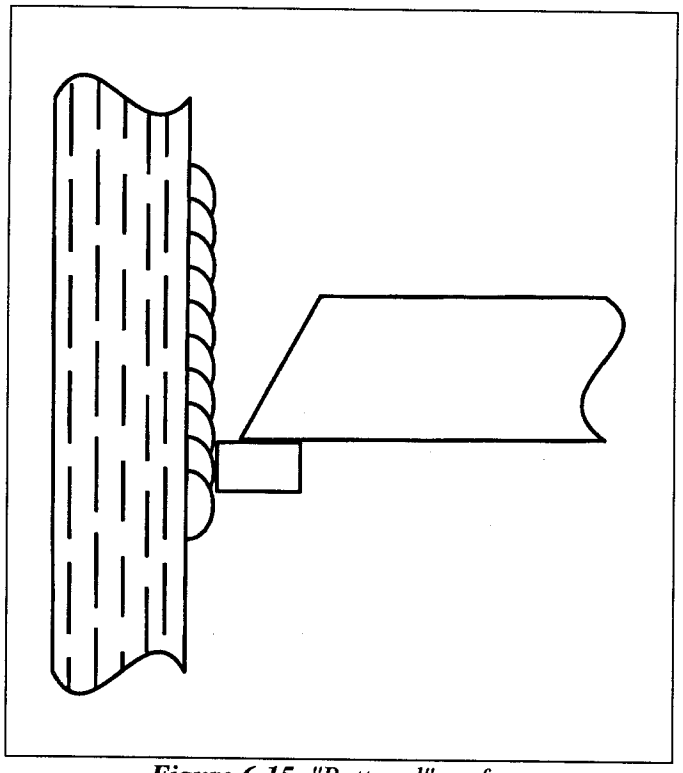

Figure 6-15 *"Buttered" surface*

Lamellar tearing tendencies are aggravated by the presence of hydrogen. When such tendencies are encountered, it is important to review the low hydrogen practice, examining the electrode selection, care of electrodes, application of preheat and interpass temperature. Additional preheat can minimize lamellar tearing tendencies.

6.4 Thermal Effects on Metallurgy

The mechanical properties of weld deposits will be largely determined by chemical composition and the thermal history experienced by the material. The major variables of preheat, interpass temperature and heat input determine the strength and toughness of weld deposits.

6.4.1 Preheat

Preheat refers to the temperature of the steel immediately before the arc is struck on the steel. The primary purpose of preheat is to slow the cooling rates that are experienced in the heat affected zone, preventing unacceptable hardening. This was also discussed under **5.3.2**. Preheat has many corollary advantages including: drying the joint of any retained moisture, burning off organic compounds, increasing the diffusion rate of hydrogen, slowing the solidification rate of the weld metal that may result in increased notch toughness, and lowering residual stresses. Overall, preheat has many significant advantages and is generally desirable. However, the following should be considered: preheat is expensive; excessively high preheats make it very difficult for the welder to perform the very best quality of work; on certain grades of steel, excessive preheats can damage the properties of the steel; and finally, weld metal properties may deteriorate when preheat or interpass temperatures exceed 550°F.

The proper level of preheat may be determined in one of several ways. The simplest and most straightforward method is to use the minimum preheat tables that have been specified in codes. For thinner sections of some grades of steel, D1.1-96 does not require any preheat, although the base metal must be at 32°F, even when no preheat is required. If the steel is below 32°F, it must be heated to 70°F minimum. These requirements, based on a history of acceptable usage, generally are sufficient to avoid heat affected zone cracking. However, codes are quick to point out that these are minimum requirements. Additional preheat may be required in situations of high restraint, enriched base metal chemistries, and adverse fabrication conditions.

A more accurate method is to base the required preheat on a specific analysis of the steel being welded. Obtaining the analysis, however, necessitates an actual test of the metal being considered. Mill test reports, for example, are not necessarily required to report all the elements that may affect hardenability. Likewise, ASTM specifications do not control all such elements. Once a chemistry is established, the composition can be used to predict the required preheat level. Myriad equations exist that have been empirically determined by various investigators. These are all based upon a hardenability or a carbon equivalency (CE) system. Carbon equivalency formulas rest on the assumption that various carbon levels and alloy contents can be empirically related to a singular number that can be used to determine required preheat levels. Based on the chemical compositions, the appropriate slower cooling rates that prohibit the formation of hard brittle microstructures can be determined.

When using these composition-based systems, it is important to keep in mind that they are empirical in nature. When determining the required preheat level for a given material, it is essential that the material be similar to those evaluated for the empirical model. Most systems are based upon carbon contents in the range of 0.12 - 0.35% and total alloy content of less than 5%. For extremely low levels of carbon, extremely high levels of carbon, or alloy contents that exceed this 5% limit, it is important to evaluate the applicability of the empirical model. Many systems will deliver a recommended preheat that is not valid for the particular steel analysis being used.

Preheat levels normally are based upon the steel being joined. In some of the newer grades of steel, it is possible to have weld metal that is higher in hardenability than the base material. Under these conditions, preheat should be based upon the filler metal composition. This is particularly true of the new generation of steels with carbon contents of less than 0.10%.

6.4.2 Interpass Temperature

Interpass temperature is identical to preheat, except that it is the temperature of the steel when the arc is re-initiated for subsequent weld passes. It has two components: minimum and maximum. The required minimum interpass temperature should be the same as the minimum specified preheat. This is the temperature below which welding should not be performed unless additional energy is added to raise the temperature of the steel. The maximum interpass temperature is that level beyond which welding should not be performed.

If a steel is hotter than the maximum interpass temperature, it should be allowed to cool to the maximum level. Water should never be applied to a weld joint to cool it, although a fan may be used to speed the cooling of a weldment.

On small weldments and short joints requiring multiple passes, there is a tendency for heat to accumulate, raising the interpass temperature. For example, preheat will be applied to bring the steel to the initial temperature required. The welding process adds additional thermal energy, which will cause the temperature of the part to rise. Welding can progress until a maximum interpass temperature is attained. Welding must then cease until the joint is cooled down to the acceptable maximum level.

Large weldments, on the other hand, generally will lose interpass temperature. This would be typical of multiple pass web-to-flange connections on plate girders. In this situation, the joint can be preheated to the acceptable level. A weld pass is placed in the joint, but due to the long length of the weld, the starting point for the second pass typically will have dropped below the minimum interpass temperature, necessitating heating the part again before welding can continue.

The minimum interpass temperature should not be lower than the preheat temperature. The maximum interpass temperature should be determined based on metallurgical requirements for the weld metal or the base material. For quenched and tempered steels, the maximum interpass temperature is controlled by the base material. This includes A514, which generally should not be allowed to exceed 450°F. On other grades, the maximum interpass temperature should be held below 550°F, unless a specific procedure qualification has been performed on test assemblies that duplicate higher interpass temperatures.

6.4.3 Heat Input

Heat input is a measure of the thermal energy added to the base metal during welding. As discussed in **6.2.2**, it also affects the weld cross sectional area. In this coverage of thermal effects, the focus will be on the energy the arc imparts to the base metal.

Excessively low heat inputs result in extremely narrow heat affected zones that are rapidly cooled. Since this can contribute to cracking and fusion problems, welding codes dictate a minimum sized weld for a given thickness of material. The specification of minimum weld size ensures that acceptable minimum levels of heat input are maintained.

Excessively high heat inputs result in high levels of energy being introduced into the base materials. This is a major concern with quenched and tempered steels, and may deteriorate properties in other steels. Most steel suppliers have guidelines limiting the heat input where this is a concern.

6.4.4 Interaction of Preheat and Heat Input

Heat input levels can be used to maintain or even increase the interpass temperature as compared to the preheat temperature. Because of the interaction of preheat and interpass temperature, some tables have been developed that allow for reduced preheats when higher heat input procedures are used.

Because of the relatively high level of heat input afforded by submerged arc welding, it is possible to use lower preheats than are required for other processes. By using these alternate approaches, the fabricator can utilize this arc energy effectively.

An extreme example of the interaction of preheat and heat input can be seen in the electroslag/ electrogas welding processes. These vertical welding processes deliver extremely high levels of heat input, frequently exceeding 1,000 kj/in. With this tremendous amount of heat input, preheat rarely is required for these welding processes. It is advisable, however, to heat the joint to ensure that any moisture or organic compounds are removed. Since the heating of the joint is being provided by the welding process, it is important that starting sumps be of dimensions that permit the welding energy to soak into the production joint before the weld puddle enters that region.

Some methods of computing the required preheat incorporate the effect of base metal chemistry, plate thickness, hydrogen level, and heat input of welding. With these systems, the energy afforded by the arc is incorporated into the required preheat, generally resulting in lower preheat requirements. However, for low heat input welding procedures, higher than ordinary preheats may be required to compensate for the lack of energy input from the welding process. The approach presented in D1.1-96 Annex IX may be used (AWS, 1996, ref. 14).

6.4.5 Applying Preheat

Preheat may be applied in several fashions; oxyfuel torches are one of the most common. One of the products of combustion is moisture. When a flame is applied to a cold steel surface, condensation of H_2O from the flame may result in a ring of moisture in the region. This has perpetuated a myth that preheat "drives the moisture out of the steel." Joints may require drying because of moisture that condenses on the surface. However, even dry steel will exhibit this condensing effect from gas flames.

As an alternate to open flames, resistance strip heaters can be applied. These frequently are powered by the same type of equipment as is used for the welding power sources and may be advantageous in situations where open flames are undesirable.

It is possible to preheat components in industrial stress relief furnaces, although it is not frequently done. For large, complex assemblies, this may be a desirable way to obtain the required preheat on the assembly. Unfortunately, such equipment is seldom available in structural fabrication shops.

When preheating is done with gas flames, it is important to make sure that the surface is not "burned" by the torches. There should be no localized melting of the steel. Moreover, when the steel is being heated, it should not exceed the transformation temperature of the steel. There is no reason for steel to exceed 1000°F during the preheating operation, and if the steel begins to change color, it is being heated too rapidly. Of course, the preheat temperature levels would not be in this range, but in the act of raising the surrounding steel to the required preheat level, locally this temperature can be attained if practices are not monitored. It is possible to inadvertently heat treat these materials while preheating. Particular caution should be exercised when quenched and tempered steels are preheated.

6.4.6 Measuring Preheat

When monitoring the preheat and interpass temperatures, temperature indicating crayons are frequently used. These devices have specific melting points which indicate the temperature of the steel. Welders typically use one crayon to indicate the minimum preheat and minimum interpass temperature, and a second to indicate the maximum interpass temperature.

Welding should begin or continue only when the lower temperature crayon melts, and the high temperature crayon does not. This assures that the preheat level has been achieved, and the maximum interpass temperature has not been exceeded. The point of measurement of preheat temperatures may be dictated by the applicable code. It is advisable to check the preheat at a distance away from the joint that is equal to the thickness of the material being joined, but not less than 3 in. in all directions, including through the thickness. Temperatures also can be read with contact pyrometers. While these may appear to be more accurate, the crayons actually are very accurate and provide an effective way to control the preheat in the fabrication environment.

6.4.7 Ambient Temperature

Ambient conditions are those localized conditions in the vicinity of the weld joint. Most welding codes indicate that welding shall not be performed when the ambient temperature is below 0°F. This is for reasons of workmanship and is independent of preheat temperatures. It is assumed that if the environ-

mental temperature is below 0°F, the welder will not be able to deliver the required quality of welding. It is possible, however, to create a new environmental ambient condition. A shelter can be erected around the joint in which the temperature can be raised to a suitable level. Even though the outside temperature may be below 0°F, welding can continue if the local ambient temperature is above 0°F, and the steel is at a minimum of 70°F, or the minimum preheat temperature, which ever is higher.

6.5 Joining Dissimilar Steels

Where structural designs require a greater capacity in one region, the designer has the option of increasing the size of the member or increasing the strength. To maintain uniform flange widths and thicknesses, steels of different strength levels may be specified in these situations. When joining dissimilar steels, it is common to require that the weld meet the requirements of the lesser of the two steels. If A572 Gr50 steel is being joined to grade A514 steel, the weld connection need only have the strength requirements of the 50 ksi material. The fabrication practice should be controlled by the more demanding of the two steels. For example, if one steel requires 125°F preheat, while the other requires only 70°F preheat, 125°F should be applied to both. Any restrictions on heat input imposed by one material should be applied to the entire joint. The lower of the maximum interpass temperatures should be applied to the joint.

If significantly dissimilar materials are to be joined, such as stainless to carbon steel, the variety of issues raised is well beyond the scope of this manual. The preceding information is applicable when common structural steels are joined to other common structural steels.

7 Distortion — Theory and Control

7.1 Why Distortion Occurs

Distortion occurs due to the non-uniform expansion and contraction of weld metal and adjacent base material during the heating and cooling cycles of the welding process. At elevated temperatures, hot, expanded weld and base metal occupies more physical space than it will at room temperatures. As the metal contracts, it induces strains that result in stresses being applied to the surrounding base materials. When the surrounding materials are free to move, distortion results. If they are not free to move, as in the case of heavily restrained materials, these strains can induce cracking stresses. In many ways, distortion and cracking are related.

It should be emphasized that not only the weld metal, but also the surrounding base material is involved in this contraction process. For this reason, welding processes and procedures that introduce high amounts of energy into the surrounding base material will cause more distortion.

Stresses resulting from material shrinkage are inevitable in welding. Distortion, however, can be minimized, compensated for, and predicted. Through efficient planning, design, and fabrication practices, distortion related problems can be effectively minimized.

7.2 Control of Distortion

7.2.1 Design Concepts to Minimize Distortion

The engineer who is aware of the effects of distortion can design measures into the welded assemblies that will minimize the amount of distortion. These concepts include the following:

Minimize the amount of weld metal. Any reduction in the amount of weld metal will result in a decrease in the amount of distortion:

- use the smallest acceptable weld size;
- use intermittent welds where acceptable;
- utilize double-sided joints versus single-sided joints where applicable; and
- use groove details that require the minimum volume of weld metal per length.

Place welds near the neutral axis. When welds are placed near the neutral axis, less longitudinal sweep or camber results. This is illustrated in Fig. 7-1.

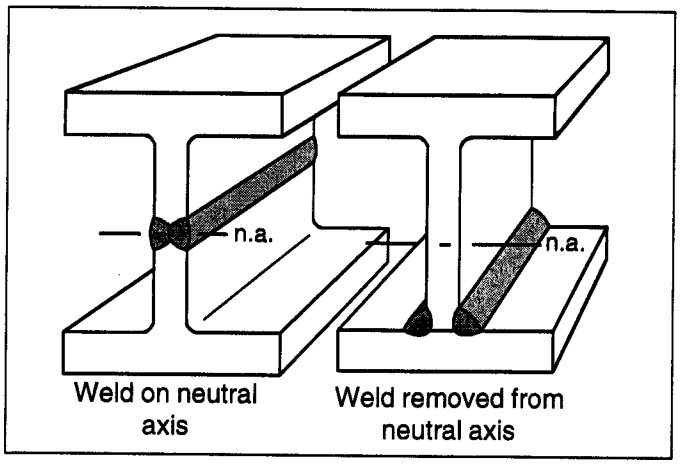

Figure 7-1 *Neutral axis*

Balance welds about the neutral axis. When welds are balanced around the neutral axis, the shrinkage force of one weld will be counteracted by the shrinkage force of another. This is illustrated in Fig. 7-2.

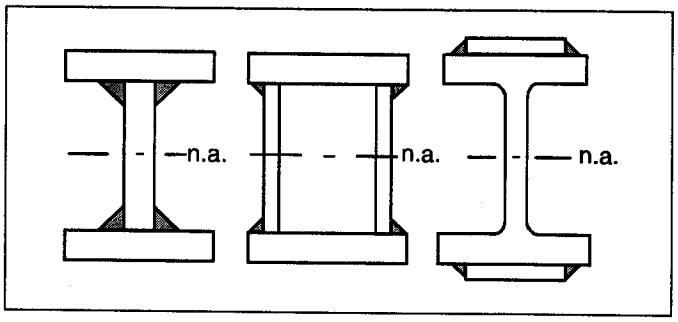

Figure 7-2 *Welds balanced about the neutral axis*

7.2.2 Fabrication Practices that Minimize Distortion

Fabricators can use techniques that will minimize distortion. These include the following:

Use as few weld passes as possible. Fewer passes are desirable inasmuch as they limit the number of heating and cooling cycles to which the joint will be subjected. The shrinkage stresses of each pass tend to accumulate, increasing the amount of distortion when many passes are used. Note that this is in direct contrast with the criterion of maximizing notch toughness, as was discussed in **6.2.2**.

Avoid overwelding. Overwelding results in more distortion than is necessary. Holding weld sizes to print requirements will help avoid unnecessary distortion.

Obtain good fit-up. Poor fit-up, resulting in gaps and larger included angles for bevel preparations, means more weld metal is placed in the joint than is required, contributing to excessive distortion.

Use high productivity, low heat input welding procedures. Generally speaking, high productivity welding procedures (those using high amperages and high travel speeds) result in a lower net heat input than low productivity procedures. At first, high amperage procedures may seem to be high heat input procedures. However, for a given weld size, the high amperage procedures are high travel speed procedures. This will result in a decreased amount of heat affected zone and reduced distortion.

Use clamps, strongbacks, or fixtures to restrict the amount of distortion. Any tooling or restraints that avoid rotation of the part will reduce the amount of distortion experienced. In addition, fixturing may be used to draw heat away, particularly if copper chill bars and clamps are used in the vicinity of the joint. The arc should never impinge on copper as this could cause cracking.

Use a well planned welding sequence. A well planned welding sequence is often helpful in balancing the shrinkage forces against each other.

Preset or precamber parts before welding. Parts to be joined may be preset or precambered before welding. When weld shrinkage causes distortion, the parts will be drawn back into proper alignment.

8 Weld Quality

A weld must be of an appropriate quality to ensure that it will satisfactorily perform its function over its lifetime. Weld "quality" is therefore directly related to the purpose the weld must perform. Codes or contract documents define the required quality level for a specific project. A quality weld, therefore, is one that meets the applicable requirements. Ensuring that the requirements have properly addressed the demands upon the weld is ultimately the responsibility of the Engineer.

8.1 Weld Discontinuities

Many welds contain discontinuities, which are defined as an interruption in the typical structure of the material, such as a lack of homogeneity in its mechanical, metallurgical, or physical characteristics (AWS, 1989, ref. 12). Such irregularities are not necessarily defects. A defect is defined as a discontinuity that is unacceptable with respect to the applicable standard or specification. Defects are not acceptable; discontinuities may, or may not, be acceptable.

Welds are not required to be "perfect," and most welds will contain some discontinuities. It is imperative that the applicable standards establish the level of acceptability of these discontinuities in order to ensure both dependable and economical structures. AWS D1.1 is the primary standard used to establish workmanship requirements. In general, these are based upon the quality level achievable by a qualified welder, which does not necessarily constitute a boundary of suitability for service. If the required weld quality for each type of weld and loading condition were specified, widely varying criteria of acceptable workmanship would be required. Moreover, acceptable weld quality (in some cases) would be less rigorous than what would be normally producible by a qualified welder (D1.1-96, para. C6.8). This suggests that, in some cases, the requirements exceed the actual requirements for acceptable performance. The Engineer can use a "fitness for purpose" type evaluation to determine alternate acceptance criteria in such situations. Some specific loading conditions require more stringent acceptance criteria than others. For example, undercut associated with fillet welds would constitute a stress riser when the fillet weld is loaded in tension perpendicular to its longitudinal axis. However, when the same fillet weld is loaded in horizontal shear, this would not be a stress riser, and more liberal allowances are permitted for the level of undercut.

A variety of types of discontinuities can exist in welds. Characteristics, causes, and cures of common examples may be summarized as follows:

Undercut is a small cavity that is melted into the base metal adjacent to the toe of a weld that is not subsequently filled by weld metal. Improper electrode placement, extremely high arc voltages, and the use of improper welding consumables encourage undercut. Changes to the welding consumable and welding procedures generally alleviate undercut.

Excess concavity or **excess convexity** are weld surface profile irregularities. These are operator- and/or procedure-related.

Overlap is the protrusion of weld metal beyond the toe of the weld where the weld metal is not bonded to the base material. Overlap usually is associated with slow travel speeds.

Incomplete penetration is associated with weld joint details that rely on melting of base metal to obtain the required weld strength. A typical example would be a square edged butt joint. Incomplete penetration occurs when the degree of penetration is inadequate, and is generally attributable to inadequate current density, improper electrode placement, or excessively slow travel speeds.

Lack of fusion, or incomplete fusion, is the result of the failure of the weld metal and the base metal to form the metallurgical bonds necessary for fusion. Lack of fusion can range from small, isolated planes, or, in extreme cases, may consist of a complete plane between the weld metal and the base metal where fusion does not exist. Improper filler metal selection, improper welding procedures, and poor surface preparation are common causes of this condition. Improper use of GMAW-s is a common cause of lack of fusion.

Arc strikes consist of small, localized regions of metal that have been melted by the inadvertent arcing between electrically charged elements of the welding circuit and the base metal. Welding arcs that are not initiated in the joint leave behind these arc strikes. Arcing of work clamps to the base metal can cause arc strikes, as can welding cables with improper insolation. SMAW is particularly susceptible to creating arc strikes since the electrode holder is electrically 'hot' when not welding. The use of properly insulated welding equipment and proper welding practices minimize arc strikes. Grinding away the affected (melted) metal is an effective way of eliminating any potential harm from arc strikes.

Slag inclusions describe the non-metallic material entrapped in the weld metal, or between the weld metal and base metal. Slag inclusions are generally attributed to slag from previous weld passes that was not completely removed before subsequent passes were applied. Slag may be trapped in small cavities or notches, making removal by even conscientious welders difficult. Proper joint designs, welding procedures, and welder technique can minimize slag inclusions.

Spatter are the roughly spherical particles of molten weld metal that solidify on the base metal outside the weld joint. Spatter is generally not considered to be harmful to the performance of welded connection, although excessive spatter may inhibit proper ultrasonic inspection, and may be aesthetically unacceptable for exposed steel applications. Excessive spatter is indicative of less-than optimum welding conditions, and suggests that the welding consumables and/or welding procedure may need to be adjusted to minimize the creation of spatter.

Porosity consists of spherical or cylindrical cavities that are formed as gases entrapped in the liquid weld metal escape while the metal solidifies. There are acceptable limits for porosity as a function of its type, size, and distribution (D1.1-96, para. 6.12.2.1). Porosity occurs as the result of inadequate shielding of the weld metal, or excessive contamination of the weld joint, or both. The products used for shielding weld deposits (gases, slags) must be of appropriate quality, properly stored, and delivered at a rate to provide adequate shielding. Excessive surface contamination such as oil, moisture, rust, or scale increases the demand for shielding. Porosity can be minimized by providing proper shielding, and ensuring joint cleanliness.

Cracking in welds is the most serious type of weld discontinuity, and is nearly always considered a defect. Weld cracking is extensively discussed in **5.3.**

8.2 Weld Quality and Process-Specific Influences

Weld discontinuities, their causes and cures, have been previously described in a general sense. Some welding processes are more sensitive to the generation of certain types of weld discontinuities, and some weld discontinuities are associated only with a few types of welding processes. Conversely, some welding processes are nearly immune from certain types of weld discontinuities. Contained below are the popular welding processes and their variations, along with a description of their associated sensitivity relative to weld quality.

8.2.1 SMAW

The unique limitations of shielded metal arc welding fall into three categories: arc length related discontinuities, start-stop related discontinuities, and coating moisture related problems. In SMAW, the operator controls arc length. Excessively short arc lengths can lead to arc outages, where the electrode becomes stuck to the work. When the electrode is mechanically broken off of the joint, the area where the short has occurred needs to be carefully cleaned, usually ground, to ensure conditions that will be conducive to good fusion by subsequent welding. The electrode is usually discarded since a portion of the coating typically breaks off of the electrode when it is removed from the work. Excessively long arc lengths will generate porosity, undercut, and excessive spatter. Because of the finite length of the SMAW electrodes, an increased number of start-and-stops is necessitated. During arc initiation with SMAW, starting porosity may result during the short time after the arc is initiated and before adequate

shielding is established. Where the arc is terminated, under filled weld craters can lead to crater cracking. The coatings of SMAW electrodes are sensitive to moisture pickup. While newer developments in electrodes have extended the period for which electrodes may be exposed to the atmosphere, it is still necessary to ensure that the electrodes remain dry in order to be assured of low hydrogen welding conditions. Lack of care of low hydrogen SMAW electrodes can lead to hydrogen induced cracking, i.e., underbead cracking or transverse cracking.

8.2.2 FCAW-g

In FCAW-g, as with all gas shielded processes, it is important to protect the gas shielding around the weld deposit. If FCAW-g gas shields are disturbed by winds, fans, or smoke exhaust equipment, porosity can result. The deep penetrating characteristics of FCAW-g are generally advantageous, but excessive penetration can lead to centerline cracking because of a poor width-to-depth ratio in the weld cross-section.

8.2.3 FCAW-ss

Excessively high arc voltages, or inappropriately short electrode extension dimensions can lead to porosity with FCAW-ss. When excessive voltages are used, the demand for shielding increases, but since the amount of shielding available is relatively fixed, porosity can result. When the electrical stickout distance is too short, there may be inadequate time for the various ingredients contained within the electrode core to chemically perform their function before they are introduced into the arc. This too can lead to porosity. Because of the extremely high deposition rate capability of some of the FCAW-ss electrodes, it is possible to deposit quantities of weld metal that may result in excessively large weld beads, leading to a decrease in fusion, if not balanced with a corresponding increase in travel speed.

8.2.4 GMAW

When solid electrodes are used, and particularly when welding out of position, the short arc transfer mode is frequently used. This can directly lead to cold-lap, a condition where complete fusion is not obtained between the weld metal and base material. This is a major shortcoming of the GMAW process and is one of the reasons why its application is restricted by the D1.1 code with respect to its prequalified status. As with all gas-shielded processes, GMAW is sensitive to the loss of gas shielding.

8.2.5 SAW

Submerged arc welding is sensitive to alignment of the electrode with respect to the joint. Misplaced or misshaped beads can result. The deep penetration of the SAW process can lead to centerline cracking due to improper width-to-depth ratios in the bead cross-section.

8.2.6 ESW

Maintaining the proper slag burden with the electroslag process is a delicate operation. Excessive flux burdens can suppress side wall fusion and can result in arc outages. Inadequate volumes of slag can result in significant porosity problems. Ultrasonic inspection of ESW welds has been incapable of detecting even massive quantities of piping porosity under specific conditions. Alternate scanning techniques and new UT equipment has helped to minimize this problem, although there continues to be among many experts a preference for RT inspection of ESW welds.

8.2.7 EGW

For true, gas-shielded EGW, the greatest problem is ensuring adequate shielding. Loss of shielding would naturally result in porosity. For the self-shielded EGW process, the greatest obstacle is maintaining the proper slag burden where, like ESW, excessive slag volumes can cause fusion problems, and inadequate shielding can lead to porosity.

9 Weld Inspection

Welds are inspected to ensure that they comply with the requirements of a given specification. Welds are acceptable when they conform to all the requirements in a given specification or code. Weld quality is directly tied to the code or specification under which the work is being performed.

9.1 The Roles of Engineers, Fabricators and Inspectors

For a full understanding of issues related to weld inspection, it is necessary to define the roles and responsibilities of various individuals involved in welded fabrication. The following definitions are taken from the AISC *Code of Standard Practice* and/or the AWS *D1.1-96 Structural Welding Code - Steel* :

Owner: The owner of the proposed structure OR that individual's designated representatives, who may be the Architect, Engineer, General Contractor, Public Authority, or others.

Architect/Engineer: The Owner's designated representative with the full responsibility for the design and integrity of the structure.

General Contractor: The Owner's designated representative with the full responsibility for the construction of the structure.

Fabricator: The party responsible for furnishing fabricated structural steel.

Erector: The party responsible for the erection of the structural steel.

Verification Inspector: The duly designated person who acts for, and on behalf of, the Owner or the Engineer in all inspection and quality matters within the scope of the contract documents. (In some codes, such as *AASHTO/AWS D1.5-95 Bridge Welding Code*, this Inspector is known as the Q.A. Inspector, that is, the Quality Assurance Inspector.)

Fabrication/Erection Inspector: The duly designated person who acts for and on behalf of the Contractor in all inspection and quality matters within the scope of the contract documents. (In D1.5, this Inspector is known as the Q.C. Inspector, that is, the Quality Control Inspector.)

Inspector: When the term Inspector is used without further qualification, it applies equally to both the Verification and Fabrication/Erection Inspector.

For the purposes of this paper, comments directed toward the Fabricator apply equally to the Erector. Since most or all of the welding will be performed by either the Fabricator or Erector, the General Contractor will not be considered in this discussion. The term Engineer will be used in lieu of Architect/ Engineer.

9.1.1 Responsibilities

The Engineer has the ultimate and full responsibility for the integrity of the structure. It is the Engineer who must establish the required quality level for all welded fabrications. This may be done by invoking a standard such as the D1.1 code. It is imperative that the Engineer understand the requirements, restrictions, and implications of the full code. The Engineer is responsible to ensure that the code provisions are adequate for the structure. Additional provisions may be required for unique structures, and these requirements must be invoked in contract documents. The Engineer is responsible for determining and specifying the level of quality required. The Engineer is also responsible to ensure that the specified level of quality is delivered by the Fabricator. The Engineer has a professional responsibility to the Owner to deliver the project in a timely fashion, and at an appropriate cost.

To assist in the quality issues, the Engineer may employ the services of a Verification Inspector. Under D1.1, this is left up to the Engineer's discretion (D1.1-96, para. 6.1.1). A Verification Inspector may be engaged either to duplicate the services of the Fabrication Inspector, or to supply spot checks. However, the Engineer may choose to rely solely upon the Fabrication Inspector to ensure the necessary quality is achieved. Many factors enter into this decision, including:

- the complexity of the structure;
- the degree of redundancy involved; and
- the relative level of confidence the Engineer has in the Fabricator.

While the Engineer must be responsible to ensure the level of quality is achieved, it is ultimately the Fabricator's responsibility to produce a quality product. To this end, the Fabricator will employ Fabrication Inspectors (Q.C. Inspectors) to monitor the welding operations and inspect the final product.

Since the Fabricator does all the welding, only the Fabricator can produce quality welds. Inspectors cannot "improve" the quality of the product that has been produced. The Inspector simply measures the level of quality achieved, and accepts those products that are within conformance.

Inspectors are responsible to ascertain that all fabrication and erection by welding is performed in accordance to the requirements of the contract documents. When contract documents invoke certain specifications or codes, the Inspector must ensure that all such requirements are met. It is important to note that the emphasis is placed on acceptance and compliance to the specification. A prevailing—but mistaken—impression of Inspectors is that their primary responsibility is to reject out-of-compliance work. This is more than an issue of semantics. The ability to reject a particular weldment is ultimately the Engineer's responsibility. The Inspector's responsibility is to accept materials that are in compliance.

9.1.2 Abuses and Errors

Abuses of, and deviations from, the philosophy outlined here are widespread. They can be perpetrated by Engineers, Inspectors or Fabricators. For instance, the Engineer may delegate engineering authority to the Inspector. The rationale for this type of decision appears to be fairly straightforward: the Engineer is not familiar with the intricacies of the code and/or fabrication process, and therefore empowers the Inspector to make decisions on his/her behalf. On the surface, this appears logical, particularly when the Inspector is highly qualified, perhaps an Engineer by training. On the other hand, another Inspector may not have the background necessary to make these types of decisions. Moreover, rarely will the Inspector have the benefit of understanding the overall structural implications of various decisions. For example, a fillet weld has been sized based upon the minimum prequalified fillet weld sizes. This

fact obviously should enter into the considerations regarding the acceptability of a slightly undersized fillet weld. In the absence of this design data, the Inspector does not have the necessary information to make the most responsible decision.

Inspectors should see that the code is followed, and report nonconformance to the Engineer. When the code requires that the "Engineer be notified" prior to some action, it is not the Inspector who should be notified. Inspectors are not in the business of deciding new acceptance criteria. That is the Engineer's responsibility. Inspectors should not be determining whether code provisions are adequate or overly restrictive. They are charged with following the established code provisions.

Many Inspectors feel they are the ultimate authority on the project. It is important to note that the Engineer has the authority to review the Inspector's credentials. Although the Fabrication Inspector is paid by the Fabricator, that Inspector's credentials and capabilities are subject to approval by the Engineer. The Engineer directly employs the Verification Inspector, who obviously is responsible to the Engineer.

Fabricators also make errors. Some companies will attempt to hide problems from the Inspector. More blatant abuses include offering bribes to Inspectors. Such activities are illegal, immoral, and unprofessional. The entire industry is hurt when a small minority thus abuses its responsibility. The Fabricator may also err by failing to utilize provisions within the code which permit deviation from standard acceptance criteria. Fabricators must know the entire code and understand what is mandatory, what is permitted, and what can be changed. Without reading the complete code, Fabricators will frequently apply one set of provisions in a universal fashion, believing it to be all-encompassing. Unnecessary increases in fabrication costs usually result. It is imperative that the whole code be understood in its entirety in order to meet the quality requirements at a reasonable cost.

Engineers are responsible for thoroughly understanding the code, the fabrication processes, and the proper roles of the Inspector and the Fabricator. If the Engineer of Record is not familiar with the intricacies of the welding processes or those of welding codes, it is imperative to consult a Welding Engineer, another professional, separate and distinct from the Inspector. The Inspector must understand how to enforce the application of the code, accept work that conforms to code requirements, and report to the Fabricator deviations from these requirements. The Inspector must know the whole code, and apply it to the situation, not "interpret" it.

The Fabricator must know the entire code, accept the Inspector's report of deficient work, and either repair deficiencies or propose an alternative to the Engineer. With the report of nonconformance, the Engineer can apply engineering judgment to resolve the problem. This approach leaves the ultimate responsibility for the project with the Engineer of Record, where it must remain. The Inspector has not exercised engineering judgment, the Fabricator has gained all the latitude necessary, and ultimately, the result is a project of the required quality at a reasonable cost.

9.2 Effective Visual Inspection (VT)

Visual inspection is the most powerful tool that can be employed to ensure weld quality. The more technologically sophisticated nondestructive processes, such as ultrasonic or radiographic inspection, can only verify that the desired quality is present once welding is complete. Effective visual inspection examines each step of the welding process, well before the weld is completed.

Everyone involved in a welding project can — and should — participate in in-process visual inspection, including the welders, Inspectors, foremen, etc. Minor discontinuities can be detected and corrected during the fabrication process, precluding the need for more expensive and complicated repair after the fabrication is complete. In order to be effective, visual inspection must take place prior to, during, and after welding. Obviously, visual inspection requires good eyesight and good lighting. Frequently, good lighting is scarce in a fabrication shop or even in certain parts of a construction site, so a simple flashlight can be a valuable aid to visual inspection.

9.2.1 Inspecting the Welding Process

Over the years, welding has been described as both an art and a science. While it is both, there has been a disproportionate emphasis on the *art* of welding. Welding is a complex science involving the interaction of many disciplines. Nevertheless, the welding process is subject to certain physical and chemical laws that allow it to be controlled and the results predicted.

The quality of a completed weld is predictable, providing the input variables are known. Unfortunately, input variables (even critical input variables) are often misunderstood, ignored, or uncontrolled, resulting in welds of unpredictable quality. Variables may be overlooked for several reasons. During procedure qualification testing for example, it is essential that critical welding parameters be evaluated and identified. During the qualification and testing of welders, the unique requirements of the specific application must be communicated to them. When all input variables are properly identified and controlled, welds of the required quality will be consistently achieved. Effective visual inspection can ensure that significant variables are controlled, resulting in welds of the required quality.

Discontinuities in welds do not occur by mere chance. They are the result of failure to identify and control for one or more critical variables. Even when critical variables are identified, they are frequently ignored or not properly communicated to the individuals involved.

While visual inspection is a powerful tool, its potency may be questioned because of past experience. Despite the application of visual inspection, weld discontinuities and defects are routinely found by nondestructive testing methods. The unfortunate fact is that visual inspection is rarely properly performed. Welding is a process, and the process must be observed throughout its application. If an Inspector arrives on the job site after the welds are complete, it is impossible to properly apply visual inspection. Because the nondestructive testing methods evaluate completed welds, Inspectors are trained to focus on finished products. Attention must be refocused on visually inspecting the process, not merely the finished result.

9.2.2 *AWS B1.11 - Guide for Visual Inspection of Welds*

To provide practical information about the requirements for conducting visual inspections, the American Welding Society has published a concise, 28-page document, *AWS B1.11 - Guide for Visual Inspection of Welds* (1988, ref. 9). Consistent with the philosophy already presented, AWS B1.11 emphasizes the importance of inspection prior to welding, during welding, and after welding. Practical suggestions, presented in a checklist format, are offered for each phase.

In Section 3.2 of B1.11, the following items are highlighted as part of inspection prior to welding:

1. Review drawings and specifications.
2. Check qualifications or procedures and personnel to be utilized.
3. Establish check points.
4. Set up a plan for recording results.
5. Review materials to be utilized.
6. Check for base metal discontinuities.
7. Check fitup and alignment of welded joints.
8. Check preheat, if required.

When appropriate attention is paid to these issues, the quality of the yet-to-be-made weld can be expected to improve as a result of the pre-welding inspection. For example, when fitup and alignment of the joint are carefully inspected, consistent uniform fusion to the root of the weld and avoidance of excessive distortion and/or residual stresses can be achieved.

Item No. 3 discusses the establishment of checkpoints, which is particularly critical for large weldments or complex projects when subsequent fabrication activities may preclude further inspection of the fabrication process. Concurrent with this idea is the development of "hold points" where approval is required before further fabrication can be continued. This must be coordinated with the various contractors involved so that the overall project can proceed as expected. Establishment of "hold points," and communication with all parties involved, are critical to maintaining both quality and the job schedule.

In Section 3.3 of B1.11, items that should be inspected during welding are outlined. These include:

1. Quality of weld root bead.
2. Joint root preparation prior to welding the second side.
3. Preheat and interpass temperatures.
4. Sequence of welding passes.
5. Subsequent layer for apparent weld quality.
6. Cleaning between passes.
7. Conformance with the applicable procedure.

The root pass, often the most critical part of the weld, frequently is made under the most difficult conditions. Maintenance of the proper preheat and interpass temperatures is critical for the metallurgical integrity of both the weld metal and the heat affected zone. Inspection of intermediate weld layers, including removal of slag between layers, is absolutely essential for applications where only visual inspection will be applied. Conformance with the maximum layer thicknesses and bead widths as governed by the applicable welding code or WPS requirements can be visually verified at this point.

The requirements for post-weld inspection are covered in Section 3.4 of B1.11. Before the checklist is provided, the following statement is made: "Many people feel that visual inspection commences once the welding has been completed. However, if all of the precedingly discussed steps have

been taken before and during welding, this final phase of visual inspection will be accomplished easily. It will simply provide a check to be sure that the steps taken have resulted in a satisfactory weld." This statement endorses the power of an effective visual inspection. The checklist of items to inspect after welding includes the following:

1. Final weld appearance.
2. Final weld size.
3. Weld length.
4. Dimensional accuracy.
5. Amount of distortion.
6. Post-weld heat treatment.

The importance of these issues is self-evident. The appearance of the weld is a strong indicator of the suitability of the actual welding procedure used, and the ability of the individual welder. More than merely a cosmetic issue, weld appearance provides some insight into how the weld was made.

9.2.3 Visual Inspection and the AWS D1.1 Code

Visual inspection is a key ingredient in the approach taken by the D1.1-96 code to ensure quality. Visual inspection is mandated by D1.1-96, para. 6.9 which states: "All welds shall be visually inspected...". In the chapter on Inspection, the following specific directions are given to the Inspector:

- The Inspector shall make certain that only materials conforming to the requirements of this code are used. (6.2)

- The Inspector shall make certain that all the welding procedures are prequalified and covered by welding procedure specification, or qualified in accordance with 4.1.1 of this code. (6.3.1)

- The Inspector shall inspect all welding equipment to be used in the work to make certain that it conforms to the requirements of 5.11. (6.3.2)

- The Inspector shall permit welding to be performed only by welders, welding operators, and tack welders who are qualified in accordance with the requirements of Section 4.(6.4.1)

- The Inspector shall make certain that only welding procedures are employed which meet the provisions of Section 3 or Section 4. (6.5.2)

- The Inspector shall make certain that electrodes are used only in the positions and with the type of welding current polarity for which they are classified. (6.5.3)

- The Inspector shall, at suitable intervals, observe joint preparation, assembly practice, the welding techniques, and performance of each welder, welding operator, and tack welder to make certain the applicable requirements of this code are met. (6.5.4)

These code requirements make it obvious that visual inspection must begin before the work is completed. This may deviate from the approach used by many Inspectors, but it is the only approach that can actually prevent the formation of welding defects. For example, when the base materials being used are examined, the Inspector can preclude the use of the wrong type of material in a specific application.

Careful examination of welding procedures will reveal the suitability of a specific procedure for a particular application. The welder's credentials will help determine the suitability of that individual for the specific application.

The AWS D1.1-96 Structural Welding Code clearly requires that inspection be performed before, during and after welding. It is the responsibility of the fabrication/erection inspector to ensure that the requirements of the contract documents are achieved, which would include the applicable sections of the D1.1 Code. A review of the various workmanship-related provisions of the Code reveals the types of operations that are to occur during these three stages of fabrication. If inspection activities occur exclusively after the welding has been completed, it is impossible to verify that some of the Code-mandated activities have actually occurred. Nondestructive testing is certainly part of an effective quality assurance program, although the nondestructive testing methods are not able to guarantee compliance with all the Code-mandated requirements. Nondestructive testing can complement but not replace effective in-process visual inspection of the various welding operations.

The following is a partial list of the activities that must be verified before welding operations begin:

- Adherence to the dimensional tolerances for prequalified joints (D1.1-96, Fig. 3.3, 3.4).
- Conformance to the tolerances of joint details qualified by test (D1.1-96, Fig. 5.3).
- Proper fitup of joints to receive fillet welds (D1.1-96, para. 5.22.1).
- Confirmation that backing is continuous for the length of the joints (D1.1-96, para. 5.10.2).
- Verification that minimum dimensions for weld access holes and copes are achieved (D1.1-96, Fig. 5.2).
- Acceptable quality of thermal cut edges (D1.1-96, para. 5.15).
- Proper cleanliness of weld joint (D1.1-96, para. 5.15).

During the welding operation, the following can be visually checked:

- The proper preheating of the joint in conformance with the WPS has been achieved (D1.1-96, para. 5.6).
- The surfaces that will be welded upon are dry (D1.1-96, para. 5.15).
- The welders are not subject to inclement conditions (D1.1-96, para. 5.12.2).
- The actual welding procedures being used conform to the WPS (D1.1-96, para. 6.5.2).
- Welders techniques are appropriate for the WPS (D1.1-96, para. 6.5.4).
- Weld layers are in conformance with the code requirements and WPS limitations (D1.1-96, Table 3.7).
- Weld beads are properly cleaned before subsequent welds are applied (D1.1-96, para. 5.30).
- For joints requiring backgouging, the resultant cavity is in substantial conformance with the groove profiles specified for prequalified groove details (D1.1-96, para. 5.22.5).

9.2.4 Inspecting the Completed Weld

Most of the emphasis to this point has been upon inspection prior to, and during welding. The quality of a completed weld can also be visually determined in many situations. The single exception to this, as previously noted, is gas metal arc - short arc transfer. With this process, a weld may have an excellent appearance and lack the essential fusion necessary for all forms of welding. In this case, extra

emphasis on process inspection and nondestructive testing will be warranted. A good-looking weld is generally a good weld. A poor-appearing weld may or may not be a poor weld. However, the presence of visually discernible criteria that deviate from good appearance is generally an indication that one or more variables are not being properly addressed. For example, excessive spatter may not detract from the quality of the weld. However, it is a sign that the process is not being controlled sufficiently.

Completed welds are inspected to ensure the completed weld meets the code imposed quality requirements. These are contained in D1.1-96, Table 6-1. The weld is acceptable providing the following conditions are met:

- The weld has no cracks.
- The weld is free of excessive undercut.
- The weld meets the geometric requirements regarding convexity, concavity and excessive reinforcement.
- The lengths and sizes of welds are as prescribed.
- The weld does not exceed the allowable limits of porosity.

The importance of visual inspection was vividly demonstrated to the author of this paper several years ago. A series of fatigue and brittle fractures that occurred on highway bridges was the subject of a professional meeting. As the organizer attempted to establish the need for more rigorous welded fabrication requirements, hydrogen cracking, brittle fracture, fracture mechanics, and fatigue details were all discussed. Most revealing, however, was a comment made by a very skilled technician, a welder, who had had no formal engineering training. His comment was as follows: "I don't understand fracture mechanics, fatigue, or hydrogen embrittlement. However, from what I see in these photographs, none of these welds that failed would have met the visual acceptance criteria of the Code." The silence in the room was deafening. The welder was correct. All of the technical issues that were being discussed had entered into these failures, but none of the welds should have ever been accepted based on simple visual inspection criteria.

9.3 Other Nondestructive Testing Methods

Nondestructive testing is an important element to any quality program. It cannot, however, replace in-process visual inspection. Before NDT is performed, the D1.1 Code requires that the welds first meet visual acceptance criteria (D1.1-96, para. 6-11).

Because of the diversity of projects that can be governed by the D1.1 Code, it is impossible to specify the exact means by which all the various required inspector functions are to be performed. This includes the extent and type of NDT to be performed. It is critical, therefore, that these items be established in advance of fabrication, under the direction of the engineer. It is the engineer's responsibility to determine whether verification inspection will be utilized, or whether reliance upon fabricator/erector inspection will be sufficient. The frequency of checks, documentation of results, establishment of hold points, and disposition of non-conformances should be established through pre-construction meetings (SAC Joint Venture, 1995, ref. 39). It is important that everybody on the project, including the various inspectors, welding supervisors, and the welders themselves, understand what is expected of them before construction begins.

9.3.1 Penetrant Testing (PT)

Liquid penetrant testing involves the application of a liquid which by a capillary action is drawn into a surface-breaking discontinuity, such as a crack or porosity (see Fig 9-1). When the excess, residual dye is carefully removed from the surface, a developer is applied, which will absorb the penetrant that is contained within the discontinuity. This results in a stain in the developer showing that a discontinuity is present.

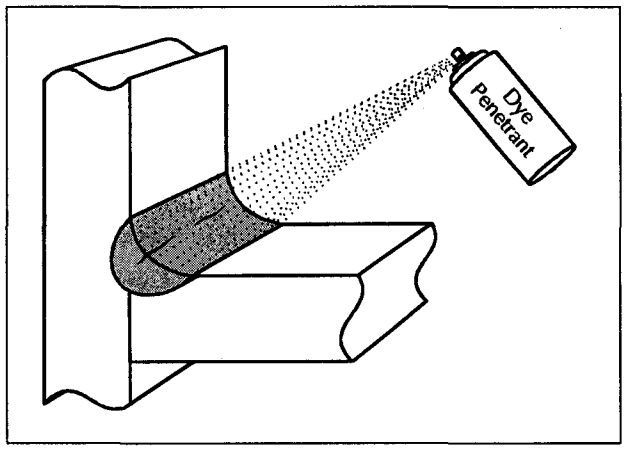

Figure 9-1 *Penetrant testing*

Dye penetrant testing is limited to surface discontinuities. It has no ability to read subsurface discontinuities, but it is highly effective in accenting the surface discontinuities that may be overlooked or be too small to detect with visual inspection. However, because it is limited to surface discontinuities, and because these discontinuities also will be observed with magnetic particle inspection, this method is not specified by most structural steel welding codes.

9.3.2 Magnetic Particle Inspection (MT)

Magnetic particle inspection utilizes the change in magnetic flux that occurs when a magnetic field is present in the vicinity of a discontinuity (see Fig. 9-2). This change in magnetic flux density will show up as a different pattern when magnetic powders are applied to the surface of a part. The process is effective in locating discontinuities that are on the surface and slightly subsurface. For steel structures, magnetic particle inspection is more effective than dye penetrant inspection, and hence, is preferred for

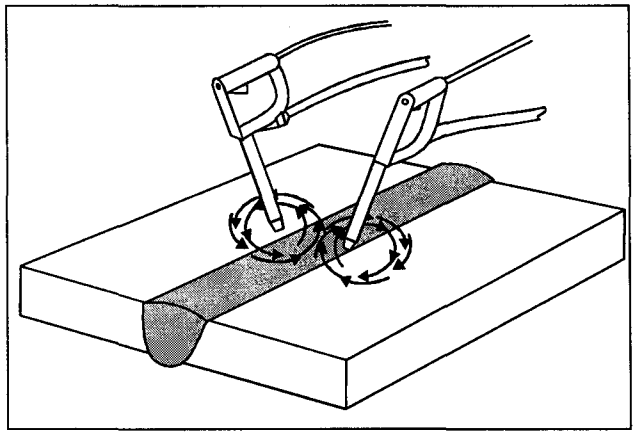

Figure 9-2 *Magnetic particle inspection*

most applications. Magnetic particle inspection can reveal cracks near surface slag inclusions, and porosity.

The magnetic field is created in the material to be inspected in one of two ways. Current is either directly passed through the material, or a magnetic field is induced through a coil on a yoke. With the first method, electrical current is passed through two prods that are placed in contact with the surface. When the prods are initially placed on the material, no current is applied. After intimate contact is assured, current is passed through. Small arcs may occur between the prods and the base material, resulting in an arc strike, which may create a localized brittle zone. It is important that prods be kept in good shape and that intimate contact with the work is maintained before the current is passed through the prods.

The second method of magnetic field generation is through induction. In what is known as the yoke method, an electrical coil is wrapped around a core, often with articulated ends. Electrical current is passed through the coil, creating a magnetic field in the core. When the ends of the yoke are placed in contact with the part being inspected, the magnetic field is induced into the part. Since current is not passed into the part, the potential for arc strikes is eliminated. Along with this significant advantage, comes a disadvantage: the yoke method is not as sensitive to subsurface discontinuities as the prod method.

Cracks are most easily detected when they lie perpendicular to the magnetic field. With the prod method the magnetic field is generated perpendicular to the direction of current flow. For the yoke method, just the opposite is true. Magnetic particle inspection is most effective when the region is inspected twice: once with the field located parallel to, and once with the field perpendicular to, the weld axis.

While magnetic particle inspection can read some subsurface discontinuities, it is best viewed as an enhancer of visual inspection. Most codes prescribe that part of the fillet welds be inspected with this method. Another common use of MT is for the inspection of intermediate passes on large groove welds, particularly in those situations that are known to be crack sensitive.

9.3.3 Radiographic Inspection (RT)

Radiographic inspection uses X-rays or gamma rays that are passed through the weld and expose a photographic film on the opposite side of the joint (see Fig. 9-3). X-rays are produced by high voltage generators, while gamma rays are produced by atomic disintegration of radioactive isotopes.

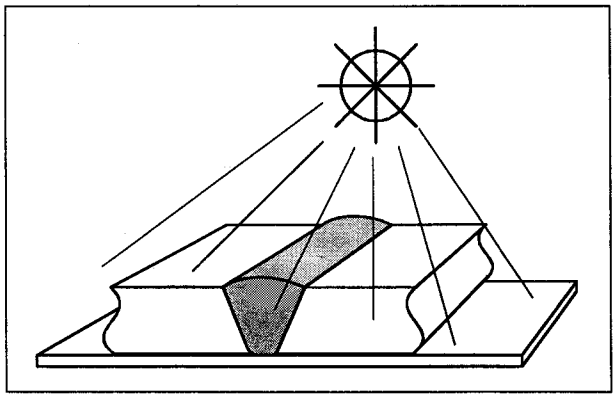

Figure 9-3 Radiographic inspection

Whenever radiography is used, precautions must be taken to protect workers from exposure to excessive radiation. Safety measures dictated by the Occupational Safety and Health Administration (OSHA), the National Electrical Manufacturer's Association (NEMA), the Nuclear Regulatory Commission (NRC), the American Society of Nondestructive Testing (ASNT) and other agencies should be carefully followed when radiographic inspection is conducted.

Radiographic testing relies on the ability of the material to pass some of the radiation through, while absorbing part of this energy within the material. Different materials have different absorption rates. Thin materials will absorb less radiation than thick materials. The higher the density of the material, the greater the absorption rate. As different levels of radiation are passed through the materials, portions of the film are exposed to a greater or lesser degree than the rest. When this film is developed, the resulting radiograph will bear the image of the plan views of the part, including its internal structure. A radiograph is actually a negative. The darkest regions are those that were most exposed when the material being inspected absorbed the least amount of radiation. Thin parts will be darkest on the radiograph. Porosity will be revealed as small, dark, round circles. Slag is also generally dark, and will look similar to porosity, but will be irregular in its shape. Cracks appear as dark lines. Lack of fusion or underfill will show up as dark spots. Excessive reinforcement on the weld will result in a light region.

Radiographic testing is most effective for detecting volumetric discontinuities: slag and porosity. When cracks are oriented perpendicular to the direction of the radiation source, they may be missed with the RT method. Tight cracks that are parallel to the radiation path have also been overlooked with RT.

Radiographic testing has the advantage of generating a permanent record for future reference. With a "picture" to look at, many people are more confident that the interpretation of weld quality is meaningful. However, reading a radiograph and interpreting the results requires stringent training, so the effectiveness of radiographic inspection depends to a great degree on the skill of the technician.

Radiographic testing is ideally suited for inspection of complete joint penetration (CJP) groove welds in butt joints. It is not particularly suitable for inspection of partial joint penetration (PJP) groove welds or fillet welds. When applied to tee and corner joints, the geometric constraints of the applications make RT inspection difficult, and interpretation of the results is highly debatable.

9.3.4 Ultrasonic Inspection (UT)

Ultrasonic inspection relies on the transmission of high frequency sound waves through materials (see Fig. 9-4). Solid, discontinuity-free materials will transmit the sound throughout a part in an uninterrupted fashion. A receiver "hears" the sound reflected off of the back surface of the part being inspected. If a discontinuity is contained between the transmitter and the back side of the part, an intermediate signal will be sent to the receiver indicating the presence of this discontinuity. The pulses are read on a CRT

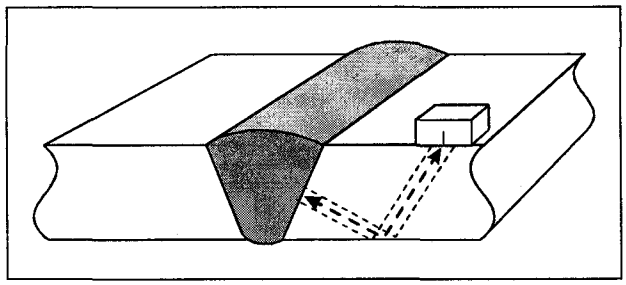

Figure 8-4 *Ultrasonic inspection*

screen. The magnitude of the signal received from the discontinuity is proportional to the amount of reflected sound. This is indirectly related to the size, type, and orientation of the reflecting surface. The relationship of the signal with respect to the back wall will indicate its location. Ultrasonic inspection is sensitive enough to read discontinuities that are not relevant to the performance of the weld. It is a sophisticated device that is very effective in spotting even small discontinuities.

UT is most sensitive to planar discontinuities, such as cracks, laminations, and non-fusion. Under some conditions, uniformly cylindrical or spherical discontinuities can be overlooked with UT.

Ultrasonic inspection is ideal for inspection of CJP groove welds. While UT inspection of PJP groove welds is possible, interpretation of the results can be difficult. UT inspection can be applied to butt, corner, and T-joints, and offers a significant advantage over RT.

A common situation in UT inspection is worthwhile noting because of the problems encountered. In tee and corner joints, with CJP groove welds made from one side and with steel backing attached, the interpretation of results is difficult at best. It is difficult to clearly distinguish between the naturally occurring regions where the backing contacts the adjacent vertical tee or corner joint member and an unacceptable lack of fusion. There is always a signal generated in this area. This of course is the situation that is encountered when steel backing is left in place on a beam-to-column moment connection. To minimize this problem, the steel backing can be removed. This offers two advantages: First, the influence of the backing is obviously eliminated; and secondly, in the process of backing removal, the joint can be backgouged and the root inspected prior to the application of the back weld and the reinforcing fillet weld.

It is also important to note that when a bottom beam-to-column connection is inspected, it is impossible for the operator to scan across the entire width of the beam flange because of the presence of the beam web. This leaves a region in the center of the weld that cannot be UT inspected. Unfortunately, this is also the region that is most difficult for the welder to deposit sound weld metal in, and has been identified as the source of many weld defects. When the beam is joined to a wide flange column, this is also the most severely loaded portion of the weld. Backing removal and subsequent backgouging operations help overcome this UT limitation since it affords the opportunity of visual verification of weld soundness.

10 Arc Welding Safety

Arc welding is a safe occupation when sufficient measures are taken to protect the welder from potential hazards. When these measures are overlooked or ignored, welders can encounter such dangers as electric shock, overexposure to radiation, fumes and gases, and fire and explosion; any of these can result in fatal injuries. Everyone associated with the welding operation should be aware of the potential hazards and ensure that safe practices are employed. Infractions should be reported to the appropriate responsible authority.

Figure 10-1 is a guide for the proper selection of an appropriate filter or shade for eye protection when directly observing the arc. Figure 10-2 consists of a series of precautions covering the major area of potential hazards associated with welding. Figure 10-3 is a checklist which gives specific instructions to the welder to ensure safe operating conditions. An Arc Welding Safety Bibliography lists published safety standards and guidelines.

Operation	Electrode Size 1/32 in. (mm)	Arc Current (A)	Minimum Protective Shade	Suggested[1] Shade No. (Comfort)
Shielded metal arc welding	Less than 3 (2.5) 3–5 (2.5–4) 5–8 (4–6.4) More than 8 (6.4)	Less than 60 60–160 160–250 250–550	7 8 10 11	— 10 12 14
Gas metal arc welding and flux cored arc welding		Less than 60 60–160 160–250 250–500	7 10 10 10	— 11 12 14
Gas tungsten arc welding		Less than 50 50–150 150–500	8 8 10	10 12 14
Air carbon arc cutting	(Light) (Heavy)	Less than 500 500–1000	10 11	12 14
Plasma arc welding		Less than 20 20–100 100–400 400–800	6 8 10 11	6 to 8 10 12 14
Plasma arc cutting	(Light)[2] (Medium)[2] (Heavy)[2]	Less than 300 300–400 400–800	8 9 10	9 12 14
Torch brazing		—	—	3 or 4
Torch soldering		—	—	2
Carbon arc welding		—	—	14
	Plate thickness			
	in.	mm		
Gas welding Light Medium Heavy	 Under 1/8 1/8 to 1/2 Over 1/2	 Under 3.2 3.2 to 12.7 Over 12.7		 4 or 5 5 or 6 6 or 8
Oxygen cutting Light Medium Heavy	 Under 1 1 to 6 Over 6	 Under 25 25 to 150 Over 150		 3 or 4 4 or 5 5 or 6

[1] As a rule of thumb, start with a shade that is too dark to see the weld zone. Then go to a lighter shade which gives sufficient view of the weld zone without going below the minimum. In oxyfuel gas welding or cutting where the torch produces a high yellow light, it is desirable to use a filter lens that absorbs the yellow or sodium line in the visible light of the (spectrum) operation.

[2] These values apply where the actual arc is clearly seen. Experience has shown that lighter filters may be used when the arc is hidden by the workpiece.

Data from ANSI/ASC Z49.1-88

Figure 10-1 Guide for shade numbers

⚠ WARNING — ARC WELDING can be hazardous.

PROTECT YOURSELF AND OTHERS FROM POSSIBLE SERIOUS INJURY OR DEATH. KEEP CHILDREN AWAY. PACEMAKER WEARERS SHOULD CONSULT WITH THEIR DOCTOR BEFORE OPERATING.

Read and understand the following safety highlights. For additional safety information it is strongly recommended that you purchase a copy of "Safety in Welding & Cutting - ANSI Standard Z49.1" from the American Welding Society, P.O. Box 351040, Miami, Florida 33135 or CSA Standard W117.2-1974. A **Free** copy of "Arc Welding Safety" booklet E205 is available from the Lincoln Electric Company, 22801 St. Clair Avenue, Cleveland, Ohio 44117-1199.

BE SURE THAT ALL INSTALLATION, OPERATION, MAINTENANCE, AND REPAIR PROCEDURES ARE PERFORMED ONLY BY QUALIFIED INDIVIDUALS.

ELECTRIC SHOCK can kill.

1.a. The electrode and work (or ground) circuits are electrically "hot" when the welder is on. Do not touch these "hot" parts with your bare skin or wet clothing. Wear dry, hole-free gloves to insulate hands.

1.b. Insulate yourself from work and ground using dry insulation. Make certain the insulation is large enough to cover your full area of physical contact with work and ground.

In addition to the normal safety precautions, if welding must be performed under electrically hazardous conditions (in damp locations or while wearing wet clothing; on metal structures such as floors, gratings or scaffolds; when in cramped positions such as sitting, kneeling or lying, if there is a high risk of unavoidable or accidental contact with the workpiece or ground) use the following equipment:

- **Semiautomatic DC Constant Voltage (Wire) Welder.**
- **DC Manual (Stick) Welder.**
- **AC Welder with Reduced Voltage Control.**

1.c. In semiautomatic or automatic wire welding, the electrode, electrode reel, welding head, nozzle or semiautomatic welding gun are also electrically "hot".

1.d. Always be sure the work cable makes a good electrical connection with the metal being welded. The connection should be as close as possible to the area being welded.

1.e. Ground the work or metal to be welded to a good electrical (earth) ground.

1.f. Maintain the electrode holder, work clamp, welding cable and welding machine in good, safe operating condition. Replace damaged insulation.

1.g. Never dip the electrode in water for cooling.

1.h. Never simultaneously touch electrically "hot" parts of electrode holders connected to two welders because voltage between the two can be the total of the open circuit voltage of both welders.

1.i. When working above floor level, use a safety belt to protect yourself from a fall should you get a shock.

1.j. Also see Items 4.c. and 6.

ARC RAYS can burn.

2.a. Use a shield with the proper filter and cover plates to protect your eyes from sparks and the rays of the arc when welding or observing open arc welding. Headshield and filter lens should conform to ANSI Z87. I standards.

2.b. Use suitable clothing made from durable flame-resistant material to protect your skin and that of your helpers from the arc rays.

2.c. Protect other nearby personnel with suitable non-flammable screening and/or warn them not to watch the arc nor expose themselves to the arc rays or to hot spatter or metal.

FUMES AND GASES can be dangerous.

3.a. Welding may produce fumes and gases hazardous to health. Avoid breathing these fumes and gases.When welding, keep your head out of the fume. Use enough ventilation and/or exhaust at the arc to keep fumes and gases away from the breathing zone. **When welding with electrodes which require special ventilation such as stainless or hard facing (see instructions on container or MSDS) or on galvanized, lead or cadmium plated steel and other metals which produce toxic fumes, keep exposure as low as possible and below Threshold Limit Values (TLV) using local exhaust or mechanical ventilation. In confined spaces or in some circumstances, outdoors, a respirator may be required.**

3.b. Do not weld in locations near chlorinated hydrocarbon vapors coming from degreasing, cleaning or spraying operations. The heat and rays of the arc can react with solvent vapors to form phosgene, a highly toxic gas, and other irritating products.

3.c. Shielding gases used for arc welding can displace air and cause injury or death. Always use enough ventilation, especially in confined areas, to insure breathing air is safe.

3.d. Read and understand the manufacturer's instructions for this equipment and the consumables to be used, including the material safety data sheet (MSDS) and follow your employer's safety practices. MSDS forms are available from your welding distributor or from the manufacturer.

3.e. Also see item 7b.

WELDING SPARKS can cause fire or explosion.

4.a..Remove fire hazards from the welding area. If this is not possible, cover them to prevent the welding sparks from starting a fire. Remember that welding sparks and hot materials from welding can easily go through small cracks and openings to adjacent areas. Avoid welding near hydraulic lines. Have a fire extinguisher readily available.

4.b. Where compressed gases are to be used at the job site, special precautions should be used to prevent hazardous situations. Refer to "Safety in Welding and Cutting" (ANSI Standard Z49.1) and the operating information for the equipment being used.

4.c. When not welding, make certain no part of the electrode circuit is touching the work or ground. Accidental contact can cause overheating and create a fire hazard.

4.d. Do not heat, cut or weld tanks, drums or containers until the proper steps have been taken to insure that such procedures will not cause flammable or toxic vapors from substances inside. They can cause an explosion even though they have been "cleaned." For information purchase "Recommended Safe Practices for the Preparation for Welding and Cutting of Containers and Piping That Have Held Hazardous Substances", AWS F4.1-80 from the American Welding Society (see address above).

4.e. Vent hollow castings or containers before heating, cutting or welding. They may explode.

Figure 10-2 Arc welding safety precautions

4.f. Sparks and spatter are thrown from the welding arc. Wear oil free protective garments such as leather gloves, heavy shirt, cuffless trousers, high shoes and a cap over your hair. Wear ear plugs when welding out of position or in confined places. Always wear safety glasses with side shields when in a welding area.

4.g. Connect the work cable to the work as close to the welding area as practical. Work cables connected to the building framework or other locations away from the welding area increase the possibility of the welding current passing through lifting chains, crane cables or other alternate circuits. This can create fire hazards or overheat lifting chains or cables until they fail.

4.h. Also see item 7c.

CYLINDER may explode if damaged.

5.a. Use only compressed gas cylinders containing the correct shielding gas for the process used and properly operating regulators designed for the gas and pressure used. All hoses, fittings, etc. should be suitable for the application and maintained in good condition.

5.b. Always keep cylinders in an upright position securely chained to an undercarriage or fixed support.

5.c. Cylinders should be located:
- Away from areas where they may be struck or subjected to physical damage.
- A safe distance from arc welding or cutting operations and any other source of heat, sparks, or flame.

5.d. Never allow the electrode, electrode holder or any other electrically "hot" parts to touch a cylinder.

5.e. Keep your head and face away from the cylinder valve outlet when opening the cylinder valve.

5.f. Valve protection caps should always be in place and hand tight except when the cylinder is in use or connected for use.

5.g. Read and follow the instructions on compressed gas cylinders, associated equipment, and CGA publication P-I, "Precautions for Safe Handling of Compressed Gases in Cylinders,"available from the Compressed Gas Association 1235 Jefferson Davis Highway, Arlington, VA 22202.

FOR ELECTRICALLY powered equipment.

6.a. Turn off input power using the disconnect switch at the fuse box before working on the equipment.

6.b. Install equipment in accordance with the U.S. National Electrical Code, all local codes and the manufacturer's recommendations.

6.c. Ground the equipment in accordance with the U.S. National Electrical Code and the manufacturer's recommendations.

FOR ENGINE powered equipment.

7.a. Turn the engine off before troubleshooting and maintenance work unless the maintenance work requires it to be running.

7.b. Operate engines in open, well-ventilated areas or vent the engine exhaust fumes outdoors.

7.c. Do not add the fuel near an open flame welding arc or when the engine is running. Stop the engine and allow it to cool before refueling to prevent spilled fuel from vaporizing on contact with hot engine parts and igniting. Do not spill fuel when filling tank. If fuel is spilled, wipe it up and do not start engine until fumes have been eliminated.

7.d. Keep all equipment safety guards, covers and devices in position and in good repair. Keep hands, hair, clothing and tools away from V-belts, gears, fans and all other moving parts when starting, operating or repairing equipment.

7.e. In some cases it may be necessary to remove safety guards to perform required maintenance. Remove guards only when necessary and replace them when the maintenance requiring their removal is complete. Always use the greatest care when working near moving parts.

7.f. Do not put your hands near the engine fan. Do not attempt to override the governor or idler by pushing on the throttle control rods while the engine is running.

7.g. To prevent accidentally starting gasoline engines while turning the engine or welding generator during maintenance work, disconnect the spark plug wires, distributor cap or magneto wire as appropriate.

7.h. To avoid scalding, do not remove the radiator pressure cap when the engine is hot.

ELECTRIC AND MAGNETIC FIELDS may be dangerous

8.a. Electric current flowing through any conductor causes localized Electric and Magnetic Fields (EMF). Welding current creates EMF fields around welding cables and welding machines.

8.b. EMF fields may interfere with some pacemakers, and welders having a pacemaker should consult their physician before welding.

8.c. Exposure to EMF fields in welding may have other health effects which are now not known.

8d. All welders should use the following procedures in order to minimize exposure to EMF fields from the welding circuit:

8.d.1. Route the electrode and work cables together - Secure them with tape when possible.

8.d.2. Never coil the electrode lead around your body.

8.d.3. Do not place your body between the electrode and work cables. If the electrode cable is on your right side, the work cable should also be on your right side.

8.d.4. Connect the work cable to the workpiece as close as possible to the area being welded.

8.d.5. Do not work next to welding power source.

Hazard	Factors to Consider	Precaution Summary
Electric shock can kill	• **Wetness** • **Welder in or on workpiece** • **Confined space** • **Electrode holder and cable insulation**	• Insulate welder from workpiece and ground using *dry* insulation. Rubber mat or dry wood. • Wear *dry, hole-free* gloves. (Change as necessary to keep dry.) • Do not touch electrically "hot" parts or electrode with bare skin or wet clothing. • If wet area and welder cannot be insulated from workpiece with dry insulation, use a semiautomatic, constant-voltage welder or stick welder with voltage reducing device. • Keep electrode holder and cable insulation in good condition. Do not use if insulation damaged or missing.
Fumes and gases can be dangerous	• **Confined area** • **Positioning of welder's head** • **Lack of general ventilation** • **Electrode types, i.e., manganese, chromium, etc. See MSDS** • **Base metal coatings, galvanize, paint**	• Use ventilation or exhaust to keep air breathing zone clear, comfortable. • Use helmet and positioning of head to minimize fume in breathing zone. • Read warnings on electrode container and material safety data sheet (MSDS) for electrode. • Provide additional ventilation/exhaust where special ventilation requirements exist. • Use special care when welding in a confined area. • Do not weld unless ventilation is adequate.
Welding sparks can cause fire or explosion	• **Containers which have held combustibles** • **Flammable materials**	• Do not weld on containers which have held combustible materials (unless strict AWS F4.1 procedures are followed). Check before welding. • Remove flammable materials from welding area or shield from sparks, heat. • Keep a fire watch in area during and after welding. • Keep a fire extinguisher in the welding area. • Wear fire retardant clothing and hat. Use earplugs when welding overhead.
Arc rays can burn eyes and skin	• **Process: gas-shielded arc most severe**	• Select a filter lens which is comfortable for you while welding. • Always use helmet when welding. • Provide non-flammable shielding to protect others. • Wear clothing which protects skin while welding.
Confined space 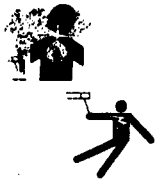	• **Metal enclosure** • **Wetness** • **Restricted entry** • **Heavier than air gas** • **Welder inside or on workpiece**	• Carefully evaluate adequacy of ventilation especially where electrode requires special ventilation or where gas may displace breathing air. • If basic electric shock precautions cannot be followed to insulate welder from work and electrode, use semiautomatic, constant-voltage equipment with cold electrode or stick welder with voltage reducing device. • Provide welder helper and method of welder retrieval from outside enclosure.
General work area hazards	• **Cluttered area**	• Keep cables, materials, tools neatly organized.
	• **Indirect work (welding ground) connection**	• Connect work cable as close as possible to area where welding is being performed. Do *not* allow alternate circuits through scaffold cables, hoist chains, ground leads.
	• **Electrical equipment**	• Use only double insulated or properly grounded equipment. • Always disconnect power to equipment before servicing.
	• **Engine-driven equipment**	• Use in only open, well ventilated areas. • Keep enclosure complete and guards in place. • See Lincoln service shop if guards are missing. • Refuel with engine off. • If using auxiliary power, OSHA may require GFI protection or assured grounding program (or isolated windings if less than 5KW).
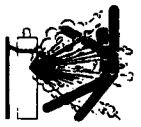	• **Gas cylinders**	• Never touch cylinder with the electrode. • Never lift a machine with cylinder attached. • Keep cylinder upright and chained to support.

Figure 10-3 Welding safety checklist

Arc Welding Safety Bibliography

ANSI Z87.1, *Practice for Occupational and Educational Eye and Face Protection,* American National Standards Institute, 11 West 42nd Street, New York, NY 10036.

Arc Welding and Your Health: A Handbook of Health Information for Welding, Published by The American Industrial Hygiene Association, 2700 Prosperity Avenue, Suite 250, Fairfax, VA 22031-4319.

NFPA Standard 51B, *Cutting and Welding Processes,* National Fire Protection Association, 1 Batterymarch Park, P.O. Box 9146, Quincy, MA 02269-9959.

The following publications are published by The American Welding Society, P.O. Box 351040, Miami, Florida 33135. Write for publications catalog:

ANSI/ASC, Standard Z49.1, *Safety in Welding and Cutting.*

AWS F1.1, *Method for Sampling Airborne Particulates Generated by Welding and Allied Processes.*

AWS F1.2, *Laboratory Method for Measuring Fume Generation Rates and Total Fume Emission of Welding and Allied Processes.*

AWS F1.3, *Evaluating Contaminants in the Welding Environment: A Strategic Sampling Guide.*

AWS F1.4, *Methods for Analysis of Airborne Particulates Generated by Welding and Allied Processes.*

AWS F1.5, *Methods for Sampling and Analyzing Gases from Welding and Allied Processes.*

AWS F4.1, *Recommended Safe Practices for the Preparation for Welding and Cutting of Containers and Piping That Have Held Hazardous Substances.*

REFERENCES

1. Alexander, Warren G. "Designing Longitudinal Welds for Bridge Members," *Engineering Journal*, Volume 28, No. 1 (1991):29-36.

2. American Association of State Highway and Transportation Officials. *Guide Specifications for Fracture Critical Non-Redundant Steel Bridge Members, 1978.* (As Revised by Interim Specifications for Bridges, 1981, 1983, 1984, 1985, 1986, and 1991.) Washington, D.C.

3. American Assocation of State Highway and Transportation Officials and American Welding Society. *Bridge Welding Code: ANSI/AASHTO/AWS D1.5-95.* Miami, Florida, 1995.

4. American Institute of Steel Construction. *Manual of Steel Construction: Load & Resistance Factor Design*, 2nd ed., Chicago, Illinois, 1994.

5. American Institute of Steel Construction. *Northridge Steel Update I.* Chicago, Illinois, October, 1994.

6. American Society for Metals. *Hydrogen Embrittlement and Stress Corrosion Cracking*, edited by R. Gibala and R. F. Hehemann. Metals Park, Ohio, 1994.

7. American Society for Metals. *Metals Handbook, Ninth Edition, Volume 6: Welding, Brazing, and Soldering.* Metals Park, Ohio, 1983.

8. American Welding Society. *A5 Filler Metal Specifications.* Miami, Florida, various dates.

9. American Welding Society. *Guide for the Visual Inspection of Welds: ANSI/AWS B1.11-88.* Miami, Florida, 1988.

10. American Welding Society. *Standard Methods for Determination of the Diffusible Hydrogen Content of Martensitic, Bainitic, and Ferritic Steel Weld Metal Produced by Arc Welding: ANSI/AWS A4.3-93.* Miami, Florida, 1993.

11. American Welding Society. *Standard Symbols for Welding, Brazing and Nondestructive Examination: ANSI/AWS A2.4-93.* Miami, Florida, 1991.

12. American Welding Society. *Standard Welding Terms and Definitions: ANSI/AWS A3.0-89.* Miami, Florida, 1989.

13. American Welding Society. *Structural Welding Code: Sheet Steel: ANSI/AWS D1.3-89.* Miami, Florida, 1989.

14. American Welding Society. *Structural Welding Code: Steel: ANSI/AWS D1.1-96.* Miami, Florida, 1996.

15. American Welding Society. "Structural Welding Committee Position Statement on Northridge Earthquake Welding Issues." Miami, Florida, November 10, 1995.

16. American Welding Society. *Welding Handbook, Eighth Edition, Volume 1: Welding Technology*, edited by Leonard P. Conner. Miami, Florida, 1987.

17. American Welding Society. *Welding Handbook, Eighth Edition, Volume 2: Welding Processes*, edited by R.L. O'Brien. Miami, Florida, 1991.

18. American Welding Society. *Welding Handbook, Eighth Edition, Volume 3: Materials and Applications, Part 1*, edited by William R. Oates. Miami, Florida, 1996.

19. American Welding Society. *Welding Handbook: Volume One, Seventh Edition: Fundamentals of Welding*, edited by Charlotte Weisman. Miami, Florida, 1976.

20. American Welding Society. *Welding Handbook: Volume Two, Seventh Edition: Welding Processes - Arc and Gas Welding and Cutting, Brazing, and Soldering*, edited by W.H. Kearns. Miami, Florida, 1978.

21. American Welding Society. *Welding Handbook: Volume Three, Seventh Edition: Welding Processes - Resistance and Solid-State Welding and Other Joining Processes*, edited by W.H. Kearns. Miami, Florida, 1980.

22. American Welding Society. *Welding Handbook: Volume Four, Seventh Edition: Metals and Their Weldability*, edited by W.H. Kearns. Miami, Florida, 1982.

23. American Welding Society. *Welding Handbook: Volume Five, Seventh Edition: Engineering, Costs, Quality and Safety*, edited by W.H. Kearns. Miami, Florida, 1984.

24. Bailey, N., Coe, F.R., Gooch, T.G., Hart, P.H.M., Jenkins, N., and Pargeter, R.J. *Welding Steels Without Hydrogen Cracking*. 2nd ed., Cambridge, England: Abington Publishing, 1973.

25. Barsom, John M., and Rolfe, Stanley T. *Fracture and Fatigue Control in Structures: Applications of Fracture Mechanics*. 2nd ed., Englewood Cliffs, New Jersey: Prentice-Hall, Inc., 1987.

26. Blodgett, Omer W. *Design of Welded Structures*. Cleveland, Ohio: The James F. Lincoln Arc Welding Foundation, 1966.

27. Blodgett, Omer W. "Details to Increase Ductility in SMRF Connections." *The Welding Innovation Quarterly*, Vol. XII, No. 2 (1995).

28. Blodgett, Omer W. "The Challenge of Welding Jumbo Shapes, Part II: Increasing Ductility of Connections." *The Welding Innovation Quarterly*, Vol. X, No. 1 (1993).

29. Boniszewski, Tad. *Self-Shielded Arc Welding*. Cambridge, England: Abington Press, 1992.

30. Lincoln Electric Company. *The Procedure Handbook of Arc Welding*. 13th ed., Cleveland, Ohio, 1995.

31. Masubuchi, Koichi. *Analysis of Welded Structures*. 1st ed., Oxford, England: Pergamon Press, 1980.

32. Miller, Duane K. "Ensuring Weld Quality in Structural Applications, Part I: The Roles of Engineers, Fabricators & Inspectors." *The Welding Innovation Quarterly*, Vol. XIII, No. 2 (1996).

33. Miller, Duane K. "Ensuring Weld Quality in Structural Applications, Part II: Effective Visual Inspection." *The Welding Innovation Quarterly*, Vol. XIII, No. 3 (1996).

34. Miller, Duane K. "Northridge: The Role of Welding Clarified." *The Welding Innovation Quarterly*, Vol. XI, No. 2 (1994).

35. Miller, Duane K. "Northridge: An Update." *The Welding Innovation Quarterly*, Vol. XIII, No. 1 (1996).

36. Miller, Duane K. *Welding of Steel Bridges*. Cleveland, Ohio: The James F. Lincoln Arc Welding Foundation, 1994.

37. Miller, Duane K. "What Structural Engineers Need to Know About Weld Metal." *1988 National Steel Construction Conference Proceedings:* 35.1-35.15. Chicago, Illinois: American Institute of Steel Construction, 1988.

38. Roeder, Charles W. *Use of Thermal Stresses for Repair of Seismic Damage to Steel Structures*. Seattle, Washington. University of Washington, 1985.

39. SAC Joint Venture. *Interim Guidelines: Evaluation, Repair, Modification and Design of Welded Steel Moment Frame Structures*. Report No. SAC-95-02 (FEMA 267). Sacramento, California, August, 1995.

40. Shanafelt, G.O. and Horn, W.B. *Guidelines for Evaluation and Repair of Damaged Steel Bridge Members*, National Cooperative Highway Research Program Report 271. Washington, D.C. Transportation Research Board, June 1984.

41. Stout, R.D. *Weldability of Steels*. 4th ed., New York: Welding Research Council, 1987.

42. Wilson, Alexander D. "Hardness Testing of Thermal Cut Edges of Steel." *Engineering Journal*, Vol. 27, No. 3 (1990): 98-105.

FRACTURE MECHANICS OF WELDED STRUCTURAL STEEL CONNECTIONS

John W. Fisher
Robert J. Dexter
Eric J. Kaufmann

LEHIGH UNIVERSITY

Abstract

Case histories of fracture in buildings illustrate the importance of weld metal toughness as the first line of defense against brittle fracture. The notch depth in typical Northridge welded steel moment frames (WSMF) connection failures includes 13 mm from the backing bar plus in some cases up to 6 mm from a lack of fusion defect. Test methods are discussed for measuring fracture toughness as well as the Charpy V-Notch toughness required to minimize the potential for brittle fracture. Metallurgical conditions, chemistry and processing, which affect fracture toughness are discussed. The fracture toughness of the E70-T4 weld metal which was commonly used in the WSMF connections falls between 45 and 50 MPa-m$^{1/2}$. Fracture mechanics analysis which could have predicted that brittle fracture would occur in these WSMF connections before yielding is explained.

Introduction

This paper is intended to: 1) summarize those aspects of fracture mechanics and the fracture resistance of structural steel and weld metal which are relevant to improving the resistance of seismically-loaded WSMF connections to brittle fracture; 2) identify aspects of building systems which affect the potential for fracture of steel connections; and, 3) demonstrate calculations which can be used to predict and minimize or avoid brittle fractures. The paper is intended for practicing structural engineers engaged in regulation, design, inspection, repair, and seismic upgrade of steel-framed buildings.

Ductility is required to allow local redistribution of stresses in members and global redistribution of forces in structures. In the AISC LRFD Specification (1993), ductility is mentioned in the Commentary, Section C-B5 (pertaining to local-buckling provisions), which states that members should have a minimum ductility factor (ratio of the rotation at failure to the rotation at yielding) of from 3 to 5, and possibly greater for structures which are likely to be seismically loaded. However, design is still carried out using stresses and a specific level of ductility is not explicitly considered in most design specifications or codes.

For example, in the AISC LRFD Manual of Steel Construction, ductility in tension is assured by allowing only specific materials. Detailing and workmanship requirements, although established for other reasons, are also crucial to assure adequate ductility. The American Society for Testing and Materials (ASTM) standard specifications for structural steel specify chemistry and minimum tensile-test elongation in order to provide adequate ductility. These properties are discussed in a companion paper in this volume by K. H. Frank. The AISC LRFD Manual states that "any of the structural steels, when

designed and fabricated in an appropriate manner, could be used for similar applications with little likelihood of brittle fracture". However, the Manual then lists a variety of conditions that should be avoided or at least warrant special consideration relative to potential brittle fracture, including low temperature, high strain rates, triaxial stress, notches, geometrical discontinuities, cold work, strain aging, welding, residual stress, weld defects, intersecting welds, and inadequate weld access holes. The Manual suggests that "for fracture-sensitive applications, notch tough base metal and weld metal should be specified". However, the AISC LRFD Manual of Steel Construction does not give any quantitative way to evaluate the potential for brittle fracture.

The earthquake which occurred on 17 January 1994 in Northridge, California severely damaged many types of structures. Although no steel-framed structures collapsed or resulted in loss of life, many structures suffered significant damage, particularly from cracking. This was surprising because steel-framed structures are considered to have superior ductility. Among the steel-framed structures, damage included fractured column base plates, buckled and fractured brace members, and fracture of beam-column connections in WSMF. The latter type of damage to WSMF, as shown in Figure 1, was predominant and alarming to many professionals. At the time of this writing, over one hundred buildings with WSMF are known to have beam-to-column connection failures. It has been noted that these fractures were "brittle", i.e. there was negligible plastic deformation prior to fracture.

Fracture mechanics provides relatively simple calculations which could have predicted the likelihood of brittle fracture of these WSMF connection welds. These calculations can be used to select materials and design welded connections that are resistant to brittle fracture.

The phenomenon of brittle fracture has been studied extensively since World War II [Shank, M. E., 1957]. More than 20 percent of the 4694 merchant ships built during the war suffered brittle fractures, and 145 ships broke in two [Irving, B., 1994]. Several of these failures occurred at very low stresses while the ships were at anchor in the harbor. As a result of these fractures, the engineering discipline of linear elastic fracture mechanics (LEFM) developed just after the war at the Naval Research Laboratory, led by George R. Irwin [Irwin, G., 1957].

Unfortunately, it seems to take catastrophes within each industry to cause that industry to recognize the possibility of brittle fracture in their structures and eventually begin to use fracture mechanics. For example, bridge engineers in the United States began to pay attention to brittle fracture after the collapse of the Point Pleasant Bridge in West Virginia in 1967 [Fisher, J. W., 1984]. In bridges, fracture is typically preceded by fatigue due to the cyclic live load. Therefore, the revision of the American Association of State Highway and Transportation Officials [AASHTO, 1978] specifications in the wake of this catastrophe emphasized fatigue design criteria and fatigue resistant details.

The connection detailing rules that are used to prevent fatigue cracking do not allow notches and other severe stress concentrations. These detailing rules are useful for the avoidance of not only fatigue but also brittle fracture as well. For example, the American Association of State Highway Transportation Officials detailing rules, for example "AASHTO LRFD Bridge Design Specifications" [AASHTO, 1994] do not permit a backing bar to be left in place. These same detailing rules are included in American Welding Society [AWS] D1.1 "Structural Welding Code - Steel" for fatigue-loaded structures. "Dynamically loaded" has been interpreted to mean fatigue loaded, therefore seismically-loaded building frames have not been required to be detailed in accordance with these rules.

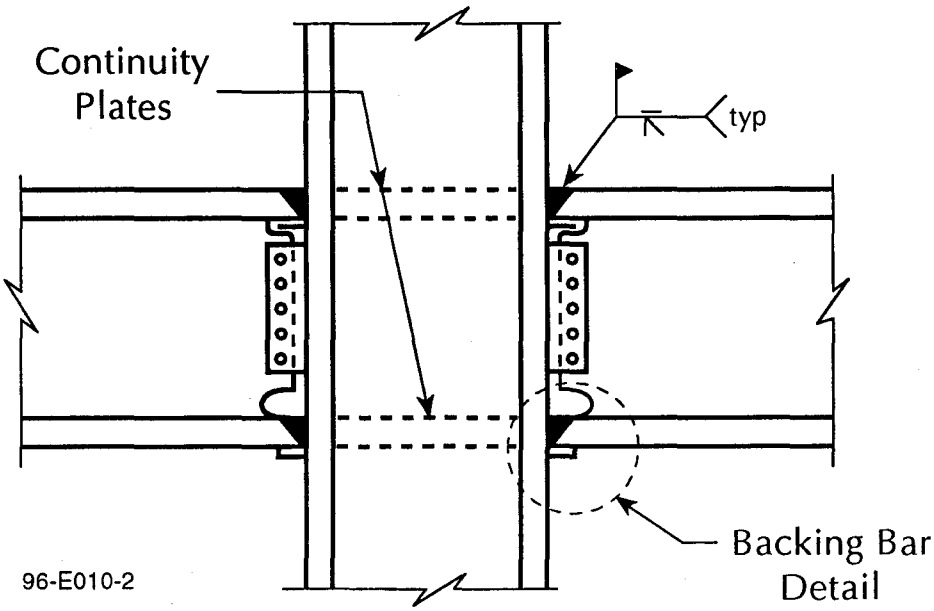

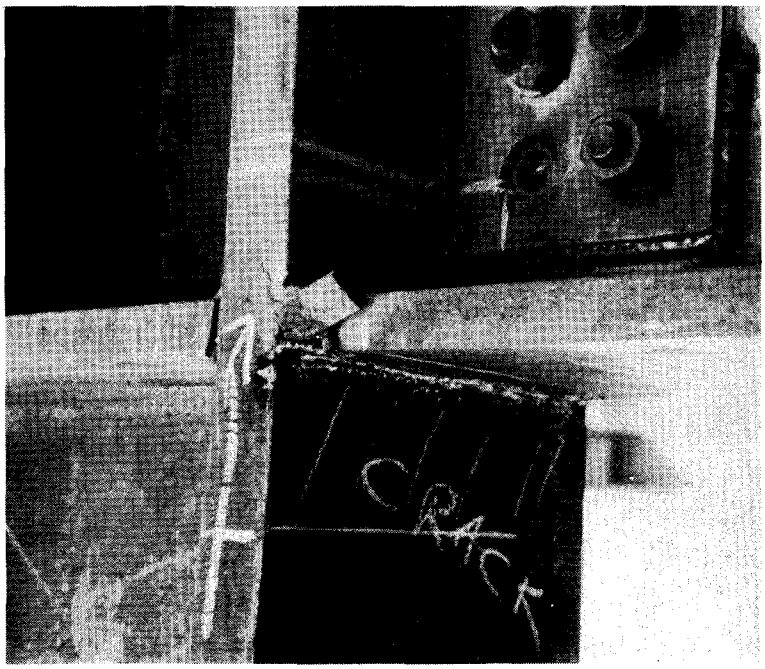

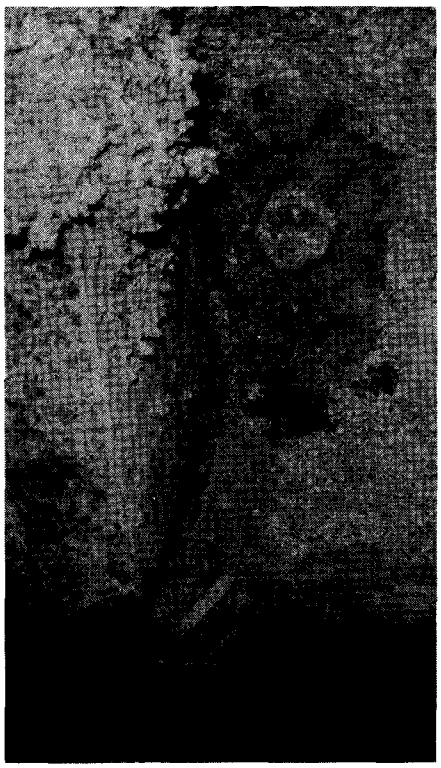

Type I: Crack Extends into Column Flange **Type II: Crack Stays in Weld or HAZ**

Figure 1 Welded Steel Moment Frame Connection and Two Typical Fractures

In addition to controlling the stress and the notch size through design, detailing, fabrication, workmanship, and inspection, the bridge fracture-control plan also strives to screen out brittle materials. Steel exhibits a transition from brittle to ductile fracture behavior as the temperature increases. For example, Figure 2 shows a plot of the energy required to fracture Charpy V-Notch (CVN) impact test specimens of A588 structural steel at various temperatures. These results are typical for ordinary hot-rolled structural steel. The transition behavior of steel is exploited as a means to screen out brittle materials. For example, the AASHTO bridge specifications ultimately required a minimum CVN energy (called notch toughness) at a specified temperature for the base metal and the weld metal of members loaded in tension or tension due to bending. As long as large defects do not exist, the notch toughness requirement assures that the fracture will not be brittle.

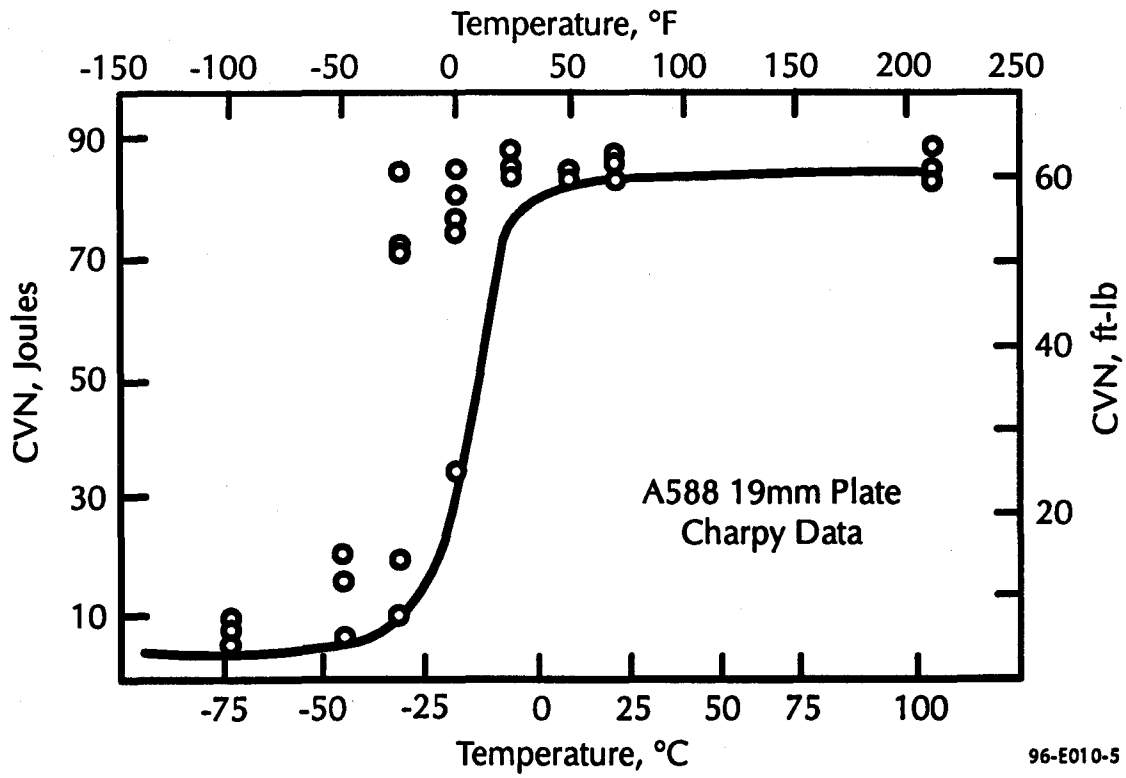

Figure 2: Typical Charpy Impact Toughness vs. Temperature Curve for Structural Steel

Since 1978, there has been an AASHTO Guide Specifications for Fracture Critical Non-Redundant Steel Bridge Members with more stringent detailing, fabrication, and notch toughness requirements for fracture critical members, i.e. those members which, if fractured, would result in collapse of the bridge. Almost two decades of experience with these bridge specifications have proved that they are successful in significantly reducing the number of fatigue cracks and brittle fractures.

Because the Charpy test is relatively easy to perform, it will likely continue to be the preferred method to measure of toughness used in steel specifications. Often the abbreviation "CVN" is used to represent the impact energy values, which in the AISC codes are given in ft-lbs, i.e. a steel with CVN 20 at a given temperature will have 27 J (20 ft-lbs) of energy. Often 34 J (25 ft-lbs), 27 J (20 ft-lbs), or 20 J (15 ft-lbs) are specified at a particular temperature. The intent of specifying any of these numbers is the same, i.e to make sure that the transition starts below this temperature.

Some of the Charpy toughness requirements for steel and weld metal for bridges and buildings are compared in Table 1. This table is simplified and does not include all the requirements. The bridge steel specifications require a CVN value at a temperature which is 38°C *greater* than the minimum service temperature. This "temperature shift" accounts for the effect of strain rates, which are lower in the service loading of bridges (on the order of 10^{-3}) than in the Charpy test (greater than 10^{1}). It is possible to measure the toughness using a Charpy specimen loaded at a strain rate characteristic of bridges, called an intermediate strain rate, although the test is more difficult and the results are more variable. When the CVN energies from an intermediate strain rate are plotted as a function of temperature, the transition occurs at a temperature at least 38°C lower for materials with yield strengths up to 450 MPa.

Table 1: Minimum Charpy Impact Test Requirements for Bridges and Buildings

Material:	Minimum Service Temperature		
	-18°C	-34°C	-51°C
	Joules@°C	Joules@°C	Joules@°C
Steel: non-fracture critical members*, **	20@21	20@4	20@-12
Steel: fracture critical members*, **	34@21	34@4	34@-12
Weld metal for non-fracture critical*	27@-18	27@-18	27@-29
Weld metal for fracture critical*, **	34@-29°C for all service temperatures		
AISC: Jumbo sections and plates thicker than 50 mm**	27@21°C for all service temperatures		
SAC: weld metal for seismic applications***	27@16°C below service temperature not to exceed-18°C		

* These requirements are for welded steel with minimum specified yield strength up to 350 MPa up to 38 mm thick. Fracture critical members are defined as those which if fractured would result in collapse of the bridge.

** The requirements pertain only to members subjected to tension or tension due to bending.

*** The Interim Guidelines suggest the use of notch tough weld metal. There was disagreement on the required impact energy and test temperature.

The temperature shift is shown schematically in Figure 3. For high-strength steels the temperature shift diminishes with increasing yield strength. For example, the temperature shift for 690 MPa yield strength steel is only 16°C. For brittle materials like some low-toughness weld metal and the core region of some jumbo rolled shapes, there is no significant temperature shift since the toughness is always on the lower shelf. The term "fracture toughness" is usually reserved for quantities such as K_c which, as explained later, are determined from a standard fracture mechanics test other than the Charpy impact test. The temperature shift as shown in Figure 3 would also occur for the fracture toughness (K_c).

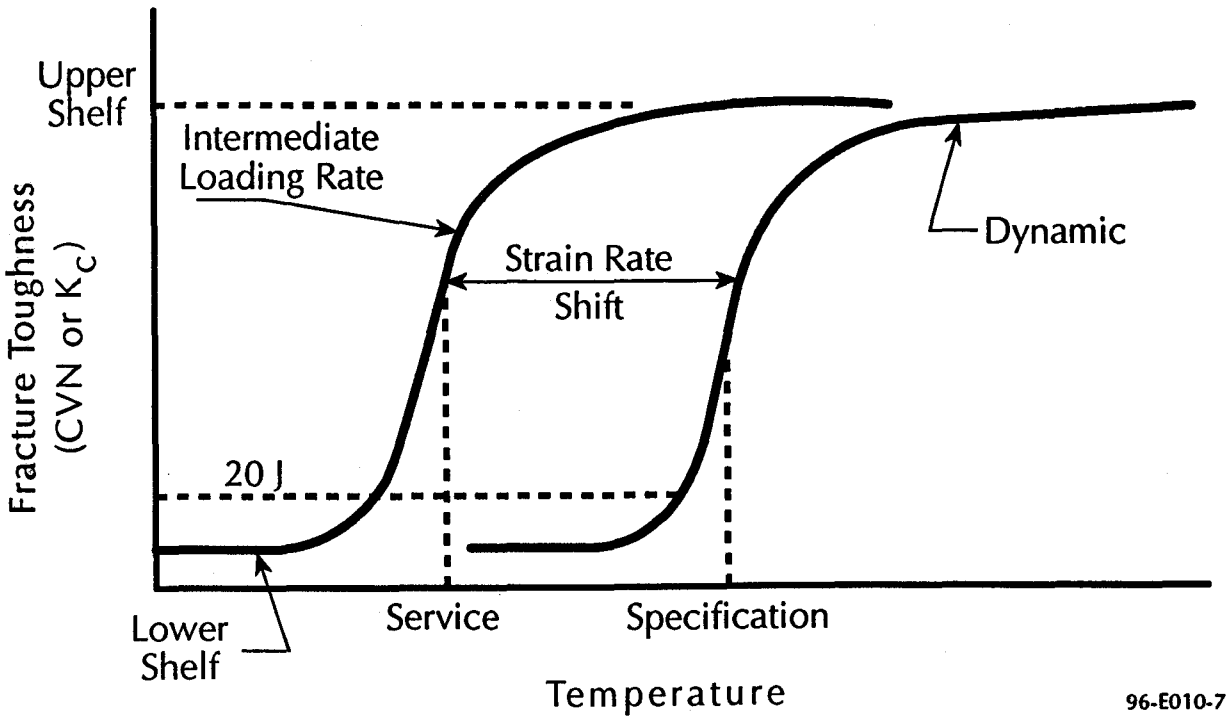

Figure 3: Schematic of the Temperature Shift Which Occurs in the CVN and K_c Fracture Toughness vs. Temperature Curves Due to the Difference in Strain Rates

Figure 4 shows some data from fracture tests on full-scale welded girders with fatigue cracks which support the temperature shift concept [Roberts, R., et al., 1977]. In these tests, the specimen was cooled to a target temperature and then the crack was grown by fatigue at 4.5 Hz until instability occurred. Figure 4 shows that for temperatures above the 38°C temperature shift, the critical surface crack length

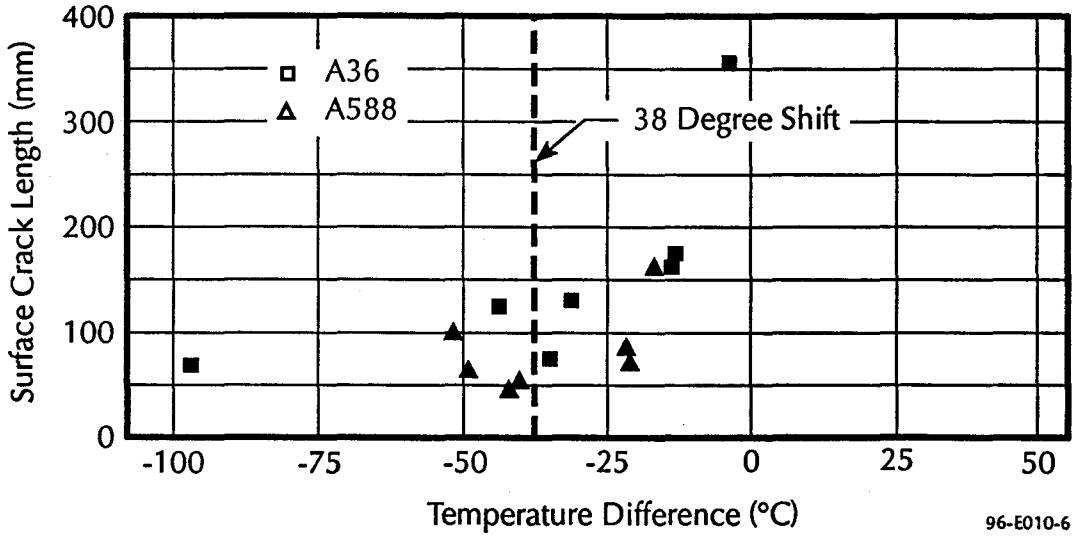

Figure 4: Results from Lehigh University Full-Scale Tests on Girders with Welded Details Showing the Critical Crack Size at Fracture as a Function of the Difference Between the Test Temperature Minus the Temperature Associated with 20 J CVN for the Steel

along the surface of the girder flange exceeded 75 mm. The depth of these larger cracks exceeded 13 mm. This size crack is considered to be detectable in inspection with some reliability. At higher temperatures the critical crack size increases rapidly in a manner analogous to the CVN vs. temperature curve

Current AISC specifications refer to ASTM specifications for structural steel such as A36, A572, and A588. Without supplemental specifications being specified, these steel specifications do not require the Charpy test to be performed. Past experience suggested that these steels provided minimum levels of fracture toughness for buildings and the supplemental specifications are seldom invoked. However, jumbo shapes, i.e. shapes in Groups 4 and 5, may have low toughness, particularly in the region of the web and flange junction. The low toughness has been attributed to the relatively low rolling deformation and slow cooling. Fractures occurred in the 1980's as these shapes began to be used for tension chords of trusses. The fractures occurred during construction at groove-weld splices or at flame-cut edges of cope holes [Fisher and Pense, 1987]. As a consequence of these fractures, AISC specifications now have a supplemental Charpy requirement for shapes in Groups 4 and 5 and (for the same reasons) plates greater than 51 mm thick, when these are welded and subject to primary tensile stress from axial load or bending. These jumbo shapes and thick plates must exhibit 27 J at 21 °C.

As shown in Table 1, the AWS D1.5 Bridge Welding Code specifications for weld metal toughness are more demanding than the specifications for base metal. This is reasonable because the weld metal is always the location of discontinuities and high tensile residual stresses. In addition, weld metal generally has a higher yield point than the base metal and greater variability in toughness will result from production welds. The commentary in the AISC LRFD Manual, Section C-A3, says weld metal is usually not critical. Similarly, there is no mandatory requirement for weld metal toughness in AWS D1.1. This lack of requirements was rationalized because typically the weld deposits exhibit greater fracture toughness than the base metal. However, this is not always the case, e.g. the E70T-4 self-shielded flux-cored arc welds (FCAW-SS) used extensively for the WSMF that fractured in the Northridge earthquake are known to have low toughness [Kaufmann]. The commentary in the AISC manual does warn that for "dynamic loading, the engineer may require the filler metals used to deliver notch-tough weld deposits".

The strain rates associated with an earthquake are intermediate, e.g. the load times are about half of a second and the maximum strain rates are on the order of 5×10^{-3}/sec. Thus, the strain rates for primary axial and flexural tensile seismic loading are essentially the same as the strain rates experienced by bridges due to truck loading. Accordingly, the AASHTO CVN requirements for weld metal in redundant (non-fracture critical) members in bridges in the highest service temperature zone (27J@-18 °C) should be more than sufficient to reduce the possibility of brittle fracture in seismic building connections, even outdoors. If it could be assured that a building will not be exposed to cold temperatures during an earthquake and its after shocks and more stringent defect sizes and quality control were imposed on building connections, then much less stringent CVN temperature requirements could be considered. Because there is no possibility of fatigue crack growth in most buildings, defects will typically be confined to the weld metal. Therefore, although weld metal CVN requirements are equally important, base metal CVN requirements are less important for buildings than for bridges.

ASTM A673 has specifications for the frequency of Charpy testing. The H frequency requires a set of three CVN specimens to be tested from one location for each heat or about 50 tons. These tests can be taken from a plate with thickness up to 9 mm different from the product thickness if it is rolled from the same heat. The P frequency requires a set of three specimens to be tested from one end of every plate, or from one shape in every 15 tons of that shape. For bridge steel, the AASHTO code requires CVN tests at the H frequency at a minimum. For fracture critical members, the guide specifications require CVN testing at the P frequency. In the AISC code, CVN tests are required at the P frequency for thick plates and jumbo

sections. A special test location in the core of the jumbo section is specified, as well as requirement that the section tested be produced from the top of the ingot.

Even the P testing frequency may be insufficient for as-rolled structural steel. In a recent report for NCHRP [Frank, K. H., et al., 1993], CVN data were obtained from various locations on bridge steel plates. The data show that because of extreme variability in CVN across as-rolled plates, it would be possible to miss potentially brittle areas of plates if only one location per plate is sampled. For plates which were given a normalizing heat treatment, the excessive variability was eliminated.

Metallurgical Factors Affecting the Toughness of Structural Steel and Weld Metal

The transition phenomena shown in Figure 2 is a result of changes in the underlying microstructural fracture mode. There are really at least three distinct types of fracture with distinctly different behavior.

1) Brittle fracture is associated with cleavage which is transgranular fracture on select crystallographic planes on a microscopic scale (see Figure 5a). This type of fracture occurs at the lower end of the temperature range, although the brittle behavior can persist up to the boiling point of water in some low-toughness materials. This part of the temperature range is called the lower shelf because the minimum toughness is fairly constant up to the transition temperature. Brittle fracture is sometimes called elastic fracture because the plasticity that occurs is negligible and consequently the energy absorbed in the fracture process is also negligible.

2) Transition-range fracture occurs at temperatures between the lower shelf and the upper shelf and is associated with a mixture of cleavage and fibrous fracture on a microstructural scale. Because of the mixture of micromechanisms, transition-range fracture is characterized by extremely large variability. Fracture in the transition region is sometimes referred to as elastic-plastic fracture because the plasticity is limited in extent but has a significant impact on the toughness.

3) Ductile fracture is associated with a process of void initiation, growth, and coalescence on a microstructural scale, a process requiring substantial energy, and occurs at the higher end of the temperature range (see Figure 5b). This part of the temperature range is referred to as the upper shelf because the toughness levels off and is essentially constant for higher temperatures. Ductile fracture is sometimes called fully-plastic fracture because there is substantial plasticity across most of the remaining cross section ahead of a crack. Ductile fracture is also called fibrous fracture due to the fibrous appearance of the fracture surface, or shear fracture due the usually large slanted shear lips on the fracture surface.

Unfortunately, these terms are often used ambiguously. For example, fracture in the transition region is often called brittle or ductile, depending on the relative toughness. Some materials go through a transition but still exhibit relatively low toughness on the upper shelf, despite a lack of cleavage and a fibrous fracture appearance. One example of such a low-upper-shelf material is the weld metal used for some girth welds in nuclear pressure vessels which has been embrittled by irradiation. A fracture in such a material at upper-shelf temperatures exhibits a fibrous fracture appearance but may be referred to as brittle because of the lack of ductility. However in this paper, unless otherwise noted, brittle fracture will imply fracture which is substantially cleavage.

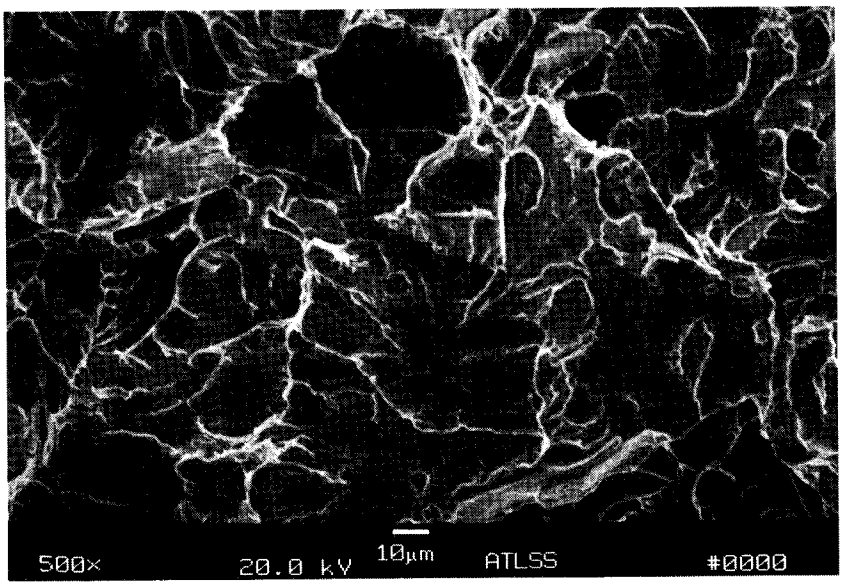

a) Typical Cleavage Fracture Features on the Weld Metal Fracture Surface from a Fractured WSMF Connection

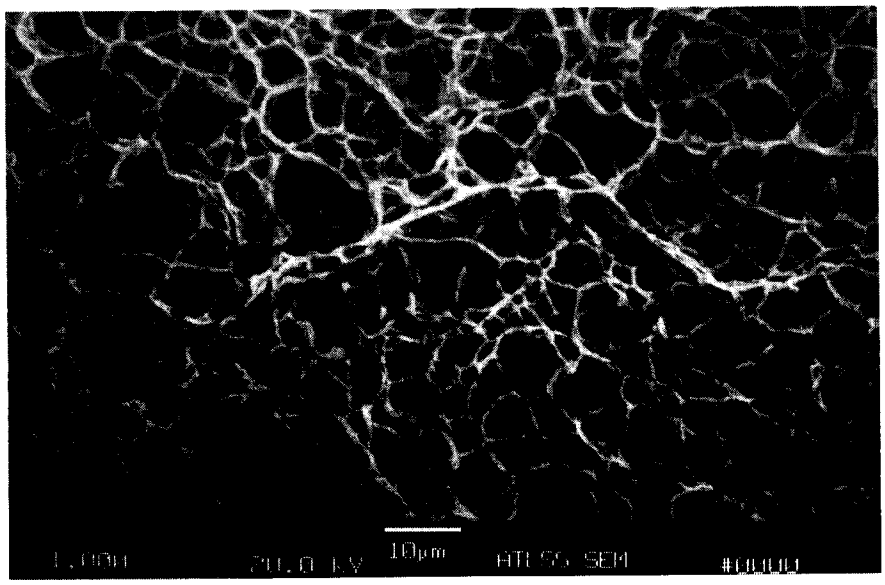

b) Typical Ductile Fracture Features on a Fracture Surface Resulting from Void Growth

Figure 5: Comparison of the Fracture Surface Features Characteristic of Cleavage Fracture and Ductile Fracture Resulting from Void Growth

Smooth specimens of structural steel or an associated filler metal will typically always fail in a totally ductile fully-plastic manner, even at low temperatures. For brittle or transition-range fractures to occur, the principal stress must exceed a critical cleavage stress, which is not related to and is much higher than the ultimate strength measured in a smooth tensile test. Therefore, brittle or transition-range fractures typically only occur when the stress is raised locally by the presence of a notch or crack.

In general, fracture toughness has been found to decrease with increasing yield strength of a material suggesting an inverse relationship between the two properties. In practice, however, fracture toughness is more complex than implied by this simple relationship since steels with similar strength levels can have widely varying levels of fracture toughness. That similar materials with the same strength level can also possess widely different fracture properties indicates that the metallurgical condition of the material has a significant influence on its fracture toughness.

The metallurgical condition of a steel is controlled through composition and processing, the combination of which can develop different strength and toughness characteristics. Composition influences fracture toughness through the development of microstructural constituents and their relative proportions. Most alloy elements are added to steels to increase strength and consequently are detrimental to fracture toughness. Of the usual alloy elements added to structural steels (C,Mn,Mo,V,Nb), carbon has the most deleterious influence on toughness. Recognition of this has led to the development of microalloyed steel compositions such as ASTM A572 which employ only small amounts of alloying elements. Newer microalloyed structural steels have since been developed with reduced carbon (<0.15 wt %) and alloy contents often combined with thermo-mechanical controlled processing (TMCP) to produce fine-grained low-carbon microstructure with high fracture toughness. ASTM A913 shapes produced by the quenching and self tempering (QST) process is an example of these new steels.

Nickel is unique as an alloy element in that it both increases strength and toughness and is frequently added to steel and weld metal (1.0-2.0 wt %) for this purpose. (Nickel alloying is only one method to improve toughness.) Unintentional or residual alloy elements in steel, such as sulfur, phosphorus, and nitrogen, can have a deleterious effect on fracture toughness. However, improved steel making practices in use today have reduced these elements to where they have only small effects on toughness. Sulfur in steel exists in the form of sulfide inclusions which tend to reduce energy absorption in CVN tests but have less influence on the ductile-brittle transition temperature of a steel. Lamellar tearing, at one time a major problem in welded fabrication, caused primarily by poor through-thickness properties in plate steels with high sulfide inclusion content, has also been reduced by controlling sulfur levels to less than 0.01 wt. % in steel.

Grain size is another factor which has a significant effect on fracture toughness. Grain refinement is unique in metallurgical processing in that it increases both fracture toughness and strength simultaneously. A simple explanation for this behavior is that the larger concentration of grain boundaries in fine grained steel provides both an impediment for plastic flow and hence increased strength and obstacles for microcracks to negotiate thus requiring increased expenditure of fracture energy. In general, finer microstructural constituents such as bainite and tempered martensite produce greater fracture resistance than coarser constituents such as ferrite and pearlite. This is the reason why quenched and tempered steels generally have superior toughness to as-rolled or normalized steels. Cooling rates largely determine the grain size of steels as well as the type of microconstituents developed. Thicker sections will tend to have coarser grain size, coarser microconstituents, and lower toughness than thinner sections. The large grain size ferrite-pearlite microstructure existing at the core region of as-rolled jumbo shapes (Figure 6) is the primary reason for the low fracture toughness measured in this area. Segregation of alloy elements to the core region resulting in alloy enrichment also contributes to low toughness.

Microalloyed steels contain elements added specifically to control ferrite grain size, e.g. niobium (Columbium) and vanadium. Aluminum, added as a deoxidizer, also limits ferrite grain size and serves as a de-nitrifier as well.

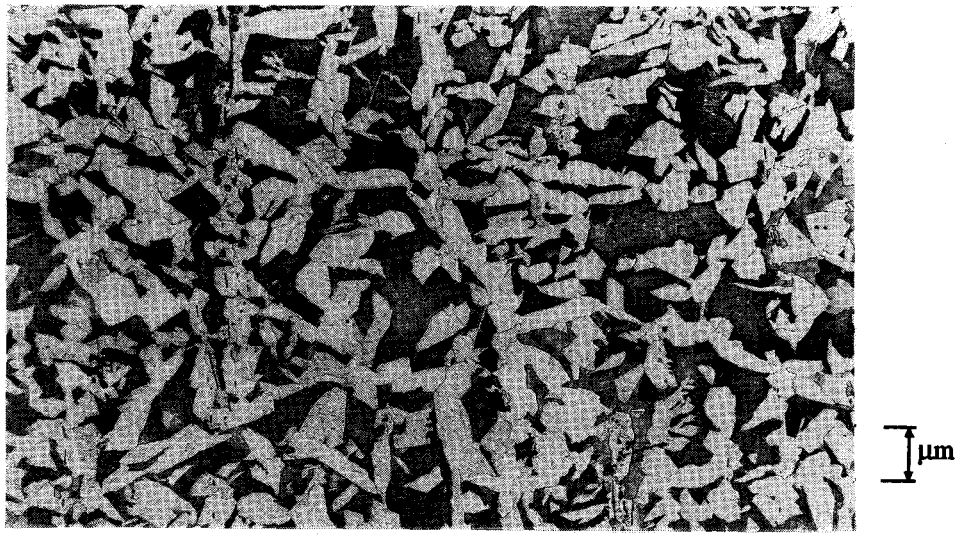

Figure 6: Typical Microstructure of the Core Region of Jumbo Shapes Showing Large Grain Size

The effect of composition and microstructure on weld metal toughness follows much the same trends as wrought steel [Easterling, K., 1983]. Toughness is still dictated by the development of desirable fine microconstituents and fine grain size. In general, weld metal toughness is usually as good or superior to plate or shape toughness largely due to the lower carbon and inherent fine grain structure and finer microconstituents which results from the high cooling rates associated with most welding processes. Only in slow-cooling high-heat-input weld processes does the resulting grain size have a detrimental effect on the weld fracture toughness. The low toughness of electroslag welds can be attributed to the coarse grain size and coarse microconstituents developed during the slow cooling of welds deposited with this very high heat input process.

More often, weld toughness is influenced by the incorporation of undesirable elements such as oxygen and nitrogen in the weld pool which reduce toughness. Controlling these elements is the role of the shielding gas and/or flux used in the weld process. Fluxes contain deoxidizers such as silicon and aluminum for this purpose.

The region with lowest fracture toughness in weldments is usually the region of base metal adjacent to the weld nugget which has been heated to high temperature but below the melting point of the base metal. This region, called the heat-affected-zone (HAZ), is composed of several sub-regions whose structure and properties reflects the highest temperature reached in that area during welding. Like weld metal, the microconstituents developed in the HAZ are influenced by the cooling rate of the weld and consequently are affected by welding procedure (ie. heat input, preheat). The sub-region nearest the weld fusion line, called the coarse grained HAZ (CGHAZ), is heated to temperatures where rapid grain growth can occur and, in the case of some steels, hard martensite microstructures can develop. These are often termed local brittle zones (LBZ's) in low carbon steels. The next sub-region beyond the CGHAZ is called the fine grained HAZ (FGHAZ) and, as the term suggests, is a region heated to a lower temperature where lessened grain growth can occur. For most wrought steels the resulting grain size is smaller than the unaffected base metal grain size and constitutes a grain refined region with superior strength and toughness compared to the base metal. In most weldments, the CGHAZ region will have lower fracture toughness than found in the unaffected base metal and lower toughness than found in most weld metals due to the coarse grain size and hard and brittle phases developed in this region. This is not the case, however, in all weldments. In weldments where the weld metal has low fracture toughness, such as produced with E70T-

4 electrodes, the CGHAZ may have equal or superior toughness compared to the weld metal and will not be the region of the weldment most susceptible to fracture.

Fracture Mechanics Analysis

Fracture mechanics is based on the mathematical analysis of solids with notches or cracks. Relationships between the material toughness, the crack size, and the stress or displacement will be derived below using fracture mechanics. Although cracks can be loaded by shear, experience shows that only the tensile stress normal to the crack is important in causing fatigue or fracture in steel structures. This tensile loading is referred to as "Mode I". When the plane of the crack is not normal to the maximum principal stress, a crack which propagates subcritically or in stable manner will generally turn as it extends such that it becomes normal to the principal tensile stress. Therefore, it is typically recommended that a welding defect or crack-like notch which is not oriented normal to the primary stresses can be idealized as an equivalent crack with a size equal to the projection of the actual crack area on a plane which is normal to the primary stresses [BSI, 1991].

Although this idealization can be made for the stable crack propagation and even the onset of unstable crack propagation, it should be noted that the direction of unstable crack propagation is sometimes erratic and random in part because of the influence of stress waves and the complexity of the residual stress fields. For example, consider the cracks which propagated from the complete penetration groove welds in the WSMF connections that fractured in the Northridge earthquake. The path of propagation of these dynamic cracks, propagating at a speed on the order of the speed of stress waves, is somewhat random. Therefore, the final orientation of these cracks should not be given too much significance.

For the purpose of the design of buildings and most other welded steel structures, it is necessary to assure that brittle fracture does not occur. When ductile fracture is the controlling failure mode on the critical net section, higher factors of safety are imposed. The degree of ductility depends on the net to gross section and the yield to tensile strength ratio. Brittle fracture occurs with nominal net-section stresses below or near the yield point. Therefore, the relatively simple principles of linear-elastic fracture mechanics (LEFM) can be used to conservatively assess whether a welded joint is likely to fail by brittle fracture rather than fail in a ductile manner.

It significantly simplifies the presentation and practical use of fracture mechanics if the discussion is confined to brittle fracture only. Worst-case assumptions are made regarding numerous factors that can enhance fracture toughness, e.g. temperature, strain rate, constraint, and notch acuity or sharpness. These assumptions eliminate the need for extensive discussion of these effects. If necessary, these effects can be considered and more advanced principles of fracture mechanics can be used to estimate the maximum monotonic or cyclic rotation before ductile tearing failure. Fracture mechanics can also be used to predict the "subcritical" propagation of cracks due to fatigue and/or stress corrosion that may be precede fracture. The influence of crack propagation from the notches in the WSMF connections due to prior low-magnitude earthquakes is a subject that should be investigated. If brittle fracture from cleavage is suppressed, there is a high probability that the connections can be made to fail from ductile cyclic rotation in the plastic range. However, available information indicates that there was little subcritical crack propagation that preceded the brittle fracture of the WSMF connections. In order to provide a thorough discussion of the brittle fracture problem in a limited number of pages, these and many other interesting topics in fracture mechanics that cannot be presented in detail. There are several excellent books on fracture mechanics which cover these topics in detail [Barsom and Rolfe, 1987], [Broek, D., 1987], [Fisher, 1984], [Anderson, 1995], [Kanninen and Popelar, 1985]. A recent review of fatigue and fracture of fabricated steel structures is particularly relevant [Kulak and Smith, 1993].

LEFM gives a relatively straightforward method for predicting fracture, based on a parameter called the stress-intensity factor (K) which characterizes the stresses at notches or cracks. The applied K is determined by the size of the crack (or crack-like notch) and the nominal gross-section stress remote from the crack. Crack-like notches and weld defects are idealized as cracks and the term crack includes crack-like notches and weld defects as well. In the case of linear elasticity, the stress-intensity factor can be considered as a measure of the magnitude of the crack tip stress and strain fields. Solutions for the applied stress-intensity factor, K, for a variety of geometries can be found in handbooks [Tada, 1985], [Rook and Cartwright, 1974], [Rooke, 1986], [Murakami, et al., 1987]. Most of the solutions are variations on standard test specimens which have been studied extensively. The following discussion presents a few useful solutions and examples of their application to welded joints.

In general, the applied stress-intensity factor is given as:

$$K=F_c*F_s*F_w*F_g*\sigma\sqrt{\pi a} \qquad (1)$$

where the F terms are modifiers on the order of 1.0, specifically:

F_c is the factor for the effect of crack shape,
F_s is the factor, equal to 1.12, that is used if a crack originates at a free surface,
F_w is a correction for finite-width which is necessary because the basic solutions were generally derived for infinite or semi-infinite bodies, and
F_g is a factor for the effect of non-uniform stresses, such as bending stress gradient.

A stress concentration factor (SCF) is defined as the ratio of the peak stress near the stress raiser to the nominal gross section stress remote from the stress raiser. SCF are often used in fracture assessments when the crack is located near a stress raiser. For example, a crack may be located at a plate edge which is badly corroded. Any SCF would also be included in F_g.

The stress intensity factor has the unusual units of MPa-m$^{1/2}$ or ksi-in$^{1/2}$. The material fracture toughness is characterized in terms of the applied K at the onset of fracture in simplified small test specimens, called K "critical" or K_c. The fracture toughness (K_c) is considered a transferable material property, i.e. fracture of structural details is predicted if the value of the applied K in the detail exceeds K_c. Equation 1 relates the important factors that influence fracture: "K_c" represents the material, "σ" represents the design, and "a" represents the fabrication and inspection.

In this paper, K_c is used as any type of critical K associated with a quasi-static strain rate, derived from any one of a variety of test methods. One measure of K_c is the plane-strain fracture toughness which is given the special subscript "I" for plane strain, K_{Ic}. K_{Ic} must be measured in specimens which are very thick and approximate plane strain. If the fracture toughness is measured in an impact test, the special designation K_d is used where the subscript "d" is for dynamic. In practice, K_c is often estimated from correlations with the result from a CVN test, because the CVN test is much cheaper to perform and requires less material than a fracture-mechanics test, and most test laboratories are equipped for the CVN test. A widely-accepted correlation for the lower shelf and lower transition region between K_d and CVN is credited to Rolfe and Barsom [Barsom and Rolfe, 1987]:

$$K_d = 11.5 * \sqrt{CVN} \quad (2)$$

where CVN is given in J and K_d is given in MPa-m$^{1/2}$. This correlation is used to construct the lower part of the curve for dynamic fracture toughness (K_d) as a function of temperature directly from the curve of CVN vs. temperature. There is a temperature shift between the intermediate load rate values of K_c and the impact load rate values of K_d which is approximately equal to the temperature shift that occurs for CVN data as shown in Figure 3. Therefore, K_c values for structural steel are obtained by shifting the K_d curve to a temperature which is 38 degrees C lower. However, on the lower shelf there is essentially no temperature shift and therefore K_c is approximately equal to K_d

There are size and constraint effects and other complications which make the LEFM fracture toughness K_c less than perfect as a material property. This is especially true when K_c is only estimated based on a correlation to CVN. Nevertheless, as illustrated in the following, a conservative lower-bound value of K_c can be used by structural engineers to avoid brittle fracture.

As previously mentioned, brittle fractures have occurred in group 4 and 5 shapes, i.e. jumbo shapes [Fisher, J. W. and Pense, A. W., 1987]. The brittle jumbo shapes had low toughness, particularly in the region of the web and flange junction. For example, Figure 7 shows some typical data for a W14x370 section which shows the gradient in CVN from the core to the plate surface. The lower bound CVN energy for the core region ranges from 4 to 14 J. The scatterband for K_c based on the Charpy data is shown in Figure 8 with some measured K_{Ic} data. Using this correlation, the scatterband for the predicted K_c ranges from 23 to 43 MPa-m$^{1/2}$. These data show that the correlation is conservative, since the actual K_{Ic} ranges from 45 to 50 MPa-m$^{1/2}$. Currently, these jumbo shapes and thick plates must exhibit 27 J at 21 °C when subjected to tension. [AISC, 1993] Using the correlation of Equation 2, 27 J gives a K_d of 60 MPa-m$^{1/2}$.

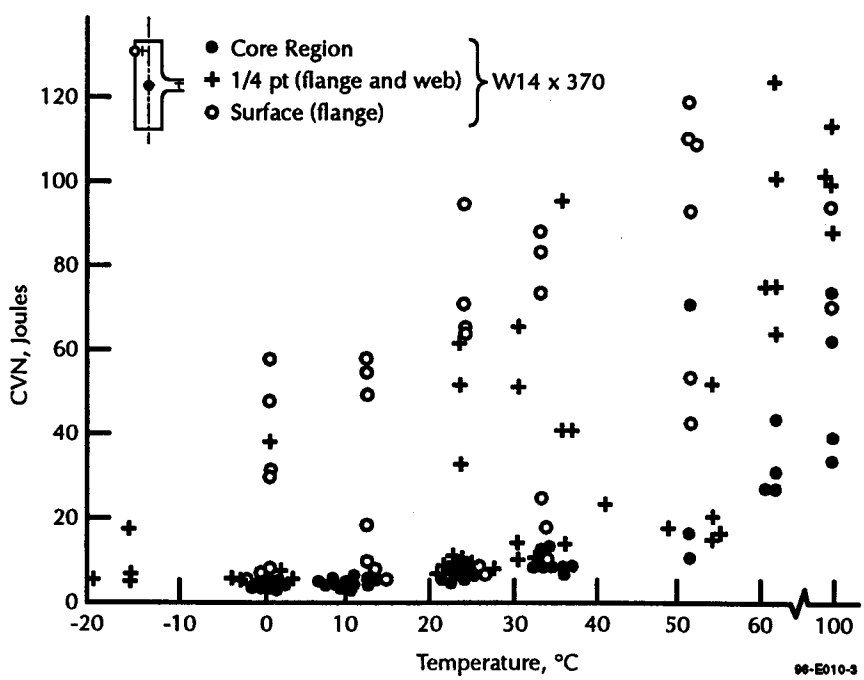

Figure 7: Typical Charpy Impact Energy Data for As-Rolled Jumbo Shapes

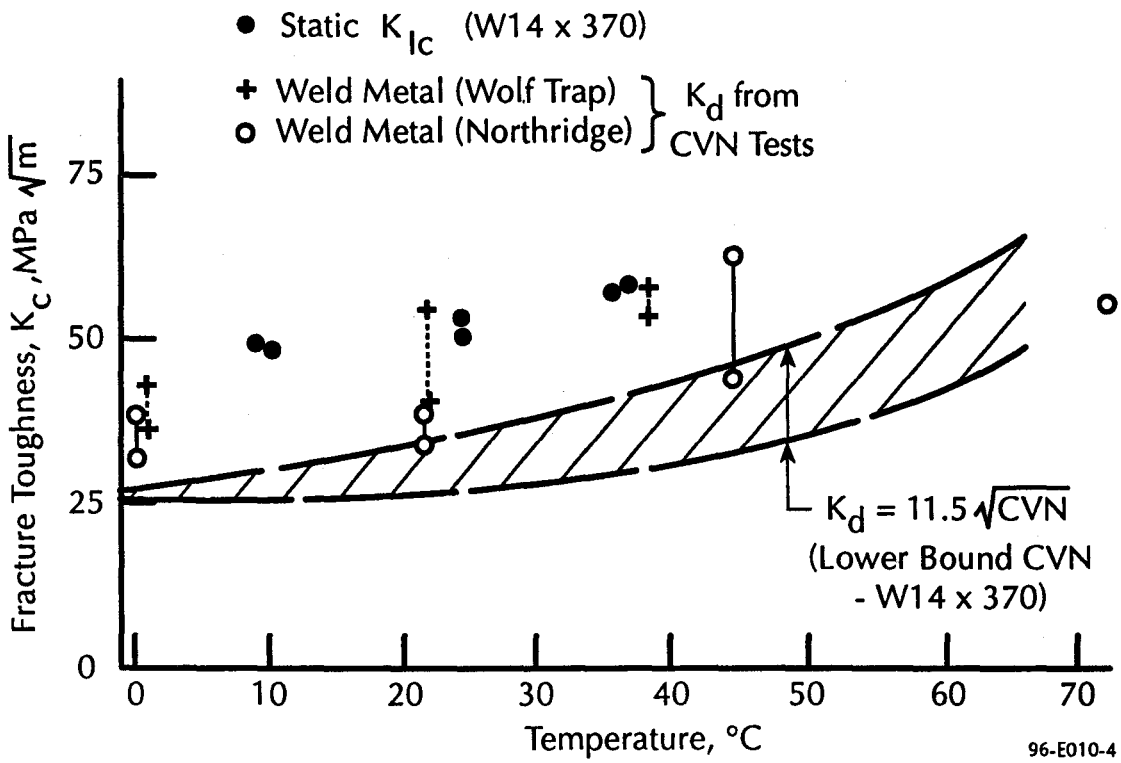

Figure 8: Comparison of K_d Lower Bound CVN Data for the W14x370 Jumbo Shape (from Figure 7) and E70T-4 Weld Medal with K_{Ic} from Fracture Mechanics Tests

In January 1986, after the temperature decreased to less than -20°C, an exposed steel box girder that supports part of the roof of the new Filene Center at Wolf Trap Farm Park in Vienna Virginia was discovered to be fractured. Figure 9 shows the fracture surface of the box girder, which exhibits the typical "herringbone" patterns that point to the origin of failure. In this case, the fracture originated from lack of fusion in the splice welds in the backing bar used for the corner longitudinal welds of the box. Typically, the welds splicing the backing bar are thought to be unimportant and are not given the same attention as the welds in the member itself. However, the backing bar is fused to the corner longitudinal weld and therefore this defect became a defect in the corner longitudinal weld. Such defects in backing bar splices have led to fatigue cracking in bridges in several cases in the past [Fisher, 1984].

The lack of fusion defects fractured the corner longitudinal groove welds because of the unusually low toughness of these welds. These low-toughness welds resulted from mixing two weld processes. Tack welds were used to place the backing bar. These tack welds were made with a self-shielded Flux-Core Arc Weld (FCAW-SS). These tack welds were partially remelted in the longitudinal Submerged-Arc Welds (SAW), giving these welds very low toughness which was comparable to the low toughness observed in core region of jumbo sections. In fact, the data are also shown on Figure 8 and it is seen that these data fall in the same region as the data from the brittle jumbo core region. As a consequence of the fracture at the Filene Center, there is now a warning in the AISC LRFD code (Section J.2.7 and commentary) regarding the mixing of weld metals.

The base metal had good static toughness and could have tolerated a rather large crack statically. However, the base metal dynamic toughness was insufficient to arrest these cracks. Cleavage cracks propagate at speeds on the order of 1000m/s and the strain rates ahead of the cracks are extremely large.

The Navy and the gas transmission pipeline industry have studied the crack arrest capability of plates. If a steel is required to arrest dynamic cracks, it must have a very high dynamic toughness. Steel with crack-arrest capability is too expensive for buildings.

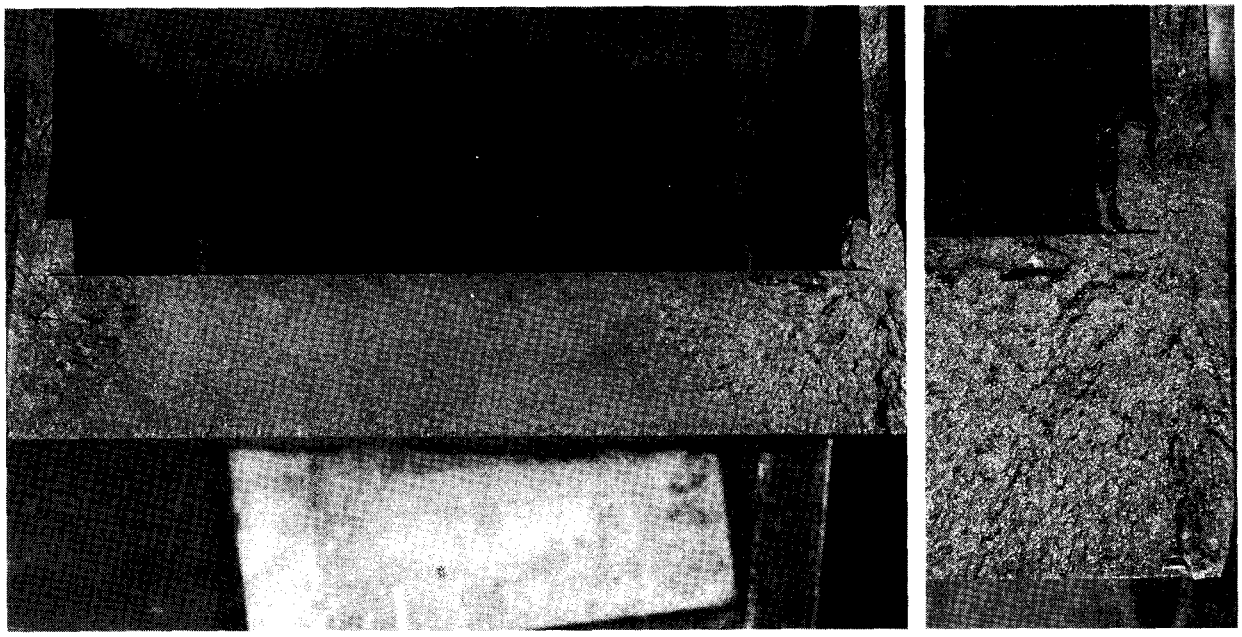

Figure 9: The fracture Surface from the Box Girder at Wolf Trap Showing Classic Cleavage Fracture Chevrons, Pointing to the Origin of the Crack in the Corner Weld

The welds in the WSMF connections were commonly made with the self-shielded flux-cored arc welding (FCAW-SS) process using an E70T-4 weld wire. For the connections which fractured in the Northridge earthquake which have been investigated so far, the weld metal CVN is plotted in Figure 10. The lower bound impact energy is between 4 and 14 J for temperatures up to 50°C. If recommended weld procedures are followed, the fracture toughness increases slightly but remains low as also indicated in Figure 10 [Kaufmann, et al., 1996].

It happens that the values of CVN and K_c toughness for this Northridge weld metal also fall within the scatterband for "lower-shelf" brittle-fracture-prone materials as shown in Figure 8. The lower bounds of the CVN and K_c data are not sensitive to temperature or strain rate because these materials do not undergo a transition at temperatures of interest. This similarity in the data suggests that a there may be a "lower-bound" value of the fracture toughness that can be assumed for brittle ferritic weld metal, structural steel, and the heat-affected zone (HAZ). The lower-bound fracture toughness reflects the worst effects of temperature and strain rate. For these materials, the lower-bound fracture toughness was between 45 and 50 MPa-m$^{1/2}$. This concept of a lower-bound fracture toughness is very useful for fracture assessment.

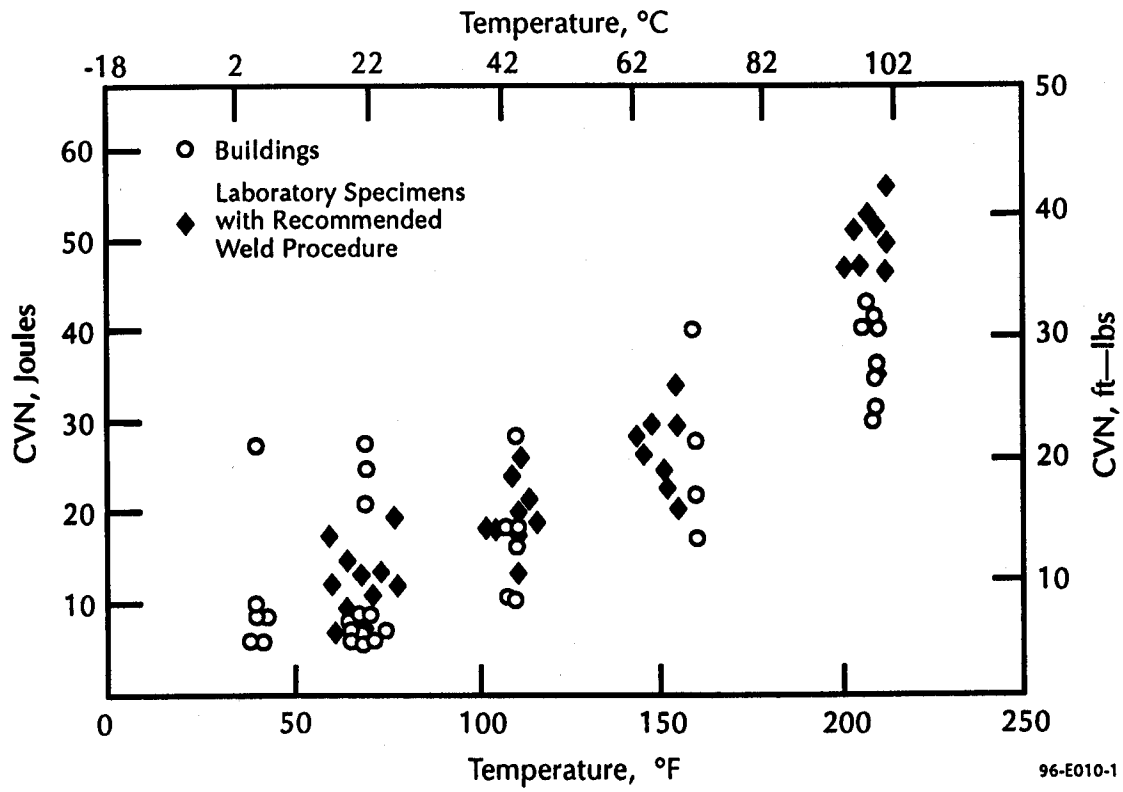

Figure 10: Typical Charpy Impact Energy from E70T-4 FCAW-S Weld Metal from WSMFConnections

Center-Crack in Tension

The solution for a plate with a through crack subject to uniform tensile membrane stress is:

$$K = F_w \sigma \sqrt{\pi a} \tag{3}$$

where:

σ = nominal gross-section stress remote from the crack,
2a = the total overall crack size.

If the total width of the panel is given as 2W, F_w for this crack geometry can be approximated by the Fedderson or secant formula:

$$F_w = \sqrt{\sec \frac{\pi a}{2W}} \tag{4}$$

This formula gives a value that is close to 1.0 and can be ignored for a/W less than about 0.3. For a/W of about 0.5, the secant formula gives F_w of about 1.2. However, the values from the secant equation go to infinity as a approaches W. The secant formula is reasonably accurate for a/W up to 0.85. The F_w may be used for other crack geometries as well.

Many common notches in welded joints can be idealized as a center-crack in tension. Figure 11 shows several defects which were revealed from cores of a WSMF flange connection which had indications from ultrasonic testing. The defect shown as in Figure 11a may be analyzed as center cracks on a vertical plane. The length of the crack is determined from the projection of the defect on the vertical plane, as shown in Figure 11a. The large pore in Figure 11a gave a much larger indication than the lack of fusion defects in Figures 11b and 11c, although it is clear that the latter defects are more critical.

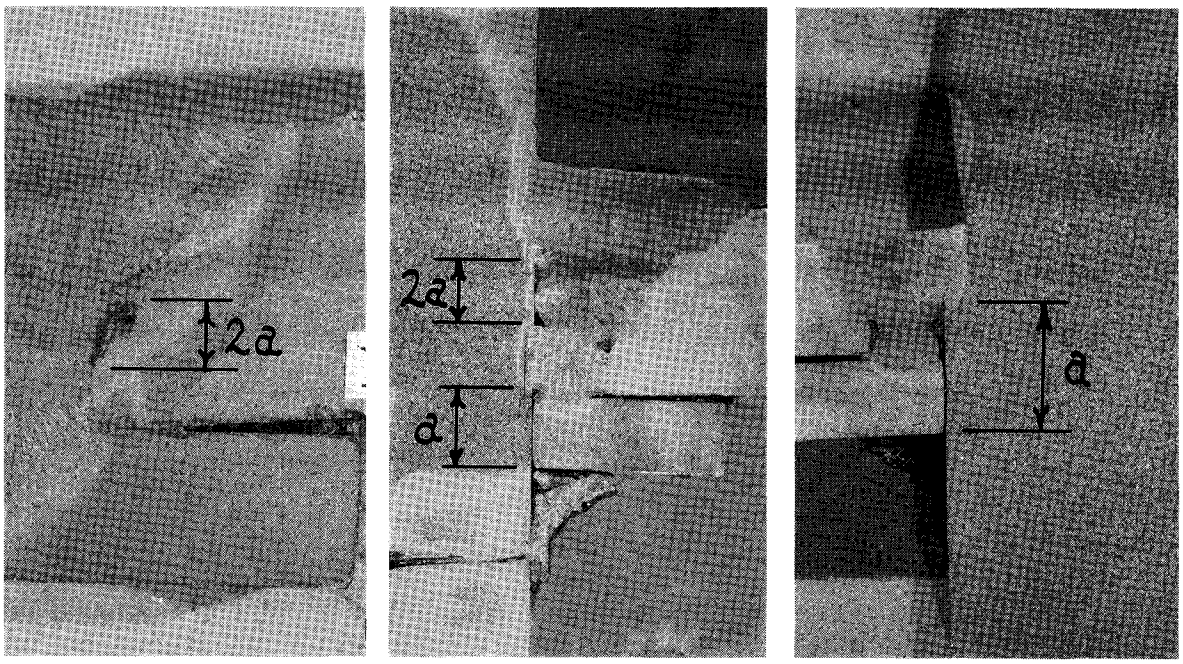

(a) (b) (c)

Figure 11: Three WSMF Weld Cross-Sections Showing Defects Detected with Ultrasonic Testing

In this case, the dimension 2a is the maximum width of the pore which is about 6 mm and the dimension 2W is the thickness of the plate or 25 mm. The a/W ratio is less than 0.25 and therefore F_w can be taken as 1.0. The stress-intensity factor can therefore be calculated using Equation 3. If the lower-bound fracture toughness of 45 MPa-m$^{1/2}$ is assumed, Equation 3 gives an allowable total (applied plus residual) stress of 460 MPa for a = 3 mm.

This area at the center of the weld is typically subjected to a compressive residual stress. However, the distribution of stress is highly variable and it is possible to have tensile residual stress. Therefore, assume a tensile residual stress of 450 MPa, which is equal to the expected yield strength for Grade 50 (350 MPa) steel. The yield point of the weld metal will equal or exceed 450 MPa. It can be seen that this type of welding defect could not possibly cause a brittle fracture before yielding. Therefore, unless the defect could grow by fatigue, this type of welding defect is inconsequential.

Another type of notch that can be idealized as a center-cracked panel is a backing bar with a fillet, as shown in Figure 12. In this case, the unfused area of the backing bar creates a crack-like notch with one tip in the root of the fillet weld and one tip at the root of the groove weld. The crack is asymmetrical but since the connection is subjected to uniform tension, the crack can be analyzed as if it were in a symmetric center-cracked panel. Of course, the applied K is higher on the crack tip which is in the root of the fillet weld because there is a high F_w for this side. Assuming the weld metal of the groove weld and the fillet

weld have comparable toughness, the fillet weld side of the backing bar will govern the fracture limit state. Therefore, the panel is idealized as being symmetric with respect to the center of the backing bar, i.e. having a width (2W) of 50 mm.

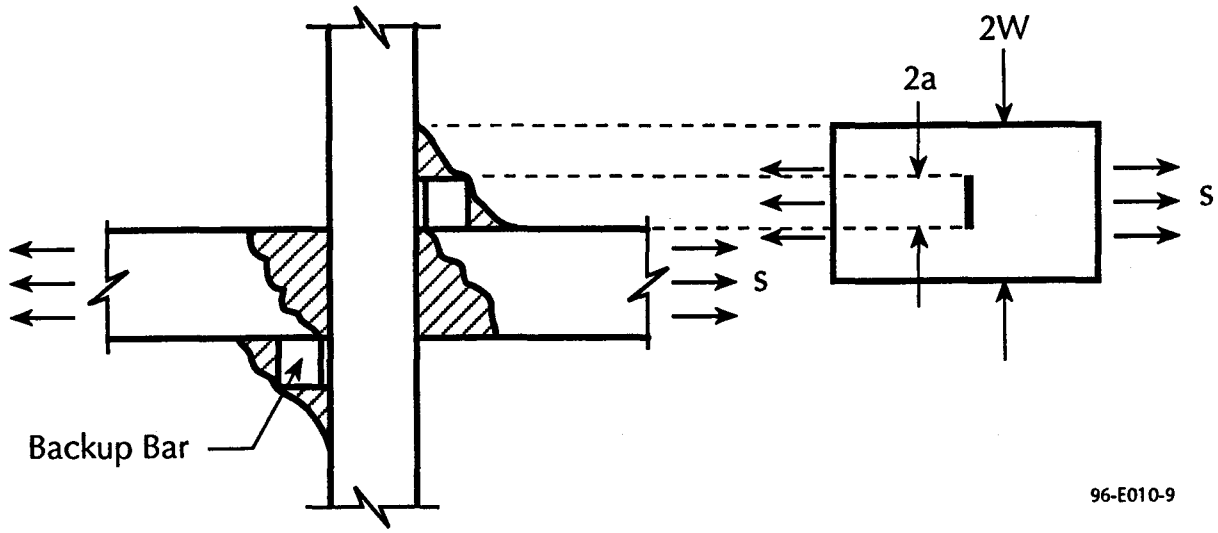

Figure 12: Idealization of Backing Bar with a Fillet Weld as a Center-Cracked Tension Panel

Assuming negligible weld root penetration, the crack size (2a)is taken as being equal to the backing bar thickness or 13 mm. Therefore, for a/W of 0.5, Equation 4 gives F_w equal to 1.2. Although this idealization seems like a gross approximation at best, the validity of the K solution for this particular weld joint was verified based on observed fatigue crack propagation rates.

If this is a Grade 50 steel, the yield strength could be up to 450 MPa. The notch tip could be subjected to full tensile residual stress. Therefore, Equation 1 is solved with the gross-section stress equal to 450 MPa, with the F_w factor of 1.2, and (a) of 6 mm, giving 74 MPa-m$^{1/2}$. It can be seen that this configuration could cause a brittle fracture for very brittle materials. However, weld metal and base steel with modest toughness could easily withstand this defect.

Edge Crack (Analysis of the WSMF Connection Welds

Figure 13 shows a cross section near the crack origin from each of the connections shown in Figure 1 which fractured in the Northridge earthquake and a fracture surface from the fracture that stayed in the weld. The fracture surfaces indicate that the fractures originate in the root of the weld, typically at a lack-of-fusion defect. This lack-of-fusion defect is difficult to avoid when the weld must be stopped on one side of the web and started on the other side. The weld fracture surface in Figure 13 shows the crack-like notch formed by the combination of a lack of fusion defect and the unfused edge of the backing bar. On a cross section at the deepest point of the lack-of-fusion defect, the total depth of the notch, including the unfused edge of the backing bar, is between 13 and 19 mm. The stress-intensity factor for this type of notch can be approximated by the formula for an edge crack, i.e.:

$$K=1.12F_w\sigma\sqrt{\pi a} \qquad (5)$$

where (σ) is the remote gross-section nominal stress and (a) is the depth of the crack-like notch. It can be seen that the edge crack equation, i.e. Equation 5, is a special case of the center-crack equation, i.e. Equation 3, where a and W are the total crack size and plate width, respectively. The F_w is approximated

by Equation 4. The factor F_s of 1.12 is applied to account for the free edge, which is not restrained as it is in the center-cracked geometry.

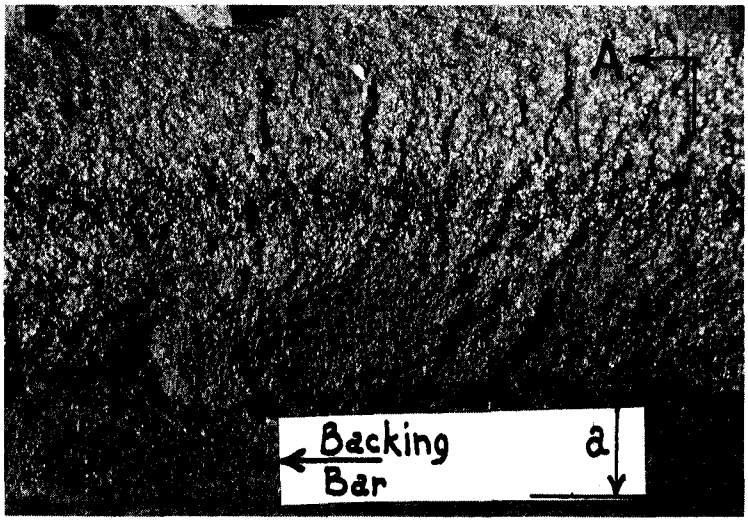

(a) Type I Crack Surface

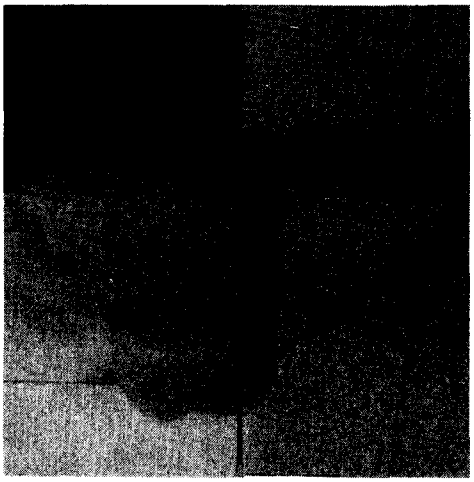

Etched Section A-A

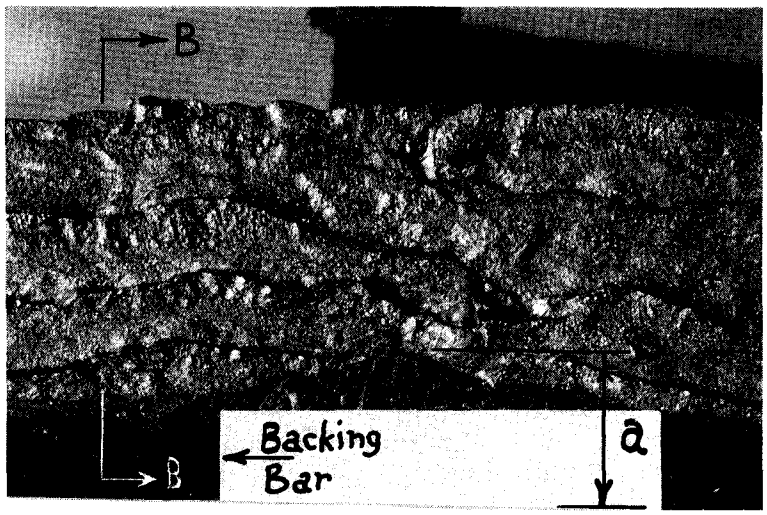

(b) Type II Crack Surface

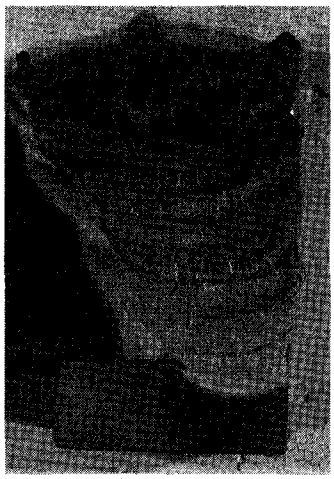

Etched Section B-B

Figure 13: Weld Cross-Sections and Fracture Surface for WSMF Connections Shown in Figure 1

As shown in Figure 8, the K_d from CVN data for the WSMF weld metal fall in the scatterband for other brittle weld metals and structural steels. Therefore it can be assumed that the lower-bound fracture toughness K_c was between 45 and 50 MPa-m$^{1/2}$. Equation 1 may be used to predict brittle fracture for the WSMF connection welds when K exceeds 45 MPa-m$^{1/2}$. For a notch depth of 13 to 19 mm, Equation 1 would predict that brittle fracture is likely to occur for gross-section stress between 160 and 200 MPa, well below the yield point. These type of LEFM calculations, had they been performed, would have predicted that brittle fracture would occur in the WSMF connections before yielding.

As explained previously in the discussion of the fracture at Filene Center at Wolf Trap, the strain rates are extremely high ahead of a propagating cleavage crack tip, making the arrest of a cleavage crack very difficult. Therefore, even if the toughness of the WSMF column section was very good, it was typically not sufficient to immediately arrest the dynamic crack emanating from the weld into the steel of the column flange and web as shown in Figure 1 and 13. The dead load compressive stress in the column and any possible uplift or tension due to bending in the column as well as residual stresses from continuity and doubler plates will have a significant influence on the path of the crack.

The scenario where a crack is initiated in a brittle material and then fractures a reasonably tough structural member (as long as there is tensile stress in the member) is common in many fractures which have been investigated, e.g. the Filene Center. Often, seemingly-insignificant but brittle tack welds are responsible. Another example which recently was investigated is a fracture due to seismic loading where a tack weld crossed the unfused abutting ends of a longitudinal backing bar for the corner welds inside a box section. This well-known scenario is exploited in one of the original fracture tests, ASTM E 208 "Standard Test Method for Conducting Drop-Weight Tests to Determine Nil-Ductility Transition Temperature of Ferritic Steel." In this test, a crack is initiated from a brittle weld bead with a notch cut in it.

The propagation path of the unstable dynamic crack is seemingly chaotic, as it is influenced by the dead load compressive stress in the column, possible uplift or tension due to bending in the column, dynamic stress waves, and complex residual stress fields. The critical event was the initiation of the unstable crack in the brittle weld. There is little significance to whether the crack propagated in the weld or turned and entered the column.

Fracture mechanics can be used to establish required levels of fracture toughness as well as limits on the size of defects. One obvious component of the solution to the WSMF cracking problem is elimination of the possibility of such large defects (i.e. $a \approx 19$ mm) that result from the backing bar and any lack of fusion defect. The backing bar removal and back gouging to minimize the lack of fusion will eliminate large crack-like conditions. Appropriate weld notch toughness requirements will avoid the use of low toughness weld metal. For fracture control, improvements in fracture toughness and decreased defect sizes are essential.

These fracture-mechanics calculations can be used to examine the expected stress intensity factor using the maximum yield strength of the furnished steel beam and defect sizes considered acceptable by AWS D1.1. The steel can be expected to have a yield strength up to 450 MPa. AWS D1.1 Section 8.15 indicates that embedded defects up to 19 mm long and edge defects up to 1.5 mm are tolerable in such a thick plate. With the embedded defect of 19 mm, (a) is equal to 9.5 mm and Equation 6 for a circumscribed crack indicates that the maximum applied K is 50 MPa-m$^{1/2}$, which, without a temperature shift, corresponds to a Charpy energy of about 20 J. Fracture toughness plus a comfortable margin can be provided when notch toughness is imposed on the weld metal. The tolerable edge crack of 1.5 mm gives an applied K of 35 MPa-m$^{1/2}$, but this assumes no backing bar is left in place.

There are certainly many other equally-important design issues that influenced these fractures. The overall lack of redundancy, i.e. the reliance on only one or two massive WSMF to resist lateral load in each direction, contribute to large forces, increase the thickness of the members, and provide high constraint at the connections. Even if brittle fracture is avoided, welds will typically fail at a lower level of plastic strain than will base metal. Therefore, it can also be argued that it is imprudent to rely upon welds for extensive plastic deformation. Several improved WSMF connections have been proposed, most of which are designed such that the plastic hinge develops out in the span away from the connection.

Nevertheless, in the event of unexpected loading, it is still desirable that these weld joints have a ductile failure mode. Therefore, while these improved connection designs may be worthwhile, the low-toughness weld metal and joint design with a built-in notch still should not be used under most circumstances, because discontinuities in the weld or at its surface can result in cleavage fracture initiation in low toughness weld metal [Kaufmann].

Note that having a fillet on the open side of the backing bar improves the edge-crack condition (such as in the WSMF connection welds). The crack size becomes equal to half the sum of the backing bar width and the lack of fusion when the fillet is added because the notch is now treated as a center crack of length (2a) rather than an edge crack of length (a). The calculations for the WSMF connection weld can be reevaluated to see what effect this would have had on the potential for brittle fracture. These calculations showed that without the fillet, a 19 mm deep notch would fail at 160 MPa stress. With the fillet, the tolerable stress could be increased to 220 MPa, which exceeds the design allowable stress but will not achieve yielding. Thus by simply adding a fillet to the backing bar, the allowable stress can be increased by 37 percent. Obviously, it would be better to remove the backup bar entirely, and to back gouge to remove defects. With or without the fillet, however, a higher-toughness weld metal would be required.

The fracture scenario of these WSMF connections is similar to the fracture scenario of the box sections at the Filene Center at Wolf Trap. Both examples illustrate the importance of weld metal toughness as the first line of defense against fracture. Building connections, like any other welded structure, are susceptible to brittle fracture, especially if the connections are likely to be loaded dynamically above the yield strength to deformations several times the yield deformations. Low temperature can also contribute to fracture when the steel is exposed.

Buried Penny-shaped Crack

Many internal weld defects are idealized as an ellipse or a circle which is circumscribed around the projection of the weld defect on a plane perpendicular to the stresses. Often, the increased accuracy obtained by using the relatively complex elliptical formula is not worth the effort, and the circumscribed penny-shaped or circular crack is always conservative. The stress-intensity factor for the penny-shaped crack is given as:

$$K = \frac{2}{\pi}\sigma\sqrt{\pi a} \qquad (6)$$

where a is the radius of the circular crack. In terms of Equation 1, the crack shape factor F_c in this case is $2/\pi$ or 0.64. Using: 1) the lower bound fracture toughness of 45 MPa-m$^{1/2}$; and, 2) an upper bound residual stress plus applied stress equal to the upper bound yield strength for Grade 50 steel (450 MPa); Equation 6 shows that a penny-shaped crack would have to have a radius exceeding 8 mm to be critical, i.e. the diameter of the allowable welding defect would be 15 mm (providing that fatigue is not a potential problem).

The crack shape factor F_c is more favorable (0.64) for buried cracks as opposed to F_s of 1.12 for edge cracks and the defect size is equal to (2a) for the buried crack and only (a) for the edge crack. These factors explain why edge cracks of a given size are much more dangerous than buried cracks of the same size.

Fracture Mechanics Test Methods

Fracture tests can be divided according to the objective or use of the data. Screening tests, like the CVN test, can rank materials and give a relative indication of toughness but the result cannot be used directly in a quantitative analysis. On the other hand, fracture mechanics tests are intended to get a quantitative value of fracture toughness that can be used directly to predict fracture in structural members. As explained previously, it is sometimes possible to indirectly infer a quantitative value of K_c from a correlation to a screening tests result like CVN.

One of the first fracture-mechanics tests was ASTM E399, "Standard Test Method for Plane-Strain Fracture Toughness of Metallic Materials". The K_c value determined from this test is given the special subscript "I" for plane strain, K_{Ic}. K_{Ic} is commonly measured on the Compact-Tension (CT) specimen such as shown in Figure 14, although edge-notched bend bars (Figure 15) may also be used. In all fracture-mechanics tests, the specimen must be fatigue precracked. The load and crack mouth displacement are monitored in the test, and K is computed from the load either at the point of instability or at some small offset from the elastic slope. In order for the test to be considered valid, the specimens must have large planar dimensions and be very thick, approximating plane strain. Specifically, the remaining ligament (b) and the thickness (B) must be:

$$b, B > 2.5 \left(\frac{K_{Ic}}{\sigma_y}\right)^2 \qquad (7)$$

This requirement is intended to assure that the specimen size dimensions are on the order of 50 times bigger than the plastic zone at the crack tip. Consider a fracture toughness level, K_{ic}, of 45 Mpa-m$^{1/2}$ (which is a lower bound for K_{ic} for structural steel and weld metal) and a yield strength of 450 Mpa. Even for these brittle materials, a specimen thickness greater than 25 mm would be required. If the plate or

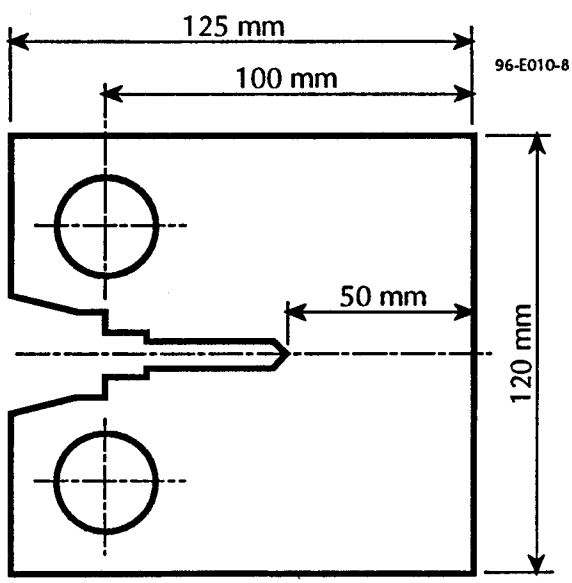

Figure 14: Typical Compact-Tension (CT) Specimen Planar Dimensions (other sizes which are proportional can also be used)

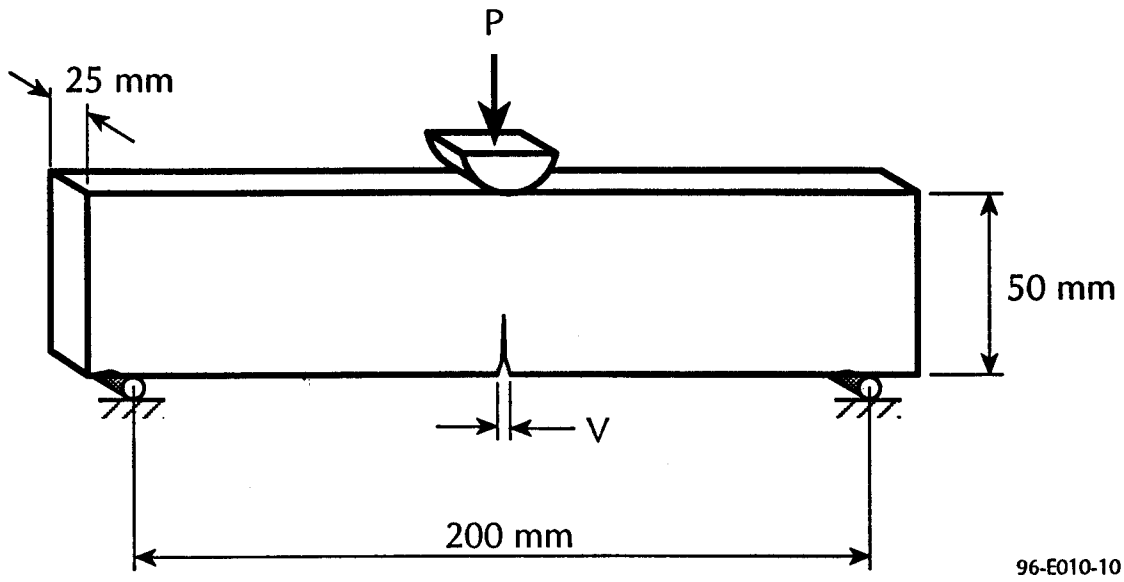

Figure 15: Single-Edge-Notched Bend (SENB) Specimen Planar Dimensions

flange thickness were less thick, valid K_{Ic} could not be obtained. Fracture toughness, greater than 100 MPa-m$^{1/2}$ for example, require specimens thicker than 120 mm. Clearly, it can be seen that this is a test which is impractical for all but the most brittle materials. Typically, invalid K_c values obtained from this test with specimens that are too small will be larger than the valid K_{Ic} However, if the test specimen and the structural member have the same thickness, invalid data often are used with caution.

The J-integral is a parameter for elastic-plastic fracture much like K is a parameter for elastic fracture. The J-integral tests were developed for elastic-plastic fracture where the fracture mode was ductile tearing rather than cleavage. The most simple of these is ASTM E813, "Standard Test Method for J_{Ic}, A Measure of Fracture Toughness" gives a value of J at the initiation of ductile tearing. This test is typically performed on CT specimens such as shown in Figure 14, although bend bars may also be used. In these J tests, the load and crack mouth displacement are monitored and J is computed from the work done on the specimen, i.e. from the area under the load displacement curve. In order to identify the initiation of ductile tearing, changes in compliance are monitored by performing periodic partial unloading of the specimen. The crack extension is determined from these compliance measurements.

J is often converted to an equivalent K by the following relation:

$$K=\sqrt{J*E} \tag{8}$$

where E is the modulus of elasticity. K_c values that are obtained from this J test are commonly given the subscript "J", i.e. K_{Jc}. The specimen size requirements for ASTM E813 are much less stringent than E399, i.e:

$$b, B>25\left(\frac{J_{Ic}}{\sigma_y}\right) \tag{9}$$

For moderate toughness of about 100 MPa-m$^{1/2}$ (J = 48 kJ/m^2), the specimen ligament and thickness are required to be greater than 3 mm, which can be easily met.

ASTM E1290, "Standard Test Method for Crack-Tip Opening Displacement (CTOD) Fracture Toughness Measurement" gives a slightly different test which is easier to perform but gives results which are more variable. This test is typically performed on single edge-notched bend bars (SENB) such as shown in Figure 15, although the CT specimen also can be used. The specimens are the full thickness of the plate or shape and there are no validity requirements. The load and crack-mouth displacement are monitored during the test, and the CTOD is inferred from the crack-mouth displacement. A variety of outcomes are possible including short propagation or pop-in of the crack without instability. The critical CTOD is either at the point of "pop-in" or at the maximum load for more ductile behavior.

The CTOD concept and test method were developed at the Welding Institute (TWI) in the United Kingdom. An empirically-based conservative fracture assessment procedure called the "CTOD design curve" was developed around the CTOD test results and was verified through extensive wide-plate tension tests of weldments. This procedure has been extensively used in the oil and gas industry for pipelines and offshore structures. In 1980, the British Standards Institute published a document called PD6493, which was revised in 1991 and is now called "Guidance on the Methods for Assessing the Acceptability of Flaws in Fusion Welded Structures" [BSI]. This document is based on fracture-mechanics fitness-for-purpose concepts, and is meant to resolve disputes about minor fabrication defects. Originally, the PD6493 procedure was based on fracture toughness measured using the CTOD test and the empirical CTOD design curve. While this approach is still embodied in PD6493:1991, the procedure was generalized to permit any measure of toughness and analysis method. The PD6493 document has an easy to follow codified procedure that can be agreed to in advance by the owner, the engineer, the regulator, and the fabricator. More economical fabrication can result when such an understanding exists beforehand. This document has been widely accepted by industry in the United Kingdom, and by the oil and gas industry around the world. Further full-scale wide-plate testing and now more than 15 years of experience with this document establishes the reliability of this approach.

As CTOD testing procedures became more sophisticated in the 1980's, tests were performed where the notch was placed precisely in the coarse-grained region of the heat-affected zone (HAZ) of weldments. It was found that low values of toughness can be obtained, called local brittle zones (LBZ). Most welded structures have such LBZ. Yet to date there have been no significant failures that can be attributed to such LBZ. Laboratory fatigue tests of full-scale welded details have had cracks which propagated through such zones, yet never experienced any distress or crack instability. Such small brittle regions are of little consequence because even if these LBZ are assumed to be cracks, nearby tough material in the weld and in the base metal do not allow instability.

The CTOD can be related to J and also to K, and therefore CTOD fracture toughness values are often converted to equivalent K values using:

$$J = 1.7 * \sigma_y * CTOD \tag{10}$$

substituting Equation 11 into Equation 9 gives:

$$K = \sqrt{1.7 * \sigma_y * E * CTOD} \tag{11}$$

Recognizing that all of these tests are performed on similar specimens and that all of the various fracture toughness measures can be related, BSI has recently developed a unified testing procedure BS 7448, "Fracture Mechanics Toughness Tests". Using this method, a test is performed and then, based on the results, it is decided how the test should be interpreted. ASTM is currently working on a similar unified test method.

Guidelines for Evaluating Fractures in Steel Frame Connections

It is usually desirable to remove part of the crack in order to assist with the investigation of its cause. However, prior to the removal, data needs to be acquired on the size, location, and orientation of the crack. This should be accomplished by: 1) detailed sketches showing the crack location and dimensions of the crack and member (these sketches should also indicate the orientation of the crack with regard to the primary stresses in the member); and, 2) photographs showing the visible crack conditions and its location relative to the detail at which it formed.

After documentation, a portion of the crack can be removed to permit the origin of the cracking to be evaluated where it is not obvious or apparent. There are generally two types of samples that can be removed. If the material characteristics need to be determined, then a large segment can be removed, as illustrated in Figure 16. In this case the entire tension flange of the beam and the cracked column flange is removed. Often, only one crack surface needs to be removed if the beam flange is cracked from the column as illustrated in Figure 1 and 13.

During removal, steps should be taken to insure that the crack surfaces do not come into contact, as that will damage the surface and destroy important information.

The material in the cracked component will usually have documentation available on the chemical composition and mechanical properties. However, fracture toughness data will often be unavailable, because mandatory Charpy V-notch data was not required at fabrication. Furthermore, seldom are toughness data available on production weld metal.

If material is available such as shown in Figures 16, such tests can be carried out. It is recommended that the following tests be carried out if material is available.

1. Standard Charpy V-notch tests should be carried out on the weld metal and base metal. Twelve to 18 specimens should be prepared and tested at several temperature increments for the base metal. Three specimens are desirable at each test temperature. It is recommended that tests be carried out at -20, 0, 20, and 40°C. Where only limited amounts of material are available such as the weld metal, the tests should be carried out at 0 and 20°C.

2. Standard ASTM 0.505 inch (12.8 mm) or 0.252 inch (6.4 mm) tensile tests should be made depending on the material thickness. Two or three specimens should be fabricated and tested for the beam flange and column flange.

3. A chemistry check analysis should be carried out on drillings from the sample. The available chemical analysis may fail to include some elements that are significant.

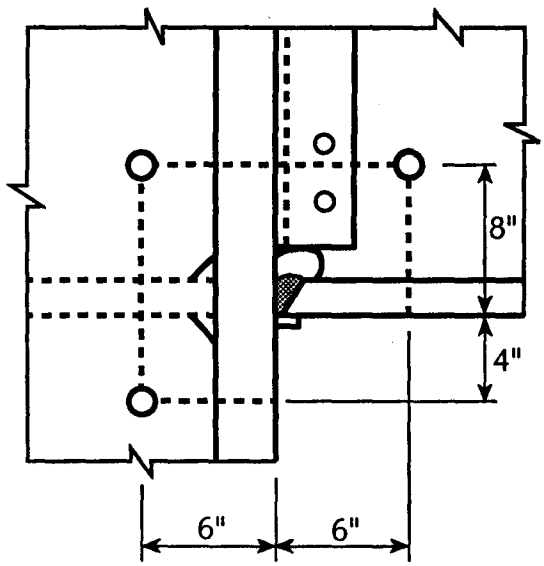

Beam Bottom Flange Detail

1. Identify Location
2. Drill 1" Holes in Web
3. Cut Straight Lines Between Holes in Web and Through Column and Beam Flanges
4. Provide Full Width of Column and Beam Flanges
5. Provide any Information Available on Materials and Welding Procedures (base metal & welds)

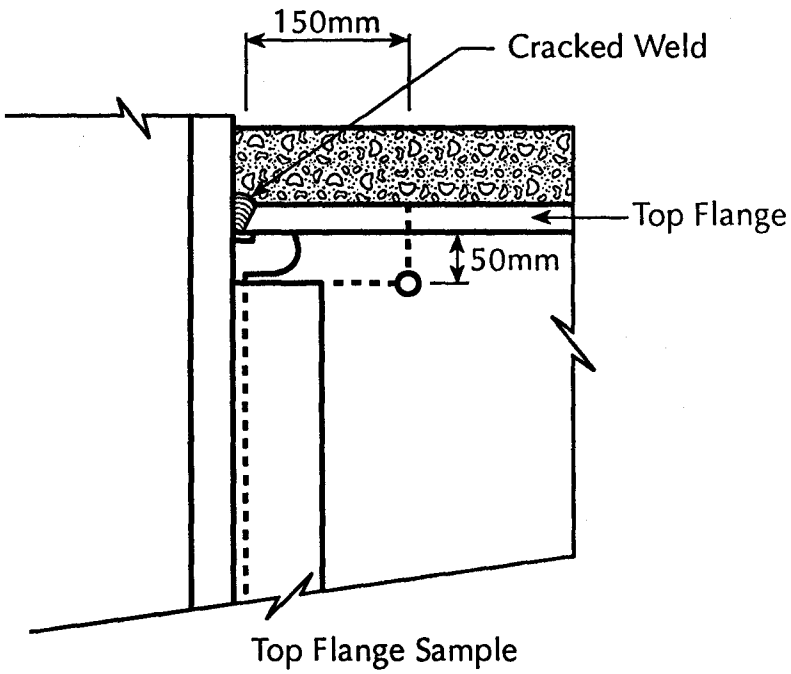

Figure 16: Removal of Samples from Damaged Beam-Column Joint

The location and layout of the test specimens should be documented by suitable sketches and dimensions. Also, it is usually desirable to cut the piece and remove the fracture surface from the segment. Saw cutting should be used in order to minimize damage to the available material and prevent damage to the fracture surface. A heavy spray coating of Krylon applied to the crack surface prior to sawing will guard it against damage from the sawing operation.

Metallographic Examinations

It is desirable to determine the weld profile and plate microstructure. If this is carried out on a segment not in the proximity of the crack origin, it can reveal the profile, heat affected zone and weld passes. It can also provide information on the plate microstructure.

The section to be polished and etched should be cut only after the origin of the crack has been established. Prior to polishing and etching, the crack should be sealed with an inert wax on the core surface in order to prevent damage to the crack surfaces. Figure 13 showed the polished and etched surface of a section weld root which shows that a crack has formed at the backing bar (which was removed after the fracture).

Generally, the macroscopic examinations of the core or plate surfaces are made at magnifications between 1 and 100X. Suitable photographs of the exposed features should be obtained.

If the crack surfaces are not exposed like the case shown in Figure 13, it will generally be necessary to saw cut the sample into segments, so that the crack surfaces can be exposed. This will depend upon the estimated size of the uncracked segment of the piece. The surface should be exposed only after the piece has been cooled in the liquid nitrogen bath, so that it can be readily broken apart. Care should be exercised in exposing the crack, so that the saw cuts do not destroy the crack tip.

Where possible a direct visual examination of the fracture surface will be very beneficial in defining the cause of cracking. Adequate photographic documentation should be obtained prior to cutting the crack surface into segments or clearing off corrosion product.

Brittle fracture surfaces most often will exhibit chevron-type markings such as in Figure 9. These chevrons point back to an origin of the brittle fracture initiation. Often, shear lips will be apparent at the plate surface of a brittle fracture.

After the as-received surfaces are examined and photographed, the Krylon clear lacquer protective coating and loose corrosion product can be removed with an organic solvent such as acetone that does not affect the crack surface. This will often reveal surface fractures that were obscured. A soft toothbrush or equivalent type of brush can be used to remove the coating and loose corrosion product.

Considerable success has been achieved on corroded crack surface examinations by stripping areas of the crack surface "clean" using solvent-softened replica tape. The softened tape is pressed against the surface and removed after it has hardened. This strips away oxides and other corrosion products. If this procedure is repeated, most of the oxide and corrosion product eventually can be cleaned form the crack surface. The final replicas can be examined with the Transmission Electron Microscopic (TEM) as the replica will carry with it the reverse impression of the crack surface. Alternatively, the cleaned surface can be examined in a Scanning Electron Microscope (SEM). Where surfaces are protected from the elements, the corrosion product will often be removed in an ultrasonic bath. Thereafter the surface can be examined with a SEM to determine the source of cleavage facets and the cause of initial defects. Generally, the SEM will be used at magnifications between 5X and 1000X

Summary

1. Building connections, like any other welded structure, are susceptible to brittle fracture. Many interrelated design variables can increase the potential for brittle fracture including lack of redundancy,

large forces and moments with dynamic loading rates, thick members, geometrical discontinuities and high constraint of the connections Low temperature can be a factor for exposed structures.

2. Many factors in fabrication can increase the potential for brittle fracture including notches, misalignment and other geometrical discontinuities, cold work, thermal cutting, flame straightening, weld heat input, weld joint design particularly backing bars, weld sequence and residual stress, non-destructive evaluation and weld defects, intersecting welds, and inadequate weld access holes. In general, these factors are much more difficult to control in field welding. The notch depth in typical Northridge WSMF connection failures includes 9 mm from the backing bar plus in some cases up to 9 mm from a lack of fusion defect.

3. The K_d from CVN data for the WSMF weld metal fall in the scatterband for other brittle weld metals and structural steels with lower-bound fracture toughness between 45 and 50 MPa-m$^{1/2}$. Given the notch depth, fracture mechanics calculations show that brittle fracture is likely to occur for gross-section stress between 160 and 200 MPa, well below the yield point. Fracture mechanics calculations could have predicted that brittle fracture would occur in the WSMF connections before yielding. The fracture mechanics calculations show that welds with discontinuities which are currently acceptable by AWS D1.1 must have a fracture toughness of at least 50 MPa-m$^{1/2}$, which with no temperature shift corresponds to a Charpy energy of about 46 J. Bridge structures use a 38°C temperature shift for steel with a yield point less than 450 MPa. For weld metal the temperature shift is less. Several examples of fracture in buildings illustrate the importance of weld metal toughness as the first line of defense against fracture. Unless there is fatigue loading to propagate the crack out of the weld into the base metal, the toughness of the base metal is less important. Of course, brittle base metal such as in jumbo sections without mandatory toughness must not be welded or flame cut and subjected to tension. Research during the second phase of SAC will likely examine the issues of acceptable flaw size and the required level of toughness of weld metal.

Appendix: References

American Association of State Highway and Transportation Officials, "Guide Specifications for Fracture Critical Non-Redundant Steel Bridge Members", AASHTO, Washington D.C., 1978.

American Association of State Highway and Transportation Officials, "LRFD Bridge Design Specifications," 1st Ed., AASHTO, Washington, D.C., 1994.

Anderson, T.L., Fracture Mechanics - Fundamentals and Applications, Second Edition, CRC Press, Boca Raton FL, 1995.

"Load and Resistance Factor Design (LRFD) Specification for Structural Steel Buildings" from the American Institute of Steel Construction (AISC), 1993.

ASCE-WRC (1971), Plastic Design in Steel, A Guide and Commentary, Second Edition, Joint Committee of the Welding Research Council and the American Society of Civil Engineers, ASCE, New York, 1971.

American Welding Society (1992), D1.1-1992, Structural Welding Code.

Barsom, J.M., and Rolfe, S.T., Fracture and Fatigue Control in Structures, Second Edition, Prentice-Hall, Englewood Cliffs, New Jersey, 1987.

Broek, D. Elementary Fracture Mechanics, Fourth Edition, Matinus Nijhoff Publishers, Dordrecht, Netherlands, 1987.

BSI, Guidance on the Methods for Assessing the Acceptability of Flaws in Fusion Welded Structures, PD 6493: 1991, Published by the British Standards Institution (BSI), 1991.

Easterling, K., Introduction to the Physical Metallurgy of Welding, Butterworths Monographs in Materials, London, 1983.

Fisher, J.W., Fatigue and Fracture in Steel Bridges, John Wiley and Sons, New York, 1984.

Fisher, J.W. and Pense, A.W., "Experience with Use of Heavy W Shaapes in Tension", Engineering Journal, American Institute of Steel Construction, Vol 24 No 2, 1987.

Frank, K.H., et al, Notch Toughness Variability in Bridge Steel Plates, NCHRP Report 355, National Cooperative Highway Research Program, 1993.

Irving, Bob "Way Back When", Welding Journal, Sept. 1994, pg 22

Irwin, G.R., and Kies, J.A., "Critical Energy Rate Analysis of Fracture Strength of Large Welded Structures", Welding Journal, Vol. 33, Research Supplement, pp. 193s-198s, April, 1954.

Irwin, G.R., "Analysis of Stresses and Strains Near the End of Crack Traversing a Plate", Transactions, ASME, Journal of Applied Mechanics, Vol. 24, 1957, also reprinted in ASTM volume on classic papers.

Kanninen, M.F., Popelar, C.H., Advanced Fracture Mechanics,Oxford University Press, New York, 1985.

Kaufmann, E.J., Xue, M., Lu, L.-W., and Fisher, J.W., "Achieving Ductile Behavior of Moment Connections", Modern Steel Construction, Vol. 36, No. 1, pp. 30-39, January, 1996.

Kulak, G.L., and Smith, I.F.C., Analysis and Design of Fabricated Steel Structures for Fatigue: A Primer for Civil Engineers, Univ. of Alberta, Dept. of Civil Engr., Structural Engr. Report No. 190, July 1993.

Murakami, Y., et al, (eds.), Stress Intensity Factors Handbook (Vol.1 and 2), Pergamon Press, Oxford, U.K., 1987.

Roberts, R., Fisher, J.W., Irwin, G.R., Boyer, K.D., Hausammann, H., Krishna, G.V., Morf, V., and Slockbower, R.E., "Determination of Tolerable Flaw Sizes in Full Size Welded Bridge Details", Report FHWA-RD-77-170, Federal Highway Administration, Washington, D.C., December 1977.

Rooke, D.P., and Cartwright, D.J., Compendium of Stress Intensity Factors, Her Majesty's Stationery Office, London, 1974.

Rooke, D.P., Compounding Stress Intensity Factors, Research Reports in Materials Science (Series One), The Parthenon Press, Lancashire U.K., 1986.

Shank, M.E. (ed) Control of Steel Construction to Avoid Brittle Fracture, Welding Research Council, New York, 1957.

Tada, H., The Stress Analysis of Cracks Handbook, Paris Productions, Inc., Saint Louis, 2nd Ed.., 1985.

SEISMIC STEEL BEAM-COLUMN MOMENT CONNECTIONS

K.C. Tsai[1] and Egor P. Popov[2]

ABSTRACT

Numerous Northridge earthquake failures of steel moment resisting connections attracted world wide attention. In this paper, the research in this area in the U.S. is reviewed. Some parallel work done at the National Taiwan University which in most respects is similar to that done in the U.S. is discussed. This relates to the experiments and their interpretation on conventional and modified beam-to-column moment connections. In addition, a probability-based design approach incorporating the demand versus capacity principle and the statistical variations of material strength is discussed. Possible enhancement of such connections with special details is described. Such enhanced connection designs, incorporating capacity-enhancement and demand-reduction principles, show experimentally that adequate plastic beam rotations can be achieved.

1. INTRODUCTION

Steel moment resisting frames (MRFs) have been widely accepted as a viable system for earthquake-resistant structures. However, fractures of beam-to-column moment connections were discovered in more than 100 steel MRFs following the 1994 Northridge earthquake. None of the buildings collapsed because of the failure of steel moment connections. However, their performance has caused great concern not only about how to repair or strengthen these connections, but also about how to design and construct new MRFs. As a result, a coordinated research program has been launched in order to examine the full range of issues associated with steel MRFs (SAC 1994).

This paper attempts to assess the possible causes and solutions for these damaged connections by first reviewing the historical performance of steel beam-column moment connections observed in experimental tests. In particular, experimental results obtained from tests conducted at the University of California at Berkeley, the University of Texas at Austin and the National Taiwan University for beam-column moment connections using bolted web welded flange (BWWF) details are evaluated. The test procedures and the test specimens (including the material, sizes and the fabrication details) employed in some tests are discussed in detail. Based on these experimental results, it is observed that the rotational capacity of conventional steel BWWF beam-column moment connections is rather erratic. The flexural strength of a BWWF connection often exceeds the beam plastic moment capacity, however, it appears to be limited by the ultimate flexural strength of the beam flanges, $Z_f F_u$. Thus, in addition to the fabrication quality, the beam flange-to-entire section plastic modulus ratio, Z_f / Z, and the material yield ratio, F_y / F_u,

---

1 [1] Professor of Civil Eng., National Taiwan University, Taipei, Taiwan

[2] Professor Emeritus, Dept. of Civil Eng., University of California at Berkeley

are recognized as the important factors affecting the ductility of conventional BWWF beam-column connections. The strength demand versus capacity principle of the seismic BWWF connections is then studied. The practical implications for the seismic-resistant design of steel beam-column moment connections are assessed.

Using the strength demand versus capacity principle, the experimental results obtained from post-Northridge testing conducted both in the U.S. and at the National Taiwan University are also discussed. It is illustrated that if a large strain hardening factor is applied in estimating the connection strength demand, and well detailed flange stiffeners are used in strengthening the connection, the inelastic response of the connection can be effectively confined to a region away from the beam-column juncture. As a result, the strength and the rotational capacities of the stiffened connection are greatly enhanced. Alternatively, confined or controlled yielding of the beam can be achieved by using a reduced beam section in the proximity of a moment connection. This paper illustrates recent experimental results indicating that the rotational capacity of two BWWF connections is significantly enhanced by drilling holes in the beam flanges near the connection. Based on these test results, the paper concludes with practical recommendations for the design of steel beam-column moment connections intended to withstand severe seismic events.

2. HISTORICAL EVOLUTION AND EXPERIMENTAL EVIDENCE

It is important to look back at how the design standards in place immediately prior to the Northridge earthquake were established. In retrospect, it is surprising how limited a database led to the code established criteria. Before the BWWF details became widely used, all-welded connection details were often adopted for steel moment connections prior to 1970. The first series of tests to assess cyclic behavior were conducted at the University of California on five W18 × 50 and three W24 × 76 beam sections (Popov and Stephen 1972). The objectives of these tests were to determine their cyclic behavior and to assess the difference in the performance of these two types of connections. In this series of tests, all connections showed strength in excess of capacities determined by the elastic-perfect-plastic theory. The hysteretic loops in all cases were remarkably stable in shape under repeated loading cycles. All welded connections showed excellent ductility while the BWWF type connections also behaved well, but were less ductile (Fig. 1). At that time, sophistication regarding the required cyclic performance of members was lacking, and a rather marginal performance, by current standards, was considered acceptable. The performance of these cost-effective BWWF connection details was considered adequate by practicing structural engineers of the time. Since then, BWWF moment connections employing field web bolting and full-penetration beam flange welds had become the industry standard for constructing steel frames in seismic regions in the U.S. and many other countries in the world. It is important to note that the yield stresses for the A36 W24 × 76 beam specimens used in these tests were 36 ksi (248 MPa) and 37 ksi (255 MPa) for the flange and the web, respectively. Their tensile strengths were 62.3 and 61.3 ksi (430 and 423 MPa) for the flange and web, respectively. The yield to tensile strengths ratio, F_y / F_u, of the steel used in this series of tests is substantially lower than that found in current statistical data on shapes produced by the industry (SSPC 1994). The effects of the steel F_y / F_u ratio on the performance of moment connections will be discussed later in greater detail.

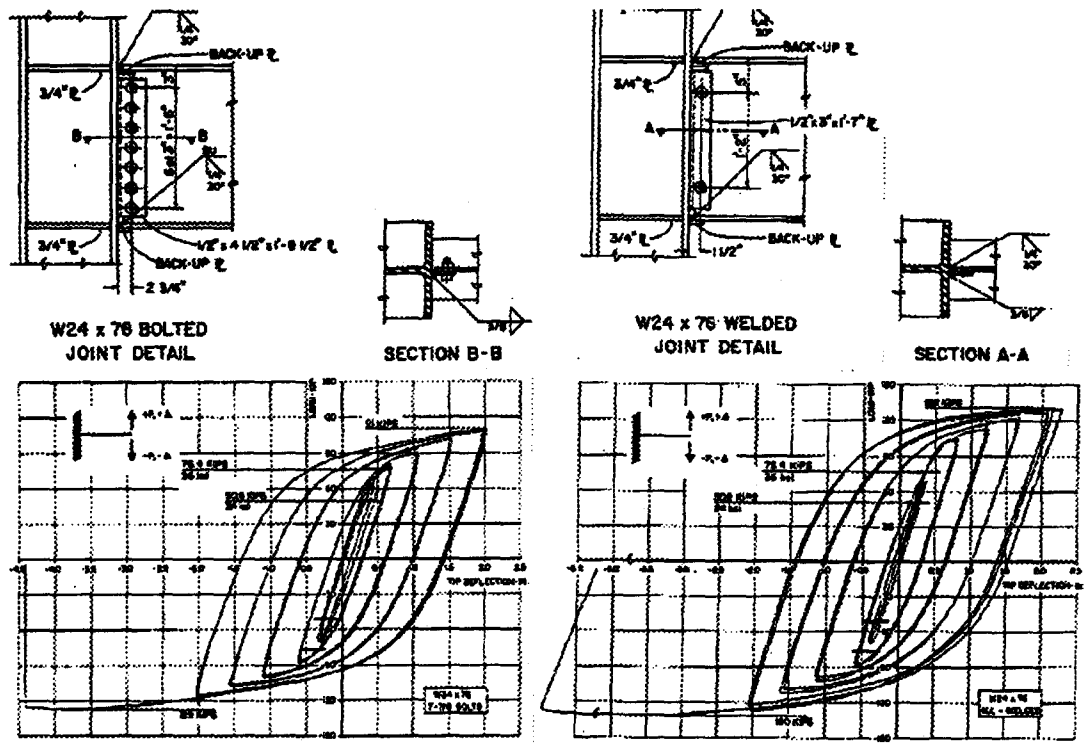

Figure 1 - Fabrication Details & Hysteresis Loops for BWWF and All-welded Connectiosn

Normally, a shear tab is shop welded to the column flange, then high tension bolts are used to attach the beam web to the shear tab before full-penetration welds are made for the beam flanges. The welding procedures used for the beam flange welds can vary from case to case. Later two experimental investigations (Krawinkler 1978, Popov *et al.* 1985) on the behavior of BWWF beam-column connections considered the effects of panel zone shear yielding. In particular, the second series of tests (Popov *et al.* 1985) employed self-shielded flux-cored arc welding (FCAW) on beam flange welds for eight large beam-column subassemblies. Each subassembly consisted of two beam specimens framing into both flanges of the column. During the tests, column specimens were placed vertically and subjected to an axial compression in order to assess its effects on the performance of panel zone joints under cyclic beam moments. The beams were A36 W18 × 40, W18 × 71 and W21 × 93 sections. The overall size of the specimens was the largest ever tested in the U.S. for this kind of study. The effects of continuity plates on the cyclic behavior of deep beam-to-column flange connections were also investigated in this series of tests. Test results indicated that continuity plates are essential to maintain the ductile behavior of beam-to-column flange connections. Test results also revealed that panel zone yielding can provide very stable energy dissipation characteristics. It should be noted that the yield stresses of the A36 beam flange plates ranged from 38 to 46.4 ksi (262 to 320 MPa).

It is primarily because of these two major studies that design requirements for supplemental web welding, panel zone joint and continuity plates were prescribed in a draft of the seismic design recommendations for steel MRFs (SEAOC 1986). Results obtained from the 1985 tests indicated that the rotational capacity of the standard BWWF connections is rather erratic. Subsequently, the so called "70-20 rule" requirements of web welding were arbitrarily established in a SEAOC code meeting. It prescribed that supplemental web welds be provided between the beam web and the shear tab for beam sections having

a beam flange plastic modulus ratio, Z_f / Z, of less than 0.7. Furthermore, a significantly reduced design moment was allowed for proportioning column panel zones (PZs) in order to induce inelastic PZ deformations. Several later versions of model seismic building codes (*Uniform* 1988, 1991 and 1994, *Specifications* 1992) retained these provisions for the construction of steel beam-to-column moment joints. In the meantime, key issues in the seismic design of beam-to-column moment connections and panel zones remained not fully resolved. While the requirements associated with the modulus ratio of 0.7 have not been found to be completely effective (Tsai and Popov 1988, Engelhardt and Husain 1993), analytical studies have shown that a weak PZ design can result in an MRF that is much more flexible than a conventional one (Tsai and Popov 1990). And, most unfavorably, the weak PZ greatly reduces the structural overstrength, an essential factor for MRFs to survive a major earthquake. Based on the behavior of the continuity plates observed in the 1985 tests, a significantly increased design load (a factor of 1.8) was codified for the design of column flange continuity plates.

Before the Northridge earthquake, additional tests were conducted at the National Taiwan University on large beam-to-box column BWWF connections. Test results indicated that the beam moment at the connection is transmitted primarily through the beam flanges (Tsai *et al.* 1992). This resulted from the rigidity of the column diaphragm plates. These test results also indicated that the flexural strength of the beam flanges, $Z_f F_u$, alone can accurately predict the ultimate moment capacities of the beam-to-box column BWWF connections. As a result, a beam section strength requirement of $Z_f F_u > 1.2 Z F_y$ for a beam connected to either a box or wide flange column using the BWWF detail was proposed, and has been adopted in the recommended provisions for the design of seismic steel MRFs (*Recommended* 1991). The factor of 1.2 in this requirement represents the effect of strain hardening. It has also been suggested (Tsai *et al.* 1995) that if this strength requirement is violated, supplemental web welds capable of carrying a bending moment of $1.2 Z F_y - Z_f F_u$ may be effective in enhancing the rotational capacity of a BWWF connection. The following paragraphs summarize the results of tests on ten beam-to-wide flange column BWWF connections (Tsai *et al.* 1995). It illustrates that a strengthened BWWF connection, employing the proposed strength requirement for the supplemental web welds, may be acceptable for steel MRFs having moderate section sizes and inelastic demand. These tests done at the National Taiwan University were similar to those done in the U.S. in most respects, and should help to interpret the behavior as well as their implications on the design of conventional BWWF beam-to-column moment connections(Tsai *et al.* 1995).

EXPERIMENTAL PROGRAM

The objectives of this study were to collect additional data on the behavior of BWWF connections and assess the effectiveness of the proposed supplemental web weld designs. All beam-column connection tests were conducted on specimens fabricated as cantilevers attached to column stubs. As shown in the experimental set-up in Fig. 2, the column was placed horizontally, and the cyclic loads were applied laterally through an actuator mounted between the reaction wall and the beam end. This set up is similar to that used in other tests (Tsai and Popov 1988, Engelhardt and Husain 1993). As summarized in Table 1, a total of ten specimens with different beam sections and web connection details were used. Beam sections W21 × 50, W21 × 62, W21 × 83 and W21 × 101 were built up from plates with Z_f / Z ratios of 0.65, 0.72, 0.74 and 0.80, respectively. All beam sections fabricated from plates were of A36 material, and all beams of the same size were made from the same sheet of plate. All beams were 2.11-m long, measured from the point of applied load to the top column flange. This results in a length-to-depth ratio of about 3.9. All column stubs were built-up W14 × 159 (H380 × 395 × 19 × 30 mm) sections of A572 Grade 50. This section was chosen to provide a relatively strong panel zone so that, except in Specimens TH1 and TH2,

limited inelastic deformations could occur in the PZ before significant flexural yielding developed in the beam sections. An 8-mm-thick double plate was welded to the column panel zone for Specimen TH1.

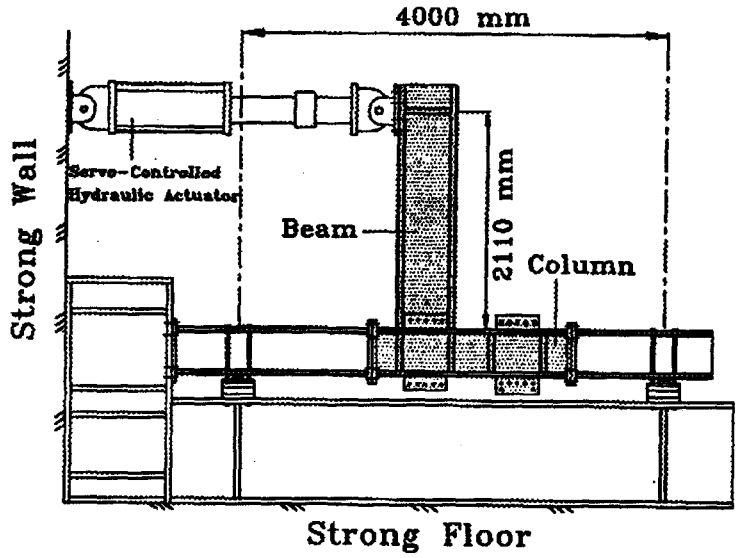

Figure 2 - Typical Experimental Setup for Steel Moment Connection Tests

Table 1 Schedule of Speciments

Specimen	Beam	Section (A36) (mm)	Z_f/Z	Web Connection (A325-X Bolt)	t_s (mm)
TH1	W21X101	(H545X315X13X20)	0.80	5-7/8"ϕ	12
TH2	W24X83	(H545X215X13X21)	0.74	5-3/4"ϕ	10
TH3	W21X62	(H535X210X10X15)	0.72	5-3/4"ϕ, slotted holes	10
TH4	W21X62	(H535X210X10X15)	0.72	5-3/4"ϕ	10
TH5	W21X62	(H535X210X10X15)	0.72	5-7/8"ϕ	12
TH6	W21X62	(H535X210X10X15)	0.72	5-3/4"ϕ + $(1.2M_p\text{-}Z_fF_u)$ Web Welding	12
TH7	W21X50	(H530X160X10X14)	0.65	5-3/4"ϕ, slotted holes	10
TH8	W21X50	(H530X160X10X14)	0.65	5-5/8"ϕ	10
TH9	W21X50	(H530X160X10X14)	0.65	7-7/8"ϕ	18
TH10	W21X50	(H530X160X10X14)	0.65	5-5/8"ϕ + $(1.2M_p\text{-}Z_fF_u)$ Web Welding	18

Connection details for all specimens are illustrated in Fig. 3. All specimens were provided with continuity plates of a thickness equal to the beam flange thickness. All continuity plates were welded to columns using partial penetration double-bevel groove welds. Web copes were torch cut and ground smooth. Complete penetration single-bevel groove welds were used to connect the beam flanges to the

column flange in all specimens. The web connection details (Table 1 and Fig. 3) included 1) bolted shear connections using standard holes (Specimens TH1, TH2, TH4 and TH8); 2) bolted shear connections using slotted holes (Specimens TH3 and TH7); 3) bolted shear connections with supplemental web welds (Specimens TH6 and TH10); and 4) bolted web with larger bolts (Specimen TH5) or supplemental web bolts (Specimen TH9). All web bolts for shear were designed for bearing using the LRFD specifications (1993). All bolts of different diameters (Table 1) were of A325-X. They all satisfied the requirements to resist a beam shear that corresponds to a bending moment of 1.2 M_p developed at the connection. For types 3 and 4 web connection details, either supplemental web welds or supplemental web bolts were designed to carry an unbalanced bending moment of $1.2\,Z\,F_y - Z_f F_u$. For Specimens TH5 and TH9, the web bolts given in Table 1 were designed for a combined shear and unbalanced moment as described. Accordingly, the shear tabs for types 3 and 4 details were designed to carry the design shear and the unbalanced moment. The thicknesses, t_s, of the shear tabs are given in column 5 of Table 1. Although the bolts were designed for bearing, all bolts were carefully tightened before making flange welds. All bolts were pretensioned, as is required for a slip critical connection (*Load* 1993), by using a calibrated torque wrench.

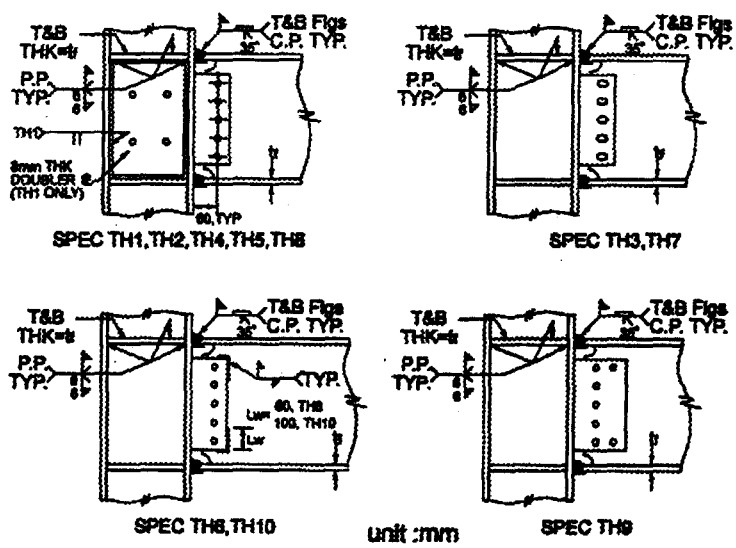

Figure 3 - Typical Connection Details for Specimens

Details of the complete penetration groove welds and the web copes are shown in Fig. 4. It should be noted that the bottom web cope is larger than the top one in order to perform bottom flange groove welds effectively. A 9 mm × 25 mm cross-section backing bar was provided for each flange groove weld. The backing bars were 100 mm wider than the beam flange width, and remained in place after the welds were completed. All flange welds were made by using Self-shielded Flux Cored Arc Welding procedures. The weld electrodes were E70T-7, 2.8 mm-diameter of NR-311 grade, made by Lincoln Electric Company. This electrode does not have rated toughness. Ultrasonic tests (UT) were conducted for all flange groove welds, and they all satisfied the code prescribed acceptance criteria for statically loaded structures (*Structural* 1992).

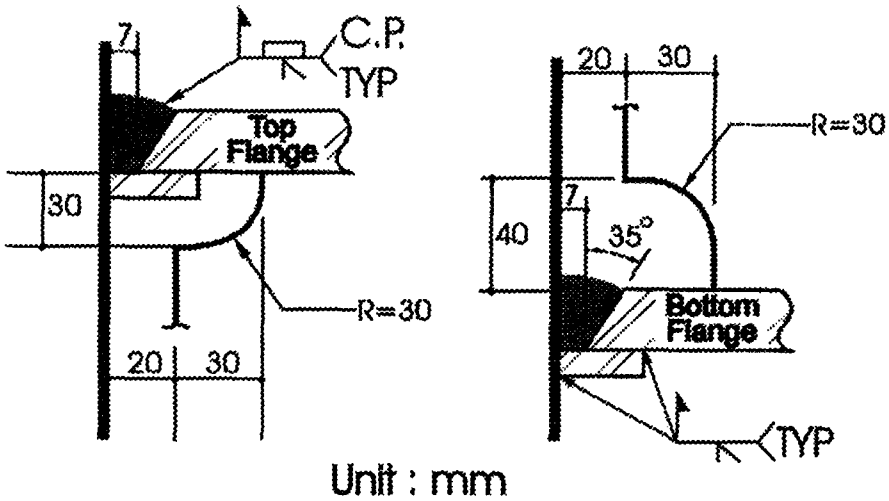

Figure 4 - Details of Beam Flange Groove Welds

EXPERIMENTAL RESULTS

All specimens were tested by imposing cyclically increasing displacements at the cantilever end. The cantilever displacement increments between each cycle were 6 mm. This is very similar to the procedures used in several earlier studies (Tsai and Popov 1988, Engelhardt and Husain 1993). All tests were conducted using a hydraulic actuator, with a pre-programmed displacement history, until failure occurred. The beam plastic rotation versus cantilever load relationships for all specimens are plotted in Fig. 5. Positive force indicates the beam bottom flange under tension. Except in Specimen TH1, where a through-column flange thickness type of fracture occurred near the beam top flange, all other fractures occurred either in the flange groove welds or in the adjacent beam flange heat affected zones.

Table 2 gives the tensile coupon strengths of the flange and the web for each specimen. Table 3 summarizes the maximum beam plastic rotations, θ_p, and maximum cantilever loads, P_u, attained before failures occurred in all specimens. In Table 3, load indices P_p and P_f are obtained by dividing the flexural strength of the entire beam section ($Z_f F_{yf} + Z_w F_{yw}$) and the beam flanges ($Z_f F_u$), respectively, by the beam length, L_b. In terms of plastic deformation, Specimen TH10 possessed the best rotational capacity (0.018 radian) and Specimen TH5 had the worst (0.009 radian). None of the specimens obtained the 0.03 radian capacity recommended by the SAC Interim Guidelines (SAC, 1995). In terms of strength, it is evident that all specimens developed the beam plastic moment capacity computed from the measured yield strength (Table 2). Column panel zone rotation versus the beam moment relationships for Specimens TH1 and TH2 have been documented (Tsai *et al.* 1995).

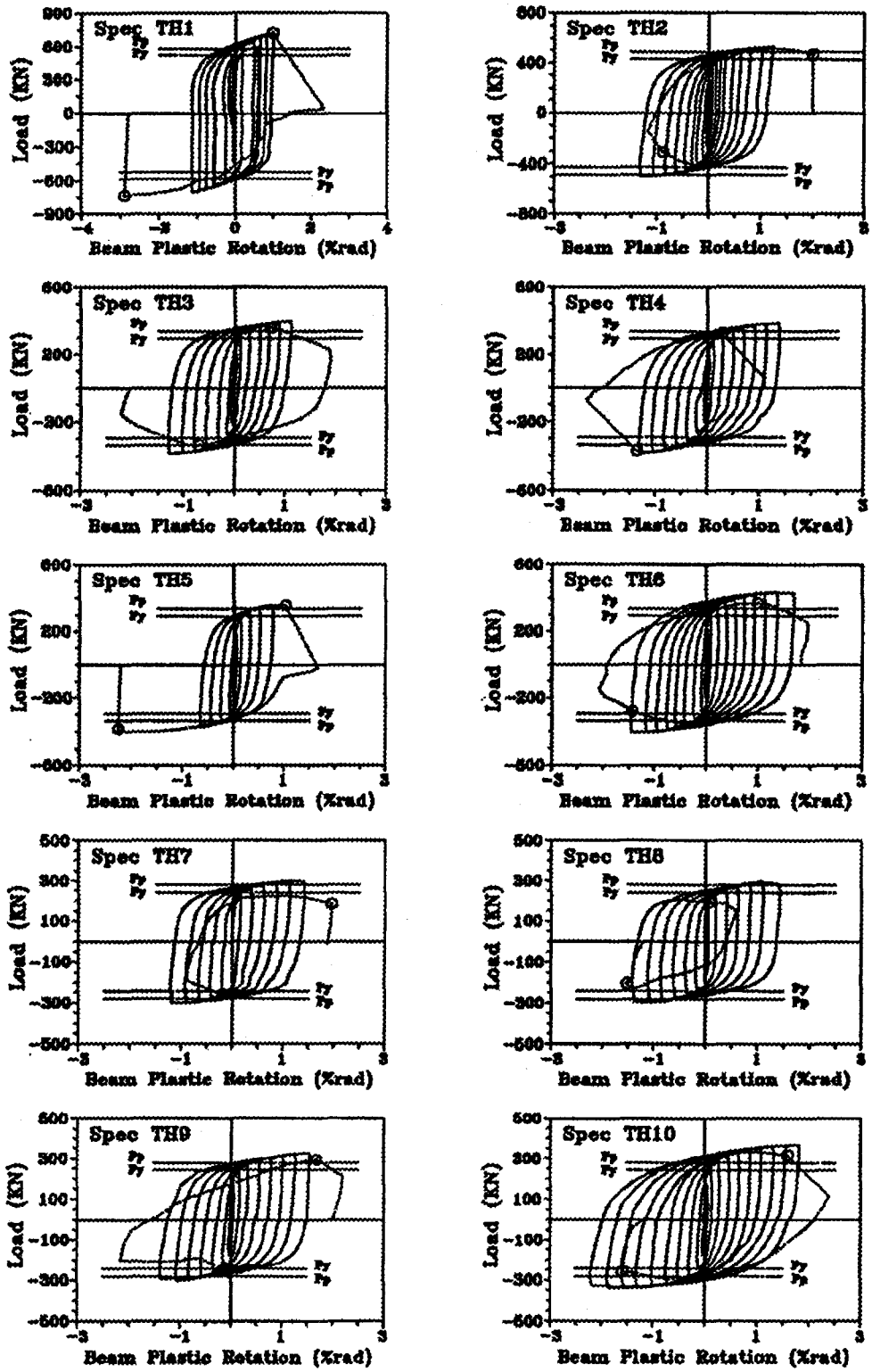

Figure 5 - Beam Plastic Rotation Versus Cantilever Load Relationships

Table 2 - Summary of Tensile Coupon Test Results for All Specimens

Section	Location	F_y (MPa)	F_u (MPa)	Elongation (%)
W21x101	Flange	296.3	478.7	29.6
	Web	295.3	481.7	28.0
W21x83	Flange	329.6	476.8	30.1
	Web	300.2	489.5	26.7
W21x62	Flange	312.0	480.7	29.0
	Web	308.0	496.4	26.1
W21x50	Flange	335.5	491.5	27.2
	Web	306.1	494.5	29.7
W14x159	Flange	420.8	593.5	26.9
	Web	390.4	538.6	26.4

DISCUSSION OF SPECIMENS' PERFORMANCE

Quality of Beam Flange Groove Welds

Difficulties in assuring good quality groove welds for beam bottom flanges often arise when the beam web bottom cope is not made big enough (Engelhardt and Husain 1993). This has commonly been identified as a contributory cause of many of the Northridge earthquake failures (SAC, 1995). Of the ten specimens tested, five specimens experienced the first flange fracture in the beam's top flange. Thus, either the quality of the groove welds for all the beam top flanges appears to be about the same as that for the bottom flanges in this series of tests or, if adequate quality welds are made other factors including material toughness, yield/tensile ratios, relative strength of beam and column materials, panel zone deformability, etc. may control the behavior. The backing bars project 50 mm beyond both sides of the flange. Runoff tabs were provided so that each pass of flange groove welds was initiated, and terminated when possible, at a point outside the flange edge. This was done to prevent poor quality welds, normally occurring at the initiation of the weld, from entering the beam flange-to-column juncture. However, several beam fractures initiated at the edges of the flange, right at the weld-beam interface, and then spread across the flange width. It appears that the quality of the flange groove welds, adjacent to the beginning and end points of each pass of these welds, may need to be viewed with suspicion. Having observed the fractured surface in Specimen TH5, it is judged that a lack of fusion not detected by the UT might have attributed to the premature fracture of the bottom flange.

Strength of Specimens

As noted above, all connections developed the beam plastic moment capacity (Table 3). In addition, it appears in Table 3 that, except for Specimens TH6 and TH10, where supplemental web welds were used, the ultimate moment capacity of the BWWF moment connections is satisfactorily predicted by the ultimate beam flange flexural strength, Z_f / F_u. The ultimate strength of connections using supplemental web bolts (Specimen TH9) is not necessarily larger than the one without them (Specimen TH7). Nevertheless, the effects of supplemental web welds on the strength of the BWWF connection is evident when comparing either Specimens TH6 with TH3 or Specimens TH10 with TH7.

Table 3 - Summary of Test Results for All Specimens

Specimen	θ_p (% rad)		P_u (KN)		P_u/P_p		P_u/P_f	
	+	-	+	-	+	-	+	-
TH1	1.14	2.89	718.8	742.4	1.24	1.28	0.96	0.99
TH2	1.24	1.29	532.4	499.4	1.09	1.03	1.00	0.94
TH3	1.12	1.28	400.7	382.2	1.20	1.14	1.07	1.02
TH4	1.38	1.29	385.4	388.8	1.15	1.16	1.03	1.04
TH5	0.92	2.25	355.9	397.6	1.06	1.19	0.95	1.07
TH6	1.68	1.44	428.8	405.9	1.28	1.21	1.15	1.09
TH7	1.42	1.19	295.1	299.1	1.05	1.07	1.07	1.08
TH8	1.33	1.27	386.9	296.5	1.02	1.06	1.04	1.07
TH9	1.56	1.38	292.4	326.8	1.04	1.16	1.06	1.18
TH10	1.82	2.21	367.0	324.7	1.31	1.16	1.33	1.18

Beam Plastic Rotational Capacity

From Table 3 and Fig. 5, it can be seen that the cyclic beam plastic rotational capacity, θ_p, of all specimens ranges between about 0.009 and 0.018 radian. Before the Northridge earthquake, this range of plastic rotational capacities was considered to be fair to satisfactory, compared with other earlier test results (Tsai and Popov 1988, Engelhardt and Husain 1993). It is worth noting that the plastic rotational capacities of the ten specimens tested did not bear an apparent relationship to the beam section modulus ratios. For example, Specimens TH2 ($Z_f / Z = 0.74$) and TH8 ($Z_f / Z = 0.65$) possessed similar plastic rotational capacities of 1.29% and 1.27%, respectively. In either the W21 × 62 (TH3-TH6) or W21 × 50

(TH7-TH10) series of beam specimens, however, it is evident that supplemental web welds have enhanced the beam plastic rotational capacities.

Beam Cumulative Deformation Capacity

The area enclosed by the hysteresis loops shown in Fig. 5 for each specimen represents the energy dissipated through the inelastic deformations of the beam and the connection. For specimens of identical deformation history, the amount of energy dissipated is directly proportional to the beam's strength. Recall that the strength of beam flanges provides a good indication of the flexural strength of the BWWF connections. Thus, the energy dissipated in each beam specimen is advantageously normalized by beam flange yield moment capacity, $Z_f F_y$:

$$\theta_{pa} = \frac{\int P L_b \, d\theta_p}{Z_f F_y} \tag{1}$$

where P and L_b are the cantilever beam load and the beam length, respectively. The resulting deformation, θ_{pa}, shown in Fig. 6 for all specimens, represents the cumulative plastic rotational capacity of the beam specimen. Recall that supplemental web welds have been used in Specimens TH6 and TH10, and premature fracture has occurred in TH5. In terms of cumulative plastic rotational capacity (Fig. 6), specimens using standard bolts (TH4 and TH8) are slightly better than those using slotted holes (TH3 and TH7); the beam specimen using supplemental web bolts (TH9) is slightly better than the one using standard web bolts (TH8). However, it should be noted that among all BWWF connection specimens, regardless of whether standard, slotted or supplemental web bolts are used, the actual variations of θ_{pa} are not very pronounced (Fig. 6). Again, in either the W21 × 62 (TH3–TH6) or W21 × 50 (TH7–TH10) series of beam specimens, it is evident that supplemental web welds have significantly enhanced the beam cumulative plastic rotational capacities. Although the cumulative rotational capacity described herein bears no direct relationship to any other analytical or experimental investigations conducted in this context, it is somewhat indicative of the cumulative ductility capacity of the BWWF connections.

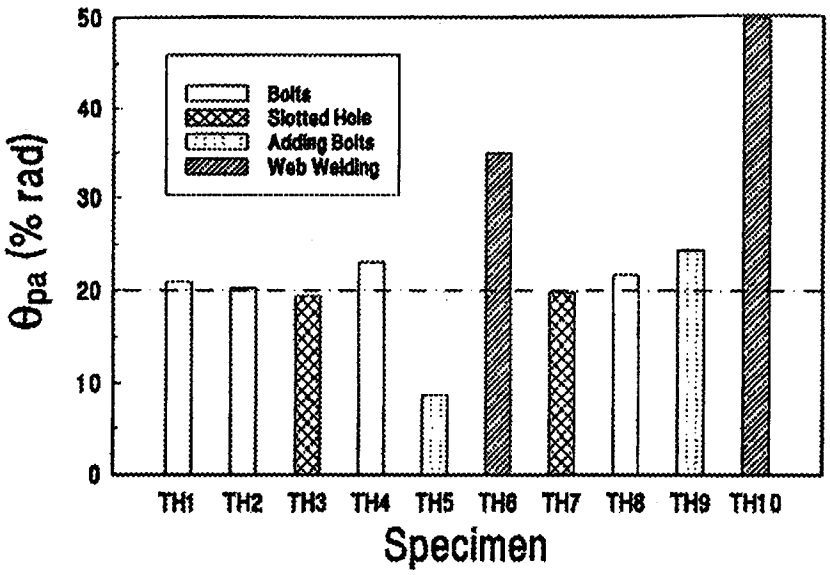

Figure 6 - Beam Cumulative Plastic Rotation Capacities

Effects of Web Connection Details

For all bolted web type moment connections using either standard or slotted holes, the difference in performance is not pronounced. The supplemental web welds, but not the supplemental web bolts, significantly enhanced the strength, ductility and energy absorbing capacity (Table 3 and Figs. 5 and 6) of the beam-column connections. The proposed design strength, $1.2\,Z F_y - Z_f F_u$, for the supplemental web welds appears to be effective in improving the performance of seismic beam-column connections. However, this measure by itself does not appear adequate to provide the plastic rotational capacity recommended by the Interim Guidelines.

SUMMARY

Historical perspectives, including some recent test results, for the BWWF connection have been discussed in detail. Recall that the ultimate beam flange flexural strength, $Z_f F_u$, accurately predicted the ultimate moment capacities of the BWWF connections. Thus, for a BWWF connection where the beam flanges are welded to the column flange using full penetration welds and the web is bolted to the shear tab to resist the design shear only, the strength criterion given as follows may be applicable for structures designed to withstand only moderate inelastic demands.

$$Z_f F_u \geq \alpha Z F_y \tag{2}$$

where α stands for the effects of strain hardening. Figure 7 illustrates the sectional modulus ratio Z_f / Z versus the strength ratio F_u / F_y relationship for various strain hardening factors, α.

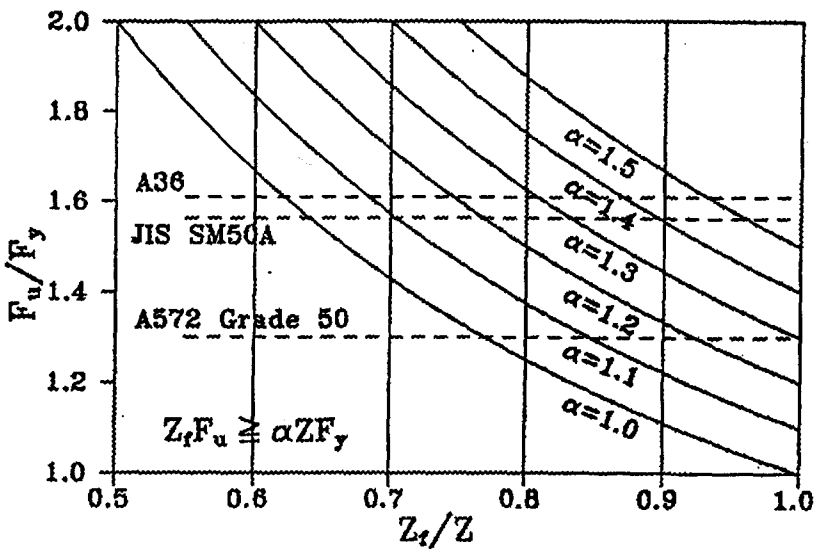

Figure 7 - Strength Ratio Versus Section Modulus Ratio Relationships for α Values

Based on $\alpha = 1.2$, $F_y = 248$ MPa and $F_u = 400$ MPa for A36 steel, it is clear that if the modulus ratio Z_f/Z is smaller than 0.74, a beam-to-column connection using the conventional BWWF details may not be able to sustain the beam flexural demand. In such a case, i.e. $Z_f F_u < \alpha Z F_y$, the beam web can be welded to the column flange or shear tab to improve connection strength and obtain moderate improvement in inelastic deformation capacity. The design strength of the welds should be at least $\alpha Z F_y - Z_f F_u$, continuously varying with the sectional modulus ratio Z_f/Z. This minimum design strength of supplemental web welds can be described in terms of the beam web plastic moment capacity $Z_w F_y$ as follows.

$$\frac{\alpha Z F_u - Z_f F_u}{Z_w F_y} = \frac{\alpha - f(F_u/F_y)}{1-f} \qquad \text{where} \quad f = Z_f/Z \qquad (3,4)$$

Figure 8 illustrates the required minimum strength of supplemental web welds as a function of Z_f/Z. From Eq. 3 or Fig. 8, it can be seen, that for an A36 steel beam section of modulus ratios Z_f/Z of 0.7 and 0.6, $1.2\,Z F_y - Z_f F_u$ should be $0.24\,Z_w F_y$ and $0.58\,Z_w F_y$, respectively. Thus, it appears that the code prescribed design strength (*Uniform* 1994, *Specifications* 1992) of $0.2\,Z_w F_y$ for the supplemental web weld is inadequate for beam sections having a Z_f/Z ratio less than 0.7. The differences in the two requirements are more pronounced for beam sections of high strength steel where the strength ratio F_u/F_y is substantially lower than that for A36.

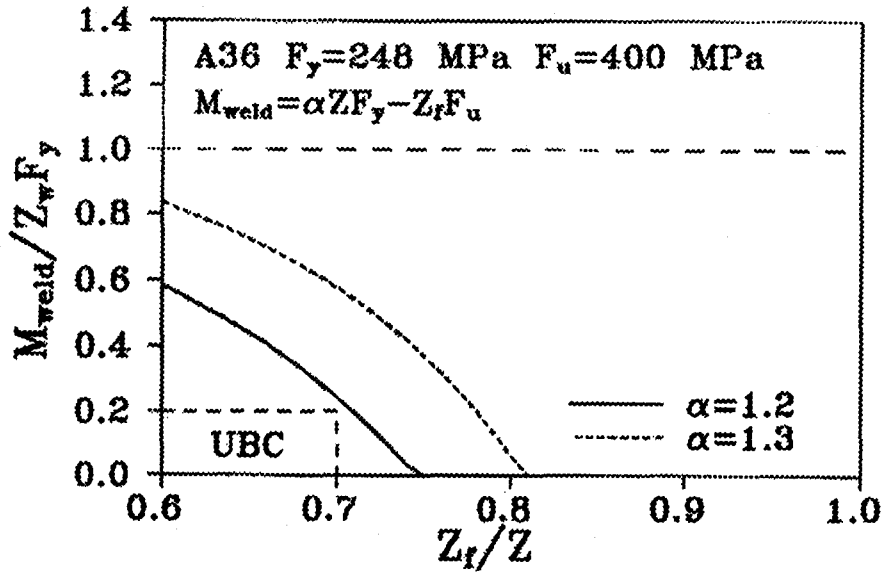

Figure 8 - Supplemental Web Weld Strength Values Versus Sectional Modulus Relationships

3. STRENGTH DEMAND VS. CAPACITY PRINCIPLE

STRENGTH CAPACITY

It is noted in Table 3 that, except for Specimens TH6 and TH10, where supplemental web welds were used, the ultimate moment capacity of the BWWF moment connections can be satisfactorily predicted by the ultimate beam flange flexural strength, $Z_f F_u$. In addition, all connections developed a bending moment substantially greater than the beam plastic moment capacity (Table 3). In order to gain insight into the key parameters affecting the flexural demand imposed on the steel moment connection, an analytical model was constructed for cantilever beams (Tsai and Liu 1992).

STRENGTH DEMAND

The relationship between the strength demand at the beam-column connection and the beam plastic rotation was studied (Tsai and Liu 1992) using cantilever beams subjected to a concentrated load monotonically applied at the beam end as shown in Fig. 9. It is assumed that the beam plane section remains plane under the bending, and the beam flange and web possess identical tensile or compressive stress-strain characteristics. It is also assumed that the variation of bending stress across the flange thickness can be ignored, and the beam shear does not affect the yield moment capacity of the beam. Based on a tri-linear stress-strain material model for steel as shown in Fig. 10, it has been found that the relationship between the fixed end moment, M_J, and the beam plastic rotation, θ_p, can be simplified as:

$$a = \frac{M_J}{M_p} = \frac{3}{2}(1 - uv) + \frac{1}{3}v(2+f) + \frac{Ev(2+f)}{2F_y r}\theta_p \tag{5}$$

where $u = \epsilon_{st} / \epsilon_y$, $v = E_{st} / E$, $f = Z_f / Z$, $r = L / (d - 2\,t_f)$, L, d, and t_f are the length, the beam depth and the flange thickness, respectively. Plastic rotation θ_p is defined by dividing the plastic cantilever displacement by the beam length.

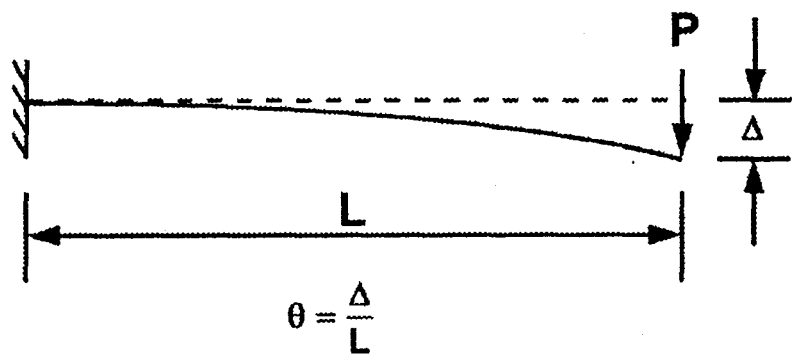

Figure 9 - Cantilever Model for Study of Moment - Rotation Relationships for Beam

In Eq. 5, a stands for the effects of strain hardening and Z is the plastic modulus of the beam section. $M_p = Z\,F_y$ and the meaning of F_y, ϵ_y, ϵ_{st}, E and E_{st} are shown in Fig. 10. Based on Eq. 5, the relationships between the beam total rotation and the fixed end moment amplification factor, M_J / M_p, for two W27 × 114 beams 3.81-meters long, are illustrated in Fig. 11. The material properties used to construct Fig. 11 are listed in Table 4 (Salmon and Johnson 1990). Since a plastic rotational capacity on the order 0.015 radian was considered as a minimum for a typical beam-column connection in MRFs with strong beam-column panel zones (Tsai and Popov 1988), a θ_p of 0.015 radian for Eq. 5 was chosen for evaluating the strength demand on the beam-column connection. Results of extensive parametric studies (Fig. 12) indicate that the moment amplification factor a in Eq. 5 ranges from 1.05 to 1.28 for a rotational demand of $\theta_p = 0.015$. It is much more sensitive to the beam length-to-depth ratio r and the critical strain ratio u than to the modulus ratios f and v. The material properties used to construct Fig. 12 are listed in Table 4. It appears that, with other parameters unchanged, the smaller the beam length-to-depth ratio, the larger the flexural strength demand will result at the support. Note that the moment amplification factor indicated in Eq. 5 is formulated for a perfectly fixed cantilever beam under monotonically applied loads. It is believed that the growth of the fixed end moment due to the material strain hardening is deformation-path dependent. In general, it can be accelerated under the cyclically applied loads. It is illustrated in Fig. 13 that a critical strain ratio u of 3 and a material modulus ratio v of 0.031 have to be adopted for Eq. 5 in order to predict the trend of the cyclic strain hardening effects. Therefore, it is evident that the cyclically applied load may rapidly build-up the flexural demand imposed on the beam-column moment connection as the critical strain ratio u has been reduced (Fig. 13).

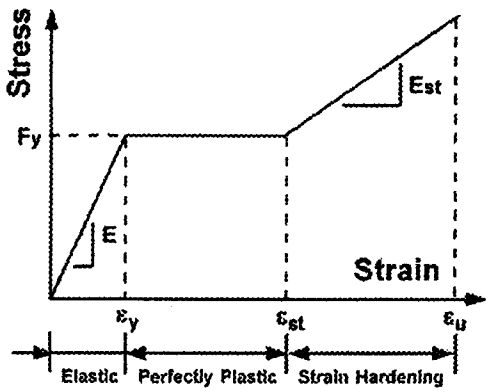

Figure 10 - Tri-linear Stress Strain Relationship for Steel

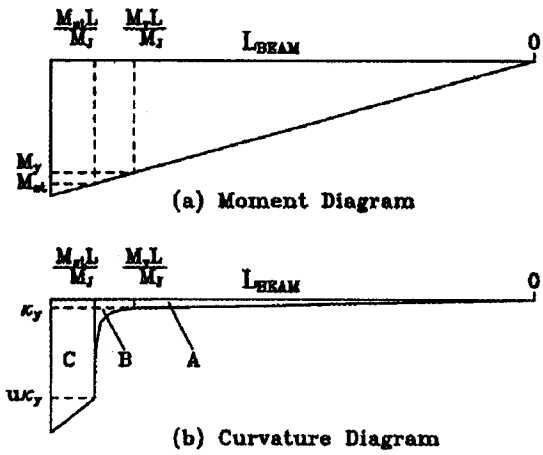

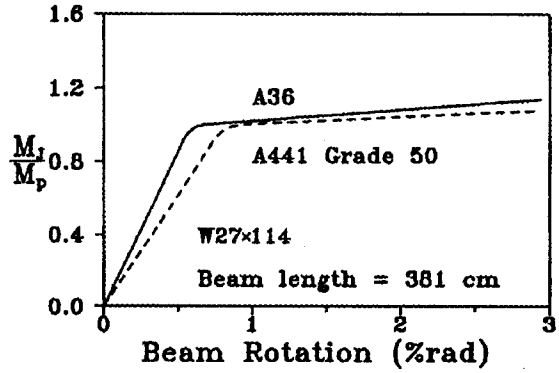

Figure 11 - Fixed End Moment versus Plastic Beam Rotation Relationships for Two Beams

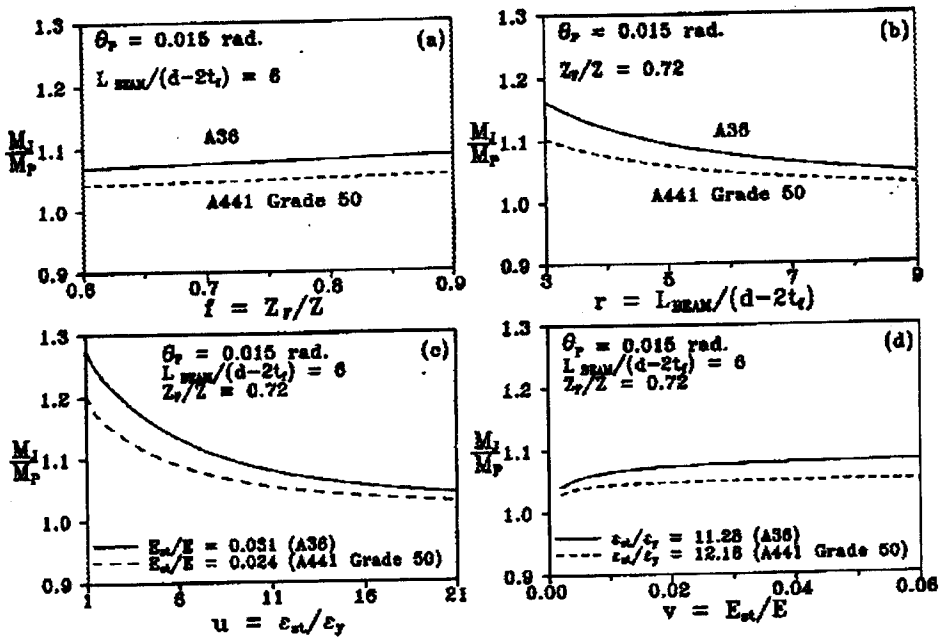

Figure 12 - Effects of Various Parameters on Amplification of Fixed End Plastic Moment

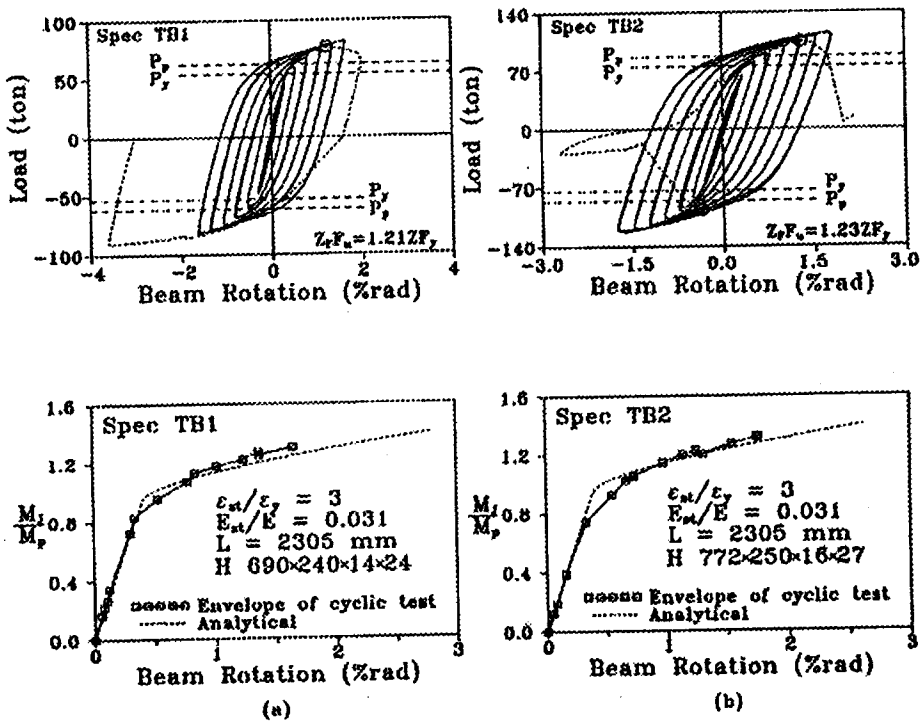

Figure 13 - Cyclic Response of Two BWWF Connections and the Predicted Skeleton Curves

Table 4 - Typical Mechanical Properties of Two Steel Grades

Material Type	F_y (t/cm^2)	F_u (t/cm^2)	ε_{st}	E_{st} (t/cm^2)	E (t/cm^2)	G (t/cm^2)
A36	2.53	4.08	0.014	63.3	2039	787
A441 Gr. 50	3.52	4.92	0.021	49.2		

LRFD IMPLICATIONS

As noted previously, the flexural capacity of the BWWF moment connection is limited by the beam flange flexural strength, while the flexural demand imposed on the seismic moment connection is often greater than the beam plastic moment capacity. The strength criterion, $Z_f F_u \geq a\, Z\, F_y$, must be met in order to sustain the beam bending moment as inelastic beam rotation develops. Therefore, the design strength of the connection is $R = Z_f F_u$ and the generalized load effect is $Q = a\, Z\, F_y$. In order to achieve specific probability of safety in the connection, the variations between the actual strength and the nominal strength must be taken into account. It follows that a probabilistic model (Ang and Tang 1984) is:

$$\mu_R \geq \varphi \mu_Q \; ; \quad \text{or} \quad Z_f\, \mu_{F_u} \geq \varphi\, a\, Z\, \mu_{F_y} \tag{6,7}$$

$$\varphi = \frac{(1-\beta^2 \rho_{RQ} \delta_R \delta_Q) + \sqrt{(1-\beta^2 \rho_{RQ} \delta_R \delta_Q)^2 - (1-\beta^2 \delta_R^2)(1-\beta^2 \delta_Q^2)}}{1-\beta^2 \delta_R^2} \tag{8}$$

where μ, δ, ρ and β are mean value, coefficient of variation (COV), correlation coefficient and safety index, respectively. Note that if the variations of the beam sectional properties are negligible, then only the variations of F_y and F_u, for the load and the resistance, respectively, needs to be considered. The resulting load and resistance factor design (LRFD) criterion for the strength limit state of seismic steel BWWF moment connections is therefore:

$$Z_f\, (F_u)_n \geq \alpha\, Z\, (F_y)_n \tag{9}$$

$$\alpha = \varphi \frac{V_y}{V_u} a \quad \text{and} \quad V_u = \mu_{F_u} / (F_u)_n \; ; \quad V_y = \mu_{F_y} / (F_y)_n \tag{10,11,12}$$

where $(F_y)_n$ and $(F_u)_n$ are nominal tensile yield strength and nominal ultimate tensile strength, respectively. Figure 14 illustrates the effects of each variable on the design coefficient α in Eq. 9, while the remaining variables are kept constant as shown in the corresponding figures. Note that the design coefficient α is almost linearly proportional to the safety index as shown in Fig 14(a). Figures 14(b), 14(c) and 14(d) correspond to a safety index of 3. It is apparent that a positive correlation between F_y and F_u will require a smaller factor for the design load (Fig. 14(b)). The larger the variation of material strength, the larger the load factor that must be used for the design (Figs. 14(c) and 14(d)). If a safety index $\beta = 1.75$ for seismic design (*Load* 1993) and statistical data for A36 steel given in Table 5 are adopted, a design coefficient α =

1.23 can be obtained. Note that it is based on $Z_f / Z = 0.85$, $L/d = 5$ and material properties given in Table 4 in computing the moment amplification from Eq. 5. A correlation coefficient, $\rho_{F_U F_Y}$, of 0.0 is also assumed.

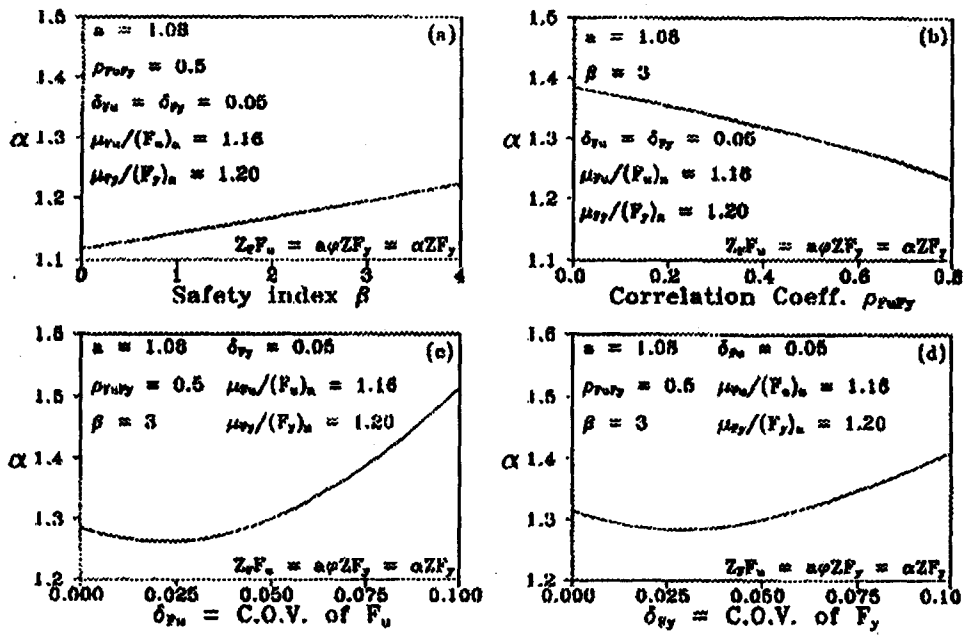

Figure 14 - Effects of Various Statistical Parameters on Design Coefficient α Values

Table 5 - Typical Statistical Data or Material Properties

Material Type	$\mu_{Fu}/(F_u)_n$	$\mu_{Fy}/(F_y)_n$	μ_{Fu}/μ_{Fy}	δ_{Fu}	δ_{Fy}
A36, SS41	1.173	1.186	1.594	0.025	0.055
A572, Gr. 50	1.222	1.124	1.405	0.025	0.050
JIS SM50A	1.121	1.1263	1.388	0.024	0.050

Applying Eq. 8, the limitations on the variation of the material strength (COV of F_u and F_y) can be investigated for given sets of design load factor φ, safety index β and correlation coefficient ρ. Comparing Figs. 15(a) and 15(c), or Figs. 15(b) and 15(d), it is shown that the larger the design load factor φ adopted, the larger the variations of material strength that can be accommodated for a specific safety index. Again, comparing Figs. 15(a) and 15(b), 15(c) and 15(d), it is shown that a positive correlation between F_u and F_y will reduce the demand imposed on the design load factor for given degrees of variations on the material strength.

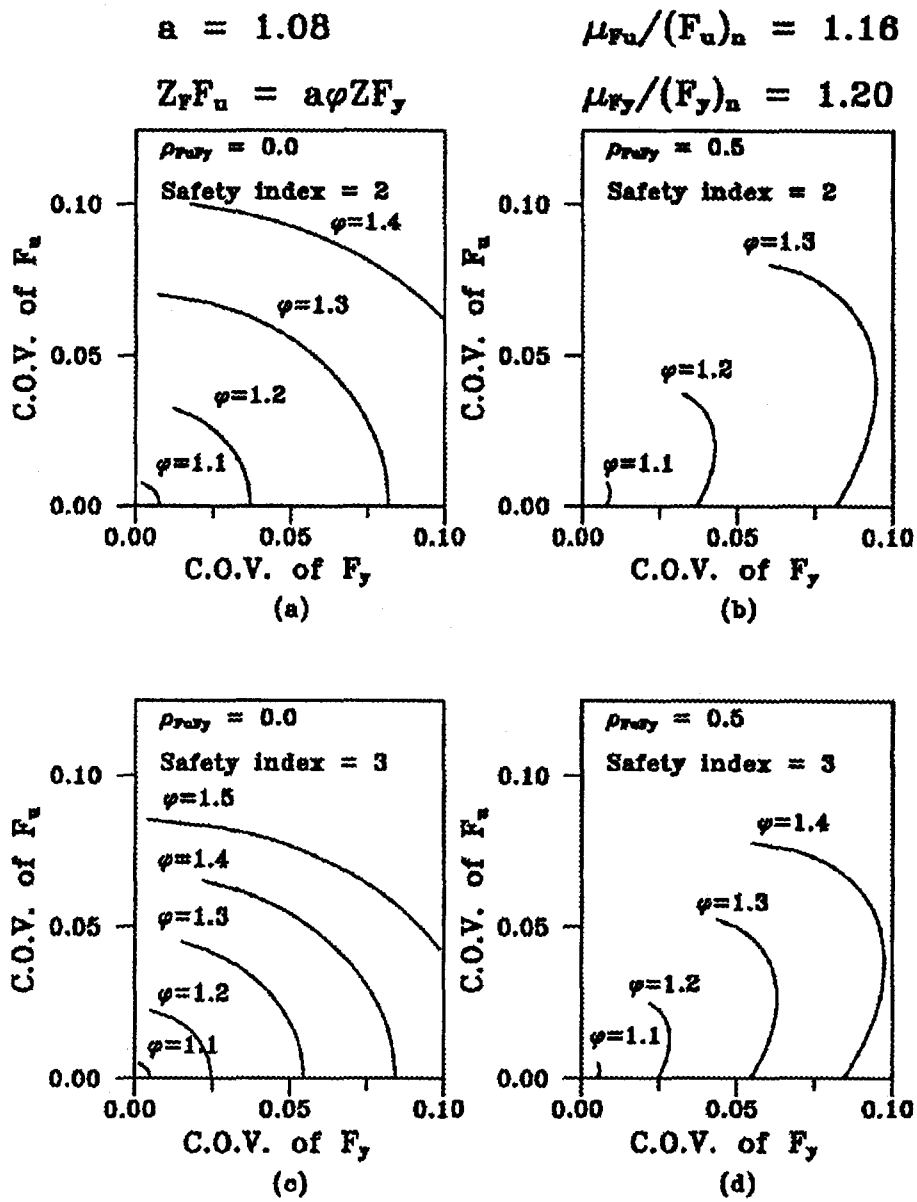

Figure 15 - Strength Variation Limitations for Specific Design Load Factors and Safety Indices

Note that the yield strength F_y affects the moment amplification factor defined in Eq. 5. Therefore, the derivations of the design criterion given in Figs. 9 and 10 are not strictly correct. However, Figs. 14 and 15 somewhat indicate the effects of material strength variation on the design load factor and the safety index. In addition, it is important to note that if the weld strength or the column flange through-thickness strength is weaker than the beam flange ultimate strength, then the statistics of the weaker one should be considered in Eqs. 8, 10 and 11. In addition, the full penetration flange welds are highly stressed under the beam moment. Therefore, the high quality of the full penetration welds in attaching the beam flange to the

column flange is essential to obtain successful earthquake-resistant beam-to-column connections (SAC 1995).

4. POSSIBLE CAUSES OF AND SOLUTIONS TO CONNECTION FAILURES

As noted above, the maximum beam moment that possibly can develop in the beam connected to a column depends on a great number of parameters. The experimental results and some important parameters discussed previously should help to better interpret the behavior, and their implications on the design, of steel moment connections. However, these parameters may be very difficult to explicitly evaluate in the practice of connection design. In addition, the maximum moment that can be developed in the beam may be limited by the shear strength of the panel zone joint or the bending strength of the column. Nevertheless, there are indications that flange connections fractured in cases where the beam stress level is clearly below yielding but the panel zone joint yielded in shear. Many of the connection failure modes observed in the Northridge earthquake (SAC 1995) were not frequently observed in experimental studies. Researchers generally attribute connection failures to welding-material- and design-related causes. Now, after more than two and half years of many experimental and analytical studies since the Northridge earthquake occurred, it has become very clear that the problem is not a simple one, and no single factor can be made fully responsible for the connection failures. Research and professional developments on many aspects of the problem are in progress and have already led to many conclusions that can be implemented on an interim basis. Many papers discussing possible sources of problems and solutions to the connection failures have been published (Krawinkler 1995, Popov 1995, Chen and Yamaguchi 1996). The SAC joint venture has completed the first phase of an extensive program directed towards the development of guidelines and solutions to the problem. SAC has already published several design advisories and an Interim Guidelines (SAC 1995). In the following discussion advantage is taken of the knowledge generated in the aforementioned efforts. Some possible causes of the connection failures are discuss below, and more detailed enumeration can be found in the references (SAC 1995, Krawinkler 1995).

POSSIBLE CAUSES OF CONNECTION FAILURES

(1) A recent statistical survey (SSPC 1994) indicates that the mean yield strength of A36 steel in the U.S. is about 35% higher than the nominal yield value while the mean tensile strength of the flange material is about 1.9 times the nominal yield strength. Applying this increase in yield stress and the cyclic hardening factor, the maximum beam moment may be significantly higher than its nominal strength. Considering large variations in the material strength, it is extremely questionable whether the conventional BWWF connection can reliably sustain the beam flexural demand imposed by the Northridge earthquake.

(2) Rolled structural shapes or plates are not isotropic. The most ductile characteristic of steel is exhibited in the direction of rolling, the least in the direction orthogonal to the thin element (through-thickness properties). The thicker the column flange, the greater potential for the through thickness properties to become more inferior. Some experiments at the University of California at Berkeley showed that even for laterally unstrained steel, the ductility in the through thickness direction was only half as large as that in the direction of rolling (Adams and Popov, 1976). Considering that the mean tensile strength (obtained in the rolling direction) of A572 steel, which is most commonly used for columns, is only

about 10% higher than the mean tensile strength of A36 steel, there are possibilities of fractures on the column side of welds even without the presence of stress concentrations.

(3) Restraining steel by welding or by preventing free expansion or contraction of the material can cause brittle behavior under stress. In the case of the most common BWWF connections, the weld itself is highly restrained through the length and in the transverse direction. This makes the connection extremely rigid and precludes yielding. As a result, any fracture that would occur would be expected to be brittle, even though the steel and the weld metal are ductile.

(4) In a large number of connections, the backing bar below the beam bottom flange has been removed and the welds back-gouged and repaired wherever defects were noted. UT inspection for welds behind the backing bar and particularly behind the beam web is not entirely reliable. Many of the detects found in connections were of a size that should have been rejected per AWS D1.1 if they could have been detected during the construction. The inclusions were particularly large in the middle of the flange width. This is the place where the weld has to be interrupted because of the presence of the beam web. Slag inclusions are equivalent to initial cracks, which are prone to crack propagation at lower stress level and may result in fracture. It is important to keep in mind that the distribution of bending stress across the width of the beam flange connection is not uniform and it is higher in the center.

(5) The relative strength of beams, columns and the panel zone at a joint have a significant effect on the distribution of inelastic deformations. If the beams are the weak elements, inelastic deformations will be concentrated in plastic hinge regions of the beams and flange connection welds must be able to transfer very high forces to the joint. If the columns are the weak elements, high vertical strains are likely to exist on the column side of the connection, which may initiate horizontal cracking across the column flange. If the panel zone is the weak element, it will yield in shear before the beams or columns attain their bending strength. Although panel zone yielding itself can be a stable energy dissipation mechanism as noted earlier, excessive shear yielding may not be desirable as it may lead to local kinking at the four corners of a panel zone joint (Krawinkler 1978). Local kinking may result in high strains and curvatures at these locations where beam flanges are connected by welding, and lead to cracking at the welds.

(6) The effects of the concrete slab are usually ignored in the design of steel MRFs. Under a positive bending moment, the top of the slab will be subjected to compression and the neutral axis will be raised. Recent test results (Hajjar and Leon 1996) indicate that the strains in the bottom flange are significantly larger than those near the top flange. This may partially explain the predominance of bottom flange failures observed in the Northridge earthquake

POSSIBLE SOLUTIONS

As a result of the far reaching concerns raised by the Northridge damage, the American Institute of Steel Construction (AISC) initiated a short-term intensive testing program to provide guidelines for improving connection details in as short a time as possible. Researchers at the University of Texas at Austin conducted experiments on single cantilever-type specimens using nine different connection designs (Engelhardt and Sabol 1994). Since then, many additional experiments have been performed on beam-column subassemblies with various connection configurations. In many cases large size specimens were used, with beams as large as W36 × 245 and columns as large as W14 × 455. The SAC Interim Guidelines

(1995) contains the important experimental results as well as their implications for the repair, modification and design of welded steel moment frame structures. The general consensus is that the presently used BWWF moment connection can not provide adequate inelastic rotational capacity with sufficient reliability. Many alternative have been proposed and several have been tested and found effective to sustain a large cyclic plastic rotational demand greater than 0.03 radian.

The SAC interim guidelines give detailed recommendations on many issues related to welding. Proper welding and weld inspection is a necessary but not sufficient condition for adequate performance of welded connections to sustain larger inelastic deformations. The general concept of these alternatives is to move the plastic hinge region into the beam and away from the connection; and to control the stress level at the beam flange welds. The minimum strength requirement for the connection can be computed by considering the maximum bending moment capacity at the plastic hinge location using statics. It was previously stated that the maximum bending capacity of the beam section can be significantly higher than its nominal strength due to the material overstrength and cyclic hardening. A factor of 1.7 for this value has been adopted to estimate the beam maximum bending capacity.

The alternatives which have been widely advocated include: cover plated connections, bottom haunch connections, connections with vertical ribs and connections with a reduced beam section. Many experimental tests have been conducted with cover plated connections. The most widely used configuration employs a wide rectangular cover plate for the bottom beam flange while using a tapered one for the top beam flange (Engelhardt and Sabol 1994). Another alternative is the spliced beam connection where either splice plates are welded to the column flange or T-sections are bolted to the column flange, and forces are transferred from the beam flange to the plates by means of high strength bolts in slotted holes. A bronze shim in the shear transfer plane provides for a controlled friction force. This connection limits the amount of force that can be transferred to the column and acts like a rotational friction damper for moment connections (Yang and Popov 1995). Another alternative is the use of side-plated connection in which the beam flange forces are transferred through welds first to horizontal plates then to vertical side plates outside the column flanges, and back into the column through horizontal stiffeners welded to the column flanges and web (Uang and Latham 1995). All of these alternatives have their advantages and disadvantages. But there is enough evidence to testify that steel moment connections which perform much better than the conventional BWWF connections can be built. Applying the demand versus capacity principle described previously, most of these alternatives can be conveniently divided into two categories: the capacity-enhancement scheme and the demand-reduction scheme.

The following discussions give additional examples for the design and construction of ductility-enhanced steel moment connections by applying these two schemes. These experimental tests were conducted at the National Taiwan University during the past two years in order to find additional data toward the construction of steel MRF structures with reliable seismic performance characteristics.

5. CAPACITY-ENHANCEMENT AND DEMAND-REDUCTION

Judging from the actual range of the modulus ratios Z_f / Z of standard AISC sections (Fig. 16) and that required to sustain a larger load factor α (Fig. 7), it is apparent that most of the AISC sections may not be able to pass the strength criterion proposed in Eq. 9. Since it is difficult to immediately change the material properties of the steel currently available in the market, possible solutions to enhance the beam rotational capacities include: 1) increase the strength capacity by increasing the effective flange modulus Z_f

at the connection, or 2) reduce the strength demand by decreasing the effective section modulus Z in the proximity of the connection. Both schemes must effectively reduce the stress in or near the flange welds in order to allow the development of large beam plastic rotations.

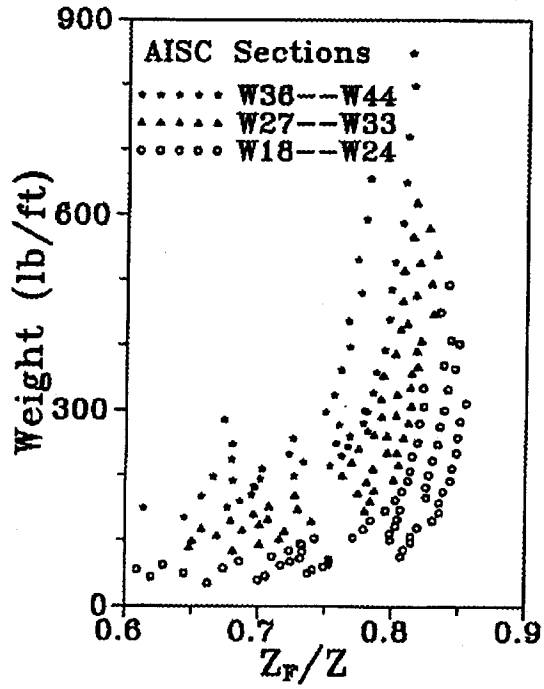

Figure 16 - Distribution of Modulues Z_f/Z for Standard AISC Wide Flange Sections

The strengthening schemes can be accomplished by adding flange ribs, or cover plates, and/or fully welding the beam web as described previously. The weakening of the beam section can be achieved by shaving the beam flanges (Plumier 1990, Chen and Yeh 1994, Popov 1996) or drilling holes in the beam flanges (Yang and Popov 1995). In order to collect additional data for the two aforementioned schemes, twenty-four (twelve W21 × 62 and twelve W27 × 94) additional modified BWWF moment connections have been tested at the National Taiwan University (Tsai and Chen 1996, Tsai and Lin 1996). The welding details and the procedures for all beam flange full penetration welds are the same as those previously described for Specimens TH1 through TH10. This paper discusses the test results for the four specimens.

CAPACITY-ENHANCEMENT

Figures 17 and 18 give the fabrication details of two W21 × 62 beam-to-column connections where a widened beam flange (Specimen WB1) and fully-welded beam web (NB2) details are used, respectively. It should be noted that a thickened shear tab (25 mm as opposed to 15 mm for WB1) has been provided for NB2 to develop the design shear and a bending moment equal to the beam web plastic moment capacity Z_w F_y. Figure 19 indicates that widened beam flanges have effectively enhanced the rotational capacity of the BWWF connection before flange local buckling occurred at the starting end of the widened flange. Figure 20 shows that the welded beam web-to-thickened shear tab scheme effectively delayed the beam flange

fracture until a large beam plastic rotation developed. The design methodologies used for the two stiffened specimens are illustrated in Fig. 21. It is found from using the tensile coupon strength (F_y = 317 and F_u = 487 MPa) that α values greater than 1.4 can be sustained for both Specimens WB1 and NB2. For cases where column flange through-thickness strength is weak, or variations of the steel beam strength are too large, a specifically selected steel plate of low strength or variation may be considered for the widened flanges. In this manner, a confined yielding of the beam in the proximity of the connection can be assured.

DEMAND-REDUCTION

Experimental evidence has indicated that the rotational capacity of steel moment connections can be effectively enhanced by reducing the beam flange width in the proximity of the connection (Plumier 1990, Popov 1996). In addition, controlled beam flexural yielding can be better achieved if the moment gradient imposed on the beam is considered in reducing the beam strength (Chen and Yeh 1994). Similar effects can be achieved by drilling holes in the beam flanges, thereby yielding the beam in the connection proximity before a large flexural demand builds-up at the beam-column juncture. This may be particularly useful in cases where drilling is more favorable than flame cutting in an existing building. Nonlinear finite element analyses have confirmed that the stress concentrations near each hole are reduced due to the presence of the adjacent holes (Tsai and Chen 1996, Zekioglu *et al.* 1995).

Figures 22 and 23 give the fabrication details of two A36 W27 × 94 beam Specimens HB1 and HB2, respectively, in which holes are drilled in the top and bottom beam flanges near the connection. It is evident in Figs. 24 and 25 that rotational capacities of these two BWWF connections were greatly enhanced before beam flange cracks initiated near the web copes. Under increasing cyclic loads, the inelastic hinges developed in the region where the beam cross sectional area has been reduced by the presence of the flange holes. In addition, no fracture or crack occurred across the flange holes.

Figure 26 shows the design basis for the holes drilled in the beam flanges. The design review indicates that the remaining plastic moment capacities across the flange holes have been reduced to 82% and 78% of the critical moments (M_A or M_B) for Specimens HB1 and HB2, respectively. Considering the actual material strength, it can be found that the strain hardening factors, α, of 1.32 and 1.38 can be accommodated in the prefabricated hinges for Specimens HB1 and HB2, respectively. Figures 24 and 25 reveal that the beam specimens have first been yielded at a moment smaller than the yield moment M_y as expected. However, the ultimate moment capacities developed at both connections are still greater than the beam plastic moment capacity. Analyses performed on both the finite element model and the simplified model using an equivalent moment of inertia for the hole-drilled section have indicated that the percentage loss of elastic beam rotational stiffness is no more than 7% for these two cases.

It is confirmed in the tests that ductile behavior of high strength steel beam-to-column moment connections can be further assured if both the capacity-enhancement and the demand-reduction schemes are applied simultaneously (Tsai and Lin 1996). Connection details employing reduced beam flange width scheme of flange holes of varying diameters in conjunction with flange ribs at the connection have been extensively studied for the design of a medical center (Zekioglu *et al.* 1995). Nonlinear finite element analyses have confirmed that the flexural stress at the beam-column juncture can be effectively reduced by properly detailed flange holes and beam flange ribs as significant cantilever deformations develop.

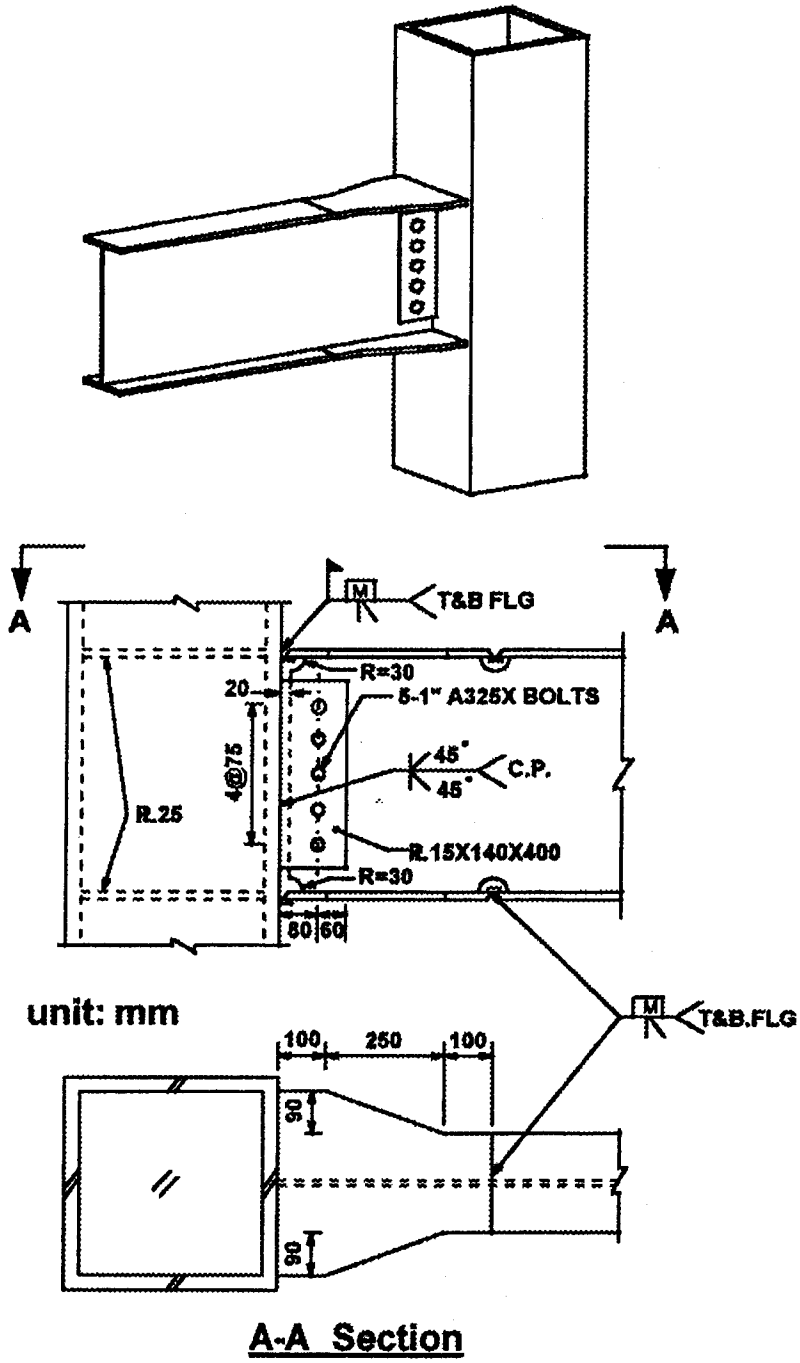

Specimen WB1

Figure 17 - Fabrication Details of Specimen WB1

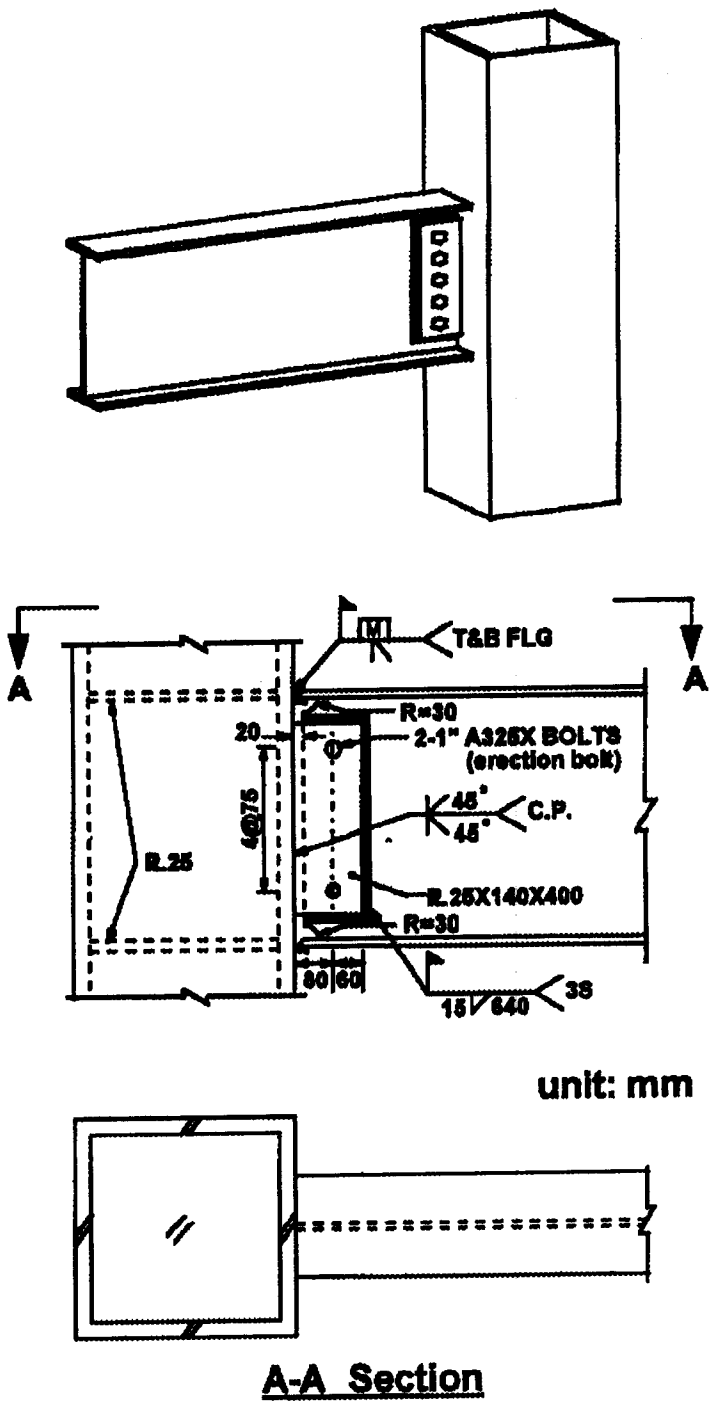

Specimen NB2

Figure 18 - Fabrication Details of Specimen NB2

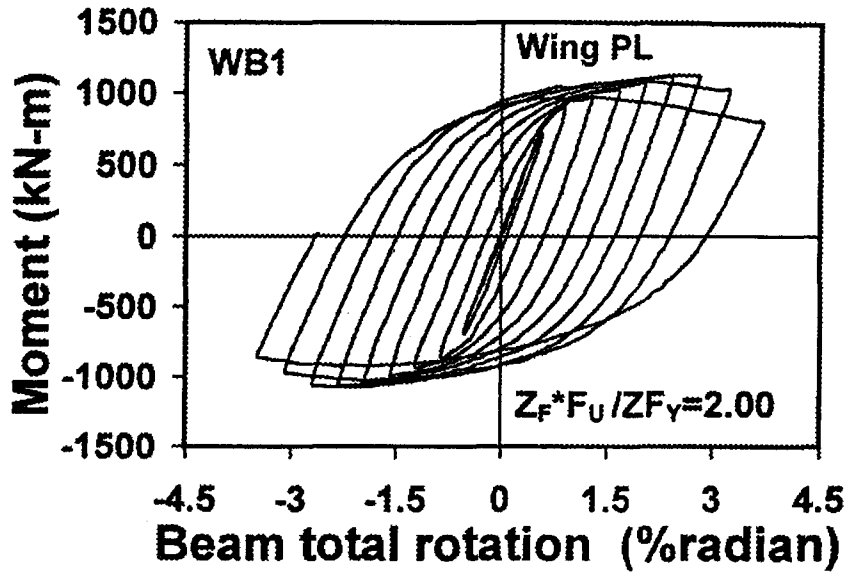

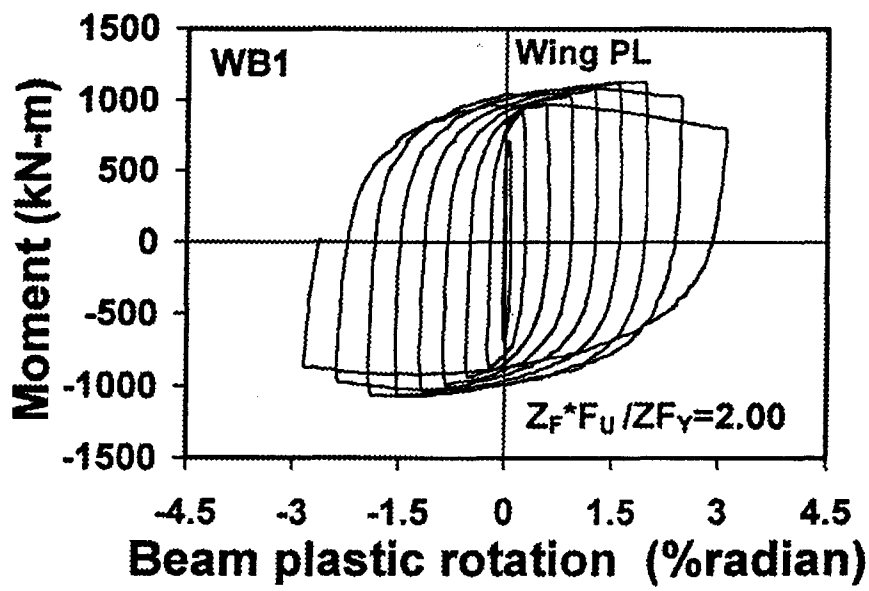

Figure 19 - Moment Versus Beam Rotation Relationships for Specimen WB1

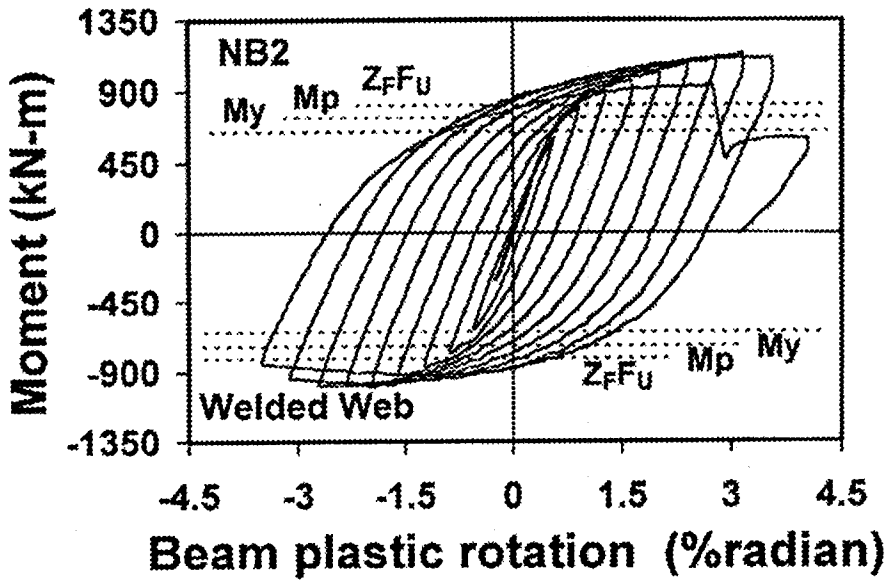

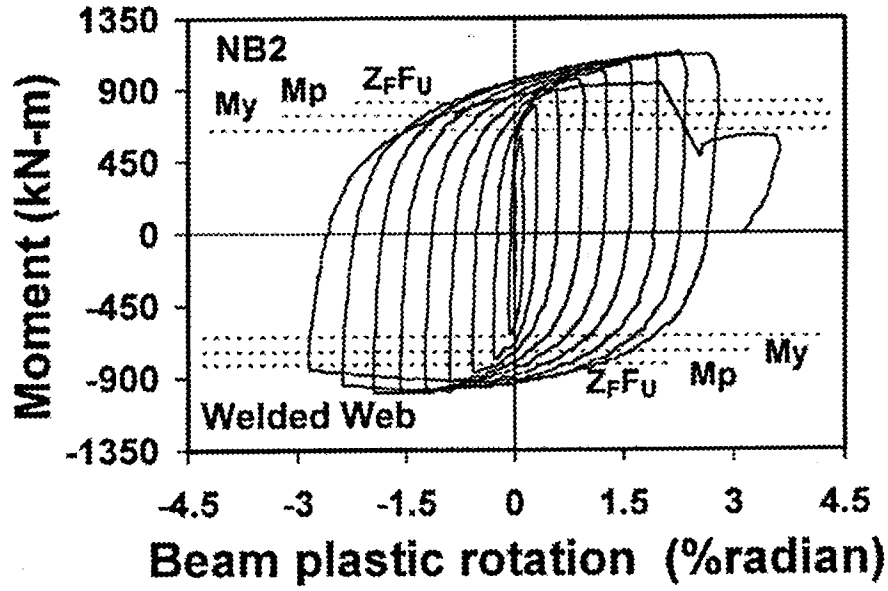

Figure 20 - Moment Versus Beam Rotation Relationships for Specimen NB2

Ductile Steel Beam to Column Connection

- **Flexural Demand: αM_P**
- **Increase Flexural Capacity**

1. Using Flange Stiffeners:

$$Z_F^* F_U > \frac{L_{bn}}{(L_{bn} - L_S)} \alpha M_P$$

$$Z_F^* = Z_F + Z_C$$

2. Using Thickened Shear Tab and Web Welds:

$$Z_F F_U + M_{Weld} > \alpha M_P$$

$$M_{Weld} = Z_W F_Y$$

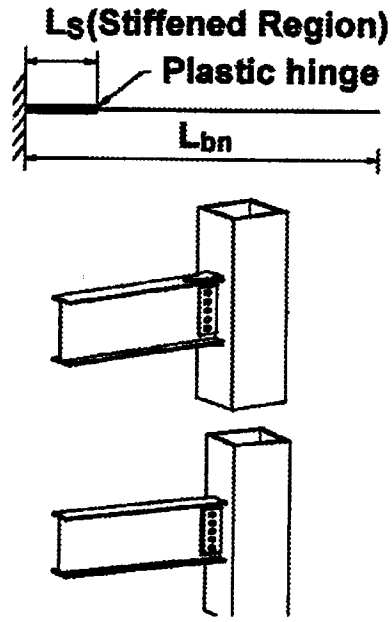

Figure 21 - Design Bases for Stiffening Beam Flanges and Welding Beam Webs

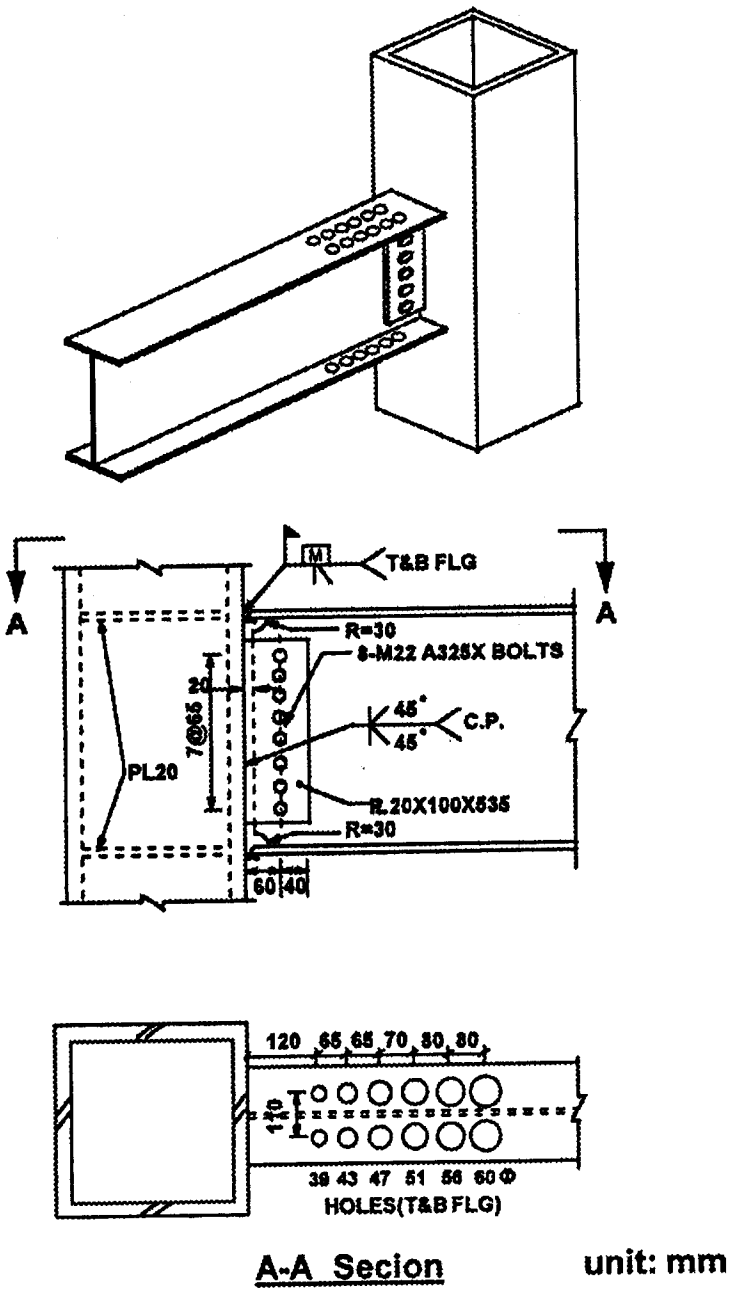

Specimen HB1

Figure 22 - Fabrication Details of Specimen HB1

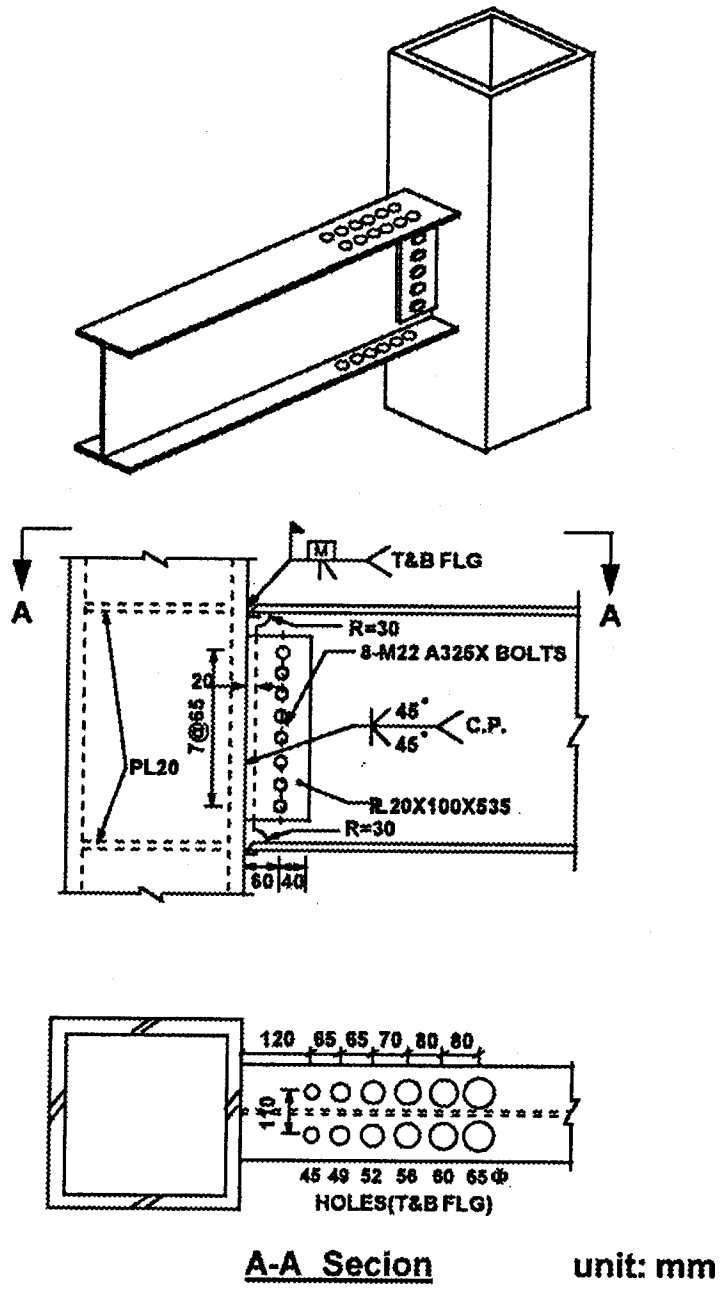

Specimen HB2

Figure 23 - Fabrication Details of Specimen HB2

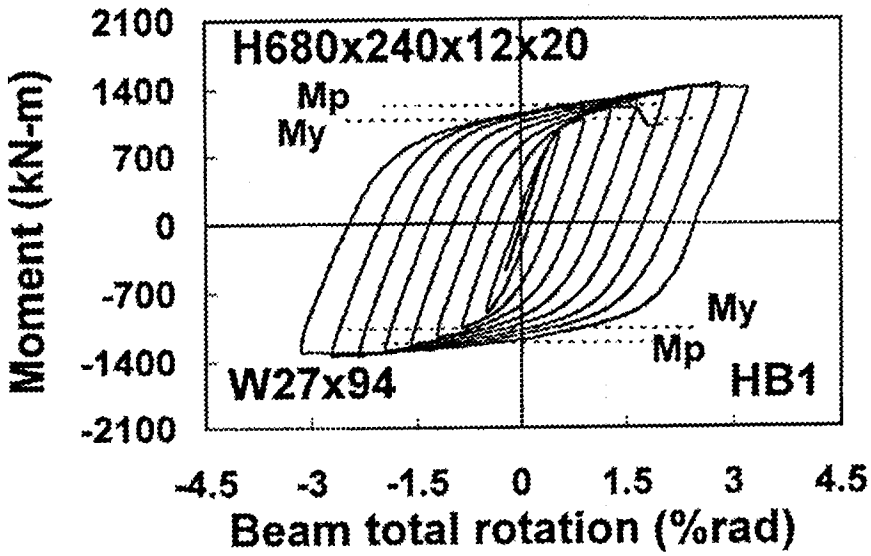

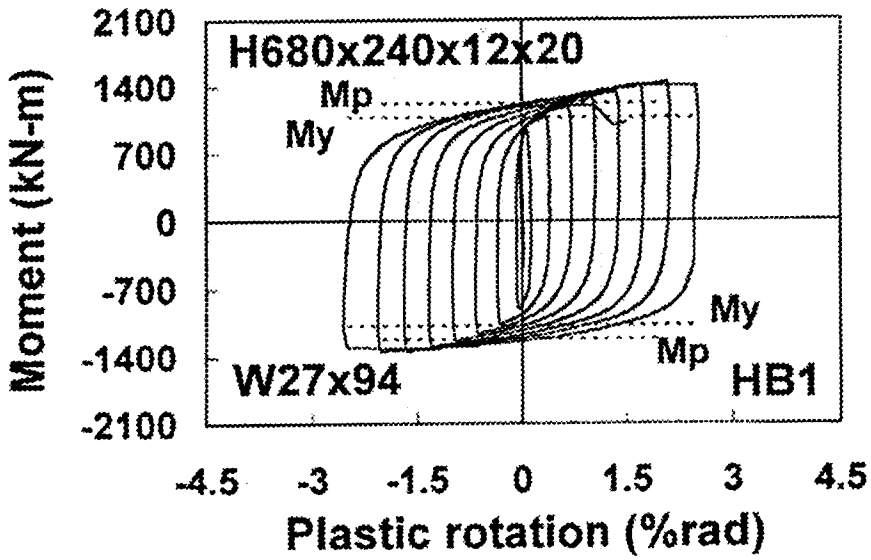

Figure 24 - Moment Versus Beam Rotation Relationships for Specimen HB1

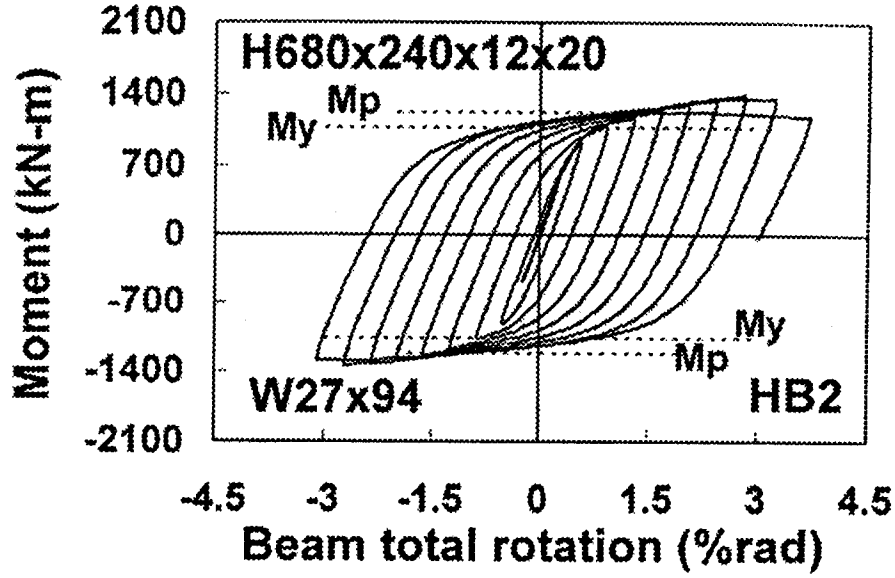

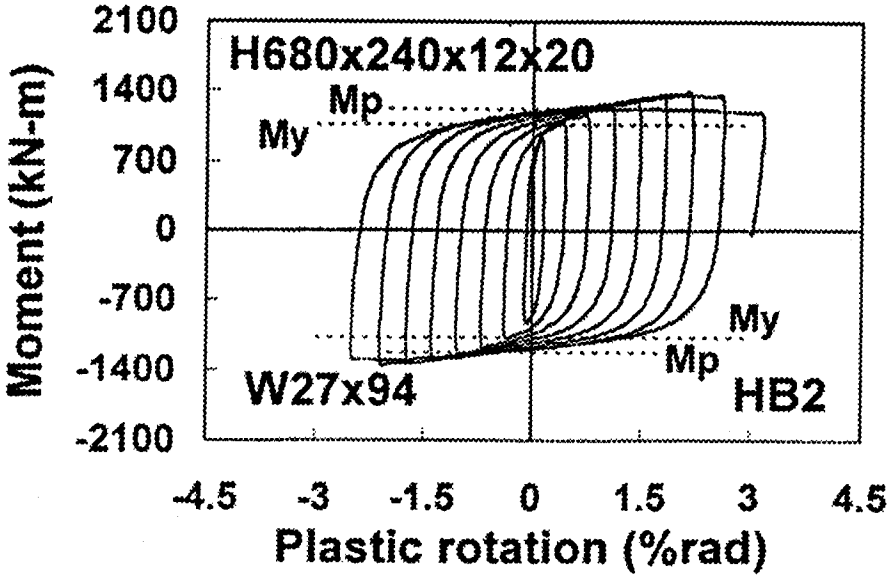

Figure 25 - Moment Versus Beam Rotation Relationships for Speciment HB2

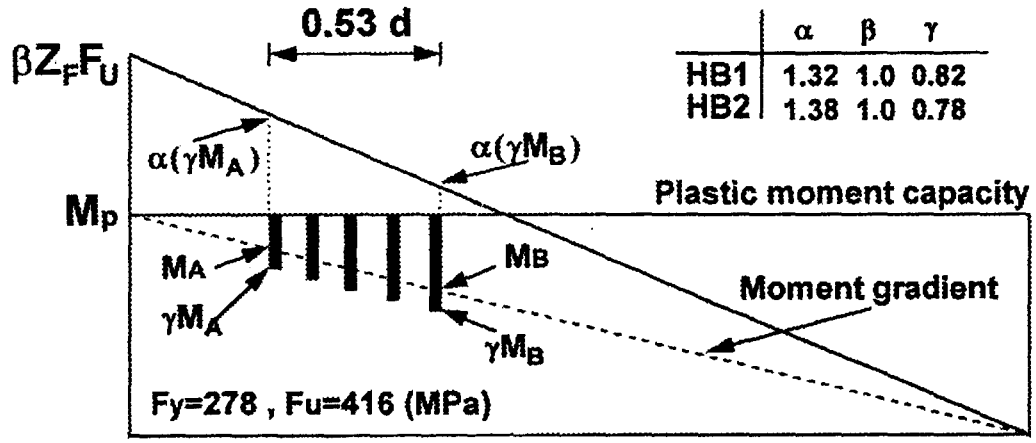

	α	β	γ
HB1	1.32	1.0	0.82
HB2	1.38	1.0	0.78

Design Bases for Drilling Holes on Beam Flanges

6. CONCLUSIONS

Having tarnished the reputation of welded steel moment resisting frames, the Northridge earthquake has given the building industry the opportunity to thoughtfully assess the causes of their unacceptable performance. This paper does not intend to address the full range of issues on welded steel moment connections. Rather, it assesses the possible requirements on the material strength and beam sectional properties. Test results demonstrate that well-proportioned supplemental web welds can effectively enhance the ductility of a conventional BWWF connection. Therefore, a well strengthened BWWF connection, employing the proposed strength requirement for the web welds, may still be acceptable for steel MRFs having moderate inelastic demand. However, it is advisable that other modified connection details be considered when the rotational demands imposed on the beam-column connection may be expected to exceed 0.015 radian, as is the case for most current designs in zones of high seismicity.

Test results have shown that the performance of conventional BWWF connections can be significantly enhanced by: (1) increasing the connection strength capacity by stiffening the beam flanges at the beam-to-column juncture or by fully welding the beam web to the thickened shear tab, or (2) decreasing the connection strength demand by reducing the beam strength in the proximity of the connection. Based on recent test results, it appears that the proposed connection strength demand versus capacity principle can be conveniently adopted for either scheme. However, it is advisable that a statistically based estimate of the expected actual values of material strengths F_y and F_u be considered. For steel with actual values of F_y and F_u significantly different from the minimum specified strength, it appears justifiable that both the capacity-enhancement and the demand-reduction schemes be considered simultaneously for the connection. Simultaneously using flange cover plates and a reduced beam section has been shown effective to prevent flange connection fractures (Popov 1996).

It is important to keep in mind that both schemes have their advantages and disadvantages. The consequence of moving the beam plastic hinge away from the connection is that the column flange will no longer provide lateral support to the beam at the location of highest inelastic deformations. In particular,

large inelastic strains will occur in a region where the beam bottom flange is laterally unsupported. Therefore, additional lateral support may be required in order to prevent lateral torsional buckling. Strengthening the beam at the connection will increase the maximum moment that can be transferred to the panel zone and the column. In present design, it is already likely that panel zone joint will yield in shear before beams attain their beam plastic moment capacity. Connection capacity-enhancement schemes may further increase this likelihood. If the panel zone has to undergo large inelastic deformations, the connection performance may be greatly affected due to the local kinking of column flanges as noted previously. If the connection capacity-enhancement scheme leads to the development of plastic hinges in columns, undesirable story mechanisms may occur. Having these concerns, demand-reduction schemes appear to be a safe and cost-effective way of reducing the stresses in the flange welds. However, it must be considered that the floor slab contributes to the beam strength and the strength reduction may not be completely realized. In addition, the lateral torsional stability of the beam may be greatly reduced due to the partial removal of beam flanges.

Steel moment resisting frames designed according to the current seismic building codes are expected to deform well into the inelastic range, thereby dissipating seismic energy. However, an emerging consensus has suggested that highly stressed moment connections are extremely sensitive to even minor imperfections in the welds as well as material property variations. The welded moment connection, unlike the bolted connection, lacks crack resisting redundancy. Further research on crack preventing details is required. Moreover, a small variation from the design strength for the column or the beam will render a completely different energy dissipation mechanism and can cause severe damage. In addition to the minimum strength, a narrow range of steel yield and ultimate strength variations should be regulated by the material specifications.

ACKNOWLEDGMENTS

The authors would like to thank the SAC Joint Venture for their support of this paper. The authors gratefully acknowledge the financial support provided by the National Science Council of the Republic of China for the experimental research conducted at the National Taiwan University. The authors also thank Messrs. K.C. Lin, M.C. Liu, S. Wu, C.Y. Chen and K.D. Lin for their excellent work during their graduate studies. The authors are also grateful to Dr. S. C. Liu, an NSF Program Director, who over a period of years provided the financial support for carrying out the research in this area. The opinions expressed herein are those of the authors and do not necessarily reflect the opinions of others involved in this effort.

REFERENCES

Adams, C.J. and Popov, E.P., (1976). "Through Thickness Fatigue Properties of Steel Plate," Welding Research Council, Bulletin No. 217, pp. 1–13.

Ang, A. H-S. and Tang, W.H., (1984). "Probability Concepts in Engineering Planning and Design," John Wiley and Sons, Inc.

Chen, S.J. and Yeh, C.H., (1994). "Enhancement of Ductility of Steel Beam-to-Column Connections for Seismic Resistance," Proceedings, SSRC Annual Technical Session, Bethlehem.

Chen, W.F. and Yamaguchi, E., (1996). "Spotlight on Steel Moment Frames," Civil Engineering, ASCE, March.

Engelhardt, M.D. and Husain, A.S., (1993). "Cyclic-Loading Performance of Welded Flange-Bolted Web Connections," Journal of Structural Engineering, ASCE, Vol. 119, No.12.

Engelhardt, M.D. and Sabol, T.A., (1994). "Testing of Welded Steel Moment Connections in Response to the Northridge Earthquake," Progress Report to the AISC Advisory Subcommittee on Special Moment Resisting Frame Research, University of Texas at Austin.

Executive Summary, Interim Observations and Recommendations of AISC Special Task Committee on the Northridge Earthquake, (1994). American Institute of Steel Construction, Chicago, Ill.

Hajjar, J.F. and Leon R.T., (1996). "Effect of Floor Slabs on The Performance of SMR Connections," Paper No. 656, Proceedings, Eleventh World Conference on Earthquake Engineering, Acapulco.

Krawinkler, H., (1978). "Shear in Beam-Column Joints in Seismic Design of Steel Frames," Engineering Journal, American Institute of Steel Construction, Vol. 13, No. 3.

Krawinkler, H., (1995). "Earthquake Design and Performance of Steel Structures," Proceedings, Pacific Conference on Earthquake Engineering, Melbourne.

Plumier, P., (1990). "New Idea for Safe Structures in Seismic Zones," Proceedings, IABSE Symposium, Brussels.

Load and Resistance Factor Design Specifications for Structural Steel Buildings, (1993). American Institute of Steel Construction, Chicago, Ill.

Popov, E.P. and Stephen R.M., (1972). "Cyclic Loading of Full Size Steel Connections," Bulletin No. 21, American Iron and Steel Institute, Washington, D.C.

Popov, E.P., Amin, N.R., Louis, J.J.C. and Stephen, R.M., (1985). "Cyclic Behavior of Large Beam-Column Assemblies," Engineering Journal, 23(1), pp. 9-23.

Popov, E.P., (1995). "What Went Wrong With Steel Connections at Northridge," 4th International Symposium on Steel Structures, Guanajuato.

Popov, E.P., (1996). "UCB Specimen DB1 Test Summary Memorandum," and "ADP Specimen No. 5 Test Summary Memorandum," University of California at Berkeley.

Recommended Ductility Requirements and Commentary for Building Structures, (1991). A Report to Building Research Institute, Ministry of Interior of Republic of China, Chinese Society of Structural Engineering, (CSSC), Taipei, Taiwan.

Salmon, C.G. and Johnson, J.E., (1990), "Steel Structures, Design and Behavior," Harper Collins Publishers, New York.

SAC, (1994) *Proceedings, Invitational Workshop on Steel Seismic Issues*, SAC Joint Venture, Sacramento, CA.

SAC, (1995) "Interim Guidelines: Evaluation, Repair, Modification and Design of Welded Steel Moment Frame Structures," Report No. SAC-95-02, SAC Joint Venture, Sacramento, CA.

Specifications of Seismic Provisions for Structural Steel Buildings, (1992). American Institute of Steel Construction (AISC), Chicago, Ill.

SEAOC, (1986) "Tentative Lateral Force Requirements and Commentary," Seismology Committee, Structural Engineers Association of California, San Francisco, CA.

SSPC, (1994) "Statistical Analysis of Tensile Data for Wide Flange Structural Shapes," Steel Shape Producers Council.

Structural Welding Code-Steel, (1992). American Welding Society, Miami, Fla.

Tsai, K.C. and Popov, E.P., (1988). "Steel Beam-Column Joints in Seismic Moment Resisting Frames," Report No. UCB/EERC 88/19, Earthquake Engineering Research Center, University of California at Berkeley.

Tsai, K.C. and Popov, E.P., (1990). "Seismic Panel Zone Design Effects on Elastic Story Drift of Steel Frames," Journal of Struct. Eng., ASCE, 116(12).

Tsai, K.C. and Liu, M.C., (1992). "A study of Ductility Requirements for Steel Beam-Column Connections," Report No. CEER/NTU R81-07, Center for Earthquake Engineering Research, National Taiwan University.

Tsai, K.C., Lin, K.C. and Liu, M.C., (1992). "Seismic Performance of Steel Beam-to-Box-Column Connections," Proceedings, Tenth World Conference on Earthquake Engineering, Madrid.

Tsai, K.C., and Popov, E.P., (1993). "Seismic Design of Steel Beam-to-Box Column Connections," Structural Engineering in Natural Hazards Mitigation, Proceedings of Structures Congress, ASCE.

Tsai, K.C., Wu, S. and Popov, E.P., (1995). "Experimental Performance Seismic Steel Beam-Column Moment Joints," Journal of Struct. Eng., ASCE, 121(6), pp. 925–931.

Tsai, K.C. and Chen, C.Y., (1996). "Experimental Performance of Ductile Steel Beam-to-Column Moment Connections," Paper No. 405, Proceedings, Eleventh World Conference on Earthquake Engineering, Acapulco.

Tsai, K.C. and Lin, K.D., (1996). "Experimental Performance of High Strength Steel Moment Connections," Report No. CEER/NTU R85-03, Center for Earthquake Engineering Research, National Taiwan University.

Uniform Building Code, (1994). International Conference of Building Officials, Whittier, CA.

Uang, C.M. and Latham, C.T., (1995). "Cyclic testing of full-scale MNH-SMRF Moment Connections," Structural Systems Research, University of California at San Diego.

Yang, T.S. and Popov, E. P., (1995). "Behavior of Pre-Northridge Moment Resisting Steel Connections," Report No. UCB/EERC 95/08, Earthquake Engineering Research Center, University of California at Berkeley.

Zekioglu, A., Mozaffarian, H. and Chang, K. L., (1995). *Structural Design for High Desert Medical Center*, Ove Arup and Partners California, Los Angeles.

SEISMIC PERFORMANCE OF BOLTED AND RIVETED CONNECTIONS

Roberto T. Leon
GEORGIA INSTITUTE OF TECHNOLOGY

1. Introduction

This article presents a state-of-the-art review of the performance of steel bolted connections under reversed cyclic loads. It is divided into three parts. The first part deals with general issues regarding connection design, with emphasis on connections in unbraced frames. This section describes in general terms many of the connection design issues that have led to problems such as those encountered with welded moment connections during the Northridge earthquake. The intent is to stimulate discussion and hopefully effect changes in the way connection design is carried out. The second part presents a review of the experimental data available for bolted and riveted connections, including composite slab effects. This review is not intended to be comprehensive and instead centers on some of the test series that are less accessible to the practicing engineer. The last part presents a review of current design provisions for bolted connections in seismic areas.

The experimental data reviewed in this report indicates that bolted and composite partially restrained connections represent a viable alternative to current fully restrained, welded moment connections. Bolted and composite connections are particularly attractive for low-rise structures with large footprints, where much of the current steel construction is taking place. In these systems the smaller initial stiffness and ultimate strength provided by many of these connections can easily be compensated by activating many more frames and connections for lateral resistance. From the economic and quality control standpoint this is desirable because most of the work can be done in the shop at relatively little additional cost as compared to current simple shear connections. For areas of low to moderate seismicity and for ordinary moment frames, several types of connections (T-stub, end plate, thick top-and-seat angle, and composite connections) can be detailed to provide the required lateral resistance. For areas of high seismicity, these same connections provide a large structural strength reserve capacity, as the survival of many heavily damaged moment frames during the Northridge earthquake attests. Widespread utilization of partially restrained and composite bolted connections should be encouraged in the context of backup structural systems since they provide great redundancy and toughness. For areas of high seismicity, past and on-going experimental work clearly indicates that column welded, flange bolted plate connections, as well as T-stub and thick end plate bolted

connections, can provide equal or better performance to welded moment connections for a wide range of beam sizes.

The two principal obstacles to the use of bolted connections are the perceived lack of design guidelines and the need for more complex structural analyses during the design phase. To address the first obstacle, a more methodical and realistic approach to connection design is described in the first part of this paper. This approach is based on mechanistic models and a sound understanding of connection behavior. The first step in this process is a careful qualitative evaluation of possible failure modes. This is followed by a design process where a hierarchy of failure modes is enforced through the use of reliability-based rules that quantify the strength of the different failure modes. It is evident from the format of the current steel design specifications (AISC 1994) that this type of fundamental approach is the way its writers intended connection design to proceed. The specifications do not deal with any specific connection type, only with connection element (weld, bolts, and base material) failure modes. The linkage between connection element performance and connection behavior is made through the structural model used for the connection design. In essence, a connection is a small structure whose behavior is controlled by that of its elements (or members). Unfortunately the large number of design aids available for steel connections, which in fact do check for most of the applicable failure modes, has led designers to think of many types of connections as a single element with well-defined characteristics. In reality, the myriad of geometric, material, and structural modeling options available to connection designers precludes this type of assumption.

The issue of the additional analysis, which would be required since most of the bolted connections to be discussed here do not provide fully rigid performance, can be addressed from two perspectives. The first one is that the traditional first-order, linear, elastic analysis used for the design of moment-resisting frames can no longer be considered sufficient even for the design of regular frames. More refined analysis, in the form of at least an inelastic, second-order, static analysis (pushover), will be required in the future even for fully-rigid frames. For irregular frames and zones of high seismicity, even more onerous requirements are likely. Thus the need for more advanced analysis cannot be considered, by itself, to be an important drawback to the use of bolted connections. The second perspective is that advanced analytical tools are readily available in the commercial arena to handle many of the problems posed by partially-restrained connections, and many more are becoming available everyday. The problem is not one of availability of analytical tools, but of the additional time required for data input and post-processing of results. In the case of partially restrained connections the only additional need is the moment-rotation curves for the connections. These can be incorporated explicitly into design-analysis programs as has been done in Europe (Jaspart et al., 1996) relieving the engineer from this tedious task.

A final, important caveat is needed. The main current limitation for both bolted and welded connections is that the effect of important variables such as cyclic loads, high strain rates, alternating plasticity, and stress raisers are generally not incorporated in calculating the design strengths present in our codes. Much work is needed in this area, particularly in the transfer of experimental results into design guidelines. However, our understanding of connection element

behavior is such that reliable methodologies for handling these uncertainties can be incorporated into specifications within a relatively short time.

In summary, to increase connection reliability in the future, the design of connections will have to be carried out at a far more fundamental level than is typically done today. This essentially returns the responsibility for connection design and detailing to the structural engineer. This report advocates the use of a rational methodology to achieve that goal. It is felt that this objective is reachable within three to five years and should form the basis for the development of codes for the next century.

1.1. Capacity Design for Connections

The conceptual design for steel and reinforced concrete (R.C.) moment-resisting frames (MRFs) subjected to large seismic excitations is based on ideas that can be summarized by the capacity design approach (Paulay, 1978). Capacity design implies that only selected areas of a structure, labeled "hinging areas," will be targeted for plastification and energy dissipation during major seismic excitation. The rest of the structure will remain essentially elastic even at the maximum drifts envisioned in design. Capacity design intends to insure that the design concept, generally a weak beam-strong column mechanism for most MRFs, is matched by a set of design provisions consistent with the design assumptions.

There are at least three basic steps in assuring a successful implementation of capacity design. First, and most important, the designer needs to identify all mechanisms, both brittle and ductile, that can govern the performance of the "hinging areas." The design provisions must address all of these mechanisms and particularly insure that brittle modes of failure are excluded. Since some forms of brittle failure cannot be avoided altogether, capacity design requires that ductile mechanisms act as fuses and limit the force input so that extensive redistribution of forces and large deformations occur before any of the brittle mechanisms begins to control. Second, in capacity design it is necessary to carefully evaluate both the possible understrength and overstrength of these "hinging areas." The "hinging areas" must be designed to carry at least the level of forces required by the analysis, but must not be so strong so as to either (a) unintentionally overstress other areas of the structure that are intended to remain elastic, or (b) inadvertently shift failure modes in the "hinging areas." Finally, the "hinging areas" require special detailing to insure adequate ductility and to limit strength and stiffness degradation under very large displacements. The necessary detailing provisions can only be developed through a combination of laboratory testing, advanced analysis, and surveys of field performance. Special attention must be paid to the interfaces between hinging and elastic regions to insure a smooth transfer of forces.

Capacity design procedures have been extensively discussed in the literature with respect to R.C. MRFs (Priestley and Paulay, 1992). Capacity design-type studies have also been conducted with respect to steel MRF's, but with more limited scopes (Bertero et al., 1972; Popov and

Bertero, 1973; Tsai and Popov, 1988)[1]. Just as for concrete R.C. MRFs, the studies on steel frames have shown that careful attention must be paid to the mechanisms involved in the inelastic action for these structures. Current design provisions (AISC, 1992) imply that there are two main areas where steel MRF's are permitted to deform plastically and dissipate energy: in beam hinges adjacent to the connections and in the connection panel zones. In addition, column bases, if designed as fixed, must also be able to undergo hinging just like the beam ends. The connection elements themselves, the welds in the case of the connections that suffered severe damage during the Northridge earthquake, are not assumed to provide any of the required ductility. They are only intended to provide sufficient strength so that the beams and the panel zones can yield and strain harden, providing stable strength and stiffness behavior during large seismic excitations.

In hindsight many of the problems encountered by steel MRF's during the recent Northridge earthquake can be traced to violations of fundamental capacity design concepts. These violations include, but are not limited to:

(a) inadequate ductility and toughness of the connection elements (welds), due both to poor selection of materials and an underestimation of the deformation demands on the connection as the beam sizes increased above what had been tested in the past.

(b) lack of consideration in design of brittle modes of failure, including weld fractures, fractures in the HAZ, and the possibility of through-thickness material problems.

(c) underestimation of the actual forces in the structures due to material overstrength (yield stresses generally were far higher than the minimum specified yield strength assumed in design).

(d) poor detailing practices, such as leaving backing bars in place, that result in stress raisers that are inconsistent with the design assumptions.

In the following section the author will endeavor to show why some of these shortcomings, which are inherent to fully restrained (FR) welded connections as designed today, cannot be easily overcome from either a technical or economical point of view. In the process of doing this the advantages and shortcomings of both FR bolted and partially restrained (PR) bolted and composite connections will be highlighted.

1.2. Connection Modeling

Connection design is the key to the design of a safe, economical structure. To discuss connection design it is useful to develop a simple mechanistic model for the connection behavior such as that advocated by current Eurocodes (Eurocode 3, 1992; Eurocode 4, 1994). In general,

[1] In most cases reference will be made only to representative works. It is impossible in this context to make citations to all pertinent sources.

connections transfer a combination of flexural, axial, shear and torsional forces. In most FR connection designs torsional and axial forces are ignored since they are assumed to be small and thus most designs are carried out for a combination of shear and flexural forces only. In most cases these two types of forces are decoupled for design since their interaction is assumed to be small in the design of the beams. In the case of a typical FR welded connection the flexural and shear forces are assigned to different components of the connection (the flexural forces to the beam flanges and the shear forces to a shear tab, angles, or other web connections). The interaction between the different components of force is generally considered only in the design of the fasteners and welds.

For the purposes of discussion, it will be assumed that the most important behavioral characteristics of a connection can be summarized in a single moment-rotation curve for the nodal zone (Leon and Zandonini, 1992). The nodal zone is defined as the area encompassing the connection elements (welds, plates, angles, bolts) and the surrounding parts of the connection (panel zone and parts of the beams and columns adjacent to the connection). A moment-rotation curve for this nodal zone is assumed to provide an adequate representation of the connection behavior that can be used in a simplified non-linear dynamic or push-over analysis of a structure.

Fig. 1 shows a simple mechanistic model for a FR welded connection. Springs are used to indicate the sources of deformation, and each spring may represent several components.

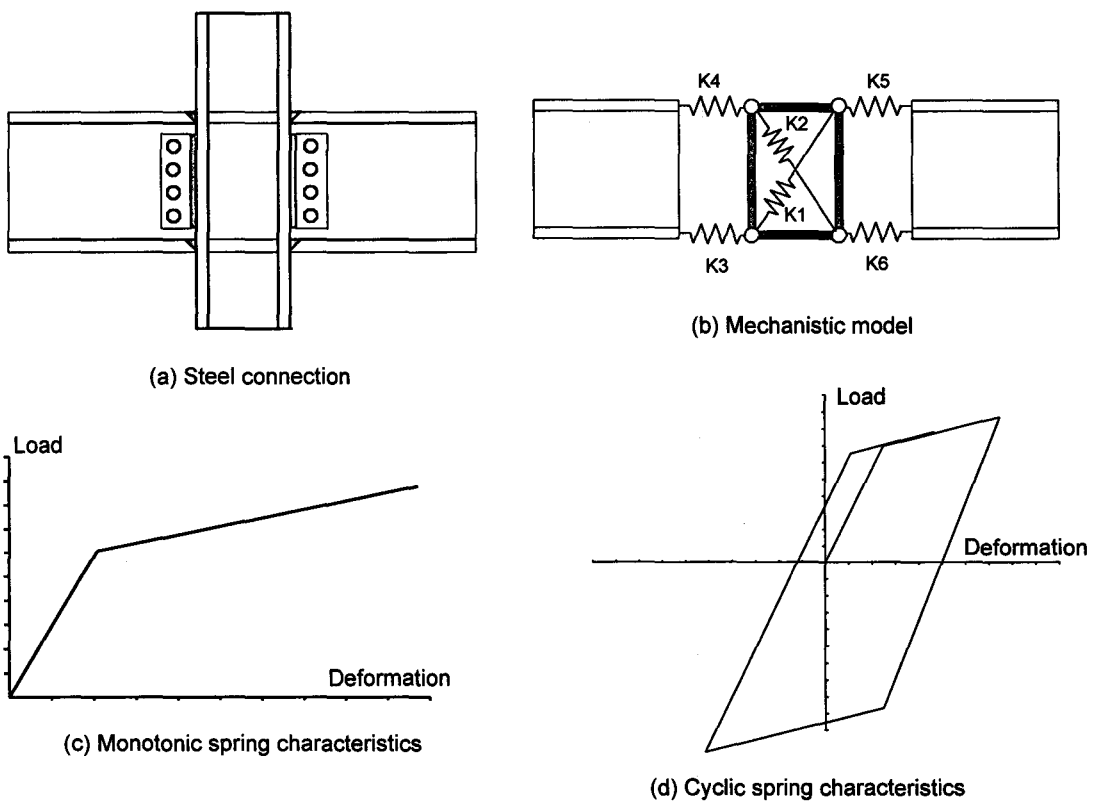

Figure 1 - Simple mechanistic model for a steel FR welded connection.

In Fig. 1(b) springs K1 and K2 represent the shear flexibility of the panel zone, while springs K3 through K6 represent the flexibility of the beam flanges outside the connection zone. The solid rectangles represent the nominally rigid boundaries provided by the column flanges, welds, and continuity plates. If the properties of the springs are known, generally in the form of a bi-linear force-deformation relationship that includes a yield point and a small positive stiffness for the plastic region (Fig. 1(c)), it is a relatively simple matter to derive a moment-rotation curve for this connection that includes both the shear yielding of the panel zone and the plastic hinging in the beam. Even for the case of cyclic loads (Fig. 1(d)), simple but accurate hysteretic rules can be established to model moderate hardening and softening of the elements.

The model in Fig. 1 represents well what current American design provisions for FR welded connections aim to achieve, and is probably reasonable for connections between very strong columns (larger than W12x120 and W14x99) to small to intermediate beams (smaller than W21x62). Although this range of steel shapes is somewhat arbitrary, it is possible in general for these types of connections to satisfy the criteria assumed in the model shown in Fig. 1(b) by rational application of current design provisions, careful selection of materials, and good detailing and inspection (AISC, 1992).

When the members exceed this range of sizes or when a more realistic model of the connection is desired, one that incorporates the floor slab for example (Fig. 2(a)), a more complex model is necessary. Such a model is shown in Fig 2(b), where the springs on the left hand side represent mostly flexural deformations and the springs on the right hand side represent mostly the shear deformations.

Springs K1 and K2 represent the shear flexibility of the panel zone. K3 and K4 represent the axial flexibility of the column web and continuity plates. K5 and K6 represent the flexibility of the welds; K7 and K8 represent the flexibility of the beam flanges for an arbitrary distance along the beam (generally $d_b/2$ to d_b, where d_b is the beam depth). K9 and K10 represent the bending stiffness of the web connection. K11 and K12 represent the bending stiffness of beam web. K13 represents the flexibility of the slab and any slab reinforcement and K14 the shear flexibility of the shear studs. Spring K13 does not show a connection since the boundary conditions for this element are strongly dependent on the detailing of the connection. Spring K15, on the right hand side, represents the shear stiffness of the beam web. K16 and K17 represent the shear flexibility of the web connection and the frictional and bearing resistance of the bolts, respectively. Finally, K18 and K19 represent the shear flexibility of the column flanges near the continuity plates. Although the shear springs are shown for simplicity as axial springs, their deformation is assumed to be of a shear type. The model shown in Fig. 2(b) is neither self-consistent nor stable for all load configurations and is used only to illustrate the complexity of the joint behavior. As an example, the open circles shown in the rigid links between springs K1 and K12 are meant to represent rotational springs. These are used to indicate that in the area adjacent to the connection plane sections do not necessarily remain plane. Finally, it should also be noted that one or more types of failures can be associated with each spring.

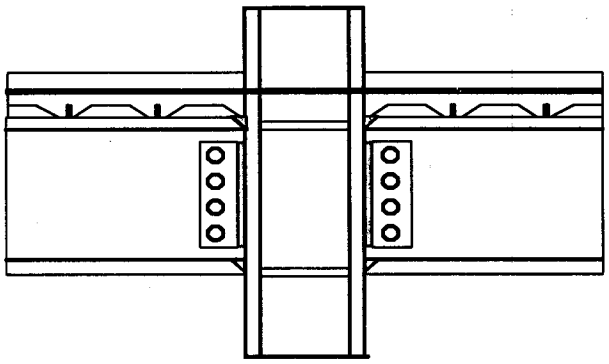

(a) Steel connection with composite slab

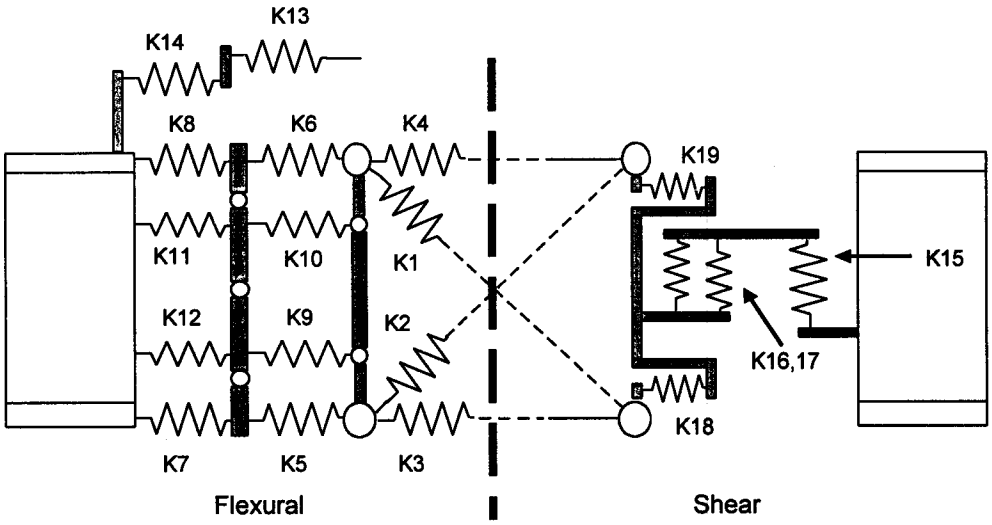

(b) Mechanistic model

Figure 2 - Complex model for a steel FR welded composite connection.

The force-deformation relationships for these springs are also much more complex (Fig. 3) since they need to represent such different phenomena as flange buckling, web crippling, bolt shearing, and slab contributions under monotonic loads. Under cyclic loads some of these modes of failure exhibit extreme pinching and strength degradation (Fig 3(b)). The behavior for springs K16 and K17 in this figure is significant because the slip that takes place in bolted connections, as will be discussed latter, is an important source of ductility and energy dissipation (Astaheh-Asl, 1995).

Obviously routine design office use of the model shown in Fig. 2 is impractical since most of the spring characteristics cannot be provided today by even the most specialized of researchers. However, this model is of great qualitative importance because it shows the myriad of failure modes that are possible in this type of connection. It is only by looking at both the demands on the connection as well as the resistance of its individual components in a qualitative model of this type that a rational design procedure for connections can be derived. By making rational assumptions about the ratios of the different stiffnesses and strengths for all the springs shown , most modes of failure can be discarded. Design provisions for the remaining modes of failure can then be determined and a desired hierarchy established. The detailing necessary to insure this behavior must be verified by experimental testing and advanced analysis.

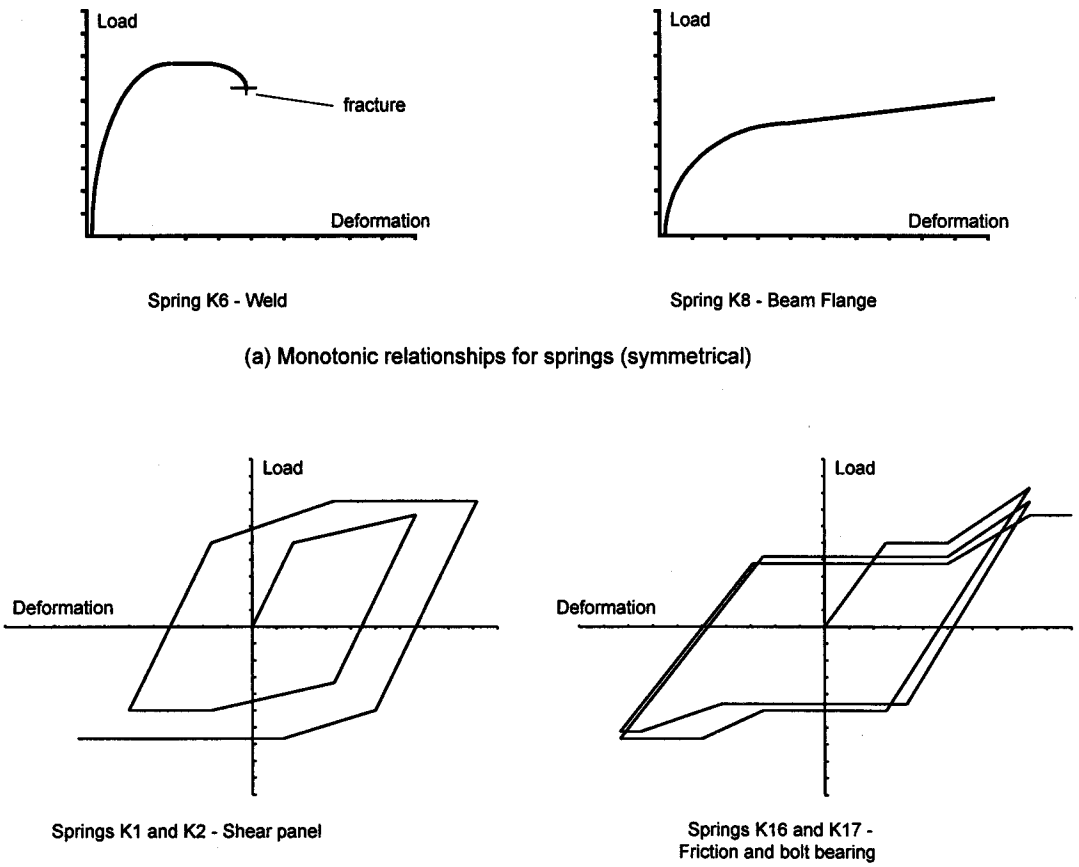

Figure 3 - Spring models for a steel FR welded connection.

1.3. Connection Classification

Current design procedures for steel MRF's imply that the designer knows the moment-rotation (M-θ) characteristics of the connections under design. A schematic set of moment-rotation curves for some typical FR, PR, and simple shear connections used in steel frame construction is

shown in Fig. 4(a). Some types of connections, end plates for example, can be detailed to provide a wide range of performance based on the thickness of the end plate and number of bolts to the column flange.

The following comments need to be kept in mind when looking at M-θ curves such as those shown in Fig. 4(b):

- Almost all connection moment-rotation curves are nonlinear from the onset of loading. However, for design purposes, the use of a linear approximation for the stiffness (K_{conn}) at the service level is generally acceptable. This assumption is justified based on the concept that the connections have "shaken down." This means that the connections have undergone many cycles of loading and unloading in the service range and that under this load regime the connections will eventually reach a linear behavior[2].

- The selection of the numerical value for K_{conn} is not a simple matter. While there are several data banks of moment-rotation curves available (Kishi and Chen, 1986; Attiogbe and Morris, 1991), most of the tabulated initial stiffnesses were derived from curve fitting to tests where little data was obtained at the beginning of the tests and which did not include loading and unloading cycles at low amplitude. Thus the tabulated values can overestimate the real value of K_{conn}. In general for design it is recommended that the value of K_{conn} be taken as the tangent stiffness to some arbitrary rotation, say 0.0025 radian (Leon et al., 1996).

- For FR construction the connection is assumed to be perfectly plastic, so that the initial stiffness can be assumed as infinite ($K_{conn} = \infty$). In "simple shear framing" the initial stiffness is assumed to be so small that it can be ignored in design ($K_{conn} = 0$). For PR construction the connection stiffness must be known.

- The definition of PR, FR and simple behavior cannot be made with reference to the absolute M-θ curve alone. This classification should depend at a minimum on the ratio (α) of the connection stiffness to the stiffness of the beam framing into it ($\alpha = K_{conn} L_b / E I_b$). Typical values for FR connections are $\alpha > 20$ and for simple connection $\alpha < 0.5$; for $20 < \alpha < 0.5$, the connection can be considered to be PR.

- Most connections actually fall under the PR category (see Fig. 4(b)) but accounting for the PR behavior in the analysis and design is not simple unless advanced analysis tools are

[2] Shakedown is an important part of plastic design theory and is used to account for the application of numerous cycles of load into the inelastic range. The reader is referred to D. G. Eyre and T. V. Galambos, "Shakedown Tests on Steel Bars and Beams," ASCE J. of the Structural Div., Vol. 96, No. 7, 1970, pp. 1287-1304 and Section 6.4 of the ASCE-WRC Plastic Design in Steel: A Guide and Commentary , ASCE, 1971 for a good introduction to the subject. For a complete treatment of the subject, see J.A. Konig, Shakedown of Elasto-Plastic Structures, Elsevier/PWN, Warsaw, 1987.

available. In the past design specifications have resorted to artifices such as the Type 2 "wind connections" to overcome this obstacle (Ackroyd and Gerstle, 1977; 1982). Given the advances in both computational capacity and knowledge of connection behavior, more realistic modeling and analysis of PR connections should be encouraged.

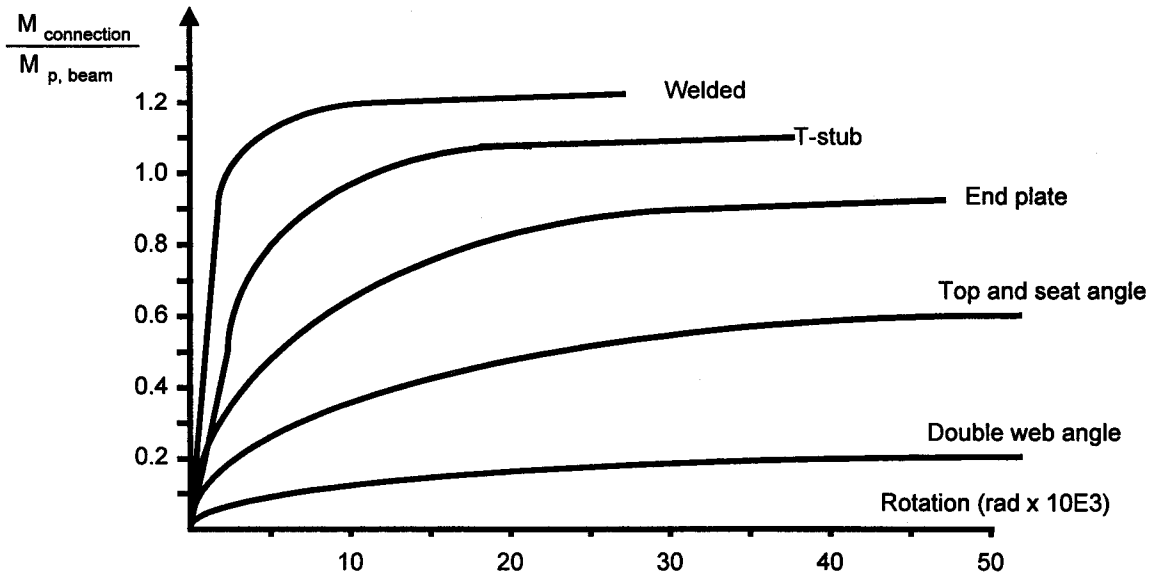

(a) Moment-rotation characteristics for typical connections

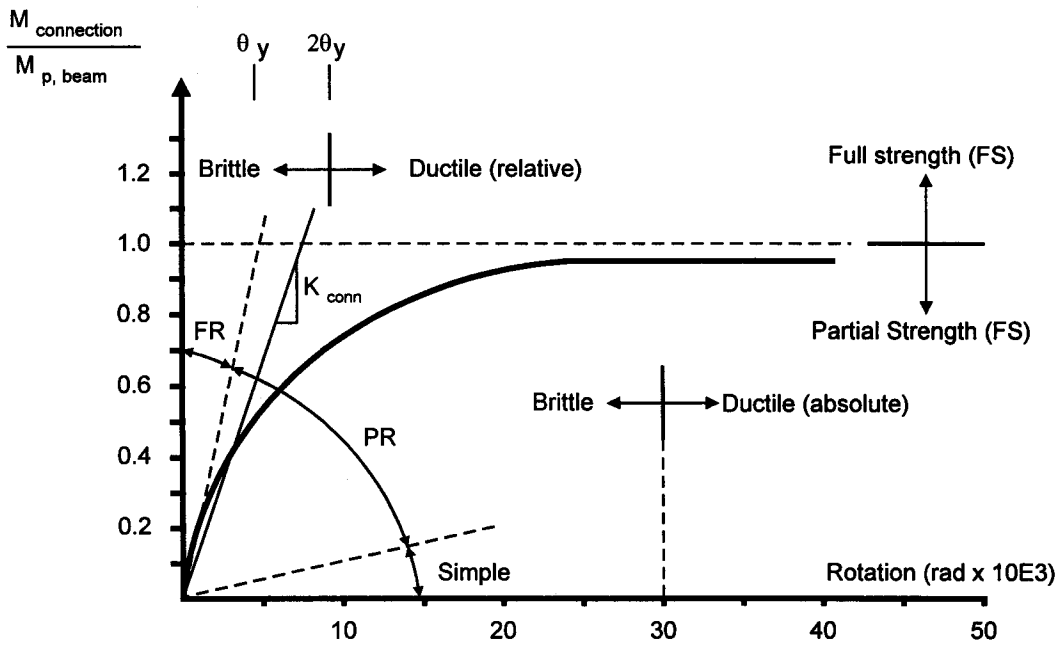

(b) Definition of connection characteristics

Figure 4 - Schematic moment-rotation curves and definitions

- Even connections whose behavior will classify them as simple will have an important role in the performance of a frame if they are numerous and tied to the main lateral load-resisting system through a rigid diaphragm.

- An important warning for designers regarding the strength predicted by many of the M-θ equations in the existing data bases is that those equations are generally tied to only one mode of failure (typically flexural yielding of the connecting elements). Thus, for example, the equations proposed in most data bases for top and seat angle connections do not contain the bolt size as a variable. Thus, these equations cannot predict when bolt shear, as opposed to yielding of the angle, may begin to govern the strength of the connection (i.e., there is no limit on the flexural strength due to bolt shear strength).

- Another important warning with respect to moment-connection curves is that in general they have been derived from tests on small or medium-size specimens. Until recently there were few tests with beams larger than W24 for FR connections.

Monotonic M-θ curves such as those shown in Fig. 4 do not tell the whole story for seismic design for at least three important reasons. First, connection behavior in the monotonic range needs to be classified with respect to stiffness, connection strength, and rotational ductility in a non-dimensional fashion. For example, the two limits between brittle and ductile behavior shown in Fig. 4(b) are arbitrary. An absolute limit of 0.03 radians was selected to be consistent with the SAC interim guidelines for new connections, while a relative limit of $2\theta_y$ as proposed for older construction by ATC-33 is also shown. For the latter type of classification, a reference rotation is needed. Second, connection behavior under cyclic loads needs to include not only considerations related to strength and ductility but also to energy dissipation, unloading and reloading stiffness, and slip plateaus. Finally, curves such as those shown in Fig. 4 are derived typically from simplified tests where the boundary conditions are very different from those in real buildings and without the presence of floor slabs. Each of these issues will be addressed briefly in the next paragraphs.

1.3.1 Monotonic Connection Classification

A proposed non-dimensional connection classification, based on the Eurocode 3 [Eurocode 3, 1992] is shown in Fig. 5. For this type of classification:

- A connection is said to have reached its nominal moment capacity (M_{ult}) if the moment in the connection is at or near the flat portion of the M-θ curve (Fig. 4(b)). Connection strength, however, is only relevant when compared to the strength of the framing beam. Thus connection strength is defined as either full strength (FS) or partial strength (PS) depending on whether the connection strength exceeds or does not exceed the plastic moment of the connecting beam (M_p). A connection is partial strength if (M_{ult} / M_p) < 1.0 and full strength otherwise. Current seismic design procedures for welded and bolted connections

address only FS connections. However, in the author's view, there is no compelling evidence to show that PS connections are inherently less reliable or would result in worse frame performance than FS connections under cyclic loads. In fact, the author would argue that these are ideal connections for areas of low to moderate seismicity (Leon, 1996) and perhaps for zones of high seismicity (Astaneh-Asl and Nader, 1992).

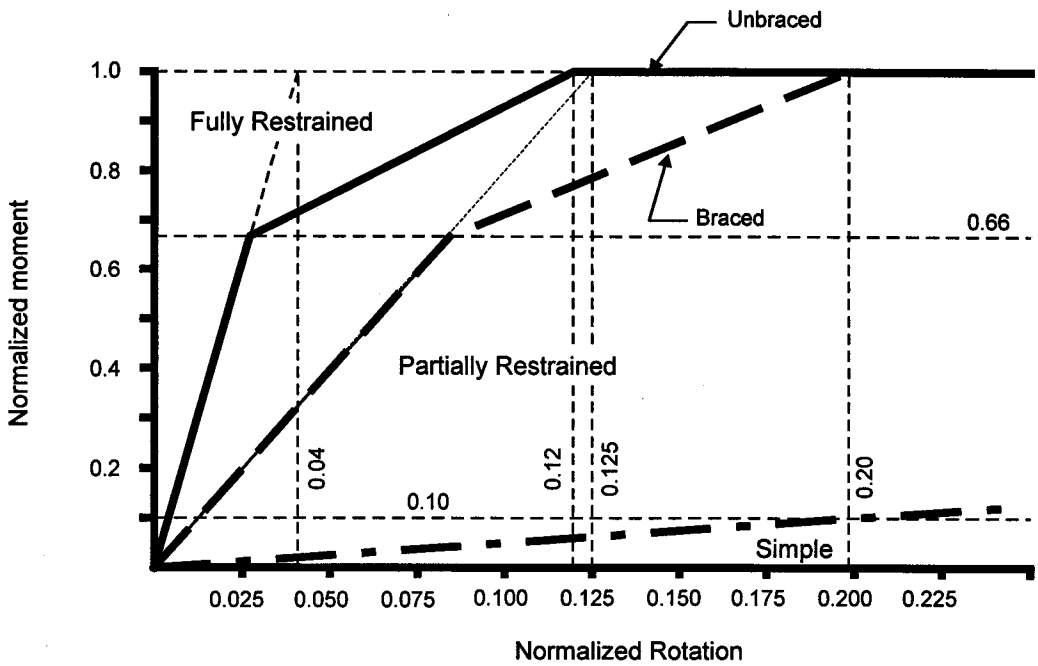

Figure 5 - Normalized moment (M_{conn}/M_p) vs. rotation (ϕ / ϕ_p) classification.

- The ductility of the connection is a key parameter in connection design since current design procedures assume that some limited yielding will take place in the nodal zone at service loads, and that much of the inelastic action at ultimate will be concentrated here. However, it is not clear for seismic design how the rotation achieved during a test should be non-dimensionalized, i.e., whether this should be related to an absolute rotation (say 0.03 radians) or to a relative one. An example of the latter [Eurocode 3, 1992] is the rotation reached in a beam when it attains its plastic moment ($\phi_p = M_p L/ EI$). Traditionally has been assumed in plastic design that if a section were capable of reaching $3\phi_p$ it would provide sufficient rotation for the formation of overall structural mechanisms. This definition seems adequate for monotonic loading. It should be noted, again, that the classification is made based on the connection being attached to a particular beam. The shape of the curve and therefore the overall classification of the connection behavior can change drastically if the same connection is attached to a small (W16x31), long beam or a large (W36x200), short one.

- Regardless of how the rotations are non-dimensionalized, both the ductility (μ) and the absolute rotation capacity are important. Ductility can be defined as $\mu = \theta_u / \theta_y$, where θ_u is the rotation at failure and θ_y is arbitrarily defined (i.e., the rotation at which extrapolation of K_{conn} intersect M_p). Connections should possess ductilities on the order of 10 and absolute

rotation capacities of greater than 0.05 radians under monotonic loads. Note that an assumption of a perfect plastic mechanism, as is done for strong column-weak beam systems, implies that the average rotation at the beam ends is equal to the story drift (i.e., 2.5% drift is 0.025 radian). Non-linear dynamic analysis for steel frames indicates that it is difficult in practice to achieve a perfect plastic mechanism and that the hinges do not necessarily form at the beam ends. Thus the designer must be conscious that modified beam mechanisms and local mechanisms, with rotational requirements that are much higher than the average, should be accounted for in design.

- Insofar as stiffness is concerned, connections have traditionally been considered rigid if α is greater than 20 and simple if α is less than 2 ($\alpha = K_{conn} L_b / E I_b$). The dividing line between full and partial restraint is arbitrarily assumed to occur when the consideration of connection stiffness results in a decrease larger than 5% from the buckling load of a similar rigid frame. A non-dimensional classification such as the Eurocode one shown in Fig. 5 clearly shows that the dividing line also depends on whether the frame is braced or unbraced. For the former case it is possible to reduce the required stiffness substantially, to an $\alpha = 8$. For a rigorous classification the relative stiffness between beams and columns also plays a role, but that issue will not be discussed here.

1.3.2 Cyclic Connection Classification

There are currently no existing proposals for the classification of connection behavior under cyclic loading. While the strength, stiffness, and ductility of the monotonic curve can be assumed to provide a benchmark, it is clear from tests that other connections characteristics are important under cyclic loads. These include unloading and reloading stiffness, energy dissipation capacity and slip plateaus that are typical of bolted connections subjected to simulated cyclic loads (Fig. 6). It should be emphasized that the slip plateaus shown in exaggerated fashion in Fig. 6 are not necessarily detrimental to the behavior if the frictional component can be maintained and the slip plateaus do not grow excessively. Fig. 6 shows the worst condition for behavior, where the slip plateaus keep growing and the strength continues to degrade. This will not be the case in properly designed bolted connections.

Experimental evidence shows that for some types of connections the unloading stiffness is proportional to the maximum rotation achieved [Leon and Shin, 1995] and not necessarily equal to the original stiffness. In addition, the stiffness, length of the slip plateau, and energy dissipation capacity are strongly dependent on the load history used and the detailing of the connection. Load histories such as those utilized for testing by ECCS [ECCS, 1986] and proposed by ATC [ATC-24, 1992], which use a series of increasing amplitude cycles, may result in more degradation than load histories with large cycles imposed at the beginning of the load history. Since the typical earthquake resembles more the latter type of load history, testing protocols, when possible, should address both types of load histories.

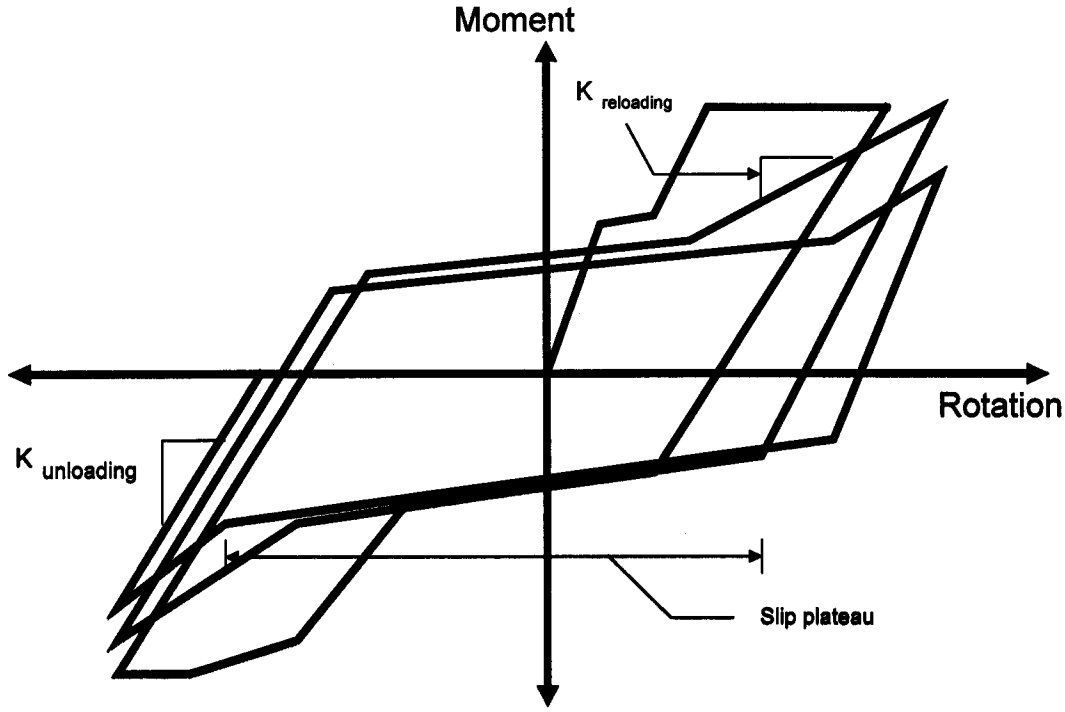

Figure 6 - Cyclic connection properties.

While there are no specific guidelines for cyclic performance of connections, tentative recommendations can be made. The author believes that connections to be used in areas of high seismicity should possess ductilities on the order of 6 and absolute rotation capacities of greater than 0.03 radians while retaining (a) more than 80% of their maximum strength, (b) more than 60% of their initial stiffness, (c) slip plateaus less than $\theta_u/2$, and (d) retaining at least 35% of their elasto-plastic energy absorption capacity. These are very stringent demands but consistent with the many assumptions made for capacity design.

1.3.3 Effect of Floor Slabs

In many situations engineers assume that ignoring the additional strength and stiffness provided by a floor slab is conservative in design. This is incorrect because:

- The field and laboratory experimental evidence reveals that a large amount of interaction will occur even if there are relatively few or no shear studs or mechanical connectors. For example, most older steel beam bridges behave compositely far beyond the service range even if there is no mechanical attachment between the beams and slab (Leon et al., 1993). This interaction arises primarily because of friction in older steel bridges and because of the puddle welds and steel deck used in modern steel construction. While it would be unreasonable to believe that this interaction will last through very severe cyclic loading unless very careful detailing of the shear studs and slab reinforcement is carried out, it must be recognized that it is the first large inelastic cycle that will probably cause the most

damage. In this context, the considerable overstrength that can occur due to the slab must be accounted for in design.

- While the amounts of slab reinforcement provided for flexural strength are generally small or non-existent in the lateral load resisting frames, there is generally reinforcement placed above the girders as (a) part of the mechanism to transfer diaphragm action and (b) to limit cracking above the girders and beams and around the column. This steel will participate in carrying the loads whether its effect is included in design or not. Clearly, from a capacity design standpoint, this steel reinforcement cannot be neglected because if some degree of interaction exists, the stiffness and strength ratios between beams and columns will shift. In particular, the ratio of column to beam flexural strength will decrease leading to the possibility of column hinging rather than beam hinging.

- The current design philosophy for MRF's assumes that the beams will be bent in double curvature. If the beam is composite, the real beam stiffness for one-half of the span will correspond to the positive moment of inertia of the composite section. The stiffness for the other half can be taken as either the stiffness of the steel beam alone, or that of the steel beam and slab reinforcement if the latter is present. This will significantly increase the effective moment of inertia of the entire cross-section. From a bending strain energy analysis, for example, for a beam bent in double curvature and having moments of inertia of I and 2I over each half of the span, the equivalent I for use in a lateral drift analysis would be 1.33I (Leon and Forcier, 1992). Thus consideration of the effect of the slab can result in substantial reductions of beam sizes. This reduction is more pronounced for the smaller and medium size beams (W16 to W21), where the typical ratios of I for bare steel to composite sections range from 1.6 to 2.0. For analysis of PR frames with composite beams the author has suggested that an equivalent I equal to 0.4 I(negative) + 0.6 I(positive) be used when a single element is used to model the beams (Leon and Forcier, 1991).

- There is new evidence that the presence of a slab will considerably affect the local strains. In a recent series of tests, the strains in a fully welded connection with a composite floor slab were one order of magnitude greater at yield at the bottom flange than at the top flange (Leon and Hajjar, 1996). This helps explain the preponderance of failures in bottom flanges observed during the Northridge earthquake and should serve as warning to designers that slabs play an important role in connection behavior. As further evidence, while bottom flange failure occurred in over 90% of the connections damaged in the Northridge earthquake (where floor slabs were in place), laboratory testing without floor slabs has resulted in a nearly random distribution of top and bottom flange failures.

The effect of the floor slab will be significantly influenced by the detailing (primarily anchorage) of the slab reinforcement and how the slab is formed around the column. Fig. 7 shows a strut-and-tie mechanism describing how the tensile forces in the slab on one side of the connection are transferred to the column by bearing on the other side. Note that transverse slab reinforcement is needed in order to maintain the force transfer and that the transfer mechanism can be improved by infilling the area between the column flanges with concrete.

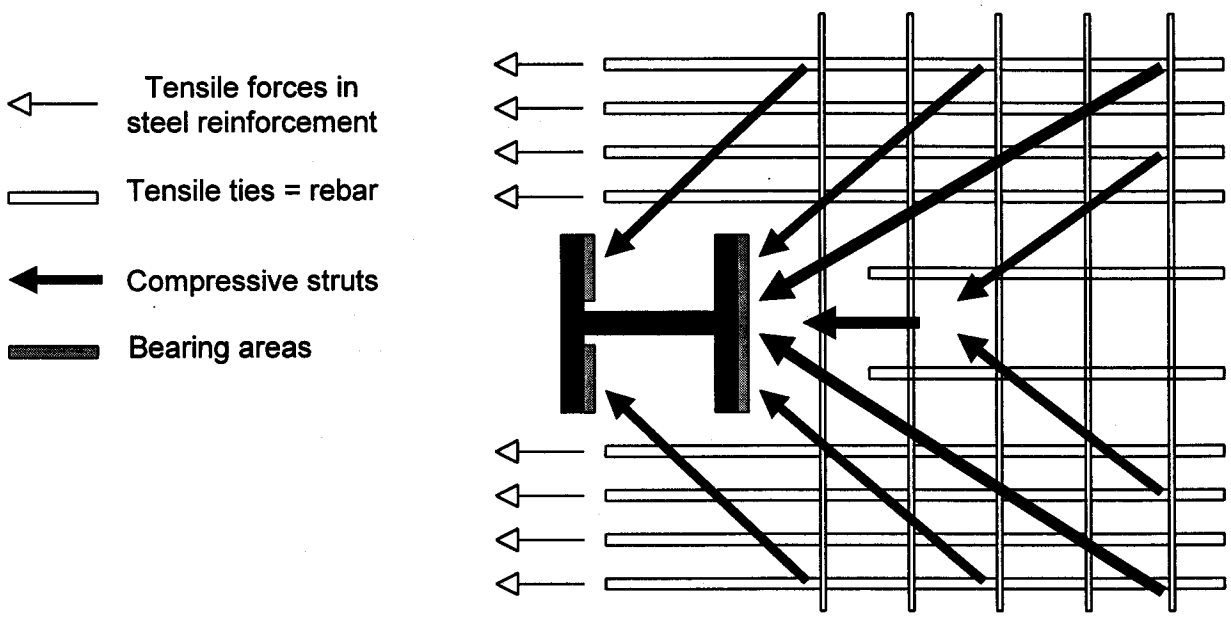

Figure 7 - Strut-and-tie mechanism for force transfer from the slab to the column.

If the slab is not in full contact with the column flanges this mechanism may not exist or be fully effective. In fact, isolating the slab from the column may be a good way of dealing with some of the overstrength problems described above . The key point, however, is that designers must account for the effect of the floor system in their connection design and that to ignore its effect is unconservative. An additional factor to consider is the presence of transverse beams (not shown in Fig. 7) which will help in the force transfer particularly if their connections possess some torsional strength. While the tendency will be to ascribe negligible torsional restraint to the beam framing into the weak axis of the column, the presence of the slab precludes this assumption. Unfortunately there is very little experimental or analytical work in this area, and it is not possible to formulate design recommendations on how to handle this effect.

1.3.4 Testing Limitations

Finally, designers must realize that much of what is known about connection design stems from structural testing that can only idealize the real conditions. Examples of these idealizations include the fixed position of inflection points in the test setups, lack of horizontal restraints at beam ends, loading schemes with constant moment/shear/axial load ratios, application of systematic cyclic loading regimes, and the lack of consideration of the effects of secondary structural and non-structural elements (Leon and Deierlein, 1996). These effects must be considered, in addition to some of the scaling problems associated with most experimental research, when assessing experimental results.

1.4 Frame Analysis Considerations

The above discussion of connection modeling necessarily leads to more complex frame analysis since in many instances the moment-rotation characteristics of the connection will need to be included explicitly. In the writer's opinion this is not necessarily the case for preliminary design, and the level of advanced analysis required for a final check should be commensurate with the importance of the structure and the level of seismic excitation expected at the site.

For example. for the case of partially restrained frames in zones of low to moderate seismicity, it is likely that drift due to wind will actually control the design. In this case the design for service can be carried out using linear springs to model the connection behavior. The use of linear springs, as noted before, is justified by shakedown theory. Linear spring models are present in many commercial analysis programs and the only unknown remains the spring stiffness. In most cases it is conservative and adequate for preliminary design to assume a connection stiffness equal to the secant stiffness to a rotation of 0.0025 radians. The latter value is based on the assumption of a perfectly plastic mechanism with all hinges at the beam ends and an allowable drift of H/400. Parametric studies (Leon and Forcier, 1991) indicate that this approach is also valid in areas of low to moderate seismicity if the structure has a regular distribution of mass and stiffness (see NEHRP 1994 definitions), it is under 8 stories in height, and utilizes partially restrained composite connections.

For preliminary design, a second-order plastic analysis can be used to check the ultimate strength of the frame (Leon et al., 1996). Parametric studies can be used to determine multipliers to account for second-order effects, considerably simplifying the analysis. Once the frame has been proportioned, a final check can be performed. In areas of low to moderate seismicity it is likely that a non-proportional pushover analysis to collapse will yield a good indication of the adequacy of regular frames (Leon and Forcier, 1991; Leon and Shin, 1995). In this case at least a trilinear approximation to the moment-rotation curve should be used. Parallel elasto-plastic springs can be used to model the connection until more sophisticated multi-linear models are available in commercial programs. For irregular frames or for frames in zones of high seismicity, time history analyses should be conducted (Astaneh-Asl and Nader, 1992; Leon and Shin, 1995). The latter are not as time consuming as one may think, except for the input phase. For example, a run for a six-story, four bay frame subjected to the first 20 seconds of the El Centro N-S record with time intervals of 0.02 seconds and incorporating trilinear degrading springs takes less than one hour in a Pentium 100 Mhz machine (Leon and Shin 1995). It will not be long before this type of program is commercially available, considerably simplifying the analysis of frames with PR connections.

2. Review of Past Research

Excellent bibliographies of early research on steel connections can be found in the work of DeJonge (DeJonge, 1945) for riveted connections, and Fisher and Beedle (Fisher and Beedle, 1964; Fisher et al., 1966; ASCE, 1967) and Munse (Munse, 1976) for both bolted and riveted connections. Four of the most important test series related to riveted joints described in those bibliographies are summarized in the next section. There has not been, to the author's knowledge, any similar bibliographies published recently for modern bolted connections although extensive synthesis of the data available can be found in the numerous connection databases produced in the 1980's and early 1990's (Frye and Morris, 1975; Goverdhan, 1984; Nethercot, 1985; Kishi and Chen, 1985; Attiogbe and Morris, 1991). A recent book even incorporates a diskette with one of these databases (Chen and Toma, 1994). In addition, SSRC Task Group 20 has an extensive bibliography on PR connection tests, analysis, and design (SSRC, 1987). The reader is referred to those sources for detailed information on test results.

There has been an upsurge in interest in steel connection behavior in the past 15 years that has led to several important international conferences and monographs (Howlett et al., 1982; Chen, 1987; Bjorhovde et al., 1988, 1992, 1996; IABSE, 1989; Narayanan, 1989; Lorenz et al., 1992; Dowling et al., 1994a,b; Mazzolani and Giouncu, 1995). However, with some notable exceptions (Mazzolani and Giouncu, 1994), the majority of the publications deal with monotonic design of connections and, from the European side, mostly for design in braced frames. In addition, there has been extensive research conducted in Japan on steel and composite connections under seismic loading (Kato, 1982; Wakabayashi, 1987); unfortunately there does not exist a comprehensive synthesis in English of that work and the information remains mostly in proceedings from joint US/Japan workshops (Morino and Nishiyama, 1992). Most recently Astaneh-Asl (Astaneh-Asl, 1995) has produced an excellent summary of the state-of-the-art in design of bolted connections, including some innovative solutions. Since this paper endeavors not to repeat what is contained in that publication, except for what is necessary to make this a self-standing document, readers are strongly encourage to also carefully read that reference. In addition readers are strongly urged to consult the classical work by Kulak et al. for fundamental issues related to bolt and rivet behavior (Fisher and Struik, 1974; Kulak et al., 1987).

2.1 Riveted Connections

Until high strength bolts proved their economic superiority in the late 1950's, hot driven rivets were the fasteners of choice for field connection of steel members. Riveted connections present several important characteristics that set them apart from bolts insofar as connection behavior is concerned:

- During installation the repeated blows of the pneumatic hammer or other installation tool cause the rivet shank to diametrically expand and to fill completely the hole in which it is being installed. Since the holes are completely filled, slip is limited to the deformation of the rivet itself (minimal for service loadings).

- While cooling the rivet shank contracts and the rivet heads exert a clamping force on the joined steel plates. The initial stress in rivets has been found to be generally greater than 70% of the yield-point strength of the steel from which the rivets were made (Wilson and Oliver, 1930). Thus there is a large amount of uncontrolled pretension in the rivets. As the experience with riveted railroad bridges shows, this pretension can be maintained through a very large number of small cyclic excursions, resulting in excellent fatigue performance for these bridges.

- The properties of driven (installed) rivets differ from the properties of rivet bar stock. Generally installation by pneumatic hammers increases the yield and ultimate strength by as much as 20% based on the nominal diameter of the rivets (Hechtman, 1948). Differences in installation procedures seem to have little influence on the final properties (Wilson and Oliver, 1930; Hechtman, 1948). It is interesting to note that Wilson (Wilson and Oliver, 1930) purposely did tension tests with rivets having poorly formed heads that would not have passed ordinary inspection, and obtained reliable tensile behavior.

- For most steel construction prior to the 1950's, fire protection was assured by encasing the main steel members in masonry or concrete. The concrete cover was generally substantial, on the order of 3 to 4 in., but it did not contain significant amounts of transverse reinforcement. Depending on the quality of the concrete, this encasing can have a very significant effect on connection performance by adding additional stiffness and strength as well as delay or preventing local buckling of the members (Roeder et al., 1994).

Structural rivets are made of A502 steel (ASTM A502-91, 1991). This material was formerly designated as ASTM A141. This type of steel is available in three grades. Grade 1 is for standard structural applications. Grade 2 is for use with high-strength carbon and high strength low-alloy structural steels. Grade 3 is similar to Grade 2 but has enhanced corrosion resistance. ASTM does not specify any strength or hardness requirements for rivets in the driven state. ASTM does however specify some hardness requirements applicable to the rivet bar stock. Kulak et al. (Kulak et al., 1987) proposed lower bounds for the ultimate tensile strength (σ_u) of rivet material: (1) σ_u = 60 ksi for Grade 1 rivets, and (2) σ_u = 80 ksi for Grade 2 or 3 rivets. They also proposed design formulas for the evaluation of the strength of rivets in tension and shear. The nominal tensile strength (B_u) of a rivet is:

$$B_u = A_b \sigma_u$$

The nominal shear strength (S_u) of a rivet is:

$$S_u = 0.75\, m\, A_b\, \sigma_u$$

where A_b is the undriven cross section area of the rivet shank, σ_u is the rivet tensile capacity, and m is the number of shear planes passing through the rivet. For cases where both tension and shear forces are acting on the rivets an elliptic interaction curve fitted to test results was developed (Munse and Cox, 1956):

$$\frac{x^2}{(0.75)^2} + y^2 = 1.0$$

where x is the ratio of the shear stress on the shear plane to the ultimate tensile strength, and y is the ratio of the tensile stress to the ultimate tensile strength.

2.1.1 Monotonic Tests of Riveted Connections

There have been numerous investigations into the behavior of riveted connections under monotonic loadings. A complete bibliography can be found in ASCE Manual 48 (ASCE, 1967), and only the most important test series will be discussed briefly here. The earliest comprehensive testing of connections was reported by Wilson and Moore who tested a series of 12 full scale steel beam-to-column joints (Wilson and Moore, 1917). All joints were riveted, and most of them connected built-up riveted members. The authors pointed out that for many of the connections tested the standard assumption of perfect compatibility of rotation between the connected columns and beams (FR behavior) was significantly in error. The PR behavior of the connections was clear despite the fact that some of the connections contained as many rivets as would have been practical to install, and thus would have been considered rigid by most designers.

Similar conclusions were drawn from the definitive study of connection behavior carried out in Great Britain by the Steel Structures Research Committee headed by Batho and Baker in the 1930's (Batho and Rowan, 1934a,b). From these beam-to-column connection tests, which included top-and-seat angles and T-stub connections, it became apparent that most connection types had nonlinear moment- rotation response, even for low load intensities. As part of the same research effort, Batho and Lash (Batho and Lash, 1936) studied the effect of monotonically increasing loads on 13 bolted top-and-seat angle beam-to-column connections encased in concrete. The resulting moment-rotation curves showed that concrete encasement effectively increases the stiffness relative to bare steel specimens; the increase depended on the amount of reinforcement in the concrete. In these tests the increase in stiffness was due to the confining effect of the concrete, which prevented the vertical legs of the angles attaching the beam flanges in tension from separating from the column. Once the concrete cracked parallel to the column flanges, the stiffness of the connection became the same as the stiffness of the bare specimens. Tests to destruction showed that encasement did not increase appreciably the ultimate strength of the subassemblies. Further experiments on concrete encased connections reported by Batho (Batho, 1938) examined the influence of loading sequence. In these experiments he compared behavior of specimens loaded from a virgin state to that of specimens that underwent limited load reversals. The conclusions were that whatever the loading sequence, the stiffness of the encased specimens became the same as the bare steel specimens when the concrete confining the vertical legs of the angles attached to the tension flanges cracked. The most important result of the investigations carried out by the Batho and Baker team was the development of the original tools, the beam-line concept in particular, to analyze PR connections (Batho and Rowan, 1934b). Simultaneously in the US, Rathbun presented the experimental results of tests on 18 beam-to-column connections (Rathbun, 1936). All the specimens were bare steel and fastened by rivets.

He investigated the moment-rotation properties of web angle, top-and-seat angle, and T-stub connections. Most of the beam-to-column connections in this case were experimentally modeled as center line beam splices, and the specimens were tested as simply supported beams loaded monotonically at midspan. The main observations was that even weak riveted beam-to-column connections offer non-negligible restraint and result in nonlinear behavior.

Hechtman and Johnston (Hechtman and Johnston, 1947) conducted a large study on 47 different subassemblies. The purpose of their research project was to demonstrate that many connections that were considered to be pinned in practice offer a non-negligible amount of restraint. Accounting for this restraint could lead to considerable savings in structural steel. Hechtman and Johnston also divided the total rotation they measured in various components, and found that slip between plates is often the major contribution to rotation.

Munse et al. (Munse et al., 1959) tested web angle connections, and compared the effects of using hot-driven rivets versus using modern high-strength bolts. The main conclusions of this study were that the connections using high-strength bolts were stiffer, and that the rivets connecting the angle legs to the column flanges experienced permanent elongation at lower connection moments than did the high-strength bolts.

2.1.2 Cyclic Tests of Riveted Connections

Information about the behavior of riveted assemblages subjected to large load reversals is rather scant. During the investigation following the collapse of the first Québec Bridge in 1907 many experiments were conducted on various riveted details (Government Board of Engineers, 1919). Fig. 8 shows the experimental results of a cyclic uniaxial test performed on a riveted shingle joint. The figure shows a series of progressively larger cycles being applied to the specimen. Each division in the horizontal axis corresponds to an elongation of 0.01 in a 20 in. gage length or a strain of 0.0005. Each division in the vertical axis corresponds to 10,000 psi shear stress on the nominal area of the rivets. The evolution of the response of the joint to load is very interesting. The responses for the initial small load reversals are linearly elastic. With higher load amplitude, hysteresis develops, the response becomes very pinched, and a low stiffness slipping zone develops. The engineers noted that although there was a considerable variation of stiffness during a given cycle, the nominal strength of the joint was unaffected. Very similar behavior was described by Young and Jackson for small amplitude cyclic tests on riveted T-stub connections (Young and Jackson, 1934). They observed that even for cycles having rotation amplitudes smaller than 4 milliradians the behavior was not elastic and significant hysteresis was occurring.

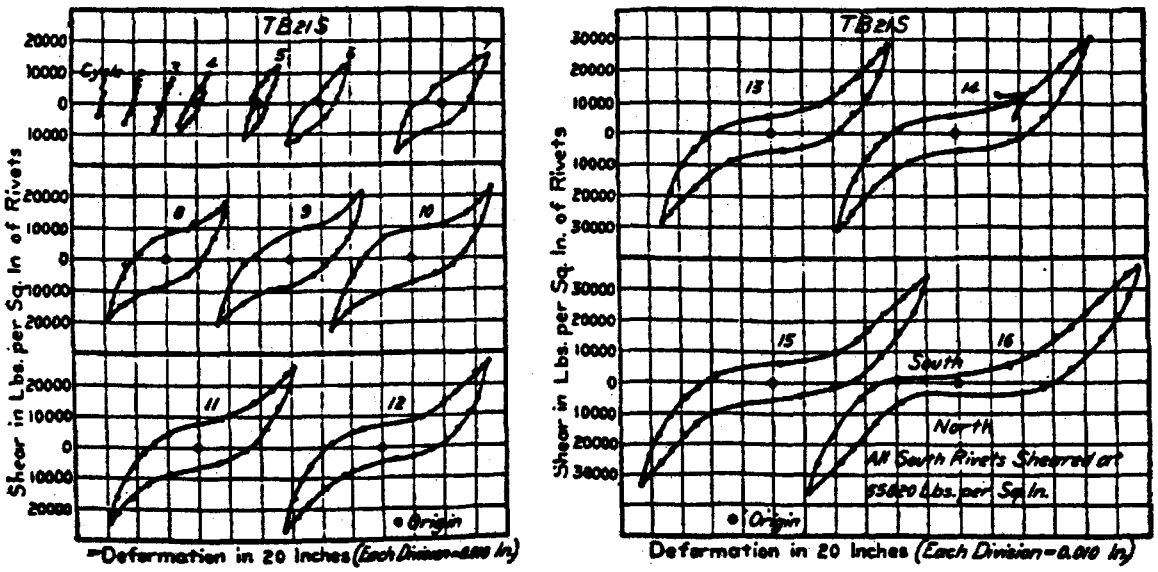

Figure 8 - Degradation of rivet shear behavior with cycling (Government, 1919).

More recently Roeder et al. (Roeder, 1994) conducted a large project aimed at assessing the strength, stiffness, and ductility of older riveted connections, including the effect of encasements. The specimens tested by Forcier and Leon (Forcier, 1994) compared the behavior of riveted and bolted connections. The specimens were interior T-stub connections, with 13 ft. high W14x99 columns and W18x50 beams. The flange connections were made with WT13.5x47, with eight 3/4" bolts or rivets in each T-stub to both the beam and column. The web connection was made with pairs of L8x6x0.5 with six bolts on each leg. Full details of the complete test series, which provides essential data for the strength evaluation of older steel frames including the effect of concrete encasement, are available elsewhere (Roeder et al., 1994).

The first three tests run by Leon and Forcier were on all-steel specimens, with the only variable being the connector type: rivets (A502 Grade 1) for specimen B4CR2, black bolts (A307) for B4CR1, and slip-critical bolts (A325) for B4CR3. Figure 9 illustrates the moment-rotation behavior of these specimens. The pronounced pinching behavior in the riveted specimen was surprising and contrary to what many researchers had assumed in the past. The pinching was due primarily to slip at the shear interface where very large local deformations had taken place. This in turn led to an elongation of the rivet and a rapid loss of any clamping action. The energy dissipation capacity decreased rapidly with increasing deformations, but the connection regained stiffness and strength once the rivets went into bearing. Typically these hysteresis loops would be considered unsatisfactory. However, the load history imposed was severe and in the real structure the connection would have benefited from additional restraints and force redistribution. Thus the performance of a structure incorporating these connections would probably be better than that determined from this type of isolated connection test.

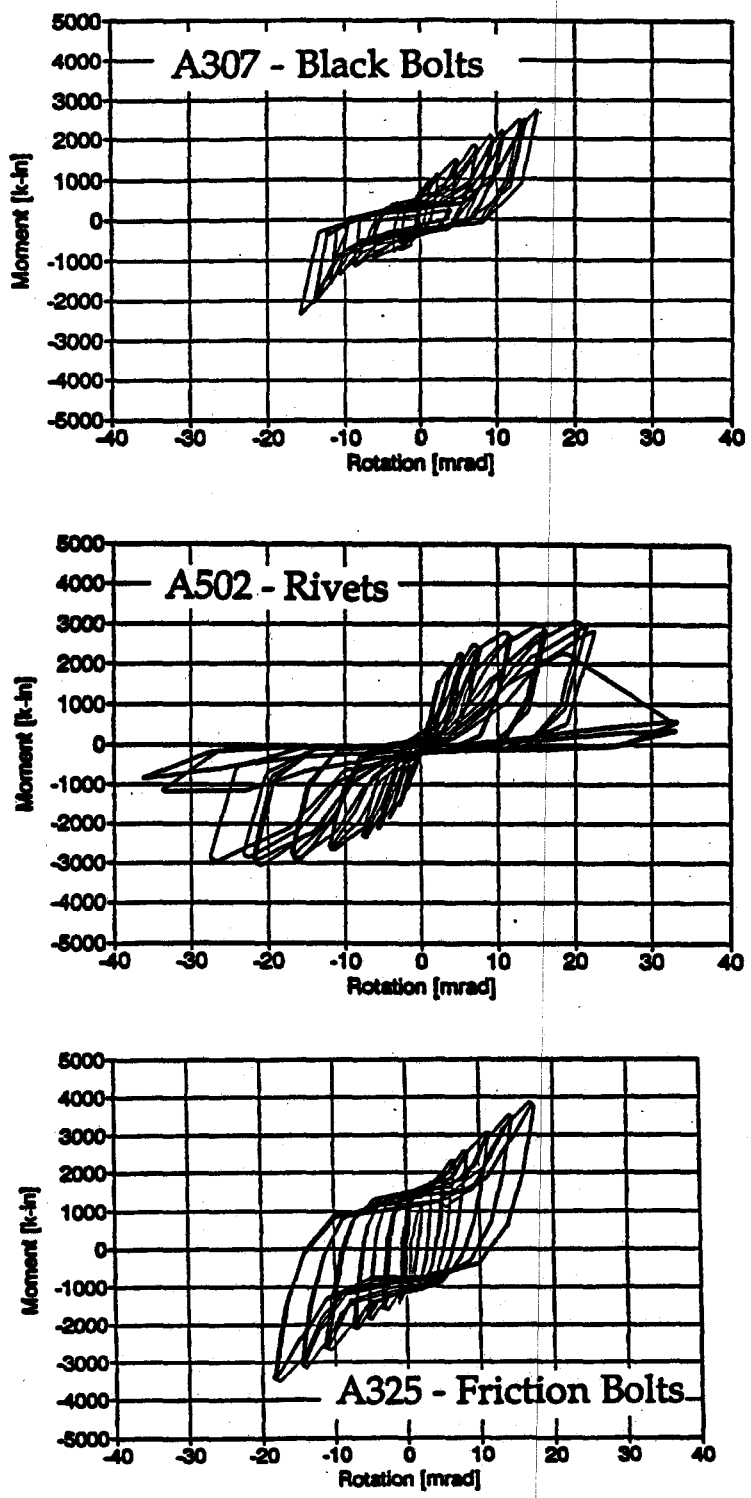

Figure 9 - Comparison of behavior for T-stub connections with A307 bolts, A325 bolts and A502 rivets.

In the remaining tests by Leon and Forcier, which included stiffened seats and the effect of encasement and floor slabs, the behavior improved markedly. The encasement increased both the strength and stiffness of the specimens even though there were no shear studs in the beam or column. In fact, the measured response indicated that the sections behaved as fully composite under cyclic loads until the concrete cover began to crush around drifts of 2.5%. The beneficial effect of the concrete cover was also surprising since the confinement steel was minimal (only 6x6x10-10 mesh around the flanges). The concrete also acted to restrain the slip. Although a crack formed at the beam-column interface early in the load history, it did not grow appreciably resulting in smaller rotations for the encased specimens than for the all-steel specimens. Two mechanisms can be postulated to explain this behavior. First, in the compression side of the connection the concrete transferred most of the force by bearing directly into the end of the T-stub and the column directly. Thus no appreciable shears were induced in the rivets and the resulting slip was very small. Second, in the tension side of the connection the rivet heads provided an additional load transfer mechanism by bearing, which in addition to the friction between the two materials, resulted in only the first few rivets being loaded to their yield in shear. As the loading progressed the web of the T-stub began to yield resulting in a stable hysteretic response. Connections governed by yielding in the beams or connecting plates performed better but at large deformations loss of cover resulted in large strength losses.

Another specimen tested as part of this series, Specimen B3RC5, had a riveted stiffened seat connection. During the fully reversed load cycles most of the subassemblage drift for this specimen originated from the beam-to-column connection rotations. The connection rotations in this specimen were dominated by flexure of the T-stub flanges and stretching of the tensile rivet groups connecting the T-stub to the column flange rather than shear deformations of the rivets connecting the T-stub to the beam. At the maximum drift of 6.5%, during the final monotonic load imposed on this specimen, the strength was beginning to decrease and both the reinforced panel and the steel girders were yielding.

Another important series of experiments, still underway, examining the performance of riveted connections under cyclic loading is that being conducted by Sarraf and Bruenau (Sarraf and Bruneau, 1994). In this case four stiffened seat angle connections taken directly from a 1910 building that was demolished in 1992 were tested and retrofit schemes proposed.

2. 2 Bolted Connections

2.2.1 Monotonic Tests

The feasibility of using bolts rather than rivets for steel connections was demonstrated first by Batho and Bateman (1934), and the feasibility of welded connections was shown shortly afterwards (Lyse and Gibson, 1936). In the US the impetus for the development of bolted connections was provided by the formation of the Research Council on Riveted and Bolted Structural Joints in 1947. The first ASTM standard for bolt material was issued in 1949 and appeared in 1951 as ASTM A325. There was a major effort in the early 1950s aimed at understanding the behavior of bolted connections and developing design guidelines. These

efforts were centered on issues related to static strength, fatigue, and control of pretension. They resulted in the widespread acceptance of bolted connections. An excellent overview of those efforts is given in (ASCE 1967; Kulak et al., 1987). Monotonic behavior of bolted connections will be discussed in latter sections of this paper in relation to design provisions.

Although bolted connections seemed to provide a substantial improvement over riveted ones, their widespread use in MFR's was short-lived. In the mid 1950's and early 1960's the interest in plastic design led to the development of welded moment connections (Pray and Jensen, 1956; Graham et al. 1959; Beedle and Cristopher 1964; ASCE-WRC 1971). The shift to fully welded connections seems to have accelerated in the late 1960's and early 1970's when welding technology made field welding feasible and economical. It is interesting to note that even at this stage a careful analysis of tests comparing bolted and welded connections would probably not have indicated a superior structural performance for the latter. Consider the data shown in Fig. 10 (Huang et al., 1971) which compares the behavior of a fully welded connection (C11) to that of two connections with plates welded to the column and bolted to the beam (C8 is a connection with friction bolts and C9 is a bearing connection).

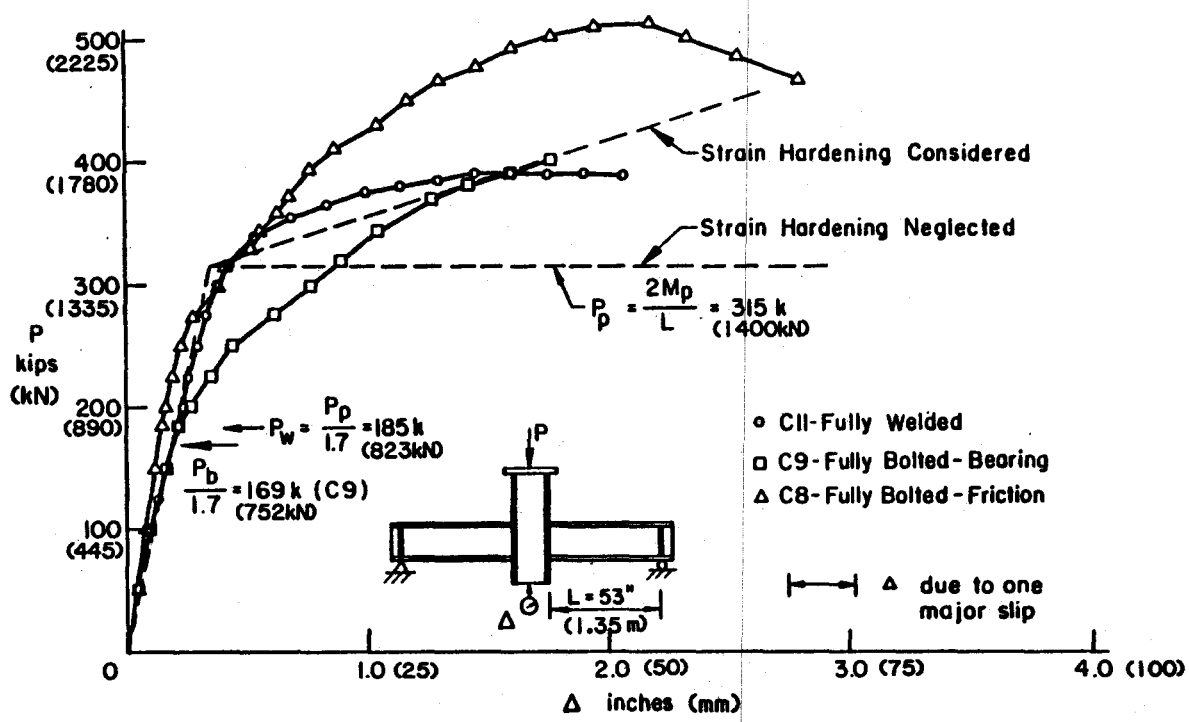

Figure 10 - Comparison of monotonic behavior between fully welded and welded-bolted connections (Chen and Lui, 1987).

All connections were between W24x61 beams and a W14x136 column stub. The friction bolted connection (C8) exhibits larger strengths and ductilities than the corresponding welded one, although the stiffness of the bolted connections decreased earlier than for the welded one. Even the bearing bolted connection (C9) provides surprising strength and ductility, with only moderate losses of stiffness.

2.2.2 Cyclic Performance

The interest on the cyclic performance of steel connections grew in the late 1960's and came to the fore in the early 1970's partially as the result of the increased research following the San Fernando earthquake. Much of the early work was carried out at the U. of Tokyo (Kato 1982), Lehigh University (Huang et al., 1971; Standig et al. 1975, 1976; Carpenter and Lu, 1973) and UC- Berkeley (Pinkney and Popov, 1967, Popov and Pinkney, 1969; Krawinkler et al., 1975; Krawinkler and Popov, 1981; Popov et al. 1985, 1993). The experimental work was complemented by analytical studies that led to the development of the design philosophy (Bertero and Popov, 1973) for welded connections that has predominated for the past 20 years. The behavior of the connections tested at UC-Berkeley has been reexamined in detail recently (Bertero et al., 1994) and that analysis will not be repeated here. In the next few paragraphs some experimental studies on bolted connections that are not well known will be highlighted. The intent is to provide some data that can be used for design.

2.2.2.1 Top-and-Bottom Plate Moment Connections

Most of the tests on FR connections have been carried out on all-welded connections, while some had plates welded to the column flange and bolted to the beams with high-strength bolts (Pinkney and Popov, 1967; Astaneh-Asl, 1995; Tsai and Popov, 1988). Pinkney and Popov's specimens consisted of a cantilever W8x20 beam connected to a W8x48 column stub with 0.5 in. thick plate welded to the column and bolted to the beam with ten 5/8" A325 bolts. In this series all specimens responded with stable and reproducible hysteretic behavior when cycled beyond their elastic limits. The bolted specimens had different hysteresis loops due to slippage at the plate-beam flange interface (Fig. 11). Final failures were by local buckling of the beam flanges and fracture of the net area of the connecting plates.

Similar results have recently been reported by both Tsai and Popov (1988) and Astaneh-Asl (1991). Details of the three specimens tested by Astaneh-Asl are given in Fig. 12 and the performance of the specimen is shown in Fig. 13.

Test results such as those shown in Fig. 13 indicate that properly detailed top-and-bottom plate bolted moment connections provide similar initial stiffnesses to fully welded connections. As the inelastic cycling increases the unloading stiffness of the bolted specimens decreases slightly, but the strength of the specimens continues to increase.

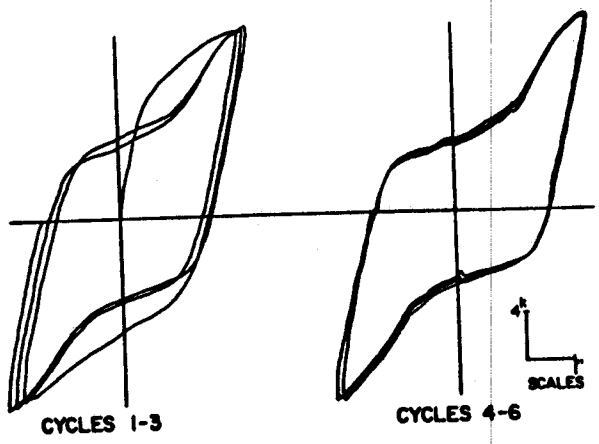

Figure 11 - Cyclic performance of welded-bolted connections (Popov and Pinkney,1969).

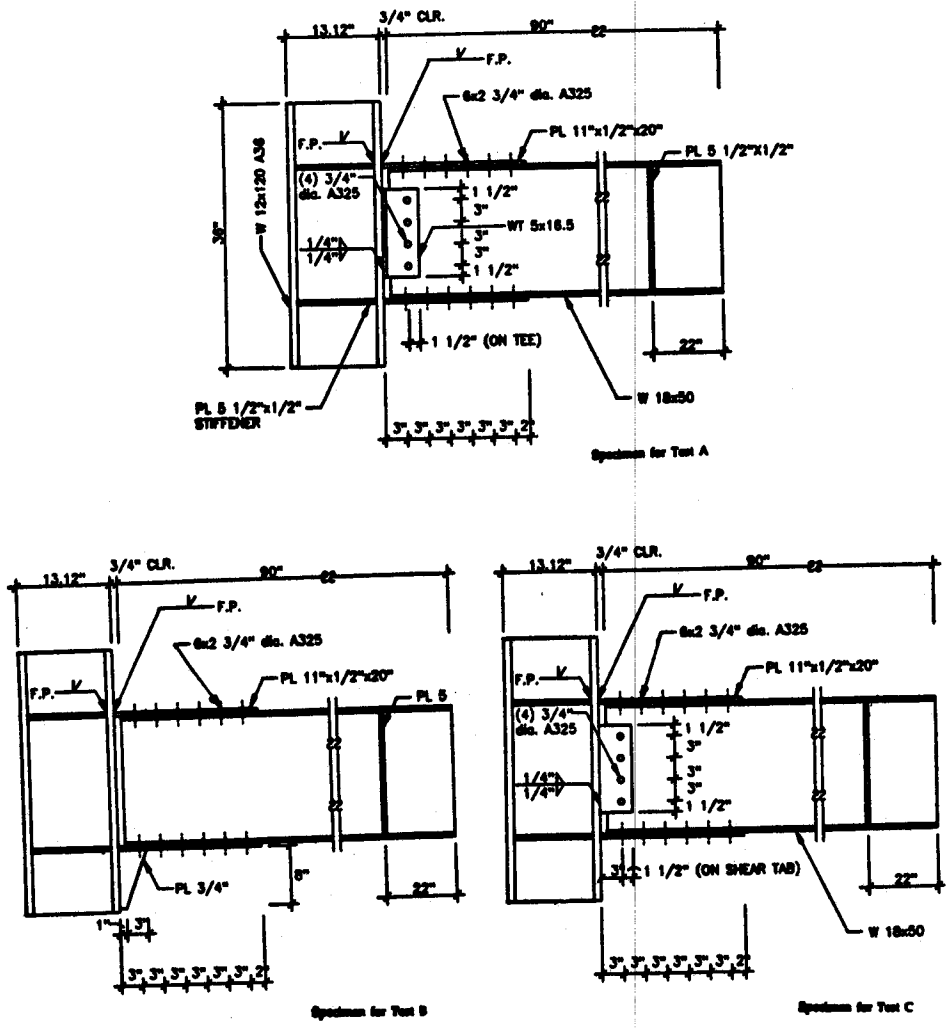

Figure 12 - Details of specimens tested by Astaneh-Asl (Astaneh-Asl et al., 1991)

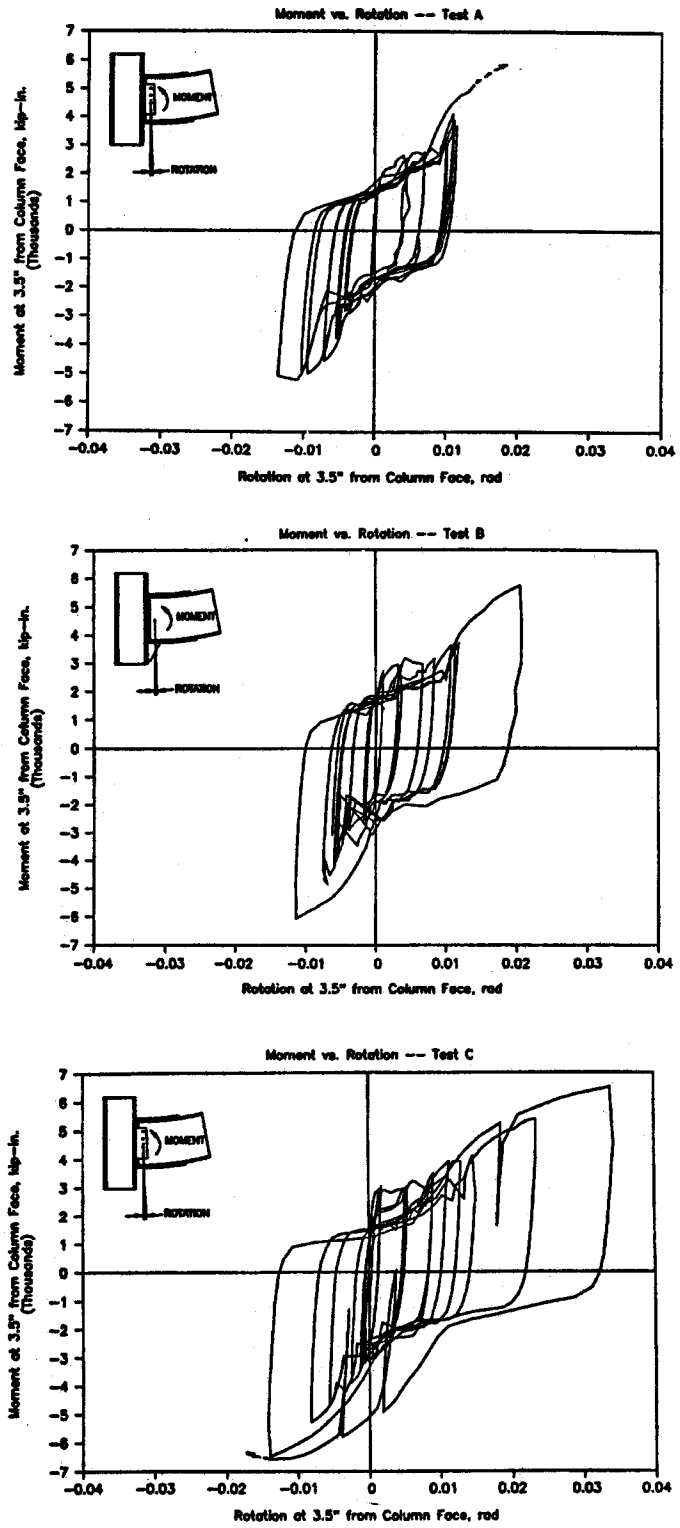

Figure 13 - Results of cyclic tests on welded-bolted connections (Astaneh-Asl et al., 1991).

The slip plateaus observed were stable and contributed to overall ductilities on the order of twice that of comparable fully welded specimens. The specimens with bolted connections, moreover, exhibited very little local buckling. Probably the most important behavioral observation from these tests is that when the connection is loaded in compression most of the yielding is concentrated between the first row of bolts and the column. When the load is reversed and the connection is loaded in tension, most of the yielding is concentrated in the plate between the first two rows of bolts. The fact that the energy absorption capacity of two different regions is being activated is the primary reason for the large ductilities achieved in these tests (Astaneh-Asl, 1995).

2.2.2.2 T-Stub Connections

As shown in Fig. 3, T-stubs are one of the strongest and stiffest bolted connections that can be economically built. Unfortunately there is a dearth of cyclic test data on this type of connection. Some of the most recent and carefully documented tests are those carried out in conjuction with a project on riveted connections (Thomas, 1992; Knetchel, 1992; Severson, 1993; Forcier, 1994; Roeder et al, 1994). Forcier's specimen B4CR1, whose details are given in Section 2.1.2, had A307 bolts installed in standard holes. The load-deflection response for this specimen was shown in Fig. 8(a). The behavior of this subassemblage was strongly influenced by local slipping of the bolts and by the yielding of the unreinforced panel zone. The evolution of the connection response can be described as follows: (1) during the first low amplitude cycles the connections responded linearly with a high initial stiffness, (2) at higher load amplitudes the frictional resistance of the T-stub web A307 bolt groups was overcome, and the T-stubs slipped with little resistance, (3) if the connection rotation was increased, all the bolt shanks eventually started to bear against the sides of the oversized holes and the stiffness increased again, and (4) unloading within the bearing zone occurred at a stiffness almost as high as the initial stiffness, and unloading at this high stiffness continued until the frictional resistance was overcome in the other direction. The frictional resistance diminished as the damage in the bolt groups increased. With diminishing frictional resistance the unloading behavior within the slipping zone changed from unloading at a stiffness of the same magnitude as the initial stiffness to unloading at the slipping stiffness. At the end of the experiment the bolts installed through the T-stub webs were loose and could be removed without tools.

Specimen B4RC3 was identical to B4RC1 except that it was assembled with A325 torque control bolts and the column panel zone was reinforced to prevent any yielding in that area (Fig. 8(c)). The specimen and its components showed no major deterioration or pinching for the range of displacements imposed upon it. The connection deformation process can be described as follows. Originally the bolts are not necessarily in bearing against the walls of the oversized holes. Until the frictional capacity of the T-stub web bolt groups is reached the connection assembly responds with high stiffness. Once the frictional capacity was attained the T-stub webs and the girder flanges slipped relative to each other until all the bolt shanks bore against the sides of the holes. With A325 bolts the slipping stiffness remained constant. While bearing against the hole sides the connection responded with increased stiffness. Upon unloading from this bearing condition the connection responded with stiffness of the same magnitude as the initial

stiffness. Unloading continued at this high stiffness until the slipping load was attained in the other direction. Here again the overall behavior of the connection was a direct consequence of the local behavior at the T-stub web-girder flange interface. The experimental data indicated that the slip resistance of the group of 8 bolts was about 70 kips or 8.75 kips/bolt, while the LRFD manual (LRFD, 1994) indicates a design value of 7.51 kips/bolt. Even with modern high-strength bolts the principal causes of deformation for the B4 connections were slips at the T-stub webs. The reversed cyclic response did not degrade because the high-strength bolts did not loose their pretension during the slipping motion. The deformations in the flanges of the T-stub were small and therefore the additional forces in the column bolts due to prying forces were assumed to not have influenced the behavior significantly.

The results of the work at the U. of Washington, where two similar but smaller specimen were tested (Thomas, 1992; Knechtel, 1992; Roeder et al. 1994), showed similar failure modes. These specimens consisted of S15x42.9 beams fastened to W12x79 columns with a T8x28.5 section and eight 3/4" A307 bolts to the beam and four similar bolts to the column flange. The bolt holes were carefully machined to ensure a very tight fit of the bolts so that the action of rivets, where there is no hole clearance, could be modelled. In addition the bolts, which were A325, were tightened to simulate the clamping force of the rivets. One of the specimens (Specimen T1) was tested monotonically and one (T2) cyclically, and both failed due to shearing of the bolts. Companion encased specimens (T3 and T4) showed similar performance to the unencased ones, but with increasing strength and stiffness until the concrete crushed at drifts of 2.5% to 3%. Specimen T6 was, similar to T4, subjected to 4 cycles rather than 2 at each deflection level and showed excellent toughness. Specimen T5, with a reduced number of bolts (six instead of eight) resulted in yielding of the tension bolts and flexural yield of the T-stub. The results obtained in these specimens were consistent with those of Batho and Rowan (1934a).

2.2.2.3 End Plate Connections

Another type of bolted connection that can provide nearly FR connection performance is the thick end plate. Numerous monotonic tests on this type of connection have been reported in the past decade, but until recently there were only a handful of cyclic tests. End plate connections require good control of materials and fabrication tolerances. As such, some fabricators have preferred other types of moment connections. With the increasing use of CNC fabrication equipment, end plate connections have consistently gained popularity. In addition, end plates have traditionally not been considered desirable for seismic applications because the pretension in the bolts to the column may be lost early on in the cyclic loading and prying forces can lead to unexpected failures of the bolts in tension. Careful design, however, can prevent this problem.

Astaneh-Asl (1995) tested two end plate connections between a A36 W18x40 and a rigid column stub (Fig. 14). These connections, which were fillet welded, were designed following the existing AISC recommendations which were not meant for seismic applications. The first specimen, designed as above, showed excellent cyclic behavior with yielding occurring in the beam and the final failure controlled by local buckling at rotations exceeding 0.014 radians (Fig. 15(a)).

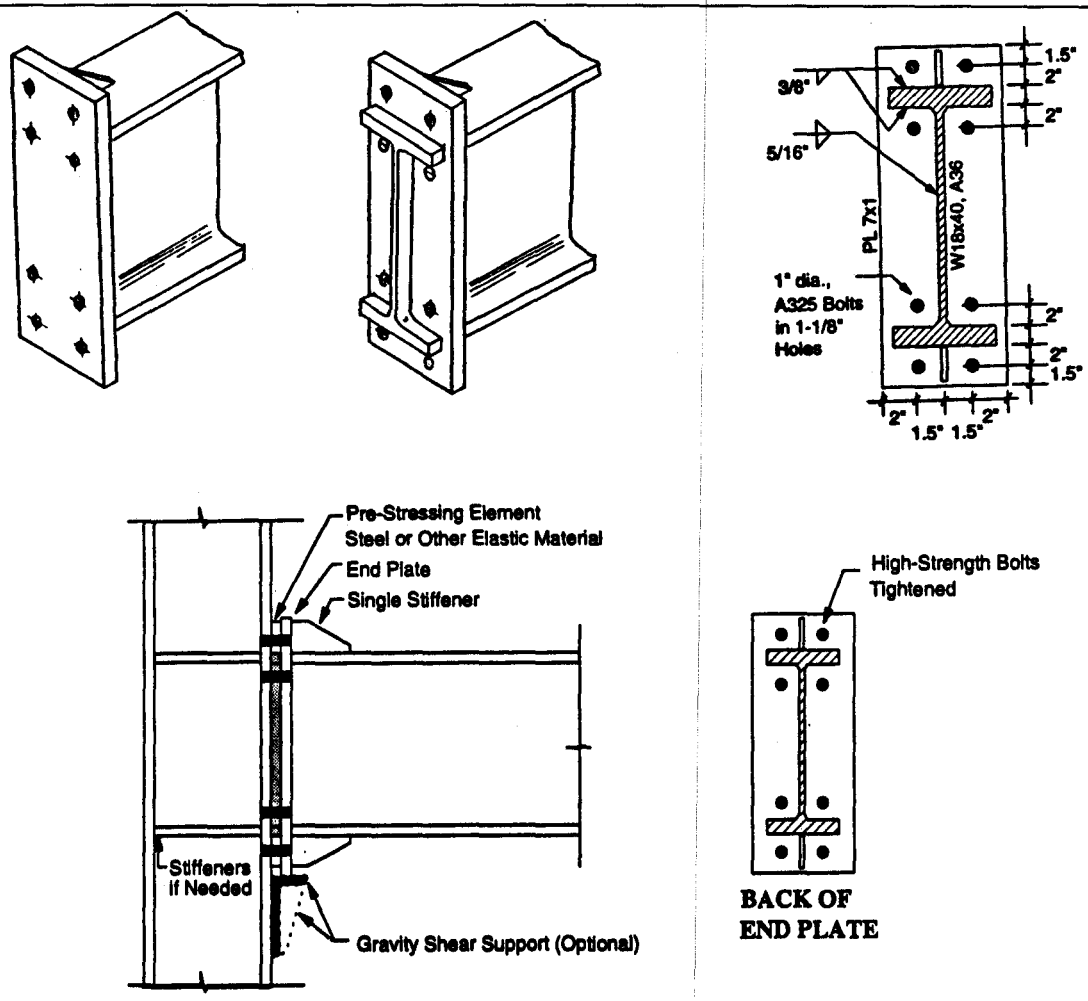

Figure 14 - End-plate specimens tested by Astaneh-Asl (Astaneh-Asl, 1995).

The second specimen was designed to obviate some of the fit-up and loss of pretension objections often raised when end plate connections are specified. In this case the beam is fabricated 1/2" to 3/4" shorter than needed and the gaps behind the plates were filled with a thin I-shape plate cut from the same beam size. This small plate is precompressed when the bolts are fully tensioned, eliminating both prying action and extreme variations in bolt tension under seismic loading. The performance of the specimen was excellent until the thin I-shape began to yield in compression, leading to loss of pretension in the bolts. Final failure was again primarily due to local buckling after the connection rotations exceeded 0.01 radian (Fig. 15(b)). The author concluded that the concept is sound but that a larger and/or stronger spacer element will be needed in order to preserve the elastic behavior of that component.

Chasten et al. (Chasten et al., 1989) also carried out tests on six large end plate connections to examine the effect of fully pretensioned bolts vs. snug tight ones. Their specimens included W27x94 beams attached to W14x193 columns with 1" and 3/4" thick end plates. Their tests indicate that under static load reversals the difference in performance due to bolt tightening were small, and that in fact snug tight connections may perform better if the additional bending and prying forces that arise in thin end plates are accounted for in design.

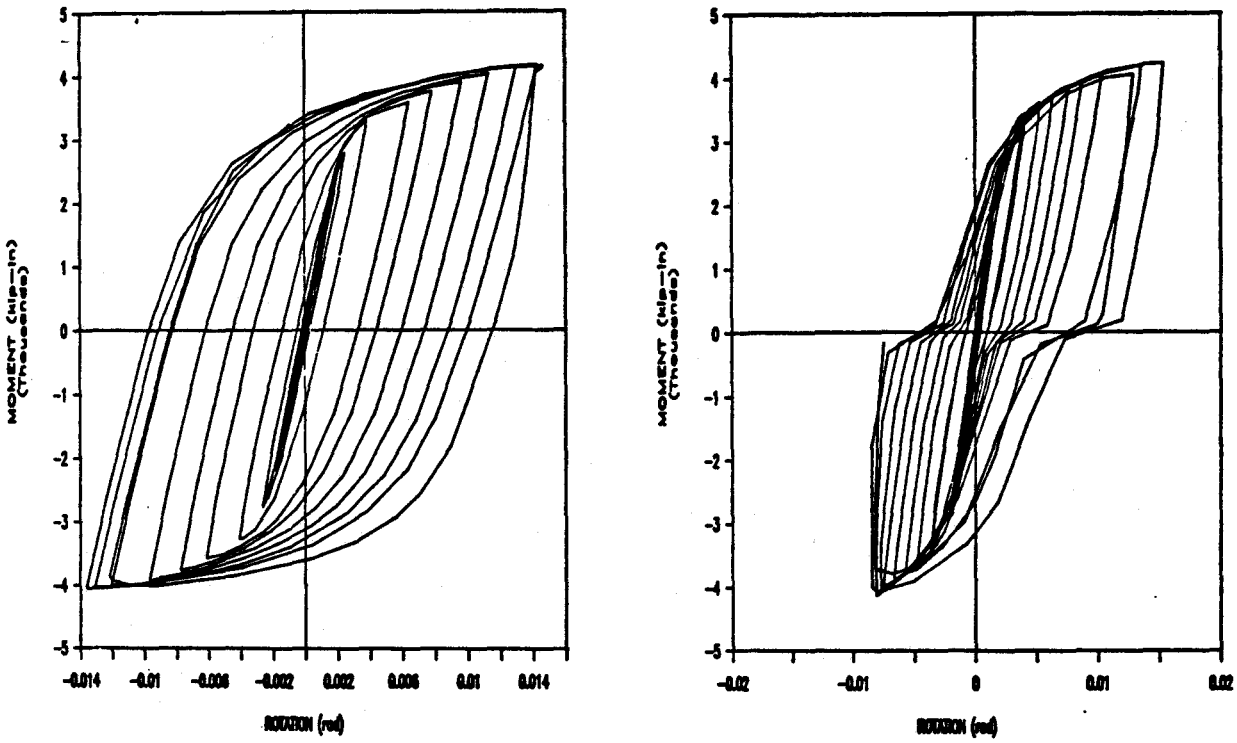

Figure 15 - Behavior of end-plate connections (Astaneh-Asl, 1996).

More recently Ghobarah et al. (1990, 1992) and Osman et al. (1993) have reported on an extensive research effort looking at the cyclic performance of end plate connections. The first series of test consisted of five cantilever-type specimens with a W14x30 beam framing into a W14x43 column stub. In these specimens a doubler plate was used to eliminate panel zone shear deformations. All connections consisted of a full penetration welded end plate connected to the column with eight 1" diameter A490 bolts. The first specimen (A-1) had a 1 in. thick end plate and no column flange stiffeners. It behaved well initially but as the tip displacements exceeded 50 mm large local deformations of the column flange were observed. This led to the loss of pretension in the bolts and the final failure was attributed to the excessive lateral deflection of the column flange. Specimen A-2 had a 1 in. thick end plate and column stiffeners to obviate some of the problems observed in Specimen A-1. Specimen A-2 performed well but beam web buckling began at tip displacements of about 50 mm. Flange local buckling and loss of pretension in the bolts was also observed as the displacement increased above 50 mm. Specimen A-3 was similar to A-2 but incorporated two triangular stiffeners 3/8" thick on the exterior of the end plate to stiffen the connection. This additional stiffener shifted the local buckling away from the end plate but led to a failure by local and lateral torsional buckling of the beam. Specimen A-4 was similar to A-1 except that the end plate thickness was reduced to 3/4", resulting in an end plate that was somewhat underdesigned according to some present recommendations (Morris and Packer, 1987). The specimen performed well initially, but a

cleavage crack initiated at the toe of the weld between the end plate and the beam flange at tip displacements of about 50 mm resulting in a progressive loss of strength with cycling. Specimen A-5 was similar to A-3 but had a 5/8" thick end plate. The performance, again, was excellent and similar to A-3. Near the end of the test a crack developed at the toe of the weld between the beam flange and the end plate stiffener. The main conclusion from these tests was that a properly detailed end plate connection can perform well even when subjected to large seismic excitations.

Ghobarah et al. followed with work with four additional tests in which the emphasis was on panel zone deformations (Ghobarah et al., 1992). This work showed that energy dissipation in the panel zone provided a very stable energy-dissipation mechanism. On the other hand the authors found that current design recommendations for panel zones, originally devised for fully-welded connections, did not work well for end plate connections.

Finally, Murray et al. (Murray and Meng, 1996) are conducting a study on the behavior of large beams with end plate connections. At least 27 tests are contemplated as part of this effort. The tests are being carried out on cantilever specimens with three combinations of beams and columns: W18x35 beams to W14x145 columns; W24x62 and W24 x76 beams to W14x287 columns; and W36x135 beams to W14x311. In addition to the standard rolled beams some 24" deep built-up welded sections are also being tested, and some of the weld details are being varied from one specimen to the next. The connections consist of thick end plates with four or eight large diameter (1" and 1-1/4") bolts (both A325 and A490) top and bottom. The failure modes observed include local flange buckling, flange fracture, and fracture of the flange-to-web weld in the built-up sections. Flange fracture occurred only in the specimens which had weld access holes. All of the hot-rolled specimens without weld access holes failed by local flange buckling. The preliminary conclusions are that end plate connections can provide good seismic performance if properly designed, but that care is needed in the welding and detailing. Fig. 16 shows the behavior of a connection between a W24x62 beam to a W14x287 column with a 1.5" thick end plate. This data shows that a properly designed end plate connection can provide excellent ductility and energy dissipation.

2.2.2.4 Top-and-Seat Connections

There are numerous cyclic tests on top-and-seat angle connections, which is one example of the more flexible kind of PR bolted connections available (Fig. 3). The most comprehensive test series is that by Almann, Azizinamini et al. (Altmann et al., 1982; Azizinamini et al., 1985; Radziminski and Azizinamini, 1986) who tested 18 subassemblies with varying sizes of components. The specimens were of cruciform shape, and consisted of two girders attached to a central column stub. The free ends of the girders were simply supported, and the load was applied vertically at the column stub. The main conclusions of this study were that (1) connections have an early nonlinear response, and (2) when subjected to cyclic load reversals, the bolted top-and-seat angle connections respond with stable and reproducible hysteresis loops.

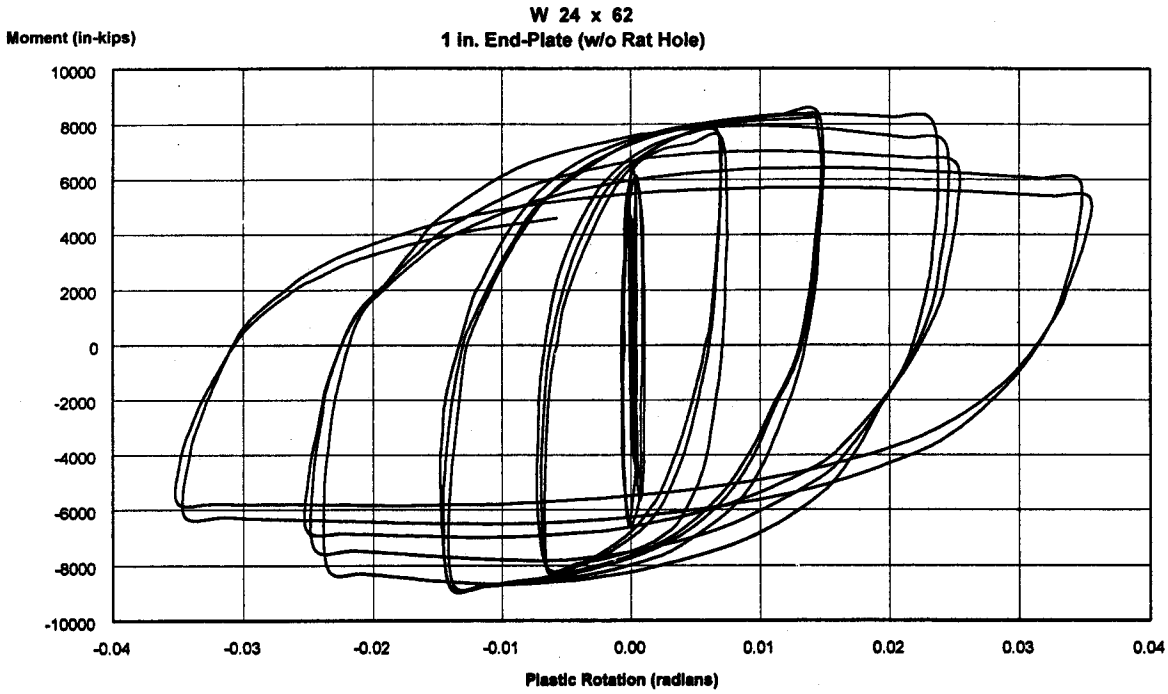

Figure 16 - Behavior of large end-plate connection.

Since the angles work by creating hinges next to the first bolt line in the beam and column, care must be exercised in detailing. The discrete sizes of angles available effectively limit the force that can be transferred, making this an ideal partial strength connection for areas of low to moderate seismicity. Another controlling factor is the number of bolts that can be installed in an angle leg, since as the thickness of the angles increase the bolt shear strength may begin to govern. Some of these detailing issues have recently been addressed by Mander et al. (Mander, 1994) who found that the inelastic fatigue life of these connections depended strongly on the location of the formation of the first yield line. In situations where tight clearances occur, as is often the case with this type of connection, even the orientation of the bolt and/or nut head appears to have a significant impact on the fatigue resistance.

The viability of using this type of connection has been also verified by extensive work at the University of Colorado by Gerstle et al. (Moncarz and Gerstle, 1981; Marley and Gerstle, 1982, Stelmark et al., 1986) who conducted tests on both isolated specimens and one- and two-story subassemblages as well as extensive analytical frame studies. Similar results have been reported by Leon and Shin (Leon and Shin, 1995) who tested a half-scale, two-story, two-bay PR steel frame under slow cyclic lateral loading (Fig. 17).

The frame contained partial strength top-and-seat angle connections with stiffness characteristics in the middle of the partially restrained range of connection behavior. In addition to the frame, three isolated connections similar to those used in the frame were tested to obtain moment-rotation curves. Based on the isolated connection test results a hysteresis model for these semi-rigid connections was developed. This model was used a priori to

predict the behavior of the two-story frame. The numerical results using the connection model showed excellent agreement with the experimental results.

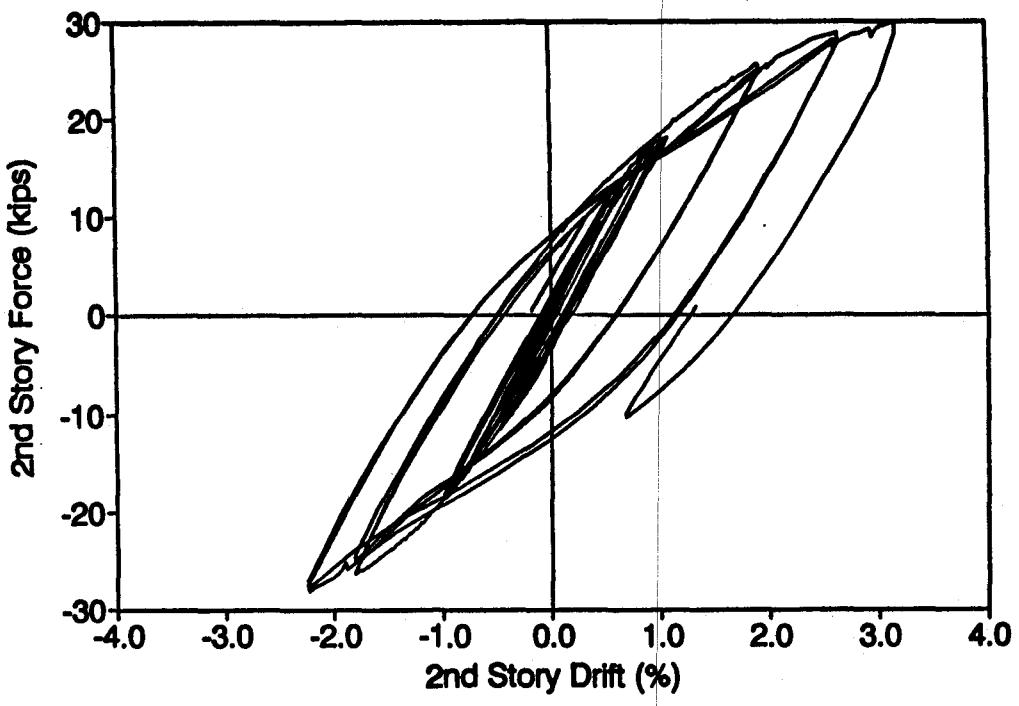

Figure 17 - Load-deflection response for the second floor of a PR frame (Leon and Shin, 1995).

The experimental results showed large redistribution of forces and good stiffness, energy dissipation capacity and hysteretic response. The load-deformation response of the frame shown in Fig. 16 indicates that if numerous of these connections are used in an unbraced frame, the system will perform well under reversed cyclic loads.

Another interesting series of 10 tests on top-and-seat angels was conducted by Roeder et al. (Roeder et al. 1994; Thomas, 1992, Knetchnel 1993). These tests were run to simulate older riveted connections, but used tightly fitted steel bolts instead of rivets. The specimens were about 85% of full scale for small connections in a 1926 building still in use in San Francisco. The beams were W14x22, the columns were W10x66, and the top-and-seat angles were L5x3.5.5/8 for the flanges and L3.5x3x5/16 for the web. Both encased and unencased specimens were tested and the number and strength of the connectors varied. For connections with A307 bolts, with two 3/4" bolts to the column and four 5/8" to the beam, the behavior was governed by the shear yielding of the connectors. Substituting A490 bolts for all of the A307 ones resulted in a shift of failure mode to flexural yielding of the angles. Substituting the bolts to the beam with A490 bolts and decreasing the connection to the column to two 1/2" A307 bolts resulted in a failure mode governed by yielding of the tensile connectors. In most specimens the effect of encasing was very large, with large increases in strength and stiffness. Fig. 18 shows a typical comparison of monotonic curves for bare vs. encased specimens. The monotonic results provided a good envelope for the cyclic tests. It should be noted that once the concrete crushed, generally at drifts of 2.5% to 3.0% , the behavior reverted to that of a bare specimen. The

increases in stiffness and strength below this level, however, have important implications for seismic design and evaluation. A clear indication of the effects of shifting failure modes is seen in Fig. 19 which compares the energy dissipation capacity with accumulated rotation for three encased specimens. The desirability of obtaining flexural yielding in the connection elements is obvious from this data.

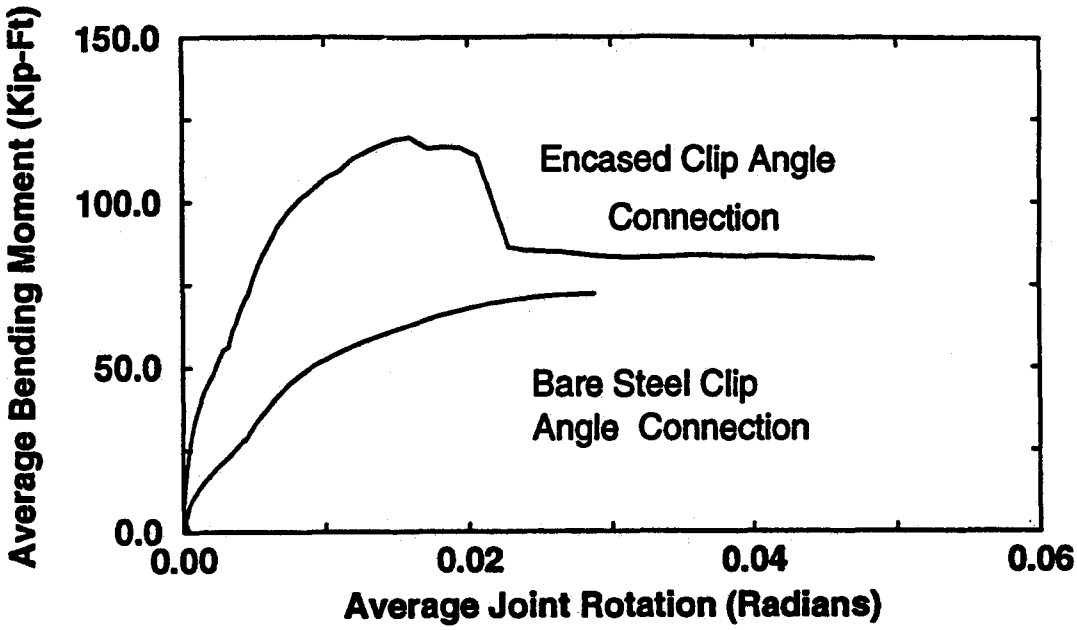

Fig. 18 - Comparison of bare steel and encased moment-rotation behavior (Roeder et al., 1994).

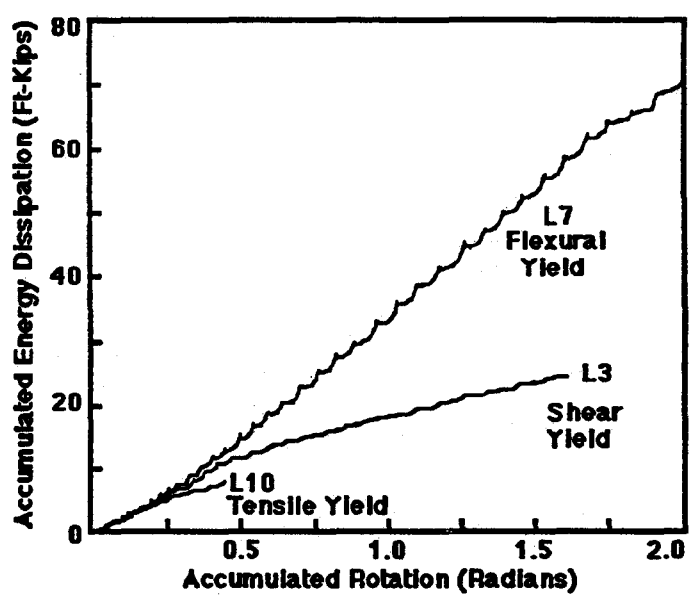

Figure 19 - Comparison of energy dissipation capacity for different failure mechanisms for encased top-and-seat angle connections (Roeder et al., 1994).

2.2.3 Additional Studies

One of the greatest drawbacks of the existing research on the behavior of steel connections under cyclic loading is that there exist very few if any test series in which a systematic variation of connection details allows the reader to make meaningful comparisons. The only exception is a series of tests conducted by Ballio et al. [1987] in Italy in the mid 1980's. Although this test series contains some detailing that is not common in the US and was conducted on relatively small specimens, it will be discussed here because it clearly shows that small changes in detailing can have a significant impact on performance. The series consisted of fourteen exterior connections between IPE 300 beams and columns. An IPE 300 has b_f= 150 mm (6 in.), t_f = 10.7 mm (0.42 in.), h = 300 mm (12 in.) and t_w = 7.1 mm (0.28 in.); it corresponds roughly to a W12x30. The nominal yield strength was Fe360 (52.2 ksi), roughly the equivalent of a A572/50 section. The columns were 2.7 m high (106 in.) and the beams were 1.35 m. (53 in.) long and were subjected to a series of cycles at increasing amplitude following the ECCS recommended load history (ECCS, 1986). The latter is very similar to the ATC-24 protocol currently being used in the US (ATC-24, 1992).

Series A (Fig. 20): This series comprised four specimens of connections welded to the column and bolted to the beam flanges. The connection plates used were 14 mm (0.55 in.) for the flanges and 12 mm (0.48 in.) for the webs. All bolts were 20 mm, Type 8.8 (0.8 in. diameter, A490 bolts). All specimens included 14 mm (0.55) thick continuity plates in the columns. The performance was as follows:

(a) Specimen A1 was the control specimen and did not incorporate any additional details. Beginning around a deformation of 50 mm (2 in.) large panel zone deformations were noted, along with failures of some of the fillet welds in the continuity plates . At a deformation of 60 mm (2.4 in.) the welds between the column flange and the beam plate began to crack, leading to a complete failure during cycling to 100 mm (4 in.). The pinching of the hysteresis loops observed from early in the tests is due to bolt slippage. The slip resistance, from design specifications of that time, would have been 45 kN (including a ϕ factor of 0.7), while the nominal shear strength would have been 173 kN.

(b) Specimen A2 included a diagonal 10 mm (0.48 in) thick stiffener in the panel zone in order to limit the large shear deformations observed in specimen A1. The hysteresis loops indicate that slippage began at the displacement of 20 mm (0.8 in) . Cracking of the welds between the column and the beam began at 30 mm (1.2 in.) and the specimen failed when the bolts sheared at 60 mm (2.4 in.).

(c) Specimen A3 included 12 mm. (0.48 in.) thick doubler plates in the beam as internal cover plates and performed similar to Specimen A1. The behavior of A3 was similar to that of A1, with large shear deformations observed in the panel zone at 40 mm (1.6 in.), some weld cracking in the connection plate observed at 60 mm (2.4 in), alternating shear buckling of the panel zone, some damage to the beam web and necking of the connection plate at 100 mm (4 in.).

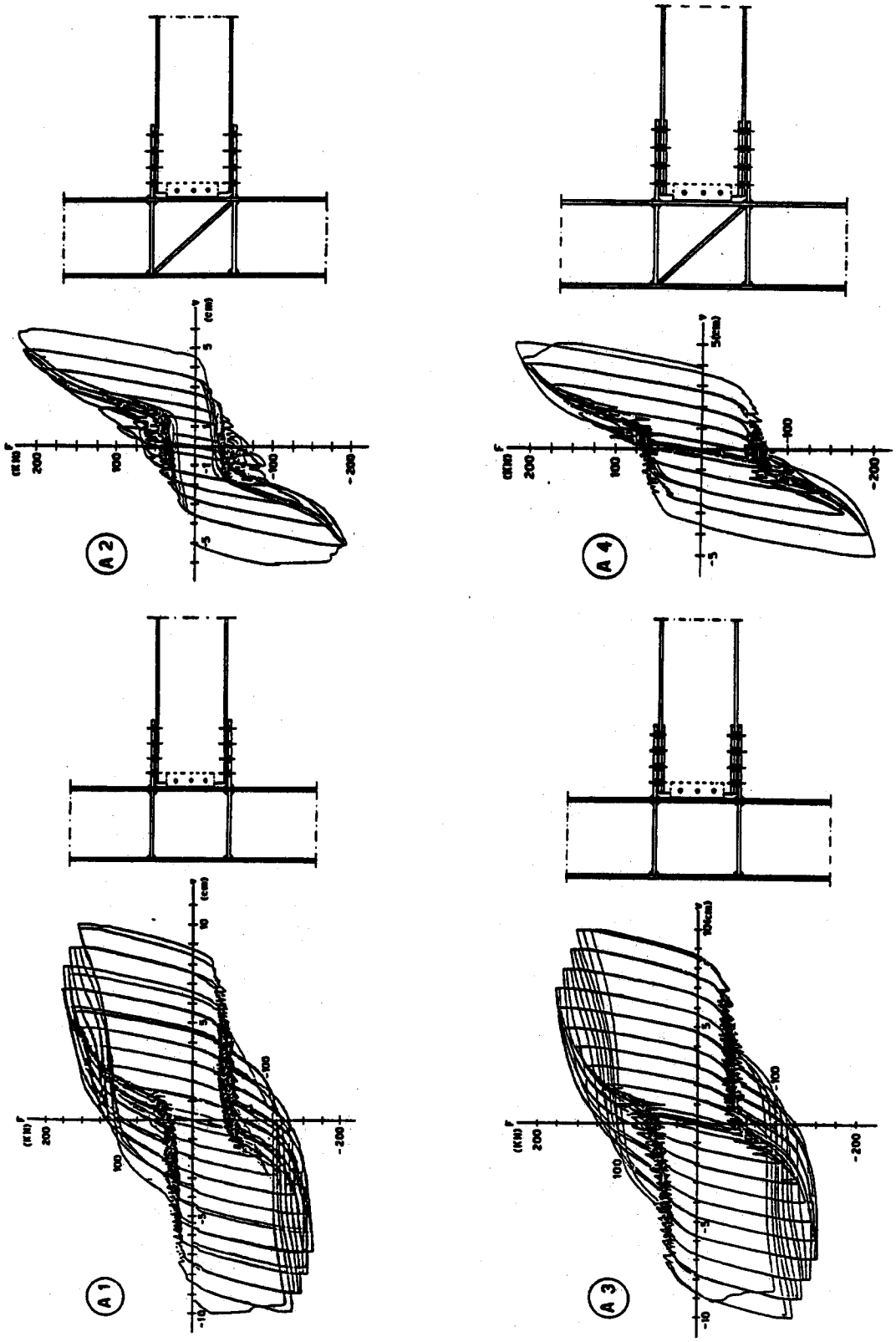

Figure 20 - Performance of welded-bolted connections (Ballio et al., 1987).

(d) Specimen A4 included both of the details used in A2 and A3. It behaved like A2, with slipping of the bolts starting early in the test, followed by some weld cracking, necking of the connecting plate at 40 mm (1.6 in.) and failure due to shearing of the external bolts.

Series B (Fig. 21): This series comprised four specimens of top-and -seat angle connections. The flange angles were 100 x 150 x 14 mm (4 x 6 x 0.55 in.; roughly a L 6 x 4 x 9/16), 150 mm (6 in.) wide, while the web angles were 60 x 60 x 8 mm (2.36 x 2.36 x 0.31 in.; roughly a L 2.5 x 2.5 x 5/16) , 200 mm (8 in.) wide. Four 20 mm, Type 8.8 (0.8 in., A325) bolts were used for the connection to the each beam flange, while two 24 mm (1 in.) bolts were used for the connection to the column and 16 mm. (0.63 in.) diameter bolts for the webs. The behavior was as follows: (a) Specimen B1 was the control specimen. The slippage of the bolts and the large relative flexural deformations between the connection elements observed early in the test are characteristic of this type of connection. Deformations between the angle and beam flanges reached 6 mm (1/4 in.) at beam end displacements of 30 mm (1.2 in.). Large flexural deformations of the angles were then observed as the cycling progressed, with the failure occurring at 70 mm (2.8 in.) due to the formation of a large crack in the angle.

(b) Specimen B2 included small stiffeners welded to the column flange and web to improve the prying action behavior. The local effects due to these stiffeners resulted in local deformation of the column flanges, including the portion between the angles. The large deformations in the angles beginning at 30 mm (1.2 in.), led to progressive cracking of the angles at the heel and ultimately to failure due to a large crack in the angle heel next to the first row of beam bolts.

(c) Specimen B3 included diagonal stiffeners in the angles aimed at limiting the deformation of the angle legs. The addition of these stiffeners resulted in larger deformations in the column flanges adjacent to the bolts, leading to some cracking of the stiffener welds in that area. The bolts to the columns showed large flexural deformations (60 mm or 2.4 in.), and the welds in the stiffening plates in the angles began to fail at deformations of 70 mm (2.8 in.). The final failure occurred by a crack propagating through the column flange at the upper corner of the panel zone next to one of the angles at a deformation of 90 mm (3.7 in.).

(d) Specimen B4 included both of the details of B2 and B3. The welds of the stiffening plates added to the angles began to crack at 30 mm (1.2 in.), and one of them failed on the column side at displacements of 60 mm (2.4 in.). The final failure mechanism was similar to that of B3.

Series C (Fig. 22): This comprised four end plate specimens with continuity plates. The column flanges and webs were thickened in the connection region in order to limit the flange distortions and improve the ability to model analytically the behavior of the joints. The thickened column flanges were made from a 20 mm thick Fe 510 (0.8 in, Fy = 75 ksi) plate, while the end plate thickness were 20 mm (0.8 in.) for specimens C1 and C2 and 30 mm (1.2 in.) for specimens C3 and C4.

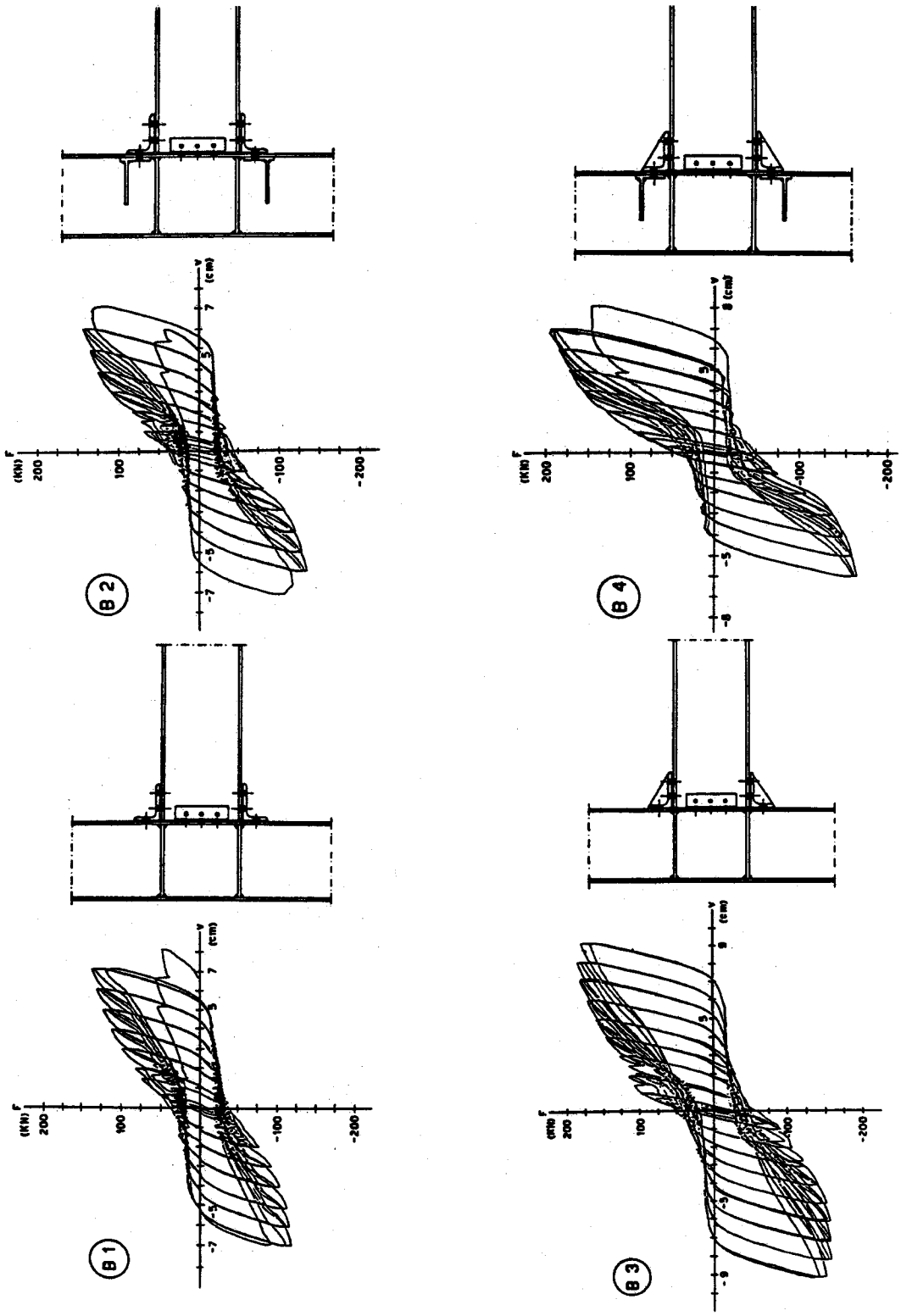

Figure 21 - Performance of top-and-seat angle connections (Ballio et al., 1987).

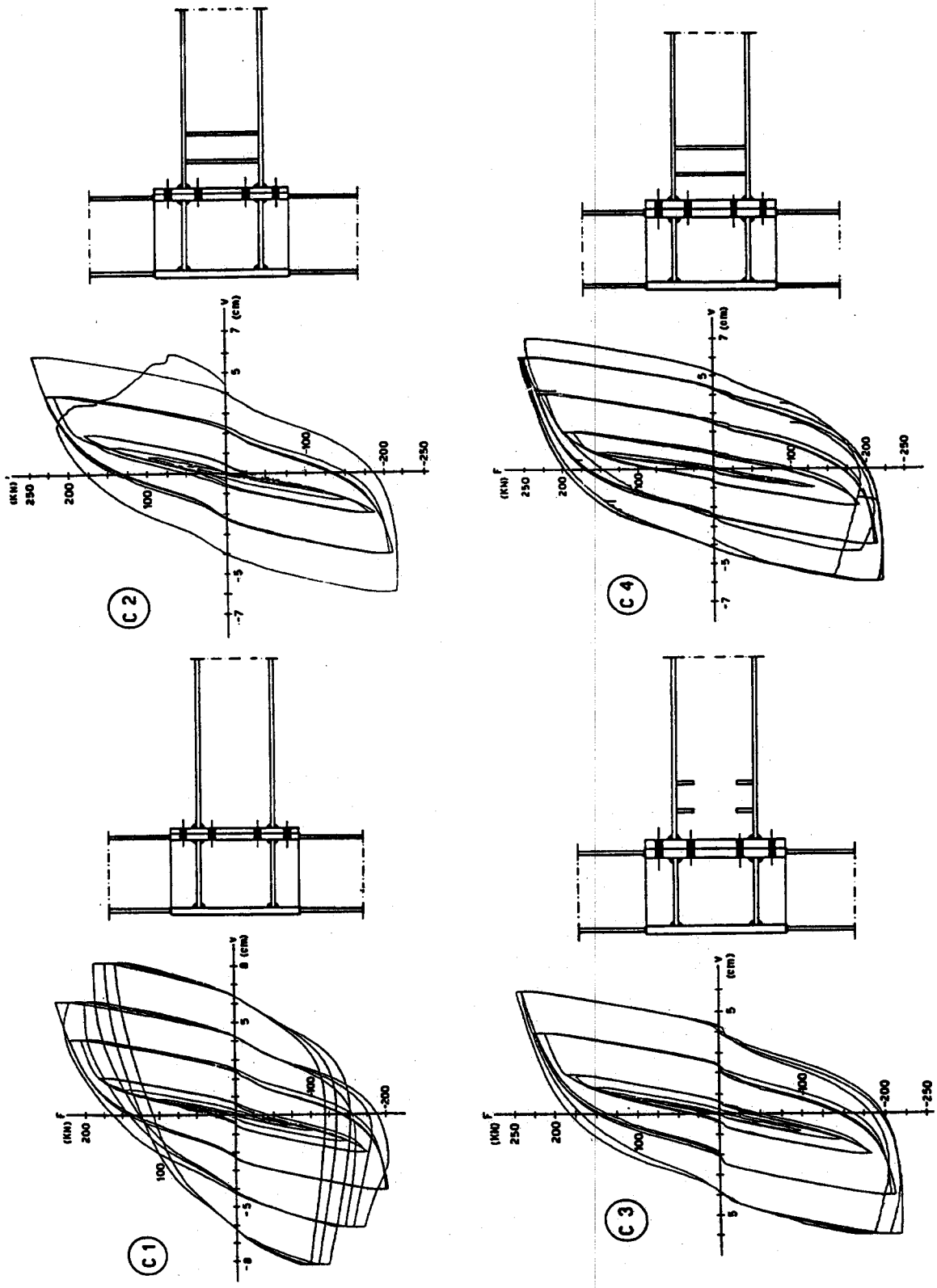

Figure 22 - Performance of end-plate connections (Ballio et al., 1987).

(a) Specimen C1, with a 20 mm (0.8 in.) end plate performed very well, with good energy dissipation and relatively little loss of strength up to 50 mm (2 in.) At 60 mm. (2.4 in.) the beam flanges began to buckle, leading to a progressive loss of strength. Very large deterioration began to occur at 80 mm (3.2 in.) when the local buckles became excessive.

(b) Specimen C2 included two full 10 mm thick stiffeners in the beam aimed at limiting the local buckling in that region. It behaved very much like B1 up to 40 mm (1.6 in.), but with cycling at 60 mm (2.4 in.) one of the welds between the beam flange and the end plate began to crack leading to an early failure.

(c) Specimen C3 had 30 mm (1.2 in.) thick end plates and included partial, triangular stiffeners in the web in order to control the local buckling. The intent was to provide some relief to the local buckling without providing as much stiffening as the full stiffeners used in C2. This connection behaved like B1 but shifted the local buckles away from the connection face. This resulted in very stable behavior with excellent energy dissipation capacity and no loss of strength.

(d) Specimen C4 had 30 mm (1.2 in.) thick end plates and contained full stiffeners. Its behavior mirrored that of C2.

Series D (Fig. 23) This series consisted of fully welded connections:

(a) Specimen D1 was the typical fully welded connection. The deformations were mostly by panel zone shear which led to very stable, large hysteretic loops. The final failure occurred by fracture of the main welds at 90 mm (3.6 in.) of displacement.

(b) Specimen D2 had a large stiffening plate (248 x 500 x 10 mm, 10 x 20 x 0.4 in.) in the column web. The stiffening effect of this plate led to a shifting of the failure mode to local buckling of the flanges in the beams, beginning at displacements of 60 mm (2.4 in.). This led to a progressive loss of strength and final failure of the specimen by excessive deformations in this area.

Conclusions: Based on the results obtained above, the researchers noted that often there is a tradeoff between strength and energy dissipation capacity. Fig 24 shows a comparison of the energy dissipated (Ω), the maximum strength (F_{max}) and strength at ultimate (F_u), and the maximum displacement (v_u) for the entire test series. This figure shows, for example, that adding the diagonal stiffener in the joint in series A leads to higher maximum strengths but significantly lower energy dissipation capacity. Careful interpretation of all the results leads to the conclusion that if connections of Type A1/A3 and C3 can be detailed to prevent or delay final weld failure, connections with excellent energy dissipation capacity can result.

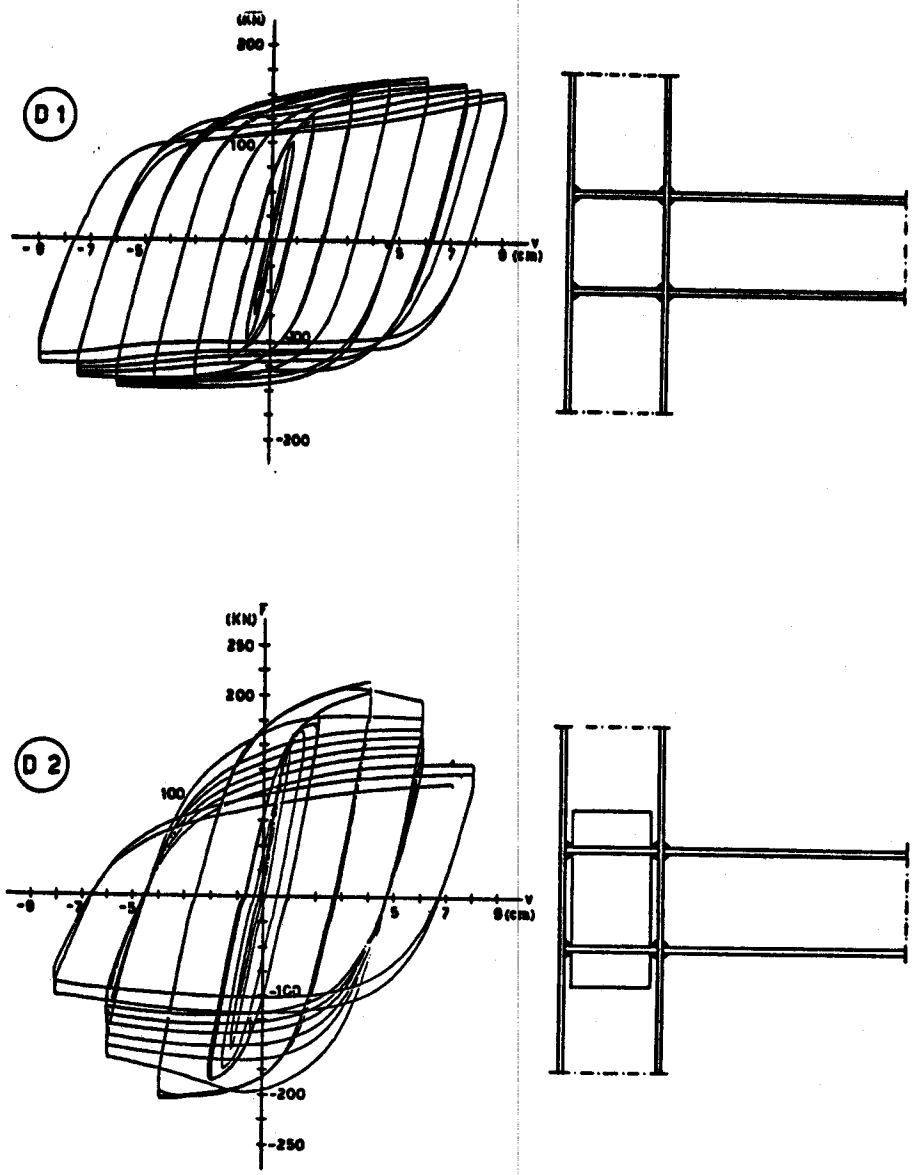

Figure 23 - Performance of fully-welded connections (Ballio et al., 1987).

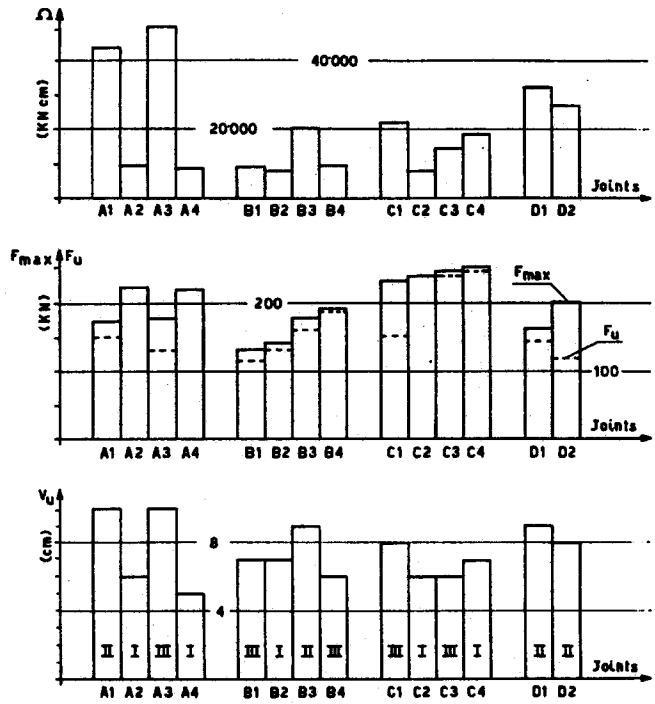

Figure 24 - Comparisons of the strength and energy dissipation capacity (Ballio et al., 1987).

It should be noted that this work has been followed by a very large comprehensive series of tests on composite connections utilizing the so-called ARBED system. In this type of construction the spaces between the flanges of the members are filled with well-confined concrete. In the follow-up work 18 exterior and 22 interior connections were tested at Milan by Ballio; three two-bay, two-story frames, including one with eccentric braces, were tested at Darmstadt by Boukamp et al.; three one-story, two-bay subassamblages were tested at Liege by Plummier; and three one-story, one bay subassemblages were tested at Wuppertal by Klingsch. The work is summarized in (Schleich and Pepin, 1992). While much of this research is not directly applicable to design in the US due to differences in construction practices, the well-coordinated approach used in these studies, where the best researchers from different countries are involved, should serve as an example for future SAC work. In addition, much of the fundamental experimental and analytical work developed in Japan, Europe and the Far East in the past few years needs to be incorporated into American design practice.

2.2.4 Composite Connections

Earlier in this review, it was pointed out that floor slabs play an important role in the behavior of FR connections. Fig. 25 shows a comparison of the strains measured near the welds at the top and bottom of a typical pre-Northridge connection between a W27x94 beam and a W14x211 column utilizing typical pre-Northridge details (Leon and Hajjar, 1996). The figure shows the strains during three cycles at 0.75 and 1.0% drift. The large strain concentration at the bottom is obvious, with almost an order of magnitude difference in the measurements. This information

is new and did not emerge from previous studies on composite fully welded connections (Daniels et al., 1970, Daniels and Wenk, 1979; Daniels and DuPlessis, 1979; Lee and Lu, 1989).

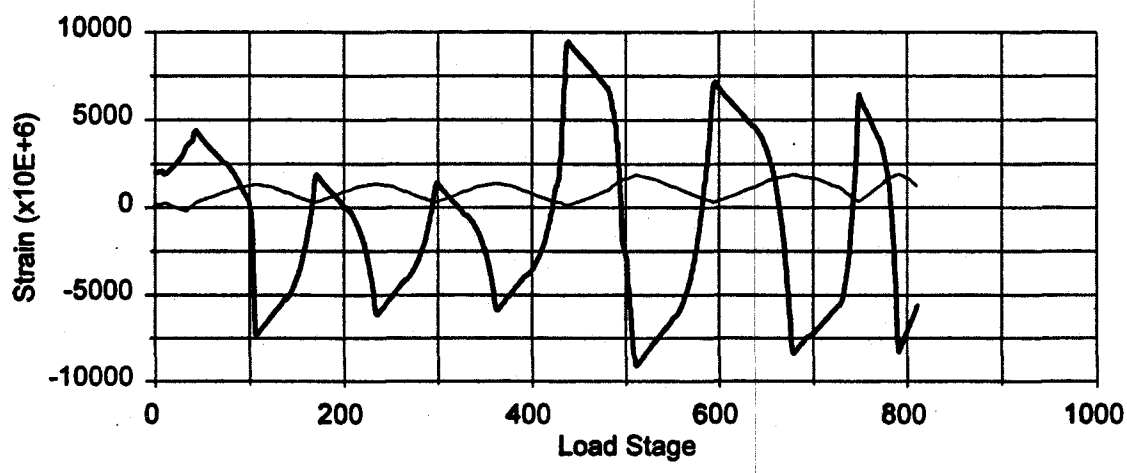

Figure 25 - Comparison of strain on top and bottom flanges of a composite connection (Leon and Hajjar, 1996).

The connections described this far are all examples of full strength, fully restrained (FS/FR) ones. Recent studies have pointed out that partial strength, partially restrained (PS/PR) connections (Deierlein and Yhao, 1992; Leon and Shin, 1995) and full strength, partial restrained (FS/PR) ones (Ghobarah, 1992; Astaneh-Asl and Nader, 1992; Deierlein and Yhao, 1992) can perform well under reversed cyclic loads.

As part of a large project aimed at assessing the feasibility of PS/PR connections, ten full-scale partially-restrained composite connections (PR-CC) were tested under both monotonic and reverse cyclic loads by Leon et al. (Ammerman and Leon, 1987; Leon et al., 1987; Leon 1990, Leon, 1994). PR-CC's are traditional steel PR connections whose strength and stiffness has been increased by adding shear studs and slab reinforcement in the negative moment regions adjacent to the columns. The additional strength and stiffness are present only after the slab hardens, and thus the sequence of construction needs to be incorporated into the design so that the connections and members are not overstressed at any stage (Ammerman and Leon, 1990, Leon and Ammerman, 1990). The slab transfers most of its compressive force directly by bearing of the slab against the column flange (Fig. 7). If the space between the flanges is filled with concrete an even more efficient force transfer can be achieved.

Four different types of connections have been investigated, utilizing mostly interior connections between W18x35 beams and W14x99 columns. In some of the specimens somewhat large beams were used (W21x62), and one large one-story, two-bay subassemblage has also been tested:

Type I: These consists of a typical seat angle, a double angle shear connection to the web, and continuous slab reinforcement across column lines. Under gravity loads the latter provides the tension part of the couple, while the angle in bearing acts as the compression member. Because of

the increase in steel strength (Grade 60 vs. A36 or A572) and lever arm, this connection adds significant moment capacity to the connection over a typical top and seat angle one. There are also significant stiffness gains because the slab steel yields in almost pure tension and at a higher stress than a top angle. Additional stiffness gains accrue from the use of friction bolts and, at large rotations, from the presence of web angles. Under seismic loading, however, the bottom angle will pullout at relatively low loads resulting in unsymmetrical and degrading hysteresis loops. Thus for seismic applications the thickness of the bottom angle should be increased to yield a connection with more symmetrical moment-rotation characteristics. Figure 26 shows a typical moment-rotation curve for this type of connection, indicating very good initial stiffness, excellent energy dissipation capacity, only minor pinching of the loops as rotations exceed 10 milliradians, and hardening behavior to rotations in excess of 30 milliradians. Extensive guidelines for the design of these connections have recently been published (Leon et al., 1996) and readers are referred to that document for more details.

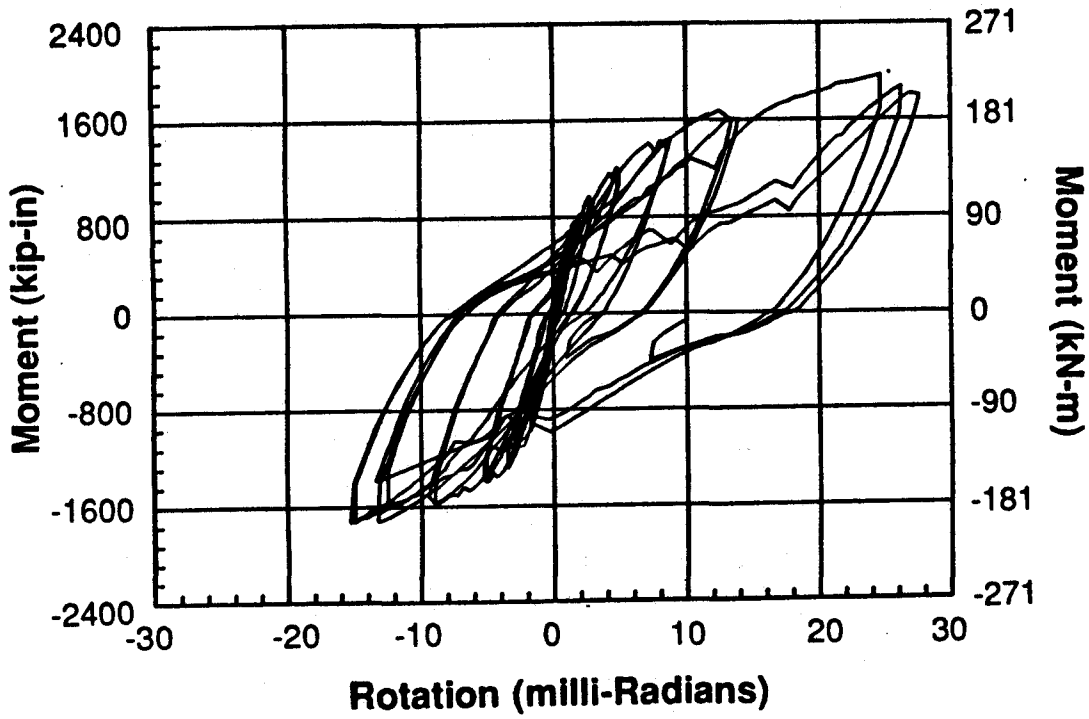

Figure 26 - Moment-rotation curve for a PR-CC (Leon, 1990).

Type II: These consist of a welded bottom plate, web angles for shear, and continuous slab reinforcement. This is a very stiff, economical connection possible because the bottom angle, which in Type I connections was the weak link, has been substituted with a welded plate. This plate carries the tensile and compressive forces basically as axial loads, resulting in a very stiff and non-degrading connection. The same results can be achieved by welding the plate to the column in the shop and bolting it to the beam with high strength friction bolts in the field. The welds must be detailed to insure full transfer of moment and to eliminate the possibility of weld fracture. This connection offers very large initial stiffnesses and symmetrical behavior under cyclic loading. Care

must be taken to eliminate the possibility of concrete crushing as a failure mode. In addition, the bottom plate must be designed to yield before either the welds or bolts fail. The bottom welded plate can be substituted by a T-stub or a partial end plate to achieve various degrees of strength and stiffness.

Type III: These consist of connections similar to Type I, except that the web angles are missing. This results is a connection with a much flatter inelastic region, because there are no web angle to provide additional restraint once the seat has yielded. In addition careful attention must be paid to the stability of the bottom angle and the beam web. As for Type I, the thickness of the seat angle is the controlling parameter.

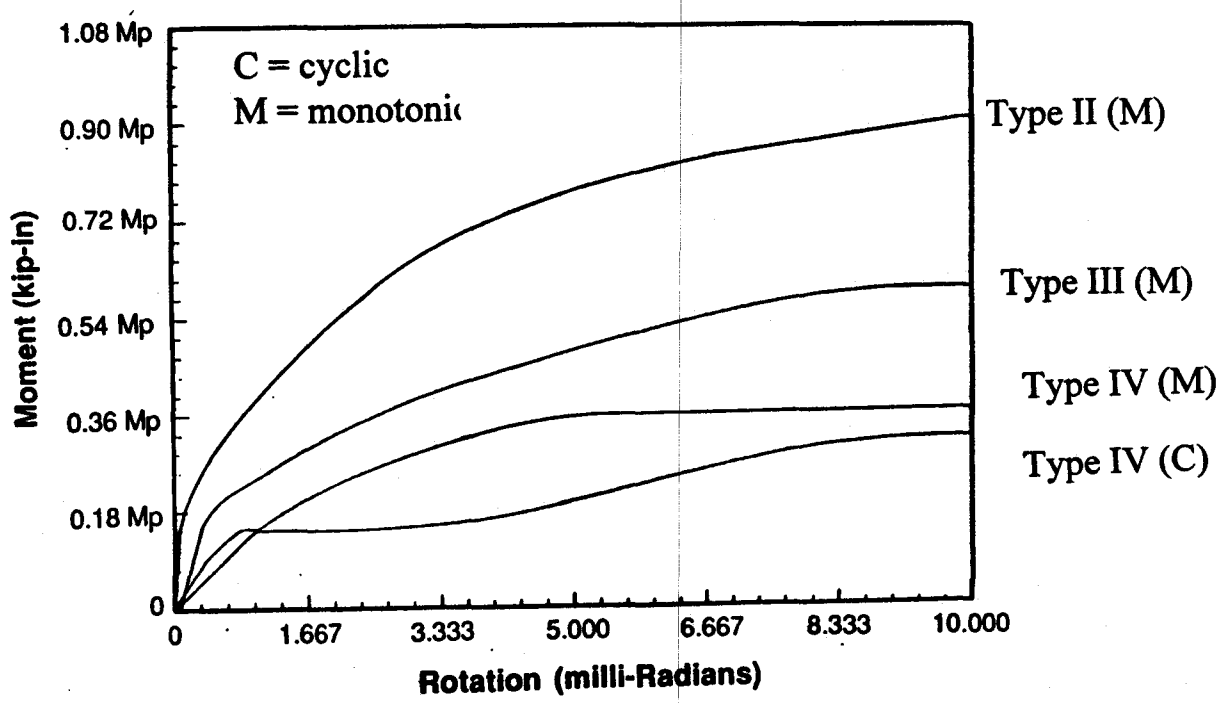

Figure 27 - Comparison of envelopes of cyclic performance for several composite connections (Leon, 1990).

Type IV: These consist of combining the simplest shear connection used in steel frames (bolted double web angles) with the slab reinforcement. Although the angles are relatively weak, the moment capacity of the composite connection can be substantially improved by increasing the thickness of the angle and lowering its position towards the bottom of the beam web. Since the web angles are carrying both shear and moment care must be taken to prevent any type of block shear failure.

Figure 27 shows a non-dimensionalized strength vs. rotation comparison for the four types of connections.

The tremendous effect of the slab on nominally weak connections can be seen in a comparison of three tests run by Leon and Forcier (unpublished) and shown in Fig. 28. The columns was a W12 X 90 and the beams were W21 X 57. The first specimen was shear connection made from a pair of

of L5 X 3.5 X 0.25 connecting the beam web to the column flange with five 7/8" A325 torqued bolts. This connection is considered simple but even under cyclic loads it exhibits some strength (0.2 Mp) and excellent ductility (Fig. 28(a)). The second connection was a typical top-and-seat angle one. It consisted of 9" long, L6 X 6 X 0.5 fastened with four 7/8" A325 bolts on each leg. The shear connection for this specimen was similar to that of the first specimen. Fig. 28(b) shows a considerable improvement in strength and stiffness over the shear connection, but probably not enough to provide good lateral restraint when subjected to a large earthquake. The third specimen was a composite one, where the top angle was removed and replaced with a 66" wide, 4 in. thick slab with six #4 (Grade 60) bars. The details of the bottom and web connection were similar to those of Specimen 2. This connection performed very well, indicating that with small changes in detailing connections that are currently not considered to participate in resisting lateral loads can provide a large portion of the lateral resistance in a moment-resisting frame. The first test confirmed that web angle type connections are very flexible, and that designers do not make a large error by considering them as pins. The second test showed that top-and-seat angle connections have a greater potential for providing lateral restraint of frames. The third test shows that replacing the top angle of a top and seat angle connection by continuous reinforcement across the column creates a stiff connection that has a favorable cyclic behavior. The amount of reinforcing steel required is not much more than is required for concrete crack control. The slab in this composite connection had only about twice the minimum amount of reinforcement (0.18%) that ACI 318 requires for temperature and shrinkage crack control.

The use of composite action in frames has been extensively studied experimentally (Johnson and Lam, 1982; Echeta and Owen, 1982; Van Dalen and Godoy, 1982; Benussi et al., 1986, 1989; Puhali et al., 1990; Tschermmeneg, 1990; Altmann et al. 1991, for example). The readers are referred to Lorentz and Chen (Lorentz and Chen, 1993) and Leon and Zandonini (1994) for a complete review of the research in this area.

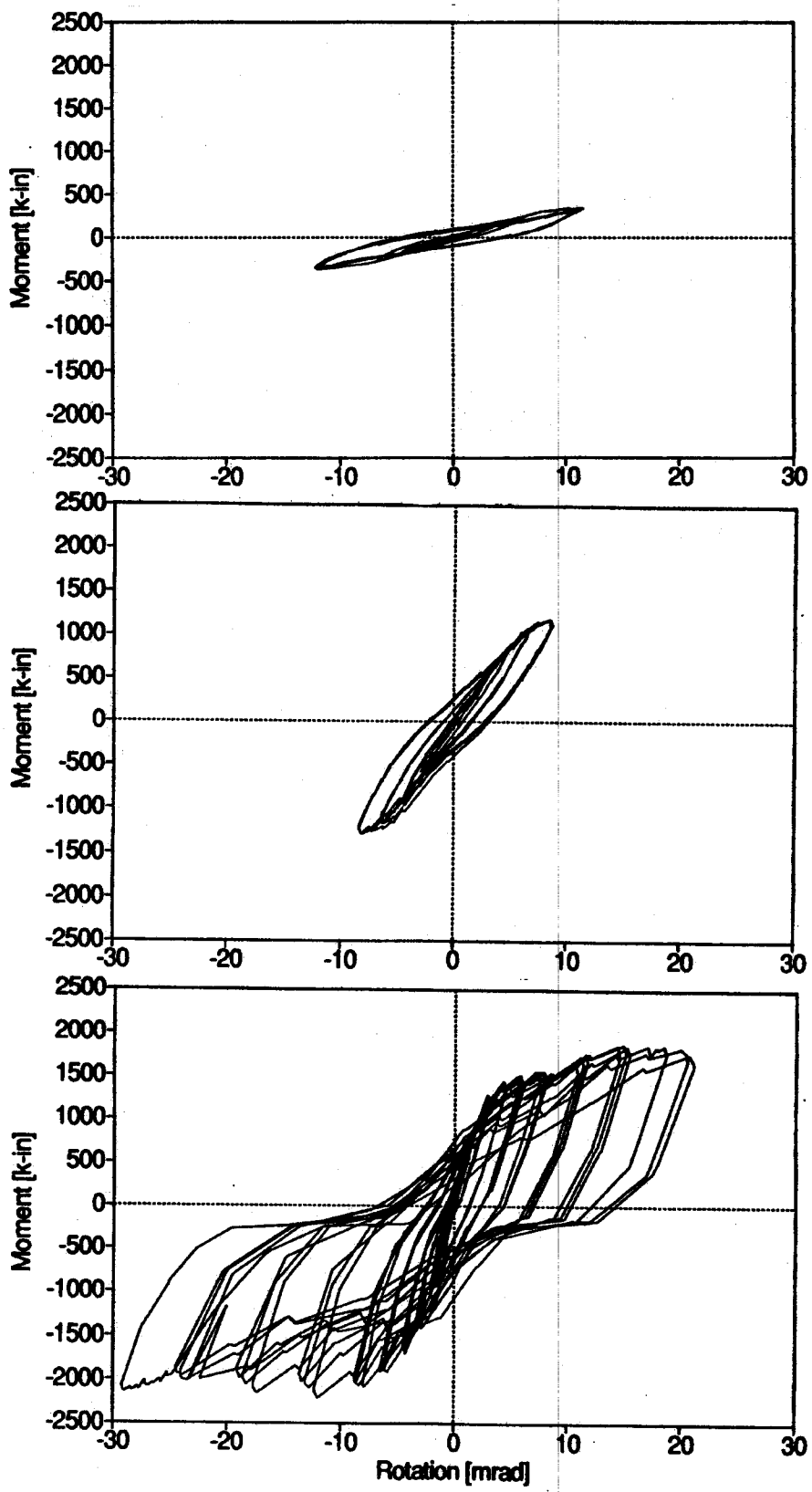

Figure 28 - Comparison of moment-rotation curves for specimens with weak connections.

3.0 Design of Bolted Connections

As discussed in Section 1.1, the first step in designing connections is to identify all important failure modes. Table 1 lists some of the many possible failure modes for the connections to be discussed in this section: column welded-beam bolted (CW-BB), column- and beam-bolted or T-stub (CB-BB), end plates (EP), top-and seat connections (TS), and partially-restrained composite connections (PR-CC). The table indicates the type of failure associated with each mechanism (ductile, semi-ductile, or brittle), and lists the ductile and semi-ductile mechanisms in descending order of desirability. The latter is an arbitrary hierarchy and designers are encouraged to develop their own lists and rankings. It is difficult, if not impossible, to insure that a perfectly ductile failure will occur since the criteria for the prevention of many of these failure modes under severe reversed loading have not been firmly established. Thus the designer will need to exercise his professional judgment when designing many of these connections.

In this section the fundamentals of design for full strength, fully restrained (FS/FR) bolted connections will be discussed first, followed by that for partial strength, partially restrained (PS/PR) ones. An important premise of this section is that the current design provisions for bolted connections, as stated in both AISC (1992) and ICBO (1994), provide neither sufficient guidance nor adequate provisions for insuring ductile behavior of bolted connections. Therefore the emphasis will be on understanding the basic steps in connection design and developing an understanding of the crucial mechanisms governing their behavior.

3.1 Full-Strength, Fully Restrained Connections

When designing connections in MRFs the first important differentiation is between ordinary moment frames (OMF) and special moment frames (SMF). The latter will be discussed here in detail, while some considerations for OMF will also be provided. To qualify under this category according to the parameters discussed in Section 1.2, the connection must (a) be able to transfer at least the plastic moment (M_p) of the beam, (b) must provide a connection stiffness $\alpha > 20$ ($\alpha = K_{conn} L_b / E I_b$), and (c) provide adequate ductility and rotation capacity. The current code requirements (ICBO, 1994) and design recommendations (AISC, 1992) for steel connections in seismic areas provide explicit guidelines only for strength but not stiffness or ductility. The latter two are implicitly assumed to be satisfied by the detailing requirements. These design provisions assume that the ductile behavior of the system will come from the formation of a plastic hinge in the beams outside the nodal zone, shear yielding of the panel zone, or a combination thereof. At this stage the provisions for both the beam yield criteria and panel zone yielding are under review, particularly for connections between large beams (W27 and greater) and heavy columns (FEMA, 1995). The current detailing requirements for bolted connections are based on a relatively small database and should be reviewed based on results of tests currently underway as part of the SAC effort as well as other efforts (AISC, AISI, NSF, NIST and others). Thus only systems in which the beam or connection elements yield will be reviewed here. Three types of connections will be addressed: column welded-beam bolted (CW-BB), column- and beam-bolted or T-stub (BC-BB), and end plates (EP).

Table 1 - Failure Modes for Bolted Connections.

Connection Type	CW-FB	CB-FB	EP	TS	PR-CC
Strength (FS or PS)	FS	FS	FS/PS	PS	PS
Stiffness (FR or PR)	FR	FR/PR	PR	PR	PR
DUCTILE:					
Slippage of slip-critical (friction) bolts	1	1			2
Flexural beam yielding adjacent to nodal zone	2	2	1		
Yielding of connecting elements in tension	3	3		2	
Formation of yield lines in connecting elements		4	2	1	3
Yielding of slab reinforcement in tension					1
Panel zone yielding	4	5	3	3	4
Limited local buckling	5	6	4	4	5
SEMI-DUCTILE:					
Elongation of bolt holes due to bearing	6	7		5	6
Yielding of bolts to column flange in tension	8	9	5	6	7
Shear yielding of bolts to beam flange	7	8		7	8
Severe local buckling of beam flange	9	10	6	8	8
BRITTLE:					
Fracture of welds between column and plate	A				
Fracture/failure of shear connection to web	A	A	A	A	A
Bearing/crushing failure of concrete					A
Fracture of shear studs and rebar					A
Fracture of beam flange due to local buckling	A	A	A		
Shear failure of bolts	A	A	A	A	A
Tensile failure of bolts (including prying action)		A	A	A	A
Fracture of beam through net section		A	A	A	A
Fracture of connecting element through net section		A	A	A	A
Column web failure (yielding, crippling, buckling)	A	A	A	A	A
Edge distance or spacing failure of bolts	A	A	A	A	A
Block shear	A	A	A	A	A

A indicates a brittle failure mode that should be carefully checked in design.

CW-FB = column welded, flange bolted connections
CB-FB = column bolted, flange bolted
EP = end plate
TS = top-and-seat angles with double web angles
PR-CC = partially restrained composite connection

3.1.1 Column Welded-Beam Bolted:

The mechanistic model for this type of connection is conceptually very similar to that shown in Fig. 2. A much simplified version of that figure, intended to show a design model for a CW-BB connection, is shown in Fig. 29. Here only the flexural components have been shown and the possibility of panel zone deformation eliminated by assuming the presence of doubler plates if needed. Springs K1 through K4 refer to the deformations of the flanges, while springs K5 through K8 refer to deformations of the web. The smaller circles in the bars between the springs represent rotational springs and are intended to highlight the fact that plane sections do not remain plane in the area adjacent to the connection.

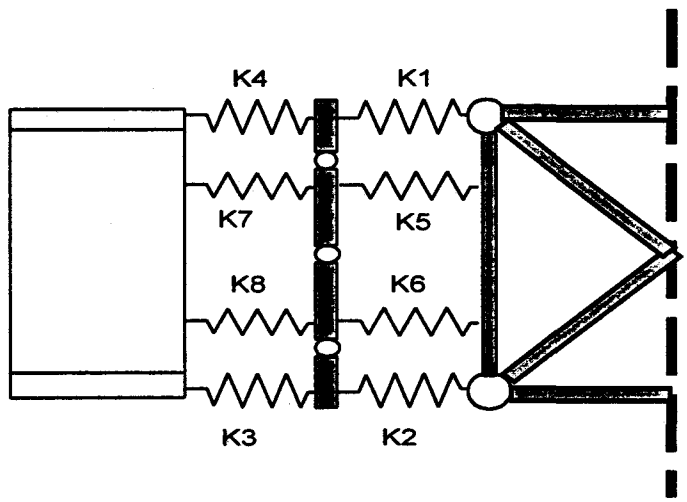

Figure 29 - Simplified design model for a CW-BB connection

For design, it will be assumed that springs K1 and K2, which will represent the welds, are much stiffer and stronger than K3 and K4. The latter two springs represent the sum of the deformations in the plate, the beam flange, the bolts, and any slip that may occur. The primary deformation modes desirable in this type of connection are bolt slippage, yielding of the gross section of the beam, and yielding of the gross section of the connecting plate. All of these are very ductile, stable mechanisms. The next desirable deformation mode is by shear deformation of the bolts. After that more brittle failure modes, including fracture in the net areas of either the beam flange or plate and fracture of the welds, will take over. For the web, springs K5 and K6, which represent a weld to a one-sided plate, are much stronger and stiffer but less ductile than springs K7 and K8, which represent the force transfer by bearing of the bolts. In general springs K3 and K4 will be much stronger and somewhat stiffer than K5 through K8. This implies that if there is a sudden failure in either K3 and K4, the web will not be able to carry the load and the connection will fail. This points out that this type of connection, which shares many similarities with the welded moment connections that performed poorly during the Northridge earthquake, does not provide a very redundant design. From the economical and practical standpoint it would be very difficult to increase the strength and stiffness of K5 through K8 to provide some degree of redundancy. Providing some continuous slab reinforcement and shear studs may be a much more efficient solution if a degree of reserve capacity is desired.

The design of CW-BB connections has recently been extensively discussed by Astaneh-Asl (Astaneh-Asl, 1995) , who proposed a model very similar to the one described above. Only some of the highlights will be repeated here:

(a) Flange Connection Design: Whenever possible the yield strength of the connection elements (top and bottom plates) should be matched to that of the beam flange so that excessive yielding does not occur in the beam flange. If this occurs, it is likely that severe local buckling will ensue, resulting in an early fracture of the beam flanges. Astaneh-Asl (Astaneh-Asl, 1995) recommends that for yielding on the gross section:

$$b_p t_p \left(F_{y_p} \right) \cong b_f t_f \left(F_{y_f} \right)$$

where b and t are the width and thickness, F_y is the actual yield strength, and the subscripts p and f refer to the plate and beam flange respectively. Since it is impossible to know the actual yield strength of the components during the design phase, according to capacity design principles an overstrength factor must be applied to undesirable modes of failure. For the design of the bolt groups and for checking failures of the net sections, a yield strength overstrength factor of 1.25 has been suggested by Astaneh-Asl (Astaheh-Asl, 1995). Since currently the dual A36/A572 steel routinely gives yield strengths in the neighborhood of 48 to 50 ksi, it would seem that an overstrength factor of 1.33 (48/36) would be more prudent. However, both net section fractures and bolt shear strength carry understrength factors (0.75) lower than yielding (0.9) so that in effect the reliability against these undesirable failure modes is higher than the nominal overstrength factor applied. Thus the 1.25 factor seems reasonable. This leads to a requirement for the ratio of the effective area (A_e) to the gross area (A_g) of the plate:

$$\frac{A_e}{A_g} \geq \frac{1.25\, F_y}{F_u}$$

This represents a slight increase over the current provisions in Sect. 2212 of the UBC code (ICBO, 1994) that requires only an 1.2 factor if F_u / F_y is less than 1.5. However, the author advocates that the 1.25 factor on beam strength discussed above should be applied to all semi-ductile and brittle modes of failure regardless of the F_u / F_y ratio.

It should be clear, however, that one of the most pressing needs in connection design is to apply reliability principles to this type of problem in order to develop reasonable overstrength design factors. This 1.25 factor, also used in reinforced concrete for the design of beam-column joints (ACI 352-R91, 1991), is only a starting point since it will be necessary to develop a different factor for each failure mechanism. In the end, and for design purposes, a single factor may be recommended. Designers should understand that currently the

quantitative data necessary to develop this information is either unavailable or has not been compiled in a useful manner.

The design of the welds to the columns, another key subject, falls within the recent recommendations by FEMA (FEMA, 1995) and will not be discussed here.

(b) Local Buckling Criteria: The current limits suggested by AISC (AISC, 1992) of $52/\sqrt{F_y}$ for b/t in beam flanges seems to provide a reasonable limit to ensure that sufficient rotational ductility is available. The typical buckle that forms when this criteria is met generally is a smooth, small local buckle. This precludes the development of a sharp buckle that may lead to fracture under reversed inelastic loading. The current limits on web slenderness (AISC, 1992) also seem to provide reasonable limits although the actual performance will be tied to the detailing of the web connections and whether composite action is expected. The slenderness of the connection plates, measured between the weld to the column flange and the centerline of the first row of bolts, should also be kept as low as practicable to prevent the formation of a local or global buckle in this area. Current criteria for unsupported compression elements are applicable in this case.

(c) Bolts: The bolt group should be designed not only to prevent a shear failure of the connectors but also to provide adequate performance during the slipping phase of the moment-rotation behavior. Since slip provides a good energy dissipation mechanism, it is prudent to design the connection such that the slip occurs well above the service load but also below the ultimate strength of the connection. To meet this criteria, Astaneh-Asl (Astaneh-Asl, 1995) recommends that the slip resistance ($F_{slippage}$) be apportioned as follows:

$$1.25F_{service} \leq F_{slippage} \leq 0.80F_{ultimate}$$

where $F_{service}$ corresponds to the nominal slip strength of the bolt group and $F_{ultimate}$ corresponds to the nominal shear strength of the bolts.

(d) Web Connection Design: The design of the web connection is usually made without much regard to the contribution of this part of the connection to the flexural strength of the joint unless the flange connections carry less than 70% of the total moment (AISC, 1992). It is clear from the performance of MRF's during the Northridge earthquake that careful attention should be paid to insure that the web connection is detailed to provide rotational ductility and strength that are compatible with the action of the flanges. Astaneh-Asl (Astaneh-Asl, 1995) suggests that the shear plates be designed to develop the plastic moment strength of the web:

$$h_p t_p \left(0.6F_{y_p}\right) \geq h_{gw} t_{gw} \left(0.6F_{y_{gw}}\right)$$

$$h_p^2 t_p \left(F_{y_p} \right) \geq h_{gw}^2 t_{gw} \left(F_{y_{gw}} \right)$$

where h and t are the depth and thickness, F_y is the yield strength, and the subscripts p and gw refer to the shear plate and the beam web respectively. Here again, allowances should be made for the steel overstrength (say $\alpha = 1.25$). Failure modes to be avoided include bolt shear, block shear, net area fractures and weld fractures.

A complete design example for this type of connection is included as Appendix B in (Astaneh-Asl, 1995) and the reader is referred to that publication for complete details.

3.2.2 Column Bolted-Beam Bolted (T-Stubs or CB-BB)

T-stub connections used to be a popular alternative in the 1950s and 1960s before field welded connections became economical. The mechanistic model for this type of connection is essentially the same as that shown in Fig. 29 for a CW-BB connection. The important conceptual difference between the two is that for T-stubs the springs K1 and K2 have lower strength and stiffness since they represent the flexural deformations that can take place in the flanges of the tee as well as any axial deformation of the bolts to the column flange. The latter can be increased by prying action. Clearly, a range of strength and stiffnesses are available for K1 and K2 depending primarily on the thickness of the flanges and the location of the bolts to the column. The big advantage of this type of connection over a CW-BB one is that springs K1 and K2 can provide a much larger deformation capacity than a weld would. A T-stub connection can thus provide a good balance between strength, stiffness, and ductility.

The design of a T-stub connection essentially follows the same steps as for the CW-BB connections described above, with important additional design provisions for prying action, bolt tensile elongation capacity, local effects on the column flange, and bolt shear strength (Agerskov, 1975; 1977; Roeder et al., 1994; 1996). The strength of the connection to the column, taking into account prying action, is limited by:

- the bending strength of the flanges of the T - this depends primarily on the thickness of the flanges and the exact location of the bolt holes.

- the ultimate tensile strength of the stem of the T - the net area generally governs over the gross area criteria because the width of the stem at the critical section for net area is not too different from that of the critical section for gross area.

- the tensile strength of the bolts - this is influenced primarily by the prying action.

- the shear strength of the bolts - it is difficult to fit more than 8 to 10 bolts in the stem of a conventional T (cut form a W shape) and thus large bolts may be needed.

Each of these failure modes must be checked individually and the lowest strength taken as the controlling value. Guidelines for these calculations are given in the AISC Manual (AISC, 1994), textbooks (see for example, pp. 848-856 of (Salmon and Johnson, 1996)), and in the standard references (Kulak et al., 1987). An excellent review of the design, including some of the numerical problems that can be encountered is given by Thorton (1985).

The effect of the reversed cyclic loading, as noted during the discussion of behavior of T-stub and end plate tests, is to progressively decrease the tension in the bolts to the column flange. Because of prying action, the stress range in these bolts is probably significantly larger than that calculated based on the simplified models used for design. This can result in either low cycle fatigue failures or in fracture of the bolt due to excessive elongation.

The design of a T-stub connection to resist seismic loads is included as Appendix A.

3.2.3 End Plate Connections

The mechanistic behavior of the end plate connection of an ideal end plate connection can again be represented by the model in Fig. 29, but with some important modification in the definitions of the springs. For an end plate connection, springs K3 and K4 represent only the deformation of the beam flanges, while springs K7 and K8 represent the flexural deformation of the web. Springs K1, K2, K5, and K6 now represent the stiffness of the end plate. Typically K1 and K2 will provide marginally larger strength and stiffness than K5 and K6 because most end plates are extended beyond the beam flanges and bolts provided in that area to stiffen the connection. The primary problem in modeling end plates is to determine the spring constants for the springs modeling the end plate. The stiffness of the springs is a function of the thickness of the plate and the bolt hole geometry. If the plate is thin or of moderate thickness compared to the column flange, yield lines will form between the holes in the plate forming a plastic mechanism. If the end plate is thick the behavior will shift to that of a thick T-stub. In the latter case care sure be exercised in not overstressing the column flanges.

An excellent review of the development of end plate connections is given by Griffiths (Griffiths 1984), and detailed design guidelines and design aids for their design under monotonic loading are available (Murray, 1990). While many models of end plate behavior exist[1], there is relatively little work on the design of end plates for cyclic loads (Whittaker and Walpole, 1982; Tsai and Popov, 1988, 1990; Ghobarah et al., 1992; Astaneh-Asl and Nader, 1992). Astaneh and Nader (1992) reviewed the available data and proposed design provisions. They listed plastic yield line formation in the end plate and column flange bending as the most desirable failure modes. For developing design provisions the end plate can be separated into two T-stubs

[1] See Krishnamurthy (1978) and associated discussions (Agerskov et al., 1979) for a flavor of the different approaches available for end-plate design.

(Morris and Packer, 1977) and thus results in a very similar approach to design to that developed in the previous section. The design forces can be calculated from free-body diagrams such as those shown in Fig. 29 (Astaneh-Asl, 1995).

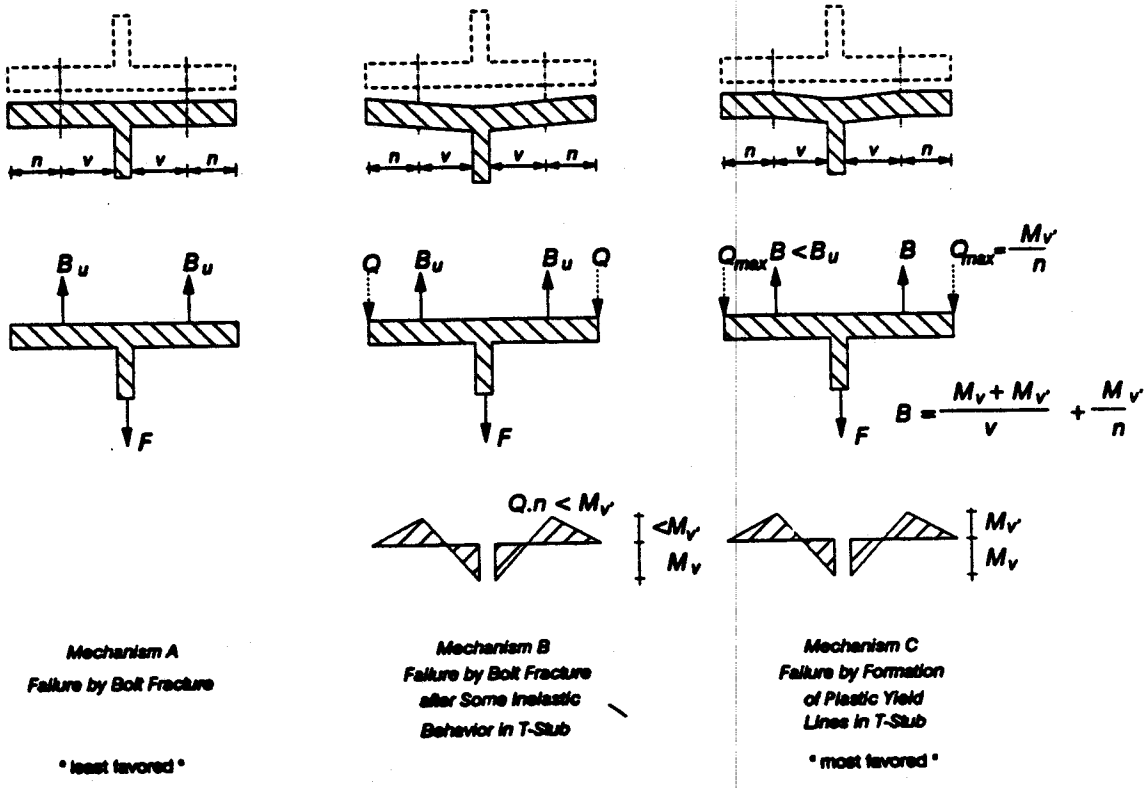

Figure 30 - Mechanism of force transfer in equivalent T-stubs (Astaneh-Asl and Nader, 1992).

From equilibrium of forces in Fig. 30:

$$\phi_b F_{ep} = \alpha \phi_b F_{fb}$$

$$\phi_b \frac{(2)(M_v + M_{v'})}{v} = \alpha \phi_b \frac{M_{pb}}{(d_b - t_{fb})}$$

$$\phi_b \frac{(2)(M_v + M_{v'})}{v} = \frac{M_{yc}}{(d_b - t_{fb})}$$

$$M_v = \frac{b_p t_p^2}{4} f_y \text{ and } M_{v'} = \frac{\left(b_p - (N/2)D'\right) t_p^2}{4} f_y$$

where α is the ratio of the connection yield moment to the plastic moment capacity of the beam, ϕ_b is the resistance factor for the bolts, F_{ep} is the force in the flange corresponding to yielding of the end plate, F_{fb} is the axial force in the beam flange corresponding to the plastic capacity of the beam, b_p is the width of the end plate, t_p is the thickness of the end plate, N is the number of bolts, and D' is the diameter of the bolt holes.

For end plates, it is recommended that two yield line patterns be checked on the column flange (Fig. 31). One consists mostly of straight lines and the other incorporates curved ones (Morris and Packer, 1977; Astaneh-Asl and Nader, 1992).

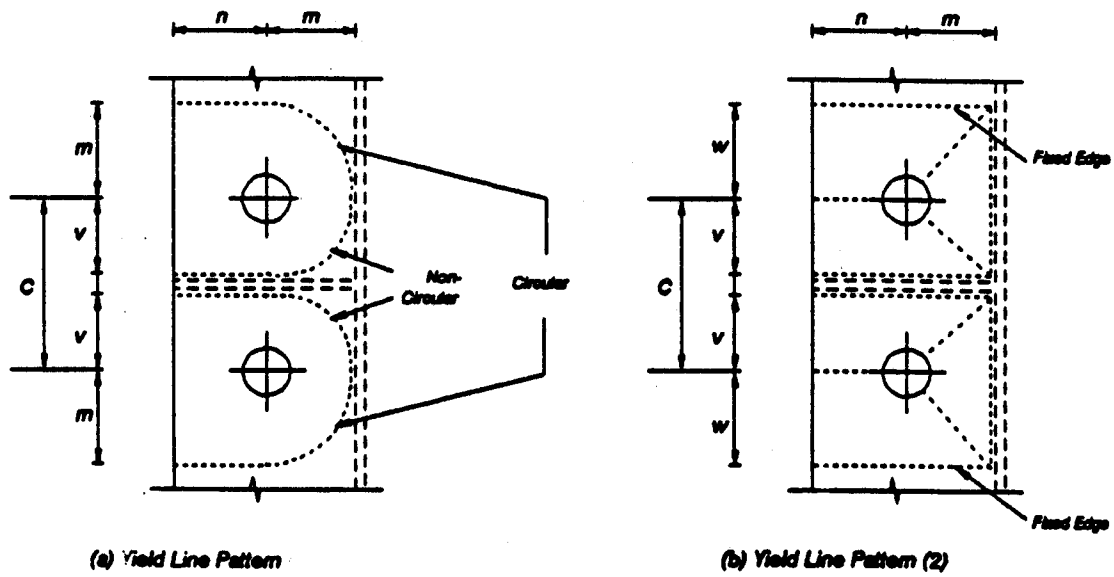

Figure 31 - Yield lines in column flanges (Astaneh-Asl and Nader, 1992).

From Fig. 31:

$$F_{f1} = t_{fc}^2 f_y \left\{ \frac{n}{v} + \frac{n}{m} + (n - 0.5D')\left(\frac{1}{v} + \frac{1}{m}\right) + \pi + \pi \sec^2\left(\tan^{-1}\left(\frac{2}{\pi}\ln\left(\frac{v}{m}\right)\right)\right)\right\}$$

$$F_{f2} = t_{fc}^2 f_y \left\{ \left\{\frac{1}{v} + \frac{1}{w}\right\}(2m + 2n - D') + \frac{(2v + 2w + -D')}{m} \right\}$$

$$w = \sqrt{(m(m + n - 0.5D'))}$$

To ensure that no out-of-plane bending occurs (Astaneh-Asl and Nader, 1992):

$$\phi_b F_{fb} = \phi_b \frac{M_{pb}}{(d - t_{fb})} \leq \begin{cases} \phi_b F_{f1} \\ \phi_b F_{f2} \end{cases}$$

$$\begin{cases} \text{if } \dfrac{b_p}{b_{fc}} = 1.0 \quad \text{then } t_{fc} \geq t_p \\ \text{if } \dfrac{b_p}{b_{fc}} = 0.5 \quad \text{then } t_{fc} \geq 0.65\, t_p \end{cases}$$

where M_{pb} is the plastic capacity of the beam, t_{fb} is the thickness of the beam flange, d is the distance between flange centerlines, and b_{fc} is the width of the column flange. Interpolation is permitted between b_p / b_{fc} values of 1.0 and 0.5.

Recently Murray et al (Murray el al., 1996) have suggested a direct formula for calculating the thickness of an end plate (Fig. 32):

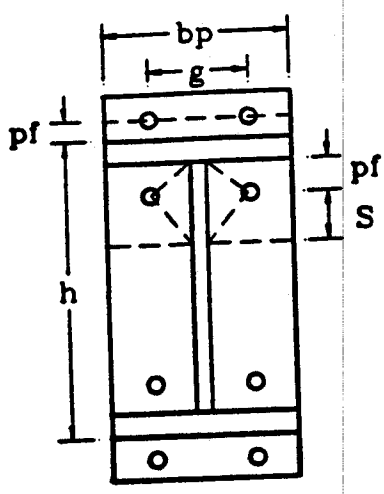

Figure 32 - Yield line patterns as proposed by Murray and Meng (1996).

$$t_p = \left[\frac{M_u / F_{py}}{\left(\frac{b_f}{2}\left(\frac{1}{p_f} + \frac{1}{s}\right) + (p_f + s)\left(\frac{2}{g}\right)\right)(h - t_f - p_f) + \frac{b_f}{2}\left(\frac{h}{p_f} + \frac{1}{2}\right)} \right]^{1/2}$$

$$s = \sqrt{b_f g/2}$$

$$t_p = \sqrt{8B_t p_f / \left(F_{py} b_p\right)}$$

where F_{py} is the yield stress of the end plate material and t_p is the thickness of the plate, B_t is the specified bolt pretension force, and the subscripts b and f refer to the plate and flange respectively.

The other pertinent design equations are given in Appendix A as part of the T-stub design example and will not be repeated here. Finally, it must be reemphasized that there is an extensive literature on end plate behavior and design. The reader is referred to Sherbourne (1961), Douty and McGuire (1965), Nair et al. (1969), Kato and McGuire (1973), Agerskov (1975, 1977), Parfitt and Morris (1977), Phillips and Packer (1981), Murray and Kukreti (1985), Moore and Sims (1986), Yee and Melchers (1986), Murray (1990) and Astaneh-Asl (1991) for additional details.

3.3 Partial Strength, Partially-Restrained Connections

Since the design of PR frames has not been common in high seismic regions, some considerations related to their analysis will be made first. The common practice for analysis of multi-story frames assumes that joints are rigid and beam and columns intersect at their centerline. Using this method there is no allowance for connection and panel zone flexibility, the spans of the beam and columns are overestimated, and the joints have no physical size and are reduced to a point. Since the PR behavior of most connections was recognized early, several modifications have been proposed to classical linear analysis techniques to account for connection flexibility. The first attempts involved modifying the slope-deflection method by adding the effect of linear rotational springs at beam ends (Batho and Rowan, 1934; Rathbun, 1936). Johnston and Mount (Johnston and Mount, 1941) gave a complete listing of coefficients to be used in the slope-deflection method including both the flexibility of the connections and the finite widths of the members. These methods were for hand calculations, and thus were limited to the analysis of relatively small structures. In an exception to this, Sourochnikoff (Sourochnikoff, 1950) used the beam line method along with experimental results obtained by Rathbun (Rathbun, 1936) to compute the nonlinear cyclic response of a one story one bay partially restrained frame. Monforton and Wu (Monforton and Wu, 1963) incorporated linear connection flexibility into the computerized direct stiffness method. This development permitted the analysis of large structures, but was still limited to linear analysis where the connections have constant stiffness. Lionberger and Weaver (Lionberger and Weaver, 1969) published the results from a program that performed fully dynamic lateral load analysis on plane frames. The connections in their program were modelled by a non-degrading bilinear model, which included

the sizes of the rigid panel zones. Moncarz and Gerstle (Moncarz and Gerstle, 1981) used a non-degrading trilinear model to analyze steel partially restrained frames subjected to lateral load reversals. When the first databases for connections were developed (Frye and Morris, 1975; Ang and Morris, 1984; Nethercot, 1985; Kishi and Chen, 1986), non-linear expressions for moment-rotation curves became widely available. This led to the development of numerous computer programs that modelled the non-linear behavior of PR connections. Shin (Shin, 1991; Shin and Leon, 1992) devised hysteresis rules for non-symmetrical composite connections with degradation of the unloading stiffness based on the maximum attained rotation, and implemented them in a dynamic nonlinear plane frame analysis program. The dynamic performance of frames incorporating partially restrained composite connections has been studied by Nader and Astaneh-Asl (1991; 1992) and Leon and Shin (1995). The numerical results obtained by Leon and Shin (1995) using a modified tri-linear degrading model showed excellent agreement with test results from a two-story, two-bay, half-scale frame. The analytical studies for PR frames showed good seismic performance for ground motions expected in zones of low to moderate seismicity. In particular they showed less problems with local buckling of members and equal or better energy dissipation capacity than rigid frames. In addition these studies showed that the lateral drifts of PR frames were within +/-20% of those of companion rigid frames when 4, 6 and 8 story frames were subjected to the El Centro, Parkfiled, and Pacoima ground motions. The results of these studies confirmed those of Astaneh-Asl and Nader (1992), and verified their shake table results. Further verification of the good performance can be found in the work of Osman et al. (Osman et al., 1993) who presented the analysis results for 8 story frames with end-plate connections and flexible panel zones of various thickness.

In the design of PR frames for seismic areas, the designer faces several obstacles:

(a) Codes currently do not permit the use of PR connections in SMRF's in seismic zones, except (a) if verification tests or advanced analysis are conducted, or (b) to the extent that PR connections that are not part of the lateral load-resisting system must comply with deformation compatibility requirements (UBC Section 2211.7.1 (IBCO, 1994)). However, it should be noted that the use of PR connections is an excellent idea for a backup structural system. This concept was clearly borne out by the good performance of many of the steel frames whose welded connections failed during the Northridge earthquake. The "simple" connections actually provided enough restraint to perform as weak PR connections. They compensated for their relatively low stiffness and strength with sheer numbers, preventing excessive drifts and non-structural damage. Based on the relative low cost of turning nominally simple connections into PR-CC's ones by adding slab reinforcement and shear studs, designers are advised to incorporate these connections into their design even if the code does not currently recognize their contribution. Of course, care should be exercised so that the overstrengths provided by these connections are accounted for in design.

(b) In general, codes will allow the use of alternate connections based on tests and analysis. The only types that would meet this criteria are some of the ones described in the new Chapter 7 of the 1994 NEHRP provisions (NEHRP, 1994). Readers are urged to peruse this reference for ideas on alternate connections and structural systems for use in seismic areas. In particular, two of the connections mentioned in the NEHRP Chapter 7 deserve further

consideration: the partially restrained composite connections described in Section 7.4.1 and the composite systems described in Sections 7.4.2 and 7.4.3 (ASCE Task Committee, 1994). There is an extensive literature associated with both systems, but only the former falls within the scope of this paper.

(c) Codes (AISC, 1993) require that the moment-rotation characteristics of PR connections be known and incorporated into the design. For PR-CC's these relationships are available for the Type I connections described in Section 2.2.4. Under negative bending (slab steel in tension):

$$M_n^- = C1\,(1 - e^{-C2\,\theta}) + C3\,\theta$$

where,

$C1 =$ $0.18(4*A_sF_{yrb} + 0.857A_lF_y)\,(d + Y3)$
$C2 =$ 0.775
$C3 =$ $0.007(A_l + A_{wl})F_y\,(d + Y3)$
$\theta =$ girder end rotation, radians
$d =$ girder depth, in
$Y3 =$ distance from the top flange of the girder to the centroid of the reinforcement, in
$A_s =$ steel reinforcing area, in^2
$A_l =$ area of bottom angle, in^2
$A_{wl} =$ gross area of double web angles for shear calculations, in^2
$F_{yrb} =$ yield stress of reinforcing, ksi
$F_y =$ yield stress of seat and web angles, ksi

Since the connection behavior is not symmetrical with respect to either strength or stiffness, a similar expression is needed for positive bending (bottom angle in tension):

$$M_n^+ = C1\,(1 - e^{-C2\,\theta}) + (C3 + C4)\,\theta$$

where,

$C1 =$ $0.2400 * [(0.48*A_{wl}) + A_l] * (d + Y3) * F_y$
$C2 =$ $0.0210 * (d + Y3/2)$
$C3 =$ $0.0100 * (A_{wl} + A_l) * (d + Y3) * F_y$
$C4 =$ $0.0065 * A_{wl} * (d + Y3) * F_y$

(d) To calculate design forces based on an equivalent lateral loads analysis, the period of the structure must be known, at least approximately. Astaneh-Asl and Nader (Astaneh-Asl and Nader, 1992) recommend that the first period (T_1)for a PR structure be calculated as:

$$T_1 = 0.0463\,h_n^{(1.0-\alpha/5)} \quad \text{for } \alpha \le 0.5$$

$$T_1 = 0.035\,(1 + 0.375/\alpha)^{0.5}\,h_n^{(0.85-\alpha/120)} \quad \text{for } 0.5 \le \alpha \le 18$$

$$T_1 = 0.035\, h_n^{(1.0-\alpha/5)} \text{ for } \alpha \geq 18$$

where $\alpha = K_{conn} L_g / E_g I_g$. These proposed expression are consistent with the results obtained by the author (Leon and Shin, 1995). It should be noted that it will be difficult to design frames with $\alpha < 10$ since meeting the wind drift conditions at service becomes difficult in that range.

(e) The response modification factors for structures with PR connections are very similar to those for rigid frames. For the practical range of α (say $\alpha > 10$) studies show that R = 8 (based on pre-Northridge provisions for SMRF) is a reasonable assumption (Astaneh-Asl and Nader, 1992; Leon and Shin, 1995). For the design of composite PR frames, the provisions in NEHRP (FEMA 1994) suggest an R = 6 as an intermediate performance between that of an ordinary moment frame and that of a special moment frame is expected.

(f) The calculation of deflections and stability effects are complicated for PR frames within the context of equivalent lateral loads. For zones of low or moderate seismicity, the service drift due to wind loads will generally control the design. This is due to the incorrect assumption in current codes that the force reduction and deflection amplification factors are not a function of the detailing level used in design (i.e., an ordinary steel moment-resisting frame has the same factors whether it was designed to satisfy the additional requirements for a zone of high seismicity as for a zone of low seismicity where no seismic detailing is done). Since the static wind load case governs because of the generous allowances for drift under seismic loading, as the connection stiffness decreases the designer has to provide more frames to resist the lateral loads. This results in PR frames with lower tributary masses and thus better dynamic characteristics.

(f) The conclusion that PR frames will not drift appreciably more than rigid ones has led to the recommendation that the displacement amplification factor for PR frames be taken as equal to that of SMRF ($C_d = 5.5$).

The design of frames with PR-CC's is the subject of a recent design guide (Leon et al., 1996) and interested readers are referred to that source for additional information and the complete design example for a four-story frame in a zone of moderate seismicity.

3.4 Considerations for Ordinary Moment Frames (OMFs)

The discussions above were meant primarily for the use of bolted and composite connections in special moment frames (SMF) and partially-restrained composite frames. All of these connections can, of course, be used for OMFs without any modifications. Because much of the discussion centered on finding overstrength and understrength factors to satisfy the capacity design approach for "hinging" zones, it is likely that following the recommendations in Sects. 3.2 and 3.3 will result in connection detailing requirements which would be uneconomical for

design approach for "hinging" zones, it is likely that following the recommendations in Sects. 3.2 and 3.3 will result in connection detailing requirements which would be uneconomical for OMFs. It is not possible, at this stage, for the author to provide guidance as to which specific recommendations can be relaxed and by how much for use in OMFs. The principal reason is that the performance criteria for OMFs are not clearly established, and therefore it is not possible to establish the desired reliability index. From past performance and following the mechanistic approach described in this paper, designers should be able to develop reasonable variations of the connections discussed for use in zones of lower seismicity and for less important structures.

3.5 Summary

This paper has discussed the fundamentals of bolted and riveted connection design. The first part of the paper presented a thorough discussion of connection behavior and classification for the monotonic loading case. Possible extensions to the cyclic loading case were discussed and the importance of slab effects was emphasized. The second part of the paper contained a review of experimental work on bolted and riveted connections. The information on the latter is important for evaluation and rehabilitation of older structures. The discussion on bolted connections points out that, with few exceptions, some of the scaling and detailing problems encountered in welded connection research and code development will probably also have to be resolved for bolted ones. However, it is clear that properly detailed bolted connections can provide equal or superior seismic performance to that of fully welded ones. Finally, proposed design provisions for bolted connections were reviewed. It is clear that a new, more fundamental and comprehensive approach is needed in current codes so that bolted connections can be properly designed in areas of moderate to high seismicity.

Acknowledgments

The author would like to thank all the researchers who have kindly provided experimental data and design provisions for this work. The material provided by Prof. H. Astaneh-Asl of the U. of California-Berkeley was extremely helpful, and much of it is reproduced with his kind permission.

Disclaimer

The opinions presented here are solely those of the author and should not be construed as being those of SAC, FEMA or any other organization.

LIST OF REFERENCES

ACI 318-95, 1995. "Building Code Requirements for Reinforced Concrete (ACI 318-95)," American Concrete Institute, Detroit.

ACI 352-R91, 1991. "Recommendations for Design of Beam-Column Joints in Monolithic Reinforced Concrete Structures (ACI 352R-91)," American Concrete Institute, Detroit.

Ackroyd, M.H., and Gerstle, K., 1977. "Strength and Stiffness of Type 2 Steel Frames", Report to AISC under Project No.199, Department of Civil Environmental, and Architectural Engineering, University of Colorado, Boulder, CO.

Ackroyd, M.H., and Gerstle, K., 1982. "Behavior of Type 2 Steel Frames", J. of the Structural Division, ASCE, Vol. 108, No. ST7, pp. 1541-1558.

Agerskov, H., 1976. "High Strength Bolted Connections Subject to Prying", J. of the Structural Division, ASCE, Vol. 102, ST1, pp.161-175.

Agerskov, H., 1977. "Analysis of Bolted Connections Subject to Prying", J. of the Structural Division, ASCE, Vol. 103, ST11, pp. 2145-2163.

Agerskov, H. et al.., 1979. "Discussion to - A Fresh Look at Bolted End-Plate Behavior and Design," Engineering Journal, AISC, Vol. 16, 2nd Quarter, pp. 54-64.

AISC, 1994. Manual of Steel Construction--Load and Resistance Factor Design, Second Edition, 2 Volumes, American Institute of Steel Construction, Chicago.

AISC, 1993, Load and Resistance Factor Design Specification for Structural Steel Buildings, American Institute of Steel Construction, Chicago.

AISC, 1992. Seismic Provisions for Structural Steel Building, Load and Resistance Factor Design, American Institute of Steel Construction, Chicago.

Altman, R. T., Maquoi, R., Jaspart, J.-P., 1991. "Experimental Study of the Non-Linear Behaviour of Beam-to-Column Composite Joints," Journal of Constructional Steel Research, Vol. 18, pp. 45-54.

Altman, W.G., Jr., Azizinamini, A., Bradburn, J.H., and Radziminski, J.B., 1982. "Moment Rotation Characteristics of Semi-Rigid Steel Beam-Colum Connections", Struct. Res. Studies, Dept. of Civil Engineering, University of South Carolina, Columbia, SC.

Ammerman, D.A., and Leon, R.T., 1987, "Behavior of Semi-Rigid Composite Connections", Engineering Journal, AISC, Vol.24, 2nd Quarter, pp. 53-62.

Ammerman D.J, and Leon R., 1990. "Unbraced Frames with Semi-Rigid Composite Connections", Engineering Journal, AISC, Vol. 27, 1st Quarter, pp. 1-10.

Ang, K. M., and Morris, G. A., 1984. "Analysis of Three-Dimensional Frames with Flexible Beam-Column Connections," Canadian Journal of Civil Engineering, Vol. 11, pp. 245-254.

ASCE, 1967. "Bibliography on Bolted and Riveted Structural Joints," Manuals and Reports in Engineering Practice No. 48, ASCE, New York.

ASCE-WRC, 1971. "Plastic Design in Steel." ASCE Manuals and Reports on Engineering Practice No. 41, ASCE-WRC, New York.

ASCE Task Committee on Design Criteria for Composite Structures, 1994. "Guidelines for the Design of Joints between Steel Beams and Reinforced Concrete Columns," J. of Structural Engineering, ASCE, Vol. 120, No. 8, pp. 2330-2357.

Astaneh-Asl, A., Nader, M.N., and Malik, L., 1989. "Cyclic Behavior of Double Angle Connections", J. of Structural Engineering, ASCE, Vol. 115, No. 5, pp. 1101-1118.

Astaneh-Asl, A., Nader, M.N., and Harriott, J.D., 1991. "Seismic Behavior and Design Considerations in Semi-Rigid Frames", Proceedings of the 1991 National Steel Construction Conference, AISC, Chicago.

Astaneh-Asl, A., and Nader, M.N., 1992. "Seismic Behavior and Design of Semi-Rigid Steel Frames," UCB/EERC-92/06, Earthquake Engineering Research Center, UC-Berkeley, Berkeley.

Astaneh-Asl, A., 1994. "Seismic Behavior and Design of Steel Semi-Rigid Structures," Proceedings, First International Workshop and Seminar on Behavior of Steel Structures in Seismic Areas, F. Mazzolani and V. Giouncu (eds.), E & FN Spon, Chapman & Hall, London.

Astaneh-Asl, A. , 1995. Seismic Design of Bolted Steel Moment-Resisting Frames, Steel Tips, Structural Steel Education Council, Moraga, CA, 82 pp.

ASTM A502-91, 1992. "Steel Structural Rivets," ASTM Designation A502-91, American Society for Testing and Materials, Philadelphia, PA.

ATC-24, 1992. "Guidelines for Cyclic Seismic Testing of Components of Steel Structures," Applied Technology Council, Redwood City, CA.

Attiogbe, E., and Morris, G., 1991. "Moment-Rotation Functions for Steel Connections," J. of Structural Engineering, ASCE, Vol. 117, No. 6, pp. 1703-1718.

Azizinamini, A., Bradburn, J. H., and Radziminski, J.B., 1985. "Static and Cyclic Behavior of Semi-Rigid Steel Beam-Column Connections," Technical Report, Dept. of Civil Engineering, Univ. of South Carolina, Columbia, SC.

Ballio, G., Calado, L., De Martino, A., Faella, C., and Mazzolani, F., 1987. "Cyclic Behavior of Steel Beam-to-Column Joints: Experimental Research", Costruzione Mettaliche, Vol. 39, No. 2, pp. 69-90.

Batho, C., and Lash, S. D., 1934a. "Further Investigations on Beam and Stanchion Connections, Including Connections Encased in Concrete; Together with Laboratory Investigations on a Full-Scale Steel Frame," Final Report of the Steel Structures Research Committee, Department of Scientific and Industrial Research, His Majesty's Stationery Office, London, pp. 276-363.

Batho, C., and Rowan, H. C., 1934a. "Investigations on Beam and Stanchion Connections," Second Report of the Steel Structures Research Committee", Department of Scientific and Industrial Research, His Majesty's Stationery Office, London, pp. 61-137.

Batho, C., and Rowan, H. C., 1934b. "The Analysis of the Mon ents in the Members of a Frame Having Rigid or Semi-Rigid Connections, Under Vertical Loads," second report of the Steel Structures Research Committee", Department of Scientific and Industrial Research, His Majesty's Stationery Office, London, pp. 177-199.

Batho, C., and Bateman, E.H., 1934. "Investigations on Bolts and Bolted Joints" Second Report of the Steel Structures Research Committee", Department of Scientific and Industrial Research, His Majesty's Stationery Office, London.

Batho, C., 1938. "The Effect of Concrete Encasement on the Behaviour of Beam and Stanchion Connections," The Structural Engineer, Dec. , pp. 427-447.

Beedle, L.S., and Cristopher, R., 1964. "Test of Steel Moment Connections," Engineering Journal, AISC, Vol. 1, No. 4, pp. 116-125.

Benussi F., Puhali R., and Zandonini R., 1986. "An Experimental Investigation into Joint in Composite Frames", Proc. of the International Conference on Steel Structures, Budva, Yugoslavia, M. Pavlovic (ed.), Elsevier Applied Science, London.

Benussi F., Puhali R., and Zandonini R., 1989. "Semi-Rigid Joints in Steel-Concrete Composite Frames", Costruzioni Metalliche, Vol. 41, No. 5, pp 1-28.

Bertero, V. V., Popov, E. P., and Krawinkler, H., 1972. "Beam-Column Subassemblages Under Repeated Loading," J. of the Structural Division, ASCE, Vol. 98, No. ST5, pp. 1137-1157.

Bertero, V., Anderson, J.C., and Krawinkler, H., 1994. "Performance of Steel Building Structures During the Northridge Earthquake," UCB/EERC 94/09, EERC, University of California, Berkeley, CA.

Bjorhovde, R. Brozzetti, J., and Colson, A. (eds.), 1988. Connections in Steel Structures: Behaviour, Strength and Design , Proceedings of the Workshop on Connections held at the Ecole Normale Superiere, Cachan, France, May 1987, Elsevier Applied Science, London.

Bjorhovde, Colson, A., Haaijer, G., and Stark, J.W.B. (eds.), 1992. Connections in Steel Structures II: Behaviour, Strength and Design , Proceedings of the Workshop on Connections held at Pittsburg, April 1991, AISC, Chicago.

Bjorhovde, Colson, A., and Zandonini, R. (eds.), 1996. Connections in Steel Structures III: Behaviour, Strength and Design , Proceedings of the Workshop on Connections held at Trento, Italy, May, 1995, Elsevier Applied Science, London (in press).

Carpenter, L.D. and Lu, L.-W., 1973. "Reversed and Repeated Load Tests of Full-Scale Steel Frames." Bulletin No. 24, American Iron and Steel Institute, New York.

Chasten C., Fleischman, R., Lu, L.-W., and Driscoll, G., 1989. "Top and Seat Connections and End Plate Connections: Snug vs. Fully Pretensioned Bolts," Proc. of the 1989 National Steel Conference, AISC, Chicago, pp.4.1-4.29

Chen, W.F., 1987. Joint Flexibility in Steel Frames, W.F. Chen (Ed.), Elsevier Applied Science, London, 290 pp.

Chen, W.F., and Lui, E., 1991. Stability Design of Steel Frames, CRC Press, Boca Raton, FL, 380 pp.

Chen, W.F. and Toma, S., 1994. Advanced Analysis of Steel Frames, CRC Press, Boca Raton, FL.

Chen, W.F., 1995. Stability Design of Semi-Rigid Frames. J. Wiley and Sons, New York.

Daniels, J.H, Kroll, G.D., Fisher, J.W., 1970. "Behavior of Composite-Beam to Column Joints", J. of the Structural Division, ASCE, Vol. 96, No. ST3, pp. 671-685.

Daniels, J.H, and duPlessis, D.P., 1979. "Strength and Stiffness of Composite Beam-to-column Connections", in Plastic Analysis and Tests for Rigid High-Rise Composite Frames, Bulletin No. 28, AISI, Washington, DC.

Daniels, J.H, and Wenk, T., 1979. "Composite Assemblage Experiments", in Plastic Analysis and Tests for Rigid High-Rise Composite Frames, Bulletin No. 28, AISI, Washington, DC.

Deierlein, G.C., and Yhao, 1992. "Static and Dynamic Analysis of Steel Frames with Non Linear Connections and Joint Effects," Structures Congress 92: Compact Papers, ASCE, New York, pp. 975-978.

DeJonge, A.E.R., 1945. "Riveted Joints: A Critical Review of the Literature Covering their Development", ASME, New York.

Douty, R. T., McGuire, W., 1965. "High Strength Bolted Moment Connections," J. of the Structural Division, ASCE, Vol. 91, No. ST2, pp. 101-128.

Dowling, P., Harding, J. and Bjorhovde, R. (eds.), 1992a. Constructional Steel Design: An International Guide, Elsevier Publishers, London.

Dowling, P., Harding, J., Bjorhovde, R., and Martinez-Romero, E. (eds.), 1992b. Constructional Steel Design: Worldwide Developements, Elsevier Publishers, London.

ECCS, 1986. "Recommended Testing Procedure for Assssesing the Behavior of Structural Steel Elements under Cyclic Loads," Technical Group 1.3 - Seismic Design, European Committee for Constructional Steel, Brussels.

Echeta, C.B., & Owens, G.W., 1981. "A Semi-Rigid Connection for Composite Frames - Initial Test Results", in Proc. Int. Conf. on Joints in Structural Steelwork, J.H. Howlett et al. (eds.), Pentech Press, London, pp 6.93-6.121.

Eurocode 3, 1992. "Design of Steel Structures, Part 1: General Rules and Rules for Buildings," ENV 1993-1-1:1992, Comite Europeen de Normalisation (CEN), Brussels.

Eurocode 3, 1994. "Design of Steel Structures, Part 1: Revised Annex J: Beam to Column Connections," supplement to ENV 1993-1-1:1992, Comite Europeen de Normalisation (CEN), Brussels.

Eurocode 4, 1992. "Design of Composite Steel-Concrete Strucutres," ENV 1994-1-1:1992, Comite Europeen de Normalisation (CEN), Brussels.

FEMA, 1994. "NEHRP Recommended Provisions for the Development of Seismic Regulations for New Buildings," FEMA 222/223, FEMA, Washington, D.C.

FEMA, 1995. "Interim Guidelines: Evaluation, Repair, Modification, and Design of Welded Steel Moment Frame Structures," FEMA 267, FEMA, Washigton, DC.

Fisher, J.W. , and Beedle, L.S., 1964. "Bibliography on Bolted and Riveted Structural Joints," Report No. 302.1, Fritz Engineering Laboratory, Lehigh University, Bethlehem, PA.

Fisher, J.W., Kormanik, R., and Allan, R.N., 1966. "Supplement to the Bibliography on Bolted and Riveted Joints," Report No. 302.1, Fritz Engineering Laboratory, Lehigh University, Bethlehem, PA.

Fisher, J.W., and Struik, J.H.A., 1974. "Guide to Design Criteria for Bolted and Riveted Joints," John Wiley and Sons, New York.

Forcier, G. P., 1994. "Seismic Performance of Older Steel Frames," Ph.D. Thesis, The Graduate School, University of Minnesota, Minneapolis, MN.

Frye, M. J., and Morris, G. A., 1975. "Analysis of Flexibly Connected Steel Frames," Canadian Journal of Civil Engineering, Vol. 3, No. 3, pp. 280-291.

Ghobarah, A., Osman, A., and Korol, R.M., 1990. "Behavior of Extended End-Plate Connections under Cyclic Loading", Engineering Structures, Vol. 12, No. 1, pp. 15-27.

Ghobarah, A., Korol, R.M., and Osman, A., 1992. "Cyclic Behavior of Extended End-Plate Joints", J. of Structural Engineering, ASCE, Vol. 118, No.5, pp. 1333-1353.

Goverhan, A.V., 1984. "A Collection of Experimental Moment Rotation Curves Evaluation of Predicting Equations for Semi-Rigid Connections," M.Sc. Thesis, Vanderbilt University, Nashville, TN.

Government Board of Engineers, 1919. The Quebec Bridge, Vol. 1, Department of Railways and Canals, Ottawa.

Graham, J.D., Sherbourne, A.N., Kabbaz, R.N., and Jensen, C.D., 1959. "Welded Interior Beam-to-Column Connections", AISC, New York.

Griffiths, J.D., 1984. "End-Plate Moment Connections - Thier Use and Misuse," Engineering Journal, AISC, Vol. 21, 1st Quarter, pp. 32-34.

Hechtman, R. A. and Johnston, B. G., 1947. "Riveted Semi-Rigid Beam-to-Column Building Connections," Progress Report No.1, Committee of Steel Structures Research, AISC, New York.

Hechtman, R. A., 1948. A Study of the Effects of Heating and Driving Conditions on Hot-Driven Structural Steel Rivets, Ph. D. thesis, Department of Civil Engineering, University of Illinois, Urbana, IL.

Howlett, J.H., Jenkins, W.M., and Stainsby, R. (eds.), 1981. Joints in Structural Steelwork, Proceedings of the International Conference held at Teesside Polythechnic, Middlesbrough, Halstead Press, John Wiley & Sons, New York.

Huang, J.S., Chen, W.F., and Regec, J.E., 1971. "Test Program of Steel Beam-to-Column Connections," Fritz Engineering Laboratory Report 333.15, Lehigh University, Bethlehem, PA.

IABSE, 1989. "Bolted and Special Connections," Proceedings of the International Colloquium held in Moscow, USSR, May 1989, VNIPIP, 4 Vols., IABSE, Zurich.

ICBO, 1994. The Uniform Building Code, Volume 2, The International Conference of Building Officials, Whittier, CA.

Jaspart, J.P., Zandonini, R., and Colson, A., "The SPRINT Results," Proc. of the Third Intl. Workshop on Steel Connections (R. Bjorhovde et al. , eds.), Elsevier, 1996 (in press).

Johnson, R.P., and Law, C.L.C., 1981. "Semi-Rigid Joints for Composite Frames," in Proc. Int. Conf. on Joints in Structural Steelwork, J.H. Howlett et al. (eds.), Pentech Press, London, pp. 3.3-3.19.

Johnston, B., and Mount, E. H., 1941. "Analysis of Building Frames with Semi-Rigid Connections," Transactions of ASCE, Vol. 107, March, pp. 993-1019.

Kato, B., 1982. "Beam-to-Column Research in Japan," J. of the Structural Division, ASCE, Vol. 108, ST2, pp. 343-360.

Kato, B., and McGuire, W., 1973. "Analysis of T-Stub Flange-to-Column Connections," J. of Structural Division, ASCE, Vol. 99, No ST5, pp. 865-888.

Kishi, N., and Chen, W. F., 1986. "Data Base of Steel Beam-to-Column Connections," Vol. 1 & 2, Structural Engineering Report No. CE-STR-86-26, School of Civil Engineering, Purdue University, West Lafayette, IN.

Knechtel, B. A., 1992. "The Effect of Concrete Encasement on the Strength, Stiffness and Ductility of T-stub Beam-to-Column Connections," M.S. Thesis, University of Washington, Seattle, WA.

Krawinkler, H., Bertero, V. V., and Popov, E. P., 1975. "Shear Behavior of Steel Frame Joints," J. of the Structural Division, ASCE, Vol. 101, No. ST11, pp. 2317-2336.

Krawinkler, H., 1978. "Shear in Beam-Column Joints in Seismic Design of Steel Frames," Engineering Journal, AISC, Third Quarter, pp. 82-91.

Krawinkler, H., and Popov, E. P., 1982. "Seismic Behavior of Moment Connections and Joints," J. of the Structural Division, ASCE, Vol. 108, ST2, pp. 372-390.

Krishnamurthy, N., 1979. "A Fresh Look at Bolted End-Plate behavior and Design," Engineering Journal, AISC, Vol. 15, 2nd Quarter, pp. 39-49.

Krishnamurthy, N., 1980. "Modelling and Prediction of Steel Bolted Connection Behaviour," Computers and Structures, Volume 11, pp. 75-82.

Kulak, G. L., Fisher, J. W., and Struik, J. H. A., 1987. Guide to Design Criteria for Bolted and Riveted Joints, 2nd Edition, John Wiley & Sons, New York.

Lee, S.-J., and Lu, L.W., 1989. "Cyclic Tests of Full-Scale Composite Joint Subassemblages", J. of Structural Engineering, ASCE, Vol. 115, ST8, pp. 977-1998.

Leon, R. T., Ammerman, D. J., Lin, J. and McCauley, R. D., 1987. "Semi-Rigid Composite Steel Frames," AISC Engineering Journal, 4th Quarter, pp. 147-155.

Leon, R. T., 1990. "Semi-Rigid Composite Construction," Journal of Constructional Steel Research, Vol. 15, Nos. 1 & 2, pp. 99-120.

Leon R., and Ammerman D.J., 1990. "Semi-Rigid Composite Connections for Gravity Loads", AISC, Engineering Journal, 1st Quarter, pp. 12-21.

Leon, R.T., 1991. "Towards New Bond and Anchorage Provisions for Interior Joints," in SP-123: Design of Beam-Column Joints for Seismic Resistance (J.O. Jirsa, ed.), American Concrete Institute, Detroit, pp. 425-442.

Leon, R.T., and Forcier, G.P., 1991. " Performance of Semi-Rigid Composite Frames," Proc. of the 1991 Annual Technical Session, SSRC, Bethlehem, PA, pp. 259-270.

Leon, R.T., and Forcier, G.P., 1992. " Parameteric Study of Composite Frames, " In Steel Connections II, R. Bjorhovde et al. (eds.), AISC, Chicago, pp. 152-159.

Leon, R.T., 1992. "Semi-Rigid Composite Connections," in Semi-Rigid Connections in Steel Frames, R. Lorentz et al. (eds.), SB-43, Council on Tall Buildings, Lehigh, PA.

Leon, R.T., and Zandonini, R., 1992. "Composite Connections," in Steel Design: An International Guide (P. Dowling, J. Harding and R. Bjorhovde, eds.), Elsevier Publishers, London, pp. 501-522.

Leon, R.T., Galambos, T.V., Schmit, J.J., and Teng, A.L., 1993. "Field Instrumentation of Steel Highway Bridges," Report MN/RC-94/15, Minnesota Department of Transportation, St. Paul, MN, 153 pp.

Leon, R.T., 1994, "Composite Semi-Rigid Construction," Engineering Journal, AISC, Vol. 31, 2nd Quarter, pp. 57-67.

Leon, R.T., and Shin, J.K., 1995. "Performance of Semi-Rigid Frames," in Restructuring: America and Beyond, Proc. of the Structures Congress XIII, ASCE, New York, pp. 1020-1035.

Leon, R.T., and Deierlein, G.G., 1996. "Considerations for the Use of Quasi-Static Testing," Earthquake Spectra, EERI (in press - to appear March 1996).

Leon, R.T., Hoffman, J., and Staeger, T., 1996. "Design of Partially-Restrained Composite Connections," AISC Design Guide 9, American Institute of Steel Construction, Chicago.

Leon, R.T., and Hajjar, J.F., 1996. "Effect of Floor Slabs on the Performance of Steel Moment Connections," to appear in Proceeedings of the 11WCEE, Elsevier, 1996.

Lionberger, S. R., and Weaver, W., 1969. "Dynamic Response of Frames with Nonrigid Connections," J. of the Engineering Mechanics Division, ASCE, Feb., pp. 95-114.

Lorentz, R.F., Kato, B., and Chen, W.F. (eds.), 1993. Semi-Rigid Connections in Steel Frames, Council on Tall Buildings and Urban Habitat, Bethlehem, PA.

Lyse, I., Gibson, G.J., 1936. "Welded Beam-Column Connection," American Welding Society Journal, Vol. 15, No. 10, pp. 34-40.

Mander, J.B., Pekcan, G., and Chen, S.T., 1995. "Low-Cycle Variable Amplitude Fatigue Modelling of Top-and-seat Angle Connections," Engineering Journal, Vol. 32, 2nd Quarter, AISC, Chicago, pp. 54-62.

Marley, M.J., and Gerstle, K.H., 1982. "Analysis and Tests of Flexibly-Connected Steel Frames," Report to AISC under Project 199, Department of Civil Engineering, U. of Colorado, Boulder, CO.

Mazzolani, F. M., and Giouncu, V. (eds.), 1995. Behavior of Steel Structures in Seismic Areas, STESSA '94 - First International Workshop and Seminar on Behavior of Steel Structures in Seismic Areas, Timisoara, Romania, June-July 1994, E & FN Spon, Chapman & Hall, London.

Moncarz, P. D., and Gerstle, K. H., 1981. "Steel Frames with Nonlinear Connections," J. of the Structural Division, ASCE, Vol. 107, ST8, pp. 1427-1441.

Monforton, G. R., and Wu, T. S., 1963. "Matrix Analysis of Semi-Rigidly Connected Frames," J. of the Structural Division, ASCE, Vol. 89, ST6, pp. 13-42.

Moore, D.B., and Sims, P.A.C., 1986. "Preliminary Investigations into the Behavior of Extended End Plate Steel Connections with Backing Plates," J. Constructional Steel Research, Vol. 6, pp. 95-122.

Morino, S., and Nishiyama, I., 1992. "Hybrid Structures in Japan," in Composite and Hybrid Structures, Goel, S., and Yamanouchi, H. (eds.), Department of Civil and Environmental Engng., The University of Michigan, Ann Arbor, MI.

Munse, W.H., 1976. "Fifty Years of Riveted, Bolted, and Welded Steel Construction," J. of Construction Division, ASCE, September, 1976, Vol. 102, CO3, pp. 437-447.

Munse, W. H., Bell, W. G., and Chesson, E., 1959. "Behavior of Riveted and Bolted Beam-to-Column Connections," J. of the Structural Division, ASCE, Vol. 95, ST3, pp. 29-51.

Munse, W. H., and Cox, H. L., 1956. "The Static Strength of Rivets Subjected to Combined Tension and Shear," Engineering Experiment Station Bulletin No. 437, University of Illinois, Urbana, IL.

Murray, T.M., and Kukreti, A.R., 1988. "Design of 8-Bolt Stiffened End Plate Moment Connections," Engineering Journal, AISC, Vol. 25, 2nd Quarter, pp. 45-53.

Murray, T. M., 1990. "Extended End-Plate Moment Connections," Steel Design Guide Series 4, Publ. No. D804, AISC, Chicago.

Murray, T.M., and Meng, R.L., 1996. "Seismic Testing of Moment End-Plate Connections," presenetd at the SAC Workshop on Nov. 11-12, Richmond, CA.

Murray, T.M., and Watson, D.P., 1996. "Strength of Moment End-Plate Connections with Multiple Rows at the Beam Tension Flange, in Connections in Steel Structures III: Behaviour, Strength and Design , R. Bjorhovde et al. (eds.), Elsevier Applied Science, London (in press).

Nader, M.N., and Astaneh-Asl, A., 1991. "Dynamic Behavior of Flexible, Semi-Rigid and Rigid Steel Frames," Journal of Constructional Steel Research, Vol. 18, pp. 179-192

Nader, M.N., and Astaneh, A., 1992. "Seismic Design Concepts for Semi-Rigid Frames," Structures Congress 92: Compact Papers, ASCE, New York, pp. 971-974.

Nair, R.S., Birkemoe, P.C., and Munse, W.H., 1969. "Behaviour of Bolts in Tee Connections Subjected to Prying Action," Structural Research Series No. 353, University of Illinois, Urbana, IL.

Narayanan, R., 1989. Structural Connections: Stability and Strength, R. Narayanan (ed.), Elsevier Applied Science, London, 452 pp.

Nethercot, D.A., 1985. "Joint Action and the Design of Steel Frames," The Structural Engineer, Vol. 63A, No. 12, Dec., pp. 371-379.

Nethercot, D.A., 1985. "Steel Beam to Column Connections -- A Review of Test Data and Their Applicability to the Evaluation of the Joint Behaviour of the Performance of Steel Frames," CIRIA, London.

Osman, A., Ghobarah, A., and Korol, R. M., 1993. "Seismic Performance of Moment Resisting Frames with Flexible Joints," Engineering Structures, Vol. 15, No. 2, pp. 117-134.

Packer, J.A., and Morris, G.A., 1987. "A Limit Design Method for the Tension Region of Bolted Beam-Column Connections," J. of the Institution of Civil Engineers, Vol. 55, No. 10.

Parfitt, J.A., and Morris, L. J., 1977. "A Limit State Design Method for the Tension Region of Bolted Beam-Column Connections," The Structural Engineer, Vol. 55, No. 10, Oct., pp. 446-458.

Park, R. and Paulay, T., 1975. Reinforced Concrete Structures, J. Wiley & Sons, New York.

Paulay, T., 1978. "Capacity Design of Reinforced Concrete Ductile Frames," in Earthquake-Resistant Reinforced Concrete Building Construction, V. Bertero (ed.), Vol. III, pp. 1043-1075, University Extension, UC-Berkeley, Berkeley, CA.

Phillips, J., and Packer, J.A., "The Effect of Plate Thickness on Flush End-Plate Connections," Proc. Int. Conf. on Joints in Structural Steelwork, J.H. Howlett et al. (eds.), Pentech Press, London.

Pinkney, R.B., and Popov, E.P., 1967. "Behavior of Steel Building Connections Subjected to Repeated Inelastic Strain Reversal--Experimental Data", Report No. UCB/SEMM 67-31, Dept. of Civil Engineering, University of California, Berkeley, CA.

Popov, E. P., and Pinkney, R. B., 1969. "Cyclic Yield Reversal in Steel Building Connections," J. of the Structural Division, ASCE, Vol. 95, ST3, pp. 327-353.

Popov, E. P., and Bertero, V. V., 1973. "Cyclic Loading of Steel Beams and Connections," J. of the Structural Division, ASCE, Vol. 99, ST6, pp. 1189-1204.

Popov, E. P., 1980. "Seismic Behavior of Structural Subassemblages," J. of the Structural Division, ASCE, Vol. 106, ST7, pp. 1451-1475.

Popov, E. P., Amin, N. R., Louie, J. J. C., and Stephen, R. M., 1985. "Cyclic Behavior of Large Beam-to-Column Assemblies," Earthquake Spectra, Vol. 1, No. 2, pp. 203-237.

Popov, E. P., Kasai, K., and Englehardt, M., 1993. "Some Unresolved Issues in Seismic Codes", Proceedings of the 1993 Structures Congress, ASCE, New York, pp. 421-426.

Pray, R.F., and Jensen, C.D., 1956. "Welded Top-Plate Beam Column Connections," The Welding Journal, Vol. 35, No. 7. .

Priestley, M.N.J. , and Paulay, T., 1992. Seismic Design of Reinforced Concrete and Masonry Buildings, J. Wiley & Son, New York, 744 pp.

Puhali, R., Smotlak, I., and Zandonini, R. 1990. "Semi-Rigid Composite Action: Experimental Analysis and a Suitable Model," Journal of Constructional Steel Research, Vol. 15, Nos. 1&2, pp. 121-152.

Radziminski, J.B., and Azizinamini, A. 1986. "Low Cycle Fatigue of Semi-Rigid Steel Beam-to-Column Connections," Proc. of the Third U.S. National Conference on Earthquake Engineering, Vol. II, EERI, El Cerrito, CA, pp. 1285-1296.

Rathbun, J. C., 1936. "Elastic Properties of Riveted Connections," Transactions of ASCE, Vol. 101, pp. 524-563.

Roeder, C.W., Leon, R.Y., and Preece, F.R., 1994. "Strength, Stiffness, and Ductility of Older Steel Structures under Seismic Loading," Report SGEM 94-4, Department of Civil Engineering, U. of Washington, Seattle.

SAC, 1994. "Invitational Workshop on Steel Seismic Issues", Proceedings, Workshop by SAC Joint Venture held in Los Angeles, September, 1994, SAC, Sacramento, CA..

Salmon, C. G., and Johnson, J.E., 1996. Steel Structures: Design and Behavior, Haper-Collins, New York.

Sarraf. M. and Bruneau, M., 1994. "Experimental Study on Cyclic Behavior of Riveted Stiffened Seat Angle Connections," Report OCEERC 94-01, Ottawa-Carleton Earthquake Engineering Research Center, Ottawa.

Schleich, J.B., and Pepin, R., 1992. "Seismic Resistance of Composite Structures," EUR 14428, Directorate-General Science, Research and Development, Commission of the European Communities, Brussels.

Severson, B. E., 1993. "Comparison of Riveted and Bolted Beam-to-Column T-Stub Connections," M. S. Thesis, University of Minnesota, Minneapolis, January 1993.

Sherbourne, A.N., 1961. "Bolted Beam to Column Connections," The Structural Engineer, Vol. 39, No. 6, June, pp. 203-210.

Shin, K. J., 1991, "Seismic Response of Frames with Composite Semi-Rigid Connections," Ph.D. Thesis, The Graduate School, University of Minnesota, MN.

Shin, K.J., and Leon, R.T., 1991. "Seismic Response of Frames with Semi-Rigid Composite Connections," Proceedings of the Pacific Conference on Earthquake Engineering, New Zealand, Vol. 3, pp. 57-68.

Shin, K.J., 1992. "Seismic Response of Semi-Rigid Composite Frames," Structures Congress 92: Compact Papers, ASCE, New York, pp. 645-648.

Sourochnikoff, B., 1950. "Wind Stresses in Semi-Rigid Connections of Steel Frameworks," Transactions of ASCE, Vol. 115, pp. 382-402.

SSRC, 1987. "Connections Bibliography," Task Group 25 (G. Morris, ed.), Structural Stability Research Council, Bethlehem, PA.

Standig, K.F., Rentschler, G.P., and Chen, W.F., 1975. "Tests of Bolted Beam-to-Column Moment Connections," Fritz Engineering Lab, Report No. 333.31, Lehigh University, Bethlehem, PA.

Standig, K.F., Rentschler, G.P., and Chen, W.F., 1976. "Tests of Bolted Beam-to-Column Flange Moment Connections," Welding Research Council Bulletin No. 218, August 1976, pp. 1-17.

Stelmack, T.W., Marley, M.J., and Gerstle, K.H., 1986. "Analysis and Tests of Flexibly Connected Steel Frames," J. of Structural Engineering, ASCE, Vol. 112, No. 7, pp. 1573-1588.

Thomas, E. D., 1992. "The Effect of Concrete Encasement on the Strength, Stiffness and Ductility of Steel Seated-Beam Connections," M.S. Thesis, University of Washington, Seattle, WA.

Thorton, W.A., 1985. "Prying Action - A General Treatment," Engineering Journal, AISC, Vol. 22, 2nd Quarter, pp. 67-75.

Tsai, K.-C., and Popov, E. P., 1988. Steel Beam-Column Joints in Seismic Moment Resisting Frames, Report No. UCB/EERC-88/19, Earthquake Engineering Research Center, University of California at Berkeley, CA..

Tsai, K.-C., and Popov, E. P., 1990. "Cyclic Behavior of End-Plate Moment Connections", J. of Structural Engineering, ASCE, Vol. 116, No. 11, pp. 2917-2930.

Tsai, K.-C., and Popov, E. P., 1990. "Seismic Panel Zone Design Effect on Elastic Story Drift in Steel Frames," J. of Structural Engineering, Vol. 116, No. 12, pp. 3285-3301.

Tschemmernegg, F., 1990. "The Moment Rotation Behavior of Composite Joints," IABSE Symposium on Mixed Construction, Vol. 60, IABSE, Zurich, pp. 83-88.

Van Dalen, K., and Godoy, H., 1982. "Strength and Rotational Behaviour of Composite Beam-Column Connections," Canadian Journal of Civil Engineering, Vol. 9, No. 2, pp. 313-322.

Wakabayashi, M., 1987. "A Historical Study of Research on Composite Construction in Japan," in Composite Construction in Steel and Concrete, I.M. Viest and D. Buckner (eds.), ASCE, pp. 400-427.

Whittaker, D., and Walpole, W.R., 1982. "Bolted End-Plate Connections for Seismically Designed Steel Frames," Research Report 82-11, Department of Civil Engineering, University of Canterbury, New Zealand.

Wilson, W. M., and Moore, H. F., 1917. "Tests to Determine the Rigidity of Riveted Joints of Steel Structures," University of Illinois Engineering Experiment Station, Bulletin No. 104, Urbana, IL.

Wilson, W. M., and Oliver, W. A., 1930. "Tension Tests of Rivets," University of Illinois Engineering Experiment Station, Bulletin No. 210, Urbana, IL.

Yee, Y.L., and Melchers, R., "Moment-Rotation Curves for Bolted Connections," J. of Structural Engineering, Vol. 112, No. 3, 1986, pp. 615- 635.

Young, C. R., and Jackson, K. B., 1934. "The Relative Rigidity of Welded and Riveted Connections," Canadian Journal of Research, Vol. 11, No. 1, pp. 62-134.

Zandonini, R., 1989. "Semi-Rigid Composite Joints," in Structural Connections: Stability and Strength, R. Narayanan (ed.), Elsevier Applied Science Publishers, Barking, 1989, pp. 63-120.

Appendix A - T-Stub Connection Design Example

Design an interior connection between W24 x 94 A36 beams and a W14 x 283 A572/50 column. The connection consists of T-stubs for moment transfer and web angles for shear transfer. The connection will be a partial restraint, full strength one.

a) Check beam compactness criteria:

$$\text{Flange:} \quad \frac{52}{\sqrt{Fy}} = 8.66 > 5.2, \text{O.K.}; \qquad \text{Web:} \quad \frac{253}{\sqrt{Fy}} = 42.1 > 41.9, \text{O.K.}$$

The 52 and 41.9 are taken directly from p. 1-31 of the 1994 LRFD Manual. A very conservative value was assumed for web compactness since the amount of axial load is unknown.

b) If all bending moment is carried by the tees and assuming that the beam can develop a force of 1.25 M_p, the force in the tees will be:

$$F \cong \frac{M_u}{d_b} = \frac{1.25 \cdot 254 \cdot 36}{24.31} = 470.2 \text{ kips}$$

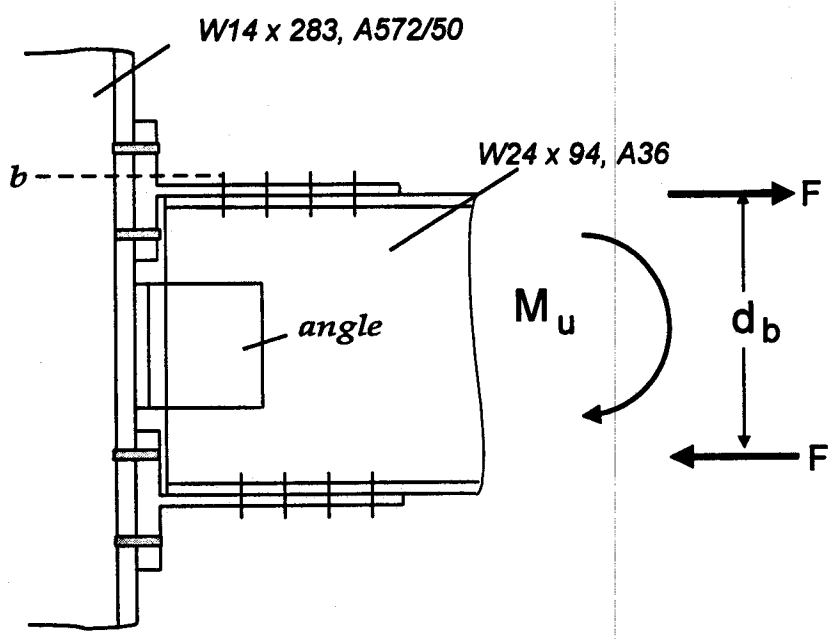

Fig. A.1 - Preliminary configuration.

Note that the assumption that the total resistance in this connection comes from the flanges is flawed. In fact the flanges transmit only 73.2% of the bending forces (Z_x for the beam is 254 in.^{3} but for the flanges alone it is 185 in.^{3}).

Thus for design for brittle modes:

$$F = (0.732)(470.2) = 344.1 \text{ kips}$$

For design for ductile modes of failure:

$$F = (0.732)(470.2) / 1.25 = 275.3 \text{ kips}$$

c) Determine the minimum number of bolts (N) required to carry the tensile force to the column flange. Assume that prying forces will be large and will use about 20% of the tensile strength. From LRFD J3.6 and Table J3.2, and assuming 1 in. A325 bolts:

$$\phi\, r_n = \phi\, F_t\ A_b = (0.75)(90)\ (0.785) = 53.0 \text{ kips / bolt}$$

$$N = 344.1\ (1.2) / 53.0 = 7.8 \text{, say 8 bolts}$$

The bolt strength is consistent with that given in the LRFD Vol. II, Table 8-15, p. 8-27. Note that because prying forces will need to be checked once the connection geometry is known, it is best at this stage to have a conservative number of bolts to the column flange.

d) Determine the number of bolts (M) required to transmit the forces from the tee to the beam flanges through shear (bolts are in single shear). From LRFD J3.6 and Table J3.2, and assuming 1 in. A490-X bolts:

$$\phi\, r_n = 0.75\, F_v\ A_b = 0.75\,(75)\,(0.7856) = 44.2 \text{ kips / bolt}$$

This strength is consistent with that given in the LRFD Vol. II, Table 8-11, p. 8-24.

Check bearing strength by Eq. (J3-1a):

$$\phi\ r_u = \phi\,(2.4)\ d \cdot t \cdot F_u = 0.75\ (2.4)\ (1)\ (t\ )\ (58) \geq 104.4t$$

Shear will govern if the thickness of the T-stub is greater than:

$$t_w \text{ (stem of T-stub)} = 44.2\ / 104.4 = 0.42 \text{ in.}$$

This is small so bearing probably will not govern; this will be checked latter. Thus:

$$M \geq \frac{344.1 \text{ kips}}{44.2 \text{ kips}} \geq 7.8 \qquad \rightarrow \qquad \text{Use 8 bolts}$$

Thus for design for brittle modes:

$$F = (0.732)(470.2) = 344.1 \text{ kips}$$

For design for ductile modes of failure:

$$F = (0.732)(470.2) / 1.25 = 275.3 \text{ kips}$$

c) Determine the minimum number of bolts (N) required to carry the tensile force to the column flange. Assume that prying forces will be large and will use about 20% of the tensile strength. From LRFD J3.6 and Table J3.2, and assuming 1 in. A325 bolts:

$$\phi\, r_n = \phi\, F_t\, A_b = (0.75)(90)\,(0.785) = 53.0 \text{ kips / bolt}$$

$$N = 344.1\,(1.2) / 53.0 = 7.8 \text{, say 8 bolts}$$

The bolt strength is consistent with that given in the LRFD Vol. II, Table 8-15, p. 8-27. Note that because prying forces will need to be checked once the connection geometry is known, it is best at this stage to have a conservative number of bolts to the column flange.

d) Determine the number of bolts (M) required to transmit the forces from the tee to the beam flanges through shear (bolts are in single shear). From LRFD J3.6 and Table J3.2, and assuming 1 in. A490-X bolts:

$$\phi\, r_n = 0.75\, F_v\, A_b = 0.75(75)(0.7856) = 44.2 \text{ kips / bolt}$$

This strength is consistent with that given in the LRFD Vol. II, Table 8-11, p. 8-24.

Check bearing strength by Eq. (J3-1a):

$$\phi\, r_u = \phi\,(2.4)\, d \cdot t \cdot F_u = 0.75\,(2.4)\,(1)\,(t)\,(58) \geq 104.4t$$

Shear will govern if the thickness of the T-stub is greater than:

$$t_w \text{ (stem of T-stub)} = 44.2 / 104.4 = 0.42 \text{ in.}$$

This is small so bearing probably will not govern; this will be checked latter. Thus:

$$M \geq \frac{344.1 \text{ kips}}{44.2 \text{ kips}} \geq 7.8 \qquad \rightarrow \qquad \text{Use 8 bolts}$$

e) Check beam flange capacities:

For gross area: $\phi A_g F_y = 0.9 (9.065 \times 0.875) (36) = 257.0$ kips
For effective area: $\phi A_e F_u = 0.75 [(9.065 - 2(1.125)) \times 0.875)] (58) = 259.4$ kips

Note that these values are not inconsistent with the forces F calculated above. If the ϕ factors are removed and the overstrength factor accounted for in the yielding criteria, then the yield force for the beam is 356.9 kips and the fracture force is 345.8 3 kips. Thus a design force of 344.1 kips seems reasonable.

f) Determine thickness (t_w) required to transmit tension on the stem of the tee [LRFD, D1]:

1) The connection is to a heavy W14, so assume that the T-stub will be 16 in. wide at the column face and taper to 9 in. at its end. The width of the beam flange is just over 9 in. so this configuration is reasonable. With this taper, and using four rows of 1 in. bolts, the minimum length of the stem is:

l_s = 3 (min. bolt spacing) + 2 (min. edge distance) + clearance + flange thickness

$l_s = 3 (3) + 2 (1.5) + 0.5 + 1.5 = 14$ in., so at least a WT15 will be needed.

The required tee stem thickness for strength controlled by gross area yielding, assuming the thickness at the critical section is 12.9 in., is:

$$A_g \geq \frac{T_u}{0.90F_y} \geq \frac{275.3}{0.9 \cdot 36} \geq 8.50 \text{ in}^2 \text{ , so } t_w = 8.50 / 12.9 = 0.65 \text{ in.}$$

2) Assume that the net area is given by the total width at the location of the first line of bolts (12.5 in.) minus two bolt holes (2 x 1.125 = 2.25) or 10.25 in. Then the required tee stem thickness for strength governed by net area fracture is:

$$A_n = \frac{T_u}{0.75 \cdot F_u} \geq \frac{344.1}{0.75 \cdot 58} \geq 7.91 \text{ in}^2, \text{ so } t_w = 7.91 / 10.25 = 0.69 \text{ in.}$$

These checks are intended to ensure that yielding on the gross area will occur before fracture in the net area. The above calculations indicate that it is possible to obtain a good balance between yielding and fracture with a tee stem thickness of around 0.7 in.

g) Determine the flange thickness (t_f) for the tee section. Prying action must be taken into account. For details see the AISC Manual (AISC, 1994), Vol. II, pp. 11-5 to 11-

16. For this purpose, we can use the equation proposed by Thornton (AISC Engineering Journal, Vol. 22, No.2, pp. 67-76):

$$t_t \geq \sqrt{\frac{4Tb'}{\phi_b w F_y (1+\alpha\,\delta)}} \qquad \phi_b \geq 0.9$$

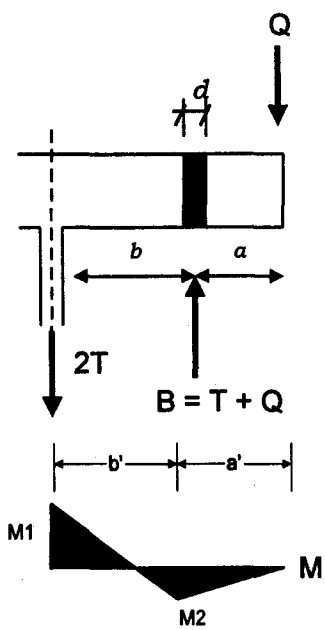

Fig. A.2 - Prying action definitions.

where,

w = tributary width of resisting section

$\alpha = M_1 / \delta\, M_2$

δ = ratio of net area at bolt line to gross area at M_1

The minimum gage (g) that can be used with is about 4 in. ($2k_1 + c_3$, where c_3 is given on p. 8-13 of the LRFD Manual):

$b = (g/2) - (t_w/2) \approx 1.75$ in

$b' = b - (d/2) = 1.25$ in.

Salmon and Johnson, following Thorton, recommend to compute β as a function of $\alpha\,\delta$:

$$\beta = (\frac{B}{T} - 1)\frac{a'}{b'} = (\frac{53.0}{43.0} - 1)(1.25) = 0.29$$

For purposes of this calculation the force B can be taken, as an upper bound, as the bolt capacity in tension (53.0 kips). The force T is the part of the total tension force going to each bolt (344.1 / 8 bolts = 43.0 kips). The value of a' is a guess since we have not chosen a tee yet. Use α as follows:

if $\beta \geq 1$, use $\alpha = 1 \rightarrow$ large prying force

if $\beta < 1$, use α = lesser of $\frac{1}{d}(\frac{\beta}{1-\beta})$ and 1.0

Estimate :

$$\delta = \frac{\text{net width at bolt line}}{\text{gross width at critical section near web face}}$$

$$\delta = \frac{16 - (4 \text{ x } 1.125)}{16} = 0.719$$

$$\frac{1}{\delta}\left(\frac{\beta}{1-\beta}\right) = \frac{1}{0.719}\left(\frac{0.29}{1-0.29}\right) = 0.57 \quad \rightarrow \alpha = 0.57$$

$$t_f \geq \sqrt{\frac{4(344.1/2)1.75}{0.9 \cdot 16 \cdot (36) \cdot (1 + 0.57 \cdot 0.719)}} = 1.28 \text{ in.}$$

A quick check of this value can be made from Table 11-1 in the LRFD Manual. For a thickness of 1.25 in. and a "b" of 2.25 in., the table gives 22.5 kips per linear inch. In this case we have about 16 in. which gives a total force of 360 kips, very close to the desired value of 344.1 kips.

Try a WT 15 x 95.5 :

t_w = 0.71 in. (slightly greater than 0.69 in. required for net area failure in tension)

t_f = 1.185 in (slightly less than the 1.28 in. required)

The flanges of the tee must be cut to meet the required distances. For this size WT the minimum gage will be 4.25 in., so the assumed values of "a" and "b" can be achieved. The total width of the flange should be about ((2 x 2.25 x 1.75) + tw) or 8.6 in. Thus we need to trim about 3.5 on each flange. Note that several design trials assuming that the flanges were not trimmed did not produce satisfactory results. This is due to the large increase in prying forces and required flange thickness if the values of "a" and "b" are not kept as low as possible.

h) Check the prying force using the formula proposed by Salmon and Johnson:

$$Q \geq T\left(\frac{\alpha\,\delta}{1+\alpha\,\delta}\right)\left(\frac{b'}{a'}\right)$$

$$Q = T\left(\frac{0.57 \cdot 0.719}{1 + (0.57 \cdot 0.719)}\right)\left(\frac{1.40}{2.54}\right) = 0.16\ T$$

$$T + Q = 1.16\ T$$

$$1.16 \cdot T_u = 1.16 \cdot 43.0 = 49.9 \text{ kips} \leq f\ R$$

<u>The entire design must now be rechecked (not shown)</u>

<u>For uniformity and constructability reasons, all bolts should be 1 in. A490-X</u>

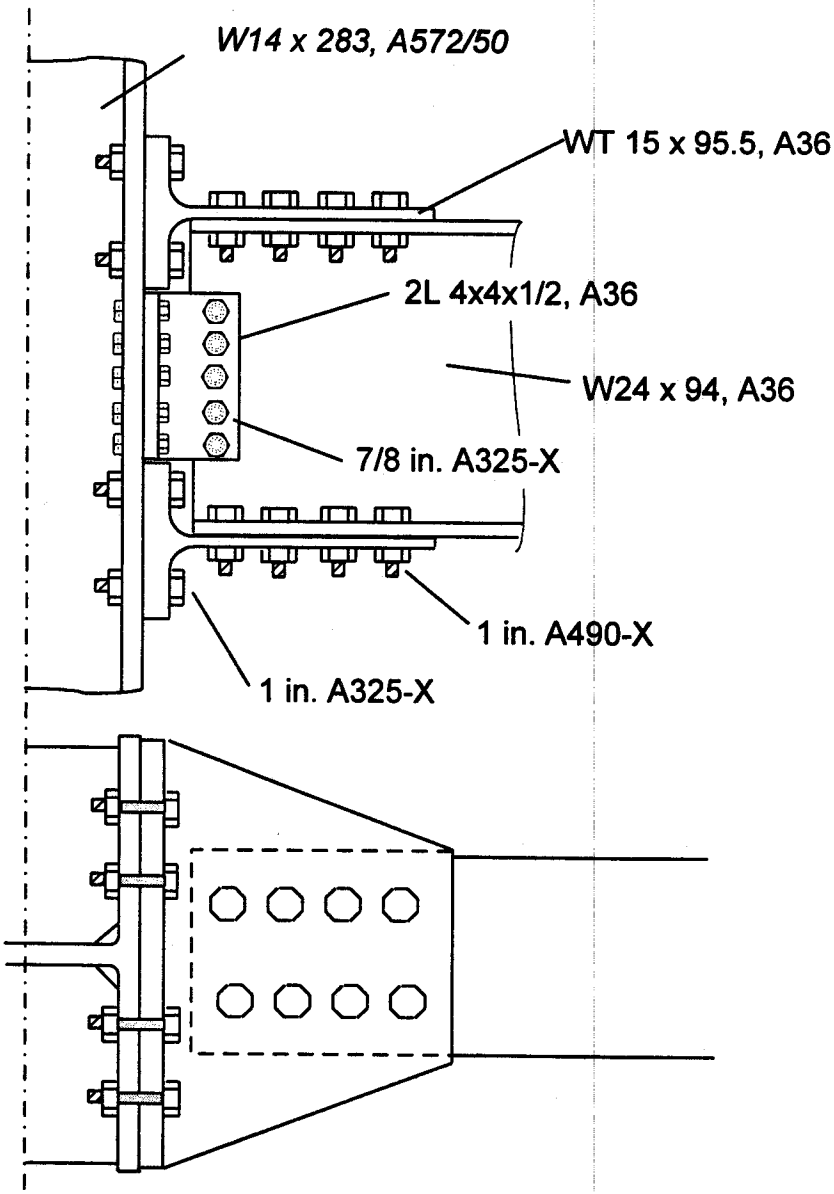

Figure A.3 - Final Design

i) Design the angles for shear transfer for either the maximum shear from lateral loads (assume beam length = 28 ft.):

i) Design the angles for shear transfer for either the maximum shear from lateral loads (assume beam length = 28 ft.):

$$\mathbf{V_u = 1.25 \cdot 2M_n / L = 78.4\ kips}$$

or the maximum reaction (from the Load Tables, p. 4-44 of the LRFD Manual):

$$\mathbf{V_u = 256\ kips\ \ (controls)}$$

From p. 9-54 of the LRFD Manual, 7 rows of 7/8" diameter A325N bolts with a 3/8 angle will work.

$$\rightarrow \quad \mathbf{Use\ 2L \cdot 4 \times 4 \times 3/8 \times 1'\text{–}9''\ with\ 7\ A325N\ bolts}$$

j) Check service level forces:

Design resistance at service = 16.5 kips/bolt (AISC Manual, p. 8-29)

$F_{service}$ = 132.0 kips

Check that this is greater than 1.25 $M_{service}$ (not specified for this problem) and less than 0.8 M_p (= 220 kips, O.K.)

k) Check panel zone shear:

$$\mathbf{V_u \geq 0.9 \sum \phi M_p / d_c = 884.9\ kips}$$

The capacity, from Eq. 8-1 of ASCE (1992) is:

$$\mathbf{Vu = 0.75 \cdot 0.6 \cdot 36 \cdot 16.74 \cdot 1.29 \cdot 1.24 = 435 kips.}$$

Doubler plates are needed - Use a 5/8 plate on each side of the web.

l) Continuity plates:

$$\mathbf{P_{bf} = \phi_b 6.25 \cdot t_{fc}^2 \cdot F_{yc} = 0.9 \cdot 6.25\,(2.07)^2 \cdot 36 = 867.7\quad kips}$$

Check vs. Section 8.5 of ASCE (1992):

$P_{required} = 1.8\ F_{yb}\ b_f t_{bf} = 1.8 \times 36 \times 16.11 \times 2.07 = 2{,}160$ kips

Continuity plate 1.25" thick are required.

m) Check if stiffeners in column are required for gravity loads:

To avoid stiffeners, the column web must be checked for:

(a) Compression zone:

(1) K.1.3 - Local Web Yielding:

$$P_{bf} = \phi(5k + t_{fb})F_{y_c} \cdot t_{w_c} \geq (1.0)\ (5 \cdot 2.75 + 0.875)\ (36)\ (1.29) = 679.2 \text{ kips}$$

(2) K1.4 - Web Crippling:

$$P_{bf} = \phi 135 t_{wc}^2 [1 + 3(\tfrac{t_{fb}}{d})(\tfrac{t_{wc}}{t_{fc}})^{1.5}]\sqrt{\tfrac{F_{yc} t_{yc}}{t_{wc}}}$$
$$= 0.75 \cdot 135\,(1.29)^2\ [1 + 3(\tfrac{0.875}{16.74})(\tfrac{1.29}{2.07})^{1.5}]\sqrt{\tfrac{36 \cdot 0.875}{1.29}} = 896.\text{k}$$

(3) K1.5 - Compression Buckling of the Web:

$$R_n = \frac{4{,}100\ t_w^3\ \sqrt{F_{yc}}}{d_c} = \frac{4{,}100\,(1.29)^3\ \sqrt{36}}{16.74 - (2 \cdot 1.25)} = 3708 \quad \text{kips}$$

Thus none of the capacities are exceed; stiffeners are not required. Note, however, that the continuity plates already exist so this check is presented only for illustrative purposes!

(b) Tension zone:

(4) K1.2 - Local Flange Bending:

$$P_{bf} = \phi_b\, 6.25 \cdot t_{fc}^2 \cdot F_{yc} = 0.9 \cdot 6.25\,(2.07)^2 \cdot 36 = 867.7 \quad \text{kips}$$

Thus P_{bf} equals the required strength and no tension stiffener are required!

SYSTEMS BEHAVIOR OF STRUCTURAL STEEL FRAMES SUBJECTED TO EARTHQUAKE GROUND MOTION

Helmut Krawinkler
STANFORD UNIVERSITY

ABSTRACT: The seismic behavior of a steel moment resisting frame structure is composed of the behavior of its elements, the interactions between elements, and the dynamic characteristics of the three-dimensional structural system. This paper addresses all three aspects, with an emphasis on inelastic behavior characteristics and methods that can be employed to predict system behavior and performance. The focus is on evaluation rather than on design, with specific consideration given to issues and problems that were raised by recently observed connection fractures.

INTRODUCTION

This paper focuses on information needed to understand the seismic behavior of steel moment resisting frame (SMRF) structures with rigid connections, and on analytical techniques that can be employed to predict this behavior. "Rigid" implies that the beam-to-column connections permit only negligible relative rotation between the end of the beam and the column. "Structures" implies that the whole three-dimensional system is considered, which consists of columns, beams framing into columns (usually, but not necessarily, in two orthogonal directions), and horizontal diaphragms that tie individual frames together at the floor levels. Diaphragms, which in SMRF structures are treated usually as rigid in their own plane, are not part of this discussion. It is assumed that sufficient shear resistance is provided between diaphragms and beams so that the seismic inertia forces generated at the floor levels can be transferred to MRFs, and shear forces generated by enforcing displacement compatibility can be transferred between MRFs.

The presentation starts with a short historical review that gives a background on the development that has led to the presently customary configurations and details of SMRFs. This background is followed by a discussion of the load-deformation behavior of individual elements, element assemblies and complete frames, directed towards an identification of those characteristics that control the seismic response of SMRFs. Next comes a discussion of ground motion characteristics and description of seismic input, which is needed to understand the seismic demands to which SMRFs may be subjected in severe earthquakes. Emphasis is then placed on a discussion of inelastic dynamic response characteristics of frames, illustrating how inelastic deformations are distributed throughout the structure and how they are dissipated, what types of hinging mechanisms may occur and how these mechanisms affect the dynamic response, and what effect higher modes may have on strength and deformation demands.

The second part of the paper is concerned with analytical predictions of the seismic demands to which SMRFs and their elements may be subjected, and with specific design considerations. The discussion on analytical predictions emphasizes techniques that can be employed in engineering practice, but tries to bring into focus the additional needs for prediction of force and deformation demands at beam-to-column connections, created by the recently observed fractures at welded connections. An attempt is made to shed some light on the possible consequences of connection fractures, but it must be emphasized that much more research is needed before these consequences are fully understood. The paper closes with suggestions for engineering practice, which are intended to provide guidance for the design of new SMRFs and to bring out specific issues of concern in the repair and retrofit of existing SMRFs.

This paper does not provide a comprehensive discussion of all important behavior and design considerations for SMRF structures. For instance, the cyclic dynamic behavior of individual elements, such as beams and columns, is reasonably well understood and is discussed extensively in the literature. It is summarized here only to the extent needed to understand its affect on system behavior. The emphasis is on system performance of SMRF structures in severe earthquakes; serviceability and damage control issues, whose importance is unquestionable, are not addressed in this discussion.

The focus of the paper is not on code design aspects but on cyclic and dynamic behavior issues that have gained much on importance because of the recently observed connection fracture problems. Standard code design has served the profession well, presuming that the deformation capacity of all elements that are expected to experience inelastic deformations is sufficiently large to tolerate large variations in expected demands, and presuming that connections fulfill their intended functions at these high demands in the elements they connect. The latter presumption appeared to be justified before January 17, 1994, the date of the Northridge earthquake. Since that date it no longer is warranted, and standard code design for SMRF structures needs to be reevaluated. This reevaluation needs to be based on a more realistic assessment of imposed demands and available capacities than was done in the past. It is expected that the profession will succeed in developing safer connection details and better structural configurations that will make future designs of SMRF structures amenable again to uncomplicated code procedures. The process of arriving at these simplified procedures needs to be based on a thorough evaluation of imposed seismic demands and available deformation capacities, and on a clear understanding of system behavior. Moreover, the assessment of the seismic safety of existing SMRF structures will have to be based on more comprehensive concepts than are contained in present code procedures. This paper attempts to summarize the state of knowledge relevant for these purposes.

HISTORICAL PERSPECTIVE

An excellent historical review of the evolution of steel frame building construction is presented in McGuire (1988). In seismic regions, steel frames have been used in building construction for more than a hundred years. In the early 20th century they were used mostly to transfer gravity loads to interior column and to exterior frames which were imbedded into masonry walls. The connections provided either only shear transfer or limited moment transfer by means of riveted partially restrained connections. Lateral stiffness was provided usually by the walls. Moment resisting frames without infill walls came into wider use when curtain walls became popular. This was the time when moment resistance and stiffness of the connections became a critical issue. Connections were usually complex and expensive, consisting of plates, angles, and/or T-sections that were riveted, or bolted, or later in part welded together. A classical example of a structurally sound but expensive connection arrangement, which was employed in the Torre Latinoamericano, is shown in Figure 1.

In the 1950's, structural welding became a widely accepted process in the building industry. This trend, together with the need for strong and stiff but economical connections, accelerated the shift from riveted or bolted partially restrained connections to welded and rigid connections. Many different types of welded connections were used, the earlier ones mostly with shop-welded/field-bolted cover plates connecting the beam flanges to the columns. But in the late 50's the field-welded direct connection between beam flanges and column flanges started to be widely used. Experimental research performed in the mid to late 50's, primarily at Lehigh University [e.g., Graham et a. (1959)], provided criteria for welding and for continuity plate requirements to prevent web crippling and column flange distortions. Experimental research performed in the mid 60's to early 70's at U.C. Berkeley [e.g., Popov and Pinkney (1969), Popov and Stephen (1970)] provided evidence that certain types of butt welded beam flange to column flange connections can behave satisfactory under cyclic loading.

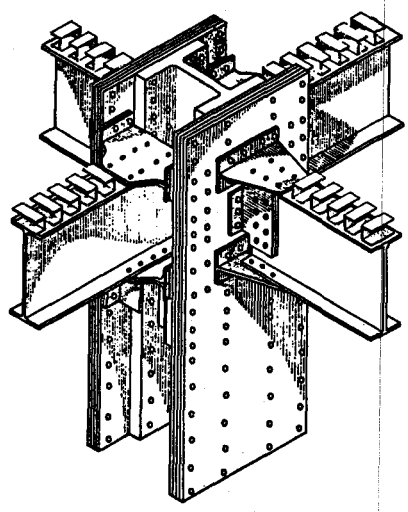

FIGURE 1. Typical Joint Detail Employed in the Torre Latinoamericano [Cuevas Barajas (1962)]

Based on the then available evidence, the engineering profession and the steel industry embraced the full penetration butt welded beam flange to column flange connection because of its simplicity and economy. It became the standard moment connection and, in concept, has remained the standard connection until 1994. However, it has to be pointed out that SMRF structures of the mid 60's to mid 70's had the following specific characteristics which no longer apply today (in most cases):

- Most (or all) connections in the structure were moment resisting connections.
- Most connections were 3- or 4-way connections in which the beams framing into the weak direction of the column were also rigidly connected.
- Because of the large number of moment connections and because of relatively small beam spans, most beam and column sections were relatively small.
- The beam material was either A-7 or A-373 (F_y = 32 ksi, phased out in 1960), or A-36 with a yield strength whose mean value was not much higher than the nominal value.
- Field welding was usually done with the Shielded Metal Arc Welding (SMAW) process.
- The joint panel zones were strong in shear (usually reinforced with doubler plates) so that little shear yielding occurred in the panel zones before the beams developed their moment capacity.

The basic type of connection has changed very little since that time, but design and construction practices have. Perhaps most important is the great reduction in the use of the 3- and 4-way connections of the type shown in Figure 2. These connections are expensive and their performance is questionable unless precautions are taken. For weak-axis connections (beams framing into the column web) it was standard for many years to weld the beam flange to a continuity plate which is welded to the web and the flanges of the column and did not extend beyond the column flanges. Tests have shown that this type of weak-axis connection is susceptible to fracture at the weld connecting the beam flange to the continuity plate [e.g., Rentschler (1980)]. This problem can be mitigated by several measures, including extending the continuity plate beyond the column flanges. Since all mitigating measures can be accomplished only at a considerable additional expense, the preferred choice today is to eliminate weak-axis moment connections.

Because of this change in design practice, and because of changes in material production, fabrication, and construction practices, most of today's SMRF structures have the following characteristics:

- Moment resisting connections are used only on two frame lines in each direction, usually at the perimeter, in order to eliminate weak-axis connections.

- Often the frames with moment resisting connections do not extend over the full length of the buildings. The number of moment resisting connections is reduced as much as possible, resulting in structures with low redundancy.
- Because of the small number of moment connections, most beam sections are relatively large. For this reason weldments are large, which increases the susceptibility to weld cracking.
- Large beam sections necessitate large column sections in order to fulfill the strong column - weak girder concept. The through-thickness properties of columns with thick flanges are inferior to those of columns with thin flanges.
- The beam material is usually A-36 steel with a yield strength whose mean value is significantly higher than the nominal value. (According to recent data [SSPC (1994)], the mean is around 49 ksi for most A-36 beam section groups.) Thus, the stress level in the welds and the column, associated with hinging in the beam, is higher than predicted.
- Columns are usually made of A-572 steel whose mean yield strength is only 15 to 20% higher than the nominal value. Thus, column hinging may occur even though the strong column - weak beam concept is fulfilled in design calculations.
- Field welding is mostly done with the Self Shielded Flux Cored Arc Welding (FCAW-SS) process. It is widely believed that this process is inferior to the SMAW process.
- In the 1985 UBC the requirement for shear strength of the joint panel zone has been relaxed considerably. Thus, in newer structures many panel zones will yield in shear long before the beams reach their bending strength, and in severe earthquakes yielding may be limited to the joint panel zones.

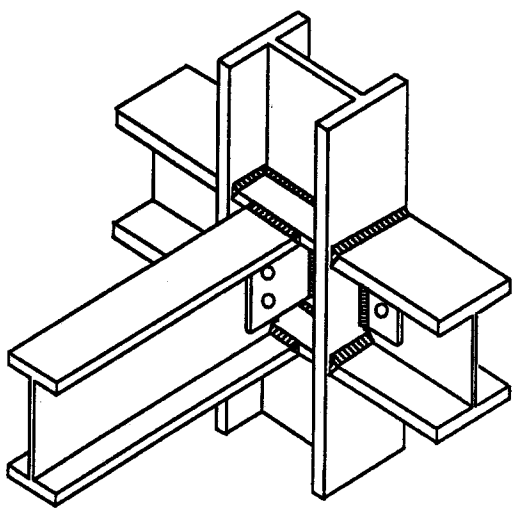

FIGURE 2. Beam-Column Joint with Strong and Weak Axis Connections

Many of the issues discussed here have a large impact on system behavior. There is little doubt that the seismic behavior of SMRF structures depends on the time of design and construction. There are also good reasons to believe that many older well designed SMRF structures with welded connections will perform better than newer ones. Time of design and construction cannot be considered in the following discussion of system behavior, but it needs to be considered in performance evaluation when capacities are compared to imposed demands.

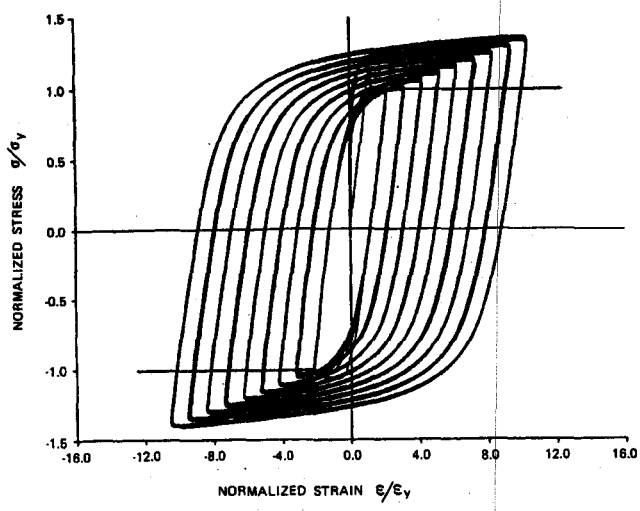

FIGURE 3. Typical Cyclic Stress-Strain Diagram of Structural Steel [Krawinkler et al. (1983)]

INELASTIC CYCLIC CHARACTERISTICS OF STRUCTURAL ELEMENTS

Elements made of structural steel have desirable as well as undesirable characteristics from the viewpoint of seismic performance in severe earthquakes. Their great advantage lies in the ability of the base material to dissipate great amounts of energy through inelastic cyclic deformations. Structural steel is a material that hardens under cyclic loading, i.e., it becomes stronger as the number of cycles and/or the deformation amplitude increases, and it exhibits large hysteresis loops. Figure 3 shows a typical cyclic stress-strain diagram of a smooth A-36 steel test specimen. Superimposed on the experimental curves is the elastic - perfectly plastic stress-strain diagram on which conventional estimates of member strengths in bending, tension, and compression are based. For the case illustrated the hardening is more than 40%. In the base material, crack initiation and propagation, which leads to deterioration and ultimately to fracture, becomes a problem only if the strain amplitude or the number of cycles is very large. Thus, steel appears to be ideally suited as a material for structures that have to dissipate seismic energy through inelastic deformations.

There are two caveats, however, to this ideal behavior characteristic. One has to do with loading in tension. Even small localized imperfections may cause very high strains when tensile stresses are applied, which in turn can lead to cracks and fracture. Imperfections may pre-exist in the base material, particularly in the through-thickness direction, or they may be created during the fabrication and erection processes. There are many sources for fabrication/erection related imperfections, but in many cases they are related to welding. Within the welds imperfections are almost unavoidable, a problem that is mitigated by the fact that the weld material is usually stronger than the base material. At the interfaces between welds and the base material imperfections may be caused by undercutting, insufficient fusion, or slag deposits. Within the base material imperfections may be caused by weld material splattering. Very high strains in the base material may also be caused around bolt holes or other points of stress concentrations. The big problem with cracks is that they propagate under cyclic loading and that they lead to unstable crack growth once a crack reaches a critical size, which may cause almost instantaneous fracture across plate elements. The result is a sudden deterioration in strength as is illustrated in Figure 4, which shows the load-deflection response of a steel cantilever beam in which fracture occurred at the toe of the weld connecting the beam flange to a column stub.

The second potential problem in steel elements has to do with loading in compression. Steel members are usually slender, which may lead to member buckling. Members are made up of individual plate elements, which are assembled into sections by hot-rolling, cold-forming, continuous or stitch

welding, or, years ago, bolting. The individual plates are susceptible to plate buckling, whose occurrence and post-buckling response characteristics depend on the plate boundary conditions and slenderness (width/thickness) ratio, material properties, the methods of plate forming and joining, and the applied cyclic loading history. The consequence of local plate buckling is a gradual deterioration in strength and stiffness of structural elements, usually of the type illustrated in Figure 5, which shows the load-deflection diagram of a steel cantilever beam with relatively thin flanges.

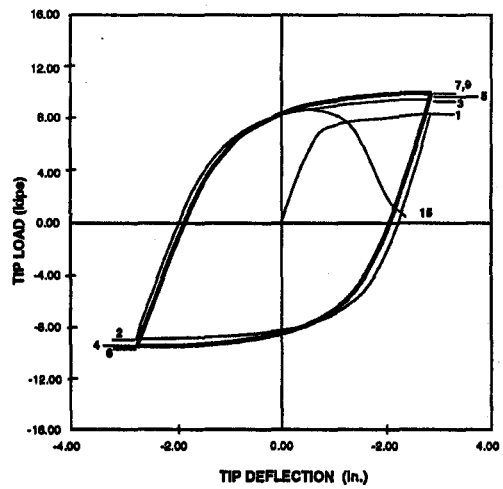

FIGURE 4. Cyclic Response of a Steel Beam with Connection Weld Fracture [Krawinkler et al. (1983)]

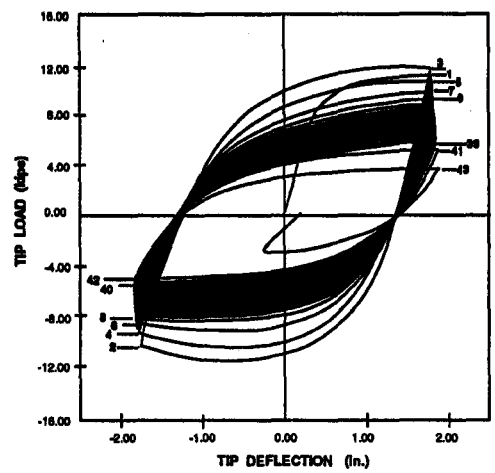

FIGURE 5. Cyclic Response of a Steel Beam with Local Buckling [Krawinkler et al. (1983)]

Many specification [e.g., LRFD (1994)] and guideline documents contain explicit criteria (usually expressed in terms of maximum permissible width/thickness ratios) to safeguard against premature local buckling, and contain also extensive lists of references on the subject. The objective of these criteria is not to prevent local buckling at all costs, but to delay local buckling to the extent that it will occur only at large strains and will not lead to unacceptable strength deterioration at strain levels expected in a severe earthquake. But it must be kept in mind that some strength deterioration due to local buckling can be expected if sections are used whose plate elements barely pass the width/thickness limitations.

Another phenomenon that will lead to deterioration in strength and stiffness of structural steel members is lateral torsional buckling. It occurs if the compression flange is inadequately braced in the

lateral direction and the member is permitted to buckle in a flexural/torsional mode. The occurrence and post-buckling behavior of this type of buckling depend on the unbraced length of the compression flange, the torsional properties of the section, the moment gradient along the member, the member boundary conditions, and the material properties. The consequences are similar to those of local buckling, which are illustrated in Figure 5, but deterioration occurs usually at a faster rate than for local buckling. Again, many specification [e.g., LRFD (1994)] and guideline documents contain explicit criteria (usually expressed in terms of maximum permissible unbraced lengths) to safeguard against premature lateral torsional buckling.

In SMRF structures the compressive deterioration modes summarized here may adversely affect the energy dissipation characteristics in plastic hinge regions of beams and columns. In regions of SMRFs in which plastic hinges are expected to form, care needs to be taken to apply the code criteria for local and lateral torsional buckling conservatively, particularly if large plastic rotation demands have to be expected. The crack propagation and fracture mode usually controls the behavior of beam-to-column connections (in SMRFs with welded rigid connections) and column splices. Since this mode leads to rapid deterioration of strength, it is believed to be the more critical deterioration mode. It should be an overriding consideration in the design process to keep the tensile stress level low at locations at which cracks may occur.

Attempts are reported in the literature to quantify the level of deformation at which onset of deterioration or unacceptable deterioration due to any of the modes discussed here occurs. Many of these attempts are based on experimental evidence obtained from monotonically loaded test specimens [e.g., Ziemian et al. (1992-1)]. These attempts may provide bounds on deformation levels but are not directly applicable to seismic loading since it is well established that under inelastic strain reversals every excursion causes damage and deterioration is a matter of cumulative damage, which depends on the number and deformation amplitude of the individual excursions. Models for cumulative damage assessment of components of steel structures have been proposed [e.g., Cosenza et al. (1990), Krawinkler and Zohrei (1983)], but the physical parameters contained in these models have not been quantified for more than a few test cases. Thus, at this time it is not feasible to provide reliable deformation levels for deterioration, or to quantify the rate of deterioration. It is believed, however, that the criteria for local and lateral torsional buckling contained in the LRFD seismic provisions [LRFD (1994)] provide adequate protection against excessive deterioration in most cases.

Beam Behavior

Under severe seismic loading, beams that are part of SMRFs consist of elastic portions and partially or completely plastified regions whose location, length, and strain distribution depend on geometric parameters (depth, span), boundary conditions, the effect of gravity loading (magnitude and gradient of gravity moment diagram), and the interstory drift demands imposed by the earthquake. In most, but not all, cases the plastified regions are located at the ends of the beam next to the column faces. These locations are desirable on one hand, because lateral bracing is provided by the column, and undesirable on the other hand because high demands are imposed on the connections.

If local and lateral torsional buckling are prevented, the moment curvature behavior at cross-sections away from the connection shows the same desirable characteristics as the material stress-strain behavior illustrated in Figure 3. In an earthquake, which causes random cycles, the response of a steel beam is as illustrated in Figure 6. This beam exhibits stable and large hysteresis loops even though some local buckling was evident late in the loading history. Thus, beams per se exhibit very desirable energy dissipation characteristics provided they are braced adequately in the lateral direction and satisfy the code compactness criteria for seismic loading. For this reason it has been a primary objective of seismic design of SMRFs to tune relative member strengths such that inelastic deformations are concentrated in

plastified regions of beams. It is questionable whether this objective is being fulfilled in many designs, as will be discussed next.

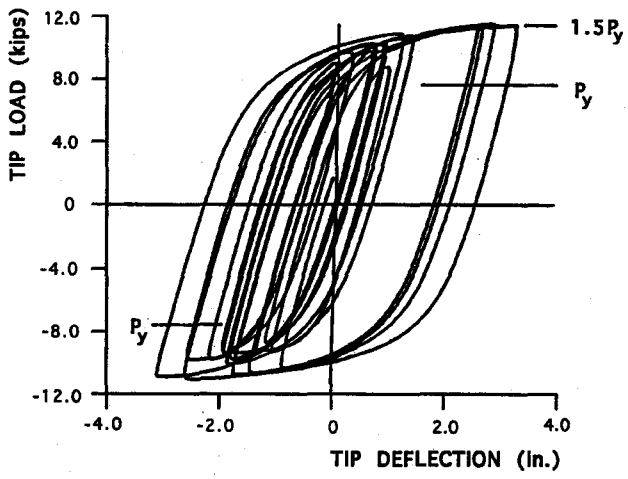

FIGURE 6. Typical Seismic Response of a Steel Beam [Krawinkler et al. (1983)]

In most engineering analyses the modeling of beams in plastified regions is greatly simplified. It is usually assumed that the moment-curvature relationship is bilinear elastic - perfectly plastic, with the "yield" value being equal to the plastic moment capacity given as F_yZ (F_y = material yield strength, Z = plastic section modulus). There are two significant consequences of these assumptions. First, plastified regions disappear and are replaced by point plastic hinges. This modeling assumption does not affect the strength of members and the structure (if the moment capacity would actually be equal to F_yZ), but it disguises the levels of stresses and strains occurring in beams and may give the engineer a misleading perception of the length and importance (particularly for lateral torsional buckling) of the plastified regions. Secondly, the computed strength value F_yZ may be significantly smaller than the true strength of a beam in a SMRF. Cyclic strain hardening will increase the strength significantly, as is shown in Figure 6 in which the load corresponding to the strength value F_yZ is indicated as P_y. Moreover, the floor slab, which is usually connected to the beam with shear studs (composite construction), contributes also to the beam bending strength [e.g., Kato et al. (1984)].

Underestimating the strength of beams in the design process may have very undesirable consequences. Firstly, it underestimates the strength demands on beam-to-column connections and therefore the stress demands on weldments. Secondly, it underestimates the maximum moments that can be transferred from beams to joint panel zones and columns. Thus, the design intent of concentrating energy dissipation in plastic hinge regions of beams is often not fulfilled. If the joint panel zones are strong in shear, the larger than predicted beam moments may cause plastic hinging in columns and may cause undesirable story mechanisms. If the panel zones are weak in shear, they may yield before plastic hinges will develop in beams. Such unplanned relocations of plastified regions change the localized stress and deformation demands around connections and the types of mechanisms that will develop in SMRFs, which affects the system behavior in severe earthquakes as will be discussed later.

Column Behavior

The presence of a significant axial force, which distinguishes columns from beams, complicates column behavior significantly compared to beam behavior, particularly if inelastic deformations occur in columns. The inelastic strain distribution and moment-curvature relationship at a cross-section become

very complicated and are greatly affected by the history of axial force that accompanies the moment history. If the axial force is high, the plastified regions may extend over a significant portion of the column length and the point hinge concept becomes a poor approximation. The plastic deformation capacity of columns subjected to moments and a significant axial force depends on many parameters and has a great variability [Nakashima (1994)]. Member P-delta effects, which are difficult to evaluate for an inelastically deformed column, accompany every column that is subjected to moments. Because of these member P-delta effects the maximum moment may be within the unsupported length of the column rather than at the end. Columns in general may be subjected to bi-axial bending and may buckle about the strong or weak axis. For plastified columns the interaction of in-plane moments and out-of-plane buckling is an extremely complex problem [Attalla et. al. (1996)].

These and many more issues make the prediction of column behavior a very difficult task in general, and in particular if moments cause plastification in the column. There are no simple methods to predict column behavior in this case. Moreover, column behavior cannot be separated from frame behavior because of structure P-delta effects. There are computer programs available that permit the evaluation of column behavior as part of frame analysis (see section on Structure P-Delta Effect and Stability), but these programs are presently difficult to implement in general design practice.

For this reason it is very good design practice to size members such that significant plastification in columns is avoided, i.e, to follow the strong column concept (intentionally the term "strong column - weak beam concept" is not used because of the joint panel zone issue discussed in the next section). If this is done, and other precautions discussed in the section on Structure P-Delta Effect and Stability are taken, the column interaction equations given in LRFD (1994) should provide adequate protection against undesirable column behavior. These interaction equations treat the columns as isolated members and constitute an approximate capacity evaluation at the factored design force level at which internal moment redistribution due to plastification is not taken into account, i.e., elastic behavior of the structure is assumed. Thus, the LRFD interaction equations do not assure that column buckling and plastic hinging will be prevented in a severe earthquake. Additional measures must be taken to prevent column buckling under overloads (discussed later). Plastification of columns is not necessarily detrimental to system behavior unless it causes lateral torsional buckling problems, adversely affects connection behavior, or occurs at sufficient locations to cause story mechanisms.

For an understanding of column behavior the reader is referred to the literature. Selected references are as follows: Cai et al. (1991), Chen and Atsuta (1976), Duan and Chen (1989), Meek and Lin (1990), Nakashima (1991), Sohal and Syed (1992), SSRC (1988), and Yura (1971).

A word of caution needs to be added here to the use of partial penetration welds in column splices. Such welds, when overstressed in bending and/or direct tension, are susceptible to brittle fracture [Bruneau and Mahin (1990-1), Popov and Stephen (1976)]. Thus, utmost care must be taken to evaluate the maximum state of stress at such welds. This stress check must be performed using maximum moments and axial forces associated with severe earthquake motions, and not those computed from seismic design loads.

Joint Shear Behavior

The transfer of moments between beams and columns causes a complicated state of stress and strain in the joint area. Within the column portion of the joint, high normal stresses are generated in the flanges and high shear stresses are generated in the joint panel zone. The forces applied to the joint are shown in Figure 7, and amplified deformations occurring in the joint panel zone are illustrated in Figure 8. If the joint panel zone starts to yield in shear before the bending capacity of the beam(s) framing into the joint is attained, plastification may occur in both the beam(s) and the panel zone, or in the panel zone alone.

An experimental result for a case in which yielding is limited to shear yielding of the joint panel zone is shown in Figure 9.

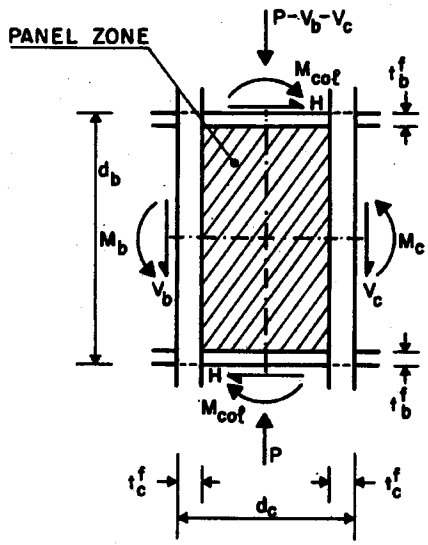

FIGURE 7. Forces Applied to Joint

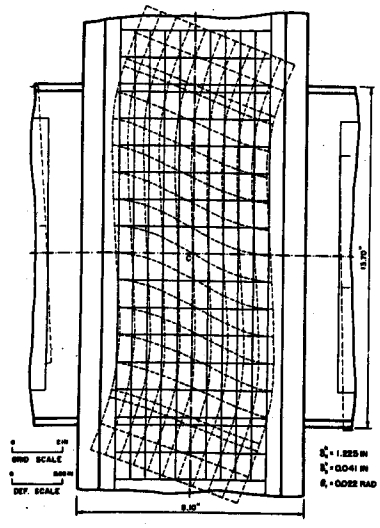

FIGURE 8. Deformations in Panel Zone [Krawinkler et al. (1971)]

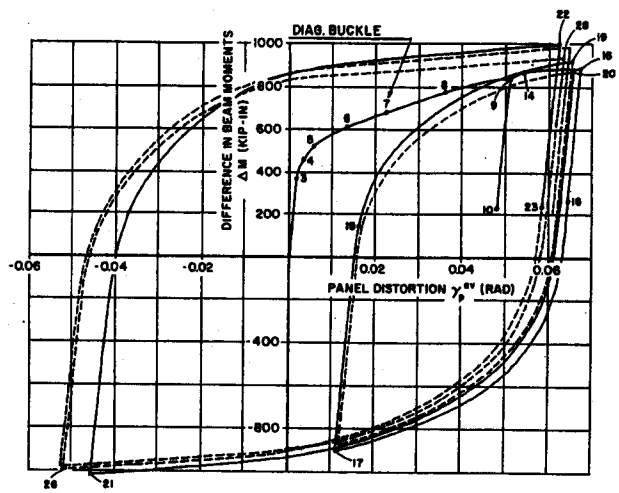

FIGURE 9. Load - Shear Distortion Diagram for a Joint Panel Zone [Krawinkler et al., 1971]

Joint shear behavior exhibits very desirable hysteretic behavior, characterized by a considerable increase in strength beyond first yielding, significant cyclic hardening, and large and stable hysteresis loops. Yielding start usually at the center of the panel zone and propagates towards the four corners, deforming the panel zone globally into a parallelogram shape. The average angle of shear distortion, *g*, (measured between the four corners of the panel zone) versus the applied beam moment difference (*DM* in Figure 9) or the joint shear force estimated from the forces shown in Figure 7 are usually employed to describe the joint shear behavior. Because of the desirable hysteretic characteristics of joint panel zones it is attractive to have joints participate in the energy dissipation during severe earthquakes. This can be achieved by tuning the relative strength of members framing into the joint as will be discussed later.

The fact that joint panel zones deform in shear has a significant effect on the lateral displacements of SMRFs, and may have also a significant effect on the lateral load resistance if the shear strength of joints is low. As Figure 10 illustrates, lateral displacements in SMRF subassemblies are caused by flexural deformations in beams (d_r) and columns (d_c), and by panel zone shear deformations (d_p). The displacement component caused by panel zone shear deformations, which can be estimated as

$$\delta_p = \gamma(h - d_b) \tag{1}$$

is in most practical cases a significant component of the total lateral displacement, particularly if the panel zone is weak in shear and will yield under earthquake loading [Krawinkler and Mohasseb (1987), Tsai and Popov (1990-1)].

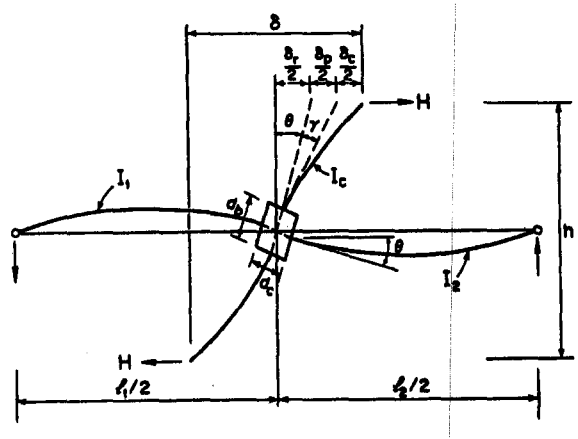

FIGURE 10. Components of Lateral Displacement in Beam-Column Subassembly [Krawinkler (1978)]

It is widely used practice to ignore the effects of joint shear distortion and shear strength on the lateral stiffness and strength of SMRFs, and to perform analysis with centerline dimensions of beams and columns. In stiffness (or lateral displacement) calculations the argument is that the use of centerline dimensions compensates for the disregard of panel zone shear deformations and that stiffness estimates based on bare frame properties are only approximations anyway because of the disregard of nonstructural contributions. In strength calculations the argument is that an accurate evaluation of strength is desirable but not critical in the evaluation of seismic performance.

These arguments need to be disputed for several reasons. In stiffness calculations the use of centerline dimensions gives a very distorted picture of the relative importance of beam versus column stiffness in drift control. If centerline dimensions are used for columns rather than clear span dimensions, the contributions of the column flexural deformations to interstory drift can easily be overestimated by a factor of two or more. In strength calculations the disregard of the joint shear strength may give a very distorted picture of the locations of plastified regions in a SMRF. Joint panel zones that fulfill present code design requirements may be so weak in shear that they yield long before the plastic moment capacity of the beams framing into the column are attained. In such cases it is possible that all plastic deformations are located in joint panel zones and the beams will never attain their bending strength and will remain essentially elastic in severe earthquakes. Again, one may want to argue that this is not critical since the shear behavior of joint panel zones is very ductile. However, in view of recently observed failures at welded beam-to-column connections, it becomes an important issue to find out where plastification around the joint area occurs. If joints are called upon to dissipate all the energy

imparted to a structure in a severe earthquake, they may have to undergo very large inelastic shear distortions. This may not cause undesirable behavior within the joint panel zone, but may create problems at weldments since very large panel zone shear distortions will cause very high strains at the corners of the joints where beam flanges are welded to the column flanges. This behavior, which is illustrated in Figure 11, has led to weld fractures in the study reported by Krawinkler et al. (1971).

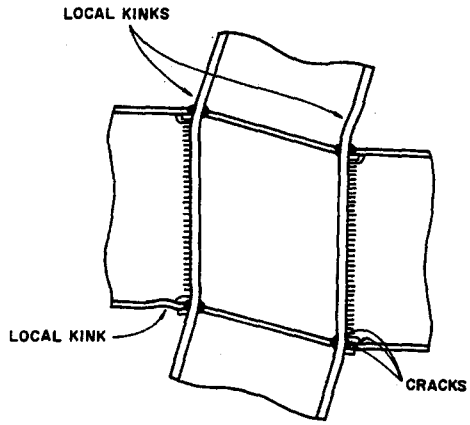

FIGURE 11. Effects of Excessive Joint Shear Distortions [Krawinkler et al., 1971]

These observations point out the need for a performance assessment of SMRF structures that include the effects of joint shear behavior. This requires analytical modeling of joint shear behavior as well as incorporation of these models in computer analysis programs. The latter is feasible in most standard nonlinear programs as will be discussed later; the former is discussed next.

Several models have been proposed in the literature to describe the load - shear distortion behavior of joint panel zones [e.g., Krawinkler (1978), Lu et al. (1988), Tsai and Popov (1988), Kim (1995)]. The models differ somewhat in the representation of inelastic behavior, but agree essentially in the representation of the elastic shear stiffness, K_e, and the yield strength in shear, V_y. Summarized here is the model proposed in Krawinkler (1978). In this model the shear force in the panel zone is estimated as

$$V = \left(\frac{\Delta M}{0.95 d_b} - V_{col} \right) \tag{2}$$

where $DM = M_b + M_c$ is the moment difference at the joint as shown in Figure 7, and d_b is the depth of the beam. The elastic stiffness is given by

$$K_e = \frac{V}{\gamma} = 0.95\ d_c t G \tag{3}$$

where d_c is the depth of the column, t is the thickness of the joint panel zone (including doubler plates if used), and G is the shear modulus of the column material. This equation is valid until $g = g_y = F_y/(\sqrt{3}\,G)$. When this value is substituted into Eq. (3), the yield shear force is obtained as

$$V_y = 0.55\ F_y d_c t \tag{4}$$

Additional shear resistance, which is mobilized primarily after yielding of the panel zone, is attributed to the resistance of the column flanges at the joint corners, which have to bend in order to accommodate the shear distortion mode of the panel zone. The full plastic shear resistance of the joint, V_p, is estimated as

$$V_n = V_y\left(1 + \frac{3b_c t_{cf}^2}{d_b d_c t}\right) = 0.55 F_y d_c t\left(1 + \frac{3b_c t_{cf}^2}{d_b d_c t}\right) \tag{5}$$

where the second term in parentheses identifies the increase in shear resistance due to column flange bending, which depends on the column flange width b_c and thickness t_{cf}. Equation (5), which is neither a lower nor an upper bound solution, is used in the 1994 UBC seismic provisions to define the shear strength of a joint. In Krawinkler (1978) it is assumed that this strength is attained at a distortion of $4g_y$. In this manner a post-elastic stiffness is defined, which terminates at $4g_y$. Beyond $4g_y$ an appropriate strain hardening stiffness may be assumed. Thus, the shear force - shear distortion behavior of a joint is defined by a trilinear diagram.

Connection Behavior

This issue is most critical in view of the recently observed fractures at welded connections. It is treated in detail in other publications of this series and will not be dealt with in this paper. In the following discussions it is assumed that all moment connections are fully rigid, an assumption that is never totally fulfilled. All connections permit relative rotations between beams and columns, and it is only the degree of rigidity that distinguishes rigid connections from semi-rigid and simple shear connections. It is an interesting but unresolved question why specifications and design practice have essentially eliminated semi-rigid (partially restrained) connections in highly seismic regions. Stiffness requirements may be the controlling issue. But one can easily argue that several frames with relatively stiff partially restrained connections could provide the same stiffness as only two frames with rigid connections. One can argue further that seismic behavior could be improved by increasing the redundancy through the use of many moment resisting connections. After Northridge one can make even good arguments that the ductility of certain partially restrained connections may be superior to that of rigid connections.

There are good reasons to take a careful look at the relative merits of rigid versus semi-rigid connections, from a performance as well as economical perspective. A good argument against the use of partially restrained connections is the uncertainty in predicting their stiffness and strength. Time and research can greatly reduce this uncertainty. Today much more is known about the stiffness and strength properties of semi-rigid (and simple) connections than was known at the time when rigid connections became the standard in highly seismic regions. Familiarity with the literature on semi-rigid connections is much encouraged. Good examples of papers on the behavior of semi-rigid connections and the seismic performance of frames with such connections are: Ackroyd and Gerstle (1977), Altman et al. (1982), Astaneh-Asl et al. (1991), Attiogbe and Morris (1991), Bjorhovde et al. (1990), Deierlein and Yhao (1992), Frye and Morris (1975), Ghobarah et al. (1990), Kishi and Chen (1990), Leon and Forcier (1991), Murray and Kukreti (1988), Sivakumaran and Chen (1994), and Tsai and Popov (1990).

STRENGTH AND INELASTIC DEFORMATION CHARACTERISTICS OF SMRF STRUCTURES

Importance of Relative Strength of Elements at a Joint

At every joint of a SMRF four types of "elements" exist: beams, columns, a joint panel zone, and connections (see Figure 12). The stress and deformation demands at the connections depend strongly on the relative strength of these members. If the beam is the weak element, it will develop a plastic hinge and the connection is expected to transfer the beam bending strength, with appropriate strain hardening, to the joint. For a welded beam flange connection this implies the transfer of very high horizontal stresses generated by yielding and strain hardening of the beam flange. If the column is the weak element, it will develop a plastic hinge and the beam may remain in the elastic range even under severe earthquake loading. For a welded beam flange connection this implies very high vertical stresses and strains in the column flange near the weld root. If the joint panel zone is the weak element and it yields in shear, neither the beam nor the column may reach their yield strength. For a welded beam flange connection this implies a state of stress and strain that may be controlled by localized yielding of the column flange due to large shear distortions in the joint panel zone (see Figure 11).

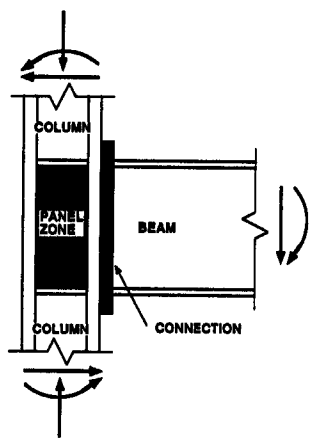

FIGURE 12. Elements Framing into a Joint

These different conditions will greatly affect the global response of the structure as well as the local behavior of a welded connection. At this time the effects of relative element strength on the behavior of welded beam flange connections cannot be evaluated with confidence; research is needed to address this issue. But awareness of this issue is needed in designs of new SMRF structures and in the evaluation of existing ones. The writer believes that excessive panel zone shear distortions (and perhaps severe plastic hinging in columns) can have a very detrimental effect on the behavior of welded connections and should be avoided. Thus, protecting the weld from excessive beam stresses (i.e., moving the potential plastic hinge away from the beam end) may not be a solution to the weld fracture problem if joint panel zones or columns are the weak elements.

In SMRF structures with rigid connections the customary design intent is to assign relative member strengths in a fashion that forces inelastic deformations into beams and joint panel zones and protects the columns from plastic hinging. This strong column concept is implemented in the UBC seismic provisions [UBC (1994)] through the following design requirement.

At moment frame joints at least one of the following two conditions needs to be fulfilled (with exceptions as noted later):

$$\frac{\Sigma Z_c(F_{yc} - f_a)}{\Sigma Z_b F_{yb}} \geq 1.0 \qquad \text{or} \qquad \frac{\Sigma Z_c(F_{yc} - f_a)}{1.25 \Sigma M_{pz}} \geq 1.0 \tag{6}$$

The subscripts b and c refer to beams and columns, respectively, and f_a is the axial stress in the column. ΣM_{pz} is the sum of beam moments associated with the panel zone shear strength as expressed in Eq. (5). The numerator is an estimate of the sum of the bending strengths of the columns above and below the joint (accounting for the effect of an axial load on the column bending strength), and the denominator is an estimate of the sum of the maximum moments that can be transferred from the beams to the columns. The first equation applies when the beams are weaker than the joint panel zone, and the second equation applies when the panel zone is weaker than the beams. There are several exceptions to this requirement, as stated in Section 2211.7.5 of the 1994 UBC.

The exceptions, and also the rule as expressed in Eq. (6), permit plastic hinging in columns in many cases. If Eq. (6) is intended to protect against plastic hinging in the column, it should be modified to include the contribution of the floor slab to the beam strength and to reflect recent developments in steel production. In a recent statistical study performed for the steel industry [SSPC (1994)] it was found that A-36 steel (used mostly for beams) has a mean yield strength that is about 35% higher than the nominal strength, whereas for A-572 the mean strength is only about 15 to 20% higher than the nominal one. Thus, beams are relatively much stronger than is reflected in Eq. (6), particularly if strain hardening during cyclic loading is considered.

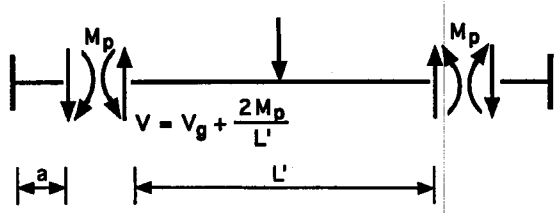

FIGURE 13. Internal Forces at Plastic Hinge Location

There is an associated issue in regard to the maximum beam moment that may develop at the column face, which has come about as a consequence of repair and retrofit procedures implemented recently in response to problems with welded connections. In many cases the connection and the region of the beam close to the connection are strengthened in order to move the beam plastic hinge away from the connection. This may be a desirable process for the connection, but has the consequence that the maximum beam moment for consideration in the design of the connection, the joint panel zone, and the column increases as given in the following equation (see Figure 13):

$$M_{max} = M_p\left(1 + \frac{2a}{L'}\right) + aV_g \tag{7}$$

In this equation a is the distance the plastic hinge has moved, L' is the span length between plastic hinge locations in a beam, and V_g is the gravity load shear force in the beam (with appropriate sign). For a realistic estimate of the maximum moment, M_p should be the bending strength of the beam at the plastic hinge location accounting for slab contribution, cyclic strain hardening, and expected rather than nominal yield strength.

This brief discussion indicates that present code design practice does not safeguard against plastic hinging in the columns. The consequences may be acceptable, unless a sufficient number of column hinges form to develop an undesirable story mechanism, or unless column hinging has a detrimental effect on connection behavior. The latter needs to be found out through focused research. The Interim Guidelines [FEMA 267 (1995)] recognize the need for a realistic estimate of the maximum beam moment in the check for the strong column - weak beam condition.

Even if plastic hinging in the columns is prevented, there is no assurance that energy in a severe earthquake will be dissipated through plastic hinging in beams. In many present code designs joint panel zones will yield in shear before beams attain their yield strength. Most present codes do not place restrictions on the relative strength of beams and joint panel zones, except for the basic shear strength design requirement for panel zones, which is applied at the design load level. Since beam sizes are often affected significantly by gravity loading and/or stiffness requirements, it can be expected that in many practical cases the panel zones are the weak elements and much or maybe all the plastification at beam-to-column joints is limited to panel zone shear deformations and the associated plastification in the columns flanges at the panel zone corners. Panel zone shear distortion is usually a very ductile mode of deformation (see Figure 9), but very large inelastic deformations in joint panel zones may have undesirable consequences on connection behavior as has been discussed earlier.

There is a basic dilemma in the assignment of relative strength between beams and joint panel zones. If the joint panel zones are very strong, all inelastic deformations will be concentrated in plastic hinge regions of beams and the demands on plastic hinge rotations and on beam-to-column connections may become very high in severe earthquakes. If the joint panel zones are weak in shear compared to the bending strength of the beams, the associated large distortions may have undesirable consequences on the connections. Thus, the concept of sharing of inelastic deformations between beams and panel zones is a very desirable one and should be implemented whenever feasible. This concept cannot be implemented at an elastic force level, even when factored loads are used. It needs to be implemented at the structure strength level and with estimates of the <u>expected</u> strengths of the elements and not nominal strengths.

A realistic performance assessment of steel structures should include the evaluation of inelastic deformations in beams, joint panel zones, and columns. This is a relatively straight forward process (see section on Methods to Predict Seismic Behavior) if panel zones are much stronger or much weaker than beams. If the elements are of comparable strength, the distribution of inelastic deformations to the individual elements is sensitive to the mathematical models assumed in the analysis. The capability to predict the real force-deformation behavior of elements with great accuracy does not exist, and likely will not exist in the future, because of the variability in yield strengths and the uncertainties in floor slab contributions to beam strength and stiffness.

The impact of prediction inaccuracy needs to be minimized by good judgment or by executing analyses with upper and lower bounds of member strengths. It may be tempting, but is inappropriate, to avoid this prediction problem by ignoring the panel zone shear behavior as is done in most routine analyses. The problem exists only when yielding in panel zones and beams occurs close to simultaneously. In many cases, particularly at interior joints with two beams framing into a joint, yielding in the panel zones occurs much earlier than in the beams. If this happens, yielding may be limited to the panel zone, beam inelastic rotations may not occur, and the strength of the structure may be much lower than predicted by ignoring the panel zone shear strength limitation. The latter would severely distort the behavior evaluation of a frame structure.

Global Strength and Deformation Characteristics

The effects of absolute and relative member strengths on the behavior of a typical SMRF are illustrated in the following example. Figure 14 shows the base shear - roof displacement relationship for an SMRF that is part of an existing 4-story structure in the Northridge area. This diagram was obtained by subjecting the frame to monotonically increasing lateral loads, using a triangular load pattern (pushover analysis). The base shear V is normalized to the seismically effective weight W, and the roof displacement d_t is normalized to the structure height H. Also shown is the design base shear, V_d, at the LRFD strength design level (i.e., using $R = 8$).

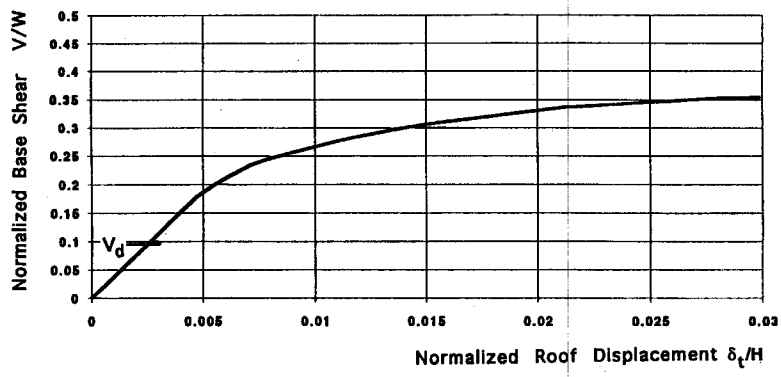

FIGURE 14. Normalized Base Shear - Roof Displacement Diagram of an SMRF [Krawinkler et al. (1995)]

The design base shear is much lower than the elastic strength of the structure, and is a fraction of the ultimate strength. This is not unusual for modern SMRF structures because of drift requirements and the selection of larger than required member sizes because of constructibility and detailing considerations. Thus, SMRF structures have often significant "overstrength", which reduces the inelastic deformation demands.

The response is multi-linear because of successive yielding of individual elements. In this structure, first yielding occurs simultaneously in several panel zones, as is illustrated in Figure 15(a). This figure shows the moments at beam and column ends, and the shear forces in joint panel zones close to first yielding, with the forces normalized to the strength of the individual elements. It is evident that in this example the elastic column moments are rather low and many of the panel zones are stressed much higher than the beams framing into the joints. In the second and third floor interior joints the beam moments are only about half of the bending strength when the panel zones start to yield in shear. These elastic results indicate already that plastic deformation demands will be concentrated in joint panel zones.

This indication is confirmed in Figure 15(b), which shows plastic deformation demands when the frame is pushed to a global drift of 0.03. All interior panel zones have to undergo large plastic shear distortions whereas most beams at the interior joints remain in the elastic range. It should be noted that in this frame many of the connections at these joints did exhibit fractures after the Northridge earthquake. If yielding in the panel zones is ignored in the analysis, a completely erroneous picture of plastic deformation demands is obtained, as is shown in Figure 15(c). In this case plastic deformations are concentrated at plastic hinge locations in beams, and considerable plastic rotation demands are indicated.

This example is presented for the following reasons. A global drift of 0.03 is very large but is not an unrealistic expectation in view of the severe ground motions recorded in recent history. In well designed SMRF structures, in which inelastic deformations are distributed over the height of the structure and are

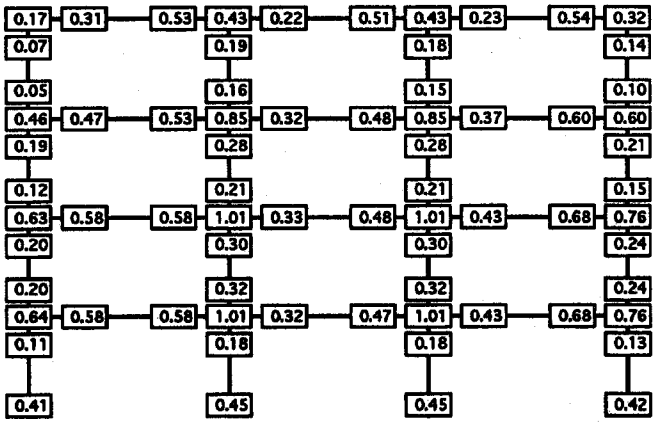

(a) Normalized Element Forces Close to First Yielding

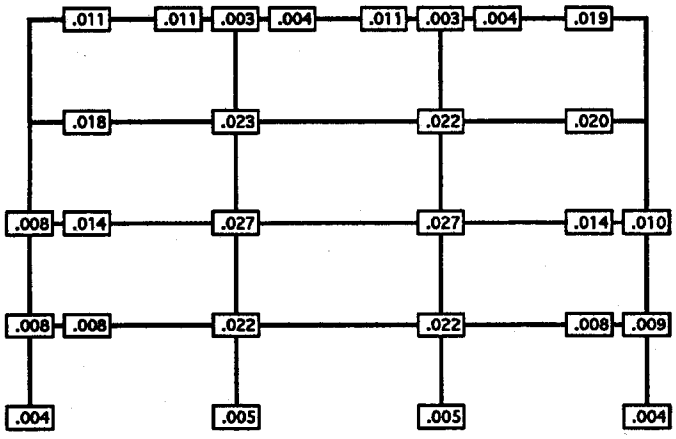

(b) Plastic Deformation Demands at Global Drift of 0.03

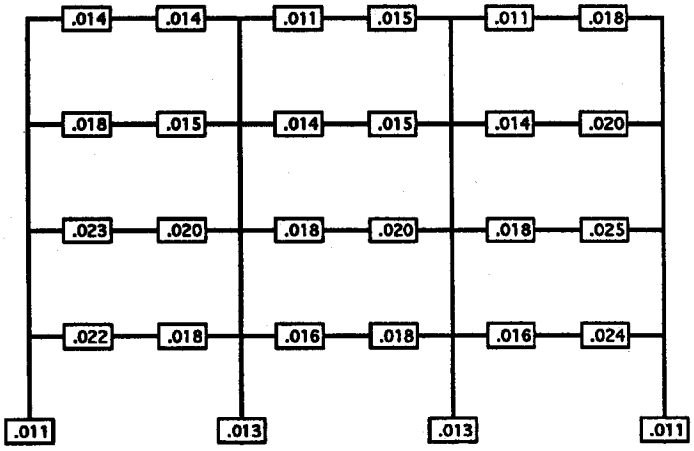

(c) Plastic Deformation Demands at Global Drift of 0.03 - Without Yielding of Panel Zones

FIGURE 15. Force and Plastic Deformation Demands from Pushover Analysis of a 4-Story SMRF [Krawinkler et al. (1995)]

not concentrated in a weak story, the plastic deformation demands (in terms of beam plastic rotations and panel zone plastic shear distortions) may be in the range of values shown in Figs. 15(b) and (c). Expectations are that in well designed beams plastic rotations in the order of 0.02 should be sustainable without much deterioration, and that in panel zones a plastic shear distortion in the order of 0.025 should not pose a major problem either. There is no reason to question these expectations for the elements per se. However, many weld fractures were observed in this frame, even though the dynamic plastic deformation demands were likely smaller than those shown in Figure 15(b). [The latter conclusion is drawn from a series of time history analyses using 9 representative ground motion records.] Thus, the fractures did occur clearly within the expected range of element deformations, and many of them did occur at states at which the beams have not yielded but the joint panel zones have undergone plastic shear distortions. This points out the need for an analysis that accounts adequately for the strength and deformation characteristics of all elements at joints. If these characteristics are not accounted for, the differences in predictions illustrated in Figs. 15(b) and (c) can show up.

Global overstrength, represented by the difference in the design force level and the structure strength has certainly an effect on plastic deformation demands, particularly if these demands are relatively low. If the demands are in the order of magnitude of the illustrated example, the importance of overstrength on plastic deformation demands diminishes in comparison to the importance of relative member strength. However, overstrength may be of critical importance in the context of structure P-delta and overloading of individual elements that have little or no ductility capacity. For SMRF structures this may occur through overloading of columns due to seismic overturning moments.

Structure P-Delta Effect and Stability

There are two closely related issues that may be critical in the seismic performance of SMRF structures, which are usually rather flexible and may be subjected to relatively large lateral displacements. One is the structure P-delta effect caused by gravity loads acting on the displaced configuration of the structure. The other has to do with stability of the 3-dimensional structural system and of individual columns in the structure.

Structure P-delta effect has consequences from the perspectives of statics and dynamics. In a static sense this effect can be visualized as an additional lateral loading that causes an increase in member forces and lateral deflections, reduces the lateral resistance of the structure, and may cause a negative slope of the lateral load - displacement relationship at large displacements. The monotonic lateral load (H) versus lateral displacement (D) response of a simple portal frame that is much more flexible than permitted by present codes is shown in Figure 16 for illustration. From a static perspective the maximum lateral load that can be applied to the structure is a critical quantity since this load cannot be maintained as displacements increase, and a sidesway collapse is imminent. From a dynamic perspective this maximum load is not a critical quantity since seismic "loading" implies energy input, and stability is maintained as long as energy can be absorbed within the structural system. In concept, collapse will not occur unless the displacement associated with zero lateral resistance is reached.

An accurate determination of the static inelastic response that includes all aspects of member and structure P-delta effects is possible only through a distributed plasticity finite element analysis (FEA). To be reliable, this analysis should incorporate also local and flexural torsional buckling effects. The response determination under cyclic loading is even more complex.

From a dynamic perspective the structure P-delta effect may lead to a significant increase in displacement response if the displacement demands are high enough to enter the range of negative lateral stiffness. This is illustrated in Figure 17, which shows the dynamic response of an idealized single degree of freedom (SDOF) system whose hysteretic behavior is bilinear but includes P-delta effects that lead to a negative post-elastic stiffness. The presence of the negative stiffness leads to drifting of the

displacement response, which brings the SDOF system close to collapse. In real structural systems a negative stiffness occurs when the P-delta effect exceeds the hardening effect prior to or during mechanism motion. A negative stiffness may also be created by deterioration in the load-deformation response of individual elements, which may be caused by local instabilities, localized fractures, or member buckling.

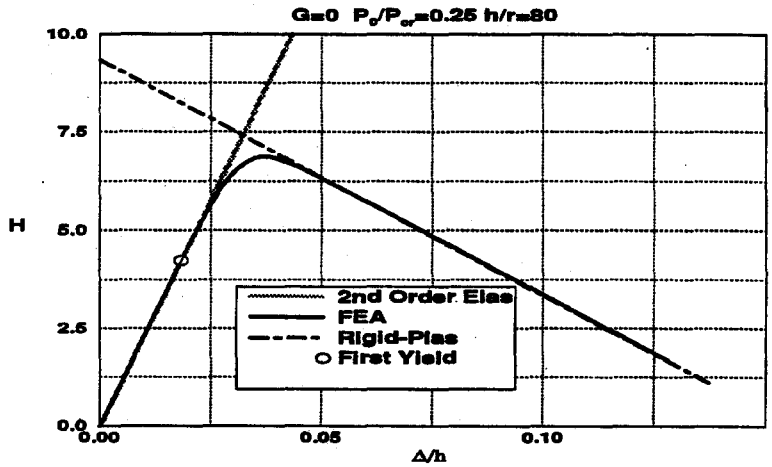

FIGURE 16. Lateral Load Response of a Portal Frame with Axial Loads on Columns [Kilic (1996)]

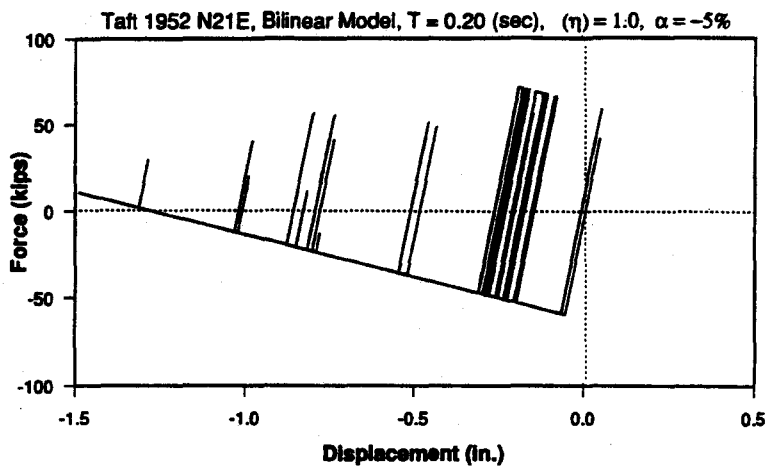

FIGURE 17. Dynamic Response of SDOF System with Negative Post-Elastic Stiffness [Rahnama (1993)]

Much more work needs to be done to evaluate the structure P-delta effect for realistic structural configurations. For bilinear and stiffness degrading SDOF systems the displacement amplifications for systems with negative post-yield stiffness ($a = K_y/K_e$ is negative) compared to systems with $a = 0\%$ (elastic - perfectly plastic) have been evaluated statistically [Rahnama and Krawinkler (1994-2)]. Mean values for bilinear systems with $a = -5\%$ and different strength reduction factors R (R = elastic strength demand over yield strength) are shown in Figure 18. It is evident that the displacement amplification depends strongly on the yield strength (R-factor) and the period of the SDOF system. Particularly for short period systems with low yield strength the amplification can be substantial.

Another important stability related problem is the possibility of buckling of individual columns due to axial overloads caused by seismic overturning moments. This type of buckling, which may occur in-plane or out-of-plane with respect to the overturning moment, is a possibility if a SMRF has a large

height to width ratio and has to resist a large portion of the structure overturning moment. An approximate evaluation of this problem can be accomplished by computing the maximum axial column force from an inelastic pushover analysis and using standard column buckling equations. More accurate solutions again necessitates a distributed plasticity analysis.

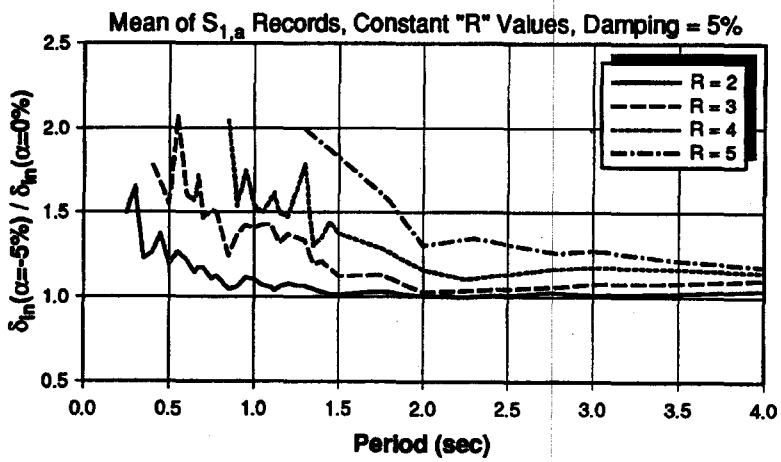

FIGURE 18. Displacement Amplification Caused by Negative Post-Elastic Stiffness

The general realization in regard to P-delta and stability problems is that at this time no simple tools exist that permit an accurate evaluation of these problems. Accurate tools do exist or are under development [e.g., Ziemian et al. (1992-1 and 1992-2), Liew et al. (1993-1 and 1993-2), Kilic (1996)], but they are rather complex and their implementation in engineering practice will take time. For the time being we will have to live with simplified rules. The following are the authors comments and recommendations.

- Structure P-delta effects need to be investigated, particularly if the structure may experience a negative lateral stiffness below the level of lateral displacement expected in a design earthquake. The FEMA 272 NEHRP Guidelines [FEMA 272 (1996)] provide simplified recommendations on this issue.
- SMRFs must resist the P-delta effects tributary to the complete structure. The P-delta effects in simple frames are transferred to the SMRFs through the floor diaphragm.
- Elastic structure P-delta effects are reasonably represented by the B_2 factor in the LRFD beam-column interaction equation, provided this factor is computed with incorporation of the axial loads tributary to simple frames. A second order analysis that includes geometric stiffness terms provides a better means to evaluate elastic structure P-delta effects.
- SMRF structures are three-dimensional systems in which individual frames are coupled by rigid floor systems. Thus, an individual frame cannot "buckle" in a sidesway mode; the complete structure deforms in a sidesway mode.
- The use of an effective length factor of K = 1.0 in the evaluation of the buckling load for use in the beam-column interaction equation, as permitted by recent codes, is reasonable except if the applied axial load is close to the buckling load.
- It is important to safeguard against buckling of columns due to axial overloads caused by overturning moments. The maximum expected axial force from overturning moments should be estimated from a rational inelastic analysis, such as a pushover analysis or a simple mechanism analysis, rather than employing an arbitrary load factor (such as $3R_W/8$) for seismic loading.

Applying these recommendations will improve safety against excessive P-delta effects or instability problems. The issue of structure P-delta needs particular attention in the safety evaluation of structures

with fractured connections, since such fractures will reduce the lateral strength and stiffness and therefore will increase the structure P-delta effects.

CHARACTERISTICS AND DESCRIPTION OF SEISMIC INPUT

Recent history has shown that different earthquakes create different surprises in regard to severity and frequency contents of ground motions. The lesson that has been learned rather clearly is that the ground motion spectra on which today's code designs are based should not be perceived as representative of the maximum motions a structure may experience. The Loma Prieta earthquake has shown that soft soil amplification of motions may be much higher than expected around frequencies excited by the soil columns. The Northridge earthquake has demonstrated that thrust fault earthquakes of medium magnitude may generate ground motions whose spectra may exceed the design ground motion spectrum by a considerable margin in wide frequency ranges. This is illustrated in Figure 19, which shows acceleration (elastic strength demand) spectra for four Northridge motions together with the ATC-3 ground motion spectrum for soil type S_2. This earthquake has taught also the lesson that near-source motion may have pulse-type characteristics that can excite structures much more violently than anticipated in the past [Heaton et al. (1995)].

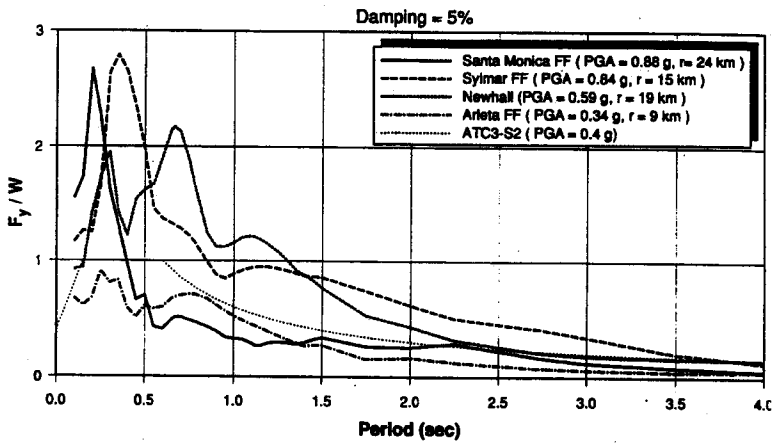

FIGURE 19. Northridge Ground Motion Spectra Together with ATC-3 Spectrum

These observations may not invalidate the presently employed design ground motion spectra, but they drive the lesson home that these spectra are no more than targets that provide a common reference frame, but do not represent the maximum expected demands for elastic structural systems. This lesson must be foremost in a designer's mind so that he/she is fully aware that the actual demands on accelerations, velocities, or displacements may be significantly higher than represented in the design ground motion spectrum.

Moreover, the designer needs to be aware that the information contained in an elastic response spectrum may be a poor measure of the demands imposed on an inelastic structural system. This applies particularly to spectra of recorded ground motions, which exhibit usually large peaks and valleys. These peaks and valleys are not indicative of proportionally large or small demands on inelastic systems. This is illustrated in Figure 20, which shows elastic and inelastic strength and displacement demand spectra for a ground motion whose elastic spectra exhibit a large peak around 0.7 seconds. This large peak diminishes for inelastic systems, leading to much smoother inelastic spectra. This illustrates that the large strength demand for an elastic system with T = 0.7 sec. decreases rapidly for inelastic systems

because of the associated period shift. Also, the displacement demand for inelastic systems at this period is much smaller than for elastic ones.

At this time design and usually also performance assessment are based on elastic SDOF spectra, which are used to estimate strength and stiffness demands for structures. The observations made in the previous paragraph lend strength to the argument that inelastic considerations should enter in the demand description whenever spectra are employed to estimate demands. Baseline information on the required strength and expected maximum displacement of structures can be obtained from inelastic strength and displacement demand spectra, which represent the required strength, $F_y(m)$, and the corresponding displacement, respectively, of SDOF systems whose ductility is limited to a predefined target value m. Spectra of this type are shown in Figure 20.

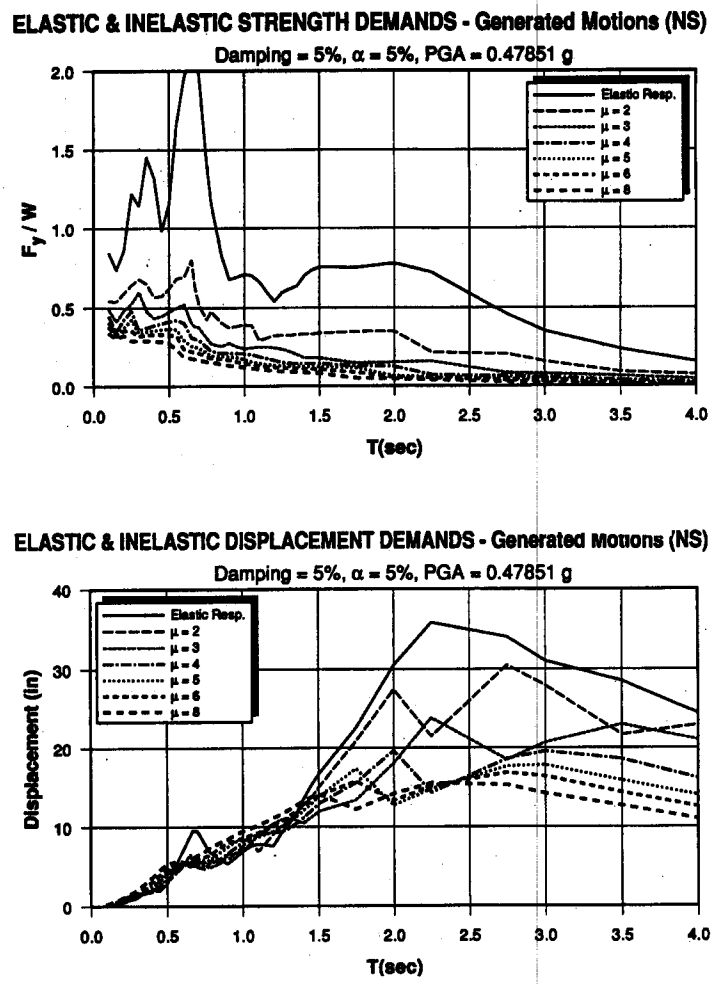

FIGURE 20. Elastic and Inelastic Strength and Displacement Demand Spectra [Krawinkler et al. (1995)]

The need for incorporation of inelastic concepts in design, together with the now widely acknowledged concept that the inelastic response of structures is controlled more by displacements and energy considerations rather than strength [Akiyama (1985), Bertero et al. (1991), Fajfar and Krawinkler (1992), Moehle (1992)], has led to rapid advances in the development of inelastic design and performance evaluation methods and supporting spectral information [e.g., Bertero and Bertero (1992), Bertero and Uang (1992), Krawinkler (1994), Osteraas and Krawinkler (1990)]. The supporting

information includes consistent data on strength, displacement, and energy spectra [e.g., Fajfar and Vidic (1994), Miranda (1993), Nassar and Krawinkler (1991), Vidic et al. (1994)], the effects of soft soils on these spectra, [e.g., Miranda (1993-1), Rahnama and Krawinkler (1994-1)], and spectral ratios that quantify the effects of plasticity on strength demands (strength reduction factors) and displacement demands [e.g., Miranda and Bertero (1994), Nassar and Krawinkler (1991), Rahnama and Krawinkler (1993), and Uang (1991)]. Examples of such spectral ratios are shown in Figures 21 and 22.

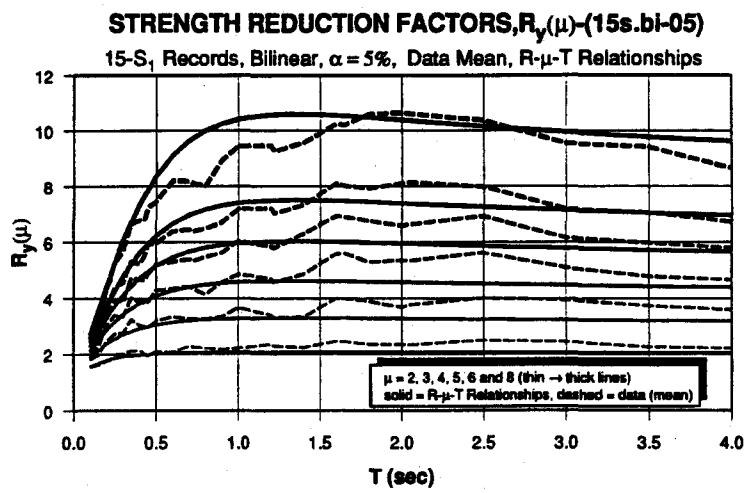

FIGURE 21. Mean Strength Reduction Factors for Soil Type S_1 [Rahnama & Krawinkler (1993)]

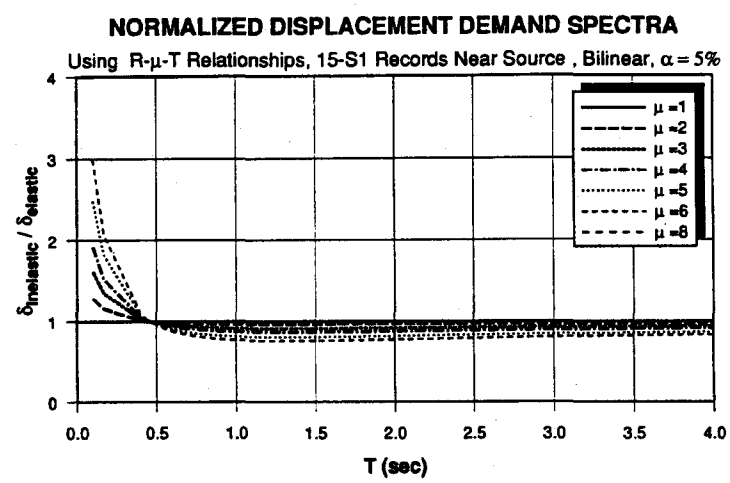

FIGURE 22. Mean Ratios of Inelastic to Elastic Displacements for Soil Type S_1 [Rahnama & Krawinkler (1993)]

Information referenced in the previous paragraph is useful for design, and it helps also in the understanding and quantification of seismic demands imposed on SDOF systems. Dynamic characteristics of multi degree of freedom three-dimensional systems must be accounted for separately. Some of the relevant issues are discussed briefly in the next section. In the process of evaluating seismic performance these issues are addressed explicitly in inelastic dynamic time history analysis. Such an analyses requires the availability or generation of ground motion records that are representative of the types of motions the structure may experience. The motions must be compatible with the hazard level for which performance is to be evaluated and should account for faulting mechanisms, source-site travel path and distance, site soil conditions, and variations in frequency content. No single ground motion

record can fulfill all these requirements, and every motion has spectral peaks and valleys that will favor or penalize structures of specific periods. Thus, a suite of ground motions needs to be employed in a performance evaluation rather than a single record. More research is needed to develop consistent suites of ground motions representative for conditions existing at specific sites.

INELASTIC SEISMIC RESPONSE OF SMRF SYSTEMS

The response of SMRF structures, when subjected to severe ground motions, is controlled by the three-dimensional strength, stiffness, and energy dissipation characteristics of the structural system and its components. It is affected by higher mode effects, torsional effects, distribution of inelastic deformations in the structure, and effects of strength and stiffness irregularities. For structures that are regular in plan and elevation, and whose story shear strengths vary over the height in accordance with the code design shear force distribution, the inelastic dynamic response characteristics will follow a predictable pattern. When significant strength or stiffness irregularities exist, the inelastic dynamic characteristics may change drastically. In such cases it must be acknowledged that even a reasonable prediction of the inelastic dynamic response will necessitate the use of inelastic three-dimensional analysis. The latter cannot be addressed here in detail. Thus, the purpose of this section is merely to point out a few discernible dynamic response characteristics that should be helpful in understanding inelastic seismic response.

2-D Dynamic Response Characteristics

If a structure were a single degree of freedom system, inelastic strength and displacement demands could be predicted accurately from elastic response spectra and information of the type presented in Figs. 21 and 22. Most structures are multi-degree of freedom systems in which higher mode effects will alter the dynamic response. Elastic higher mode effects can be assessed by means of a modal analysis using a representative elastic response spectrum and accepted superposition procedures such as SRSS or CQC. It should not be expected, however, that even careful tuning of story strengths and stiffnesses to the elastic modal analysis requirements will result in evenly distributed inelastic deformation demands over the height of the structure. This is illustrated in Figs. 24 and 25, which show interstory displacement ductility demands (maximum interstory displacement over yield displacement) for frames with a first mode period ranging from 0.22 to 2.05 seconds.

In the design of these frames the base shear strength is tuned to the inelastic strength demand, $F_y(m)$, of the first mode SDOF system for specific target ductility ratios m. Three types of frames are designed. In the first type plastic hinging is limited to beam ends (BH Model), and in the second type plastic hinging is limited to column ends (CH Model). In both types the member strengths are tuned such that uniform yielding occurs over the height of the structure under the UBC load pattern, resulting in the mechanisms shown in Figures 23(a) and (b). In the third type plastic hinging is limited to the columns in the first story, and the rest of the structure is made strong enough to remain in the elastic range, thus creating a weak story (WS Model, see Figure 23(c)). The frames were subjected to a set of 15 recorded ground motions whose spectra represent, in average, the ATC-3 ground motion spectrum for soil type S_1 [ATC-3 (1978)].

Figure 24 shows the mean and mean ± s values of the story ductility demands for BH and CH frames with a period of 1.22 seconds. The ductility demands vary significantly over the height even though the story strengths are tuned to the code shear force pattern. The demands exceed the target value of 4 in the bottom stories, are much lower than the target value in the middle stories, and approach the target value in the upper stories. Thus, a great variation of ductility demands over the height has to be anticipated in

structures designed according to present codes, and the maximum demand is expected to be larger than the target value. The reason is higher mode effects.

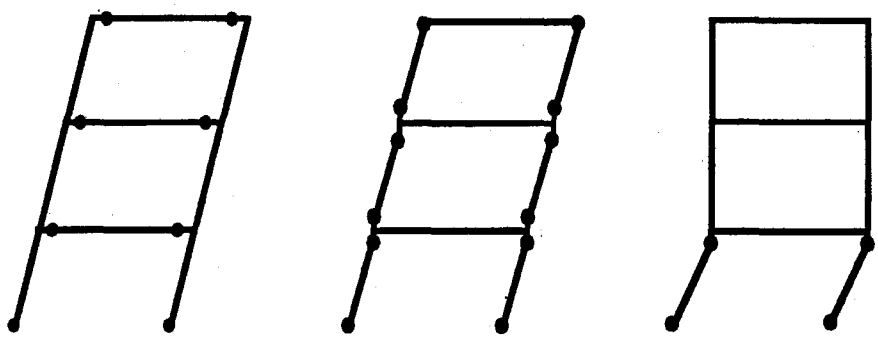

(a) Beam Hinge (BH) Model (b) Column Hinge (CH) Model (c) Weak Story (WS) Model

FIGURE 23. Basic Types of Mechanisms {Nassar & Krawinkler (1991)]

The effect of higher modes and of the structure mechanism on the maximum story ductility is illustrated in Figure 25, which shows mean values of the ratio of maximum story ductility to the SDOF target ductility for the three types of frames. Except for short period and high strength structures, the maximum story ductility is larger than the target value. The amplification of the ductility demand depends on the period of the structure and the type of mechanism that will develop. The figure illustrates the advantage that can be achieved through implementation of the strong column - weak beam concept (BH Model) compared to permitting distributed story mechanisms (CH Model). The figure demonstrates also clearly that weak stories may lead to large amplifications of ductility demands (WS Model).

The results presented here show that even tuned code designs will not lead to a uniform distribution of inelastic demands over the height of the structure. It would be unfair to expect that code designs should result in such a uniform distribution, considering that no two ground motions are alike. The results are presented only to illustrate expected variations and to show that good designs (BH frames) will lead to smaller ductility demands.

3-D Dynamic Effects

Three-dimensional effects come from multi-component ground motions, mass irregularities, and from elastic and inelastic stiffness and strength irregularities. Accounting only for torsional effects caused by elastic mass and stiffness irregularities may be misleading since it is well established that inelastic torsional effects differ significantly from elastic ones [Goel and Chopra (1991)]. Inelastic torsional effects caused by a loss of stiffness due to attainment of strength in a lateral load resisting unit may greatly affect the dynamic response. In the context of conceptual design the complexity of the combined problems makes it very difficult to consider all three-dimensional effects simultaneously and accurately. Because of this limitation and the undesirable consequences of torsional vibrations, design should be based as much as possible on symmetry in elastic as well as inelastic strength and stiffness.

In the context of design verification and performance assessment, all important 3-D effects, whether caused by ground motions or by true or accidental torsion, can be accounted for in an inelastic time history analysis with multi-component ground motion input. At this time it is a matter of sound engineering judgment if and when such an analysis is needed. There is a belief amongst many

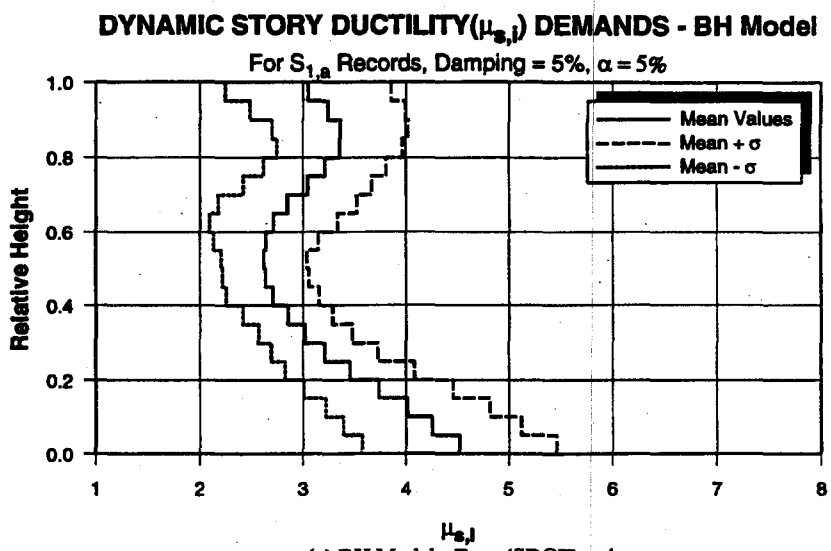

(a) BH Model - For μ(SDOF) = 4

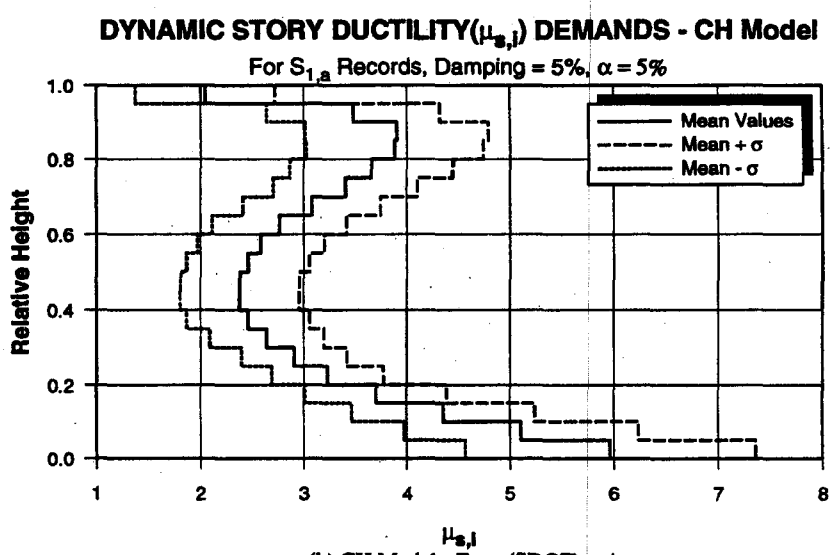

(b) CH Model - For μ(SDOF) = 4

FIGURE 24. Variation of Story Ductility Demand Over Height [Seneviratna (1996)]

earthquake engineers, including the writer, that an accurate prediction of the seismic response is desirable but often not critical in view of the uncertainties in demands and capacities. What is critical is to detect weaknesses and to obtain reasonable bounds on member forces and deformation demands. If this can be achieved with a thoughtful and carefully evaluated 2-D analysis it may be as good as the execution of a complex 3-D analysis in which a careful evaluation sometimes is very difficult to achieve because of the complexity of the computer input and output. As we improve our ability to define the seismic input more reliably, to describe the 3-D inelastic load-deformation characteristics of structural elements more accurately, and to interpret analysis results in a consistent and well managed manner, the 3-D nonlinear analysis should become the standard method of performance evaluation.

The caveat to this advocacy of a simplified prediction approach is the presence of severe strength, stiffness, or mass iregularities. To some extent, the effects of stiffness and mass irregularities can be

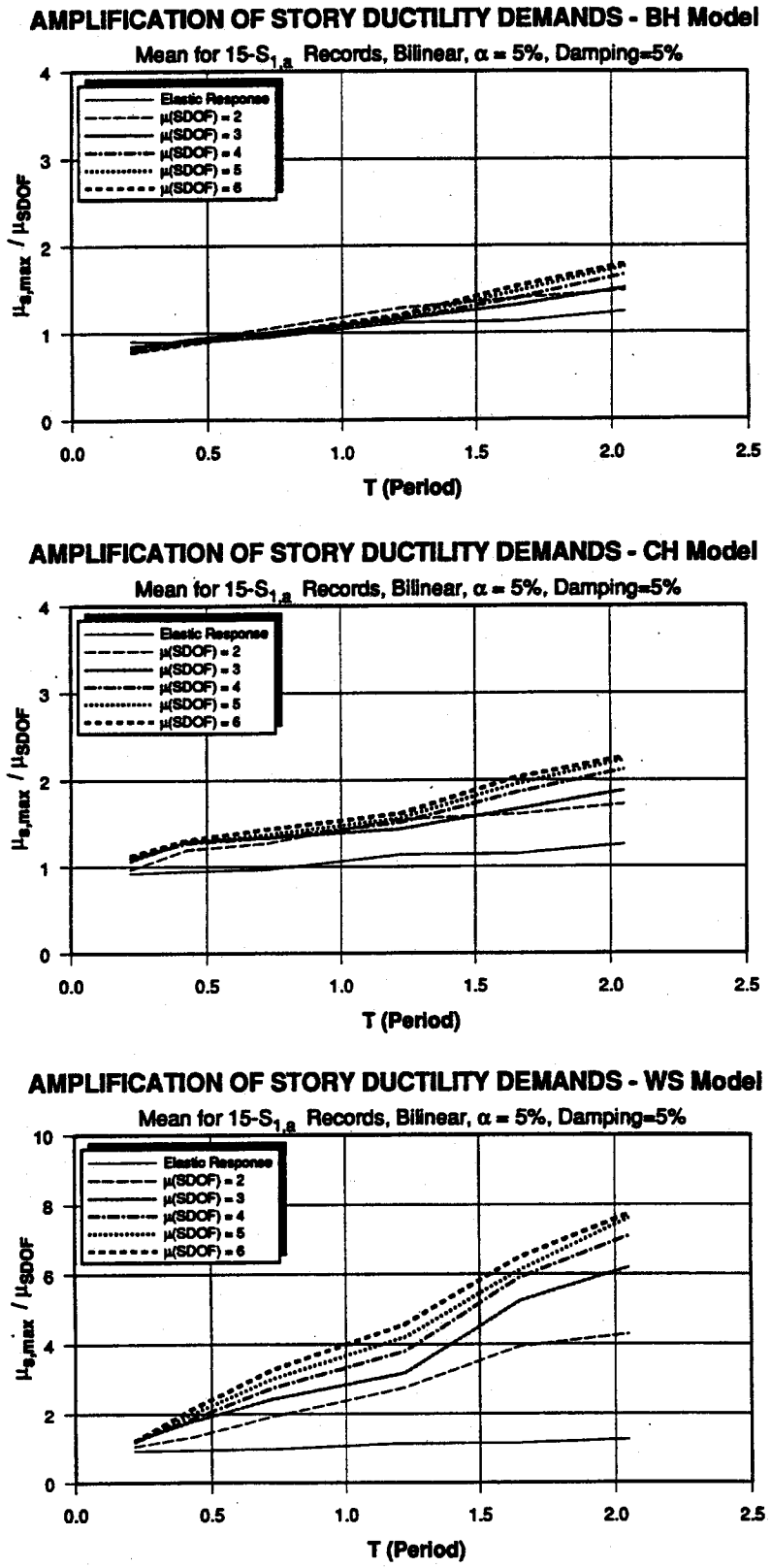

FIGURE 25. Effect of Mechanism on Maximum Story Ductility Demand [Seneviratna (1996)]

estimated by means of an elastic 3-D analysis. However, the effects of strength irregularities, which may be a consequence of stiffness or mass irregularities, cannot. In particular, strength irregularities that cause torsional inelastic response, are a problem that requires inelastic 3-D analysis.

Torsional effects and their determination and evaluation have been the subject of many studies. The literature on this subject is extensive, but certainly incomplete. Selected recent references are as follows: Bruneau and Mahin (1990-2), De La Llera and Chopra (1995), Goel and Chopra (1991), Goel and Chopra (1993), Mittal and Jain (1995), Sadek and Tso (1998), Tso and Zhu (1992), and Zhu and Tso (1992).

METHODS TO PREDICT SEISMIC BEHAVIOR

Predictive methods are always a compromise between accuracy and complexity. The simplest method that provides the desired information with reasonable accuracy is the preferred (and usually also the best) method. For engineers, analysis methods are bounded by the availability of analytical tools, the ability to model structures and their element behavior characteristics with these tools, and the types of information needed to interpret behavior. Herein it is assumed that the objective of behavior prediction (analysis) is to compute demands for a performance evaluation of SMRFs structures, with an emphasis on forces and inelastic deformations around beam-column joints, and forces in elements such as columns that need to be protected from excessive overloads.

The available methods include elastic and inelastic static and dynamic analyses. In this context the terms inelastic and dynamic need to be clearly defined. In general, analysis should consider geometric as well as material nonlinearities. In the context of this discussion inelastic analysis means consideration of material nonlinearities caused by plastification in structural elements. Geometric nonlinearities (e.g., P-delta effects) should always be considered if they are important, whether the analysis is elastic or inelastic. In elastic analysis the term dynamic implies either time history analysis or modal analysis based on response spectra. In both elastic and inelastic static analysis dynamic considerations are often employed to establish load patterns and target load or displacement values for performance evaluation.

In the following discussion the four methods are briefly summarized, and advantages as well as disadvantages are pointed out. The four methods are implemented in the FEMA 272 NEHRP Guidelines [FEMA 272 (1996)], in a similar but not necessarily identical manner as described here. Up front it must be said that a simple static code check does not qualify as a feasible method for performance evaluation. Such a check is performed with code forces (either at the allowable stress level or the member strength design level), which have no established relationship to the actual strength of the elements or the structure.

Elastic Static Analysis

In this method lateral loads of pre-established pattern and magnitude are applied to the structure together with the gravity loads that are likely to exist at the time of the earthquake. Internal forces are computed under these load combinations by means of elastic analysis, and the resulting force quantities are normalized to capacity values to estimate demand/capacity ratios and evaluate acceptability of each component.

This method is simple in implementation but has many ambiguities since it attempts to predict inelastic dynamic demands by means of an elastic static analysis. Formalization requires the development of rules that need to facilitate simplicity but will always be subject to doubts since it is impossible to place inelastic behavior consistently into an elastic framework.

The load pattern could be a code-type load pattern, and the magnitude of the lateral loads could be derived from an unreduced elastic smoothed ground motion spectrum. Except for force controlled components (components that cannot sustain inelastic deformations), the loads should be considered as a surrogate means to estimate element deformations due to the expected inelastic displacements of the structure. Since the inelastic displacements may differ significantly from the elastic ones, particularly for short period structures (see Figure 22), the loads should be multiplied with estimates of the ratio of inelastic to elastic displacements, accounting also for issues such as pinching of hysteresis loops and dynamic P-delta effects.

The analysis will result in computed demand/capacity ratios that can be employed for a performance evaluation (which requires the assignment of acceptable demand/capacity ratios), or for an estimate of the deformation demands in components. In many cases these estimates may be realistic, in others they may not since these ratios cannot account for redistribution of internal forces. In the judgment of the writer these values are preliminary, but sometimes questionable final, indicators of potential problems.

Elastic Dynamic Analysis

The use of dynamic analysis procedures adds the benefit that the elastic dynamic characteristics of the structure are represented more realistically. If modal analysis is employed using a smoothed spectrum, a clear advantage is gained compared to the static method since load effects are better represented. But all the other drawbacks of the elastic method still apply. If a site-specific spectrum with large peaks and valleys is used, or a time history analysis is performed, a trap may occur that may significantly distort the results compared to a realistic inelastic analysis. As was pointed out in the section on Characteristics and Description of Seismic Input, a site-specific elastic spectrum that exhibits large peaks and valleys, such as a spectrum of an actual ground motion, may be a poor indicator of inelastic demands (see Figure 20) if the structural period coincides with peaks or valleys of the spectrum. This poor indication will be reflected in the results of a elastic dynamic analysis of a structure.

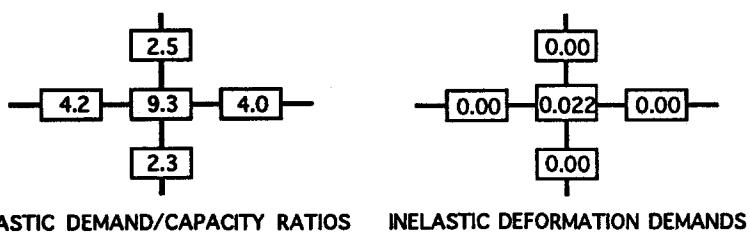

FIGURE 26 Seismic Demands at a Joint Obtained from Elastic and Inelastic Time History Analysis

An example of the type of misleading results that can be obtained from a elastic time history analysis is illustrated in Figure 26. Shown are the demand/capacity ratios obtained from a elastic analysis, and the plastic deformation demands obtained from a inelastic analysis, for the elements framing into an interior joint of a 2-story frame subjected to the same ground motion. In the inelastic analysis neither beams nor columns yield despite the large elastic demand/capacity ratios, and the joint shear distortion corresponds to a ductility ratio of 7.4.

The conclusion is that great caution must be exercised in the interpretation of a elastic dynamic analysis, particularly if site specific spectra or time history records are employed.

Modeling of Structural Elements for Inelastic Analysis

Inelastic analysis requires advanced knowledge and sound engineering judgment. There are few rigid modeling rules, and many decisions are based on the desired degree of accuracy. In the simplest case, structural elements are modeled as elastic elements with plastic point hinges at the ends. Plastic hinge rotations are most commonly described with bilinear moment-rotation relationships consisting of an elastic stiffness, a strength value, and a constant strain hardening stiffness which is a fraction (usually between 0 and 5%) of the elastic stiffness. Cyclic strain hardening and distributed plastification are usually, but not always, ignored. Advanced models with moment-rotation relationships derived from the cyclic stress-strain behavior of materials (see Figure 3) do exist [e.g., Kim (1995)]; they are excellent research tools but are rarely used in engineering practice. Distributed plasticity models, and point hinge models in which distributed plasticity is accounted for implicitly, exist also [e.g., Ziemian et al. (1992-1 and 1992-2), Liew et al. (1993-1 and 1993-2), Kilic (1996)]. It is advisable to give such models consideration if significant plastification is expected in columns with high axial loads.

To the writer's knowledge none of the commonly available tools accounts simultaneously for cyclic hardening, distributed plasticity, and localized effects such as local and lateral torsional buckling. Thus, accurate engineering analysis that eliminates the need for separate member checking is still a task for the future. Moreover, complexity is added by the need to model joint shear behavior as well as connection behavior explicitly and to account for slab contributions to the strength and stiffness of beams and connections. At this time the recommended approach is to perform first a global analysis in which the model is kept as simple as justifiable, followed by refined analytical investigations of those local regions in which the global analysis has pointed out potential problems.

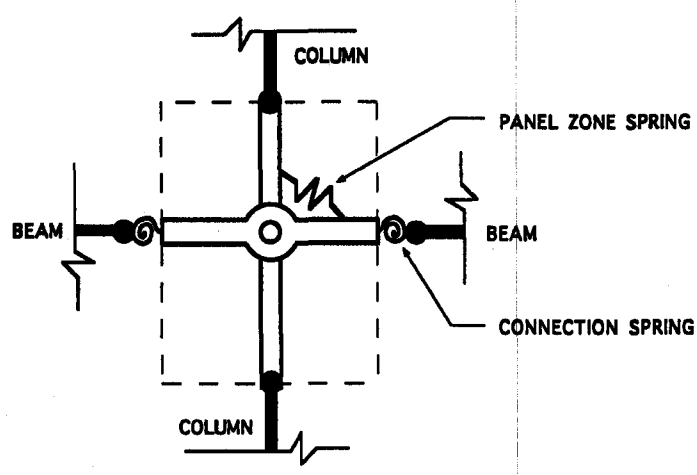

FIGURE 27. Analytical Model of Elements at Interior Joint

In the global analysis all elements and connections that contribute significantly to the seismic response need to be represented. At a typical interior beam-column joint the analytical model may include the elements shown in Figure 27. The joint panel zone can be modeled with a scissors type arrangement that permits relative rotation between two rigid elements. The rotation is controlled by a spring that relates the moment difference in the beams to the spring rotation. The moment difference can be related to the joint shear force [see Eq. (2)], and the spring rotation is equal to the joint shear distortion. Provided that distributed plasticity effects can be neglected, columns and beams can be modeled as standard beam-column elements with plastic hinges and appropriate M-P interaction diagrams defining the element strength. Connection behavior, which in general should be separated from beam behavior (a necessity for partially restrained connections), can be modeled by means of a spring

inserted between the beam end and the column face (joint panel zone). The question is what properties to assign to this connection spring.

The issue of connection moment rotation properties is not addressed here in detail. For welded rigid connections the need exists to account for slab contributions to connection behavior. Post-fracture behavior will have to be modeled if the performance of SMRFs with fractured welds is to be investigated. This can be done with empirical models if springs are used to represent connection behavior, or through the use of fiber elements. Of large importance becomes then the modeling of cyclic behavior, which no longer should be approximated with bilinear non-degrading properties since the behavior of connections with fractured welds exhibits history dependent strength and stiffness degradation.

Consideration should also be given to the incorporation of shear connections in the structural model. The strength and stiffness properties of these connections are not negligible because of the contribution of the floor slab. The contributions of shear connections to the strength and stiffness of the structure may be significant, particularly if a large number of moment connections have fractured and a large number of shear connections exist.

Accurate analytical modeling is complicated further by the fact that most elements, when subjected to repeated reversed inelastic loading, will deteriorate in strength and stiffness. This deterioration is a function of the applied loading history and would need to be modeled with cumulative damage models [Krawinkler and Zohrei (1983)]. The writer is not aware of any widely available computer program that incorporates deterioration based on cumulative damage models for steel structural components.

The upshot of this brief discussion is that accurate modeling of the inelastic behavior of steel frames needs much more research and development. As was mentioned previously, an accurate prediction of the seismic response is very desirable but often not critical in view of the uncertainties in demands and capacities. The simplest model that points out all important potential problems is usually the best one.

Inelastic Static Analysis (Pushover Analysis)

The pushover analysis is an evaluation method in which force and deformation demands at specified performance levels are estimated from a static, incremental, inelastic analysis, and acceptability of a structure and its components is assessed by comparing these demands to performance level dependent force and deformation capacities. The method requires a description of the seismic input in terms of response spectra that define the site dependent seismic hazard for the specified performance levels.

The process is to (1) represent the structure in a two- or three-dimensional analytical model that accounts for all important elastic and inelastic response characteristics, (2) apply lateral loads in predetermined or adaptive patterns that represent approximately the relative inertia forces generated at locations of substantial masses, and (3) push the structure under these load patterns to a specific target displacement level. The internal forces and deformations computed at the target displacement level are estimates of the strength and deformation demands, which need to be compared to available capacities.

A target displacement level is a characteristic displacement in the structure that serves as an estimate of the global displacement experienced by the structure in a design earthquake associated with a specified performance level. The roof displacement is a convenient parameter for this purpose. This displacement can be estimated with reasonable accuracy from inelastic displacement spectra, using an appropriate shape vector and the corresponding equivalent SDOF system to obtain the SDOF inelastic displacement, and transforming this displacement to the roof level of the MDOF structure.

The evaluation of a lateral load resisting system is based on an assessment of capacities and demands of important performance quantities. Such quantities include global drift, interstory drift, inelastic element and connection deformations (either absolute or normalized to a yield value), and element and connection forces (for elements and connections that cannot sustain inelastic deformations).

The method is relatively simple to implement, but hinges on a great number of assumptions and approximations that may be reasonable in many cases but unreasonable in some. Thus, the interpretation of results must be done within the context of the assumptions. In somewhat different formats the method has been proposed, formalized, and evaluated in several research studies [e.g., Fajfar & Fischinger (1988), Lawson et al. (1994), Miranda (1991), Saiidi & Sozen (1981)]. Common to all formulations is the assumption that the deflected shape of the MDOF structure can be represented by a single shape vector that remains constant throughout the time history, regardless of the level of deformation. This shape vector together with the strength and elastic stiffness of the structure is used to define the equivalent inelastic SDOF system from which the aforementioned target displacement is estimated.

This process has been shown to provide a reasonable estimate of the global deformation response for structures that respond primarily in the first mode, but it must be emphasized that the pushover analysis cannot disclose performance problems caused by changes in the inelastic dynamic characteristics due to higher mode effects. In order to bound the response behavior, it is advisable to perform the pushover analysis using several load patterns (uniform, triangular, and SRSS patterns, or adaptive load patterns that account for changes in dynamic characteristics).

Inelastic Time History Analysis

This evaluation method, which is much more labor-intensive than the other methods, is the most accurate and reliable one provided that

- the structure can be modeled realistically for inelastic time history analysis,
- the cyclic load-deformation characteristics of each element can be modeled realistically,
- the ground motion time histories used in the analysis represent the range of demands the design earthquake will impose on the structure, and
- the results of the time history analyses can be interpreted in an unambiguous manner.

At this time it is not clear that these conditions can be fulfilled in all cases.

In the context of the evaluation of SMRF structures with potential connection problems, priority needs to be given to this method, particularly when fractured connections exist and the post-fracture response of structures needs to be investigated. In such cases the response may depend strongly on the deterioration characteristics of the fractured connections and on increased P-delta effects because of the loss in stiffness and strength. In the pushover analysis the effects of deterioration and P-delta on the target displacement are difficult to evaluate accurately. Thus, much emphasis needs to be placed on the development of analysis tools that permit an efficient and reliable execution of inelastic time history analyses.

RESPONSE OF SMRF STRUCTURES WITH FRACTURED CONNECTIONS

At this time there are only few certainties about issues and problems caused by fractured connections. One is that a fractured connection constitutes a local failure state that has <u>always</u> undesirable consequences, and the other is that fractures at a few beam-to column flange weld do not necessarily bring a structure much closer to collapse in severe earthquakes. Both points need elaboration.

Let us first consider one connection only. Fracture of one weld (top or bottom of connection) or both welds (top and bottom) will always reduce the lateral strength, stiffness, and energy dissipation capacity of the structure, as well as the gravity load resistance. Alone the reduction in gravity load resistance reduces the safety factor of the structure, by definition. This reduction may be marginal unless fracture extends into the shear tab, in which case the safety factor will be greatly reduced particularly if the shear

connection fails. Even in this case some shear transfer can be mobilized through the shear resistance of the slab. The reduction in lateral strength and stiffness will most likely increase lateral displacements under earthquake (and wind) loading, which will adversely affect the serviceability behavior (drift and damage control) and is likely to reduce safety against incremental collapse. To what extent it affects collapse safety depends on the type of local failure, on system behavior, and on the characteristics of the ground motion.

The following brief discussion tries to raise awareness of possible consequences, but does not attempt to pass quantitative judgment on the severity of the consequences. At this time the information does not exist to pass such judgment.

In most earthquakes, a loss in stiffness and energy dissipation capacity will lead to an increase in displacements. Larger displacements and smaller strength will lead to larger P-delta effects, which will further amplify the displacements. The amount of displacement increase depends on the relative number of fractured versus sound connections and on the frequency characteristics of the ground motion. Larger displacements will amplify the energy dissipation demands on beams (or columns) around sound connections. These elements have limited energy dissipation capacities and may deteriorate in strength and stiffness if the demands become too large. This may increase displacements further. Moreover, the larger demands on the elements may cause more fractures at connections. In addition, a decrease in stiffness at the connection will reduce the end restraints at the columns, which increases the susceptibility to buckling. It is conceivable that the accumulation of all these consequences will lead to incremental collapse of the structure. Only extensive in depths studies will show how likely (or unlikely) such a collapse is.

The severity of the consequences depends on many considerations, some of which are enumerated next.

- The total number of moment connections and the relative number of fractured to sound connections. The larger the number of moment resisting connections per floor, the better off the structure will be.
- The number of shear connections. These connections, which have considerable stiffness and strength due to the presence of a composite floor slab, act as a back-up system when the fractured moment connections lose stiffness and strength.
- The relative importance of gravity loads compared to lateral stiffness and strength. P-delta effects are proportional to PD/h (P = gravity load on structure, D = interstory displacement, h = story height) and, in the inelastic range, increase significantly for structures with low strength (dynamic P-delta effect, see Figure 18).
- Energy dissipation capacity of beams, columns, and joint panel zones. Elements away from fractured connections are called upon to dissipate more energy through inelastic deformations.
- The type of mechanism that develops in the structure. This was discussed in the section on 2-D Dynamic Response Characteristics (see Figure 25).
- The strength and stiffness degradation characteristics of the fractured connections.
- The contribution of the floor slab to the strength and stiffness characteristics of the connections.
- The type of failure at the connections. Fracture that reduces the strength of the column (the frequently observed fracture across column flanges and sometimes even column webs) may have much more severe consequences than fractures that reduce the moment transfer from beams to columns.
- The frequency characteristics of the ground motion. As stiffness is lost, the effective period of the structure increases. Considering smooth spectra, an increase in period leads to an increase in displacements, a decrease in strength demands, and a decrease in energy dissipation demands. What smooth spectra do not show is that energy dissipation demands decrease at a slower rate than strength demands [Lawson and Krawinkler (1994)]. Actual ground motions, particularly those in soft soils, may have very different characteristics than those reflected in smooth spectra.

It is easily possible that period lengthening brings the structure into a spectral range in which strength and energy dissipation demands increase rather than decrease.

This brief discussion is intended to make it clear that there are no simple answers to the question of consequences of connection fractures. The consequences can only be addressed in the context of systems behavior. It also needs to be considered that the seismic demands, the element capacities (in particular the connection strength and deformation capacities), and the system capacities are associated with large uncertainties. Thus, a realistic safety evaluation needs to be reliability based, with due consideration given to the uncertainties inherent in demands and capacities and to the consequences of connection fractures on structural safety. This necessitates experimental work to assess the uncertainties in capacities and to develop better models for the hysteretic characteristics of fractured connections. It also necessitates analytical work to develop computer programs that permit realistic and efficient representations of post-fracture behavior, and foremost it necessitates the development of a systematic approach to the safety evaluation of buildings with SMRF structural systems.

It is fortunate that our present methods for designing SMRF structures and predicting their behavior are based on models that ignore important contributions to strength and stiffness. Foremost are the contributions of floor slabs and of shear connections, of which there are usually many in present SMRF systems. These connections, which in composite floor construction act together with floor slabs, can develop significant strength. At this time the problem is that their stiffness characteristics are difficult to predict and depend strongly on the tightness of the bolts in the shear connection. There is no doubt, however, that these connections contribute significantly to the collapse safety of SMRF structures.

REMARKS ON CONNECTION DESIGN

This paper has attempted to illustrate that the seismic behavior of SMRF structures depends on element and system behavior. SMRF structures have been and are expected to remain desirable structural systems in seismic regions.

There is a need, however, to improve system behavior by better detailing around connections. This can be achieved in several ways. If welded connections are used, the quality of welding must be improved and the stress level around the welds must be kept at a safe level. This requires consideration of the expected rather than nominal strength of the elements (including cyclic hardening), and the development of configurations in which overstressing of welds in severe earthquakes is avoided. Moving plastified regions away from the welded regions is a desirable option. When this is done by reinforcing the connection region, moments that are larger than the strength of the unreinforced beam will be transferred to the joint panel zone and the columns. The effects of these larger moments on panel zone and column behavior as well as system behavior (possible development of undesirable story mechanisms) need to be considered. Alternatively, stresses at weldments can be kept at a safe level by reducing the beam cross section away from the connection. This is often possible without increasing the beam section since beam sizes are frequently governed by stiffness considerations.

Alternatives to welded connections should be given consideration. Bolted connections are used widely in the U.S. in regions of lower seismicity. Their drawback is that relative rotations will occur between beam ends and columns, which reduces the lateral stiffness. However, there are bolted connection types in which this relative rotation is small. Using stiff bolted connections in many places might accomplish the same as using welded connections in a few places. Clearly, the ductility of bolted connections must be established to the extent that it can be quantified and is found to be sufficient for the level of deformations expected in highly seismic regions.

An overriding consideration for structural safety is redundancy. This has been known for a long time, but has been difficult to quantify in the past. The recent incidences of connection fractures make it possible now to quantify the benefit of redundancy from a system's perspective. Reliability analysis will

show this benefit explicitly in the future. Until methods for such an analysis will be common knowledge, the design emphasis should be to provide as much redundancy as is economically feasible. Designers should be encouraged to provide moment connections in several frames and not just at the perimeter, and to avoid minimizing the number of moment resisting connections.

CONCLUDING REMARKS

Because of recently observed fractures at welded connections, current design procedures for new SMRF structures need to be modified and the safety of existing SMRFs needs to be evaluated. Both activities necessitate information and procedures that go beyond current code approaches. We need to assess and advance the current state of knowledge in order to develop solutions to the problems exposed by the Northridge earthquake. This paper attempts to assess the state of knowledge in order to lay the foundation for needed advancements. The reader should not be left with the impression that an evaluation of the performance of SMRF structures necessitates always a three-dimensional inelastic time history analysis that accounts for distributed plasticity effects and for element deterioration due to cumulative damage. To the contrary, the simplest prediction method that provides a reasonable assessment of seismic demands and identifies potential weaknesses in the structural system is usually the most appropriate one. But the selection of the simplest prediction method adequate to accomplish this objective, and the interpretation of its results, require awareness of all the issues that may significantly affect the performance of the structure. It is the intent of this paper to contribute to this awareness.

REFERENCES

Ackroyd, M.H., and Gerstle, K.H. (1977). "Strength and stiffness of Type 2 steel frames," Report to AISC on Project 199, Dept. of Civil Engrg., U. of Colorado, Boulder.

Akiyama, H. (1985). *Earthquake-Resistant Limit-State Design for Buildings*, University of Tokyo Press, 1985.

Anderson, J.C., and Bertero, V.V. (1987). "Uncertainties in establishing design earthquakes," *Journal of Structural Engineering*, ASCE, Vol. 113, No. 8.

Altman, W.G., Azizinamini, A., Bradburn, J.H., and Radziminski, J.B. (1982). "Moment-rotation characteristics of semi-rigid steel beam-to-column connections," *Report*, Department of Civil Engineering, University of South Carolina, Columbia, S.C.

Astaneh-Asl, A., Nader, M.N., and Harriott, J.D. (1991). "Seismic behavior and design considerations in semi-rigid frames," *Proceedings of the 1991 National Steel Construction Conference*, AISC..

ATC-3 (1978). "Tentative provisions for the development of seismic regulations for buildings," *Applied Technology Council.*

Attalla, M.R., Deierlein, G.G., and McGuire, W. (1996). "Nonlinear frame analysis with torsional-flexural member behavior," *SSRC 5th International Colloquium*, Chicago, IL.

Attiogbe, E., and Morris, G. (1991). "Moment-rotation functions for steel connections," *Journal of Struct. Engrg.*, ASCE, Vol. 117, No. 6.

Bertero R.D., and Bertero, V.V. (1992). "Tall reinforced concrete buildings: conceptual earthquake resistant design methodology," *Report No. UCB/EERC-92/16*, Earthquake Engineering Research Center (EERC), University of California at Berkeley.

Bertero, V.V., Anderson, J.C., Krawinkler, H., and Miranda, E. (1991). "Design guidelines for ductility and drift limits," *Report No. UCB/EERC-91/15*, Earthquake Engineering Research Center (EERC), University of California at Berkeley.

Bertero, V.V., and Uang, C.M. (1992). "Issues and future directions in the use of an energy approach for seismic-resistant design of structures," *Nonlinear Seismic Analysis and Design of Reinforced Concrete Buildings,* Edited by P. Fajfar and H. Krawinkler, Elsevier Applied Science, London and New York.

Bjorhovde, R., Colson, A., and Brozzetti, J. (1990). "Classification system for beam-to-column connections," *Journal of Struct. Engrg.*, ASCE, Vol. 116, No. 11.

Bruneau, M., and Mahin, S.A. (1990-1). "Ultimate behavior of heavy steel section welded splices and design implications," *J. of Struct. Engrg.*, ASCE, Vol. 116, No. 8.

Bruneau, M., and Mahin, S.A. (1990-2). "Normalized inelastic response of structures having eccentricities in plan," *J. of Struct. Engrg.*, ASCE, Vol. 116, No. 12.

Cai, C.S., Liu, X.L., and Chen, W.F. (1991). "Further verification of beam-column strength equations," *Journal of Struct. Engrg.*, ASCE, Vol. 117, No. 2.

Chen, W.F., and Atsuta, T. (1976). "*Theory of beam-columns*", Vols. 1 and 2, McGraw-Hill, New York.

Cofie, N.G., and Krawinkler, H. (1985), "Uniaxial cyclic stress-strain behavior of structural steel," *Journal of Engineering Mechanics,* ASCE, Vol. lll, No. 9.

Cosenza, E., Manfredi, G., and Ramasco, K. (1990). "An evaluation of the use of damage functionals in earthquake resistant design," *Proceedings, 9th European Conference on Earthquake Engineering,* Moscow, July 1990.

Cuevas Barajas, L. (1962). "Comportamiento de la estuctura de la Torre Latinoamericana de la Ciudad de Mexico," published in *La Torre Latinoamericana*, 1983.

Deierlein, G.G., and Yhao D. (1992). "Static and dynamic analysis of steel frames with nonlinear connections and joint effects," *Proceedings of Structures Congress 1992*, ASCE.

De La Llera, J.C., and Chopra, A.K. (1995). "Understanding the inelastic seismic behaviour of asymmetric-plan buildings," *Earthquake Engineering and Structural Dynamics,* Vol. 24, No.4.

Duan, L., and Chen, W.F. (1989). "Design interaction equations for steel beam-columns," *Journal of Struct. Engrg.*, ASCE, Vol. 115, No. 5.

Fajfar, P. and Fischinger, M. (1988). "N2 - a method for non-linear seismic analysis of regular structures", *Proceedings of the 9th World Conference on Earthquake Engineering*, Vol. 5, Tokyo, Japan.

Fajfar, P., and Krawinkler, H. (1992). *Nonlinear Seismic Analysis and Design of Reinforced Concrete Buildings,* Elsevier Applied Science, London and New York.

Fajfar, P., and Vidic, T. (1994). "Consistent inelastic design spectra: hysteretic and input energy," *Earthquake Engineering and Structural Dynamics,* Vol. 23.

FEMA 267. (1995). "*Interim Guidelines: evaluation, repair, modification and design of welded steel moment frame structures*," Federal Emergency Management Agency.

FEMA 272 (1996). "*NEHRP Guidelines for the seismic rehabilitation of buildings*," Federal Emergency Management Agency.

Frye, M.J., and Morris, G.A. (1975). "Analysis of flexibly connected steel frames," *Canadian Journal of Civil Engineering*, 2(3).

Ghobarah, A., Osman, A., and Korol, R.M. (1990). "Behavior of extended end-plate connections under cyclic loading," *Engineering Structures*, Vol. 12, No. 1.

Goel, R.K., and Chopra, A.K. (1991). "Effects of plan asymmetry in inelastic seismic response of one-story systems," *Journal of Struct. Engrg.*, ASCE, Vol. 117, No. 5.

Goel, R.K., and Chopra, A.K. (1993). "Seismic code analysis of buildings without locating centers of rigidity," *Journal of Struct. Engrg.*, ASCE, Vol. 119, No. 10.

Graham, J.D., Sherbourne, A.N., Khabbaz, R.N., and Jensen, C.D. (1959). "Welded interior beam-to-column connections," *AISC Publication*, A.I.A. File No. 13-C.

Heaton, T.H., Hall, J.F.,] Wald, D.J., and Halling, M.W. (1995). "Response of high-rise and base-isolated buildings to a hypothetical M_W7.0 blind thrust earthquake," *Science*, Vol. 267, Jan. 1995.

Kato, B., Aoki, H., and Tagawa, Y. (1984). "Seismic behavior of steel frames with composite girders," *Proceedings, 8th World Conference on Earthquake Engineering*, San Francisco, Vol. VI.

Kilic, S.A. (1996). "Stability issues in frames under lateral loads," *Ph.D. Dissertation*, Department of Civil Engineering, Stanford University.

Kim, K. (1995). "Development of analytical models for earthquake analysis of steel moment frames," *Ph.D. Dissertation*, Dept. of Civil Engrg., Univ of Texas at Austin.

Kishi, N., and Chen, W.F. (1990). "Moment-rotation relations of semirigid connections with angles," *Journal of Struct. Engrg.*, ASCE, Vol. 116, No. 7.

Krawinkler, H., Bertero, V.V., and Popov, E.P. (1971). "Inelastic behavior of steel beam-to-column subassemblages," *Report No. UCB/EERC-71/7*, Earthquake Engineering Research Center (EERC), University of California at Berkeley.

Krawinkler, H. (1978). "Shear design of steel frame joints," *Engineering Journal*, AISC, Vol. 15, No. 3.

Krawinkler, H., et al. (1983). "Recommendations for experimental studies on the seismic behavior of steel components and materials," *John A. Blume Earthquake Engineering Center*, Report No. 61, Department of Civil Engineering, Stanford University.

Krawinkler, H., and Zohrei, M. (1983). "Cumulative damage in steel structures subjected to earthquake ground motions," *Journal on Computers and Structures,* Vol. 16, No. 1-4.

Krawinkler, H., and Mohasseb, S. (1987). "Effects of panel zone deformations on seismic response," *Journal of Constructional Steel Research,* Elsevier Applied Science Publishers, England, Vol. 8.

Krawinkler, H. (1994). "New trends in seismic design methodology," *Proceedings of the 10th European Conference in Earthquake Engineering*, Vienna, Austria.

Krawinkler, H., Alali, A., and Dunlea, J.M. (1995). "Analysis of a damaged 4-story building and an undamaged 2-story building," SAC 95-04, Part 1. *Technical Report: Analytical and Field Investigations of Buildings Affected by the Northridge Earthquake of January 17, 1994.* SAC Joint Venture.

Lawson, R. S., Vance, V. and Krawinkler, H. (1994). "Nonlinear static push-over analysis - why, when, and how?", *Proceedings of the 5th U. S. Conference in Earthquake Engineering*, Vol. 1, Chicago, IL.

Lawson, R.S., and Krawinkler, H. (1994). "Cumulative damage potential of seismic ground motion," *Proceedings of the 10th European Conference in Earthquake Engineering*, Vienna, Austria.

Leon, R.T., and Forcier, G.P. (1991). "Performance of semi-rigid composite frames," *Proceedings of the 1991 Annual Technical Session, SSRC.*

Liew, J.Y.R., White, D.W., and Chen, W.F. (1993-1). "Second-order refined plastic-hinge analysis for frame design. Part I," *J. of Struct. Engrg.,* ASCE, Vol. 119, No. 11.

Liew, J.Y.R., White, D.W., and Chen, W.F. (1993-2). "Second-order refined plastic-hinge analysis for frame design. Part II," *J. of Struct. Engrg.,* ASCE, Vol. 119, No. 11.

LRFD (1994). "Manual of Steel Construction, Load & Resistance Factor Design, volume I - seismic provisions for structural steel buildings," *American Institute of Steel Construction*, Chicago, IL.

Lu, L.W., Wang, S.J., and Lee, S.J. (1988). "Cyclic behavior of steel and composite joints with panel zone deformation," *Proceedings of the 9th World Conference on Earthquake Engineering,* Vol. IV, Tokyo-Kyoto, Japan.

McGuire, W. (1988). "Introduction to Special Issue on Steel Beam-Column Building Connections," *Special Issue on Steel Beam-toColumn Building Connections, Journal for Construct. Steel Research*, Vol. 10, Elsevier Science Publishers.

Meek, J.L., and Lin, W.J. (1990). "Geometric and material nonlinear analysis of thin-walled beam-columns," *Journal of Struct. Engrg.,* ASCE, Vol. 116, No. 6.

Miranda, E. (1991). "Seismic evaluation and upgrading of existing buildings," *Ph.D. Dissertation*, Dept. of Civil Engineering, University of California, Berkeley.

Miranda, E. (1993). "Evaluation of site-dependent inelastic seismic design spectra," *Journal of Structural Engineering*, ASCE, Vol. 119, No. 5.

Miranda, E. (1993-1). "Site-dependent strength-reduction factors," *Journal of Structural Engineering*, ASCE, Vol. 119, No. 12.

Miranda, E., and Bertero, V.V. (1994). "Evaluation of strength reduction factors for earthquake-resistant design," *Earthquake Spectra*, EERI, Vol. 10, No. 2.

Mittal, A.K., and Jain, A.K. (1995). "Effective strength eccentricity concept for inelastic analysis of asymmetric structures," *Earthquake Engineering and Structural Dynamics,* Vol. 24, No. 1.

Moehle, J.P. (1992). "Displacement based design of RC structures," *Proceedings of the 10th World Conference on Earthquake Engineering*, Vol. 8, Madrid, Spain.

Murray, T.M., and Kukreti, A.R. (1988). "Design of 8-boltstiffened moment end plate," *Engineering Journal*, AISC, Vol. 25, No. 2.

Nakashima, M. (1991). "Statistical evaluation of strength of steel beam columns," *Journal of Struct. Engrg.,* ASCE, Vol. 117, No. 11.

Nakashima, M. (1994). "Variation of ductility capacity of steel beam-columns," *Journal of Struct. Engrg.*, ASCE, Vol. 120, No. 7.

Nassar, A.A., and Krawinkler, H. (1991). "Seismic demands for SDOF and MDOF systems," *John A. Blume Earthquake Engineering Center Report No. 95*, Department of Civil Engineering, Stanford University.

Osteraas, J.D. and Krawinkler, H. (1990). "Strength and ductility considerations in seismic design", *John A. Blume Earthquiake Engineering Research Center Report No. 90*, Department of Civil Engineering, Stanford University.

Popov, E.P., and Pinkney, R.B. (1969). "Cyclic yield reversals on steel building connections," *Journal of the Structural Division,* ASCE, Vol. 95, No. 3.

Popov, E.P. and Stephen, R.M. (1970). "Cyclic loading of full-scale steel connections," *Report No. UCB/EERC-70/3*, Earthquake Engineering Research Center (EERC), University of California at Berkeley.

Popov, E.P. and Stephen, R.M. (1976). "Tensile capacity of partial penetration welds," *Report No. UCB/EERC-76/3*, Earthquake Engineering Research Center (EERC), University of California at Berkeley.

Rahnama, M., and Krawinkler, H. (1993). "Effects of soft soils and hysteresis models on seismic design spectra," *John A. Blume Earthquake Engineering Center*, Report No. 108, Department of Civil Engineering, Stanford University.

Rahnama, M., and Krawinkler, H. (1994-1). "Amplification of Seismic Demands in Linear and Nonlinear Soft Soils," *Proceedings of the 5th U.S. National Conference on Earthquake Engineering*, Vol. II, Chicago, IL.

Rahnama, M., and Krawinkler, H. (1994-2). "Effects of P-delta and strength deterioration on SDOF strength demands," *Proceedings of the 10th European Conference in Earthquake Engineering,* Vienna, Austria.

Rentschler, G.P., Chen, W.F., and Driscoll, G.C. (1980). "Tests of beam-to-column web moment connections," *Journal of the Structural Division,* ASCE, Vol. 106, No. 5.

Roeder, C.W., Schneider, S.P., and Carpenter, J.E. (1993). "Seismic behavior of moment-resisting steel frames: analytical study," *Journal of Struct. Engrg.*, ASCE, Vol. 119, No. 6.

Sadek, A.W., and Tso, W.K. (1988). "Strength eccentricity concept for inelastic analysis of asymmetric structures," *Proceedings of the 9th World Conference on Earthquake Engineering*, Tokyo, Japan.

Saiidi, M. and Sozen, M.A. (1981). "Simple nonlinear seismic analysis of R/C structures", *Journal of the Structural Division,* ASCE, Vol. 107, No. 5.

Seneviratna, G.D.P.K. (1996). "Evaluation of inelastic MDOF effects for seismic design," *John A. Blume Earthquake Engineering Center*, Report, Department of Civil Engineering, Stanford University.

Sivakumaran, K.S., and Chen, S. (1994). "Seismic behavior of type PR steel frames," *Proceddings of the Structures Congress 1994*, ASCE.

Sohal, I.S., and Syed, N.A. (1992). "Inelastic amplification factor for design of steel beam-columns," *Journal of Struct. Engrg.*, ASCE, Vol. 118, No. 7.

SSPC (1994). "Statistical analysis of tensile data for wide flange structural shapes," Steel Shape Producers Council.

SSRC (1988). "*Guide to stability design criteria for metal structures*," Structural Stability Research Council, 4th Ed., J. Wiley & Sons, New York.

Tsai, K.C., and Popov, E.P. (1988). "Steel beam-column joints in seismic moment resisting frames," *Report No. UCB/EERC-88/19*, Earthquake Engineering Research Center (EERC), University of California at Berkeley.

Tsai, K.C., and Popov, E.P. (1990). "Cyclic behavior of end-plate moment connections," *Journal of Struct. Engrg.*, ASCE, Vol. 116, No. 11.

Tsai, K.C., and Popov, E.P. (1990-1). "Seismic panel zone design effect on seismic story drift in steel frames," *Journal of Struct. Engrg.*, ASCE, Vol. 116, No. 12.

Tso, W.K., and Zhu, T.J. (1992). "Design of torsionally unbalanced structural systems based on code provisions. I: ductility demand," *Earthquake Engineering and Structural Dynamics,* Vol. 21.

Uang, C.M. (1991). "Establishing R (or (R_W) and C_d factors for building seismic provisions," *Journal of Struct. Engrg.*, ASCE, Vol. 117, No. 1.

UBC (1994). "Structural Engineering Design Provisions," *Uniform Building Code*, Vol. 2, International Conference og Building Officials.

Vidic, T., Fajfar, P., and Fischinger, M. (1994). "Consistent inelastic design spectra: strength and displacement," *Earthquake Engineering and Structural Dynamics,* Vol. 23.

Yura, J. A. (1971). "The effective length of columns in unbraced frames," *Engineering Journal*, AISC, April 1971.

Zhu, T.J., and Tso, W.K. (1992). "Design of torsionally unbalanced structural systems based on code provisions. II: strength distribution," *Earthquake Engineering and Structural Dynamics,* Vol. 21.

Ziemian, R.D., McGuire, W., and Deierlein, G.G. (1992-1). "Inelastic limit states design. Part I: Planar frame studies," *Journal of Struct. Engrg.*, ASCE, Vol. 118, No. 9.

Ziemian, R.D., McGuire, W., and Deierlein, G.G. (1992-2). "Inelastic limit states design. Part II: Three-dimensional frame study," *J. of Struct. Engrg.*, ASCE, Vol. 118, No. 9.

APPENDIX A:
SAC PROGRAM TO REDUCE THE EARTHQUAKE HAZARDS OF STEEL MOMENT FRAME STRUCTURES, AN OVERVIEW

Following the January 17, 1994 Northridge, California Earthquake, more than 150 steel buildings with welded moment-resisting frames were found to have experienced beam-to-column connection fractures. The damaged structures cover a wide range of heights ranging from one-story to 26 stories; and a wide range of ages spanning from buildings as old as 30 years of age to structures just being erected at the time of the earthquake. The damaged structures are spread over a large geographical area, including sites that experienced only moderate levels of ground shaking. Although relatively few steel buildings were located on sites that experienced the strongest ground shaking, damage to these buildings was generally quite severe.

Discovery of these extensive connection fractures, often with little associated architectural damage to the buildings, has been alarming. The discovery has also raised concern that similar, but undiscovered damage may have occurred in other buildings affected by past earthquakes. Indeed, there are isolated reports of such damage. In particular, a building at Big Bear Lake is known to have been damaged by the 1992 Landers-Big Bear, California sequence of earthquakes, and at least one building, under construction in Oakland, California at the time of the 1989 Loma Prieta Earthquake, was reported to have experienced similar damage.

Welded Steel Moment Frame (WSMF) construction is used commonly throughout the United States and the world, particularly for mid- and high-rise construction. Prior to the Northridge Earthquake, this type of construction was considered one of the most seismic-resistant structural systems, due to the fact that severe damage to such structures had rarely been reported in past earthquakes and there was no record of earthquake-induced collapse of such buildings, constructed in accordance with contemporary US practice. However, the widespread severe structural damage which occurred to such structures in the Northridge Earthquake calls for re-examination of this premise.

The basic intent of the earthquake resistive design provisions contained in the building codes is to protect the public safety; however, there is also an intent to control damage. The developers of the building code seismic provisions have explicitly set forth three specific performance goals for buildings designed and constructed to the code provisions (SEAOC - 1990). These are to provide buildings with the capacity to:

- resist minor earthquake ground motion without damage;
- resist moderate earthquake ground motion without structural damage but possibly some nonstructural damage; and
- resist major levels of earthquake ground motions, having an intensity equal to the strongest either experienced or forecast for the building site, without collapse, but possibly with some structural as well as nonstructural damage.

In general, WSMF buildings in the Northridge Earthquake met the basic intent of the building codes, to protect life-safety. However, many of these buildings experienced significant damage that could be viewed as failing to meet the intended performance goals with respect to damage control . Further, some members of the engineering profession (SEAOC - 1995b) and government agencies (Seismic Safety Commission - 1995) have stated that even these performance goals are inadequate for society's current needs.

WSMF buildings are designed to resist earthquake ground shaking, based on the assumption that they are capable of extensive yielding and plastic deformation, without loss of strength. The intended plastic deformation consists of plastic rotations developing within the beams and at their connections to the columns. Damage is expected to consist of moderate yielding and localized buckling of the steel elements, not brittle fractures. Supplemental provisions within the building code, intended to control the amount of interstory drift sustained by these flexible frame buildings, typically result in structures which are substantially stronger than the minimum base shear requirement. This design approach has been developed based on historical precedent, the observation of steel building performance in past earthquakes, and limited research that has included laboratory testing of beam-column models (albeit with mixed results) and non-linear analytical studies.

Observation of damage sustained by buildings in the Northridge Earthquake indicates that contrary to the intended behavior, in many cases brittle fractures initiated within the connections at very low levels of plastic demand, and in some cases, while the structures remained elastic. Typically, but not always, fractures initiated at, or near, the complete joint penetration (CJP) weld between the beam bottom flange and column flange (Figure A-1). Investigators initially identified a number of factors which may have contributed to the initiation of fractures at the weld root including: notch effects created by the backing bar which was commonly left in place following joint completion; sub-standard welding that included slag inclusions as well as incomplete fusion; and potentially, pre-earthquake fractures resulting from initial shrinkage of highly restrained welds during cool-down. Such problems could be minimized in future construction, with the application of appropriate welding procedures and more careful exercise of quality control during the construction process. However, it is now known that these were not the only causes of the fractures which occurred.

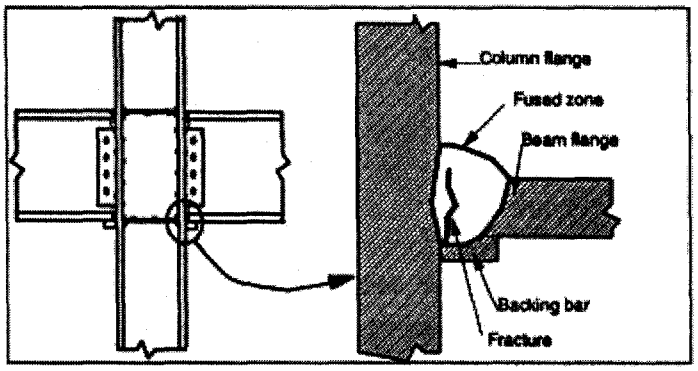

Figure A-1 - Common Zone of Fracture Initiation in Beam-Column Connection

Current production processes for structural steel shapes may result in inconsistent strength and deformation capacities for the material in the through-thickness direction. Further, the distribution of stress across the girder flange at the connection to the column is not uniform. Even in connections stiffened by continuity plates across the panel zone, significantly higher stresses tend to occur at the center of the flange, where the column web produces a local stiffness concentration. Large secondary stresses are also induced into the girder flange to column flange joint by kinking of the column flanges resulting from shear deformation of the column panel zone.

The dynamic loading experienced by the moment-resisting connections in earthquakes is characterized by high strain, tension-compression cycling. While the nature of the dynamic loads resulting from earthquakes is somewhat different than the high cycle dynamic loads for which fatigue-prone structures such as bridges are designed, similar detailing may be desirable for buildings subject to seismic loading.

The rapid rate of loading imposed by seismic events, and the complete inelastic range of tension-compression-cyclic loading applied to these connections is much more severe than typical bridge loading applications. The mechanical and metallurgical notches of stress risers created by the beam-column weld joints are a logical point for fracture problems to initiate. This, coupled with the tri-axial restraint provided by the beam web and the column flange, is a recipe for brittle fracture.

During the Northridge earthquake, once fractures initiated in beam-column joints, they progressed in a number of different ways. In some cases, the fracture initiated but did not grow, and could not be detected by visual observation. In other cases, the fractures progressed completely through the thickness of the weld, and if fireproofing was removed, the fractures were evident as a crack through exposed faces of the weld, or the metal just behind the weld (Figure A-2a). Other fracture patterns also developed. In some cases, the fracture developed into a through-thickness failure of the column flange material behind the CJP weld (Figure A-2b). In these cases, a portion of the column flange remained bonded to the beam flange, but pulled free from the remainder of the column. This fracture pattern has sometimes been termed a "divot" or "nugget" failure. A number of fractures progressed completely through the column flange, along a near horizontal plane that aligns approximately with the beam lower flange (Figure A-3a). In some cases, these fractures extended into the column web and progressed across the panel zone Figure (A-3b). Investigators have reported some instances where columns fractured entirely across the section.

a. Fracture at Fused Zone

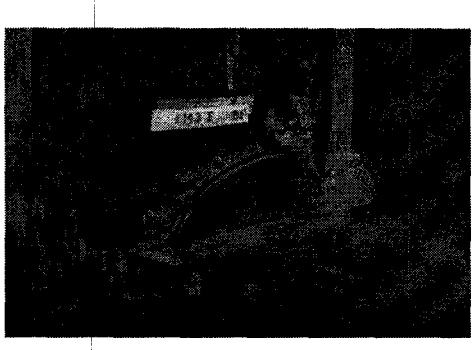

b. Column Flange "Divot" Fracture

Figure A-2 - Fractures of Beam to Column Joints

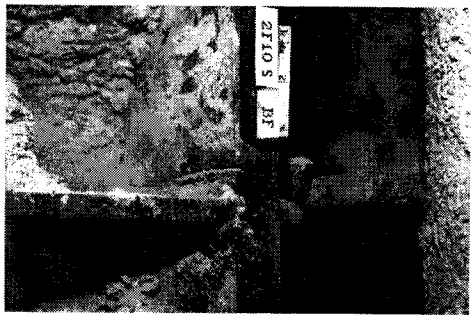

a. Fractures through Column Flange

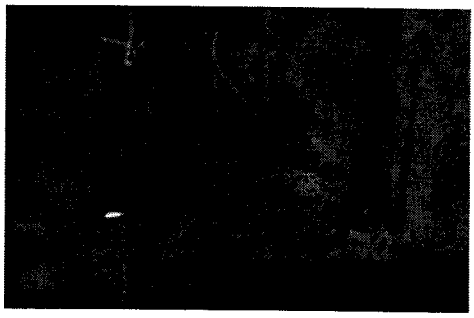

b. Fracture Progresses into Column Web

Figure A-3 - Column Fractures

Once these fractures have occurred, the beam-column connection has experienced a significant loss of flexural rigidity and capacity. Residual flexural strength and rigidity must be developed through a couple consisting of forces transmitted through the remaining top flange connection and the web bolts. In providing this residual strength and stiffness, the beam shear connections can themselves be subject to failure, consisting of fracturing of the welds of the shear plate to the column, fracturing of supplemental welds to the beam web or fracturing through the weak section of the shear plate aligning with the bolt holes (Figure A-4).

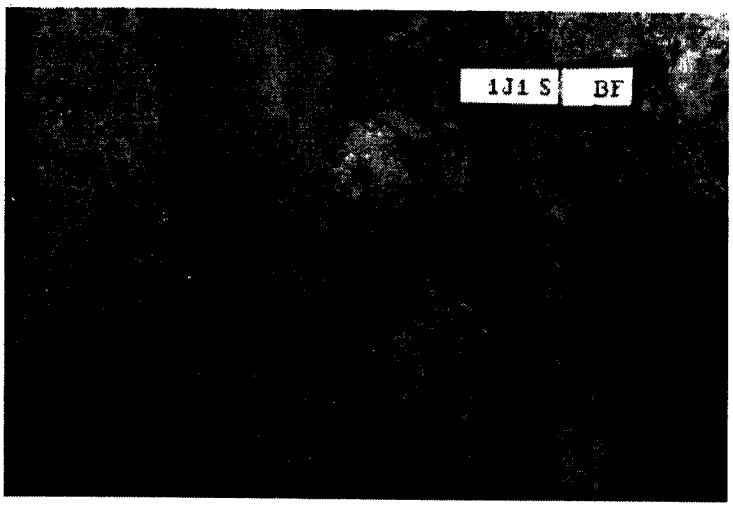

Figure A-4 - Vertical Fracture through Beam Shear Plate Connection

Despite the obvious local strength impairment resulting from these fractures, many damaged buildings did not display overt signs of structural damage, such as permanent drifts or extreme

damage to architectural elements. Until news of the discovery of connection fractures in some buildings began to spread through the engineering community, it was relatively common for engineers to perform cursory post-earthquake evaluations of WSMF buildings and declare that they were undamaged. In order to reliably determine if a building has sustained connection damage it is necessary to remove architectural finishes and fireproofing and perform nondestructive examination including visual inspection and ultrasonic testing. Even if no damage is found, this is a costly process. Repair of damaged connections is even more costly. A few WSMF buildings have sustained so much connection damage that it has been deemed more practical to demolish the structures rather than to repair them.

THE PROBLEM

The Northridge earthquake effectively invalidated the building code and professional practices used before the earthquake for the design and evaluation of steel moment frame structures. It was not clear how to repair damaged, retrofit undamaged, or design new steel moment frame structures. This left owners and structural designers in a precarious situation.

- Should a damaged building be repaired immediately, using expensive and possibly ineffectual techniques, or wait for better techniques to arrive, but risk more serious, potentially catastrophic, behavior in future earthquakes and aftershocks before it is repaired?
- Should an owner inspect the connections of a building that shows very little visible damage?
- Should a perspective owner buy or should a lender finance an existing steel building?
- Should owners with steel frame buildings awaiting construction continue on schedule, or should they change their designs to correct the apparent deficiencies uncovered by the Northridge earthquake?
- Should designers choose other structural systems until definitive answers to performance questions were known?
- How do we identify buildings that are damaged and pose increased life-safety risks in earthquakes, including aftershocks?
- How do we repair damaged buildings so that they provide life-safety?
- How do we design new buildings and retrofits for existing buildings so that they perform acceptably?

These questions were especially worrisome because the knowledge and experience needed to confidently devise good, cost-effective reliable answers was not available. Until new knowledge was generated, any action in repair, design or retrofit was fraught with the possibility of being deficient in both safety and economy. The implications of this situation were substantial for the design profession, the construction and steel industries, building officials, owners, occupants, lenders, and insurers - not only in the Los Angeles area, but throughout the U.S., and the world.

THE SAC JOINT VENTURE

SAC is a joint venture of the Structural Engineers Association of California (SEAOC), the Applied Technology Council (ATC), and California Universities for Research in Earthquake Engineering (CUREe), formed specifically to address both immediate and long-term needs related to solving the problems of the WSMF connection. SEAOC is a professional organization comprised of more than 3,000 practicing structural engineers in California . The volunteer efforts of SEAOC's members on various technical committees have been instrumental in the development of the earthquake design provisions contained in the *Uniform Building Code* as well as the *National Earthquake Hazards Reduction Program (NEHRP) Recommended Provisions for Seismic Regulations for New Buildings.* The Applied Technology Council is a non-profit organization founded specifically to perform problem-focused research related to structural engineering and to bridge the gap between civil engineering research and engineering practice. It has developed a number of publications of national significance including ATC 3-06, which serves as the basis for the *NEHRP Recommended Provisions*. CUREe's eight institutional members are: the California Institute of Technology, Stanford University, the University of California at Berkeley, the University of California at Davis, the University of California at Irvine, the University of California at Los Angeles, the University of California at San Diego, and the University of Southern California. This collection of university earthquake research laboratory, library, computer and faculty resources is among the most extensive in the United States. The SAC Joint Venture allows these three organizations to combine their extensive and unique resources, augmented by subcontractor universities and organizations from around the nation, into an integrated team of practitioners and researchers, uniquely qualified to solve problems related to the seismic performance of WSMF structures.

The goal of the SAC Joint Venture Steel Project is to:

> *Develop professional practices and recommend standards for the evaluation, repair, retrofit, and design of steel moment frame buildings so that they provide reliable, cost-effective seismic performance in future earthquakes.*

The following objectives were identified as necessary to meet these goals:

1. Characterize and understand what happened to steel moment frame buildings during the Northridge Earthquake.
2. Prepare interim procedures for professional practices and standards applicable to:
   - identification of buildings that may have been damaged and that require detailed inspection and investigation.
   - evaluation of seismically vulnerable buildings, including the characterization of the safety of inspected or damaged buildings.
   - rehabilitation of damaged buildings; and

- design of new steel frame structures

3. Conduct directed and coordinated technical investigations, analyses and research, as necessary, to develop new knowledge required to develop reliable and cost effective design guidelines and standards of practice related to steel moment frame structures.
4. Prepare recommendations for the repair, retrofit and design of buildings based on a rational understanding of seismic behavior.

The SAC Joint Venture program involves two phases. Phase 1 covers items 1 and 2 above plus initial portions of item 3. The specific tasks in Phase 1 are listed in Table A-1. Brief descriptions of each task are provided in subsequent sections. The remainder of item 3 and item 4 are to be addressed in Phase 2.

Table A-1 - Phase I Tasks

Task 1:	Organize Phase I Program and Engage Key Participants
Task 2:	Inspect and Assess How Buildings Performed During the Northridge Earthquake to Understand the Damage.
Task 3:	Perform Detailed Assessment of the Performance of Selected Buildings
Task 4:	Characterize Ground Motions at the Sites of Subject Buildings
Task 5:	Develop Design Advisories.
Task 6:	Assessment of Current Knowledge
Task 7:	Conduct Laboratory Tests of Steel Assemblies
Task 8:	Develop Draft Interim Guidelines
Task 9:	Conduct Users Workshop and Finalize Interim Guidelines
Task 10:	Publish Interim Guideline Documents and Conduct a Seminar in Southern California

PHASE I - ORGANIZATION AND MANAGEMENT PLAN

As indicated in Figure A-5, the Program Management and Organization Chart, the Phase I Program, including contract funds, have been administered by the SAC Joint Venture Management Committee, which is comprised of two representatives each from SEAOC, CUREe, and ATC. Arthur E. Ross, representing SEAOC, served as Chair of the Phase 1 Management Committee.

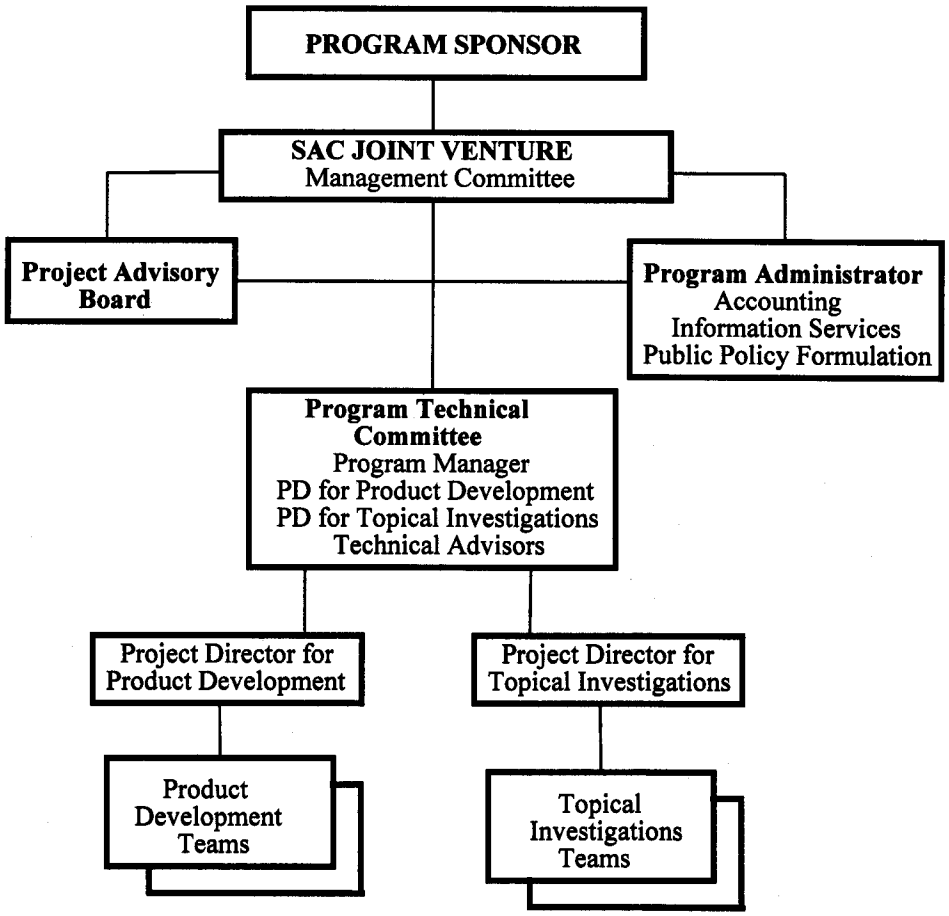

Figure A-5 - Organization and Management Chart

Following is a description of the key Joint Venture program groups and personnel and their responsibilities:

1. **Joint Venture Management Committee.** The Joint Venture Management Committee has overall responsibility for carrying out the proposed program. This includes: establishing the general scope of work to be completed under the program, developing and implementing the program management scheme, overseeing the selection and engagement of program personnel, overseeing the receipt and distribution of program funds, establishing a process for conflict resolution, and approving any contract deliverables established by the funding agencies. Table A-2 lists the members of the SAC Joint Venture Management Committee.

2. **Program Advisory Boards.** In Phase 1, two nationally representative Program Advisory Groups were established. The *Oversight Board*, composed of

Table A-2

SAC Management Committee
Chairman - Arthur E. Ross

Structural Engineers Association of California	**Applied Technology Council**	**California Universities for Research in Earthquake Engineering**
Maryann Phipps*	John Coil	Robin Shepherd
Arthur E. Ross	Christopher Rojahn	Charles Thiel, Jr.

*Replaced Ronald Nelson in February, 1995.

Table A-3

SAC Project Oversight Committee
Dr. William Hall, University of Illinois, Chair

Susan Dowty, International Conf. of Building Officials
Roger Ferch, Herrick Corporation
John Gross, National Inst. of Standards & Technology
Fred Herman, City of Palo Alto, California Seismic Safety Commission
Richard Holguin, City of Los Angeles
Nestor Iwankiw, American Inst. of Steel Construction
Roy Johnston, Brandow and Johnston Associates
William Mooseker, WHM Consultants
Joseph Nicoletti, URS Consultants
Richard Ranous, California Office of Emergency Services
M. P. Singh, National Science Foundation
John Theiss, EQE International, Inc.

representatives from FEMA, OES and other government agencies, building regulatory agencies, model code groups, steel industry and fabricators associations, and professional practice, has responsibility for monitoring the overall program, providing input from the end-users perspective, and advising the Joint Venture Management Committee. Dr. William Hall served as the Chair of the Oversight Board, whose members are listed in Table A-3. The *Technical Advisory Board*, composed of recognized specialists in the seismic design and performance of steel moment frame structures, has responsibility for providing technical overview and guidance. Table A-4 lists the members of the Technical Advisory Board.

3. **Program Manager**. The Program Manager has overall responsibility for managing all aspects of the program and reports directly to the Joint Venture

Management Committee. Dr. Stephen A. Mahin served as the Phase I Program Manager.

Table A-4

SAC Technical Advisory Board

Robert Bachman, Fluor-Daniel Corp.	William Honeck, Forell/Elsesser Engineers, Inc.
Vitelmo Bertero, Univ. of California at Berkeley	Stanley Lindsey, Stanley V. Lindsey Associates
John Fisher, Lehigh University	Hank Martin, American Iron and Steel Institute
Subhash Goel, University of Michigan	John Martin, Jr., John A. Martin and Associates
Thomas Heaton, United States Geological Survey	Duane Miller, Lincoln Electric Company
Thomas Henyey, So. California Earthquake Center	Charles Thornton, Thornton-Tomasetti, Inc.

4. **Program Administrator.** The Program Administrator has responsibility for administrative support functions and reports directly to the Joint Venture Management Committee. The Program Administrator also served as the Authorized Joint Venture Representative. This function was carried out by the SEAOC Executive Director, Allen Paul Goldstein.

5. **Project Director for Product Development..** The Project Director for Product Development has responsibility for managing and coordinating the development of products (i.e., specific deliverables such as Interim Guidelines) for the practicing design professions. Ronald O. Hamburger was the Phase 1 Project Director for Product Development.

6. **Project Director for Topical Investigations.** The Project Director for Topical Investigations has responsibility for managing and coordinating the topical investigations (e.g., investigations of welding, joint behavior, and system behavior, modeling and analytical investigations, and nondestructive testing). James O. Malley was the Phase 1 Project Director for Topical Investigations.

7. **Program Technical Committee.** The Program Technical Committee has responsibility for advising the Program Manager on day to day operations. It consists of the Program Manager, who serves as Chair, the Project Director for Topical Investigations, and the Project Director for Product Development.

8. **Task Consultants/Subcontractors.** The SAC Joint Venture engaged consultants and/or subcontractors to conduct detailed task work. The specific responsibilities for each consultant and subcontractor were defined in the Work Plan by task. The task consultants and subcontractors were supervised by the Project Director for Product Development and/or the Project Director for Topical Investigations.

TASK DESCRIPTIONS

The ten tasks completed in the Phase I program are described below. The following general considerations were applied:

1. All technical task efforts should include both researchers and practicing engineers in a meaningful way. Integration of knowledge producers (researchers) with knowledge users (practitioners) is considered to be an extremely effective mechanism in technology transfer.

2. Each technical task will have a Technical Advisory Panel (TAP) to provide advice, assist in interpreting results, facilitate coordination of efforts among different subtasks, and expedite transfer of knowledge to the user community.

Task 1: Organize Phase 1 Program and Engage Key Participants

Under this task the SAC Joint Venture Management Committee finalized the overall scope of Phase 1 of the program, wrote the Phase 1 Work Plan, finalized the Phase 1 budget, identified and resolved management issues, established a quality control program, and identified and engaged key Phase 1 participants. The Management Committee was assisted by the Program Administrator and the Program Manager in this endeavor.

Task 2: Inspect and Assess How Buildings Performed During the Northridge Earthquake to Understand the Damage

The objectives of this task were to gather quantitative information regarding the total number of damaged and undamaged steel buildings in the area of strong shaking, and especially important, of the structural configuration, materials and details of steel moment frame buildings that exhibited good and poor performance. The following subtasks were carried out: (1) surveys of performance of steel frame buildings in the Los Angeles vicinity; (2) development of maps (in a GIS environment) showing the locations of damaged buildings along with attributes of interest; (3) interviews to gather and synthesize field experience related to inspection, evaluation, repair and construction; and (4) testing and evaluation of specimens removed from buildings surveyed.

Task 3: Perform Detailed Assessment of the Performance of Selected Buildings

Detailed investigations and analyses (and material and field tests) were performed on selected buildings to identify the specific causes of failures, to assess the accuracy of available analytical methods, and to identify the conditions under which more severe, life threatening damage might occur. This activity built upon previous efforts undertaken by inspectors and engineers following the Northridge Earthquake, but was more detailed and focused. Specific investigations quantitatively assessed the ability of different types of modeling and analysis procedures to predict dynamic characteristics, and the global and local damage in the building. Also, studies were undertaken to assess the possible response of the structures considered during hypothetical aftershocks, or other types of future earthquakes to identify conditions that might lead to more

severe damage and threaten life-safety. These activities supported concurrent efforts to develop the Interim Guidelines and suggest topics for subsequent investigation related to modeling and analysis methods, evaluation procedures, and system response.

Task 4: Characterize Ground Motions at the Sites of Subject Buildings

This effort involved the generation of ground motions at sites in the Northridge area where steel buildings selected for detailed study are located. Simulated motions were generated corresponding to the January 17 event (if no records are available at the site), for aftershocks, and for hypothetical events that should be considered in design of buildings in that area. This activity relied heavily upon existing geophysical models for the fault rupture mechanism for the Northridge Earthquake as well as upon available knowledge and data from the Southern California Earthquake Center (SCEC), U.S. Geological Survey (USGS), California Strong-Motion Instrumentation Program (CSMIP) and other geotechnical specialists in the public and private sectors. Ground motion data was also provided for mapping efforts in Task 2.

Task 5: Develop Design Advisories

The objective of the task was to collect and review information from design professionals, construction inspectors, contractors, building officials, and others regarding problems in (1) identifying and inspecting potential deficient steel frame buildings, (2) developing rehabilitation plans, (3) designing new structures, and (4) executing repairs in the field. The information was gathered and reviewed in workshop settings, including the International Workshop on Steel Seismic Issues (International Workshop), which was held in Los Angeles in September 1994. The information was made available in three design advisories. *Design Advisories 1 and 2* (SAC 94-02, SAC 94-03) consists of selected information on available design recommendations and performance of steel structures; *Design Advisory 3* (SAC 95-01) contains a review of available information on design and performance. In addition, the SAC Joint Venture published the proceedings of the International Workshop (SAC 94-01).

Task 6: Assessment of Current Knowledge

Data available worldwide on performance of steel moment frame buildings during earthquakes in laboratory tests and elsewhere were compiled and presented in a form useful to practicing engineers and developers of guidelines for inspection, evaluation, analysis and rehabilitation as well as for design of new structures. Information on topics such as welding, bolting, non-destructive testing, and inspection procedures will be gathered and evaluated.

The following subtasks were performed: (1) a literature review, which will include development of an electronic database; (2) preparation of state-of-the-art and state-of-the-practice summary papers; (3) formation of topical teams to review and evaluate results from subtasks 1 and 2, identify areas of concern that should be considered during development of the Interim Guidelines (see Tasks 8 and 9), and identify specification investigation needs; and (4) development of a program to disseminate results to the user community.

Task 7: Conduct Laboratory Tests of Steel Assemblies

Preliminary experimental investigations were needed to identify the critical factors causing the observed connection fractures during the Northridge Earthquake, to establish the validity of conceptual models being developed for the design of connections, and to assess the reliability of details and procedures being considered for inclusion in the Interim Guidelines. A wide variety of parameters critically influence the performance of beam-to-column connections, including material properties, weld process and procedures, joint design and detailing, member sizes, and loading rates. During the Phase I program, it was not possible to investigate experimentally all of the issues and details involved. An initial test program was needed to begin to prioritize and clarify these issues. A short term, coordinated program was needed to begin to prioritize and clarify these issues. Tests examining repaired and new connection details and the effect of weld procedures and material properties on connection behavior were carried out. Results were used immediately to validate and refine the basic recommendations in the Interim Guidelines and to clarify longer term issues that require further investigation.

The following subtasks were performed: (1) establishment of the details of the test program; (2) full-scale tests of details for new and repaired beam-to-column connections; (3) special tests to assess factors influencing the performance of weldments; and (4) testing of material properties used in test assemblies and evaluation of specimen failure modes.

Task 8: Develop Draft Interim Guidelines

This task focused on the development of Interim Guidelines for professional practices and standards applicable to: (1) identification of buildings that may have been damaged for investigation; (2) evaluation of the safety condition of inspected buildings; (3) repair of damaged buildings to provide life-safety and pre-earthquake performance expectations; and (4) design of new steel moment frames.

The technical approach for development of Interim Guidelines was driven by the need to quickly provide guidance to practicing structural engineers in the Los Angeles region who are confronted with finding appropriate solutions for the repair of steel moment frame buildings damaged by the Northridge earthquake. The time allotted for this task prohibited the development of comprehensive guidelines that have been thoroughly evaluated and tested; rather, the guidelines are intended to provide the best-possible "stop-gap" measures, given the manpower, informational, and financial resources available, and recognizing that the Interim Guidelines will undergo review and revision during the longer term Steel Program current being planned. In fact, it is anticipated that there may be *significant* changes to the Interim Guidelines when more information becomes available at a later date.

The Interim Guidelines were written for practicing structural engineers and building officials. Due to the special regional nature of the problem at hand, the draft version of the Interim Guidelines produced under this task focused specifically on the representative types of steel moment frame buildings now located throughout the Los Angeles region. In other words, the guidelines specifically considered the design, detailing, and construction criteria and standard

followed for this type of construction in this area. While this construction type is quite common, this limited task was not able to cover all forms of steel frame construction used in the United States.

Task 9: Conduct Users Workshop and Finalize Interim Guidelines

After the completion of Task 8, the draft Interim Guidelines were evaluated in a Users Workshop to gather peer review comments, upon which the Guidelines were finalized. Participants in this workshop included those invited to a project participants workshop, plus representatives from the user community: practicing engineers, building officials, fabricators, and others. Following this workshop, the Guidelines were finalized.

Task 10: Publish Interim Guideline Documents and Conduct a Seminar in Southern California

The SAC Joint Venture published the finalized Interim Guidelines entitled, *Interim Guidelines: Evaluation, Repair, Modification and Design of Welded Steel Moment Frame Structures* (SAC 95-02), and widely announced their availability as well as that of other resource materials developed during Phase I. In addition, the SAC Joint Venture conducted a seminar in Southern California, Northern California and Washington to explain the results, findings, and conclusions of the Phase I Program. The seminars focused primarily on the Interim Guidelines.

REFERENCES

SAC, *Proceedings of the International Workshop on Steel Moment Frames, October 23-24, 1994 SAC-94-01.* Sacramento, California, December, 1994.

SAC, *Steel Moment Frame Advisory No. 1.* Sacramento, California, September, 1994.

SAC, *Steel Moment Frame Advisory No. 2.* Sacramento, California, October, 1994.

SAC, *Steel Moment Frame Advisory No. 3 SAC-95-01,* Sacramento, California, February, 1995.

SAC, *Interim Guidelines: Evaluation, Repair, Modification and Design of Welded Steel Moment Frame Structures, SAC-95-02,* Sacramento, California, September, 1995.

Structural Engineers Association of California (SEAOC), Seismology Committee, *Recommended Lateral Force Requirements and Commentary,* Sacramento, California, 1990.

Structural Engineers Association of California (SEAOC), *Vision 2000: A Framework for Performance Based Engineering of Buildings,* Sacramento, California, April, 1995.

☆ U.S. GOVERNMENT PRINTING OFFICE: 1997 – 517- 727 83612

FEDERAL EMERGENCY MANAGEMENT AGENCY

PACE AC BELLO MERITA